GENETIC AND SYSTEMIC TOXICITY INDUCED BY TITANIUM DIOXIDE AND ZINC OXIDE NANOPARTICLES AND THEIR MIXTURE IN SOMATIC AND GERM CELLS OF MICE

BY

OPEOLUWA MOTUNRAYO, FADOJU

Matric. No.: 180505

B.Sc. Cell Biology and Genetics (Lagos), MRes. Medical Genetics (Newcastle upon Tyne)

A Thesis in the Department of Zoology,
Submitted to the Faculty of Science
in partial fulfilment of the requirement for the Degree of

DOCTOR OF PHILOSOPHY

of the

UNIVERSITY OF IBADAN

NOVEMBER, 2018

ABSTRACT

Titanium dioxide (TiO_2) and zinc oxide (ZnO) nanoparticles are components of personal care products whose continuous release into the environment may enhance co-exposure, with potential risks to the ecosystem. *In vitro* studies have shown their potential to induce genetic damage. However, there is dearth of information on *in vivo* induction of DNA and systemic damage, alongside their interactive effects. This study was designed to investigate genetic and systemic toxicity and mechanism of DNA damage by TiO_2 and ZnO nanoparticles and their mixture in mice.

Male Swiss mice ($\bar{x}$=24.0±2.0g; n=80; 6-8 weeks old) were intraperitoneally exposed to distilled water (Control) and 9.4, 18.8, 37.5, 75.0 and 150.0 mg/kg concentrations of each of the nanoparticles and their mixture (1:1) for 5 days (5 mice/group) to assess micronucleus induction and cytomorphological abnormalities in the bone marrow of mice. Haematological parameters [Haemoglobin, Packed Cell Volume (PCV), Red Blood Cell (RBC) and White Blood Cell (WBC) counts] were assessed following standard procedures. Mechanism of DNA damage was evaluated by oxidative stress [Superoxide dismutase (SOD), reduced Glutathione and Malondialdehyde in the liver and kidney] parameters following standard methods. Sperm count, motility, abnormalities and concentrations of Luteinizing Hormone (LH), Follicle Stimulating Hormone (FSH) and Testosterone were evaluated in another group of mice ($\bar{x}$=30.0±2.0g; n=80; 11-15 weeks old), intraperitoneally exposed with the same nanoparticle concentrations (5 mice/group) at 35-day exposure. Liver, kidney and testis were sectioned for histopathological analysis. The Interaction Factor (IF) of nanoparticle mixture was calculated according to standard method. Data were analysed using descriptive statistics and ANOVA at $\alpha_{0.05}$.

The nanoparticles and mixture induced micronuclei, but significant only for TiO_2 (16.8±2.1-53.3±18.5) compared with the control (3.7±0.9). Blebbed, target,

hyperchromic and hypochromic erythrocytes were the observed cytomorphological anomalies. The mixture exerted a significant reduction only in the WBC count. In the liver, there was a significant decrease in SOD (unit/mg protein) activities (1.3-1.5; 1.4-2.0; and 1.2-1.6 fold for TiO_2, ZnO and mixture, respectively), with increase in Malondialdehyde (nmol/mg protein) levels (1.1-1.7; 1.2-1.8; and 1.7-1.7 fold for TiO_2, ZnO and mixture, respectively). In the kidney, there were significant alterations in SOD: 1.2-1.3; and 1.1-1.4 fold decrease for TiO_2 and ZnO, respectively; and 1.3-2.0 fold increase for the mixture. While Malondialdehyde levels increased (1.2-1.4; 1.4-1.6; and 1.7-1.9 fold for TiO_2, ZnO and mixture, respectively). Both organs showed alterations in reduced Glutathione levels (1.0-1.5 fold decrease for TiO_2; 1.0-1.1 fold increase for ZnO and mixture) indicating systemic toxicity. A significant decrease in sperm count and motility; and increase in abnormalities (1.3-8.0; 1.2-2.6; 4.6-12.1 fold for TiO_2, ZnO and mixture, respectively), with a concomitant decrease in the serum level of LH and increase in FSH and Testosterone were observed. Hepatocellular and spermatogenic cell necrosis and degeneration of tubular epithelial cells were observed. The IF indicated synergism.

Titanium dioxide and zinc oxide nanoparticles and their mixture induced genomic and systemic damage in somatic and germ cells of mice; with the mixture synergistically evoking the highest toxic response. Oxidative stress might be one of the mechanisms of cytogenotoxicity.

Keywords: Metal oxide nanoparticles, DNA damage, Germ and somatic cell mutation, Oxidative damage.

Word count: 496

DEDICATION

This thesis is dedicated to my late Father, Dr (Elder) Solomon Olugbenga Fadoju (Ph.D.) who contributed financially, morally and spiritually to the success of my Ph.D. studies before his transition to glory. You will forever remain in my heart Daddy.

ACKNOWLEDGEMENTS

I am indeed grateful to my supervisor, the current Head of Department of Zoology, University of Ibadan, Prof. A. A. Bakare for his support, encouragement, firmness, push and intellectual criticisms. I thank him for the unwavering faith he had in me despite the fact that I never did my master's programme in the University of Ibadan, yet he gave me the opportunity of being his research student. I thank him for being scrupulous in all the write-ups that I submitted throughout the period of my Ph.D. studies. I wish to thank Dr. Arno Gutleb and his group at the Environmental Research and Innovation Department, Luxembourg Institute of Science and Technology, Luxembourg for assisting with the physicochemical characterisation of the NPs and their mixture.

I appreciate Prof. O. O. Sonibare of the Department of Chemistry, University of Ibadan for providing the ultrasonicator used through out the research. My appreciation goes to Prof. O. A. Adaramoye of the Department of Biochemistry, University of Ibadan for his advice on the biochemical aspect of the research. I am grateful to Dr C. G. Alimba who has always being like an uncle and teacher since my undergraduate days; he laid the foundation of research on which I built. He believed and encouraged me, and was a contributing factor to my passion for research. I appreciate the contributions of the former Head of Department of Zoology, University of Ibadan, Prof. Adiaha A. A. Ugwumba; all the academic, non-academic and administrative Staff of the department.

I thank the Genetic Toxicology family: Dr O. A. Alabi, and Dr Mrs Ifeoluwa Oyeyemi for their advice and words of encouragement, and my colleagues and friends who we started the Ph.D. programme together, Ogunsuyi Olusegun, Gbadebo Adeyinka and Atoyebi Seun for their assistances in the research. I wish to thank Miss Olubukola Akanni who I was always calling everyday regarding the biochemical tests; she created time for me despite her busy schedule. I appreciate Mr Odeh, Mr Adejumo, Mrs Naomi Adeyemo, Mrs Rolake Afolabi, Mrs Motunrayo Coker, Miss Oluwakemi Oyetade, and Mr Samuel Odebamowo for their assistance during my Ph.D. studies. Finally, I sincerely appreciate the prayers, advice, reassurance, the constant calls,

spiritual, and financial assistance of my dear parents: Late Dr and Mrs Solomon Fadoju; the general overseer of the Mountain of Fire and Miracles Ministries Worldwide, Dr D. K. Olukoya for his constant prayers and counseling; the district superintendent of Itire District Coordinating Council, Pastor Dr G. O. Oladokun; my siblings: Olubusolami Siyanbola, Titilayo Olakunle and Oluwatoyin Fadoju; my brothers-in-Law: Mr Adebowale Siyanbola and Mr Gbenga Olakunle and my nieces and nephew: Zoe Siyanbola, Angela Olakunle, Zuriel Siyanbola and Joshua Olakunle for their love, prayers and financial supports towards the completion of my Ph.D. studies. This acknowledgement will be incomplete if I fail to appreciate 'my best friend', Isaac Ifeoluwa who stood by me during the toughest period of my life. I love you to the moon and back. God bless you.

CERTIFICATION

This is to certify that this work was carried out by FADOJU Opeoluwa Motunrayo in the Cell Biology and Genetics unit of the Department of Zoology, University of Ibadan, under my supervision.

.....

Prof. A. A. Bakare
B.Sc. (Hons.), M.Sc., Ph.D. (Ibadan)
Cell Biology and Genetics Unit
Department of Zoology
University of Ibadan, Ibadan, Nigeria

TABLE OF CONTENTS

LIST OF TABLES

LIST OF FIGURES

LIST OF ABBREVIATIONS

ALT	- Alanine aminotransferase
AST	- Aspartate aminotransferase
bw	- Body weight
CAT	- Catalase
CREA	- Creatinine
CYP	- Cyclophosphamide
DBIL	- Direct Bilirubin
DLS	- Dynamic Light Scattering
DNA	- Deoxyribonucleic Acid
FBS	- Foetal Bovine Serum
FP	- Fine particles
FSH	- Follicle Stimulating Hormone
GGT	- Gamma Glutamyl Transferase
GSH	- Reduced Glutathione
Hb	- Haemoglobin
HDL	- High Density Lipoprotein
ICR	- Imprinted Control Region

LH	- Luteinizing Hormone
LPO	- Lipid peroxidation
MCH	- Mean Cell Haemoglobin
MCHC	- Mean Cell Haemoglobin Concentration
MCV	- Mean Cell Volume
MDA	- Malondialdehyde
MN	- Micronucleus
MPs	- Microparticles
NCE	- Normochromatic Erythrocyte
NM	- Nanomaterials
NP	- Nanoparticles
OECD	- Organisation for Economic Corporation and Development
PALS	- Periarteriolar Lymphoid Sheath
PCE	- Polychromatic Erythrocyte
PCV	- Packed Cell Volume
RBC	- Red Blood Cell
RNS	- Reactive Nitrogen Species
ROS	- Reactive Oxygen Species
RPM	- Revolution per minute
SOD	- Superoxide Dismutase

TBIL	- Total Bilirubin
TCHOL	- Total Cholesterol
TEM	- Transmission Electron Microscopy
Testo	- Testosterone
TiO_2	- Titanium dioxide
TRI	- Triglycerides
WBC	- White Blood Cell
ZnO	- Zinc oxide

CHAPTER ONE

INTRODUCTION

Nanotechnology is a rapidly growing field of science that combines engineering with physics, chemistry and biology without any boundaries (Ray *et al*., 2009). In this field, atoms and molecules are being controlled, as well as dealing with structural materials within the range limit of 1 and 100 nanometer referred to as the nanoscale, where a nanometer (nm) is 10^{-9} meters or one billionth of a meter. Scientists are making materials in extraordinary ways by taking advantage of their peculiarities that occur within the natural size range. The physical and chemical properties such as colour, electrical conductivity, melting point, magnetic permeability, boiling point and optical properties at the nanoscale are altered as a result of their particle size (Boverhof and David, 2010). Thus, the physicochemical properties of a material at the nanoscale are significantly different from the same material at the bulk state (Ryu *et al*., 2014; Kim *et al*., 2014a). Therefore, new dimensions of materials, where size is taken into consideration are being opened by nanotechnology. Today, nanotechnology has reached a summit where atoms and molecules are individually manipulated and controlled by scientists and engineers with an outstanding level of accuracy (Hanley *et al*., 2009), making it one of the most important technologies in the world (Luther and Malanoswski, 2004).

Nanotechnology encompasses the synthesis of nanomaterials and by definition in accordance with the European Union (2011), nanomaterials are defined as particles in agglomerate, aggregate, or unbound state in which more than 50% of the particles show one or more external dimensions at the nanoscale level of 1 – 100 nm. Nanoparticles (NPs) exist in one of two forms, as naturally occurring nanoparticles (NNPs) that exist in combustion by-products, volcanic eruptions, storm dust and forest fires; and engineered nanoparticles (ENPs), purposely synthesised to be utilised in applications (Yah *et al*., 2012). The ENPs consist of the carbon based (carbon nanotubes, fullerenes, and

graphenes), quantum dots (selenium and cadmium), and inorganic [metal (silver, manganese, iron, and copper) and metal oxide (titanium dioxide, copper oxide, zinc oxide, iron oxide, and silicon oxide,)] (Nam *et al*., 2014). One of the most unique physicochemical properties of NPs is their small size and large surface area to volume ratio with high reactivity potential (Shukla *et al*., 2011; Baek *et al*., 2012; Cho *et al*., 2013; El-Morshedi *et al*., 2014). Thus, this unique property makes them being extensively produced on a large scale by industries that use them. Therefore, occupational and environmental settings will enhance the probability of exposure due to increased production of these particles (Handy *et al*., 2008a; Wang *et al*., 2008a; Baek *et al*., 2012; Sharma *et al*., 2012a). Subsequently, this will become a great concern and importance to the scientists and the public considering their adverse effects (Li *et al*., 2010a; Shukla *et al*., 2011; Sharma *et al*., 2012a; 2012b).

Recently, the application of NPs associated with their benefits and risks have been widely debated. Assessment of NPs in humans can be very difficult as these NPs are heterogeneous in nature. The extensive production of NPs does not give an accurate estimation on the release of NPs in the environment annually. As large amounts of these NPs are manufactured during industrial processes and nanotechnology, they become unavoidably released into the air, water and soil (Ghosh *et al*., 2010; Shi *et al*., 2013), with little or no environmental fate. The benthic organisms in the aquatic environment are contaminated with NPs in a process known as bioaccumulation, and are, therefore, fed by larger animals, thereby increasing the concentrations of NPs through the food chain in a process known as biomagnification (Begnum *et al*., 2009; Sharma *et al*., 2012a). The release of NPs into the aquatic body causing chronic behavioural alterations, organ pathologies, oxidative stress and mortality in aquatic organisms have been reported (Federici *et al*., 2007; Smith *et al*., 2007; Ramsden *et al*., 2009; 2013).

The toxicokinetics (absorption, distribution, metabolism and excretion) of NPs are influenced by exposure routes, particle size, crystalline structure, agglomeration and surface properties (Fischer and Chan, 2007; Hanley *et al*., 2009; Baek *et al*., 2012; Choi *et al*., 2013; Cho *et al*., 2013). Absorption and distribution in toxicokinetics are critical steps following the deposition of NPs at the exposure site. Blood components such as white or

red blood cells, plasma proteins, dissolved nutrients, bioactive factors, platelets and coagulation factors as well as organs and tissues interact with NPs when they reach systemic circulation (Deng *et al*., 2009; Grissa *et al*., 2015; Setyawati *et al*., 2015). The toxicokinetics of NPs are highly influenced by the binding to the plasma proteins (Hagen *et al*., 2007; Setyawati *et al*., 2015). Translocation of NPs to the systemic circulation is accumulated in the liver, lymphatic tissues and other viscera (Shi *et al*., 2013).

Titanium dioxide (TiO_2) NPs and zinc oxide (ZnO) NPs are among the available metal oxide NPs utilised in the production of consumer products (Xue *et al*., 2011; Cho *et al*., 2013; Ryu *et al*., 2014). They are widely used because of their unique properties such as photocatalysis, anticorrosion, semiconductive properties and ultraviolet adsorption. The toxicities of TiO_2 and ZnO NPs have been investigated in *in vivo* models and mammalian cells (Sharma *et al*., 2009; Huang *et al*., 2009; Yuan *et al*., 2010; Li *et al*., 2010a; Cui *et al*., 2011; Ghosh *et al*., 2012). The genotoxic effects of TiO_2 NPs have been demonstrated in plants and human lymphocytes (Ghosh *et al*., 2010; Tavares *et al*., 2014), Syrian hamster embryo fibroblasts (Rahman *et al*., 2002), human hepatoma HepG2 cells (Petkovic *et al*., 2011; Shukla *et al*., 2014), human keratinocytes (HaCaT) cells (Xue *et al*., 2011), mouse macrophages (Zhang *et al*., 2013), chinese hamster ovary (CHO) cells (Warheit *et al*., 2007a; Di Virgillio *et al*., 2010), human bronchial epithelial (BEAS 2B) cell (Falck *et al*., 2009), human epidermal (A431) (Shukla *et al*., 2011), human lung cancer (A549) cells (Srivastava *et al*., 2011; Srivastava *et al*., 2013) and human SHSY5Y neuronal cells (Valdiglesias *et al*., 2013).

Likewise, the genotoxic effects of ZnO NPs have been demonstrated *in vivo* (Sharma *et al*., 2012a, Li *et al*., 2012, Cho *et al*., 2013; Choi *et al*., 2015, Ghosh *et al*., 2016) and *in vitro* in human negroid cervix carcinoma (HEp-2) cells (Osman *et al*., 2010), human liver (HepG2) cell (Sharma *et al*., 2012b), human hepatocytes (LO2) and human embryonic kidney (HEK293) cells (Guan *et al*., 2012), HEK293 and NIH3T3 cells (Demir *et al*., 2014). Toxicity of ZnO NPs are suggestive of Zn^{2+} ions release (Franklin *et al*., 2007; Sayes *et al*., 2007; Landsiedel *et al*., 2010; Xia *et al*., 2011; Ryu *et al*., 2014), intracellular reactive oxygen species generation (Xia *et al*., 2008; Yang *et al*., 2009; Lin *et al*., 2009; Dimkpa *et al*., 2011) as well as membrane damage, intracellular Ca^{2+} influx and

mitochondrial dysfunction (Huang *et al*., 2010; Kocbek *et al*., 2010; Wu *et al*., 2010; Ahamed *et al*., 2011; Moos *et al*., 2011; Hsiao and Huang, 2011).

Direct interactions between NPs and the DNA have been demonstrated recently in *in vitro* studies. However, the studies failed to consider the genotoxic mechanisms that arise from the intercellular processes. Altered synthesis of DNA repair proteins, depletion of antioxidants and indirect DNA damage are indications of the genotoxicity of NPs (Magdolenova *et al*., 2014). Nonetheless, even though there are disparities in recent literatures, evidence shows the genotoxicity of a variety of metal oxide NPs to cultured cell *in vitro* (Zhang *et al*., 2012). Firstly, the physical and chemical properties of NPs which include the crystalline structure, size, shape, surface properties and agglomeration determine the toxicity of NPs, as these are not comprehensively characterised (Akhtar *et al*., 2012). Secondly, inter-species differences in toxic effects are as a result of the toxicological animal model utilised for such evaluations, with no certainty in the prediction of human toxicity. Different results from various laboratories using the same cell line make prediction of nanotoxicity more difficult (Hanley *et al*., 2009). Thirdly, experimental conditions such as dose, exposure time and end point assay highly differ among laboratories, thereby making it difficult to meaningfully compare results. Nevertheless, the genotoxic potential of NPs at the *in vivo* level may not be easily compared with that of the *in vitro*, due to the pharmacokinetic factors, DNA repair proteins, physiological barriers to be absorbed and metabolism that occur under the *in vivo* conditions. Furthermore, concentrations of NPs utilised at the *in vivo* study may differ from the *in vitro* study. Likewise, novel distribution, clearance, immune response and metabolism patterns are essential in the *in vivo* study as a result of the interactions of NPs with the biological systems.

1.1 Aim of the study

This study aims at investigating *in vivo*, genetic and systemic toxicity of TiO_2, ZnO NPs and their mixture using somatic and germ tissues/organs in mice.

1.2 Objectives of the study

To achieve the aim, the study seeks to accomplish the following specific objectives:

1. To determine the morphologies, hydrodynamic diameters and zeta potentials of TiO_2, ZnO NPs and their mixture using transmission electron microscopy (TEM) and Dynamic Light Scattering (DLS);

2. To assess the acute toxicity in mice treated with TiO_2, ZnO NPs and their mixture;

3. To assess DNA damage using the bone marrow micronucleus assay in mice treated with TiO_2, ZnO NPs and their mixture;

4. To assess sperm count and motility, morphology of the testes and measure steroid hormones such as luteinizing hormone (LH), follicle stimulating hormone (FSH) and testosterone in mice treated with TiO_2, ZnO NPs and their mixture;

5. To assess haematological parameters, liver and kidney function tests and lipid profile in mice treated with TiO_2, ZnO NPs and their mixture;

6. To assess the histopathology of the liver, spleen, kidney, heart, testes and brain in mice treated with TiO_2, ZnO NPs and their mixture; and

7. To determine the mechanism of DNA damage through measuring the activities of enzymatic antioxidants [superoxide dismutase (SOD) and catalase (CAT)] and non-enzymatic antioxidant [reduced glutathione (GSH)] and malondealdehyde (MDA) in mice treated with TiO_2, ZnO NPs and their mixture.

1.3 Hypotheses of the study

H0: 1 TiO_2, ZnO NPs and their mixture will not induce somatic DNA damage in mice.

H0: 2 TiO_2, ZnO NPs and their mixture will not induce germ cell toxicity in the mice.

H0: 3 TiO_2, ZnO NPs and their mixture will not induce systemic toxicity in mice.

H0: 4 TiO_2, ZnO NPs and their mixture will not induce DNA damage through direct interaction with the genetic material and or indirectly via the production of intracellular reactive oxygen species (ROS).

1.4 Justification of the study

Several concerns are raised by the public and scientific researchers on the health and environmental implications with respect to the synthesis and application of TiO_2 and ZnO NPs for biomedical, industrial and consumer products. Their ability to contaminate the environment and cause unanticipated deleterious changes is on the increase, hence immediate toxicological assessment, is required.

There is paucity of information on nanotoxicity in Nigeria despite the fact that Nigerians are continually treated with TiO_2 or ZnO NPs through natural and/or man made sources. For this reason, it is imperative to carry out toxicological assessment.

Industrial sources (run offs, effluents and waste discharge) and non-industrial sources (consumer products, food packaging and additives) that directly contain individual forms of TiO_2 or ZnO NPs may culminate in the environment (soil, water and air) as heterogeneous engineered NPs (Reeves *et al*., 2008). Therefore, it is foreseeable that both TiO_2 and ZnO NPs may aggregate and interact in the environment as a result of large scale production from the nanotechnology industries. Due to their stability, persistency and non-degradable nature, they may associate and interact with other NPs in solids or sediments, aggregate and penetrate either the food chain or different sources of drinkable water (Dobrzynska *et al*., 2014).

Consequently, the co-existence of TiO_2 and ZnO NPs in different parts of the body through the lymphatic or circulatory system from the site of exposure may induce short or long term genotoxic and cytotoxic effects. In addition, TiO_2 and ZnO NPs may interact to induce synergistic, antagonistic or additive effects when they co-exist in the biological system of humans and other lower organisms. In particular, several researches have concentrated on the genotoxicity and cytotoxicity of either TiO_2 or ZnO NPs, with no

existing studies on their co-existence. Thus, the toxicological assessment of the mixture of TiO_2 and ZnO NPs in animal models *in vivo* is essential.

The potential adverse health effects of the individual forms of TiO_2 and ZnO NPs have been investigated extensively in *in vitro* studies (Sharma *et al*., 2012a; 2012b; Baek *et al*., 2012; Morsy *et al*., 2016) but just a few exist on the *in vivo* genotoxicity studies. Hence, *in vivo* studies should be investigated to study the interaction of TiO_2 and ZnO NPs with the biological system that will elicit immune responses, absorption of physiological barriers, metabolic patterns, interaction with DNA repair processes and serum proteins (Singh *et al*., 2013; Cho *et al*., 2013).

CHAPTER TWO

LITERATURE REVIEW

Nanotechnology is undoubtedly the most significant technology of the 21st century. In 2007, commercial and consumer products were estimated to have been worth $147 billion while it was predicted to reach $3 trillion by 2015 (Koedrith *et al*., 2014). In 2008, the funding in development and research of nanotechnology attained $18.2 billion worldwide, with Japan and the United States leading in this activity (Lux Research, 2004). Approximately €600 million per year was contributed by the EU Seventh Framework Programme to support research fundings. Likewise, over 600 nanotechnology industries are present in the United Kingdom (The Nanotechnology Knowledge Transfer Network, 2009).

Many solutions to problems in medicine, engineering, energy production and environmental sustainability are provided by nanotechnology (Kwon *et al*., 2014a). The exceptional properties of nanoparticles opportunities are explored and exploited by both government and investors in nearly every industrial and technological sector. There is the likelihood that significant quantities are released into the environment, as the number of nanotechnology grows with the nanomaterial types and applications (Sharma *et al*., 2012a; 2012b; Kwon *et al*., 2014a). This, therefore, becomes pertinent in terms of the safety of the environment and human health (Zhang *et al*., 2012). The contamination of the aquatic environment with nanoparticles has become particularly vulnerable, as it serves as a plunge for other environment pollutants. Wastewater discharges, degradation and wear of products that contain nanoparticles and accidental release from factories are examples of common sources to the aquatic environment. The activities of nanoparticles in the environment, their absorption, circulation and causes on animal models are likely to occur due to their large surface area to mass ratio and extremely small size.

2.1 Brief history of Nanotechnology

Nanotechnology is defined as the organisation, manufacturing and utilisation of particles, system and structures at the nanoscale level (Williams *et al*., 2005). Nanomaterials are particles that are less than or equal to 100 nm in at least a single dimensional feature (Baek *et al*., 2012; Li *et al*., 2012; Shi *et al*., 2013; El-Morshedi *et al*., 2014; Jia *et al*., 2014). Figure 2.1 provides an illustration of a nanoscale definition compared with subcellular and cellular structures in the human body. Nanotechnology was adopted by Professor Norio Taniguchi of the Tokyo Science University, "On the Basic Concept of Nanotechnology", which was communicated in 1974 at a Japanese Conference (Taniguchi, 1974).

2.2 Applications of nanotechnology

New material application has been invented by nanotechnology. In consumer products such as the frames of tennis rackets and motorcycle helmets, nanoparticles are added to them to make them stronger, lighter and durable. Nanoparticles are also applied to fabrics to prevent bacterial growth, wrinkling and staining. The application of nanoparticles on the surfaces of computer, camera display and windows make them anti-reflective and resistant to infrared light or ultraviolet and anti-fog (U.S. National Nanotechnology Initiative).

The use of nanoparticles in medicine, also offers some endless possibilities such as building nanoparticles with antibodies that have high affinity and specificity in targeting tumour cells. Therefore, for drug delivery, small drug molecules can be encapsulated with nanoparticles forming micelles, which are transported to the desired location thereby reducing the side effects (Jain, 2010). In addition, early diagnosis of atherosclerosis is possible through the development of imaging techniques that measure the amount of antibody-nanoparticles that accumulate in plaques (Wickline *et al*., 2006). Also, the detection and cleaning up of organic solvents that pollute ground water with nanoparticles is underway in environmental sciences (Long *et al*., 2006). Environmentally friendly batteries and efficient solar cells are potentially been produced from nanoparticles (Tian *et al*., 2007). Table 2.1 gives a summary of the application of nanomaterials.

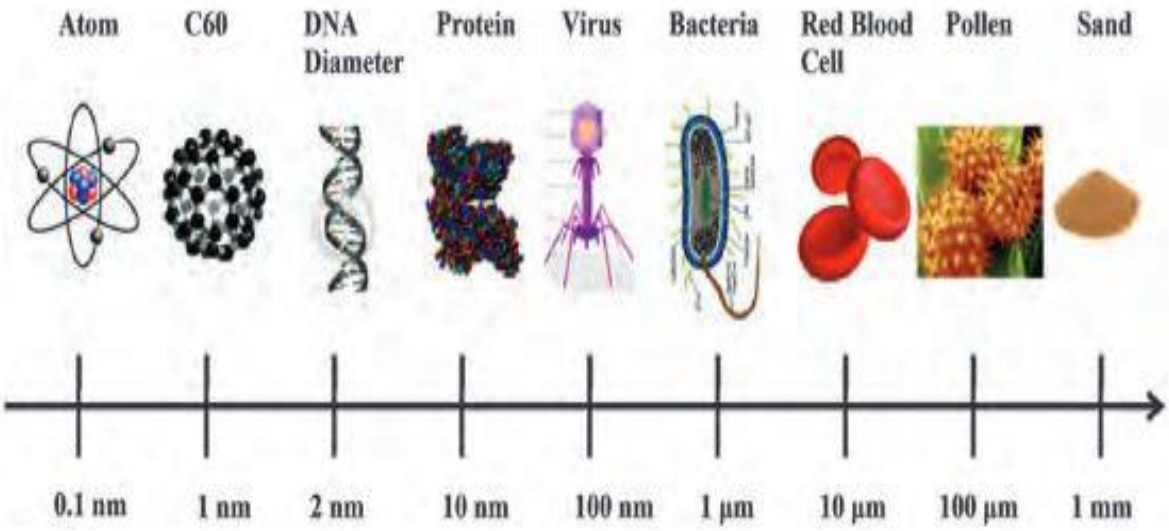

Figure 2. 1: A nanoscale showing the comparison between nanoparticles and biological components. Source: Ismail *et al*. (2016)

Table 2. 1: Applications of nanomaterials

Nanomaterials	Applications	References
Titanium dioxide (TiO_2) NPs	Osseointegration of artificial medical implants and bone, surface cleaning agents, as a photocatalyst, sunscreens, food packaging, therapeutics, biosensors, pigments, cosmetics, pharmaceuticals, paints, paper, inks, food colourant (E171), toothpastes, remediation of wastewater, plastics, ceramics and rubber.	Huang *et al*., 2010; Di Virgilio *et al*., 2010; Sadiq *et al*., 2012; Catalan *et al*., 2012; Tu *et al*., 2012; Dobrzynska *et al*., 2014; Demir *et al*., 2015; Grissa *et al*., 2015; Kansara *et al*., 2015.
Aluminum oxide (Al_2O_3) NPs	Catalyst, structural ceramics for reinforcements, polymer modification, functionalisation of textiles, heat transfer fluids, wastewater treatment, biosensors, biofiltration, antigen delivery for immunisation purposes, orthopedic materials, abrasives, wear-resistant coatings on propeller shafts of ships.	Balasubramanyam *et al*., 2009a; 2009b; Di Virgilio *et al*., 2010; Morsy *et al*., 2016; Hashimoto and Imazato, 2015.
Silicon dioxide (SiO_2) NPs	Cosmetics, varnishes, resin composites, additives to drugs, biomedical and biotechnological fields (biosensors), printer toners, DNA delivery, cancer therapy, drug delivery and enzyme immbolisation.	Hashimoto and Imazato, 2015; Sadek *et al*., 2016.
Copper oxide (CuO) NPs	Biocide properties, antimicrobial textiles, paints, plastics, heat transfer fluids, semiconductors and intrauterine contraceptive devices.	Perreault *et al*., 2012; Akhtar *et al*., 2012; Zhang *et al*., 2016.

Nanomaterials	Applications	References
Silver (Ag) NPs	Toothpastes, textiles, household cleaning products, air cleaners, coating for refrigerators, wound infections, catheters, contraceptive devices, surgical instruments, cosmetics, dental alloys, bone prostheses, shampoo, nipples and nursing bottles, toys, deodorants, kitchen utensils, food packaging, water disinfection, biocides and bandages.	Kim *et al*., 2008; Arora *et al*., 2009; Piao *et al*., 2011; Foldberg *et al*., 2011; Ghosh *et al*., 2012; Cho *et al*., 2013; Dobrzynska *et al*., 2014; Tomankova *et al*., 2015.
Magnetitie NPs	Cell separation, drug delivery systems, cancer diagnosis and treatment and magnetic resonance imaging contrast agent.	Sadeghiani *et al*., 2005.
Zinc oxide (ZnO) NPs	Cosmetics, sunscreens, food additives, food packaging, fungicides in agriculture, anticancer drugs, biomedical imaging, semiconductors, as a photocatalyst, paints, ceramics, rubber, metallurgy additives, chemical fibres, shampoos and antiperspirants.	Sharma *et al*., 2011; 2012a, 2012b; Baek *et al*., 2012; Li *et al*., 2012; Akhtar *et al*., 2012; Guan *et al*., 2012; Demir *et al*., 2014; Kwon *et al*., 2014a; Choi *et al*., 2015; Namvar *et al*., 2015.
Carbon Nanotubes (CNT) - multi walled (MWCNT)	Drug delivery systems, sensors, electronic devices, wastewater treatment, bone cell growth, high tensile strength, semi-conductive electronic properties, cancer treatment, thermal and chemical stability.	Muller *et al*., 2008; Asakura *et al*., 2010; Patlolla *et al*., 2010; Thurnherr *et al*., 2011.
Single walled (SWCNT)	Electronics, optics, imaging, drug delivery, bone cell growth and cancer treatment	Patlolla *et al*., 2016.

Nanomaterials	Applications	References
Indium tin oxide (ITO) NPs	Functional thin film material in display devices, dye-synthesised solar cells, liquid crystal displays and organic light-emitting diodes, optical devices such as camera lenses and optical functional material in energy-saving glass coating.	Akyil *et al*., 2015
Fullerenes	Energy conversion and drug delivery in industrial and medical fields.	Shinohara *et al*., 2009
Cerium oxide (CeO) NPs	As a fuel additive to promote combustion, ultraviolet-absorbing compound in sunscreen electrolyte in solid oxide fuel cells, polishing agent, and as a subcatalyst for automotive exhaust cleaning.	Kumari *et al*., 2014.
Iron oxide (Fe_2O_3) NPs	Cell tracking, cell target, heat elements for hyperthermia, cancer therapy, magnetic resonance imaging, drug delivery, and tissue repair.	Alarifi *et al*., 2014; Sarkar and Sil, 2014; Gaharwar and Paulraj, 2015; Silva *et al*., 2017.
Europium hydroxide (EH) NPs	Pro-angiogenic EH NPs could be developed as an alternative treatment for cardiovascular diseases, ischemic diseases and wound healing.	Bollu *et al*., 2016a.
Manganese oxide (MnO_2) NPs	Drug delivery, contrast agents for magnetic resonance imaging, wastewater treatment, ionisation-assisting reagent in mass spectroscopy and batteries.	Singh *et al*., 2013.

Nanomaterials	Applications	References
Platinum (Pt) NPs	Catalysis, cosmetics manufacturing and the processing of dietary supplements.	Yamagishi *et al*., 2013.
Chitosan NPs	As a carrier for oral peptide and protein drug delivery, dietary supplements, drug delivery and pharmaceutical and biomedical fields.	Tao *et al*., 2011.
Magnetic NPs	Contrast agents in magnetic resonance imaging, drug delivery, tissue repairing, hyperthermia, detoxification of biological fluids, cell separation and drug targeting.	Syama *et al*., 2014.

2.3 Nanoparticles

Nanoparticles can be broadly defined as particles having one or more dimensional feature within a nanoscale of 1 and 100 nm (Magdolenova *et al*., 2014; Kim *et al*., 2014a; Sadek *et al*., 2016). They include metal oxides, metals, carbon nanotubes and quantum dots (Nam *et al*., 2014). Metal oxide NPs are utilised in the production of electronics (Chow *et al*., 2009), as catalysts (Sharghi *et al*., 2009), remediation of contaminated ground water (Zhang, 2003), pharmaceuticals (Sun *et al*., 2008), drug delivery (Choi *et al*., 2007), biomedical imaging (Qu *et al*., 2008), fuel cells (Du and Wang, 2009) and chemical sensors (Guerrini *et al*., 2009). Titanium dioxide (TiO_2) and zinc oxide (ZnO) NPs are examples of metal oxide NPs widely utilised in consumer products, most importantly in cosmetics and personal care products. They are manufactured through the hydrolysis of the transition of metal ions (Masala and Seshadri, 2004). Silica (SiO_2), an example of a non-metal NP is synthesised via carbondioxide laser-induced decomposition of silicon hydride in a gas flow reactor, sodium metal reduction of silica salts or nonpolar organic solvent with metal silicides, or top-down laser ablation and ultrasonic methods. SiO_2 NPs are utilised in cancer therapy (Hirsch *et al*., 2003), for oligonucleotide synthesis (Zhao *et al*., 2009) and for anti-biofilm characteristics (Hetrick *et al*., 2009).

2.3.1 Types of Nanoparticles

2.3.1.1 Naturally occurring nanoparticles

i. Volcanic eruptions:

Particulate matter (nanoscale – microns) present in ash and gases are erupted into the atmosphere reaching heights of more than 18 000 meters (Figure 2.2A) (Buzea *et al*., 2007). Up to 30 million tons of particulate matter are ejected in a single volcanic eruption, resulting into enormous particles being released into the atmosphere (Taylor, 2002). The upper troposphere and stratosphere in the atmosphere may accommodate volcanic eruptions resulting to the wide spread, and affecting the earth for several years. A major consequence of volcanic eruption is the scattering and blocking of the sun's radiation.

Figure 2. 2: Examples of naturally occurring events that contain nanoparticles. (A) Volcanic eruption that occurred in Japan (www.dailymail.co.uk); (B) Forest fire in Kenya (www.ecoforum.com).

ii. Forest Fires:

Lightning strikes are the primary cause of forest fires. Particulate matter which includes nanoparticles that exceed the quality standards of the ambient air are increased during major fires that spread smoke and ash over several miles (Scown *et al*., 2010) (Figure 2.2B).

iii. Dust Storms:

The main component of environmental dust storms is nanoparticles. Dust storms produce particles ranging between 100 nm to several microns, and can reach a concentration of 1 500 particles / cm^3 when in a range of between 100 and 200 nm (Buzea *et al*., 2007).

iv. Organisms:

Bacteria (30 - 700 nm) and viruses (10 - 400 nm) are smaller than a few microns (Buzea *et al*., 2007). No supply of energy is needed by nanoparticles to remain in a stable form since they are inorganic solids. They are able to transform, dissipate and interact with their environment via chemical reactions. Both uni- and multicellular organisms through intracellular and extracellular processes produce nanoparticles (Ahmad *et al*., 2005).

2.3.1.2 Anthropogenic nanoparticles

i. Cigarette smoke:

Nanoparticles ranging from 10 nm to a maximum of 150 nm are usually present in tobacco smoke, which is a combustion product. (Figure 2.3A) (Ning *et al*., 2006). The environmental tobacco smoke is a complex composition consisting of over 100, 000 chemical compounds and components (Ning *et al*., 2006).

ii. Diesel and engine exhaust nanoparticles:

The major primary source of diesel and automobile exhaust are the atmospheric nano- and microparticles in the urban areas (Figure 2.3B) (Westerdahl *et al*., 2005). For diesel engines, the size range of particles from the vehicle exhaust is between 20 and 130 nm

Figure 2. 3: Examples of anthropogenic sources of nanoparticles (A) Cigarette smoke (www.thesceneisdead.com); (B) Exhaust fumes from vehicles (www.telegraph.co.uk).

while gasoline engines are between 20 and 60 nm. Diesel combustion by-products include carbon nanotubes (Evelyn *et al*., 2003), while, 20% of the particle mass constitute nanoparticles with diesel-generated particles taking more than 90% (Kittleson, 2001).

iii. Indoor pollution:

The indoor air pollution is 10 times greater than the out door pollution. Human activities generate a substantial amount of particulate matter indoors. Cleaning, smoking, cooking, and combustion (e.g. fire places and candles) are just a few examples of common indoor activities. Spores, cooking, dust mites, chemicals, textile fibres, skin particles, smoke from candles, and cigarettes are examples of indoor nanoparticles (Buzea *et al*., 2007).

iv. Buildings demolition:

When large buildings are demolished, high levels of concentrated nanoparticles are produced with diameter smaller than 10 microns (Stefani *et al*., 2005). At the site of demolition, wood, lead, paper, glass, respirable asbestos fibres and further toxic materials are mostly found, and travel several kilometers with the help of the dust cloud to neigbouring regions of the collapsed building (Stefani *et al*., 2005).

v. Cosmetics:

Many thousands of years in ancient Egypt, mineral powders and black soot have been utilised as cosmetics. Cosmetics which contain a large variety of nanoparticles have been extensively embraced by industries, however, these nanoparticles present in them can be absorbed into the deep layers that tend to protect the skin (Buzea *et al*., 2007). Also, synthetic peptides that instruct cells to regenerate are delivered into the skin as nutrients (Xiao *et al*., 2005). Nanoparticles help maintain a youthful appearance of the skin as a result of their antioxidant properties (Xiao *et al*., 2005). Cosmetic products such as creams contain functionalised fullerenes that have radical scavenging properties (Nohynek *et al*., 2007). A large number of cosmetics and personal care products (such as toothpaste, soap, deodorants, body creams, shampoos and hair dandruff) (Figure 2.4) contain nanoparticles that can take up and reflect ultraviolet (UV) light due to their optical propeties (Nohynek *et al*., 2007).

Figure 2. 4: Example of cosmetics that contain nanoparticles.

Source: Wilson Centre and Virgina Tech University.

www.law.widener.edu/nanolaw

2.3.2 Classification of nanoparticles

Classification can be done in a number of ways. Chemical composition is one of the broad ways of classifying nanoparticles (Buzea *et al*., 2007; Handy *et al*., 2008b). The classification includes: carbon-based structures [carbon nanotubes (CNT) and C60 fullerenes], metal oxide nanoparticles (e.g. CuO, ZnO and TiO_2) or semiconductor nanocrystals also known as quantum dots.

Another way of classifying nanoparticles is based on their dimensionality (Buzea *et al*., 2007; Krug and Wick, 2011). Nanoobjects and nanostructured materials are the two main types of nanoparticles according to the International Organisation for Standardisation (ISO). These include nanocrystalline materials (consist of nanosized crystalline grains within particles that may or may not be at the nanoscale dimensions), nanoporous materials (having nanosized pores with particles that may or may not be of the nanoscale dimesnions) and complex fliuds containing nanosized objects. Classification of nanoobjects into nanoplates, nanofibres and nanoparticles is based on the number of dimensions confined to the nanoscale range (Figure 2.5).

Nanofilms, nanolayers and nanocoatings have one dimension confined to the nanoscale. Graphene is an example of a nanoplate consisting of sheets of graphite with electronic properties (Geim and Novoselov, 2007). Nanotubes, nanorods and nanowires belong to the nanofibres with two dimensions within the nanoscale and are widely used in the area of medicine (Bianco and Practo, 2003). Nanoparticles have all their three dimensions with the nanoscale and are often spehrical in shape (Ashby *et al*., 2009; Krug and Wick, 2011).

2.3.3 Exposure routes of nanoparticles

Government agencies and scientists are more concerned about the negative impact of nanotechnology on human health and ecosystem since there is lack of knowledge in these areas (Oberdorster *et al*., 2005; Owen and Handy, 2007; Klaine *et al*., 2008). The society benefits from nanotechnology applications in terms of general consumer products, health care and environment.

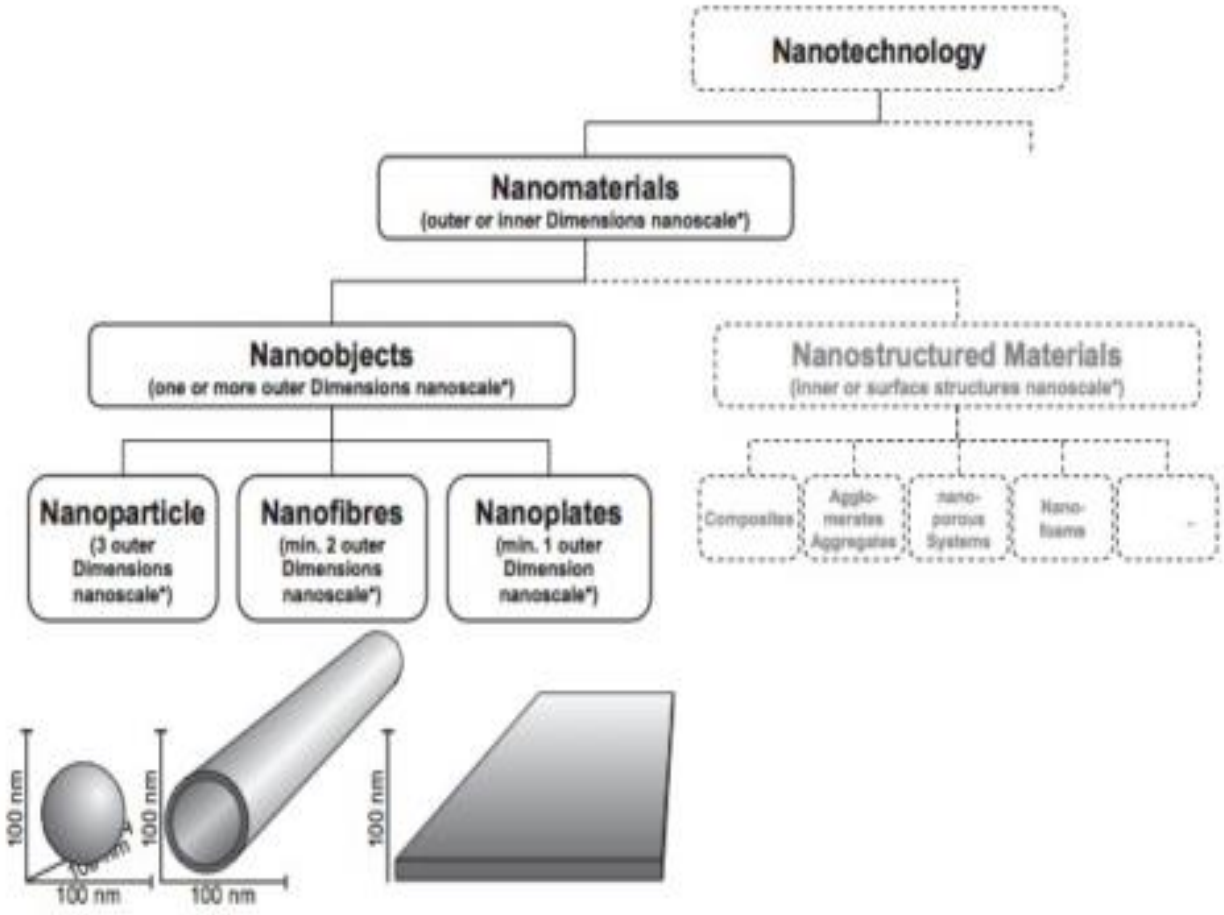

Figure 2. 5: The ISO definition of nanoobjects. The shape of nanoobjects reflects the number of dimensions confined to the nanoscale. Source: Krug and Wick (2011).

Due to the numerous applications of NPs in consumer products, the chances of human exposure through oral, inhalation and dermal may be significantly increased (Guan *et al*., 2012; Kumar and Dhawan, 2013). Human, plants and aquatic organisms may be treated with NPs through industrial (manufacturing, processing and packaging), usage (consumer products, cosmetics, medical applications) and via the envronment (polluted air, effluents, disposal and contaminated water) (Figure 2.6). Information on the behaviour of NPs in the environment, interactions with biotic and abiotic components or their potential toxic effects in living organisms is lacking. The levels of NPs in the various environmental compartments are not known and assessment to measure the NPs load is currently underway.

2.3.3.1 Nanoparticles in the atmosphere

There have been a number of studies on the atmospheric levels and the composition of nanoparticles suggesting a link between the respiratory health and nanoparticle exposure (Sioutas *et al*., 2005). Primary combustion products from motor vehicles and diesel engines are the major sources of NPs, which contribute 36 % particle numbers in the atmosphere (Shi *et al*., 2001). Nanoparticles have a long half-life in the atmosphere and can be transported to reasonable distances due to their small size. Organic compounds such as polycyclic aromatic hydrocarbons, oxidant gases and transition metals may be absorbed to the NPs surface, facilitating their co-transport (Oberdorster, 2001). Significant levels of particles are found in the indoor compared with the outdoor environment, with several studies reporting the chemical properties and concentrations of NPs indoor (Thatcher and Layton, 1995; Jones *et al*., 2000). The safety of workers in factories producing NPs has become a great concern, especially with the risk of the atmospheric movement of NPs out of the factory environment. Studies have also addressed the atmospheric transport and load of NPs (Boxall *et al*., 2007; Tsai *et al*., 2009).

2.3.3.2 Nanoparticles in soils

Mueller and Nowack (2008), proposed a modeling approach regarding the direct route of entry of Ag, TiO_2 and CNT into the soil. It was suggested that the use of sprays, cleaning

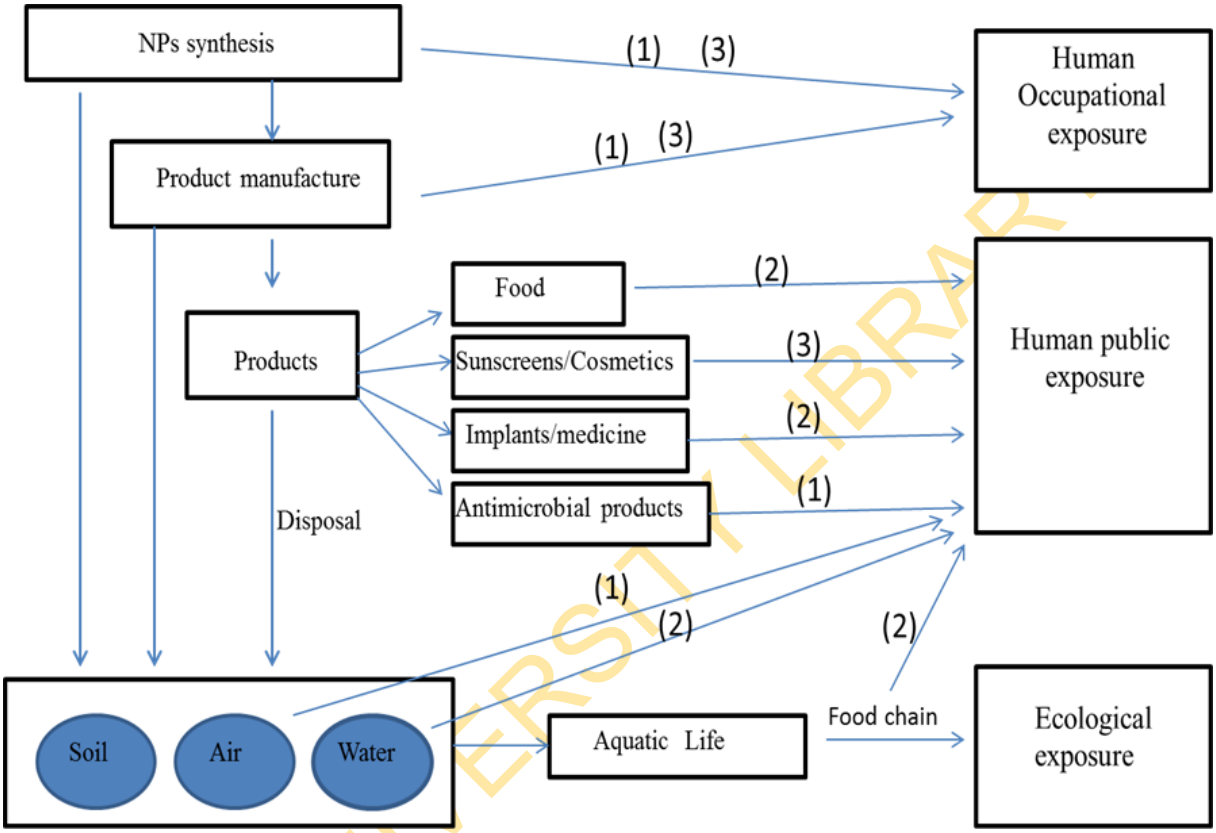

Figure 2. 6: Exposure routes of nanoparticles. Potential release, exposure and uptake of NPs in the ecosystem (1) inhalation; (2) ingestion; (3) dermal penetration

Source: Zhang *et al*. (2012)

agents, and paints lead to the release and deposition of NPs into the soil through run-offs, which makes it a major consideration. Run-off from road surfaces, accidental release from factories, and degradation of products, and leaching of NPs to the soil through landfill are entry points through which NPs accumulate in the soil. Soil and ground water remediation technologies, application of plant protection products, application of fertilizers to agriculture, land that contain sewage sludge, excretion of drugs that contain NPs and through the NP deposition from the air are the main exposure routes of NP to the soil proposed by Boxall *et al*. (2007).

Several potential implications of NP entry into the soil environment occur most especially on organisms dwelling in the soil. Terrestrial isopods (Jemec *et al*., 2008), earthworms (Scott-Fordsmand *et al*., 2008), nematodes (Wang *et al*., 2009) and soil bacterial communities (Johansen *et al*., 2008), are a few of the studies demonstrated to show the changes in the structure of their community. Various NP types in soils can affect the plant growth and agricultural produce such as seed germination inhibition (Lin and Xing, 2008), root elongation (Canas *et al*., 2008), accumulation and translocation within plant tissues (Zhu *et al*., 2008).

2.3.4 Metal oxide nanoparticles

Metal oxide NPs have been extensively utilised in the field of nanotechnology (as semiconductors and thermoelectrical materials), nanomedicine (as drug delivery systems for diagnosis and treatments) and in the decontamination of environmental pollutants (Seabra and Duran, 2015). Rapid production and utilisation of these metal oxide NPs have led to increased exposures in both human and the ecosystem. Metal oxide NPs include but not limited to Bismuth Trioxide (Bi_2O_3), Titanium dioxide (TiO_2), Zinc oxide (ZnO), Aluminium oxide (Al_2O_3), Copper oxide (CuO, Cu_2O), Iron oxide (Fe_2O_3, Fe_3O_4), Silica (SiO_2), Tin oxide (SnO_2) and Zirconia (ZrO_2) NPs. Conservative markets estimated an increase in the production of metal oxide NPs from 270,041 tons in 2012 to 1,663,168 tons by 2020 (Future Market Inc., 2013). Nam *et al*. (2014) reported that the production and utilisation of TiO_2 NPs ranged from 7,800 tons to 38,000 tons per year in the USA, while 435 tons of TiO_2 NPs was calculated to be produced in Switzerland per year (Piccinno *et al*., 2012).

2.3.4.1 Titanium dioxide nanoparticles

Titanium (Ti) is one of the most widely distributed elements on earth, with an average concentration of 4 400 $mgkg^{-1}$ (Shi *et al*., 2013). It has a high affinity for oxygen and, therefore, exists in the +4, +3 and +2 oxidation states, of which +4 is the most common oxidation state. TiO_2 is referred to as titanic acid anhydride, titanic anhydride, titania, titanium white or titanium (IV) oxide (Shi *et al*., 2013). TiO_2 is a white, fine, odourless, natural, thermally stable, non-silicate mineral oxide and nonflammable with a molecular weight of 79.9 $gmol^{-1}$, boiling point of 2972 ^oC and melting point of 1843 ^oC (Iavicoli *et al*., 2012; Shi *et al*., 2013).

Titanium dioxide NPs exist in one of the three forms: anatase, rutile and brookite (Sadiq *et al*., 2012; Cho *et al*., 2013; Chen *et al*., 2014) (Figure 2.7). Anatase has eight faced tetragonal dipyramids forming a sharp elongated point which makes it distinct from other polymorphs (Sadiq *et al*., 2012). Anatase is a stable form at the nanoscale level and has been shown to be more toxic than rutile (Sayes *et al*., 2006; Falck *et al*., 2009), which is thermally stable at the microscale level (Zhang *et al*., 2012). On the other hand, brookite is an impure form of both anatase and rutile forms. Most importantly, they possess anticorrosive and photocatalytic properties (Zhang *et al*., 2012). Their large surface area and crystallinity (anatase rather than rutile) increase the catalytic activity of TiO_2 NPs (Magdolenova *et al*., 2014). Semiconductor photocatalysis, decontamination of waste water containing hazardous by-products from industries and solar cells are examples of some of the catalytic reactions used by TiO_2 NPs (Zhang *et al*., 2012).

The most important polymorphs in relation to the utilisation in consumer products are anatase and rutile (Shi *et al*., 2013; Cho *et al*., 2013; Chen *et al*., 2014). The photocatalytic activity of anatase TiO_2 is reported to be approximately 1.5 times higher than the rutile form (Falck *et al*., 2009). It has been observed that the nanoscale anatase was 100 times more cytotoxic than the nanoscale rutile in human dermal fibroblast and human lung epithelial A549 cells (Sayes *et al*., 2006). It was suggested that the differences in the photocatalytic activity of anatase and rutile is due to the differential ability to generate ROS (Sayes *et al*., 2006). The inner structure size, surface characteristics and shape of rutile differ significantly from anatase (Andersson *et al*., 2011; Wang and Li, 2012).

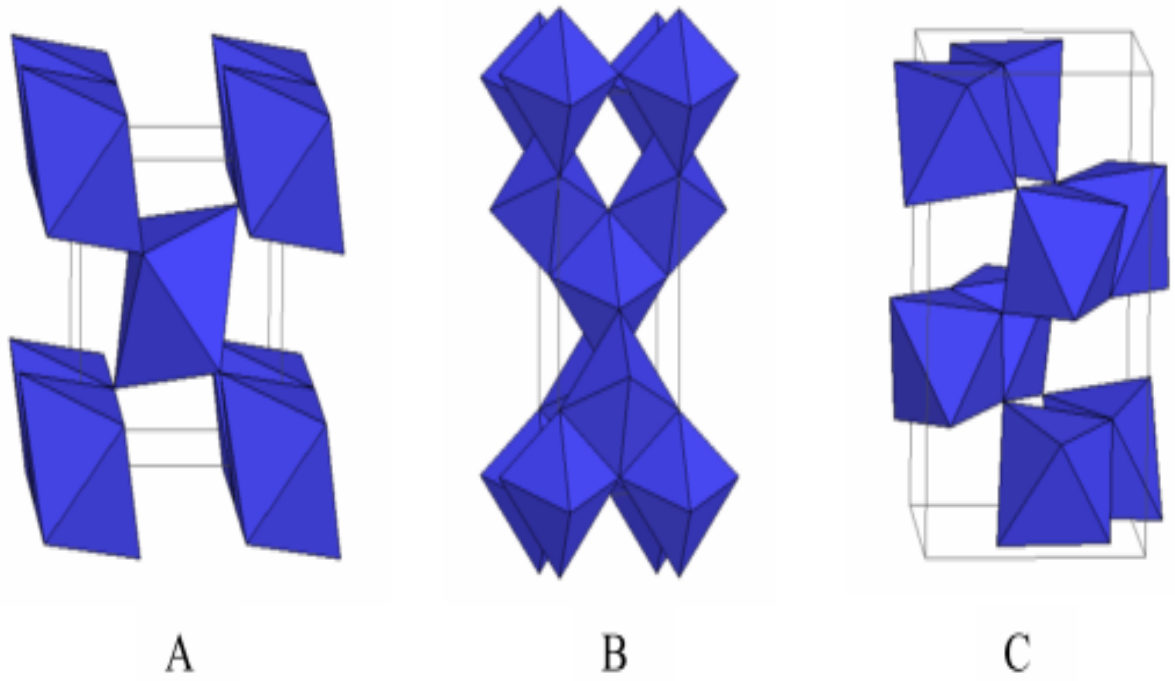

Figure 2. 7: The crystal structures of A) rutile B) anatase C) brookite. http://ruby.colorado.edu/~smyth/min/tio2.html.

2.3.4.1.1 Uses of titanium dioxide nanoparticles

Titanium dioxide (TiO_2) NPs are broadly utilised in a variety of applications due to their brightness and high refractive index (Shi *et al*., 2013; Chen *et al*., 2014). Over 70% of the total production volume is accounted for by TiO_2 NPs (Shi *et al*., 2013), with at least 36% present in food (Weir *et al*., 2012), making it one of the top five NPs utilised in consumer products (Shukla *et al*., 2011; Chen *et al*., 2014). Various properties of TiO_2 NPs have been exploited in several applications. The particle size strongly influences the absorption property of TiO_2 NPs, as they serve as either an oxidizing or reducing agent (Zhang *et al*., 2012). Manipulation of TiO_2 NPs through surface treatment is applicable to UV radiation absorption, pollutant degradation, protection of polymers and paint films from other chemical species degradation (Shi *et al*., 2013). Hence, they are widely utilised in sunscreens because they increase the sun protection factor thereby reflecting and absorbing UV light (Bondarenko *et al*., 2013). The photocatalytic property of TiO_2 NPs decompose many organic matters in waste water, and also destroy both gram negative and positive bacteria (Yin *et al*., 2012; Iavicoli *et al*., 2012). In applications where low interaction with the surrounding matrix is desired, the rutile form of TiO_2 NPs is often utilised while for photocatalytic applications, the anatase form of TiO_2 NPs is employed (ED and DuPont, 2013).

Titanium dioxide NPs are found in a variety of consumer products such as automotive products, printing inks, plastics, ointments, rubber, floor coverings, toothpaste, as food colourants (e.g. candies, sweets, coffee whitener) (Wang *et al*., 2007), confectionary (white sauces and dressings), powdered foods (Mikkelsen *et al*., 2011), absorbents, ceramics and mortar (Trouiller *et al*., 2009). They are also able to form different shades of colours such as grey and green when in combination with other pigments (Mikkelsen *et al*., 2011). In addition, windows, self-cleaning tiles, textiles and car mirrors for anti-fogging purposes are other industrial applications of TiO_2 NPs due to their photocatalytic effects (Shi *et al*., 2013).

Advanced imaging and nanotherapeutics are useful tools investigated in nanomedicine using TiO_2 NPs (Yuan *et al*., 2010). For example, photodynamic therapy can be accomplished with TiO_2 NPs utilised as a potential photosensitizer. Novel treatments such

as atopic dermatitis, hyperpigmented skin lesion, acne vulgaris, recurrent condyloma accuminata and other dermatologic diseases are being treated with TiO_2 NP-containing skin care products (Yuan *et al*., 2010; Montazer and Seifollahzade, 2011).

2.3.4.1.2 Toxicity of titanium dioxide nanoparticles

i. Acute toxicity of titanium dioxide nanoparticles

Wang *et al*. (2007) indicated that female mice treated with TiO_2 NPs (25, 80 and 150 nm; 5 g/kg bw) at a single oral administration showed no obvious acute toxicity. In contrast, mice treated with 25 and 80 nm TiO_2 NPs showed high hepatic coefficients. In addition, there were significant alterations in the levels of aspartate aminotransferase (AST), alanine aminotransferase (ALT), blood urea nitrogen (BUN), and lactate dehydrogenase (LDH), with hepatic and renal injury. No histopathological lesions were observed in the heart even with significant changes in the LDH levels in TiO_2 NPs (25 and 80 nm) treated mice, with no anomalies in ovaries, spleen and lung.

Li *et al*. (2008a) reported hemagglutination, abnormal sedimentation, and dose dependent hemolysis in erythrocytes treated with TiO_2 NPs and not TiO_2 FPs. Ma *et al*. (2009) reported liver toxicity in mice treated for 14 days with TiO_2 NPs (5 nm; 5, 10, 50, 100 and 150 $mgkg^{-1}$). There was a significant alteration in the messenger RNA (mRNA) and inflammatory pathways such as macrophage migration inhibitory factor (MMIF), nuclear factor kappa-light-chain-enhancer of activated B cells (NK-$_k$B), Tumour Necrotic Factor (TNFα), interleukin factor IL-1β, (IL)-6, IL-4, cross reaction protein, and IL-10 using the enzyme-linked immunosorbent assay (ELISA) and real-time quantitative-PCR (RT-PCR). TiO_2 NPs anatase (5, 10, 50, 100 and 150 $mgkg^{-1}$; 5 nm) intraperitoneally administered to mice for 14 days revealed pathological changes in the liver, kidneys and myocardium as well as significantly altering the levels of blood sugar, lipid, pseudocholinesterase, leucine acid peptide, ALT, total protein, albumin, uric acid and BUN (Liu *et al*., 2009a).

ii. Sub-acute toxicity of titanium dioxide nanoparticles

Bu *et al*. (2010) reported the effect of orally treated TiO_2 NPs (0.16, 0.4 and 1.0 gkg^{-1}) on the metabolomic analyses in urinalysis and serum. TiO_2 NPs elevated the levels of

trimethylamine-N-oxide (TMAO), hippurate, taurine, citrate, histidine, alpha ketoglutarate, citrulline, phenyl acetylglycine (PAG) and acetate. The levels of 3-D-hydroxybutyrate (3-D-HB), methionine, betaine, threonine, pyruvate, lactate, choline and leucine were elevated. There were reductions in glutamate, pyruvate, glutamine, methionine, glutathione and acetoacetate, as well as increases in choline, TMAO, creatinine, 3-D-HB, and phosphocholine as indicated in the metabolomics of the serum. In addition, the swelling of the mitochondria in the tissue of heart as well as elevated levels of LDH, CK and AST were induced by TiO_2 NPs in the rats. Similar to the results obtained above, Eydner *et al*. (2012) also reported inflammatory changes in the lungs, β-glucuronidase and leucopenia depletion after TiO_2 NPs inhalation. TiO_2 NPs (1 or 10 $mgkg^{-1}$) was intratracheally instilled in rats. LDH activity, malondialdehyde, total protein and leukocytes were significantly increased when treated with 10 $mgkg^{-1}$ as correlated with the control. In addition, 10 $mgkg^{-1}$ increased pulmonary inflammation in the lungs via histopathological examination.

iii. Sub-chronic toxicity of titanium dioxide nanoparticles

Bermudez *et al*. (2004) compared the pulmonary responses to aerosol concentrations of P-25; 21 nm TiO_2 NPs (0.5, 2.0 and 10 mg/m^3) for 6 hours / day, 5 days / week for 13 weeks in female rats, mice and hamsters. All three groups of rodents revealed a dose dependent increase in lung burdens with significant differences of pulmonary responses among the species. Severe inflammatory responses were developed by rats than mice when the lung burden of TiO_2 NPs was equivalent, resulting in fibro proliferative changes and progressive epithelial. Rodents treated with TiO_2 NPs (10 mg/m^3) exhibited impaired clearance of particles from the lung; where as the administration of doses did not affect the clearance of TiO_2 NPs in hamsters.

Another study by Warheit *et al*. (2006) compared 25 nm of TiO_2 NPs and 100 nm of FPs (1 and 5 $mgkg^{-1}$) with a variety of crystal structures, sizes and surface areas, which were treated via intratracheal instillation for 24 hours, 1 week and 3 months in rats. The lung inflammatory responses in both TiO_2 NPs and FPs were almost the same despite the 30 fold difference in the surface areas of TiO_2 NPs and FPs. It was concluded that the particle size and surface area do not determine the toxicity of TiO_2 particles through lung

instillation. It was suggested that the particle surface properties rather than the surface area was responsible for the toxicity of TiO_2 NPs. In another study reported by Roursgaard *et al*. (2011), TiO_2 NPs (rutile) and FPs (5, 50 and 500 µg) were intratracheally instilled once in mice for 3 months. At high doses, levels of neutrophils, total protein and interleukin – 6 (IL-6) in BALF were elevated by TiO_2 NPs and FPs. However, it was suggested that the cytotoxicity and inflammatory effects induced by TiO_2 NPs to the lungs may be similar to those induced by the FPs of similar composition.

iv. Chronic toxicity of titanium dioxide nanoparticles

Studies on the chronic lung inhalation exposure of TiO_2 FPs to pigs or rats reported pulmonary pathology which includes increased occurrences of pneumonia, squamous metaplasia (Baskerville *et al*., 1988), proliferation of pulmonary cells and responses (Warheit *et al*., 1996). Likewise, macrophage dysfunction (Warheit *et al*., 1997), alveolar epithelial metaplasia, fibroproliferative lesions (Bermudez *et al*., 2002) and accumulation of macrophages in interalveolar septa (Lee *et al*., 1985) have been reported in TiO_2 NPs-induced toxicity. Exposure of ICR mice to 5 - 6 nm of TiO_2 NPs (2.5, 5 and 10 $mgkg^{-1}$) for a period of 90 days via oral exposure resulted in severe spleen lesions with significant decreases in lymphocyte counts, platelets, immunoglobulin, haemoglobin and blood cells. In addition, notable increase in the levels of MMIF, IL-2, IL-4, IL-6, IL-8, IL-10, IL-1β, TNF-α, $NF\text{-}_kB$, transforming growth factor-β (TGF-β), CYP1A1 expression, interferon-γ, Bax, cross-reaction protein and decrease in heat shock protein 70 (Hsp 70) and Bcl-2 expression levels were also induced (Sang *et al*., 2012).

v. Dermal toxicity of titanium dioxide nanoparticles

Cosmetics and sunscreens contain TiO_2 NPs that help protect skin from harmful UV radiation. Percutaneous absorption and ROS-mediated skin aging are potential risk of general skin exposure to these applications (Menzel *et al*., 2004; Lademann *et al*., 2006; Lademann *et al*., 2008; Wu *et al*., 2009). The first line of defense from the outside world is the skin. Transdermal drug delivery is facilitated by a narrow link of capillaries that surround the hair follicles (Nohynek *et al*., 2007). The orifices of the hair follicles contain 1 % of applied TiO_2 NPs, which are difficult to remove compared with that on the skin

surface (Lademann *et al*., 2006; Lademann *et al*., 2008). The percutaneous penetration of most extraneous substances is shielded by the stratum corneum (the topmost layer of the epidermis) (Yaar and Gilchrest, 2003), however, penetration of TiO_2 NPs was shown in the stratum granulosum and stratum corneum in pigs (Menzel *et al*., 2004). So far, systemic toxicity has not occurred through the dermal exposure of TiO_2 NPs.

Most studies have reported that the outmost layer of the stratum corneum retain TiO_2 NPs, with the epidermis containing little or no TiO_2 NPs (Nohynek *et al*., 2007). Furthermore, no irritation or sensitisation of TiO_2 NPs (80/20 anatase/rutile) (129.4 nm; 175, 550, 1750 and 5000 $mgkg^{-1}$) was found in mice for the local lymph node assays, irritation and acute dermal studies (Warheit *et al*., 2007a). ROS induction and skin aging were observed after the prolonged TiO_2 NPs exposure in the presence of illumination (Wu *et al*., 2009). Only the adhesion of the cell-matrix and not cell viability were altered when human keratinocyte HaCaT cells were treated with TiO_2 NPs (< 60 µg/mL) for 24 hours (Fujita *et al*., 2009). Chen *et al*. (2010) obtained decreased cell viability and increased ROS levels induced by photo-irradiation. The penetration and toxicity of TiO_2 NPs were investigated via dermal exposure in both *in vitro* and *in vivo* studies (BALB/c hairless mice, domestic pig ears). No absorption of TiO_2 NPs via the stratum corneum in the isolated porcine skin. In another study reported by Unnithan *et al*. (2011), serum biochemical alterations were observed in Wistar rat skin atopically treated with 20 nm of TiO_2 NPs (14, 28, 42 and 56 $mgkg^{-1}$). Glutathione-S-transferase (GST) and Catalase (CAT) activities were depleted while LDH and lipid peroxidation (LPO) increased. ALT, AST, BUN and creatinine concentration increased with no histopathological alterations on the tissues.

In contrast, Wu *et al*. (2009) observed that 4 nm and 60 nm of TiO_2 NPs (24 mg of 5 % TiO_2 NPs) penetrated via the horny layer and were located in the inner epidermal layer after topical application for 30 days *in vivo*. In addition, TiO_2 NPs did not only absorb through the skin of hair mice after 60 days dermal exposure, but was also translocated, and induced several pathological lesions in major organs. Liu *et al*. (2006) treated mice at 1, 24 or 48 hours with TiO_2 NPs (1000, 2150, 4640 and 10 000 $mgkg^{-1}$) and observed no irritation tests. Likewise, Warheit *et al*. (2007b) further demonstrated the effect of TiO_2

NPs (129.4 nm; 80/20 anatase/rutile; 0, 5, 25, 50 and 100 %) dermally in rabbits and mice (CBA/JHsd) for 3 days of which no skin irritation was observed.

vi. Neurotoxicity of titanium dioxide nanoparticles

The high metabolic rate, numerous ROS targets and low capacity of cellular regeneration make the brain susceptible to oxidative stress (Zhang *et al*., 2012). The olfactory nerve is speculated to be the pathway through which NPs are intranasally transported (Dorman *et al*., 2004; Oberdorster *et al*., 2005; Elder and Oberdorster, 2006). Wang *et al*. (2008b) reported morphological alterations of the hippocampal neurons and olfactory bulb, oxidative stress and high accumulation of TiO_2 NPs. However, a slight brain lesion was induced by TiO_2 NPs via oral administration (Wang *et al*., 2007). The introduction of TiO_2 NPs via the olfactory bulb route resulted in the hippocampus being a main target, which displayed a translocation capacity in the CNS in a time-dependent manner after intranasally instilled (Wang *et al*., 2008b). The homeostatic disturbance of enzymes, trace elements, and neurotransmitter systems reduced the spatial recognition memory ability of mice treated with TiO_2 NPs. A cascade of reactions such as excessive release of nitric oxide, reduced antioxidants, reduction of glutamic acid, lipid peroxidation, and the decrease in the activity of acetylcholinesterase activity with the presence of brain injury were induced when TiO_2 NPs were translocated from the intraperitoneal cavity to the brain (Ma *et al*., 2010). The expression levels of TNF-α, IL-1β, Factor-$_k$B-inducible kinase, NF-$_k$B and I_kB kinase were upregulated while I_kB was down-regulated (Ma *et al*., 2010).

Hu *et al*. (2010b) reported that 5 nm anatase of TiO_2 NPs (0, 5, 10 and 50 $mgkg^{-1}$) intragastically instilled in ICR mice consecutively for 60 days significantly damaged the spatial recognition memory. Homeostasis of neurotransmitters, trace elements, and enzymes were distorted as well as significant alterations in the levels of K, Fe, Na, Zn, Mg and Ca. The activities of nitric oxide synthase (NOS), Ca^{2+-}ATPase, $Ca^{2+/}Mg^{2+}$ ATPase, Na^+/K^+-ATPase, and acetylcholine esterase were also significantly inhibited. In addition, TiO_2 NPs notably reduced the levels of monoamines neurotransmitters such as DOPAC, NE, 5-HT and its metabolite 5-HIAA and increased nitric oxide (NO), glutamate and acetylcholine. The effect of TiO_2 NPs (100 $mgkg^{-1}$) on the learning memory and the

hippocampal cell proliferation of the offsprings in pregnant rats (gestational day 2 to day 21) via oral gavage was investigated. Impaired learning and memory, and cell proliferation in the hippocampus of the offspring were induced by TiO_2 NPs (Mohammadipour *et al*., 2014). In another study reported by Cui *et al.* (2014), oxidative damage in the offspring brain and emotional behaviour in the adulthood were induced in TiO_2 NPs prenatal exposure. The status of the antioxidant was damaged, lipids and oxidative DNA damage were significantly increased in the new pups.

vii. Pulmonary toxicity of titanium dioxide nanoparticles

The penetration of exogenous fine particles via the respiratory system in the body induces ROS by phagocytosis in the alveolar macrophages (Abidi *et al*., 1999). Enzymatic and non-enzymatic antioxidants in the alveolar macrophages scavenge ROS; however, these antioxidants are not sufficient to prevent pulmonary damage and oxidative stress (Repine *et al*., 1997). Oberdorster *et al*. (1994) observed particle size, persistence and lung injury in rats treated via inhalation to TiO_2 NPs (20 and 250 nm) for 12 weeks. Greater pulmonary effects such as inflammation and lung injury were induced by the NPs rather than the FPs, indicating that their small size and larger surface area to mass ratio are major characteristics that conferred to the accumulation and NPs toxicity. Systemic and lung inflammation, platelet aggregation, and cardiac and pulmonary edema were induced by the acute exposure to TiO_2 NPs rods and dots for 24 hours (Nemmar *et al*., 2008). Hepatic lesions, lymph nodule proliferation, systolic hypertension, splenic congestion, thrombus tachycardia, inflammation and oxidative stress were aggravated with TiO_2 NPs coated with Fe.

Liu *et al*. (2009b) reported that intratracheally instilled rats treated with TiO_2 NPs (5, 21 and 50 nm respectively) at 0.5, 5 or 50 $mgkg^{-1}$ after 7 days revealed dose-dependent inflammatory lesions with histopathological examinations of the lung tissue. In addition, it was demonstrated that particle size was a function of pulmonary toxicity where 5 nm of TiO_2 NPs was more severe than 21 and 50 nm TiO_2 NPs. Also, Kobayashi *et al*. (2009) treated rats via intratracheal instillation to TiO_2 NPs (19 and 28 nm; 5 mg/mL) every 24 hours for 1 week; TiO_2 NPs revealed a dose-dependent distribution. Liu *et al*. (2010a) treated rats with 5 and 200 nm of TiO_2 NPs (0.5, 5 and 50 $mgkg^{-1}$) via intratracheal

instillation to evaluate the alveolar macrophages. TiO_2 NPs exposure led to alveolar macrophages dysfunction, cell structure damage, ultimately leading to immunosuppression in the rats. Oberdorster *et al*. (2000) treated rats and mice with 20 nm of TiO_2 NPs and 250 nm of fine particles (FPs) via intratracheal instillation and observed significant pulmonary response through the significant increase of LDH activity, acid-glucosidase and total protein in BALF. It was deduced that particle size was a function of the TiO_2 NPs toxicity. Rossi *et al*. (2010) treated mice with 40 nm of silicon dioxide (SiO_2)-coated rutile TiO_2 NPs (10 mg/m^3) via inhalation for 2 hours on 4 progressive days for 4 weeks. The exposure induced increased pulmonary neutrophil, neutrophil attracting chemokine (CXCL-1) and TNF-α in the tissues of the lungs. Contrastingly, the toxicity of TiO_2 NPs was attributed to the SiO_2 surface coating. Li *et al*. (2010b) treated mice via intratracheal instillation to 3 nm of TiO_2 NPs (13.2 mgkg^{-1}) once weekly for 4 weeks. After the 28 day exposure, the lung was damaged; it altered the absorptivity of the alveolar-capillary barrier. Through the systemic circulation, TiO_2 NPs were translocated to the kidneys and liver, resulting into various degrees of tissue lesions. TiO_2 NPs (0.1, 0.5 and 1.0 mg/mL) were intratracheally administered to APOE -/- mice twice/week for 6 weeks and induced dyslipidemia with atherosclerosis and plaque rupture (Hu *et al*., 2010a).

viii. Genotoxicity of titanium dioxide nanoparticles

A study by Falck *et al*. (2009) showed that TiO_2 NPs were genotoxic to human bronchial epithelial BEAS 2B cells. The cells treated with nanosized anatase (< 25 nm), SiO_2 coated nanosized rutile (10 x 40 nm) and fine rutile (< 5 µm) at 1 – 100 µg/cm^2 for 24, 48 and 72 hours revealed that nanoanatase (after 48 and 72 hours) and fine rutile (after 24 and 48 hours) induced DNA damage in a concentraion-dependent manner using the comet assay. Similarly, only nanosized anatase induced a significant increase in micronuclei frequency at 10 and 60 µg/cm^2 after 72 hours exposure. It was concluded that uncoated nanosized anatase and fine rutile, and not SiO_2 coated nanorutile were able to induce DNA damage. Only nanosized anatase was capable of slightly inducing micronuclei. Another study conducted by Kang *et al*. (2008) revealed that human peripheral blood lymphocytes treated with TiO_2 NPs (25 nm; 20, 50 and 100 µg/mL) for 6, 12 and 24 hours induced

micronuclei frequency and DNA damage in a dose and time-dependent manner. However, the genotoxic effects were via TiO_2 NPs induced intracellular generation of ROS.

It was also observed in another study that Goldfish skin cells (GFS_k-S1) treated with TiO_2 NPs alone (5 nm; 1, 10 and 100 µg/mL for 24 hours) or in combination with UVA (2.5 J/m^2 for 2 hours) had DNA damage using the alkaline comet assay (EndoIII and Fpg). TiO_2 NPs alone induced significant increase in oxidative DNA damage in a concentration-dependent manner represented by the increased levels of Fpg-sensitive sites, indicating oxidation of purine DNA bases. Similarly, UVA in combination with TiO_2 NPs further caused a significant increase in oxidative DNA damage compared with TiO_2 or UVA alone. It was observed that hydroxyl radical ($^{\cdot}OH$) and not singlet oxygen ($^1O_2$) was the most prominent radical generated by TiO_2 NPs through the electron spin resonance reacting directly with the DNA or indirectly through membrane lipid peroxidation causing biological damage in combination with UVA irradiation (Reeves *et al*., 2008).

Evaluation of TiO_2 NPs genotoxicity was also carried out by Trouiller *et al*. (2009) who treated mice with Aeroxide P25 21 nm at 5, 100, 250 and 500 $mgkg^{-1}$ for 5 days using DNA deletion, alkaline comet, micronucleus, oxidative DNA damage and γ-H2AX assays. TiO_2 NPs significantly increased frequency of DNA deletions and double strand breaks. Similarly, there was a significant increase in micronuclei frequency, DNA double strand breaks and oxidative DNA damage at 500 $mgkg^{-1}$. It was confirmed that TiO_2 NP induction of genotoxicity, oxidative DNA damage and inflammation in mice may be due to the generation of hydroxyl radical activity, which can trigger ROS causing cellular damage via interaction with the biological membranes.

In contrast to other studies that have shown positive genotoxicity of TiO_2 NPs, Bhattacharya *et al*. (2009) treated human lung fibroblast (IMR-90) and human bronchial epithelial cells (BEAS-2B) to TiO_2 NPs (< 100 nm) and observed that DNA damage as evaluated by the alkaline comet assay was not significant in IMR90-cells and BEAS-2B cells. However, 24 hours post treatment, TiO_2 NPs (5 and 10 $\mu g/cm^2$) induced DNA adduct formation in IMR-90 cells. Low frequency of genotoxic biomarkers in cells treated with TiO_2 NPs may be related to the surface charge as TiO_2 NPs were highly positively charged (+ 48.8 mV) while the ability to generate oxidative DNA adduct may be due to

the generation of ROS. Female mice treated with TiO_2 NPs (19.7 – 101.0 nm) at 0, 1 and 3 mg exhibited significant increase in micronuclei frequency in the peripheral blood at 48 hours after intraperitoneal administration. In addition to the micronuclei frequency, there was a significant induction of urinary 8-OH-dG levels after 24 hours at 3 mg of TiO_2 NPs but not in the liver DNA. Taken together, it was considered that TiO_2 NPs and other metal oxide NPs (CuO, Fe_2O_3, Fe_3O_4 and Ag) were able to induce oxidative stress through the fenton reaction, interact with the mitochondrial membrane causing loss of the membrane potential, opening of the permeability transition pores and ROS production (Song *et al*., 2012).

Human peripheral blood lymphocytes were treated with Aeroxide P25 TiO_2 NPs (20 nm) and normal TiO_2 (1 µm) at 0, 1 and 5 µg/mL for 0 – 48 hours in the absence or presence of 365 nm UVA (0.5 J/cm^2). The CBMN assay revealed that TiO_2 NPs but not normal TiO_2 induced a slight increase in micronuclei frequency, which was significantly increased at the highest concentration. Similarly, TiO_2 NPs alone and TiO_2 NPs + UVA caused a significant increase in DNA damage in a concentration-dependent manner (Kang *et al*., 2011). The genotoxicity observed in the results may be contributed to the fact that TiO_2 NPs, which are photosensitizers, can generate ROS when absorbed by the UVA light causing cell death through the mitochondria-mediated apoptotic pathway. It was observed that the detrimental effects of TiO_2 NPs increased synergism with UVA irradiation.

Shukla *et al*. (2011) investigated the genotoxicity of TiO_2 NPs (0.008, 0.08, 0.8, 8 and 80 µg/mL for 6 hours) in human epidermal cells (A431) using the Fpg-modified comet and CBMN assays. TiO_2 NPs induced a significant increase in the DNA damage at 8 and 80 µg/mL in the treated cells as evident by the comet assay through the olive tail moment and percentage tail DNA. Similarly, a significant increase in the micronuclei formation at 0.8, 8 and 80 µg/mL was observed. It can be suggested that the production of excess intracellular ROS may have been responsible for the DNA damage and micronuclei formation, as it is known that TiO_2 NPs generate ROS, leading to alterations of antioxidant enzymes causing oxidative stress and lipid peroxidation.

Turkez (2011), treated human peripheral blood lymphocytes to TiO_2 NPs (< 100 nm at 3, 5 and 10 µM) and evaluated genotoxicity using SCE, MN and comet assays. Results

revealed that TiO_2 NPs induced SCE in a concentration-dependent manner. In addition, TiO_2 NPs also caused a concentration-dependent increase (5 and 10 µM) in MN frequency at 72 hours exposure and strand breaks (0 to 10 µM). Sycheva *et al*. (2011) revealed that CBAB6F1 mice treated with TiO_2 (33 nm and 160 nm) orally at 40, 200 and 1000 $mgkg^{-1}$ daily for 7 days showed that TiO_2 NPs (33 nm) induced DNA strand breaks and micronuclei in the bone marrow cells and liver at 40 and 200 $mgkg^{-1}$ while 160 nm induced DNA strand breaks and micronuclei in the bone marrow cells only. In addition, 33 and 160 nm TiO_2 NPs increased the mitotic index in the forestomach and colon epithelial cells.

Ghosh *et al*. (2010), treated *Nicotiana tabacum* to TiO_2 NPs (100 nm; 2, 4, 6, 8 and 10 mM for 24 hours) and evaluated genotoxicity using the comet assay. TiO_2 NPs caused a significant increase in DNA damage at 2 mM, which later decreased with increased concentrations. This may possibly be due to the agglomeration property of NPs, as the number of particle interaction increases with increased concentration, reducing the ability of free TiO_2 NPs to interact with the plant system. In addition, DNA laddering also confirmed DNA fragmentation which was highest at 10 mM. The mechanism of TiO_2 NP-induced genotoxicity may have been due to the generation of hydroxyl radicals resulting to lipid peroxidation and oxidative stress. In contrast to studies that have reported genotoxicity of NPs in plant systems, Ramesh *et al*. (2014) reported that TiO_2 NPs and MPs did not induce genotoxicity to *Triticum aestivum* at 250, 500, 1000 and 2000 mg/L as evident by the mitotic index and chromosome aberration assay. The negative effect of TiO_2 NPs may possibly be due to the plant species used as genotoxicity which varies from species to species, the ability of TiO_2 NPs to agglomerate at higher concentrations thereby reducing the amount of particles in the plant organisms.

Chromosomal aberration assay was used by Catalan *et al*. (2012), to evaluate the genotoxicity of TiO_2 NPs (< 25 nm; 6.25-300 µg/mL for 24, 48 and 72 hours) in human peripheral blood lymphocytes. TiO_2 NPs induced a concentration-dependent significant chromosome and chromatid-type at 12.5, 100 and 300 µg/mL only at 48 hours. However, TiO_2 NPs at any of the exposure time did not significantly affect the mitotic index. Sadiq *et al*. (2012) showed that B6C3F1 mice treated with 10 nm TiO_2 NPs at 0.5, 5.0 and 50

$mgkg^{-1}$ for three consecutive days showed no significant increase in the percentage MN-reticulocytes across all concentrations. Similarly, phosphatidyl inositol glycan complementation group A gene (Pig-a) assay showed no increase in RBC^{CD24-} and RET^{CD24-} frequencies across all concentrations. However, the contradictory results of genotoxicity observed in this study may be attributed to the source of NP, experimental design, crystal forms of NPs, end point assay and experimental animal model used.

Magdolenova *et al*. (2012) used the alkaline comet assay (-/+ Fpg) to assess DNA damage in TK6 human lymphoblast cells, Cos-1 monkey kidney fibroblasts and EUE human embryonic epithelial cells treated with TiO_2 NPs (15-60 nm; 0.12, 0.6, 3, 15 and 75 $\mu g/cm^2$ for 2 and 24 hours) using two different dispersion protocols (DP): DP1 (5 mg TiO_2 NPs with 1 mL of 20 % FBS in PBS, sonicated for 15 minutes) and DP2 (20 mg TiO_2 NPs with 10 mL of culture medium, sonicated for 3 minutes). Results showed that no significant increase in DNA damage (SB + Fpg) levels were found in TK6 cells treated with TiO_2 NPs dispersed using DP1 after 2 and 24 hours. However, TiO_2 NPs dispersed in DP2 only showed a significant increase in oxidised DNA damage at 75 $\mu g/cm^2$ after 2 hours, while 24 hours treatment with TiO_2 NPs (DP2) did not show any significant increase in strand breaks and oxidised DNA damage. In addition, TiO_2 NPs (DP2) induced a significant increase in strand breaks at 75 $\mu g/cm^2$ after 2 and 24 hours but no significant induction in Fpg in Cos-1 cells. Also, EUE cells treated with TiO_2 NPs (DP1) showed no significant induction in strand breaks after 2 hours but a significant increase at 75 $\mu g/cm^2$ after 24 hours. The varying results obtained in different cell types treated with TiO_2 NPs (DP1 or DP2) may be attributed to properties such as dispersion method, surface area, crystal form, size, distribution, toxicity assay, cell types and exposure period, all of which can influence toxicity of NPs.

Lindberg *et al*. (2012), showed that C57BL/6J mice treated with TiO_2 NPs (21 nm; 0.8, 7.2 and 28.5 mg/m^3, 4hours per day) for five consecutive days via inhalation exhibited no significant induction of MNPCE or MNNCEs in the peripheral blood after 48 hours of last exposure. Similarly, no significant induction of DNA damage was observed across the three concentrations in the alveolar type II and clara cells, suggesting no genotoxic effects by TiO_2 NPs. The negative genotoxicity results may have been due to the short exposure

duration. However, prolonged exposure duration may have increased the retention of TiO_2 NPs in the lungs thereby stimulating the inflammatory cells to induce systemic genotoxicity.

Shukla *et al*. (2014), treated mice orally to TiO_2 NPs (2-50 nm; 10, 50 and 100 $mgkg^{-1}$) for 14 consecutive days to evaluate the genotoxicity using the bone marrow micronucleus and modified alkaline comet assays. A significant increase in MN frequency was observed at 100 $mgkg^{-1}$ and a significant dose-dependent increase in strand break and oxidative DNA damage with or without fpg at 50 and 100 $mgkg^{-1}$. This confirms the genotoxicity properties of TiO_2 NPs, all of which may be attributed to the direct interaction of TiO_2 NPs with the DNA or secondarily through ROS generation. Dobrzynska *et al*. (2014) treated wistar rats intravenously to a single dose of TiO_2 NPs (21 nm; 5 $mgkg^{-1}$) and examined the genotoxic effect after 24 hours, 1 and 4 weeks using the micronucleus and comet assays. Results showed a significant induction of MN frequency in PCE after 24 hours, which decreased with exposure time but was not significant. However, no significant induction of DNA damage in the bone marrow leukocytes across the exposure periods. The result may have been attributed to early DNA damage repair in the bone marrow of the treated rats and the ability of the reticuloenodthelial cells of the organs (liver and spleen) to phagocytose NPs leading to systemic clearance.

Browning *et al*. (2014), evaluated the genotoxicity of TiO_2 NPs (P25; 0 – 100 $\mu g/cm^2$ for 24 h) in primary human skin fibroblasts (BJ cells) and human skin fibroblast cells immortalised with hTERT (BJhTERT). It was observed that TiO_2 NPs did not induce clastogenicity as measured by chromosomal aberration assay in the treated cells even though TiO_2 NPs penetrated both the cellular and nuclear membranes. A consideration for the non-clastogenicity of TiO_2 NPs in the cells may be due to the difference in cell lines and exposure time. The human skin fibroblast was immortalised with hTERT, which might have interfered with the mechanism. In addition, the exposure time might not be sufficient enough to induce clastogenicity; likewise the chromosomal aberration assay may not be sensitive enough to detect damage. It is also important to know that different cells respond differently to the same NPs when treated (Magdolenova *et al*., 2012; Tomankova *et al*., 2015). Human peripheral blood lymphocytes were treated with four

nanosized TiO_2 (NM-102, NM-103, NM-104 and NM-105 at 2.5, 5, 15, 45, 125 and 256 µg/mL for 30 hours). Using the CBMN assay, TiO_2 NM-102 induced a significant increase of MNBC at 125 µg/mL, NM-103 at 5 and 45 µg/mL and NM-104 at 15 and 45 µg/mL. However, no significant increase was induced by NM-105. The absence of a clear concentration-dependent response in the NMs may have been due to the increasing size of the agglomerates with dose and time. This will however, affect the cellular uptake of TiO_2 NPs by the lymphocytes, thereby resulting into no dose-response (Tavares *et al*., 2014).

Kansara *et al*. (2015) treated human alveolar (A549) cell to TiO_2 NPs at 25, 50, 75 and 100 µg/mL for 6 hours. TiO_2 NPs induced a significant concentration-dependent increase in MN frequency and strand breaks at 75 and 100 µg/mL. It is known that DNA damage was as a result of excess production of hydroxyl radicals by TiO_2 NPs. The excess intracellular ROS generated may induce oxidative DNA damage leading to genetic instability and consequently cause carcinogenesis or cell death. Tomankova *et al*. (2015) treated NIH3T3 cell line (mouse fibroblasts), SVK14 (human keratinocytes) and BJ (human fibroblasts from fore skin) at IC50 concentrations (3234.4, 1744.1 and 5659.8 mg/L) of TiO_2 NPs (28 nm) and 1571.2, 508.6 and 2596.9 mg/L to Nanorutil (128 nm) for 6 hours. TiO_2 (28 nm) induced significant DNA damage in all cells with SVK14 cells as the most sensitive while NIH3T3 cells as the least sensitive. However, nanorutil caused a significant DNA damage in SVK14 and not in BJ or NIH3T3 cells. TiO_2 NPs were more genotoxic than the nanorutil because of the particle size. It is known that the particle size is a fundamental factor to toxicity as small sized NPs facilitate penetration into the cytoplasm and nucleus to interact with macromolecules (Balasubramanyam *et al*., 2009a, b; Demir *et al*., 2015). SVK14, NIH3T3 and BJ cells responded differently to TiO_2 NPs and nanorutile.

Male rats were treated with TiO_2 NPs (anatase, 5 - 12 nm) at 50, 100 and 200 $mgkg^{-1}$ for 60 days. A significant dose-dependent increase of MN frequency at 100 and 200 $mgkg^{-1}$ and a decrease of percentage PCE at 200 $mgkg^{-1}$ were observed. TiO_2 NPs also induced a dose-dependent increase of strand breaks at 100 and 200 $mgkg^{-1}$. The presence of a decrease in percentage PCE is an indication that TiO_2 NPs reached the bone marrow cells and damaged hemosynthesis. Likewise, the presence of MN showed lagging acentric

chromosomes or chromatid fragments (Grissa *et al*., 2015). Demir *et al*. (2015), treated human embryonic kidney (HEK293) and mouse embryonic fibroblast (NIH3T3) cells to TiO_2 NPs (21 and 50 nm) and microparticulate form of TiO_2 at 10, 100 and 1000 µg/mL. TiO_2 NPs induced a significant increase in MN frequency in HEK293 and NIH/3T3 at 1000 µg/mL while none was induced in both cells by the microparticulate form. Similarly, there was a significant induction in DNA damage at 1000 µg/mL obtained with both TiO_2 NPs (21 and 50 nm) in both cells while the microparticulate form did not induce any significant DNA damage. When Fpg was used in detecting oxidised DNA damage, neither TiO_2 NPs nor the microparticulate form induced a significant level of oxidative DNA damage. Using the soft-agar colony assay, TiO_2 NPs also induced a significant increase in colony only at 1000 µg/mL while no colony was observed by the microparticulate form. From this study, it is important to know that exposure to high doses of NPs becomes a risk, as it can induce genotoxicity and mutagenicity.

ix. Systemic toxicity of titanium dioxide nanoparticles

TiO_2 NPs (5 - 100 nm) have been reported to translocate across the air-blood-barrier (Geiser and Kreyling, 2010). Retention of TiO_2 NPs in the lymphatic system, liver, and further organs and tissues when translocated to the blood has been reported. In another study, 20 - 30 nm of TiO_2NPs (70/30 anatase/rutile) intravenously administered to rats was investigated for tissue distribution by Fabian *et al*. (2008). TiO_2 NPs (5 $mgkg^{-1}$) was intravenously injected once to rats and bioaccumulation was investigated at 1, 14 and 28 days later. The liver showed the highest content of TiO_2 NPs, followed by the kidneys, lung and spleen on day 1 post treatment. The liver retained TiO_2 NPs throughout the 28 days of the experiment. TiO_2 NPs levels slightly decreased in the spleen from day 1 to days 14 and 28, with the lung and kidneys having similar results to the control levels by day 14.

TiO_2 NPs levels were not detected in the brain, plasma, blood cells or lymphnodes at day 1 and days 14 and 28, suggesting the translocation and bioaccumulation of TiO_2 NPs to the lung, spleen, kidneys and liver. In another study, Chen *et al*. (2009) demonstrated the intraperitoneal injection of 80 and 100 nm of TiO_2 NPs (anatase; 0, 324, 648, 972, 1296, 1944 and 2592 $mgkg^{-1}$) in mice for 1, 2, 7 and 14 days exposure. TiO_2 NPs

bioaccumulation levels were highest in the kidneys, liver, spleen and lung following a decreasing order at 1, 2, 7 and 14 days post treatment. Similarly, Liu *et al*. (2009a) intraperitoneally treated mice for 14 days to 5 nm of TiO_2 NPs (anatase; 5, 10, 50, 100 and 150 $mgkg^{-1}$) to investigate the distribution of the TiO_2 NPs. Accumulation was in the following order: liver > kidneys > spleen > lung > brain > heart. In the liver, 50 $mgkg^{-1}$ of TiO_2 NPs was higher compared with TiO_2 NPs of the same dose in other tissues. Ma *et al*. (2010), reported that 5 nm of TiO_2 NPs (anatase; 5, 10, 50, 100 and 150 $mgkg^{-1}$) intraperitoneally administered to ICR mice for 14 consecutive days translocated to the brain inducing damage and oxidative stress. Similarly, Li *et al*. (2010b), treated mice with TiO_2 NPs once a week for 4 weeks, which passed through the blood-brain barrier. Ferin *et al*. (1992) treated rats via a single intratracheal instillation or 12 weeks inhalation to TiO_2 NPs (12 and 21 nm) and TiO_2 FPs (230 and 250 nm). Particle migration to the interstitium was related to the NP size, dose delivered and dose rate. Furthermore, TiO_2 NPs (20 nm) at acute and sub-chronic inhalation studies demonstrated access to the pulmonary interstitium compared with TiO_2 FPs (250 nm).

x. Carcinogenicity of titanium dioxide nanoparticles

Dankovic *et al*. (2007) demonstrated that TiO_2 NPs (< 100 nm; 10 mg/m^3) and TiO_2 FPs (< 2.5 µm; 250 mg/m^3) treated with rats for 2 years induced respiratory cancer at high concentrations. Heinrich *et al*. (1995) investigated the carcinogenic effect of 15 – 40 nm of TiO_2 NPs. The authors reported TiO_2 NPs to be tumourigenic at 10 mg/m^3 in rats for 2 years. The carcinogenic potential was more in TiO_2 NPs compared with TiO_2 FPs. Pott and Roller (2005) treated 21 – 25 nm of TiO_2 anatase NPs or hydrophilic to female rats via intratracheal instillation once a week for 30 weeks. TiO_2 anatase NPs or hydrophilic induced a greater significant occurrence of lung tumours (2 - 69.6 % of squamous cell epitheliomas/carcinomas and adenomas/carcinomas or their combination) compared with the controls (0 %). There was a significant induction of lung tumours (30-63.6 %) by anatase NPs compared with TiO_2 hydrophilic NPs (6.7 %). TiO_2-coated mica was investigated for its carcinogenic and toxicological properties by Bernard *et al*. (1990). Diets containing 0, 1.0, 2.0 and 5.0 % TiO_2-coated mica were given to rats for 13 weeks;

there were no carcinogenic or toxicological effects even at 5.0% of the dietary concentrations.

Xu *et al*. (2011) conducted the carcinogenic property of 20 nm of TiO_2 NPs (rutile) on Ha-ras proto-oncogene transgenic (Hras 128) rats (which are susceptible to skin cancer) treated twice weekly for 10 weeks to UV-B radiation. TiO_2 NPs (100 mg/mL) was painted on the shaved area twice weekly prior to sacrifice. TiO_2 NPs tumour-induction was not notably distinct from the controls of UV-B. However, it was proposed by the authors that skin carcinogenesis could not be induced by TiO_2 NPs due to its lack of penetration to reach skin structures through the epidermis. This study was also supported by Newman *et al*. (2009) who reported no skin cancer as a result of the lack of penetration of TiO_2 NPs into the undamaged part of the dermal tissue. Emphasis was made for further studies to stimulate UV exposure and sunburned skin, which are real-world conditions to evaluate the safety of TiO_2 NPs in sunscreens.

xi. Reproductive toxicity of titanium dioxide nanoparticles

The reproductive and endocrine effects of 5-day orally treated rats to TiO_2 NPs anatase were investigated by Tassinari *et al*. (2014). The spleen and ovaries contained increased levels of Ti; histopathological alterations were induced in the thyroid, adrenal medulla, adrenal cortex and ovarian granulosa. TiO_2 NPs induced a reduction in T_3 hormone and an elevation in testosterone levels in males. Male mice were orally treated for 90 consecutive days to TiO_2 NPs so as to investigate the alterations in gene expression profiles of the testis (Gao *et al*., 2013). TiO_2 NPs penetrated the blood testis barrier and accumulated therein, leading to histopathological lesions of the testis, alterations in sex hormones and increase in sperm malformations. Subsequently, there was up-regulation of 70 genes and down-regulation of 72 genes as indicated by microarray. The exposure of TiO_2 (UV-titan) by inhalation and carbon black (Printex90) by intratracheal instillation were investigated in male reproduction following two generations.

Reduction of sperm production counts and not daily sperm production in the F_1 generation was affected by maternal particulate exposure. Lower sperm production was found in the fathers of F_2 generation treated with Printex90 while sperm production in the males of the

F_2 generation was not affected. Gao *et al*. (2012) treated female mice for 90 consecutive days to TiO_2 NPs (10 $mgkg^{-1}$) via oral administration to investigate gene-expressed characteristics and injury in the ovaries. TiO_2 NPs induced ovarian damage as a result of accumulation of NPs in the ovaries, altered sex hormones, decreased pregnanacy rate or fertility and induced oxidative stress. There was up-regulation of 223 genes and down regulation of 65 genes in the ovaries. Pregnancy complications were observed in female mice intravenously injected with SiO_2 NPs (70 nm) and TiO_2 NPs (35 nm). SiO_2 NPs and TiO_2 NPs translocated and accumulated in the placenta, foetal liver and brain while smaller uteri and foetuses were also observed in the NPs treated mice compared with the control (Yamashita *et al*., 2011). The developmental and neurobehavioural effects of aerosolised powder of UV-titan L181 to maternal exposure via inhalation on gestation days 8 - 18 were investigated by Hougaard *et al*. (2010). Penetration of UV-titan in the lungs induced lung inflammation on day 5 when the cell counts of BAL fluid was assessed. Furthermore, moderate neurobehavioural alterations were displayed by the offsprings.

2.3.4.2 Zinc oxide nanoparticles

Zinc oxide (ZnO) NPs are white soluble inorganic compounds known as zinci oxicum, permanent white, oxydatum, ketozinc and oxozinc. They exist in one of two forms: the wurtzite and zinc blende structures, with the wurtzite structure been the most stable under ambient conditions (Figure 2.8) (Vaseem *et al*., 2010). Over 1.2 million tons of ZnO NPs are produced by more than 300 companies in the world (Kumar *et al*., 2015), thus making it the third highest producing NP globally. It has a molar mass of 81.40 $gmol^{-1}$, boiling point of 2360°C and melting point of 1975°C. They possess a high refractive index with anticorrosive, antifungal and UV filtering properties. Nanowires, nanorods and nanoparticles are a few of the variety of morphologies in which ZnO can be synthesised into (Vaseem *et al*., 2010).

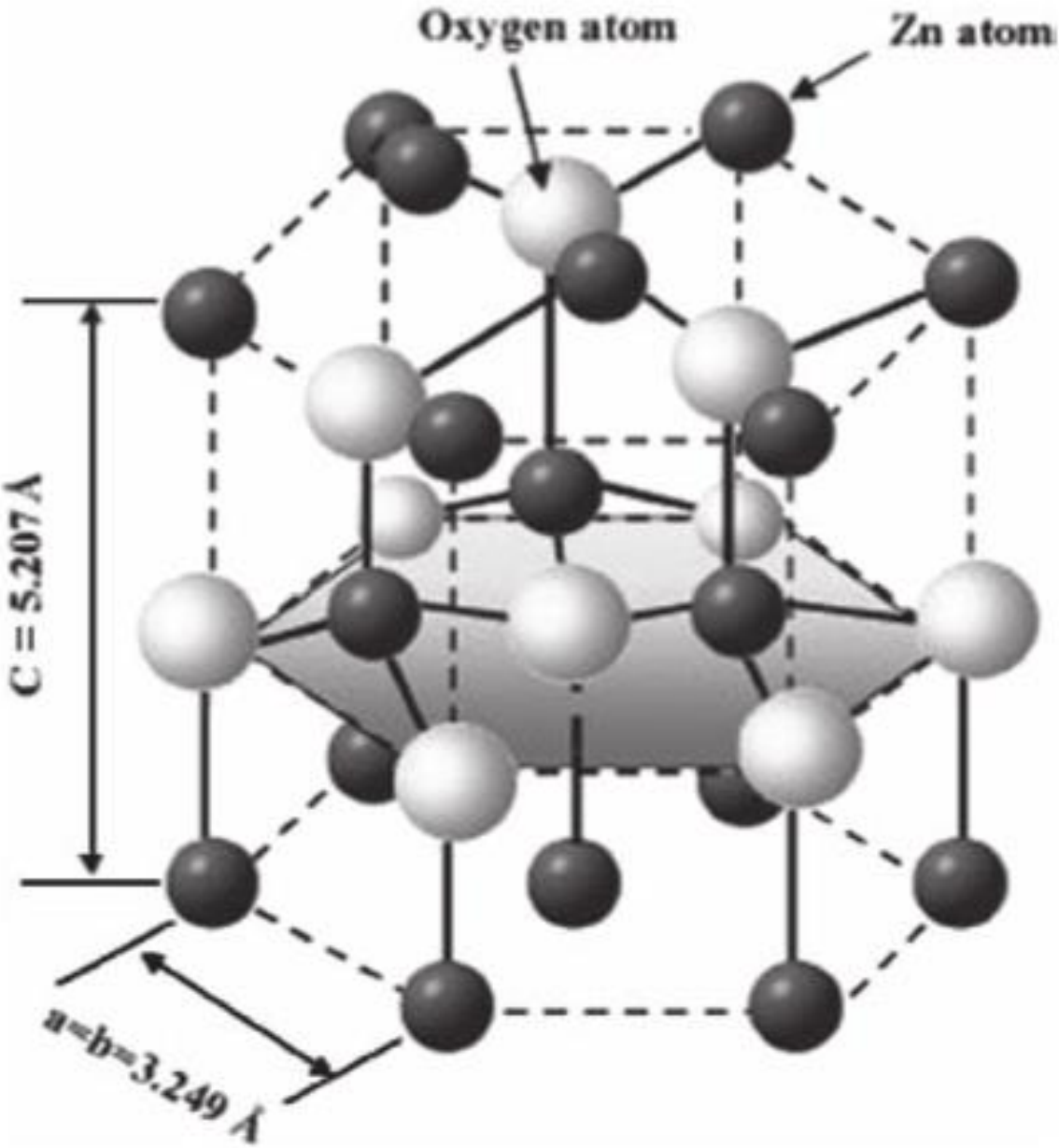

Figure 2. 8: The hexagonal wurtzite structure model of ZnO. The tetrahedral coordination of Zn-O is shown. Oxygen atoms are shown as larger white spheres while the Zn atoms are smaller brown spheres. Source: Vaseem *et al*. (2010).

2.3.4.2.1 Uses of zinc oxide nanoparticles

Zinc oxide (ZnO) NPs are a highly functional material with high chemical reactivity, very strong oxidative material and corrosive resistance, photocatalytic and strong absorptive ability to UV rays (Guan *et al*., 2012). ZnO NPs are used in various categories in consumer products because of their electrical, optical, dermatological and antibacterial properties (Adamcakova-Dodd *et al*., 2014). They are utilised in the production of sunscreens, baby powders, antidandruff shampoos, fabric treatments for UV shielding (Osmond and McCall, 2010; Burnett and Wang, 2011), creams and ointments for treating skin diseases (Sharma *et al*., 2012a; 2012b), as additives in the manufacture of concrete and ceramics, food products such as breakfast cereals. Most importantly, they are essential for anticancer therapy, drug delivery (Zhang *et al*., 2011a), and fillers in orthopedic, dental implants (Srivastav *et al*., 2016) and as essential ingredients in almost all types of antifouling agents (IPPIC, 2012).

2.3.4.2.2 Toxicity of zinc oxide nanoparticles

i. Acute toxicity of zinc oxide nanoparticles

Toxicity of nano-ZnO or fine- ZnO particle mixture was assessed by Sayes *et al*. (2007). Cytotoxicity was induced at 24 hours and 1 week after instillation by both nano- and fine-ZnO particles, though was not different from the controls instilled with PBS. Rats treated with nano- and fine ZnO particles had significant higher number of cells at the 24 hours time point compared with other time point. However, the instillation procedure led to a transient increase that diminished at the 1 week time point. Wang *et al*. (2017a) reported that ICR male mice intratracheally instilled with ZnO NPs (200, 400 and 800 µg/kg) showed bodyweight loss, total protein and hydroxyproline content in BALF. In addition, inflammatory and hyperplastic changes were observed in the lungs. Sarkheil *et al*. (2018) reported that *Artemia franciscana* nauplii exposed to ZnO NPs (1 – 30 mg/L) for 48 and 96 hours did not induce any significant acute toxicity after 48 hours, but a significant increase in the immobilisation rate after 96 hours was observed.

ii. Sub-acute toxicity of zinc oxide nanoparticles

Adamcakova-Dodd *et al*. (2014) reported an elevation of Zn^{2+} in the BAL fluid after exposure to ZnO NPs (3.5 mg/m^3, 4 hours/day, 2 weeks), which returned to baseline 3 weeks post treatment. No other toxic responses were observed except for an increase of macrophages in BAL fluid, IL-12 (p40) and MIP-1α. The toxicity of orally treated female Wistar rats to ZnO NPs (20 nm; 100, 200 and 400 mgkg^{-1}) for 14 consecutive days was demonstrated by Shokouhian *et al*. (2013). There was a significant increase in IgG, TNF-α and IL-6 and a reduction in GSH level, as well as histopathological alterations in the lungs. Ben-Slama *et al*. (2015) demonstrated that male rats treated with ZnO NPs (10 mg/kg) orally for 5 consecutive days showed significant alterations in the activities of ALT and AST. Hao *et al*. (2013) reported that juvenile carp (*Cyprinus carpio*) exposed to ZnO NPs and bulk-ZnO for 30 days showed significant hyper-bioaccumulation of 50 mg/L of ZnO NPs in the liver and gills.

iii. Sub-chronic toxicity of zinc oxide nanoparticles

Park *et al*. (2014) treated Sprague Dawley rats via oral exposure to ZnO NPs (20 nm; 125, 250 and 500 mgkg^{-1}) to investigate toxicity. Anaemia-related factors, apoptosis, increased numbers of regenerative acinar cells in the pancreas and stimulated periductular lymphoid cell filtration were induced at 500 mgkg^{-1} of ZnO NPs. Retinal atrophy was observed at 250 and 500 mgkg^{-1} while stomach lesions were observed at 125, 250 and 500 mgkg^{-1}. Increased level of Zn was observed in a dose-dependent manner in the liver, kidney, intestines and plasma. In another study by Seok *et al*. (2013), male and female rats orally administered with ZnO NPs (67.1, 134.2, 268.4 and 536.8 mgkg^{-}1) for 13 weeks demonstrated a significant decrease in the body weight at 536.8 mgkg^{-1} as well as significant alterations in the anaemia-related haematologic parameters with pancreatitis.

Negatively and positively charged ZnO NPs (100 nm) (31.35, 125 and 500 mgkg^{-1}) were treated with Sprague Dawley rats for 90 days. Significant changes in the haematological and biochemical analyses were induced at 500 mgkg^{-1} for the ZnO NPs with histopathological alterations in the pancreas, eye, stomach and prostrate gland tissues (Kim *et al*., 2014b). The pharmacokinetics and toxicokinetics of ZnO NPs (125, 250 and

500 $mgkg^{-1}$) in a 90-day oral exposure in male and female rats were investigated by Chung *et al*. (2012). Toxicity potential was indicated by the elevated plasma concentrations compared with the normal levels.

iv. Chronic toxicity of zinc oxide nanoparticles

Growth reproduction and accumulation of zinc were investigated through the exposure of ZnO NPs and $ZnCl_2$ on *Daphnia magna* in a 21-day chronic toxicity study. Extensive amounts of ZnO NPs dissolved in the medium resulting in the chronic effects on growth, reproduction and accumulation. It was however concluded by the authors that the dissolution property of ZnO NP is a contributing factor to the toxicological effects of ZnO NPs at the chronic level (Adam *et al*., 2014). Lopes *et al*. (2014) treated *Daphnia magna* to different particle sizes of ZnO NPs (30 nm and 80 - 100 nm) and $ZnCl_2$ and investigated the effect of particle sizes on the immobilisation, feeding inhibition and reproduction of ZnO NPs compared with the ZnO microsized particles. At 30 nm of ZnO NPs, feeding activity and reproductive outcome were impaired, indicating that the particle size and dissolution properties are essential factors that contribute to the toxicity of ZnO NPs.

The chronic effect of ZnO NPs on the culture media of *Escherichia coli* strain was reported by Dutta *et al*. (2013). Higher toxicity was exhibited at the minimum inhibitory concentration compared with the higher concentrations of the single exposure. Scanning Electron Microscopy (SEM) revealed cell wall deformation which confirmed membrane lipid peroxidation through the production of ROS that inhibited growth. Kool *et al*. (2011) treated *Folsomia candida* in the soil to ZnO NPs, non-nano ZnO and $ZnCl_2$. Increase in soil concentration increased the zinc concentrations, in addition, a dose-dependent reduction in reproductive capability in the exposure to ZnO NPs, non-nano ZnO and $ZnCl_2$ respectively was observed. It was concluded that Zn^{2+} ions and not the particle size contributed to the toxicity effects. In another study by Hooper *et al*. (2011), *Eisenia veneta* earthworm was exposed to soil and food dosed with uncoated ZnO NPs (< 100 nm) for 21 days. In the measured traits, $ZnCl_2$ showed more impact than ZnO NPs. In addition, *E. veneta* treated with $ZnCl_2$ showed complete inhibition of the reproduction, and reduced immune activity compared with those treated with ZnO NPs. However, it was observed

through the scanning electron microscopy that *E. veneta* accumulated ZnO in the particulate form.

v. Dermal toxicity of zinc oxide nanoparticles

Studies have shown that sunscreens that contain ZnO NPs do not penetrate beyond the stratum corneum in a healthy skin (Filipe *et al*., 2009; Schilling *et al*., 2010). Gulson *et al*. (2010) demonstrated the topical application of ZnO NPs (19 nm and 100 nm) on the skin of healthy human volunteers for 5 days. ^{68}Zn was used to prepare ZnO particles in order to distinguish it from the Zn present in the body. It was observed that approximately 0.1% of all Zn in the blood was ^{68}Zn after the application of the sunscreen containing one of the two types of particles. The blood and urine contained a higher amount of ^{68}Zn compared with the microsized particles. In another study, the dermal penetration of TiO_2 and ZnO NPs was investigated in human volunteers using the punch biopsy analysis after *in vivo* application. Skin tape stripping was used in evaluating the localisation of TiO_2 and ZnO NPs in damaged skin. Interestingly, Ti was not detected beyond the stratum corneum while Zn levels in the treated skin were similar to that of the non-treated skin (Filipe *et al*., 2009).

Monteiro-Riviere *et al*. (2011) reported the penetration of ZnO NPs (140 nm) only in one to two layers of the stratum corneum of UV-irradiated sunburned pig skin. In addition, Pasupuleti *et al*. (2012b) reported collagen loss as a result of the skin penetration of realistic doses of ZnO NPs (20 nm) 5 times/week for 28 days in rats. Meyer *et al*. (2011) reported apoptotic induction and p53 and phosphos-p38 upregulation in human dermal fibroblasts treated with ZnO NPs (23.5 nm). Moos *et al*. (2011) treated HaCaT human keratinocytes and SK Mel-28 human melanoma cells to ZnO NPs (8 – 10 nm) and ZnO particles (44 µm). No proinflammation occurred, however, there were changes in the chaperonin proteins, protein folding genes and metal metabolism as revealed by gene profiling. Kocbek *et al*. (2010) treated NCT2544 human keratinocytes to ZnO NPs (< 100 nm, 10 µg/mL) for 3 months. The vesicles within the cytoplasm, particularly the early and late endosomes and amphesomes contained the NPs. ZnO NPs exposure induced ROS generation, loss of normal cell morphology, decreased mitochondrial membrane potential activity and cell cycle disturbance. Yazdi *et al*. (2010) treated primary human

keratinocytes to ZnO NPs (15 nm). Penetration of ZnO NPs affected the skin cells while apoptosis but not inflammatory response occurred after short term exposure. Subsequently, formation of tubular intercellular structures decreased mitochondrial membrane potential activity and increased ROS generation after long-term exposure. A 90-day dermal toxicity of ZnO NPs was demonstrated in rats by Ryu *et al*. (2014). A dose-dependent irritation was observed at the site of application. The liver, small intestine, large intestine and feaces showed increased concentrations of ZnO NPs.

vi. Neurotoxicity of zinc oxide nanoparticles

Information is limited on the neurotoxicity of ZnO NPs. Deng *et al*. (2009) investigated the neurotoxicity of ZnO NPs (10 – 200 nm) on mouse neutral stem cells (NSCs). There was a dose-dependent decrease in the cell viability studies as well as apoptosis detected by the transmission electron microscopy and flow cytometry. Han *et al*. (2011) reported that intraperitoneally treated ZnO NPs (20 – 80 nm; 4 $mgkg^{-1}$) twice weekly for 8 weeks in rats altered the synaptic plasticity and changed spatial learning and memory ability. In another study by Darroudi *et al*. (2014), neuro2A cells treated with ZnO NPs showed a dose-dependent toxicity from 6 µg/mL and above.

vii. Pulmonary toxicity of zinc oxide nanoparticles

Particles phagocytosed by alveolar macrophages migrate to the tracheobronchial region via the mucociliary escalator where they are either swallowed or coughed up. If either of these mechanisms fails, clearance will no longer be available once the particles have penetrated the interstitium, leading to inflammation and fibrosis of cells (Osmond and McCall, 2010). Transient increase in the concentration of Zn^{2+} ions may occur as a result of ZnO dissolution in the acidic environment of the lung lining fluid (Osmond and McCall, 2010). Warheit *et al*. (2009) treated rats via intratracheal instillation to fine size ZnO particles (3 µm; 1 and 5 $mgkg^{-1}$) and ZnO NPs (300 nm; 1 and 5 $mgkg^{-1}$) or inhalation to aerosols of 25 or 50 mg/m^3 for 1 or 3 hours. The authors observed increased LDH, protein content, neutrophil content and transient inflammation. Lung inflammatory responses were substantially produced following the intratracheal instillation exposure to high-dose nano- and fine-ZnO particles (5 $mgkg^{-1}$) at 24 hours, which followed minimal

neutrophils through a week. Similar studies by Cho *et al*. (2012) reported eosinophilic/fibrotic/granulomatous inflammation and eosinophils and neutrophils in BAL of rats treated via a single intratracheal instillation to ZnO NPs (10 nm). Xia *et al*. (2011) demonstrated that mice treated with ZnO NPs (20 nm) doped with iron exhibited reduced neutrophil counts, interleukin-6 and heme oxygenase (HO) expression as compared with the non-doped ZnO NPs.

Wang *et al*. (2010) treated male Wistar rats via inhalation to ZnO NPs (20 nm; 2.5 $mgkg^{-1}$) twice daily for 3 days via inhalation, and observed high levels of Zn content in the liver tissues 12 hours post treatment. Activities of ALT, AST, LDH and CK were significantly reduced compared with the negative control group. Histopathological examination revealed liver and lung damage. George *et al*. (2010) treated BEAS-2B cells and RAW264.7 murine macrophages to ZnO NPs (20 nm) and observed induction of intracellular Ca^{2+} influx, lowering of the mitochondrial membrane potential and loss of membrane integrity when a cytotoxicity screening approach was used. Hsiao and Huang (2011) reported that A549 lung epithelial cells treated with ZnO NPs (32-95 nm) cores coated with TiO_2 shell exhibited reduced mitochondrial activity, increased membrane damage as indicated by increased LDH level, IL-8 production and ROS generation. Huang *et al*. (2010) reported a concentration and time-dependent cytotoxicity in BEAS-2B cells treated with ZnO NPs (20 nm). Also, increased intracellular Ca^{2+} influx, LDH release and oxidative stress were reported.

viii. Genotoxicity of zinc oxide nanoparticles

Zinc oxide nanoparticles have been demonstrated to be genotoxic both in *in vitro* and *in vivo* test systems. Osman *et al*. (2010) evaluated the genotoxicity of ZnO NPs in human negrad cervix carcinoma HEp-2 cells using the cytokinesis block micronucleus (CBMN) and comet assays. Cells were treated with ZnO NPs (10, 20, 50 and 100 µg/mL) for 2 hours (CBMN) and 4 hours (comet assay). A significant concentration-dependent increase in MN frequency was observed at 50 and 100 µg/mL and a significant concentration-dependent increase in the percentage tail DNA at 20, 50 and 100 µg/mL. It is known that ROS plays a critical role in NP-induced DNA damage and excessive intracellular ROS generation may cause single and double- strand breaks, which may lead to carcinogenesis

due to incomplete DNA repair. It is also important to know that ZnO NPs can release free hydrated zinc ions (Zn^{2+}) due to their solubility that may increase genotoxicity. Shaymurat *et al*. (2012) reported the phytotoxic and genotoxic effects of ZnO NPs (4 nm; 10, 20, 30, 40 and 50 mg/L for 8, 16 and 24 hours) on *Allium sativum*. A significant decrease in the mitotic index and increase in chromosome aberration in a concentration- and time-dependent manner were observed. It was concluded that ZnO NPs had the potential of inducing toxicity to the root cells by inhibiting DNA synthesis through the production of excess ROS that could cause membrane lipid damage resulting to lipid peroxidation (Kumar *et al*., 2015).

According to Sharma *et al*. (2012a), male Swiss mice treated orally to ZnO NPs (30 nm, 5, 50 and 300 $mgkg^{-1}$) for 14 consecutive days showed a significant increase in oxidative DNA damage at 300 $mgkg^{-1}$ for both olive tail moment (OTM) and percentage tail DNA in the liver cells. However, no significant increase in the DNA strand breaks in the kidney cells of the treated mice. Oxidative stress was proposed as the main mechanism of genotoxicity in ZnO NP-induced oxidative DNA damage in the liver cells. Excess ROS generation can result in several alterations to the DNA: DNA-protein crosslinks, oxidation of purine/pyrimidines and alkali labile sites and the like. Similar results were also obtained by Sharma *et al*. (2012b) when human hepatocarcinoma (HepG2) cells were treated with ZnO NPs (30 nm; 8, 14 and 20 µg/mL for 6 hours). The comet assay revealed a concentration-dependent increase in strand breaks and oxidative DNA damage at 14 and 20 µg/mL for both olive tail moment and percentage tail DNA. Guan *et al*. (2012) treated human hepatocyte (LO2) and human embryonic kidney (HEK293) cells to ZnO NPs (50 nm; 0, 5, 10, 25, 50, 75 and 100 µg/mL for 4, 12 and 24 hours). Comet assay showed a concentration-dependent increase in DNA strand breaks in both cell lines. Significant concentration-dependent increase was observed after 4 hours treatment at 75 and 100 µg/mL; 50, 75 and 100 µg/mL after 12 hours and 25, 50, 75 and 100 µg/mL after 24 hours treatment in LO2 cells. In HEK 293 cells, a significant concentration-dependent increase was observed at 50, 75 and 100 µg/mL after 5, 10, 25, 50, 75 and 100 µg/mL after 12 hours and 5, 10 25, 50, 75 and 100 µg/mL after 24 hours treatment.

Li *et al*. (2012) treated male mice orally to ZnO NPs (50 nm; 1.25, 2.5 and 5.0 g/kg) or ZnO MPs (> 100 nm) and evaluated genotoxicity after 24, 48 and 72 hours using the micronucleus assay. In addition, *Salmonella typhimurium* histidine auxotrophs (TA98, TA100, TA102, TA1535 and TA1537) were used in evaluating the mutagenicity of ZnO NPs and MPs. The percentages of PCE and MNPCE frequenies in ZnO NPs and MPs treated mice were not significantly different across all concentrations. Similarly, the Ames test showed no significant changes in the revertants at all concentrations of ZnO NPs and MPs treatments. The negative results in both genotoxicity and mutagenicity may be due to the sensitivity of the assay. ZnO NPs and MPs may have formed agglomeration that increased their particles sizes and prevented them from penetrating the bacterial cell wall because of its rigidity and permeability.

Demir *et al*. (2014) evaluated the genotoxicity of ZnO NPs [(≤ 35 nm and 50 – 80 nm) and ZnO MPs at 10, 100 and 1000 µg/mL] in human embryonic kidney (HEK293) cells and mouse embryonic fibroblast (NIH3T3) cells using the micronucleus, soft-agar colony and comet assays (with or without Fpg and EndoIII). Results showed that ZnO NPs induced a significant concentration-dependent increase in the frequency of MN in binucleated cells at 100 and 1000 µg/mL in both cell lines while no significant induction of MN by the ZnO MPs was observed. Similarly, there was a significant concentration-dependent increase in the induction of percentage tail DNA damage at 100 and 1000 µg/mL in both cell lines. However, no genotoxic effect was observed in cells treated with ZnO MPs. In addition, a significant concentration-dependent increase in the frequency of oxidative DNA damage at 100 and 1000 µg/mL in both cells with Fpg (purines) and EndoIII (pyrimidines) lesions were observed respectively. The net oxidative damage for both Fpg and EndoIII showed no significant difference, indicating that oxidative damage of DNA was not one of the major mechanisms of ZnO NPs. The soft-agar colony assay, a technique that determines the potential ability of a chemical to induce carcinogenesis through cell transformation showed that ZnO NPs induced a significant dose-dependent anchorage-independent growth in both cell lines at 100 and 1000 µg/mL while ZnO MPs did not.

Ghosh *et al*. (2016) reported the genotoxicity of ZnO NPs (85 nm; 0.2, 0.4 and 0.8 mg/L) on *Vicia faba* (chromosome aberration and MN assays) and *Nicotiana tabacum* roots and

leaves (comet assay). Results showed a significant decrease in mitotic index and increase in percentage chromosome aberrations and MN at all concentrations. The comet assay revealed a significant increase in percentage tail DNA damage in both roots and leaves of *N. tabacum*. However, DNA damage was higher in the roots than the shoots due to direct exposure to ZnO NP suspension. ZnO NP-induced genotoxicity in *Vicia faba* and *N. tabacum* may have been due to the free radicals directly interacting with the DNA or DNA proteins involved in cell division in the plant system. *Fagopyrum esculentum* (buckwheat) was treated with ZnO NPs (< 50 nm; 2000 and 4000 mg/L) and genotoxicity evaluated using random amplified polymorphic DNA (RAPD) assay with only four primers (OPA04, OPA08, OPB04 and OPB10). Results showed significant band changes at both concentrations. Changes in the genetic pattern induced by ZnO NPs resulted in genomic instability which may be due to large deletions or mutations (Lee *et al*., 2013).

ix. Systemic toxicity of zinc oxide nanoparticles

Esmaeillou *et al*. (2013) reported that mice treated orally to ZnO NPs (333 $mgkg^{-1}$) for 5 days exhibited a significant increase in LDH indicative of cell damage, increase in the activities of ALT and AST indicative of hepatocellular injury and a decrease in HDL level. It was concluded that within a period of 5 days, that ZnO NPs are able to induce an imbalance in lipid metabolism. Pasupuleti *et al*. (2012a) also reported altered ALT, AST, PLT, HCT, Ca^{2+} and MCV in rats treated with ZnO NPs (5.0 $mgkg^{-1}$) via oral gavage for 14 days compared with ZnO MPs. Li *et al*. (2012) reported that ZnO NPs (2.5 g/kg) intraperitoneally administered to mice were absorbed within 30 minutes after dosing into circulation and accumulated therein in the liver, spleen and kidney. Intraperitoneally administered ZnO NPs were present in the serum for 72 hours and spread to the heart, lung and testes while orally treated ZnO NPs exhibited higher absorptivity and tissue biodistribution compared with ZnO MPs. It was concluded that liver toxicity induced by ZnO NPs was as a result of its absorption, biodistribution and clearance.

Baek *et al*. (2012) reported an increase in Zn concentration after 24 hours of administration in a dose-dependent manner in rats orally treated ZnO NPs (20 nm and 70 nm). The liver, lung and kidney bioaccumulated ZnO NPs after 72 hours with majority of the NPs eliminated in the feaces. Najafzadeh *et al*. (2013) reported a significant decrease

in ALP and creatinine concentration in lamb treated with ZnO NPs for 25 days. Histopathological examination revealed cell swelling, multifocal interstitial nephritis and eosinophilic necrosis of the hepatocytes. Also, Wang *et al*. (2008a) treated mice orally to ZnO NPs (20 and 120 nm) to investigate their toxicological impact. The ZnO NPs accumulated in the liver, heart, spleen, pancreas and bone. There was a little difference in the biochemical and pathological effects between 20 nm and 120 nm ZnO NPs. Mice treated with ZnO NPs (120 nm) had histopathological lesions in the heart, spleen, gastric and liver in a dose-dependent way while mice treated with 20 nm ZnO NPs had less pathological damage in the spleen, pancreas and liver in a dose-dependent manner. Shrivastava *et al*. (2014a), reported increased ROS levels which altered the antioxidant enzyme activities, induced oxidative stress in the erythrocytes, liver and brain of male mice treated with TiO_2, ZnO and Al_2O_3 NPs (500 $mgkg^{-1}$) for 21 consecutive days. In addition, TiO_2, ZnO and Al_2O_3 NPs induced neurotoxicity in the brain through the increase in dopamine and norepinephrine levels in the cerebral cortex.

Amara *et al*. (2014) reported the accumulation of ZnO NPs and/or $ZnCl_2$ solution in the liver and kidney when treated with Wistar rats intraperitoneally for 10 days. AST activity and uric acid concentration increased with a decrease in creatinine. It was concluded by the authors that the possible toxic effect of ZnO NPs and $ZnCl_2$ injected solution may be due to the release of Zn^{2+} ion and accumulation in the target organs. Umrani and Paknikar (2014) treated streptozotocin-induced Type 1 and 2 diabetic rats to ZnO NPs (1, 10 and 30 $mgkg^{-1}$) via oral exposure to demonstrate the antidiabetic activity of ZnO NPs. Glucose tolerance, higher serum insulin (70 %), reduced blood glucose (29 %), nonesterified fatty acids (40 %) and reduced triglycerides (48 %) were reduced by ZnO NPs. The liver, adipose tissue and pancreas had elevated levels of zinc levels indicating ZnO NPs absorption. Pasupuleti *et al*. (2012a) treated rats orally to ZnO NPs (20 nm) and ZnO MPs. ALT and AST activities were significantly increased in a dose-dependent manner compared with those treated with ZnO MPs. In addition to these, histopathological alterations were observed in the liver, pancreas, heart and stomach of rats treated with lower doses of ZnO NPs compared withthose treated with ZnO MPs.

x. Carcinogenicity of zinc oxide nanoparticles

Information is limited on the carcinogenicity of ZnO NPs. The tumour promoting activity of nanoZnO was investigated by Xu *et al*. (2014). Human c-Ha-ras proto-oncogene transgenic (Hras) rats were orally treated with drinking water containing 0.2 % N-nitrobis (2-hydroxypropyl) amine (DHPN) for 2 weeks and then treated with 0.5 mL of 250 or 500 µg/mL nanoZnO particles. Using the initiating promoting protocol, DHPN-induced lung carcinogenesis was not promoted by nanoZnO particles, a dose dependent induction of epithelial hyperplasia of terminal bronchioles was observed.

xi. Reproductive toxicity of zinc oxide nanoparticles

Jo *et al*. (2013) reported reduction in numbers and body weights of born/live pups, increased foetal reasorptions and biodistribution of ZnO NPs in the tissues of dams, liver and kidney of the pups when rats were treated with ZnO NPs (< 100 nm; 500 $mgkg^{-1}$) 2 weeks before mating at postnatal day 4. In another study, the spontaneous delivery, pregnancy rates, birth numbers, survival rates and neurology development in pregnant rats and their offsprings in rats treated with ZnO NPs were investigated by Zhang *et al*. (2008). It was observed that neurology and spatial memory of the offsprings were affected, pregnancy rates were lower and birth numbers were insignificant. Pregnant dams and embryo foetal development was investigated after Sprague Dawley rats were treated with positively charged ZnO NPs (20 nm; 0, 100, 200 and 400 $mgkg^{-1}$) over a gestational period of 5 – 19 days. There was a significant reduction in the body and liver weights, with increase in adrenal gland weight in the dams at 400 $mgkg^{-1}$ as well as reduced food intake at 200 and 400 $mgkg^{-1}$. The number of implantation sites, dead foetuses, resorptions, placenta weight and litter size showed no treatment-related difference. In contrast, foetal weights were significantly decreased after 400 $mgkg^{-1}$ administration but the foetal tissues had no significant difference in the Zn content (Hong *et al*., 2014).

2.4 Effects of physicochemical properties on titanium dioxide and zinc oxide nanoparticle-induced genotoxicity

Many conflicting results on the genotoxicity of titanium dioxide and zinc oxide nanoparticles are been published despite the fact that a large number of the genotoxicity studies of NPs are increasing. Several studies lack the detailed characterisation of NPs in the testing media in spite of the fact that different media and treatment conditions alter the properties of NPs, resulting in the difficulty of comparing results (Stone *et al*., 2009; Som *et al*., 2010; Dusinska *et al*., 2011). In order to assess the toxic effects of NPs, many different NPs characteristics are taken into consideration (Figure 2.9). Many adverse health effects are attributed to the physiochemical properties of NPs which are a strong link to their biological activity (VegaVilla *et al*., 2008). The most important role exhibited by the physicochemical properties of NPs is still not known. However, it is believed that these properties including chemical composition, size, shape, crystal structure, surface area, solubility, surface chemistry, purity of the NPs and aggregation status in the medium are important in determining the adverse effects of NPs in the biological system (Hansen *et al*., 2007; Stone *et al*., 2010).

2.4.1 Size and surface area

NPs exhibit a small size and large surface area to mass ratio compared with their bulk counterparts. As the particle size decreases, the number of atoms exponentially increases (Magdolenova *et al*., 2014), thus, making them significantly reactive in biological systems. Larger particles of the same chemical composition have a lower surface energy and are less toxic in contrast to their NPs (Chan, 2006). NPs are able to disperse throughout the body, penetrate in the blood brain- and testis-barriers, capable of penetrating individual cells and interacting with biomolecules on the surface of the cells as well as within (McNeil, 2005; Chan, 2006).

The possibility of size dependent genotoxicity has been tested by different sizes of NPs (Barnes *et al*., 2008). The effect of different sizes of TiO_2 particles (anatase-10 nm, 20 nm, 200 nm, > 200 nm and rutile- 200 nm) on the induction of DNA damage was investigated by Gurr *et al*. (2005). TiO_2 NPs (10 nm and 20 nm) induced a higher potency of oxidative

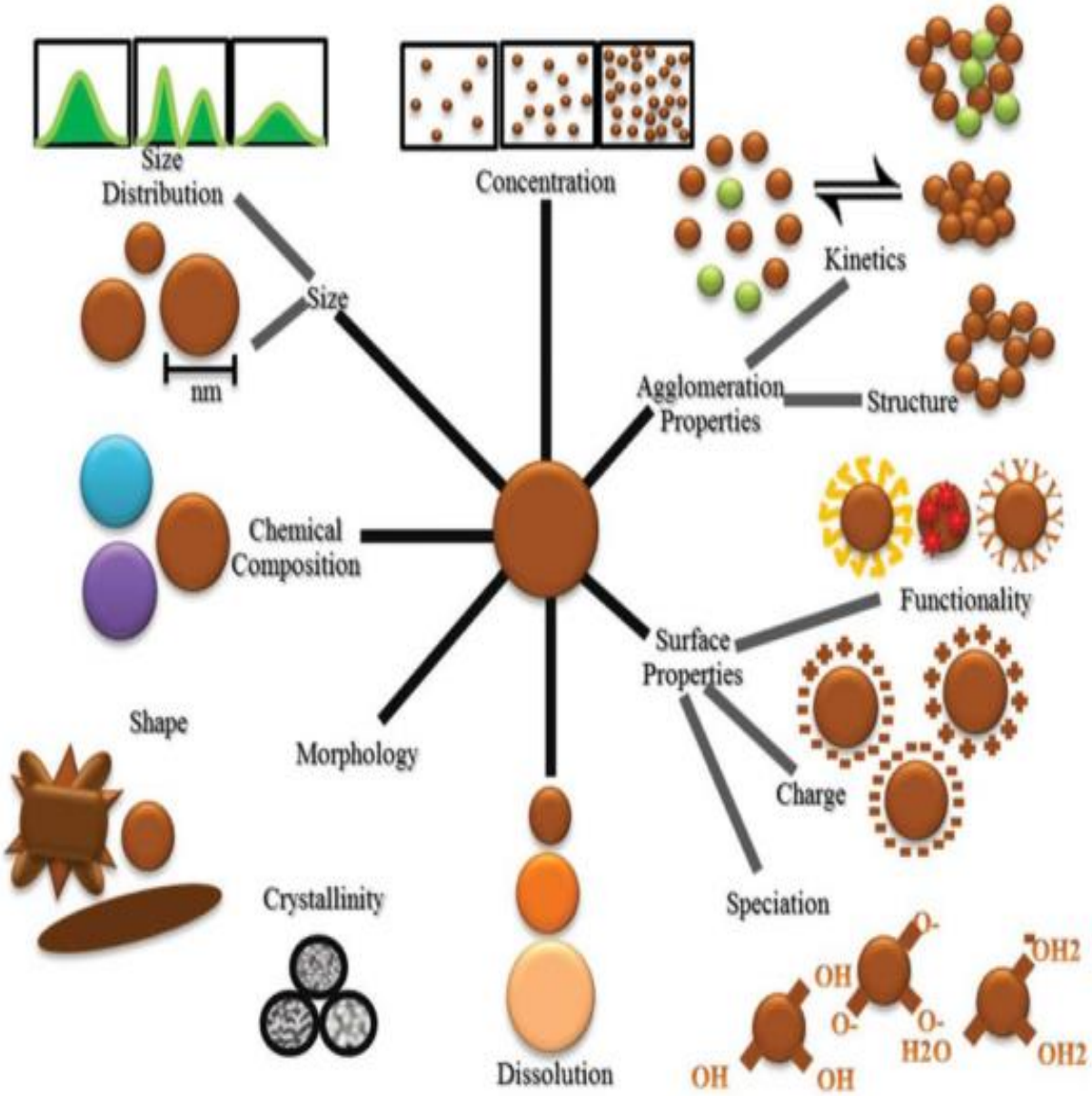

Figure 2. 9: Effects of physiochemical properties on nanoparticles induced genotoxicity. Source: Koedrith *et al*. (2014).

stress in the absence of photoactivation compared with 200 nm and > 200 nm sized TiO_2 particles. Different kinetic particles of substances are produced by different particle sizes, which enhance or reduce toxicokinetics (uptake, distribution, metabolism and elimination) (Nohynek *et al*., 2008). It is important to know that the physicochemical properties of NPs change with decrease in particle size vis-à-vis their hardness, magnetic characteristics, chemical reactivity, electrical conductivity, and biological activity (Karlsson *et al*., 2008).

The surface area of nanoparticles is directly related to their size, with larger surface area to smaller NP sizes. The number of free radicals and transient metal area increases, thus, enhancing the possible interaction of NPs with the cells. A direct association between the surface area of NPs and ROS formation was observed by Li *et al*. (2011). There was a size- dependent induction of DNA damage and ROS formation thus, making the surface area an important factor.

2.4.2 Surface properties

Surface chemistry and charge as well as other surface properties are significant factors that determine the genotoxicity of NPs. Binding of molecular, chemical and biological entities to NPs occur as a result of surface modifications (McNeil, 2005). A study carried out by Landsiedel *et al*. (2010) showed no induction of genotoxicity in lung cells of rats treated via inhalation to triethoxycaprylylsilane-coated ZnO NPs (30-200 nm). Different behaviour of NPs in solutions occurs as a result of the different surface chemistry they exhibit. Coated NPs disperse readily in surrounding medium as compared with uncoated NPs that agglomerate. Dissolution or aggregation of NPs in a medium is determined by the surface charge, which can also affect the biocompatibility and influence the penetration into biological barriers (McNeil, 2005). Studies have confirmed that the cytotoxicity and genotoxicity of NPs are influenced by the surface modifications. The surrounding medium often alters the characteristics of NPs. Adsorption of biomolecules such as polysaccharides, proteins and lipids often modify the surface of NPs in the biological environment, thereby forming a 'biomolecular corona' with the NPs surface, which is relatively stable (Monopoli *et al*., 2011). Thus, different results may occur when the same NPs are dispersed in different experimental conditions.

2.4.3 Coatings

Dispersion of NPs in aquatic media or biological compatibility or NP embedding into inert matrices is accomplished by the addition of surface coatings to NPs. However, negative implications on their biological effects have been reported. Yoshida *et al*. (2009a) reported the negative toxicity of tetramethylammonium hydroxide-coated ZnO NPs on *Salmonella typhimurium* strains TA98, TA100, TA1535 and TA1537 and *E. coli* strain WP2uvrA (-) with and without S9 metabolic activation. Another study by Singh *et al*. (2007) demonstrated that TiO_2 NPs modified on the surface by methylation had no inflammatory effects on the lung epithelial cells, but the surface area of TiO_2 NPs induced a dose dependent toxicity.

2.4.4 Agglomeration

An important feature that influences the behaviour and impact of NPs on genotoxicity is the agglomeration. Agglomerated NPs cannot penetrate into the mitochondria and nucleus unlike unagglomerated NPs that are distributed within the cell (Dhawan *et al*., 2009). Shukla *et al*. (2011) demonstrated that human skin epidermal cells internalised small sized TiO_2 NPs (30 – 100 nm) in the cytoplasm, vesicles and nucleus, compared with the larger sized particles (> 500 nm) that remained outside the cells. The surface charge (hydrophilic or hydrophobic) and interactions with the medium such as medium pH, salinity and protein content determine the dissolution or agglomeration of NPs. The cytotoxicity and genotoxicity of NPs are highly dependent on their agglomeration, as dispersion or agglomeration state brings about different outcomes of NPs (Magdolenova *et al*., 2012).

2.4.5 Solubility

The increase or decrease in the bioavailability of NPs in the biological system is highly dependent on their solubility; it is a key factor in the assessment of NPs. Their structure or presence of reactive groups in their surfaces determine their solubility. Soluble forms of NPs such as ZnO and FeO produce ions that are toxic with greater cytotoxicity compared with the insoluble forms such as CeO and TiO_2 (Franklin *et al*., 2007; Zhang *et al*., 2012).

2.4.6 Photochemistry

The toxicity of NPs can be influenced by UV radiation. ROS are generated in aqueous media when TiO_2 and ZnO NPs are treated with UV light due to their photocatalytic activities. TiO_2 and ZnO NPs illuminated by sunlight inhibited the growth of *Bacillus subtilis* and *E. coli* in the culture media. Adams *et al*. (2006) reported cell structure damage as seen in human skin fibroblasts cells treated in the presence of UV radiation as compared with those kept in the dark. UV radiation and TiO_2 concentration in the exposure of medium induced significant amount of the hydroxylation of guanine bases in calf thymus DNA. Vevers and Jha (2008) reported a significant increase in the toxicity and DNA strand breaks in rainbow trout gonadal tissue cells treated with UVA radiation in combination with TiO_2 NPs as compared with the cells treated with TiO_2 NPs only.

2.5 Conditions influencing the genotoxicity of titanium dioxide and zinc oxide nanoparticles

2.5.1 Preparation of nanoparticles

Solvents used in dispersing or dissolving NPs can influence their genotoxic effects and properties. Toxicity of NPs or their biological responses can be influenced by factors such as pH, salinity, temperature, water hardness and presence of dissolved or natural organic particles (Handy *et al*., 2008a; Vevers and Jha, 2008). Therefore, different solvents such as culture medium, water, phosphate buffered saline (PBS) and normal saline may influence NPs behaviour differently, as these can affect their uptake, cellular penetration and toxic response.

The effects of different solvents such as tissue culture medium, PBS or water on well characterised TiO_2 NPs were examined by Ververs and Jha (2008). In the medium, biomolecules such as protein surround NPs, forming a 'protein corona', which could influence the genotoxicity potential of the NPs (Gonzalez *et al*., 2010). Often times, agglomeration is prevented through the addition of proteins such as FBS or BSA to stabilise the NPs. The formation of a 'protein corona' may help disperse the NPs better in the medium. Another important factor that can contribute to agglomeration reduction is

sonication. Magdolenova *et al*. (2012) reported that sonication of TiO_2 NPs suspension may trigger ROS generation through the oxidation of Ti surface atoms.

2.5.2 Concentration of nanoparticles

An essential aspect that affects the cytotoxicity and genotoxicity potential of NPs is their concentration (Magdolenova *et al*., 2014). The exposure of NPs to humans should mimic the concentrations that are utilised in *in vitro* experiments. Due to the particle's small size and quantity present in consumer products, it is quite technically challenging to determine the quantification of NPs in the air, water and soil. Van der Waal's forces are weak hydrogen bonds that are present in NPs, which initiates agglomeration when they are in their dry form or in suspension. Furthermore, agglomeration occurs when the concentration of NPs exceeds a certain limit, thereby affecting the bioavailability of the NPs into the cell leading to false negative and false positive results.

2.5.3 Physical and chemical agents

The presence of chemical (polycyclic aromatic hydrocarbons) or physical (UV irradiation) agents can alter the toxicological responses of NPs (Vevers and Jha, 2008). Studies reported that ZnO or C60 NPs in the presence of irradiation were able to generate ROS (Shinohara *et al*., 2009; Hackenberg *et al*., 2011). The genotoxic effects of TiO_2 and ZnO NPs under visible light and UV irradiation inducing phototoxicity have been investigated (Guo *et al*., 2008; Ma *et al*., 2014).

2.5.4 Cell type

The type of cell utilised can affect the genotoxicity of NPs (Dusinska *et al*., 2012). Metabolic activities in cell types such as epithelial, connective, neural and macrophages vary differently (Ververs and Jha, 2008). The variation in cell surface receptors, antioxidants, DNA repair capabilities, metabolic pathways, and presence of different enzymes/hormones may induce cell lines of the same or different tissue origin to be more or less susceptible to NP exposure. With a particular cell type, the behaviour, fate and interaction of NPs may be affected by these aforementioned factors. In addition, different

cell lines may interact with NPs separately due to their varying forms of phagocytosis, cytoplasmic inclusion properties and internalisation.

2.5.5 Bioavailability and uptake of nanoparticles

One of the major factors that provide information on the adverse effects on the cellular system is the uptake and availability of NPs to cells and tissues. The interaction of NPs with the surrounding medium, behaviour and bioavailability determines the fate of NPs. Electrostatic, hydrogen bonding and hydrophobic interactions enable the adsorption of proteins on NPs surface, which ultimately affects the dispersity, uptake and bioavailability of NPs (Kumar *et al*., 2011).

The physicochemical properties such as size, surface charge, surface area and reactivity are usually altered when NPs agglomerate or aggregate. Besides protein, factors such as salt ions, hydrophobic surfactant and polar groups on the NPs surface can also influence aggregation. Understanding the behaviour and toxicity of NPs is an important step through the detection of internalised NPs. The transmission electron microscopy (TEM), scanning electron microscopy (SEM), confocal and fluorescence microscopy, reflection-based imaging and flow cytometry are the commonly used methods for assessing the uptake of NPs in cells (Shukla *et al*., 2011; Shukla *et al*., 2013; Sharma *et al*., 2012b).

2.6 Mechanisms of titanium dioxide and zinc oxide nanoparticle-induced genotoxicity

The interaction of NPs with the genetic material (direct) or NP-induced ROS damage and release of metal ions from soluble NPs (indirect) may induce genotoxicity (Barnes *et al*., 2008). Secondary genotoxicity can be as a result of NP-elicited inflammatory responses by phagocytes (neutrophils and macrophages) that produce ROS to attack DNA (Stone *et al*., 2009). Direct interaction with the DNA can occur when NPs cross the cell membrane and diffuse across the nuclear membrane to reach the nucleus or via the nuclear pore complexes. Di Virgilio *et al*. (2010) observed that large aggregates of TiO_2 NPs deformed the nucleus as revealed by TEM in the Chinese Hamster Ovary cells (CHOK1). Cellular vesicles were formed due to the aggregated TiO_2 NPs that affected the shape of the

nucleus. Mitotic process, segregation of chromosomes and normal functioning of the mitotic spindle and its components may unfavorably be affected when the nuclear shape is deformed.

Depending on the phase of the cell cycle, NPs may interact directly with the DNA organised in chromatin or chromosomes, once they penetrate the nuclear pore to gain access to the nucleus or during the mitotic process (Magdolenova *et al*., 2014). DNA replication and transcription of DNA to RNA can be influenced when NPs interact to bind with DNA molecules during the interphase. Chemical binding to DNA molecules can be affected when NPs mechanically disturb the mitotic process, inducing aneugenic or clastogenic effect. Likewise, mitotic spindle apparatus, centrioles or their associated proteins can interact indirectly with NPs to induce an aneugenic effect. Loss or gain of chromosomes in the daughter cells is an implication of the NPs interference with the mitotic apparatus. Huang *et al*. (2009) reported abnormal multipolar spindle formation, chromosomal alignment and segregation during anaphase and telophase at long term exposure to TiO_2 NPs. The function of protein kinases such as regulation of cell cycle events - DNA replication and cell division can be compromised when NPs interact. The mitotic checkpoint PLK1 protein responsible for cytokinesis and contractile ring formation was deregulated by TiO_2 NPs (Huang *et al.*, 2009). Aneuploidy or micronucleated cells can also occur through cytokinesis disturbance. Huang *et al*. (2009) reported ROS production, increased micronucleueated cells and ERK signaling activation in cells treated with TiO_2 NPs.

Reactive oxygen species arising from the surface of NPs can also be another contributing factor to indirect genotoxicity. Oxidative DNA damage can be induced through NP generated ROS in cells. Free radicals were generated by SiO_2, ZnO and TiO_2 NPs in aqueous suspensions (Sharma *et al*., 2009; Barillet *et al*., 2010; Shukla *et al*., 2011). Potential consequences may occur when free radicals interact with cellular biomolecules such as DNA, protein and lipids. DNA strand breaks (single and double) and purine and pyrimidine-derived oxidised base lesions may occur when ROS attacks the DNA. Mispairing in DNA replication resulting in mutation is a major consequence of DNA base lesions which can initiate the process of carcinogenesis (Cooke *et al*., 2003). ROS and

oxidative stress led to oxidative DNA damage and micronucleus formation in human skin cells treated with TiO_2 NPs (Shukla *et al*., 2011, 2013). In addition, DNA damage can be induced through toxic ions released from soluble NPs. Fenton-type reaction can produce intracellular ROS through the release of certain transition metal ions such as $Fe^{2+,}$ Ag^{+}, Cu^{+}, Mn^{2+}, Cr^{5+} and Ni^{2+} from NPs (Kruszewski *et al*., 2011).

Cellular organelles like the mitochondria and inflammatory cells (macrophages and neutrophils) can be damaged by affecting their functions when NPs interfere with them. ROS are generated by mitochnodria and neutrophils in response to stress. Kocbek *et al*. (2010) reported decreased mitochondrial activity, loss of cell morphology and disturbances in cell cycle in keratinocytes treated with ZnO NPs. TEM analysis revealed that early and late endosomes and amphisomes contained ZnO NPs. Trouiller *et al*. (2009) reported oxidative DNA damage and inflammatory responses in mice treated with TiO_2 NPs. A possible explanation for the genotoxicity observed may be due to the activation of the phagocytes. Accumulation of ROS and inhibition of antioxidants can potentially lead to DNA damage (Barillet *et al*., 2010). Reduced glutathione, increased lipid peroxidation and reduced antioxidant enzymes such as glutathione reductase and superoxide dismutase were induced by TiO_2 NPs *in vitro* (Shukla *et al*., 2011). In addition, Sharma *et al*. (2011) reported ROS generation and glutathione and superoxide dismutase depletion in ZnO NP-induced cytotoxicity and genotoxicity *in vitro*.

2.7 Review of methods

2.7.1 Characterisation of nanoparticles using the transmission electron microscopy

The biological behaviour of NPs is determined by the surface interaction between them and biological substances; essential factors such as the particle size, size distribution and shape must be studied for possible toxicological explanations (Kwon *et al*., 2014b). Furthermore, it is known that a major reason for NP's toxicity is their large surface area resulting from their small size (Baek *et al*., 2012). Thus, before toxicological evaluations, it is highly recommended to analyse the particle size, shape and size distribution. Generally, OECD WPMN's guidelines suggest the analysis of NPs using the scanning

electron microscopy (SEM), transmission electron microscopy (TEM) and X-ray diffraction (XRD), which is also supported by material scientists (Zhong *et al*., 2012).

The transmission electron microscopy is a type of electron microscope that uses electron beams (at a high resolution) focused on the sample to provide structural and chemical images of the sample (Smith, 2015; Su, 2017). These images are produced when the electrons interact with the atoms in the material (Kwon *et al*., 2014b). Several studies have utilised TEM to evaluate the particle morphology and size (Xu *et al*., 2008; Baek *et al*., 2012; Kim *et al*., 2012). The TEM and SEM are found to be the most recommended tools in evaluating the particle size and shape, since they have direct accessibility to the NPs (Kwon *et al*., 2014b).

2.7.2 The Micronucleus assay

In the 19th century, Howell and Jolly recognised the micronucleus (MN) as a small inclusion in the blood of cats and rats as well as the peripheral blood of aneamic patients. Afterwards, the MN was referred to as the Howell-Jolly body (Hayashi, 2016). In 1970, a test method was developed by Boller and Schmid, (1970) to assess the frequency of MN induction in erythrocytes during haematopoiesis by using the peripheral blood cells and bone marrow tissue of Chinese Hamster treated with trenimon, an alkylating agent. Till the mid 1970's, researchers had successfully explained the basis of the MN assay (Heddle, 1973; Schmid, 1975). In 1976, the human cultured lymphocyte was tested using the MN assay by Countryman and Heddle, (1976). However, Fenech and Morley, (1985) modified the protocol by introducing cytochalasin B.

In 1980, MN was detected in the mouse peripheral erythrocytes by MacGregor *et al*. (1980). The peripheral blood of rats and humans do not contain the MN because the spleen rapidly and effectively removes the MN from the blood. Conversely, the MN is present in the peripheral blood of mice. The acute effect of any chemical can be evaluated using the MN assay in the bone marrow while the chronic effect can be evaluated in the peripheral blood erythrocytes because the MN are still present in the mature cells up to their life span (Hayashi, 2016). In 1983, the fluorescent dyes: acridine orange and hoechst 332568 were introduced by Hayashi *et al*. (1983) and MacGregor *et al*. (1983)

respectively in identifying the MN. These contributed to the accuracy of the results of micronucleated erythrocytes over time.

Some International Organisations such as the Organisation for Economic Cooperation and Development (OECD) and the Collaborative Study Group for the Micronucleus Test (CSGMT) in the 1980s developed test guidelines for assessing the probable genotoxic effects of chemicals of which the MN assay has gained a wide recognition. Since 1984 till now, the CSGMT, which is a representative of the Environmental Mutagen Society, has evaluated and reported several factors that can influence the test results. Such studies include sex-related difference (the Collaborative Study Group, 1986), difference between intraperitonal and oral exposures (Hayashi *et al*., 1989), aging of mice (Morita *et al*., 1997), using the rat peripheral blood (Wakata *et al*., 1998) and targets to other erythropoietic tissues (Suzuki *et al*., 2005 and Hamada *et al*., 2015). These trials have contributed valuably to the standardisation of the test protocol and guidelines.

The micronuclues test is one of the numerous *in vivo* genotoxicity tests utilised in assessing the risk of cancer. Other tests such as the alkaline comet assay, gamma-H2AX, chromosome aberration assay, and bacterial reverse test are used in evaluating the consequence of cancer (Kang *et al*., 2013). A number of chromosomal aberrations are present in cancer tissues (Keen-Kim *et al*., 2008) and accumulations of genetic damage as well as genome instability are crucial steps in the initiation of cancer (Stratton *et al*., 2009). Genotoxic agents or carcinogens may exert their properties through abnormal cell growth, altered gene expression, and destruction of normal cell functioning (Pratheepa *et al*., 2008). Therefore, with the aim of assessing the risk of cancer, the genetic damage is evaluated using the *in vivo* MN assay.

Recently, several studies have shown that increased frequency of MN is an indication of cancer risk, thus it is an immediate biomarker for detecting the process of carcinogenesis (Bonassi *et al*., 2006; Murgia *et al*., 2008). The continual survival of a cell with modified DNA and abnormal genome might lead to latent cancer cells or give rise to cancer (Weisburger and Williams, 1981). Several studies have shown strong positive correlation between MN frequency and cancer development (Duffaud *et al*., 1999; Iarmarcovai *et al*.,

2008), thus suggesting that increased frequency of MN is associated to the early process of carcinogenesis (Bonassi *et al*., 2011).

The *in vivo* MN assay has advantage over the *in vitro* assay, as the *in vivo* assay considers the pharmacokinetics of chemicals, which are absolutely absent in the *in vitro* assays (Sasaki *et al*., 2002; Benigni *et al*., 2012). However, the *in vitro* assay provides a preliminary screening on a chemical while the *in vivo* genotoxicity assay provides comprehensive biological and physiological effects of the chemical (Brendler-Schwaab *et al*., 2005). Genotoxic and mutagenic effects of chemicals are detected by the MN assay as they induce DNA fragments bound with small membranes called the MN (Fenech *et al*., 1999; Fenech, 2000; Fenech, 2007). The micronucleus is briefly described as a small structure of between 1/20 and 1/5 of the main nucleus, which are cytoplasmic chromatin-containing bodies from whole chromosome loss and chromatid/chromosome fragments that were not included in the daughter nuclei at anaphase of mitosis (Krishna and Hayashi, 2000).

When undamaged chromosomes move to the spindle poles during anaphase, these chromatid and chromosome fragments may lag behind. In the telophase, the regular daughter nuclei are produced by the normal chromosomes while the lagging chromosomes are incorporated in the daughter cells with a significant portion becoming the secondary nuclei (Figure 2.10). In principle, the MN assay can detect chemicals that are capable of inducing clastogenicity (chromosome and chromatid breakage) and aneugenicity (inhibition of mitotic apparatus) (Savage, 1988).

The micronuclei formation is generally accepted through four major mechanisms: 1) Loss of acentric chromosome fragments and acentric chromatid fragments leading to structural aberrations. 2) Loss of whole chromosomes resulting to numerical aberrations. 3) Lagging chromosomes from chromosomal breakage and exchange, tangled chromosomes or inactive centromere leading to structural aberrations. 4) Apoptosis (Savage, 1988; Mateuca *et al*., 2006; Fenech, 2007; Fenech, 2010). Micronuclei analysis is particularly suitable in the erythrocytes; the nucleus is extruded during the maturation of the erythroblast to the PCE, which makes micronuclei detection easy (Chatterjee *et al*., 2010). The two cell types: the polychromatic erythrocytes (PCE) and the normochromatic

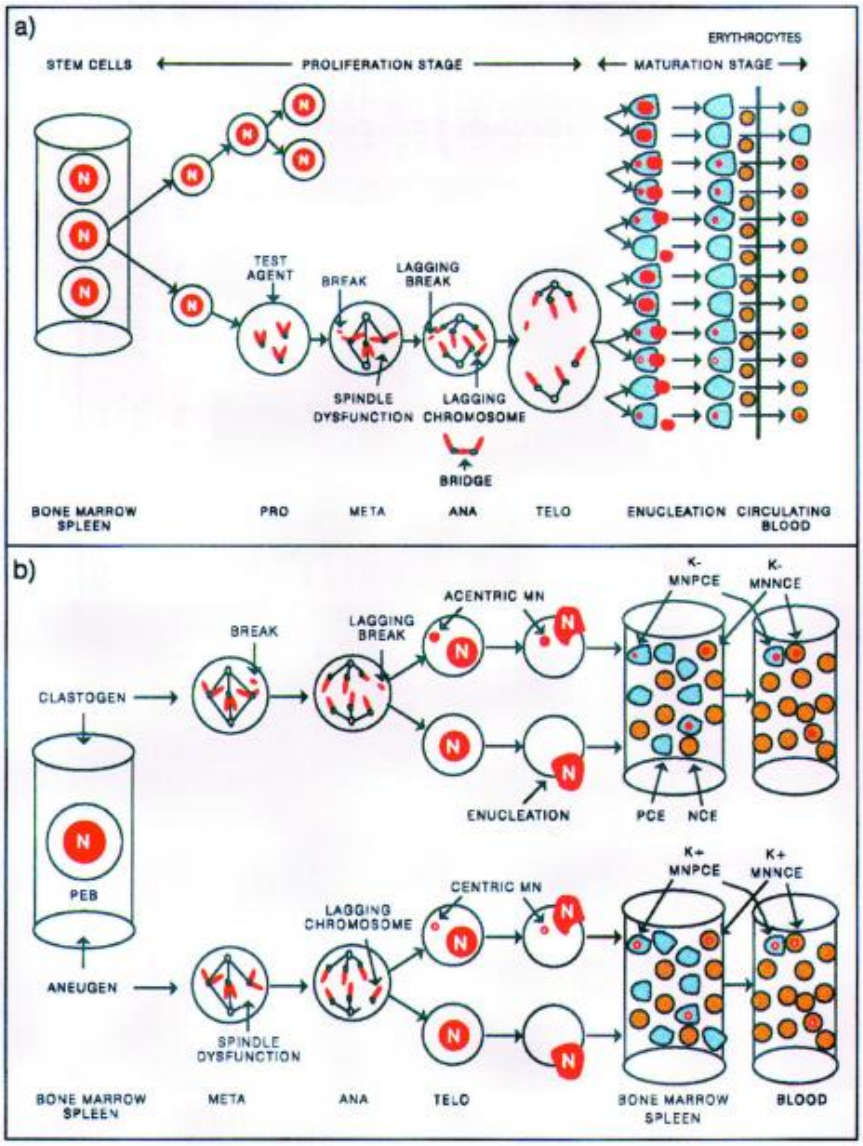

Figure 2. 10: The process of erythropoiesis *in vivo*; (b) the mechanism of micronucleus formation in the polychromatic erythrocytes (PCEs) and normochromatic erythrocytes (NCEs). Also, classification of kinetochore-positive (K+) and kinetochore-negative (K−) erythrocytes. N, nucleus; PEB, proerythroblast; MN, micronucleus

Source: Krishna and Hayashi (2000).

erythrocytes (NCE), which are present in the bone marrow, spleen and blood compartments, stain differently using the giemsa stain. The PCE (larger, immature erythrocyte, basophilic, contains RNA and stains blue purple) are synthesised in the bone marrow (major hematopoietic) tissue, hence, used for the micronucleus assay. The peripheral blood of other species can be used for micronucleated PCE (MNPCE) as evidence has shown the inability of the spleen to remove micronucleated erythrocytes. In addition, the micronulceated NCE (smaller, contain haemoglobin, acidophilic and stains light pink) (MNNCE) can be used as an endpoint when the life span of the erythrocytes does not exceed the period of the treated animals. The principal endpoint of the assay is the frequency of micronucleated erythrocytes. Mutagenicity can be assessed using the *in vivo* micronucleus assay as it considers *in vivo* metabolism, pharmacokinetics and DNA-repair processes, which differ among genetic endpoints, tissues and species.

In the *in vivo* test, the mouse is the preferred rodent as the micronucleated cells induced by clastogens and aneugens, are formed in the bone marrow and detected in the peripheral blood while the micronucleated erythrocytes are selectively eliminated by the spleen of rats, thus, making it a less sensitive test. Intraperitoneal injection or oral gavage is given to test animals. After chemical administration, appropriate time is required for the increase in the number of micronucleated erythrocytes to rise to a significant level through adsorption and metabolism of the chemical, extrusion of the erythroblast nucleus, and completion of the erythroblast cell cycle. The cytotoxicity index is calculated as the ratio of PCE to the total erythrocytes (TE) (Krishna and Hayashi, 2000). Chromosomal aberration is induced when a test chemical increases the frequency of micronucleated PCE; however, molecular cytogenetic techniques such as immunofluorescent CREST-staining or fluorescence in situ hybridisation with pancentromeric DNA probes can be used to distinguish between absence (clastogenic) and presence (aneugenic) of chromosomes.

2.7.3 Sperm morphology assay

Spermatozoa are the end products of the differentiation and maturation process of germ cells, which proliferate and divide meiotically, given rise to specialised haploid cells for reproduction (De Boer *et al*., 2015). The spermatozoon can be distinguished by having three distinctive parts: the head, midpiece and tail (Figure 2.11). The head is oval shaped

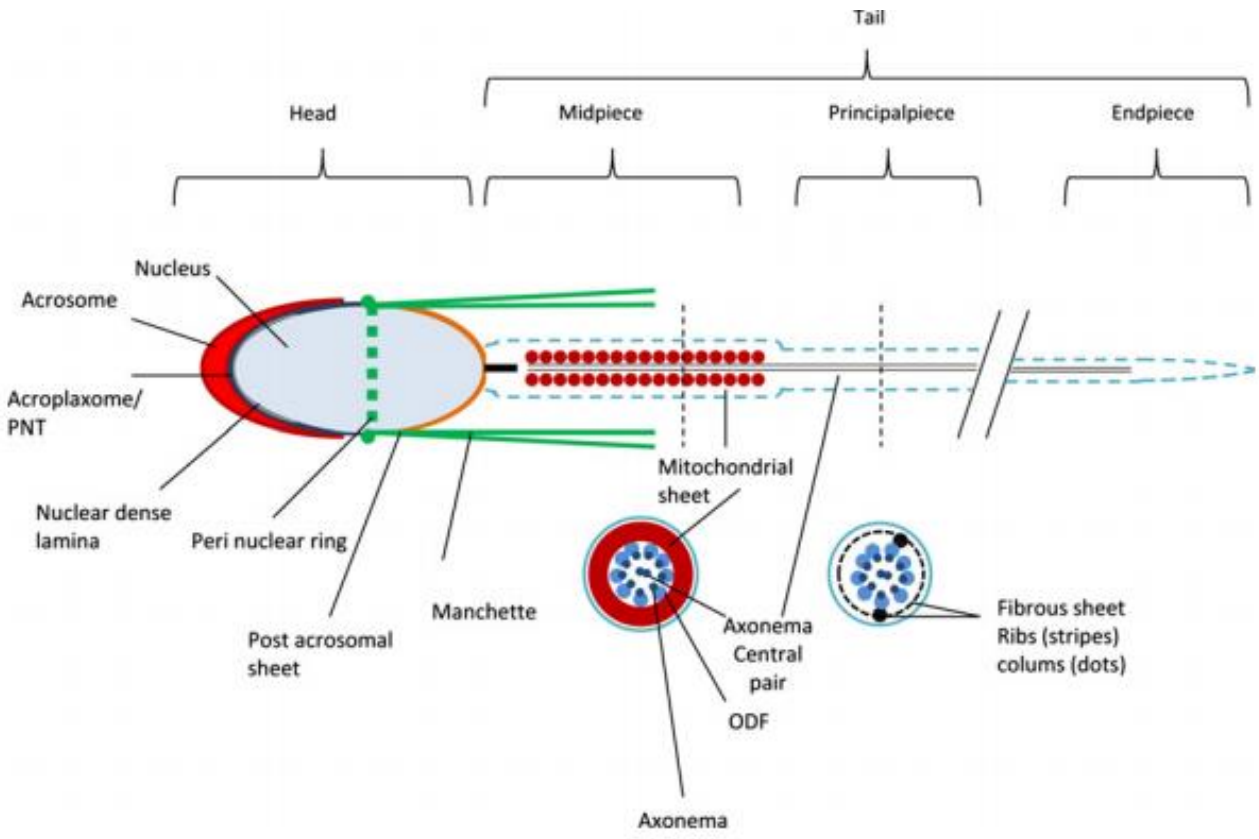

Figure 2. 11: Schematic composition of a late stage elongating spermatid contents. Source: De Boer *et al*. (2015).

with more than one-third of its acrosomal cap covering its surface. The length of the head is between 3 and 5 µm and the width between 2 and 3 µm. The head has a distinct hook, which is essential during its transportation to fertilizing the egg. The hook allows the attachment of the sperm to the walls of the oviductal isthmus (Suarez, 1987; Smith and Yanagimachi, 1990). The midpiece is approximately 7 to 8 µm long and aligned longitudinally to the axis of the head while the tail is at least 45 µm long, uncoiled with a regular outline (Sun *et al*., 2006).

The genetic information that determines the shape and the function of the spermatozoon is located in the head (Beatty, 1970). Therefore, any alterations in the genetic material of the sperm are reflected by changes in its morphology (De Boer *et al*., 2015). Abnormalities of the spermatozoa are categorised as defects in the head, midpiece or tail. Defects in the head include but not limited to amorphous, short hook, no hook, double heads, wrong-angled hook as well as the combination of any of these. Also, midpiece defects include thin or thick midpiece having no mitochondria sheath and any of these combinations while the tail defects include folded and multiple tails and any of these combinations. Numerical and structural chromosome abnormalities are common aberrations that can occur in the genetic material of the spermatozoa (Martin *et al*., 1994). Aneuploidies and polyploidies are the types of numerical abnormalities that arise as a result of a missing or meiotic non-disjunction of extra chromosome(s) while the duplication of chromosomes results in polyploidies. Chromosome breaks, gaps, translocations, inversions, deletions and acentric fragments are examples of structural abnormalities. It has been reported that fertile men have a frequency of 1-2 % of numerical chromosome abnormalities and a frequency of 7-17 % of structural chromosome abnormalities (Martin, 2003).

The mechanism involved in the alterations of the structure of the spermatid at compaction and elongation was explained by Kierszenbaum and Tres (2004). There are four elements involved in the modeling of the sperm head; (i) the stacked F-actin-containing hoops generate contractile forces in the Sertoli cell, connecting to the elongated spermatid nucleus at the apical region, (ii) the molecular characteristics of acrosome formation, (iii) formation of the acroplaxome/PNT from the assemblage of the subacrosomal cytoskeletal

plate and (iv) the relationship between the manchette (a microtubular/actin-containing structure and the acrosome-acroplaxome (Figure 2.11)

One of the most important structures of the sperm head is the manchette (Figure 2.11). The development of the manchette begins in step 8 of the spermatogenic cycle, which degenerates in step 12 and completely disappears in step 16 (Figure 2.12). It originates at the acute side in the perinuclear ring. Asides the function of shaping the nucleus, it is also involved in the transportation of the nuclear effluents (chromatin metabolism) (Kierszenbaum, 2001; 2002b) through the nuclear pores beneath the acrosome (Fawcett and Chemes, 1979). Precursor-protamine 2 (pre-P2) and protamine 1 (Prm1/P1) and transition proteins 1, 2 (Tnp1, 2) largely contribute to the chromatin remodeling, which are supplied to the nucleus. In addition to these functions, the intramanchette transport also traffic tail components (Kierszenbaum *et al*., 2011).

Sperm head morphology abnormalities may occur as a result of deletions in the Y chromosome (Ward and Burgoyne, 2006), azh mutations (Mendoza-Lujambio *et al*., 2002; Ward, 2005), genetic manipulation (Adham *et al*., 2001; Cho *et al*., 2003; Luo *et al*., 2012), and changes in the regulation of the epigenetics of the paternal genome in mice. In addition, environmental toxicants can also increase the changes in the sperm head morphology (Wyrobek and Bruce, 1975). Consequently, the sperm head morphology was developed to screen potential carcinogenic chemicals that have the ability of inducing spermatogenic dysfunction (Wyrobek *et al*., 1983).

The sperm head morphology became a standard test described by WHO for fertility clinics. Thus, normal assessment of spermatozoa is the basis for the morphology guidelines provided by WHO. Previous studies have indicated the correlation between sperm morphology and sperm functions (Liu and Baker, 1990; 1992). The percentage of sperm abnormalities are assessed by visually scoring the smears made from the sperms of the cauda epididymis of chemically treated mice (Wyrobek and Bruce, 1975). In addition, Esterhuzien *et al*. (2000) reported that evaluation of the sperm morphology, particularly the acrosome configuration, provides the necessary information for the 'sperm fertilizing ability'. Furthermore, Menkveld *et al*., (2003) demonstrated the binding of the zona pellucida and sperm cells' viability is highly correlated to the sperm morphology.

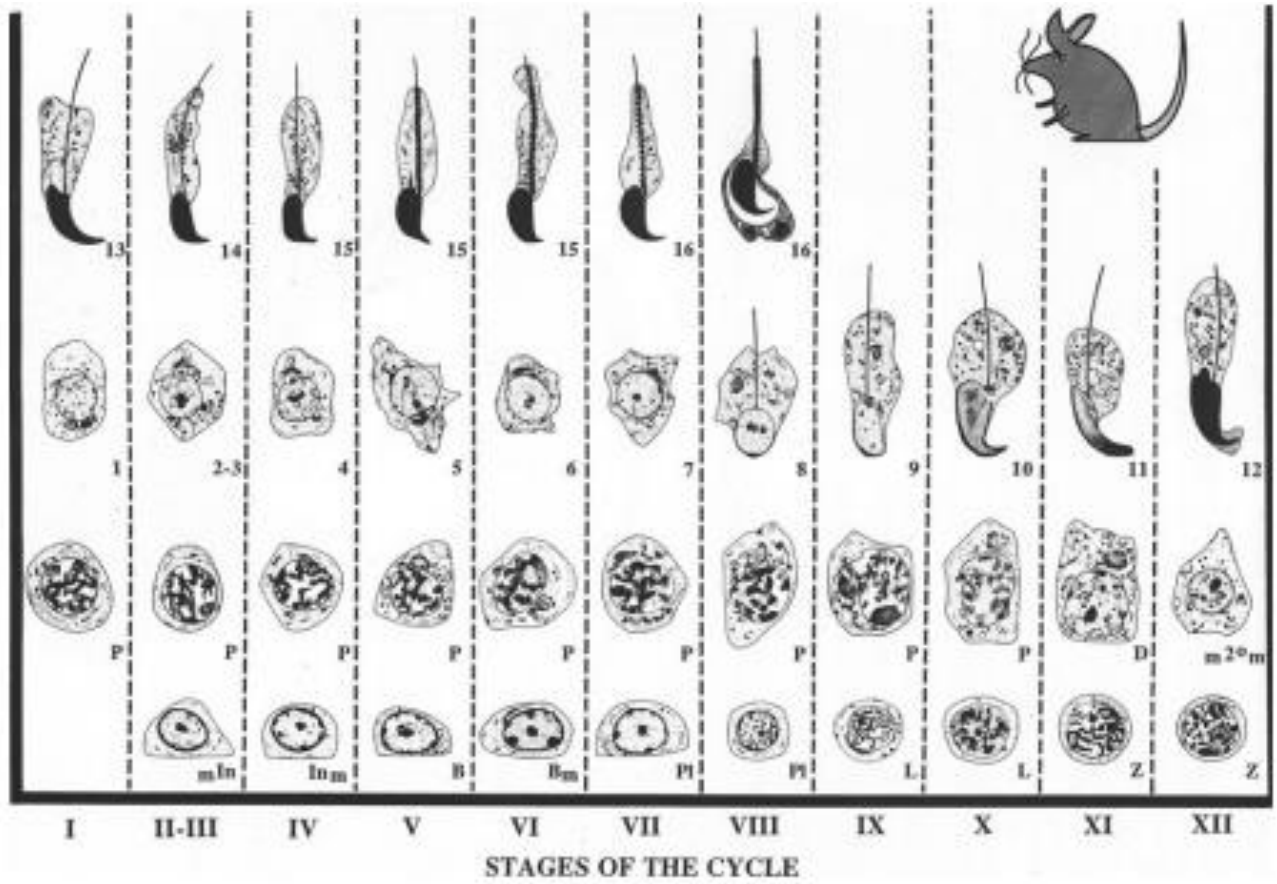

Figure 2. 12: Stages of the cycle of the mouse seminiferous epithelium.

Source: Russel *et al*. (1991).

Over the years, testicular damage and infertility in mammals have been diagnosed using the semen analysis (Amelar, 1966). The quality of the sperm production is measured directly using the sperm test in animals that are chemically treated. The genetic basis of induced sperm abnormalities in treated mice have been over emphasised in several studies that have evaluated the ability of chemicals to induce sperm abnormalities as well as their genetic consequences (Wyrobek and Bruce, 1975; Wyrobek *et al*., 1983; Brinkworth, 2000; Braydich-Stolle *et al*., 2005). Genetic damage of the germ cell is a reflection of some changes in the sperm morphology. Before the pre-meiotic stage of spermatogenesis, only DNA synthesis occurs, therefore no other changes occur in the sperm head, making it extremely stable.

Recently, a lot of focus is on the analysis of DNA damage of the sperm, which is an indicator of sperm quality (Franken and Oehninger, 2012). The single and double DNA strand breaks, oxidation of purines, inter- and intrastrand crosslinkage and DNA-protein cross links are examples of common sperm DNA damage identified (Aitken and de Luliis, 2007; 2010). Several assays such as the comet (Hughes *et al*., 1996), terminal deoxynucleotidyl transferase-mediated dUTP nick end-labelling (TUNEL) (Gorczyca *et al*., 1993), DNA breakage detection-FISH (Fernandez *et al*., 2005), chromatin structure assay (Evenson *et al*., 1991) and chromatin dispersion test (Fernandez *et al*., 2003) are the various tests utilised in identifying and quantifying DNA damage in sperms.

Advantages

1. The assay has the ability of identifying germ cell mutagens.

2. The potential adverse effects of exogenous toxicants on sperm production can easily be assessed by the assay.

3. It is quite simple, inexpensive, and less invasive and relatively rapid compared with other short term *in vivo* assays.

4. It is specific to carcinogenicity

5. Irrespective of the experimental model, exposure dose, route and duration, it has been found adaptable.

Disadvantages

1. False positive responses may be elicited through factors such as alterations in body temperature and infection.

2. No clear understanding on the consequences of mutation - induced sperm-shape abnormalities.

3. Insensitivity of the toxicants may occur due to the different strains of mice used.

2.7.4 Sperm count and motility

Sperm count and motility are vital criteria for the examination of male infertility. Low sperm count, abnormal sperm motility and function are causes that mostly contribute to male infertility worldwide (Jamsai and O'Bryan, 2011). However, evaluation of motility and count assessments has extensively been reviewed by the WHO 2010 manual. The ability of the spermatozoon to deliver correctly its chromosome to the ovum is measured indirectly through seminal analysis. In achieving this, the number, motility and morphology of the spermatozoa must be accurately produced in order for them to go through the cervix, uterus until they bind to the zona pellucida and under go nuclear decondensation (Vasan, 2011). However, defects in any of these complex processes may lead to male infertility.

Determination of sperm count is mostly done using an improved Neubauer haemocytometer. The sperm count is defined as the number of spermatozoa per unit volume (Franken and Oehninger, 2012). A microscopic examination of the freshly collected spermatozoa is reported in millions per millilitre (Vasan, 2011). According to the WHO manual 2010, the normal value of the sperm count is usually greater than 20 million/mL (normozoospermia). Therefore, any value that falls below the reference value is referred to as oligozoospermia while no spermatozoa present in the ejaculate is referred to as azoospermia.

The motility of spermatozoa determines the passage through the cervical mucus (Vasan, 2011). The WHO manual 2010 classified motility into four categories namely: rapidly progressive (class a) (forward speed of at least 25 μms^{-1}), slow progressive (class b) (forward at a speed of less than 25 μms^{-1}), non-progressive (class c) move slowly at a speed less than 5 μms^{-1} and immotile (class d) that do not make any movement at all but appear dead (Sikka and Hellstrom, 2016). Spermatozoa with head and tail are only scored during motility. A normal suspension usually should contain more than 50 % of the sum of the rapidly progressive and slow progressive. However, when the immotile spermatozoa exceed 50 %, sperm vitality test should be carried out (Vasan, 2011).When the sperm concentration and percentage of progressively motile spermatozoa are below the reference limit, it is referred to as oligoasthenozoospermia while the percentage of the progressively motile spermatozoa below the reference limit is referred to as asthenozoospermia.

2.7.5 Male reproductive hormones

The anterior pituitary gland contains the gonadotroph cells which secrete the luteinizing hormone (LH). In males, it is referred as the interstitial cell-stimulating hormone (ICSH) (Louvet *et al*., 1975). The leydig cells in the testis are stimulated by the LH to produce testosterone, and LH also acts synergistically with follicle stimulating hormone (FSH). LH exists as a heterodimer glycoprotein that is not covalently related, with each of the monomeric unit consisting of one alpha and one beta subunit. The beta subunit of LH has 120 amino acids and provides its specific biological action (Jiang *et al*., 2014).

In males, the gonadotropin-releasing hormone (GnRH) regulates LH release in the pituitary gland, which acts on the leydig cells in the testis to produce testosterone. Subsequently, the enzyme 17β-hydroxysteroid dehydrogenase which is regulated also by LH converts androstenedione to testosterone (steroid hormone primarily involved in spermatogenesis) (Guyton and Hall, 2006). The hypothalamus releases GnRH which stimulates the release of LH when the testosterone level is low. Subsequently, as the testosterone level increases, there is a negative feedback mechanism on the hypothalamus and pituitary gland which inhibits GnRH and LH release respectively. Within the menopausal period, high level of LH is expected. Patients with polycystic ovarian

syndrome, testicular failure, premature menopause and Turner syndrome usually have relatively elevated LH levels. Low levels of LH are seen in patients with hypogonadism, hyperprolactinemia and hypothalamic suppression.

The Follicle Stimulating Hormone (FSH) is another glycoprotein polypeptide secreted in the anterior pituitary gland where the gonadotroph cells are located. It is involved in the reproductive process, growth, development and pubertal maturation of the body. It has both alpha and beta subunits. The beta subunit has 111 amino acids which gives its specific biological function (Jiang *et al*., 2012). The germ cells in both male and female are stimulated by FSH. In males, the FSH also stimulates the sertoli cells to secrete androgen-binding proteins (ABPs). The anterior pituitary gland regulates the secretion of ABPs via a negative feedback mechanism.

Primary spermatocytes are stimulated by FSH to undergo first meiotic division to give rise to the secondary spermatocytes. It is also responsible for the formation of connections between the sertoli cells that form the blood-testis barrier. High levels of FSH are expected in the menopausal period, but are abnormal in the reproductive period. Premature ovarian failure (premature menopause), testicular failure, subfertility/infertility and Turner syndrome may lead to high FSH levels. Hypogonadism, polycystic ovarian syndrome, hypothalamic suppression and hyperprolactinemia often occur due to low FSH levels.

Testosterone is the principal hormone in males, which belongs to the androgen family. It is primarily secreted in the testicles of males and in an insignificant amount in females. In males, the major roles of testosterone include: development of the testis and prostate, increase muscle and bone marrow, broadened chest and presence of hair growth (Mooradian *et al*., 1987). The hormone is notably lower in females than in males, which is 7-8 times greater (Torjesen and Sandnes, 2004) and decreases gradually as men age. It is responsible for the normal development of spermatozoa, gene activation in sertoli cells stimulate spermatogonia differentiation, controls physical and cognitive energy and supports muscle tropism. The most significant amount of testosterone is produced in the testes. Testicular dysfunction or hypothalamic pituitary dysfunction can induce low levels of testosterone (hypotestosteronism) while high levels of testotsterone

(hypertestosteronism) may occur as a result of leydig cell hypertrophy or increase in steroid biosynthesis.

2.7.6 Kidney and Liver Function Tests

i. Blood Urea Nitrogen

The maintenance of physiological homeostasis is required by a healthy kidney (Dalton, 2010). Blood Urea Nitrogen (BUN) is one of the most commonly measured parameters to evaluate renal function. Urea is the main end product of the metabolism of nitrogen-containing substances formed in the liver and excreted by the kidneys (Baum *et al*., 1975). Increase or decrease in serum urea nitrogen has their clinical implications in the body system. The rates of synthesis and excretion determine the concentration of urea in body fluids. The protein in fate or tissue breakdown of urea is correlated with the rate of synthesis. Increased protein catabolism increases the urea synthesis, which relatively increases its concentration. Excess ingestion of exogenous protein or tissue protein breakdown in wasting diseases may also increase urea concentrations. The glomerular capillaries filter urea which is excreted into the tubular lumens while the blood urea concentration may increase as a result of decreased filtration. In case of low BUN levels, severe hepatic disease can lower the urea concentration since urea is synthesised in the liver (Gallagher and Seligson, 1962). Patients with severe liver disease (liver cirrhosis) with no protein intake as a result of severe anorexia elicited from liver disease or low-protein diet will markedly have low BUN level (Baum *et al*., 1975). Low BUN levels may also occur as result of urea cycle enzyme deficiencies (Jurado and Mattix, 1998).

ii. Creatinine

Creatinine is primarily a metabolite of the muscle which is excreted by the kidneys (Baum *et al*., 1975). It is also produced from creatine and phosphocreatine metabolism in the skeletal muscle (Traynor *et al*., 2006; Dabla, 2010). Serum creatinine is ideal for measuring acute or chronic kidney disease and glomerular filtration rate (GFR) of the kidney. The serum concentration of creatinine increases as the GFR declines (Dalton, 2010). Unlike the BUN, it has been found to be a more sensitive index. In addition, where

urea undergoes tubular reabsorption, creatinine is not reabsorbed but secreted by the tubules and freely filtered at the glomerulus (Traynor e*t al*., 2006; Dabla, 2010). Reduced levels of serum creatinine may be suggestive of reduced muscle mass, which may lead to the depletion of creatinine production in individuals that have renal diseases. Increased level of serum creatinine is an indication of severe renal damage (Baum *et al*., 1975).

iii. Bilirubin

Bilirubin is formed as a result of the breakdown of haemoglobin that is synthesised in the reticuloendothelial system (Limdi and Hyde, 2003; Gowda *et al*., 2009). It is released as unconjugated bilirubin and transported to the liver. It is not soluble in water and thus cannot be eliminated via the urine. It is secreted into the bile and gut, once it is conjugated to bilirubin glucuronide in the liver (Limdi and Hyde, 2003) by the enzyme UDP-glucuronyltransferase (Gowda *et al*., 2009). Subsequently, it is also broken down by intestinal flora into urobilinogen where some are reabsorbed and eliminated by the liver into the intestinal tract or via the kidney into the urine. The residue is thereafter excreted as stercobilinogen in the stool.

Serum bilirubin occurs in unconjugated form (indirect) and conjugated form (direct). It is mostly in the unconjugated form, which maintains equilibrium between synthesis and hepatobiliary excretion. The normal values of the serum total bilirubin range between 2 and 21 µmol/L (Gowda *et al*., 2009), with direct and indirect bilirubin being 8 µmol/L and 12 µmol/L respectively. Excessive production of bilirubin may be as a result of increased hemolysis (jaundice), muscle injury, erythropoietic dysfunction and haematoma resorption (Limdi and Hyde, 2003). Indirect bilirubin makes more than 85 % of the total bilirubin and occurs when there is an excessive production of bilirubin or hepatic uptake defects or inherited diseases (e.g. Gilbert's syndrome) and this is referred to as unconjugated hyperbilirubinaemia (Gowda *et al*., 2009). Increased levels of conjugated bilirubin may occur in hepatocellular damage or ischemic liver injury (Gowda *et al*., 2009). However, low serum bilirubin may occur as a result of incomplete extrahepatic obstruction due to biliary canaliculi or parenchymal liver diseases (Daniel and Marshal, 2007).

iv. Aminotransferases

The well known and measured indicators of hepatic disease are the aminotransferases (formerly referred as transaminases) (Reichling and Kaplan, 1988; Limdi and Hyde, 2003). Aspartate aminotransferase (AST) or serum glutamate oxaloacetate transaminase and alanine aminotransferase (ALT) or serum glutamate pyruvate transaminase are the most important biomarkers for hepatocellular necrosis (Gowda *et al*., 2009). Both ALT and AST are involved in gluconeogenesis where they catalyse the transfer of α-amino groups of alanine or aspartic acid to the α-keto group of ketoglutaric acid forming pyruvic acid and oxaloacetic acid respectively (Reichling and Kaplan, 1988; Limdi and Hyde, 2003).

Alanine aminotransferase is a purely cytosolic enzyme available in the kidney, liver, heart and muscle and with higher concentrations in the liver (Reichling and Kaplan, 1988; Limdi and Hyde, 2003; Gowda *et al*., 2009). AST is a cytosolic and mitochondrial enzyme, available in the kidneys, cardiac muscle, liver, brain, lungs, skeletal muscle, pancreas, leucocytes and red cells (Limdi and Hyde, 2003). Most of the activity of AST in the mammalian liver is considered to be the mitochondrial isoform (Rechling and Kaplan, 1988) while that of the serum AST activity (approximately 80 %) is of the cytosolic isoform.

Patients with all types of liver diseases such as viral hepatitis, toxin-induced liver damage (Gowda *et al*., 2009), ischemic liver injury, and all types of acute and chronic hepatitis, infections, congestion from acute and chronic heart failure, cirrhosis, alcoholic liver disease, and metastatic carcinoma and granulomatous exhibit high levels of AST and ALT (Reichling and Kaplan, 1988). Hepatocellular injury and exposure to hepatotoxins due to drug induction elicits high levels of aminotransferases. However, aminotransferase reduction does not imply recovery, but may be due to massive destruction of liver cells with little or no liver cell to sustain life (Reichling and Kaplan, 1988). Subsequently, lower-than-normal ALT activity have been utilised as a biomarker for increased risk of mortality and frailty (Ramaty *et al*., 2014). The development of frailty (muscle wastage or sarcopenia) in later life and the risk of developing a disease and dying at an early age are signs that are predicted by the lower-than-normal ALT activity. In addition, lower-than-

normal ALT activity are also found in patients that suffer from end-stage renal disease (Ramaty *et al*., 2014).

The ratio of AST to ALT is of clinical importance than the individual assessment of each enzyme (Gowda *et al*., 2009). The ratio identifies cirrhotic patients with 81.3 % sensitivity and 55.3 % specificity and progressively increases once the liver function is impaired (Giannini *et al*., 2003). Patients with advanced liver fibrosis and chronic hepatitis C infection usually have a value greater than 1. However, a value greater than 2 and 3 is an indication of alcoholic or severe liver disease (Reichling and Kaplan, 1988).

v. Gamma glutamyl transferase

Gamma glutamyl transpeptidase also known as Gamma glutamyl transferase (GGT) is a microsomal enzyme present in both liver and biliary epithelial cells (Gowda *et al*., 2009). One of its functions is to catalyse the transfer of gamma glutamyl group from one peptide to another across the cell membrane (Reichling and Kaplan, 1988; Gowda *et al*., 2009). It is expressed in many tissues like the kidney, liver, spleen, pancreas, brain and heart. The level of serum GGT significantly increases in patients with hepatobiliary and pancreatic disease. Examples of other conditions that would bring about raised GGT activity include: renal failure, myocardial infarction, diabetes, chronic obstructive pulmonary disease, hyperthyroidism, obesity, dystrophica myotonica, anorexia, alcoholism and Gullian barre syndrome (Limdi and Hyde, 2003; Gowda *et al*., 2009). In addition, drugs such as barbiturates, carbamazepine and phenytoin may also raise the levels of serum GGT. Antioxidants such as lycopene, α-carotene, β-carotene and β-cryptoxanthin are inversely related to increased levels of GGT; hence, it can be used as a marker for oxidative stress (Koenig and Seneff, 2015).

vi. Albumin

It is the most abundant, negatively charged plasma protein, primarily synthesised in the liver (Garcovich *et al*., 2009). Approximately 10 – 15 g/day of albumin is synthesised in a healthy adult with about 60 % localised in the extracellular space (Hankins, 2006). Albumin is involved in the following functions such as: maintaining colloid oncotic pressure (COP), transporting of substrates, free radical scavenging, coagulation, buffering

capacity and wound healing (Mazzaferro *et al*., 2002; Hankins, 2006). A number of factors such as urinary and gastrointestinal losses affect Albumin concentration (Limdi and Hyde, 2003). Increase or decrease in albumin concentration may occur depending on the disease state. Most times, increased level of serum albumin is clinically insignificant; however, dehydration can bring about increased albumin concentration. On the other hand, increased protein loss through wounds, burns, liver disease and malnutrition can bring about decreased levels of serum albumin (analbuminemia). Increased catabolism, decreased synthesis or a combination of both can also lead to analbuminemia (Hankins, 2006). Inflammatory processes (chronic inflammatory disorder and acute-phase responses) are a major cause of decreased albumin. The severity, prognosis of total hepatic function, acute hepatitis or cirrhosis does not correlate with Albumin concentration (Limdi and Hyde, 2003; Hankins, 2006). Excessive excretion of albumin in the urine suggests the inability of the proximal tubular cells to reabsorb albumin; hematuria or proximal tubular damage (Horne *et al*., 1991).

2.7.7 Lipid Profile

i. Total cholesterol

The most important steroid hormone synthesised by animals is the cholesterol (Razin and Tully, 1970), which is required in maintaining the integrity of the structural membrane and fluidity of the cells (Razin and Tully, 1970). The hepatic cells in humans synthesise the largest amount of cholesterol. Other functions of cholesterol include intracellular transport, nerve conduction, cell signaling processing, and lipid rafts formation in plasma membrane (Incardona and Eaton, 2000). Several biochemical pathways such as vitamin D synthesis, adrenal gland hormones (aldosterone and cortisol), all steroid hormones, and sex hormones (progesterone, testosterone and estrogens) utilise cholesterol as a precursor molecule (Hanukoglu, 1992; Payne and Hales, 2004).

Hypercholesterolemia or dyslipidemia is as a result of increased cholesterol level in the blood (Durrington, 2003). No clinical signs are induced by hypercholesterolemia, indicating that it is asymptomatic; however, atherosclerosis (hardening of the arteries) can occur as a result of the prolonged elevation of serum cholesterol, which results in the

production of artrial atheromatous plaques. The consequence results in the constriction of the arteries or clot formation and obstruction of blood flow which may lead to the rupture of the smaller arteries (Finn *et al*., 2010). Subsequently, coronary artery blockage as well as blockage of the artery supplying the brain can induce heart attack and stroke respectively. A combination of environmental (obesity, diet and stress) and genetic factors (polygenic, familial and familial combined hyperlipidemia) can bring about hypercholesterolemia (Calderon *et al*., 1999; Bhatnagar *et al*., 2008). Other conditions such as diabetes mellitus type 2, nephrotic syndrome, hypothyroidism, anorexia nervosa, cushing's syndrome and medications (thiazide, glucocorticoids and retinoic acid) also elevate cholesterol levels (Bhatnagar *et al*., 2008).

Low cholesterol levels do not have any clinical significance; however, it becomes a great concern when it falls far below the normal value (120 mg/dL). Hypocholesterolemia exists in the primary [genetic mutations resulting to hypobetalipoproteinemia and abetalipoproteinemia (Welty, 2014) and tangier disease (Bektas *et al*., 2008)] and secondary (anaemia, infection, inflammation, malabsorption, hyperthyroidism and leukemias) forms (Oztas, 2016). It has been established through clinical and experimental studies that changes in cholesterol breakdown may be correlated with tumour development and carcinogenesis (Silvente-Poirot and Poirot, 2012). In order to continue the tumour proliferation, migration and metastatic activities of cancer cells, the metabolic requirements are significantly increased (Warburg, 1956). Therefore, membrane synthesis and cell division required for cancer development ultimately alter the regulation of cholesterol transport and metabolism (Silvente-Poirot and Poirot, 2012).

ii. Triglycerides

Carbohydrates and free fatty acids are utilised by the liver to synthesise triglycerides (Cox and Garcia-Palmieri, 1990). Abnormal concentrations (increase or decrease) of triglycerides may occur due to several conditions. Hypertriglyceridemia (elevated triglyceride) may be a contributing factor to a high incidence of obesity, cardiovascular disease, type 2 diabetes mellitus, metabolic syndrome and acute pancreatitis (Hodis *et al*., 1996). Exogenous (dietary fat) and endogenous (liver) are the two main sources of plasma triglycerides (Yuan *et al*., 2007). Hypertriglyceridemia are classified into primary and

secondary. Primary hypertriglyceridemia include familial chylomicronemia (primary mixed hyperlipidemia type 5 and hyperlipoproteinemia type 1) which are distinguished by chylomicrons 12-14 h post fasting. Hepatosplenomegaly, eruptive xanthomata and lipemia retinalis are some of the clinical features of both primary mixed hyperlipidemia and familial chylomicronemia. Contrastingly, secondary hypertriglyceridemia are usually associated with metabolic disorders which include obesity, diabetes (Lemieux *et al*., 2000), alcohol, renal disease (Kaysen and de Sain-van der Velden, 1999), pregnancy (Warth *et al*., 1975), nonalcoholic fatty-liver disorder (Clark, 2006; Farrell and Larter, 2006) and medications (e.g. antiretroviral drugs) (Calza *et al*., 2004).

iii. High-density lipoproteins

High-density lipoproteins (HDL) consist of lipid (phospholipids, free cholesterol, cholesteryl esters and triglycerides) and protein (apoA-I and apoA-II) (Mendoza *et al*., 1976; Sich *et al*., 1998). HDL are involved in the reverse cholesterol transport system were they transport additional cholesterol from the tissues (fibroblasts and macrophages) to the liver (El Khoury *et al*., 2014). HDL2 and HDL3 are two subclasses of HDL, of which HDL2 has been connected with coronary artery disease. Hypoalphalipoproteinemia (reduced HDL- levels) has more clinical significance than hyperalpalipoproteinemia; considering the fact that it is significantly correlated with increased risk of coronary heart disease. Several factors such as genetic diseases (abetalipoproteinernia, tangier disease and dyslipoproteinemia), obesity, cigarette smoking, physical inactivity, oral contraceptives, cholesterol reducing diets and thiazide diuretics decrease the levels of HDL-cholesterol. Conversely, elevated HDL-cholesterol (hyperalphalipoproteinemia) is correlated with low risk of CHD. However, genetic (dominant or polygenic inheritance) or secondary (regular exercise, biliary cirrhosis and estrogen administration) factors can contribute to elevated HDL levels (Kakafika *et al*., 2008; Bermudez *et al*., 2008).

2.7.8 Oxidative stress biomarkers for systemic toxicity

Nanoparticles of various sizes, chemical composition, surface properties have been reported to attack the mitochondria, which are the organelles where redox reactions take place (Alarifi *et al*., 2014). NPs may alter the production of ROS and antioxidants,

resulting into oxidative stress. The mechanism of NP-induced toxicity is not clearly understood but it is presumed that oxidative stress is a major mechanism of nanotoxicity (Syama *et al*., 2014; Reddy *et al*., 2015; Niska *et al*., 2015; Ferreira *et al*., 2015). Oxidative stress occurs when there is an imbalance between the production of free radicals and antioxidants (Reddy *et al*., 2015). ROS are produced in the mitochondria during oxidative metabolism (Niska *et al*., 2015) and are eliminated by both endogenous and exogenous antioxidants (Pourhamzeh *et al*., 2016). ROS consist of reduced oxygen metabolites such as superoxide anions, hydroxyl radical, hydrogen peroxide, and singlet oxygen (Syama *et al*., 2014). Antioxidants (enzymatic and non-enzymatic) play important roles in cellular maintenance (Huang *et al*., 2010; Niska *et al*., 2015). Examples of antioxidant enzymes include superoxide dismutase, catalase while non-enzymatic antioxidant includes reduced glutathione. ROS are also involved in intracellular signal transduction (Yoshikawa and Naito, 2002). Conversely, excessive increase in ROS levels can induce modifications in the DNA, proteins, as well as the polyunsaturated fatty acids in cell membrane lipids (Sarkar and Sil, 2014).

i. Superoxide dismutase

The first line of enzymatic defence against free radicals is superoxide dismutase (SOD) (Niska *et al*., 2015). In eukaryotes and other mammals, SOD exhibits three isoenzymes which include SOD1 or Cu/Zn SOD localised in the cytosol, SOD2 or Mn SOD localised in the mitochondria and the extracellular SOD significantly expressed in kidney, fat tissues and lungs. In the inner mitochondrial membrane, electrons leak from the electron transport chain, which is acquired by molecular oxygen to form superoxide anion (O_2^-) (Niska *et al*., 2015). SOD catalyses the dismutation of superoxide radical (O_2^-) to hydrogen peroxide (H_2O_2) and singlet oxygen (Abdelhalim *et al*., 2015). The superoxide anion is not as reactive as the hydroxyl radical and is found within a particular environment where it is synthesised as a result of its inability to diffuse through the lipid membranes. In addition, superoxide anion and hydrogen peroxide can be converted to hydroxyl radical ($OH^{\cdot}$) through the fenton reaction.

ii. Catalase

Catalases (CAT) are dominantly localised in the peroxisomes of mammalian cells. They catalyse the decomposition of one molecule of H_2O_2 into two molecules of water and one molecule of oxygen. Oxidation of transition metals produces highly reactive $OH^{\cdot}$ from H_2O_2. Without the catalase to convert H_2O_2, metabolic processes in cell and tissues as well as the DNA macromolecule, will be significantly damaged inducing mutations that can initiate cancer process.

iii. Lipid peroxidation

Unsaturated fatty acids (cell membrane components) are oxidised in a chain reaction process known as lipid peroxidation. The free radical chain reaction proceeds when the hydrogen atom is removed from the fatty acid molecule. Radicals such as hydroxyl, hydroperoxyl, lipid peroxyl and alkoxyl are involved in the removal of hydrogen atoms from lipid molecules. The chain initiation reaction is a process in which lipids generate lipid radicals ($L^{\cdot}$) after the hydrogen atom removal (Yoshikawa and Naito, 2002). Lipid peroxyl radical ($LOO^{\cdot}$) are generated when the lipid radical ($L^{\cdot}$) reacts spontaneously with oxygen thus, the $LOO^{\cdot}$ attacks another lipid in order to remove hydrogen atom forming a lipid hydroperoxide (LOOH) and a new lipid radical ($L^{\cdot}$).This reaction continues and thereafter, accumulates lipid peroxide. An important and accepted biomarker for evaluating lipid peroxidation is the malondialdehyde, which is a secondary aldehydic product of lipid peroxidation.

iv. Glutathione

Glutathione (GSH) is an important intracellular antioxidant that is abundantly found in both plants and animals (Pompella *et al*., 2003). It contains the thiol group (-SH) that plays a role in cellular defense and aminoacids: L-glutamic acid, L-cysteine, and glycine are involved in the synthesis of GSH (Lu, 2009). GSH exists in one of two states: the reduced (GSH) and oxidised (GSSG). In the reduced state, a reducing proton is donated to other unstable molecules such as the reactive oxygen species by the thiol group of cysteine. Glutathione becomes reactive in donating a proton and forms glutathione disulphide (GSSG) with another reactive glutathione. However, the flavoenzyme

glutathione reducatse (GR) reduces oxidised GSSG to GSH in a NADPH-dependent manner (Couto *et al*., 2013).

An important indicator of cellular toxicity is the ratio of reduced glutathione to oxidised glutathione (Pastore *et al*., 2001). Reduced GSH accounts for over 90 % of the total glutathione while less than 10 % is in the oxidised state (GSSG) in the human body. Glutathione, an endogenous antioxidant is involved in a number of functions which include neutralising ROS and free radicals; maintaining vitamins C and E (both endogenous antioxidants) in their reduced forms; involved in DNA synthesis and repair, amino acid transport, protein synthesis, and enzyme activation.

CHAPTER THREE

MATERIALS AND METHODS

3.1 Laboratory Animal

Male Swiss mice (*Mus musculus*) were bred throughout the period of this study at the Department of Zoology, University of Ibadan. Mice of 6 - 8 weeks (24.0 ± 2.0 g) and 11 - 15 weeks old (30.0 ± 2.0 g) were used for the bone marrow micronucleus and sperm morphology assays, respectively. Standard laboratory animal feeds (pelleted mouse cubes) were obtained commercially and fed to the mice with drinking water *ad libitum*. They were housed in 12 hours light / 12 hours dark cycle, with appropriate temperature and relative humidity. All procedures involving the use of mice were in compliance with laboratory animal ethics (CIOMS, 1985; ILAR, 2011) and approved by the Animal Care and Use Research Ethics Committee (ACUREC) University of Ibadan, Oyo State (approval number: UI-ACUREC/App/2015/005; Appendix I).

3.2 Nanoparticles and preparation

Titanium dioxide and zinc oxide nanoparticles were procured from Sigma Aldrich, St. Louis, USA with the following specifications:

Zinc oxide (ZnO); Average Particle Size: < 100 nm; Surface Area: 15 - 25 m^2/g; and Colour: white; Chemical Abstract Service number: 1314-13-2.

Titanium dioxide (TiO_2, anatase); Average Particle Size: < 25 nm; Specific Surface Area: 45 m^2/g; Colour: white; Chemical Abstract Service number: 1317-70-0.

Nanopowdered Titanium dioxide and Zinc oxide were suspended in distilled water. Stock doses of TiO_2, ZnO NPs and their mixture (1:1) respectively were prepared in distilled water using an ultrasonic water bath (Bandelin, Sonorex digitec, Germany) to break up particle aggregates in which ultrasound energy was applied to break the intermolecular interactions for 10 minutes at 60 W (3 minutes pulse on and 30 seconds pulse off at room temperature). The nanoparticles and their mixture were further vortexed for 5 minutes to disperse the particles. NPs were freshly prepared prior to animal exposure.

3.3 Physicochemical characterisation using Transmission Electron Microscopy and Dynamic Light Scattering

3.3.1 Dispersion protocol of titanium dioxide, zinc oxide nanoparticles and their mixture

Both nanoparticles and their mixture were dispersed according to the protocol of Georgantzopoulou *et al*. (2013; 2016). In brief, the stock solutions of TiO_2, ZnO NPs and their mixture were prepared by suspending 2 mg of each of the NPs and their mixture in 1 mL of sterile MilliQ water. NP suspensions were sonicated in a sonication bath 3 times 3 minutes with 30 seconds pause in between using a UP 200S probe ultrasonicator (Hielscher, Germany). The resulting suspensions were further vortexed for 5 minutes to obtain uniform samples.

3.3.2 Morphologies of titanium dioxide and zinc oxide nanoparticles

The shapes of TiO_2 and ZnO NPs were determined using the TEM according to Georgantzopoulou *et al.* (2016). One milligram each of the NPs were first suspended in 1.5 mL of ethanol and sonicated for a minute. The suspension was dropped on a conventional TEM copper mesh grid with a carbon film as the carrier. Digital images were produced using the TEM (FEI Tecnai G2 F20) at an accelerating voltage of 120 kV and recorded in the bright-field mode using Gatan Ultrascan 2k x 2k CCD camera.

3.3.3 Size distribution of titanium dioxide, zinc oxide nanoparticles and their mixture

The particle size distribution, zeta (ζ) potential and polydispersity of TiO_2, ZnO NPs and their mixture were obtained by DLS using Zetasizer Nano Series instrument (Malvern Instruments Ltd, UK) (Cambier *et al*., 2018). The particles were prepared according to the dispersion protocol. The He-Ne laser beam (5 mW, λ= 633 nm) was used in irradiating the samples with red light and the back scattering mode (detected at 173°) to detect the intensity of the light scattered by the moving particles after irradiation. The following were taken into consideration during analyses: the viscosity (cP) of distilled water (0.8872); refractive index of distilled water (1.330); refractive indexes of TiO_2 (2.61), ZnO NPs (2.00) and their mixture (2.61) with a general absorption of 0.01. Disposable cuvettes were used in measuring both NPs and their mixture at a temperature of 25^oC, which was maintained within 0.1^oC. Data represent the calculated mean distribution from three independent repetitions for TiO_2, ZnO NPs and their mixture, respectively. The zeta potentials of TiO_2, ZnO NPs and their mixture were also carried out in triplicates of 12 sub-runs each. Data were presented as the calculated mean and standard deviation from three independent repetitions for TiO_2, ZnO NPs and their mixture respectively.

3.4 Acute toxicity for the genetox bioassay

Preliminary screening was carried out to determine the appropriate dose range for testing the NPs and their mixture for the micronucleus assay and reproductive toxicity. Acute toxicity test was carried out according to OECD guidelines 420 (OECD, 2008) for testing chemicals for the determination of lethal dose 50 (LD_{50}). Four male mice (6 - 8 weeks old) per dose were treated intraperitoneally to fixed doses of 150 and 300 $mgkg^{-1}$ of TiO_2 and ZnO NPs and their mixture and observed for changes in fur, eyes and mucous membranes, salivation, coma, lethargy, diarrhoea, convulsion, tremors. Mortality of the mice within 24 hours was recorded while living animals were observed for 14 days before termination of the study. The percentage net body weight (bw) of mice was computed as:

$$\frac{\text{Final bw of mice on sacrifice day (g)} - \text{Initial bw of mice prior to treatment (g)}}{\text{Initial bw of mice prior to treatment (g)}} \times 100$$

3.5 Treatment groups and experimental design

One hundred and seventy male mice (5 mice per group) were used for the micronucleus assay. Two exposure periods were considered, 5 and 10 days. The mice were intraperitoneally adminsitered with 0.5 mL of five doses (9.38, 18.75. 37.50, 75.00 and 150.00 $mgkg^{-1}$) at 24 hours interval for each administration. For the 10- day exposure period, mice were treated for 5 consecutive days and observed for another 5 days to assess DNA repair. Negative control mice were injected intraperitoneally with distilled water while the positive control mice were treated with 20 $mgkg^{-1}$ of cyclophoshamide (Endoxan^{TM} Mfg Lic. No. 186. Frankfurt am Main, Germany) 24 hours prior to sacrifice.

3.5.1 Blood collection

Without anaesthesising, the mice were manually restrained by using the thumb and the forefinger to apply pressure just behind the eye, pulling back the skin to protrude the eyeball. The microhaematocrit capillary tube (70 mL) was inserted directly and firmly in the medial canthus (inner corner of the eye) of the mice. Peripheral blood (1 mL) was collected in Ethylene Diamine Tetracaetic Acid (EDTA) and plane bottles respectively prior to sacrifice. Treated mice were sacrificed 6 hours after the last administration through cervical dislocation.

3.5.2 Urine collection

Mice were orally administered with 0.1 mL of tap water to induce urination. The one-handed method was used in restraining the mice. The tails of the treated mice were secured with the pinkie finger while the same hand was placed over the back to scruff them. On the last day of treating the mice with titanium dioxide, zinc oxide nanoparticles and their mixture, 0.2 mL of pure urine samples without faeces were collected 6 hours post treatment in clean plane bottles when the treated mice were held and lightly stroked on the belly.

3.6 Bone marrow preparation

Mouse bone marrow erythrocyte micronucleus test as described by Schmid (1975) and modified by Alimba and Bakare (2016) were used for the bone-marrow cell micronucleus preparations. The two femoral bones were harvested and freed of adherent tissues using a pair of scissors and forceps. By gentle traction, the distal epiphyseal portion was torn off together with the rest of the tibia and the surrounding muscles. A pair of scissors was utilised in shortening the proximal ends of the fermur until a visible opening was made. Using a 1 mL syringe, the cells of the bone marrow was aspirated with 1 mL Foetal Bovine Serum (FBS) (Sigma Aldrich, Germany) into eppendorf tubes. The bone marrow cells were dislodged properly by carefully agitating them using the micropipette. The suspended cells were spun for 5 minutes at 2000 rpm after which the FBS was aspirated. The eppendorf tube was briefly agitated using a fresh micropipette tip to disperse the clumps. The FBS (1 mL) was added again, mixed properly and spun for 5 minutes at 2000 rpm.

Fifty microlitres (0.05 mL) of FBS was added to the pellets and the cells were carefully mixed by aspiration into the capillary part of a fresh micropipette tip. For each animal, five thin smears were made by placing 10 µL of bone marrow suspension on the end of the slide and spread by pulling the suspension behind a polished cover glass held at an angle of 45° towards the end of the slide making a distance of 4 - 5 cm. The slides were allowed to dry overnight, fixed for 2 minutes with 70 % methanol and then allowed to dry completely. Fixed slides were stained with 0.4 % May-Grunwald solution for 3 minutes in coplin jars, immediately stained again in 1:1 0.4 % May-Grunwald/distilled water (v/v) for 3 minutes and then rinsed thoroughly in distilled water to remove excess stains. Slides were dried completely over night and then counter stained in 5 % Giemsa (w/v) for 5 minutes, rinsed thoroughly in distilled water and air dried overnight at room temperature.

Slides were dipped in xylene, mounted with 2 drops of Dibutyl Phthalate Xylene (DPX) mountant and screened, at 400X magnification, for regions of suitable technical quality, where the cells are well spread, undamaged and perfectly stained. The mature erythrocytes (NCE) stained light pink and blue-purple in the polychromatic erythrocytes (PCE). From each mouse, 1000 cells were examined and PCE cells with micronucleus (MNPCE) were

evaluated at 1000X magnification using the light microscope (Micromaster, Fisher Scientific, China). Only PCE with homogeneous blue/grey colour were scored while PCE: NCE ratio was used as an index of cytotoxicity (Krishna and Hayashi, 2000). Micronucleus with PCE was recognised by their characteristic size, round shape and dark blue colour. The same observer scored all slides blindly.

3.7 Assessment of organ weights

The liver, kidney, brain, spleen and heart of mice treated with TiO_2, ZnO NPs and their mixture at the 5- and 10- day exposure periods were excised and rinsed with 1.15 % potassium chloride (KCl). Morphology such as organ colour change was in comparison with the group of mice that received distilled water. The organs were blotted dry with a whatman filter paper and weighed to determine their absolute organ weights. The organ to the body weight ratio (relative organ weights) was computed as the percentage of organ (g) (wet weight) to body weight (g).

3.8 Haematological analysis

Blood collected into EDTA bottles through the retro orbital sinus of the mice treated with both NPs and their mixture at the 5- and 10- day exposure periods was used to determine the haematological indices: Red Blood Cell count (RBC) count, Haemoglobin content (Hb), percentage Haematocrit (Ht), Mean Corpuscle Haemoglobin Concentration (MCHC), Mean Corpuscle Volume (MCV), Mean Corpuscle Haemoglobin (MCH), platelets, total white blood cell count (WBC) count and differentials (lymphocytes, neutrophils, monocytes, eosinophils and basophils) (Cheesbrough, 2005).

3.9 Histopathological analysis

Histopathological evaluation of the liver, kidney, spleen, brain and heart were performed according to standard procedures. Portions of these organs were cut and fixed in 10% neutral buffered formalin solution for histopathological assessment. The formalin preserved tissues were immersed in paraffin wax, sectioned into 4 µm thickness and arranged on clean microscope slides. Haematoxylin-eosin (H & E) stains were used on the slides and observed using a light microscope at a magnification of 400X.

3.10 Biochemical assays

3.10.1 Clinical biochemistry

Urine samples collected into plane bottles were assayed for the levels of albumin and creatinine. Blood samples earlier collected was centrifuged at 3000 rpm for 10 minutes to obtain clear sera and used to determine the activities of aspartate aminotransferase (AST), alanine aminotransferase (ALT) and Gamma Glutamyltransferase (GGT); concentrations of total bilirubin (TB), albumin (ALB), Blood Urea Nitrogen (BUN), creatinine (CREA), and triglyceride (TRI); and levels of Total Cholesterol (TCHOL) and high density lipoprotein (HDL) were assessed using the Randox Diagnostic Kits following the manufacturer's instructions.

i. Assay of Aminotransferases activities

Alanine aminotransferase (ALT) and Aspartate aminotransferase (AST) enzyme activities were determined according to Reitman and Frankel (1957) protocol. The complex formed between pyruvate hydrazone and 2, 4-dinitrophenylhydrazine was measured to give the ALT value. Likewise, the complex formed between oxaloacetate hydrazone and 2, 4-dinitrophenylhydrazine was measured to give the AST value.

Preparation of working reagents and protocol (See Appendix 3)

ii. Assay of Gamma Glutamyl transferases activity

Gamma Glutamyl transferases (γ-GT) was determined according to Szasz (1969) protocol. The γ-GT in the sample converted L-γ-glutamyl-3-carboxy-4-nitroanilide in the presence of glycylglycine to 5-amino-2-nitrobenzoate.

Preparation of working reagents and protocol (See Appendix 3)

iii. Determination of Bilirubin concentration

The colourimetric method described by Jendrassik and Grof (1938) was employed. A blue coloured complex was formed when sulphanilic acid in alkaline medium reacted with

direct bilirubin. Total bilirubin was determined by the reaction of diazotised sulphanilic acid, which released albumin bound bilirubin in the presence of caffeine.

Preparation of working reagents and protocol (See Appendix 3)

iv. Determination of Albumin concentration

Albumin concentration was determined according to the method of Dumas *et al*. (1997). The measurement was based on the binding of albumin to Bromocresol green (BCG).

Preparation of working reagents and protocol (See Appendix 3)

v. Determination of Urea concentration

Urea concentration was determined according to Weatherburn (1967) protocol. In the presence of urease, urea was hydrolysed to ammonia in the serum. Berthelot's reaction was used to measure ammonia photometrically.

Preparation of working reagents and protocol (See Appendix 3)

vi. Determination of Creatinine concentration

Creatinine concentration was determined by Bartels and Bohmer (1972) protocol. A coloured complex was formed when picric acid reacts with creatinine. A direct proportion was formed between the creatinine concentration and amount of the complex formed in the solution.

Preparation of working reagents and protocol (See Appendix 3)

vii. Determination of Cholesterol level

Cholesterol concentration was determined according to Trinder (1969) protocol. Enzymatic hydrolysis and oxidation was used in determining the assay. The presence of phenol and peroxidase in hydrogen peroxide and 4-aminoantipyrine formed Quinoneimine.

Preparation of working reagents and protocol (See Appendix 3)

viii. Determination of High-density lipoprotein level

The precipitation of chylomicron fractions and low density lipoproteins (LDL) was achieved through the inclusion of phosphotungstic acid. After centrifuging the mixture, the cholesterol in the HDL fraction was determined in the supernatant.

Preparation of working reagents and protocol (See Appendix 3)

ix. Determination of Triglycerides concentration

Triglyceride concentration was determined according to Tietz (1990) protocol. The enzymatic hydrolysis with lipases determined the triglycerides. The principle is based on the production of quinoneimine from 4-aminophenazone, hydrogen-peroxide, and 4-chloropenol under peroxidase as a catalyst Jacobs and VanDemark (1960), Trinder (1969), Koditschek and Umbreit (1969).

Preparation of working reagents and protocol (See Appendix 3)

3.10.2 Oxidative stress parameters

Liver, kidney and testis of the mice treated with TiO_2, ZnO NPs and their mixture for the 5- and 10- day exposure periods were used to evaluate the oxidative stress parameters. The organs were rinsed in 1.15 % KCl to remove any red blood cell clot and homogenised in 6 volumes of cold phosphate buffer (0.1 M, pH 7.4) to obtain the homogenates respectively. Centrifugation of the homogenate was carried out at 10 000 rpm for 15 minutes at $4^{o}C$ to obtain the post mitochondrial fraction (PMF). The PMF was stored at $-20^{o}C$ until use.

3.10.2.1 Determination of protein concentration

The protocol of Gornal *et al*. (1949) was used in determining the protein concentrations of the homogenised samples. The precipitation of Cu^{2+} ions as cuprous oxide was prevented by adding potassium iodide.

Principle

A coloured complex was formed between the proteins and the cupric ions found in the Biuret reagent containing $CuSO_4$, KI and sodium potassium tartarate. A standard BSA curve was used in calibrating the procedure.

Preparation of working reagents and standard curve (See Appendix 3)

3.10.2.2 Assay of Superoxide Dismutase Activity

The SOD activity was evaluated according to the method of Mistra and Fridovich (1972).

Principle

The basis of this assay was the inhibition of the autoxidation of epinephrine at pH 10.2 by SOD. The generation of superoxide radical via xanthine oxidase reaction induced adenochrome. The increased oxidation of epinephrine yielded adenochrome per superoxide with increased pH and epinephrine concentration (Valerino and Cormack, 1971).

Preparation of working reagents and procedure (See Appendix 3)

3.10.2.3 Assay of Catalase Activity

The method of Claiborne (1985) was used in determining the catalase activity.

Principle

This activity was determined as catalase splits hydrogen peroxide while the absorbance was observed at 240 nm. Since no absorbance maximum for hydrogen peroxide, its concentration correlated well at 240 nm. The extinction coefficient used was 0.3436 $mM^{-1}cm^{-1}$ (Noble and Gibson, 1970).

Preparation of working reagents and procedure (See Appendix 3)

3.10.2.4 Determination of Reduced Glutathione level

The method of Beutler *et al*. (1963) was used in determining the level of reduced glutathione (GSH).

Principle

The bulk of cellular non-protein sulfhydryl group form most of the reduced form of glutathione. The reaction between sulfhydryl compounds and Ellman's reagent [5', 5'-dithiobis-(2-nitrobenzoic acid)] produced a stable yellow colour absorbed at 412 nm. In the test sample, there was a direct proportion of the reduced glutathione level and the complex absorbed at 412 nm.

Preparation of working reagents and procedure (See Appendix 3)

3.10.2.5 Assessment of lipid peroxidation

Lipid peroxidation was determined as described by Rice-Evans *et al*. (1986).

Principle

An end product of lipid peroxidation, which was malondialdehyde, reacted with 2-thiobarbituric acid (TBA) to generate a chromophore (pink colour), which absorbed at a maximum wavelength of 532 nm when produced on heating in an acidic pH.

Preparation of working reagents and procedure (See Appendix 3)

3.11 Germ cell toxicity

Eighty five male mice (11 – 15 weeks old) (five mice per group) were treated with TiO_2, ZnO NPs and their mixture at five doses (9.38, 18.75. 37.50, 75.00 and 150.00 $mgkg^{-1}$) each with positive and negative controls, respectively. Negative control animals were treated intraperitoneally to distilled water while positive control mice were treated with cyclophoshamide (20 $mgkg^{-1}$). Mice were treated with 0.5 mL of the nanoparticles' suspension for 5 consecutive days at a 24 hour interval. The experiment lasted for 5 weeks (35 days) from the first injection, since it takes 34.5 days for the completion of

spermatogenesis (Bartke *et al*., 1974). Cervical dislocation was used in sacrificing the animals and their cauda epididymes taken out and minced with a pair of scissors in a petri dish containing 1 mL of physiological saline (isotonic medium) to release the sperm (forming the sperm suspension).

3.11.1 Determination of Sperm Motility

Sperm motility was carried out using a fixed volume of the spermatozoa suspension (10 µL) placed on a clean glass slide and covered with a 22 x 22 mm cover slip. It was left to stabilise for 1 minute. The examination was carried out using 400X magnification to classify 200 spermatozoa into rapid progressive motility, slow progressive motility, non-progressive motility and immotility. The average of both left and right cauda was determined for the motility. According to WHO (2010), sperm motility should be 50% or more motile (rapid and slow progessive motility) or 25% or more with rapid progressive motility.

3.11.2 Determination of Sperm Count

Sperm count was determined from both the left and right cauda, using the haemocytometer method. A 1:10 dilution (5 µL of sperm suspension + 45 µL of normal saline) was made in a dish. The properly mixed suspension (10 µL) was transferred to the chamber of the haemocytometer. This was done by carefully touching the edge of the cover glass with the pipette tip and allowing the haemocytometer to fill by capillary action. The chamber was allowed to stand for 10 minutes in a humid chamber to prevent drying out. The spermatozoa were counted in 5 squares out of 25 squares (each of the 25 square is ruled into 16 boxes) at 400X magnification.

Sperm concentration/ mL = dilution factor x count in 5 squares x 0.05×10^6

3.11.3 Determination of Sperm Abnormality

Four hundred and fifty microliter (450 µl) of the sperm suspension combined with 50 µl of 1% Eosin Y aqueous resulting into a 9:1, [(normal saline solution + semen): eosin Y stain] was placed on a wash glass. After 45 minutes, sperm solution was placed on a microscope

slide. Using another slide held obliquely to the first (approximately 45° angle), it was touched against the drop of sample (away from the frosted end). After the droplet spread along the junction of the slide, the second slide was gently pulled away from the drop along the length of the first slide. The prepared smears were then allowed to dry over night. The preparation was observed with oil immersion under the bright light microscope (Micromaster, Fisher Scientific, China). Six slides were prepared from each mouse and 1000 sperm cells scored per animal (Wyrobek and Bruce, 1975; Alabi and Bakare, 2011).

3.11.4 Determination of testicular weight and histopathological examination

The testes were blotted dry with a whatman filter paper and weighed to determine their absolute weights. Histopathological evaluation of the testis was performed according to standard procedures. The bouin preserved tissues were fixed in paraffin wax, sectioned into 4 µm thickness and placed on clean microscope slides. Haematoxylin and Eosin chemicals were used in staining the slides and thereafter observed using a light microscope.

3.11.5 Luteinizing Hormone, Follicle Stimulating Hormone and Testosterone assays

Blood collected through the retro orbital sinus of the mice treated with TiO_2, ZnO NPs and their mixture for 35 days was spun for 10 minutes at 3000 rpm and the sera assessed for the concentrations of Luteinizing Hormone (LH), Follicle Stimulating Hormone (FSH) and Testosterone. An enzyme linked immunosorbent assay (ELISA) system was employed in quantifying the concentrations of LH (mIU/mL), FSH (mIU/mL) and Testosterone (ng/mL) using the Calbiotech kits (Spring Valley, CA, USA) at the Department of Veterinary Surgery and Reproductive Unit of the Faculty of Veterinary Medicine, University of Ibadan.

i. Principles of Luteinizing Hormone and Follicle Stimulating Hormone assays

The LH ELISA kit (LH231F) and FSH ELISA kit (FS232F) were solid phased assays that used streptavidin/biotin method. The samples and Anti-LH/Anti-Biotin conjugate or Anti-FSH/Anti-Biotin conjugate, respectively were added to the wells coated with streptavidin. LH or FSH in the serum formed a sandwich between specific antibodies labelled with

biotin and horse radish peroxidase (HRP). Unbound protein and HRP conjugate were washed off with the wash buffer. Upon the addition of the substrate, they were read at 450 nm using an ELISA reader. The colour intensity was proportional to the concentrations of LH or FSH in the serum.

Working reagent and procedure (See Appendix 3)

ii. Principle of Testosterone assay

The testosterone ELISA kit (TE187S) was based on the antagonistic reaction between testosterone and the HRP conjugate in the serum for a certain volume of mouse anti-Testosterone. Endogenous testosterone in the standard and samples competed with a fixed number of HRP-labeled testosterone for a number of testosterone antibody specific to the binding sites during incubation. The immunologically bound testosterone peroxidase conjugated to the well decreased as the testosterone concentration in the sample increased. The wells were washed while the unbound testosterone peroxidase conjugate also washed away. The development of a blue colour was visible after the addition of TMB reagent and incubation for 15 minutes at room temperature. The addition of a stop solution further stopped the colour development, and the absorbance was read using an ELISA reader at 450 nm.

Working reagent and procedure (See Appendix 3)

3.12 Statistical analyses

Probit analysis (SPSS 20.0) (IBM SPSS Statistics for Windows, Version 20.0 Armonk, NY: IBM Corp) was used in determining LD_{50} of TiO_2, ZnO NPs and their mixture. Body weight (g), absolute (g) and relative (%) organ weights of the treated mice were statistically compared with the mice treated with distilled water using one way ANOVA followed by Dunnett post-hoc test. Frequencies of MNPCEs of the micronucleus assay were calculated and the PCE: NCE ratio served as a function of the cytotoxicity index. For both 5- and 10- day exposure periods, the significance of frequencies of the micronuclei at the different dose levels was in comparison with their corresponding groups of mice treated with distilled water using one-way ANOVA followed by Dunnett test. Two-way

ANOVA with Bonferoni test was used in analysing the differences between the 5- and 10-day exposure periods where nanoparticles treatments and exposure periods served as factors.

For the sperm parameters and reproductive hormonal assay (LH, FSH and Testosterone), the one-way ANOVA followed by a Dunnett test was used in analysing their frequencies in comparison at different dose levels against the group of mice treated with distilled water. Haematological and biochemistry parameters of the different doses were in comparison with the mice treated with distilled water. SOD, CAT, GSH and MDA were analysed using two-way ANOVA with Bonferoni test where nanoparticles treatments and exposure periods served as factors. Analyses were performed using GraphPad Prism version 5.01 for Windows, GraphPad Software, San Diego California, USA and IBM Statistical Package for Social Sciences (SPSS) version 20 at 0.05 level of significance.

Effects of the mixture of TiO_2 NPs and ZnO NPs, known as interaction factor (IF), were calculated according to Katsifis *et al*. (1996) and Demir *et al*. (2014) as follows:

$$IF = TZ - T - Z + C$$

$$SE_{IF} = \sqrt{(SE_{TZ})^2 + (SE_T)^2 + (SE_Z)^2 + (SE_C)^2}$$

Where TZ is mean of the mixture of TiO_2 NPs and ZnO NPs, T is the mean of TiO_2 NPs, Z is the mean of ZnO NPs and C is the mean of the mice treated with distilled water. SE_{IF} is the standard error of the interaction factor, SE_{TZ} is the standard error of the mixture of TiO_2 NPs and ZnO NPs. SE_T is the standard error of TiO_2 NPs, SE_Z is the standard error of ZnO NPs and SE_C is the standard error of the mice treated with distilled water. A negative IF value represented antagonism, a positive IF value represented synergism while a zero IF value represented additivity.

CHAPTER FOUR

RESULTS

4.1 Physicochemical characterisation using Transmission Electron Microscopy and Dynamic Light Scattering

The physicochemical characteristics of TiO_2, ZnO NPs and their mixture are presented in Figure 4.1. The TEM revealed spherical and irregular shapes for the TiO_2 NPs and ZnO NPs, respectively (Figure 4.1 Ai-ii).

Both NPs and their mixture showed larger hydrodynamic diameters (mean size distribution) than the particle sizes of TiO_2 (< 25 nm) and ZnO NPs (< 100 nm) (Figure 4.1 B (i)-B (iii)). The hydrodynamic diameters of TiO_2, ZnO NPs and their mixture were 1492 nm, 482.7 nm and 882.8 nm respectively indicating that the aqueous medium (MilliQ water) had an influence on the sizes of both NPs and their mixture. TiO_2 and ZnO NPs formed agglomerates, which were 60 and 5 times larger, respectively, than their particle sizes. These further corroborated the results of the polydispersity index (PDI) values of TiO_2, ZnO NPs and their mixture with 0.822, 0.649 and 0.729, respectively. Therefore, the results of the polydispersity index indicated that the distribution of both NPs and their mixture consisted of heterogenous samples in the aqueous medium.

The zeta potential values of TiO_2, ZnO NPs and their mixture in the aqueous medium were +17.2 ± 3.52 mV, +21.4 ± 3.45 mV and +14.7 ± 5.25 mV (Figure 4.1 C (i) - C (iii)) respectively. Normally, the stability of a dispersed NP occurs when the zeta potential is higher than + 30 mV or lesser than – 30 mV. However, values obtained for the zeta potential revealed that TiO_2 NPs and their mixture were less stable while ZnO NPs were closely stable in the aqueous medium.

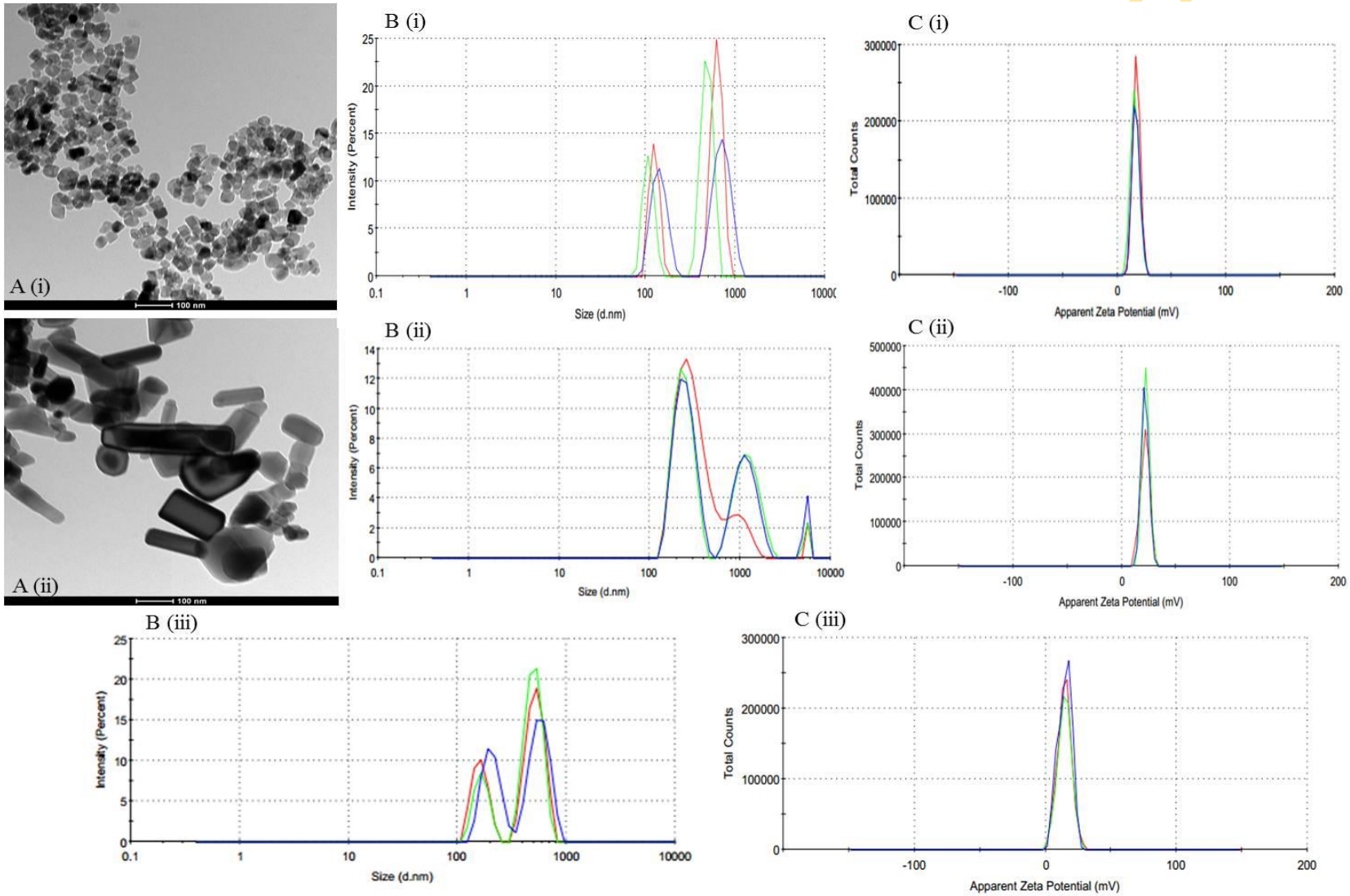

Figure 4. 1: Particle characterisation of TiO_2, ZnO NPs and TiO_2 + ZnO NPs. (A) TEM images of (i) TiO_2 NPs < 25 nm and (ii) ZnO NPs < 100 nm. Scale bar: 100 nm. (B) Hydrodynamic size and (C) ζ potential determination of the different NPs: (i) TiO_2 NPs, (ii) ZnO NPs and (iii) TiO_2 + ZnO NPs.

4.2 Acute toxicity of TiO_2, ZnO NPs and their mixture in *Mus musculus*

Table 4.1 shows the percentage net body weight of mice treated with TiO_2, ZnO NPs and their mixture. No significant differences were observed in the percentage body weight of mice treated with 150 $mgkg^{-1}$ of both NPs and their mixture. In contrast, a significant ($p < 0.001$) reduction in the percentage body weight of mice treated with 300 $mgkg^{-1}$ of ZnO NPs in comparison with the mice treated with distilled water was observed. Mortality was not seen in mice treated with 150 and 300 $mgkg^{-1}$ of TiO_2 NPs; 150 $mgkg^{-1}$ of ZnO NPs and their mixture.

Table 4.2 shows the various clinical signs exhibited by mice treated with NPs and their mixture. Animals treated with 300 $mgkg^{-1}$ of TiO_2 NPs had severe clinical signs that included excess mucus secretion at the anus (Figure 4.2). Mice treated with 150 $mgkg^{-1}$ of ZnO NPs showed signs of toxicity such as severe mucus secretion at the anus, and diarrhoea during the first few hours after exposure (Figure 4.2). When the dose of ZnO NPs was increased to the 300 $mgkg^{-1}$, one mouse died less than 24 hours after administration while another died 8 days later. Partial paralysis was observed in 2 mice 2 hours post treatment, however, this partial paralysis was reversed after 24 hours in one of them. Severe mucus discharge, abscesses in the fore and hind limbs and hard scrotum were observed in this group (Figure 4.2). Severe weight loss was observed in 25 % of the mice treated with ZnO NPs through out the 14 day exposure suggesting that the organs weights may have been affected also. The calculated LD_{50} for ZnO NPs was 299.9 $mgkg^{-1}$.

Table 4. 1: Percentage net body weights of mice treated with titanium dioxide, zinc oxide nanoparticles and their mixture for 14 days

Doses ($mgkg^{-1}$)	Negative Control	TiO_2 NPs	ZnO NPs	Mixture
150.00	19.99 ± 3.93	16.61 ± 7.94	17.85 ± 3.97	20.15 ± 2.87
300.00	19.99 ± 3.93	6.02 ± 2.37	-31.42± 12.88***	-

*** $p < 0.001$ in comparison with mice treated distilled water. Negative control (NC) = Distilled water

Table 4. 2: Clinical signs of acute toxicity observed in mice treated with titanium dioxide, zinc oxide nanoparticles and their mixture

Doses (150 / 300 $mgkg^{-1}$)	Dullness	Moribund	Active Movement	Feeding	Diarrhoea	Mucus Discharge	Aggressive Behaviour	Calmness	Bright coloured eyes	Swollen Limbs
TiO_2 NPs	-/+	-/-	+/-	+/+	+/+	+/++	+/+	-/-	+/+	-/+
ZnO NPs	-/+	-/++	+/-	+/-	+/++	+/++	+/++	-/-	+/+	+/+
Mixture	-	-	+	+	+	+	-	+	+	-

+: represents presence of mild clinical signs.

++: represents presence of severe clinical signs.

–: represents absence of clinical signs.

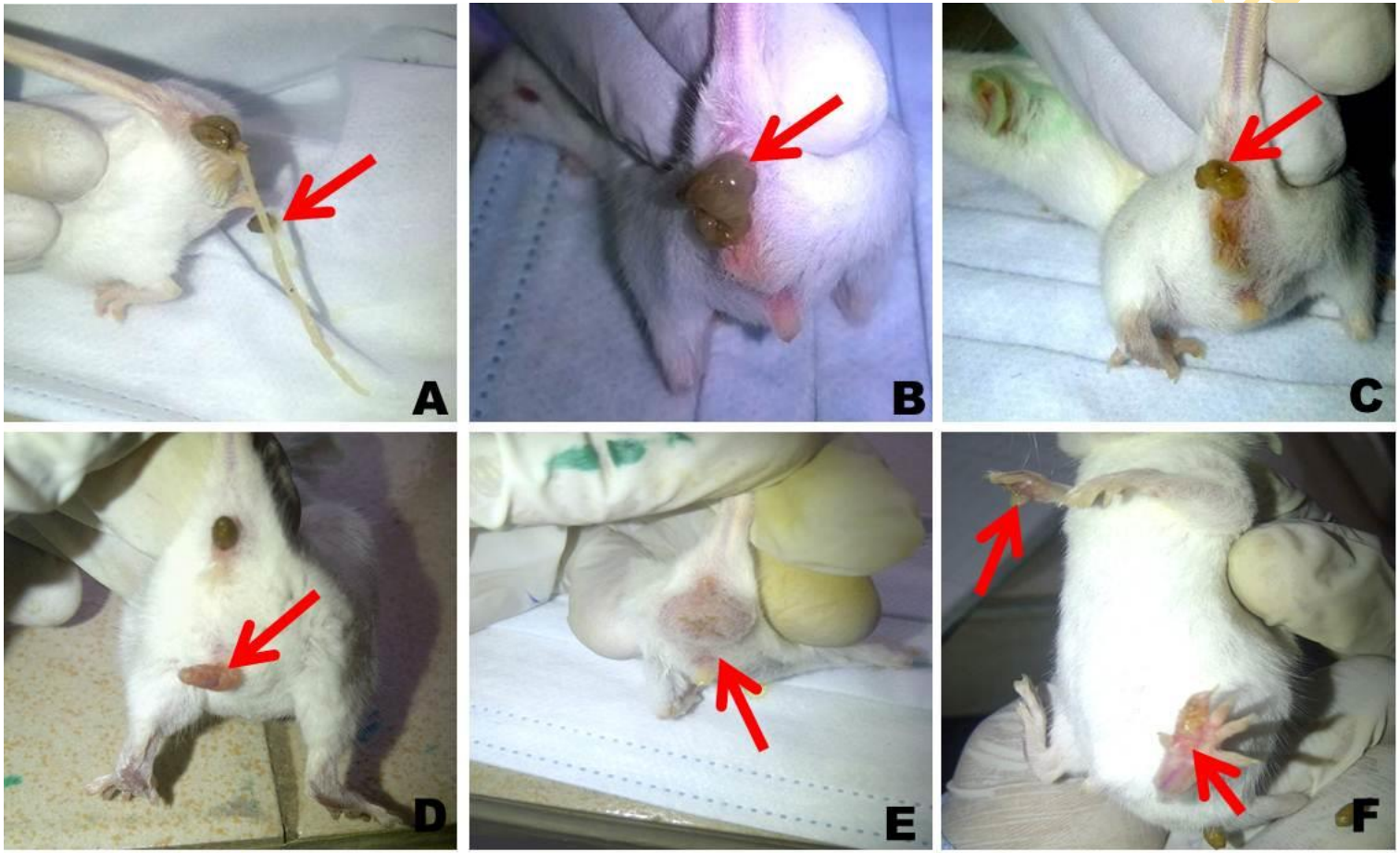

Figure 4. 2: Representatives of some clinical signs of acute toxicity. Mice treated with 300 $mgkg^{-1}$ of TiO_2 NPs exhibited severe mucus discharge 96 hours post treatment (A); mice treated with 150 $mgkg^{-1}$ of ZnO NPs exhibited severe stool 2 hours post treatment (B); mild mucus discharge 24 hours post treatment (C); and those treated with 300 $mgkg^{-1}$ of ZnO NPs exhibited swollen penis 12 days post treatment (D); hard scrotum (E); and abscesses in both fore and hind limbs (F) 10 days post treatment.

4.3. Micronuclei induced by titanium dioxide, zinc oxide nanoparticles and their mixture in mice for 5 and 10 days

The frequencies of micronucleus induced in the bone marrow cells of mice treated with TiO_2, ZnO NPs and their mixture are presented in Figures 4.3 – 4.8. The frequency of micronucleated polychromatic erythrocyte (MNPCE) (Figure 4.9) in mice treated with TiO_2 NPs at doses of 9.38, 18.75, 37.50, 75.00 and 150.00 $mgkg^{-1}$ for 5 days was 16.75 ± 2.14, 20.25 ± 1.89, 30.00 ± 2.31, 31.33 ± 5.55 and 36.00 ± 9.29 respectively. A dose-dependent increase was found in the frequency of MNPCEs, which was significant at 18.75 ($p < 0.05$), 37.50 ($p < 0.01$), 75.00 ($p < 0.01$) and 150.00 $mgkg^{-1}$ ($p < 0.001$) when in comparison with mice treated with distilled water (3.67±0.88). For the 10-day exposure period, the frequency of MNPCEs observed in the mice was 4.25 ± 1.03, 6.33 ± 0.88, 8.67 ± 1.45, 9.25 ± 0.63 and 22.00 ± 1.53 corresponding to the respective doses. However, there was a significant increase only at the 150 $mgkg^{-1}$ ($p < 0.001$) in comparison with the mice treated with distilled water (7.00 ± 1.16). Consequently, there was a significant difference between the 5- and 10- day exposure periods of MNPCE induced at the 9.38 ($p < 0.05$), 18.75 ($p < 0.05$), 37.50 ($p < 0.001$), 75.00 ($p < 0.001$) and 150.00 $mgkg^{-1}$ ($p < 0.05$) of TiO_2 NPs administered to the mice (Figure 4.3).

The percentage PCE: NCE in mice treated with TiO_2 NPs at the doses of 9.38, 18.75, 37.50, 75.00 and 150.00 $mgkg^{-1}$ for 5 days was 99.21 ± 4.18, 88.20 ± 11.75, 81.85 ± 8.75, 55.79 ± 7.06 and 39.22 ± 6.32 respectively. Statistical analysis showed a significant decrease of PCE at 9.38 ($p < 0.05$), 18.75 ($p < 0.01$), 37.50 ($p < 0.01$), 75.00 ($p < 0.001$) and 150.00 $mgkg^{-1}$ ($p < 0.001$) in comparison with the mice treated with distilled water (151.7 ± 19.88). For the 10-day exposure period, there was a 178.9 ± 26.87, 70.52 ± 7.49, 64.02 ± 9.94 and 61.01 ± 8.24 reduction of PCEs in the mice treated with 18.75, 37.50, 75.00 and 150.00 $mgkg^{-1}$, except for 9.38 $mgkg^{-1}$ (223.8 ± 26.98) that showed no signifanct increase. A significant decrease was observed only at 37.50 ($p < 0.001$), 75.00 ($p < 0.001$) and 150 $mgkg^{-1}$ ($p < 0.001$) when in comparison with the mice treated with distilled water (188.7 ± 16.65). Furthermore, significance was observed between the 5- and 10- day exposure period of percentage PCE: NCE at the 9.38 $mgkg^{-1}$ ($p < 0.001$) and 18.75 ($p < 0.001$) of TiO_2 NPs administered to the mice (Figure 4.4).

The frequency of MNPCE in mice treated with ZnO NPs at the doses of 9.38, 18.75, 37.50, 75.00 and 150.00 $mgkg^{-1}$ for 5 days was 3.00 ± 1.00, 5.50 ± 1.19, 7.00 ± 0.58, 6.75 ± 0.63 and 5.00 ± 1.53 respectively. For the 10- day exposure period, the frequcency of MNPCEs observed in the mice was 2.75 ± 0.75, 4.75 ± 0.48, 5.00 ± 0.71, 6.00 ± 0.71 and 8.00 ± 1.16 corresponding to the respective doses. A decrease was observed across all treatment groups, with a statistical significance ($p < 0.05$) only at the 9.38 $mgkg^{-1}$ in comparison with mice treated with distilled water (Figure 4.5).

The percentage PCE: NCE in mice treated with ZnO NPs at the doses of 9.38, 18.75, 37.50, 75.00 and 150.00 $mgkg^{-1}$ for 5- days was 173.4 ± 17.45, 142 ± 13.47, 117 ± 8.95, 160.3 ± 8.54 and 37.10 ± 14.18. Statistical analysis showed a significant decrease ($p < 0.001$) of PCE only at the 150.00 $mgkg^{-1}$ in comparison with the mice treated with distilled water (151.7 ± 19.88). For the 10- day exposure period, there was a 94.91 ± 19.87, 108.3 ± 34.53, 157.7 ± 33.82, 226.7 ± 44.81 and 219.4 ± 75.03 reduction of PCEs in the mice treated with the respective doses. Subsequently, significance was observed between the 5- and 10- day exposure periods of PCE: NCE at the 150 $mgkg^{-1}$ ($p < 0.01$) of ZnO NPs administered to the mice (Figure 4.6).

The frequency of MNPCE in mice treated with the mixture at the doses of 9.38, 18.75, 37.50, 75.00 and 150.00 $mgkg^{-1}$ for 5 days was 2.67 ± 0.33, 1.00 ± 0.00, 0.75 ± 0.25, 0.50 ± 0.29 and 0.75 ± 0.25, respectively. There was no significant decrease ($p > 0.05$) at tested doses in comparison with the mice treated with distilled water. For the 10- day exposure period, the frequency of MNPCEs observed in the treated mice was 7.33 ± 0.88, 11.33 ±1.33, 10.33 ± 1.45, 8.67 ± 0.88 and 8.67 ± 0.88 corresponding to the respective doses. Significance was observed between the 5- and 10- day exposure period of MNPCE induction at the 9.38 ($p < 0.05$), 18.75 ($p < 0.001$), 37.50 ($p < 0.001$), 75.00 ($p < 0.001$) and 150 $mgkg^{-1}$ ($p < 0.001$) of their mixture administered to the mice (Figure 4.7).

The percentage PCE: NCE in mice treated with the mixture at the doses of 9.38, 18.75, 37.50, 75.00 and 150.00 $mgkg^{-1}$ for 5 days was 110 ± 25.84, 232.2 ± 15.96, 226.7 ± 41.79, 192.8 ± 43.02 and 132 ± 16.7. For the 10- day exposure period, there was a 91.21 ± 7.98, 44.18 ± 16.60, 75.27 ± 15.03, 42.47 ± 9.60 and 111.3 ± 31.04 reduction of PCEs in the treated mice corresponding to the respective doses. Statistically, there was no significant

difference across all doses except at the 9.38 $mgkg^{-1}$ where there was a slight decrease in comparison with the mice treated with distilled water for the 5- day exposure period. In contrast, a significant decrease was observed at 9.38 ($p < 0.01$), 18.75 ($p < 0.001$), 37.50 ($p < 0.001$), 75.00 ($p < 0.001$) and 150.00 $mgkg^{-1}$ ($p < 0.05$) in comparison with the mice treated with distilled water at the 10-day exposure period. Consequently, significance between the 5- and 10- day exposure period of PCE: NCE was shown at the doses of 18.75 ($p < 0.001$), 37.50 ($p < 0.001$) and 75.00 ($p < 0.001$) administered to the mice (Figure 4.8).

4.3.1 Cytomorphological alterations induced by titanium dioxide, zinc oxide nanoparticles and their mixture in the bone marrow cells of mice.

Morphological changes detected in the bone marrow cells in mice treated with TiO_2, ZnO NPs and their mixture are presented in Figure 4.10. The majority of the erythrocytes observed were normochromic normocytic with very few blebbed NCEs at the 9.38 $mgkg^{-1}$ of TiO_2 NPs; microcytic normochromic with few hypochromic NCEs and blebbed NCEs at the 18.75 $mgkg^{-1}$ of TiO_2 NPs. Microcytic normochromic with few hypochromic and normocytic NCEs were observed in mice treated at the 37.50 $mgkg^{-1}$ of TiO_2 NPs. In addition, microcytic normochromic and few macrocytic NCEs and blebbed NCEs were observed in the bone marrow cells in mice treated at 75.00 $mgkg^{-1}$ of TiO_2 NPs. NCEs observed were dimorphic having a combination of macrocytic and microcytic NCEs, with hyperchromic and blebbed NCEs at 150.00 $mgkg^{-1}$ of TiO_2 NPs. Normochromic normocytic NCEs were observed at 9.38, 18.75 and 37.50 $mgkg^{-1}$ of ZnO NPs. Normochromic, microcytic with few hyperchromic and macrocytic NCEs were observed at 75.00 and 150.00 $mgkg^{-1}$ of ZnO NPs.

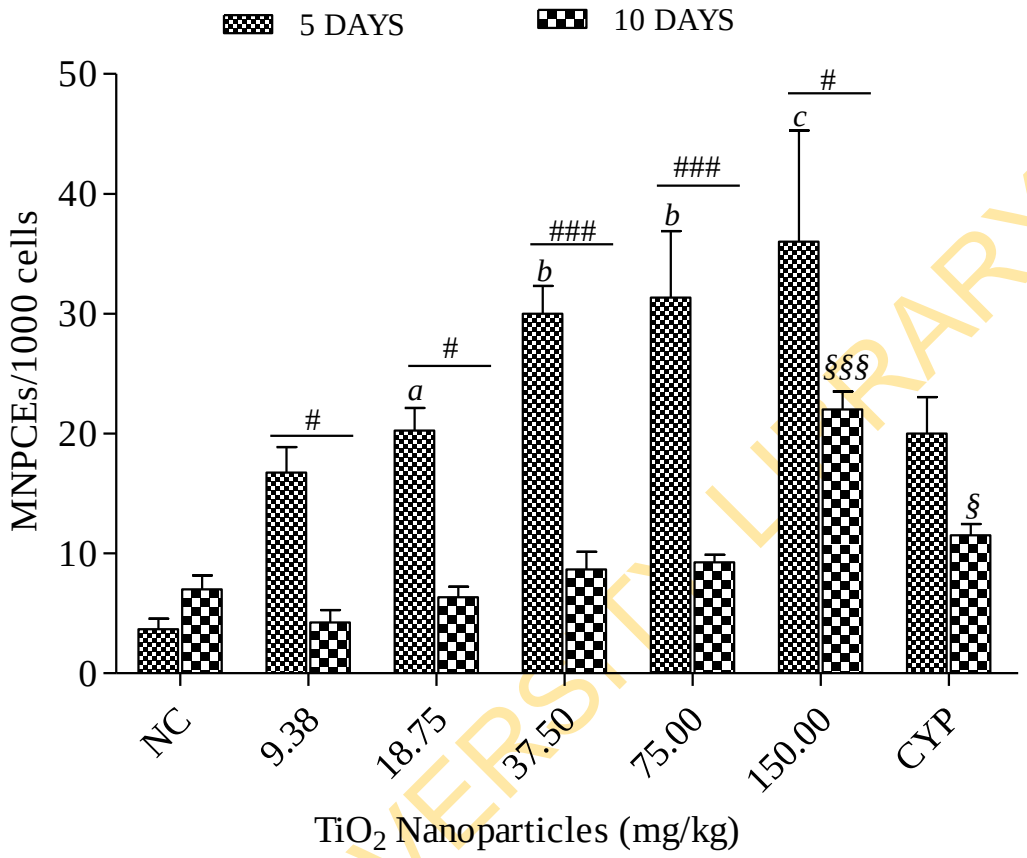

Figure 4. 2: Frequency of MN induction in the bone marrow cells of mice treated with TiO_2 NPs at 5- and 10-days.

NC = distilled water, CYP = cyclophosphamide (positive control). Data represents mean ± SE (n=4).

[a] $p < 0.05$, [b] $p < 0.01$ and [c] $p < 0.001$ in 5-days exposure

[§] $p < 0.05$ and [§§§] $p < 0.001$ in 10-days exposure

[#] $p < 0.05$ and [###] $p < 0.001$ for the comparison between 5- and 10-days exposures

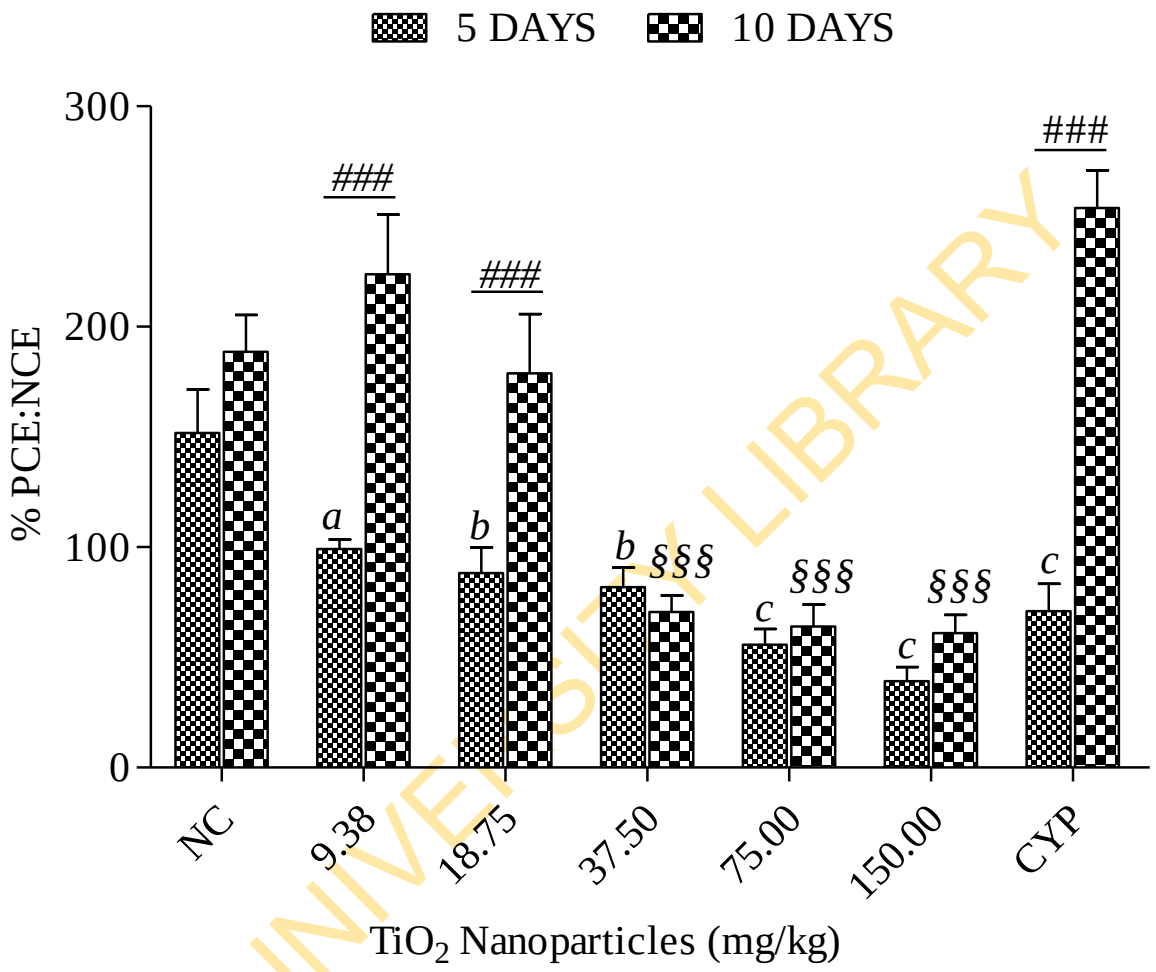

Figure 4. 3: Percentage PCE: NCE in the bone marrow cells of mice treated with TiO_2 NPs at 5- and 10-days.

NC = distilled water, CYP = cyclophosphamide (positive control). Data represents mean ± SE (n=4).

[a] $p < 0.05$, [b] $p < 0.01$ and [c] $p < 0.001$ in 5-days exposure

[§§§] $p < 0.001$ in 10-days exposure

[###] $p < 0.001$ for the comparison between 5- and 10-days exposures

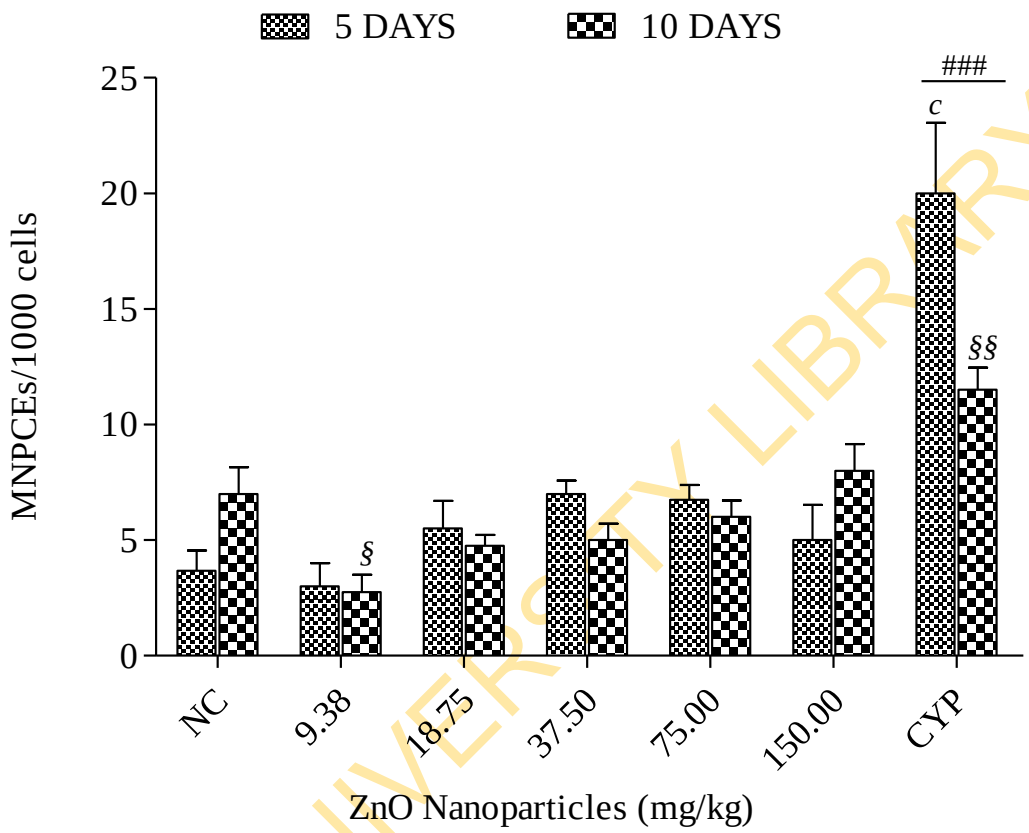

Figure 4. 4: Frequency of MN induction in the bone marrow cells of mice treated with ZnO NPs at 5- and 10-days.

NC = distilled water, CYP = cyclophosphamide (positive control). Data represents mean ± SE (n=4).

[c] $p < 0.001$ in 5-days exposure

[§] $p < 0.01$ and [§§] $p < 0.01$ in 10-days exposure

[###] $p < 0.001$ for the comparison between 5- and 10-days exposures

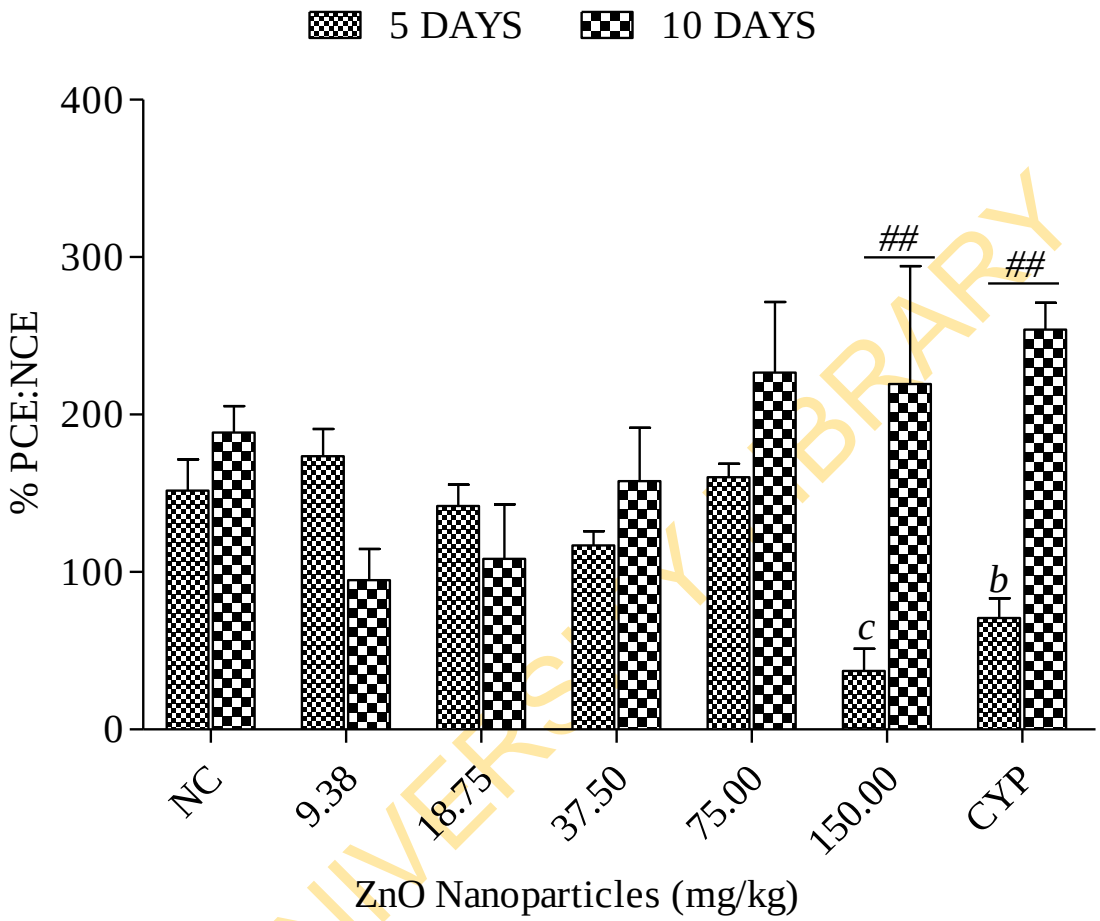

Figure 4. 5: Percentage PCE: NCE in the bone marrow cells of mice treated with ZnO NPs at 5- and 10-days.

NC = distilled water, CYP = cyclophosphamide (positive control). Data represents mean ± SE (n=4).

[b] $p < 0.01$ and [c] $p < 0.001$ in 5-days exposure

[##] $p < 0.01$ for the comparison between 5- and 10-days exposures

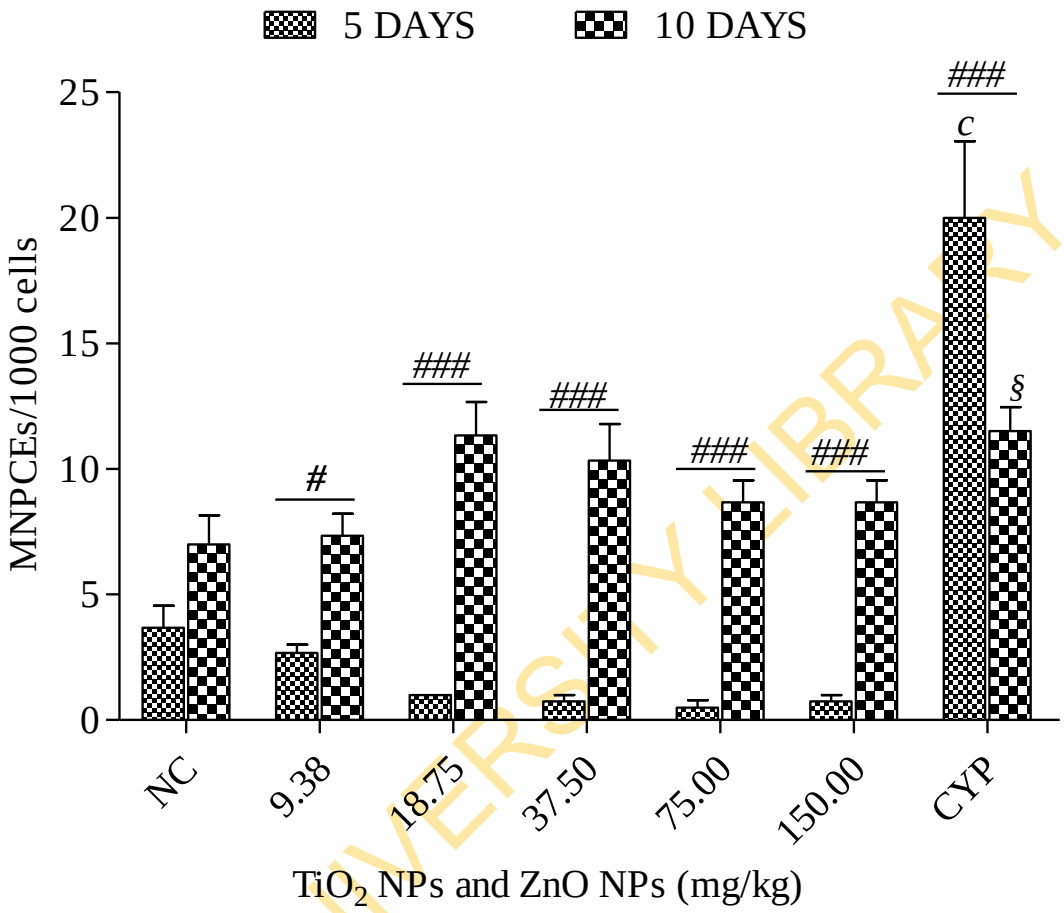

Figure 4. 6: Frequency of MN induction in the bone marrow cells of mice treated with TiO_2 and ZnO NPs at 5- and 10-days.

NC = distilled water, CYP = cyclophosphamide (positive control). Data represents mean ± SE (n=4).

[c] $p < 0.001$ in 5-days exposure

[§] $p < 0.05$ in 10-days exposure

[#] $p < 0.05$ and [###] $p < 0.001$ for the comparison between 5- and 10-days exposures

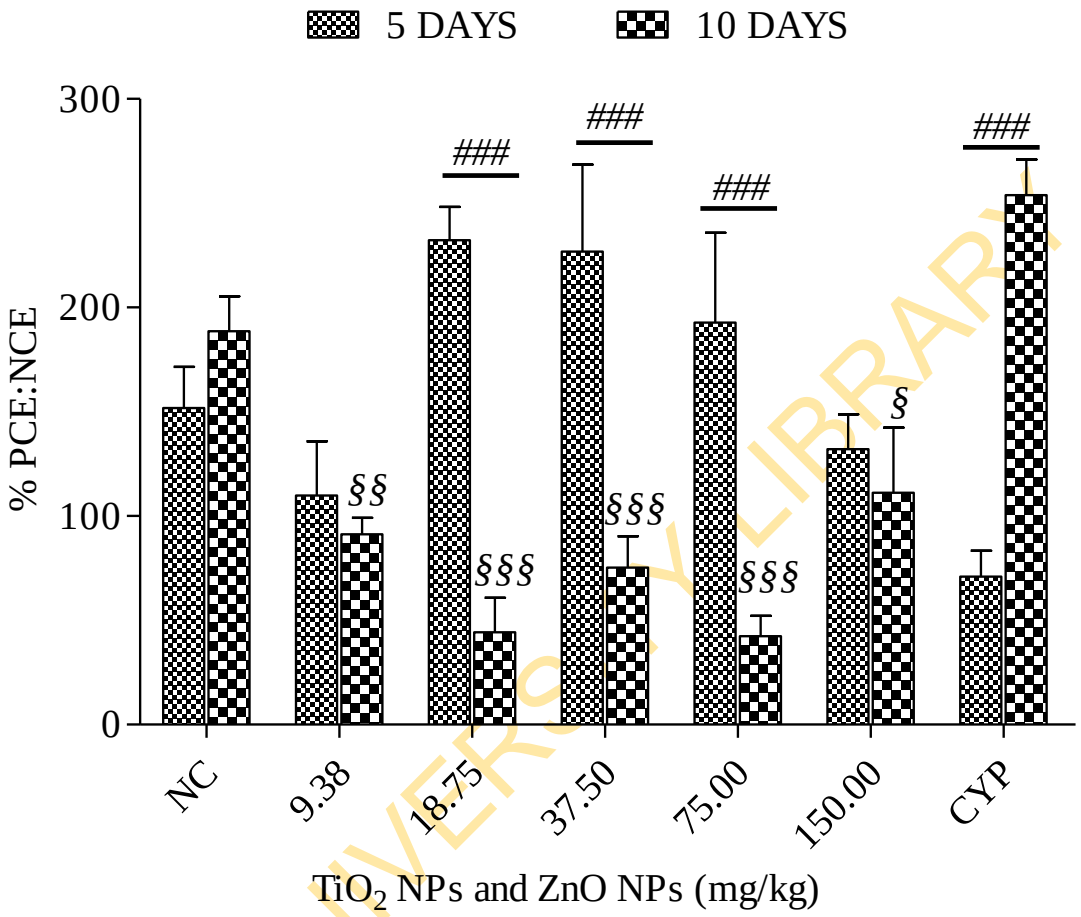

Figure 4. 7: Percentage PCE: NCE in the bone marrow cells of mice treated with TiO_2 and ZnO NPs at 5- and 10-days.

NC = distilled water, CYP = cyclophosphamide (positive control). Data represents mean ± SE (n=4).

§ $p < 0.05$, §§ $p < 0.01$ and §§§ $p < 0.001$ in 10-days exposure

$^{\#\#\#}$ $p < 0.001$ for the comparison between 5- and 10-days exposures

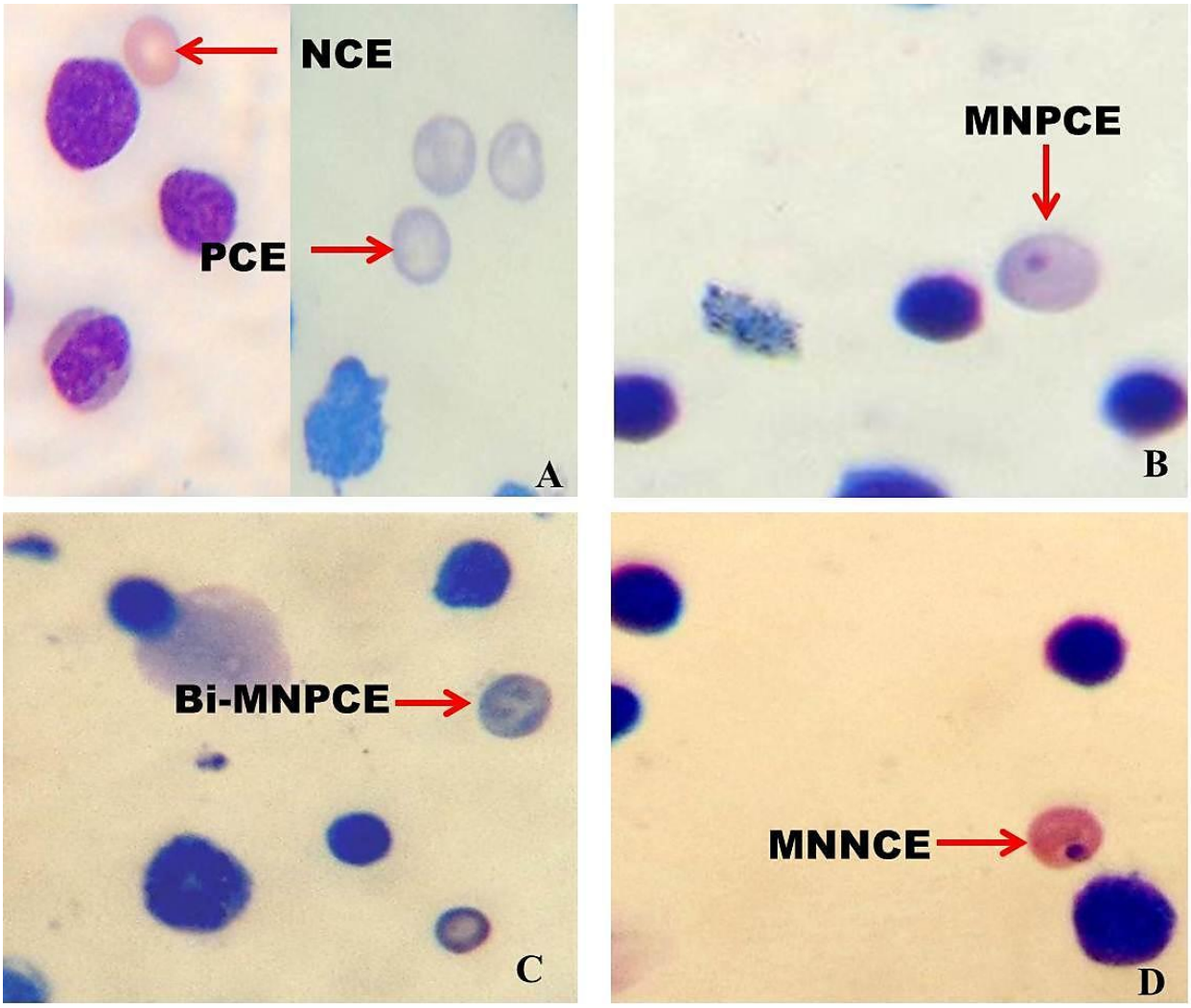

Figure 4. 8: Bone marrow cells stained with May-Grunwald and Giemsa stains. NCE: normochromatic erythrocyte, PCE: polychromatic erythrocyte, MNPCE: micronucleated polychromatic erythrocyte, Bi-MNPCE: bi-micronucleated polychromatic erythrocyte and MNNCE: micronucleated normochromatic erythrocyte.

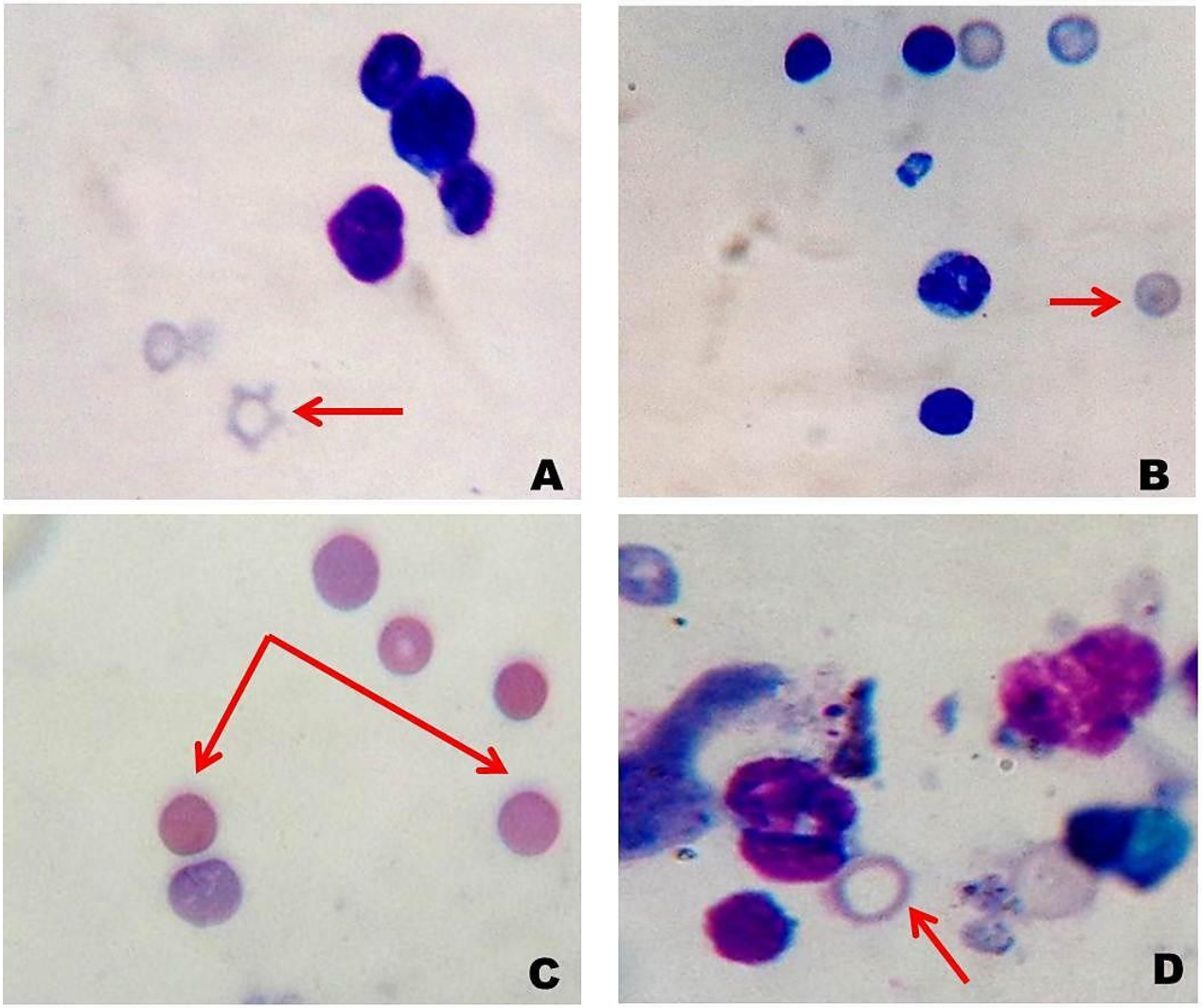

Figure 4. 9: Bone marrow cells stained with May-Grunwald and Giemsa stains showing cytomorphological alterations. A: blebbed PCE; B: target NCE; C: hyperchromic macrocytic NCEs; D: hypochromic NCE.

4.3.2 Interactive effects of titanium dioxide and zinc oxide nanoparticles for 5 and 10 days

The interaction factors (IF) for the frequency of MNPCE and percentage PCE: NCE is presented in Table 4.3. An antagonistic effect at all doses was obtained in the MNPCE and a synergistic effect at all doses except the 9.38 $mgkg^{-1}$ for the percentage PCE: NCE of the bone marrow cells of the mice for the 5- day exposure period. However, a synergistic effect was obtained at doses of the 9.38 to 75.00 $mgkg^{-1}$ and an antagonistic effect at 150.00 $mgkg^{-1}$ in the frequency of MNPCE while an antagonistic effect was observed at 9.350; 18.75 and 75.00 $mgkg^{-1}$ and a synergistic effect at 37.50 and 150.00 $mgkg^{-1}$ for the 10- day exposure period.

4.4 Systemic toxicity induced by titanium dioxide, zinc oxide nanoparticles and their mixture in mice for 5 and 10 days

4.4.1 Macroscopic examinations and gross pathology in treated mice

All mice in the treated groups appeared to be in good health and behaved no differently from the negative control. After sacrifice, it was observed that both NPs and their mixture were found to have agglomerated around the organs within the abdominal cavity at doses of 37.50, 75.00 and 150.00 $mgkg^{-1}$ (Figure 4.11). However, little or no residues of agglomerated NPs were present around these organs of the treated mice for the 10- day exposure.

Gross pathology of the liver and spleen in the mice treated with TiO_2, ZnO NPs and their mixture are presented in Figures 4.12 and 4.13.The liver is reddish brown in colour with a shiny surface (Figure 4.12A) while the spleen is highly vascularised and appears dark red in colour (Figure 4.13A). The liver and spleen of the mice treated with TiO_2 NPs at the 5- and 10- day exposure periods were macroscopically normal across tested doses. However, mice treated with 150.00 $mgkg^{-1}$ of ZnO NPs for 5 days showed that their livers were pale in colour with accentuated lobular pattern (Figure 4.12B) while their spleens were abnormally enlarged having lymphoid follicles (Figure 4.13B). Subsequently, mice treated with 9.38 – 75.00 $mgkg^{-1}$ of ZnO NPs at the 5- and 10- day exposures did not show any abnormal macroscopic appearance of the organs.

Table 4. 3: Interaction factor (IF) of titanium dioxide and zinc oxide nanoparticles calculated using the MNPCE and percentage PCE: NCE in mice for 5 and 10 days

EXPOSURE PERIODS	**5 DAYS**		**10 DAYS**	
Doses ($mgkg^{-1}$)	MNPCE IF ± SE_{IF}	% PCE: NCE IF ± SE_{IF}	MNPCE IF ± SE_{IF}	% PCE: NCE IF ± SE_{IF}
9.38	-13.41 ± 2.54	-10.91 ± 37.21	7.33 ± 1.93	-38.80 ± 38.26
18.75	-21.08 ± 2.40	153.70 ± 31.14	7.25 ± 2.03	-54.32± 49.67
37.50	-32.58 ± 2.55	179.55± 47.94	3.66 ± 2.46	35.75 ± 41.27
75.00	-33.91 ± 5.66	128.41 ± 48.67	0.42 ± 1.74	-59.55 ± 49.76
150.00	-36.58 ± 9.46	207.38 ± 30.25	-14.33 ± 2.41	19.58 ± 83.30

Also, mice treated with 9.38 - 37.50 $mgkg^{-1}$ of their mixture at both 5- and 10- days did not show any macroscopic abnormalities except at the 75.00 $mgkg^{-1}$ for the 10- day exposure which induced a massive tumour in the liver (Figure 4.12C) and a small spleen with dark red colouration (Figure 4.13C).

4.4.2 Absolute and relative organ weights of mice treated with titanium dioxide, zinc oxide nanoparticles and their mixture

The absolute and relative organ weights of the liver, kidneys, spleen, brain and heart of treated mice for 5 and 10 days are presented in Tables 4.4 – 4.13. Generally, mice treated with TiO_2, ZnO NPs and their mixture for the 5- day exposure period did not show any significant ($p > 0.05$) reduction in the absolute liver weights except at the 37.50 and 150.00 $mgkg^{-1}$ of TiO_2 NPs; and 75.00 $mgkg^{-1}$ of their mixture, which showed increased weights in comparison with the mice treated with distilled water. A significant ($p < 0.01$) reduction was observed only at the 150.00 $mgkg^{-1}$ of the mixture. Likewise, a significant ($p < 0.05$) reduction of the relative liver weight was observed only at the 75.00 and 150.00 $mgkg^{-1}$ of ZnO NPs; and 18.75 $mgkg^{-1}$ of their mixture in comparison with the mice treated with distilled water (Table 4.4).

TiO_2 and ZnO NPs administered to the mice did not induce significant ($p > 0.05$) reduction of both absolute and relative spleen weights except at the 75.00 $mgkg^{-1}$ of TiO_2 NPs compared with mice treated with distilled water for the 5- day exposure period. However, a significant reduction was observed at the 9.38 ($p < 0.01$), 18.75 ($p < 0.01$) and 37.50 $mgkg^{-1}$ ($p < 0.001$) of their mixture for the absolute spleen weights; at the 9.38 ($p < 0.01$), 18.75 ($p < 0.01$), 37.50 ($p < 0.001$) and 75.00 $mgkg^{-1}$ ($p < 0.05$) of their mixture for the relative spleen weights of the treated mice (Table 4.5). For the 5- day exposure period, mice treated with both NPs and their mixture exhibited a significant ($p < 0.01$) increase in the absolute kidney weight at the 37.50 and 150.00 $mgkg^{-1}$ of TiO_2 NPs; at the 75.00 and 150.00 $mgkg^{-1}$ of ZnO NPs; and at the 75.00 $mgkg^{-1}$ of their mixture. However, a significant increase of relative kidney weight was observed only at the 75.00 ($p < 0.01$) and 150.00 $mgkg^{-1}$ ($p < 0.05$) of ZnO NPs administered to the mice compared with those treated with distilled water (Table 4.6).

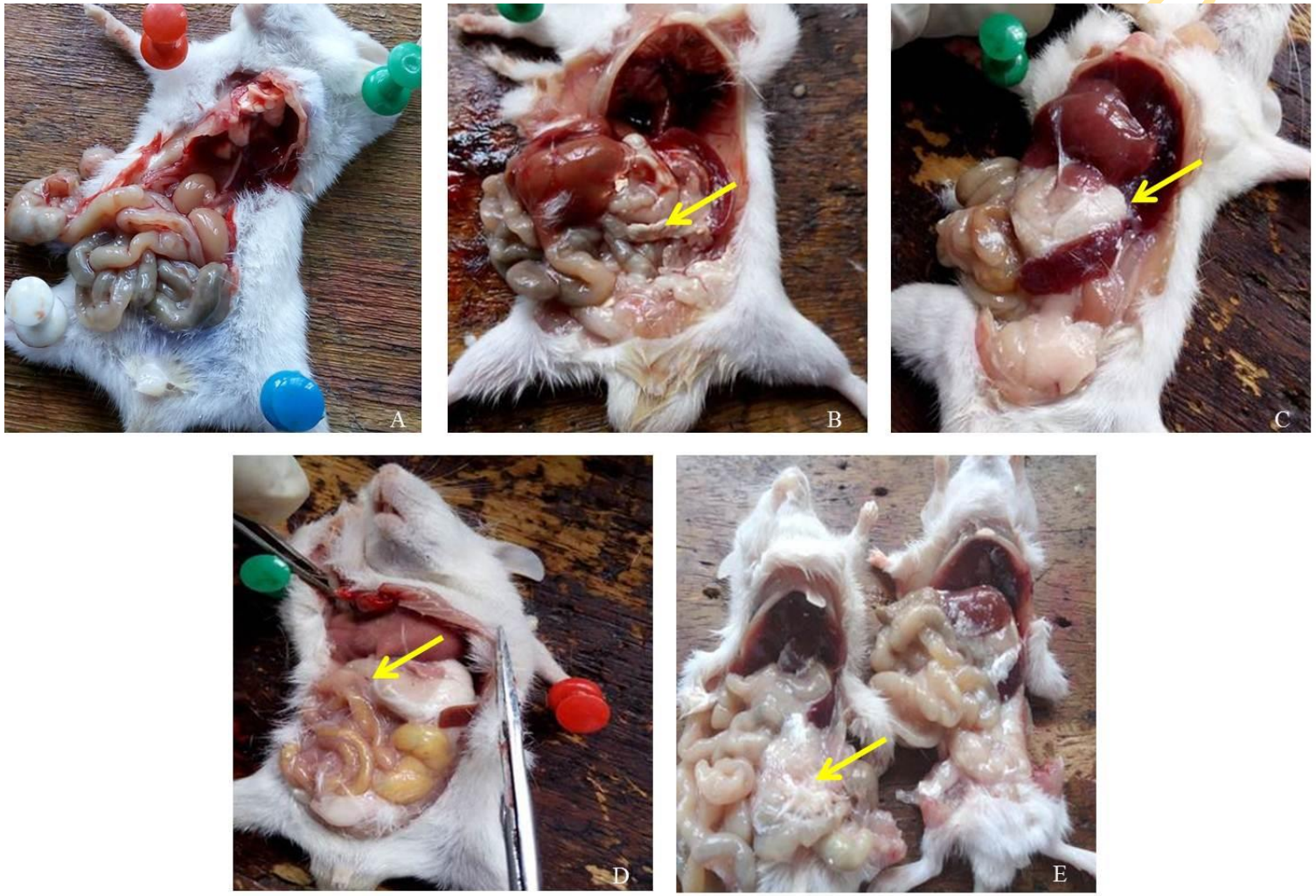

Figure 4. 10: Mouse treated with distilled water (A); mice showing residues of agglomerated 150 $mgkg^{-1}$ of TiO_2 NPs (yellow arrow) (B); 75 $mgkg^{-1}$ of ZnO NPs (C); 150.00 $mgkg^{-1}$ of ZnO NPs (D) 150.00 $mgkg^{-1}$ of their mixture (E) after 5- days exposure.

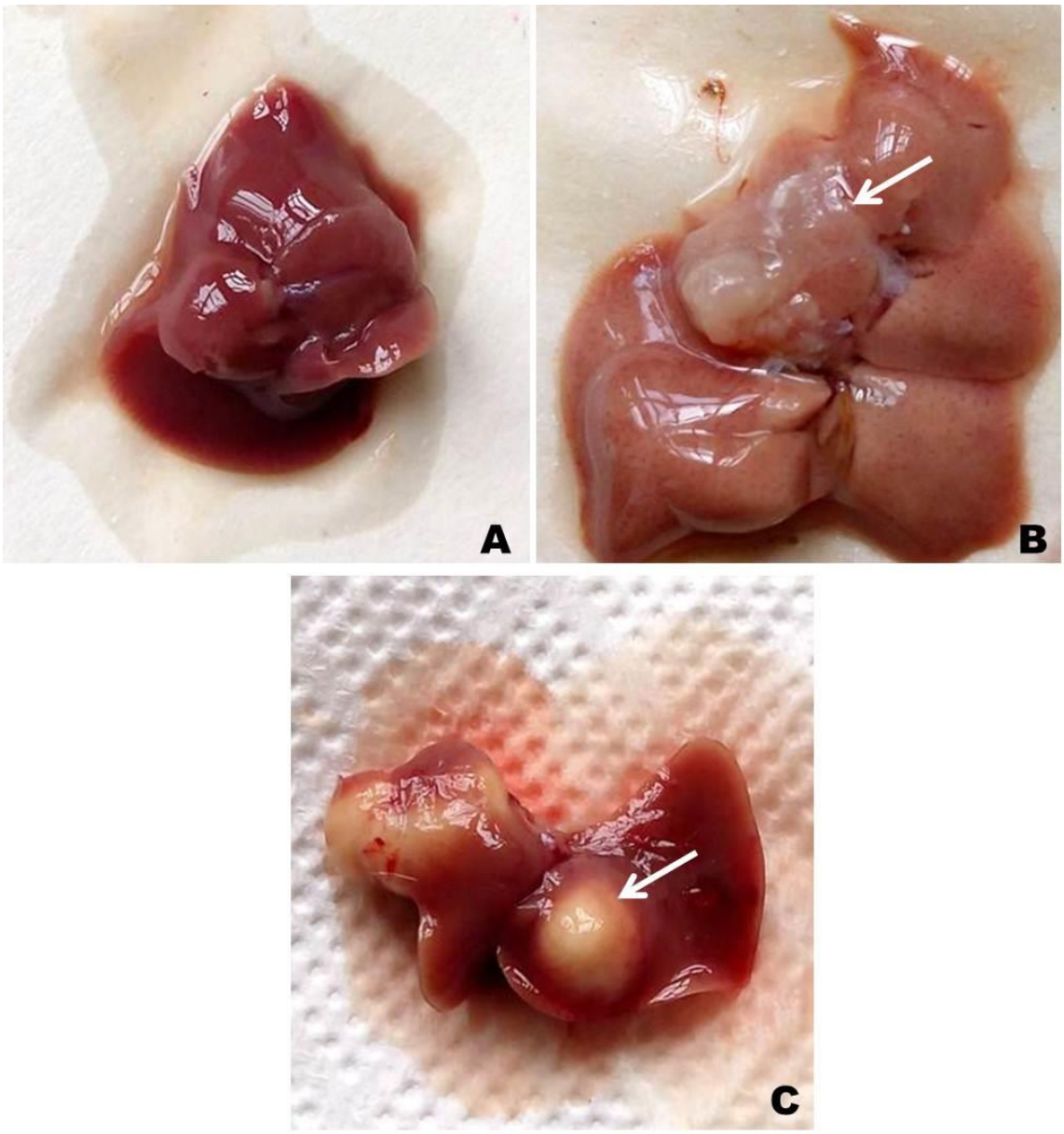

Figure 4. 11: Gross pathology of the liver of treated mice. Liver of mouse treated with distilled water (A); mouse treated with 150 $mgkg^{-1}$ of ZnO NPs after 5 days showing discolouration of the liver with accentuated lobular pattern (B); mouse treated with 75.00 $mgkg^{-1}$ of their mixture after 10- days showing a liver with a tumour (C). Scale bar: 1.05 x 10^{8} nm.

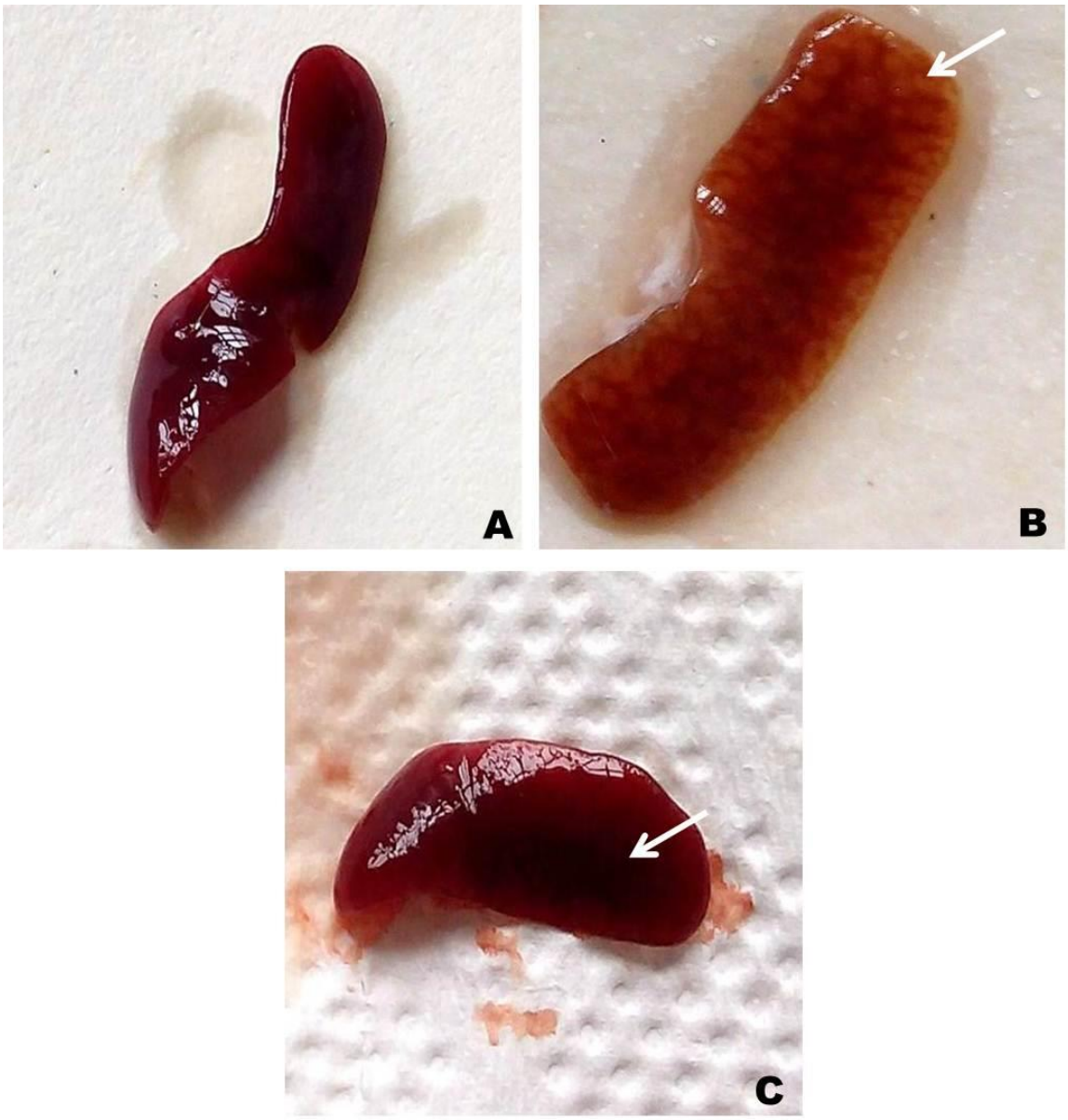

Figure 4. 12: Gross pathology of the spleen of treated mice. Spleen of mouse treated with distilled water (A); abnormal enlargement of the spleen with lymphoid follicles (B) in mouse treated with ZnO NPs (150.00 $mgkg^{-1}$) after 5 days exposure. Abnormally darkened spleen (C) of mouse treated with their mixture (75.00 $mgkg^{-1}$) after 10 days exposure. Scale bar: 1.35 x 10^{8} nm.

TiO_2, ZnO NPs and their mixture induced no significant ($p > 0.05$) decrease in the absolute weights of the brain of the treated mice except at the 75.00 $mgkg^{-1}$ of ZnO NPs that caused a significant ($p < 0.05$) reduction in comparison with the mice treated with distilled water. In addition, no significant ($p > 0.05$) decrease in the relative brain weight was observed across tested doses in mice treated with both NPs and their mixture except at the 9.38 $mgkg^{-1}$ of TiO_2 NPs and ZnO NPs, and 150 $mgkg^{-1}$ of their mixture (Table 4.7). For the 5- day exposure period, TiO_2 NPs administered to the mice did not induce a significant ($p > 0.05$) increase in the absolute weight of the heart at the 18.75, 37.50 and 150.00 $mgkg^{-1}$ and a decrease at the 9.38 and 75.00 $mgkg^{-1}$; ZnO NPs induced no significant ($p > 0.05$) decrease at the 9.38, 18.75 and 37.50 $mgkg^{-1}$ and an increase at the 75.00 and 150.00 $mgkg^{-1}$; and their mixture induced no significant increase at the 9.38 and 75.00 $mgkg^{-1}$ and a decrease at the 18.75, 37.50 and 150.00 $mgkg^{-1}$ in comparison with the mice treated with distilled water. Likewise, no significant ($p > 0.05$) reduction of the relative heart weights was observed across tested doses except at the 37.50 and 150.00 $mgkg^{-1}$ of TiO_2 NPs; at the 75.00 and 150.00 $mgkg^{-1}$ of ZnO NPs; and at the 9.38 and 150.00 $mgkg^{-1}$ of their mixture, which induced no significant ($p > 0.05$) increase in comparison with the mice treated with distilled water (Table 4.8).

For the 10- day exposure period, mice treated with TiO_2 NPs exhibited a significant ($p < 0.05$) reduction in the absolute liver weight only at the 37.50 and 150.00 $mgkg^{-1}$ in comparison with the mice treated with distilled water. In addition, a significant reduction in the relative liver weight was observed only at the 75.00 $mgkg^{-1}$ ($p < 0.01$) of TiO_2 NPs; and 9.38 ($p < 0.001$), 18.75 ($p < 0.001$), 37.50 ($p < 0.01$), 75.00 ($p < 0.05$) and 150.00 ($p < 0.05$) $mgkg^{-1}$ of their mixture in comparison with the mice treated with distilled water (Table 4.9). Mice treated with both NPs and their mixture exhibited no significant ($p > 0.05$) reduction in the absolute spleen weight across tested doses except at the 37.50 $mgkg^{-1}$ ($p < 0.01$) of TiO_2 NPs, which showed a significant reduction in comparison with mice treated with distilled water. Also, a significant ($p < 0.05$) reduction in the relative weight of the spleen was observed only at the 37.50 and 150.00 $mgkg^{-1}$ of TiO_2 NPs; 9.38 $mgkg^{-1}$ of ZnO NPs; and 75.00 $mgkg^{-1}$ of their mixture in the treated mice in comparison with mice treated with distilled water (Table 4.10).

TiO_2 NPs administered to mice induced no significant reduction ($p > 0.05$) in the absolute kidney weight across all doses; no significant ($p > 0.05$) decrease at the 18.75 and 37.50 $mgkg^{-1}$ while an increase at the 9.38, 75.00 and 150.00 $mgkg^{-1}$ of their mixture. In contrast, no significant ($p > 0.05$) increase at the 9.38, 18.75, 37.50 and 150.00 $mgkg^{-1}$ and a decrease at the 75.00 $mgkg^{-1}$ of ZnO NPs in comparison with the mice treated with distilled water was observed. Subsequently, TiO_2, ZnO NPs and their mixture also induced no significant ($p > 0.05$) reduction in the relative kidney weight across all doses except at the 37.50 $mgkg^{-1}$ of TiO_2 NPs; and 18.75 and 37.50 $mgkg^{-1}$ of ZnO NPs that showed increase in comparison with the mice treated with distilled water (Table 4.11). TiO_2, ZnO NPs and their mixture administered to mice induced no significant ($p > 0.05$) reduction in the absolute weights of the brain across tested doses in comparison with the mice treated with distilled water. In addition, no significant ($p > 0.05$) reduction in the relative brain weight was observed across tested doses except at the 18.75 $mgkg^{-1}$ of both ZnO NPs and their mixture that showed significance ($p < 0.05$) in comparison with the mice treated with distilled water (Table 4.12).

TiO_2 NPs administered to mice induced no significant ($p > 0.05$) decrease in the absolute heart weight across tested doses except at the 150.00 $mgkg^{-1}$ that showed an increase; ZnO NPs induced no significant ($p > 0.05$) increase at the 18.75, 37.50 and 150.00 $mgkg^{-1}$ while a decrease at the 9.38 and 75.00 $mgkg^{-1}$; and their mixture induced no significant ($p > 0.05$) increase across all the doses. Similarly, both NPs and their mixture administered to the mice induced no significant ($p > 0.05$) reduction of the relative heart weight across all the doses except at the 75.00 $mgkg^{-1}$ of their mixture that induced no significant ($p > 0.05$) increase in comparison with the mice treated with distilled water (Table 4.13).

Table 4. 4: Absolute and percentage relative liver weight in mice treated with titanium dioxide, zinc oxide nanoparticles and mixture for 5 days.

TiO_2 NPs		
Doses ($mgkg^{-1}$)	**Absolute liver weight (g)**	**Relative liver weight (%)**
NC	1.32 ± 0.07	6.07 ± 0.34
9.38	1.14 ± 0.05	6.00 ± 0.28
18.75	1.21 ± 0.09	5.47 ± 0.56
37.50	1.56 ± 0.08	5.75 ± 0.27
75.00	1.29 ± 0.10	5.85 ± 0.51
150.00	1.35 ± 0.19	5.14 ± 0.91
CYP	1.30 ± 0.14	6.34 ± 0.59
ZnO NPs		
NC	1.32 ± 0.07	6.07 ± 0.34
9.38	1.19 ± 0.04	5.66 ± 0.17
18.75	1.32 ± 0.08	5.65 ± 0.27
37.50	1.22 ± 0.06	5.58 ± 0.27
75.00	1.07 ± 0.10	4.65 ± 0.33*
150.00	1.15 ± 0.11	4.62 ± 0.31*
CYP	1.30 ± 0.14	6.34 ± 0.59
Mixture		
NC	1.32 ± 0.07	6.07 ± 0.34
9.38	1.31 ± 0.03	5.73 ± 0.20
18.75	1.14 ± 0.05	4.61 ± 0.10*
37.50	1.18 ± 0.09	4.98 ± 0.18
75.00	1.39 ± 0.08	5.12 ± 0.32
150.00	0.97 ± 0.06**	5.10 ± 0.45
CYP	1.30 ± 0.14	6.34 ± 0.59

Data represent Mean ± SEM (n=5). * $p < 0.05$ and ** $p < 0.01$ in comparison with the mice treated with distilled water. Negative control (NC) = distilled water, CYP = cyclophosphamide (positive control).

Table 4. 5: Absolute and percentage relative spleen weight in mice treated with titanium dioxide, zinc oxide nanoparticles and mixture for 5 days.

TiO_2 NPs		
Doses ($mgkg^{-1}$)	**Absolute spleen weight (g)**	**Relative spleen weight (%)**
NC	0.22 ± 0.03	1.02 ± 0.14
9.38	0.11 ± 0.01	0.59 ± 0.06
18.75	0.15 ± 0.03	0.74 ± 0.12
37.50	0.20 ± 0.04	0.72 ± 0.14
75.00	0.23 ± 0.06	1.04 ± 0.31
150.00	0.22 ± 0.02	0.83 ± 0.04
CYP	0.16 ± 0.02	0.79 ± 0.06
ZnO NPs		
NC	0.22 ± 0.03	1.02 ± 0.14
9.38	0.18 ± 0.04	0.85 ± 0.19
18.75	0.20 ± 0.02	0.88 ± 0.12
37.50	0.21 ± 0.04	0.95 ± 0.17
75.00	0.17 ± 0.03	0.76 ± 0.12
150.00	0.15 ± 0.04	0.58 ± 0.12
CYP	0.16 ± 0.02	0.79 ± 0.06
Mixture		
NC	0.22 ± 0.03	1.02 ± 0.14
9.38	0.11 ± 0.01**	0.50 ± 0.05**
18.75	0.12 ± 0.02**	0.48 ± 0.07**
37.50	0.10 ± 0.01***	0.43 ± 0.04***
75.00	0.17 ± 0.02	0.63 ± 0.11*
150.00	0.16 ± 0.02	0.82 ± 0.09
CYP	0.16 ± 0.02	0.79 ± 0.06

Data represent Mean ± SEM (n=5). * $p < 0.05$, ** $p < 0.01$ and *** $p < 0.001$ in comparison with the mice treated with distilled water. Negative control (NC) = distilled water, CYP = cyclophosphamide (positive control).

Table 4. 6: Absolute and percentage relative kidney weight in mice treated with titanium dioxide, zinc oxide nanoparticles and mixture for 5 days.

TiO_2 NPs		
Doses ($mgkg^{-1}$)	**Absolute kidney weight (g)**	**Relative kidney weight (%)**
NC	0.29 ± 0.02	1.31 ± 0.09
9.38	0.30 ± 0.02	1.61 ± 0.13
18.75	0.31 ± 0.02	1.38 ± 0.13
37.50	0.43 ± 0.05**	1.58 ± 0.17
75.00	0.29 ± 0.01	1.32 ± 0.06
150.00	0.41 ± 0.02**	1.55 ± 0.11
CYP	0.31 ± 0.02	1.54 ± 0.10
ZnO NPs		
NC	0.29 ± 0.02	1.31 ± 0.09
9.38	0.30 ± 0.02	1.44 ± 0.06
18.75	0.33 ± 0.03	1.39 ± 0.11
37.50	0.33 ± 0.01	1.49 ± 0.03
75.00	0.39 ± 0.02**	1.73 ± 0.08**
150.00	0.43 ± 0.05**	1.73 ± 0.17*
CYP	0.31 ± 0.02	1.54 ± 0.10
Mixture		
NC	0.29 ± 0.02	1.31 ± 0.09
9.38	0.32 ± 0.01	1.40 ± 0.02
18.75	0.31 ± 0.01	1.25 ± 0.05
37.50	0.35 ± 0.03	1.52 ± 0.21
75.00	0.39 ± 0.02**	1.41 ± 0.02
150.00	0.28 ± 0.01	1.47 ± 0.06
CYP	0.31 ± 0.02	1.54 ± 0.10

Data represent Mean ± SEM (n=5). * $p < 0.05$ and ** $p < 0.01$ in comparison with the mice treated with distilled water. Negative control (NC) = distilled water, CYP = cyclophosphamide (positive control).

Table 4. 7: Absolute and percentage relative brain weight in mice treated with titanium dioxide, zinc oxide nanoparticles and mixture for 5 days.

TiO_2 NPs		
Doses ($mgkg^{-1}$)	**Absolute brain weight (g)**	**Relative brain weight (%)**
NC	0.40 ± 0.02	1.85 ± 0.11
9.38	0.38 ± 0.02	1.98 ± 0.10
18.75	0.36 ± 0.03	1.75 ± 0.22
37.50	0.38 ± 0.04	1.41 ± 0.15
75.00	0.33 ± 0.02	1.48 ± 0.08
150.00	0.42 ± 0.02	1.61 ± 0.18
CYP	0.39 ± 0.01	1.91 ± 0.16
ZnO NPs		
NC	0.40 ± 0.02	1.85 ± 0.11
9.38	0.40 ± 0.00	1.89 ± 0.04
18.75	0.39 ± 0.01	1.69 ± 0.07
37.50	0.40 ± 0.01	1.84 ± 0.09
75.00	0.34 ± 0.02*	1.50 ± 0.12
150.00	0.39 ± 0.01	1.59 ± 0.11
CYP	0.39 ± 0.01	1.91 ± 0.16
Mixture		
NC	0.40 ± 0.02	1.85 ± 0.11
9.38	0.39 ± 0.01	1.70 ± 0.04
18.75	0.38 ± 0.01	1.52 ± 0.03
37.50	0.40 ± 0.02	1.67 ± 0.04
75.00	0.41 ± 0.01	1.51 ± 0.13
150.00	0.38 ± 0.03	1.98 ± 0.13
CYP	0.39 ± 0.01	1.91 ± 0.16

Data represent Mean ± SEM (n=5). * $p < 0.05$ in comparison with the mice treated with distilled water. Negative control (NC) = distilled water, CYP = cyclophosphamide (positive control).

Table 4. 8: Absolute and percentage relative heart weight in mice treated with titanium dioxide, zinc oxide nanoparticles and mixture for 5 days.

TiO_2 NPs		
Doses ($mgkg^{-1}$)	**Absolute heart weight (g)**	**Relative heart weight (%)**
NC	0.11 ± 0.00	0.52 ± 0.01
9.38	0.08 ± 0.01	0.43 ± 0.03
18.75	0.13 ± 0.01	0.48 ± 0.07
37.50	0.14 ± 0.01	0.53 ± 0.03
75.00	0.11 ± 0.00	0.50 ± 0.02
150.00	0.16 ± 0.02	0.62 ± 0.08
CYP	0.13 ± 0.01	0.65 ± 0.03
ZnO NPs		
NC	0.11 ± 0.00	0.52 ± 0.01
9.38	0.11 ± 0.01	0.52 ± 0.01
18.75	0.11 ± 0.01	0.48 ± 0.03
37.50	0.11 ± 0.00	0.49 ± 0.02
75.00	0.13 ± 0.01	0.59 ± 0.04
150.00	0.14 ± 0.01	0.56 ± 0.03
CYP	0.13 ± 0.01	0.65 ± 0.03*
Mixture		
NC	0.11 ± 0.00	0.52 ± 0.01
9.38	0.12 ± 0.00	0.53 ± 0.03
18.75	0.11 ± 0.01	0.45 ± 0.02
37.50	0.10 ± 0.01	0.44 ± 0.02
75.00	0.14 ± 0.01	0.52 ± 0.02
150.00	0.11 ± 0.00	0.59 ± 0.02
CYP	0.13 ± 0.01	0.65 ± 0.03**

Data represent Mean ± SEM (n=5). * $p < 0.05$ and ** $p < 0.01$ in comparison with the mice treated with distilled water. Negative control (NC) = distilled water, CYP = cyclophosphamide (positive control).

Table 4. 9: Absolute and percentage relative liver weight in mice treated with titanium dioxide, zinc oxide nanoparticles and mixture for 10 days.

TiO_2 NPs		
Doses ($mgkg^{-1}$)	**Absolute liver weight (g)**	**Relative liver weight (%)**
NC	1.48 ± 0.04	6.21 ± 0.21
9.38	1.31 ± 0.09	5.43 ± 0.36
18.75	1.28 ± 0.07	5.33 ± 0.22
37.50	1.12 ± 0.05*	5.80 ± 0.38
75.00	1.18 ± 0.05*	4.11 ± 0.61**
150.00	1.37 ± 0.06	5.35 ± 0.244
CYP	0.98 ± 0.11***	5.41 ± 0.20
ZnO NPs		
NC	1.48 ± 0.04	6.21 ± 0.21
9.38	1.36 ± 0.12	5.10 ± 0.38
18.75	1.62 ± 0.12	5.38 ± 0.371
37.50	1.60 ± 0.08	5.51 ± 0.13
75.00	2.00 ± 0.85	7.42 ± 0.25
150.00	1.39 ± 0.10	4.47 ± 0.18
CYP	0.98 ± 0.11	5.41 ± 0.20
Mixture		
NC	1.48 ± 0.04	6.21 ± 0.21
9.38	1.22 ± 0.06	4.56 ± 0.20***
18.75	1.29 ± 0.03	4.53 ± 0.15***
37.50	1.24 ± 0.02	4.70 ± 0.12**
75.00	1.48 ± 0.07	5.16 ± 0.27*
150.00	1.55 ± 0.01	5.16 ± 0.29*
CYP	0.98 ± 0.11***	5.41 ± 0.20

Data represent Mean ± SEM (n=5). * $p < 0.05$, ** $p < 0.01$ and *** $p < 0.001$ in comparison with the mice treated with distilled water. Negative control (NC) = distilled water, CYP = cyclophosphamide (positive control).

Table 4. 10: Absolute and percentage relative spleen weight in mice treated with titanium dioxide, zinc oxide nanoparticles and mixture for 10 days.

TiO_2 NPs		
Doses ($mgkg^{-1}$)	**Absolute spleen weight (g)**	**Relative spleen weight (%)**
NC	0.24 ± 0.04	1.01 ± 0.16
9.38	0.14 ± 0.03	0.59 ± 0.11
18.75	0.18 ± 0.04	0.80 ± 0.18
37.50	0.10 ± 0.01**	0.50 ± 0.07*
75.00	0.16 ± 0.03	0.62 ± 0.12
150.00	0.14 ± 0.01	0.55 ± 0.06*
CYP	0.11 ± 0.02*	0.59 ± 0.11
ZnO NPs		
NC	0.24 ± 0.04	1.01 ± 0.16
9.38	0.12 ± 0.02	0.43 ± 0.05*
18.75	0.15 ± 0.03	0.51 ± 0.10
37.50	0.17 ± 0.03	0.59 ± 0.09
75.00	0.21 ± 0.11	0.76 ± 0.34
150.00	0.12 ± 0.01	0.37 ± 0.02
CYP	0.11 ± 0.02	0.59 ± 0.11
Mixture		
NC	0.24 ± 0.04	1.01 ± 0.16
9.38	0.16 ± 0.03	0.68 ± 0.10
18.75	0.16 ± 0.02	0.57 ± 0.06
37.50	0.15 ± 0.01	0.58 ± 0.04
75.00	0.20 ± 0.03	0.53 ± 0.07*
150.00	0.21 ± 0.05	0.71 ± 0.19
CYP	0.11 ± 0.02*	0.59 ± 0.11

Data represent Mean ± SEM (n=5). * $p < 0.05$ and ** $p < 0.01$ in comparison with the mice treated with distilled water. Negative control (NC) = distilled water, CYP = cyclophosphamide (positive control).

Table 4. 11: Absolute and percentage relative kidney weight in mice treated with titanium dioxide, zinc oxide nanoparticles and mixture for 10 days.

TiO_2 NPs		
Doses ($mgkg^{-1}$)	**Absolute kidney weight (g)**	**Relative kidney weight (%)**
NC	0.37 ± 0.02	1.53 ± 0.07
9.38	0.34 ± 0.02	1.43 ± 0.06
18.75	0.32 ± 0.04	1.33 ± 0.14
37.50	0.30 ± 0.03	1.55 ± 0.08
75.00	0.36 ± 0.01	1.45 ± 0.08
150.00	0.34 ± 0.01	1.32 ± 0.05
CYP	0.29 ± 0.03	1.63 ± 0.07
ZnO NPs		
NC	0.37 ± 0.02	1.53 ± 0.07
9.38	0.39 ± 0.03	1.46 ± 0.11
18.75	0.47 ± 0.01	1.57 ± 0.10
37.50	0.49 ± 0.02	1.69 ± 0.08
75.00	0.35 ± 0.06	1.36 ± 0.10
150.00	0.47 ± 0.05	1.51 ± 0.12
CYP	0.29 ± 0.03	1.63 ± 0.07
Mixture		
NC	0.37 ± 0.02	1.53 ± 0.07
9.38	0.37 ± 0.02	1.38 ± 0.07
18.75	0.36 ± 0.01	1.26 ± 0.02
37.50	0.30 ± 0.07	1.15 ± 0.27
75.00	0.40 ± 0.01	1.39 ± 0.07
150.00	0.43 ± 0.02	1.42 ± 0.06
CYP	0.29 ± 0.03	1.63 ± 0.07

Data represent Mean ± SEM (n=5). Negative control (NC) = distilled water, CYP = cyclophosphamide (positive control).

Table 4. 12: Absolute and percentage relative brain weight in mice treated with titanium dioxide, zinc oxide nanoparticles and mixture for 10 days.

TiO_2 NPs		
Doses ($mgkg^{-1}$)	**Absolute brain weight (g)**	**Relative brain weight (%)**
NC	0.42 ± 0.01	1.78 ± 0.04
9.38	0.41 ± 0.02	1.70 ± 0.09
18.75	0.42 ± 0.05	1.76 ± 0.14
37.50	0.39 ± 0.01	2.01 ± 0.06
75.00	0.40 ± 0.01	1.55 ± 0.05
150.00	0.37 ± 0.01	1.45 ± 0.04
CYP	0.39 ± 0.01	2.22 ± 0.16*
ZnO NPs		
NC	0.42 ± 0.01	1.78 ± 0.04
9.38	0.41 ± 0.01	1.55 ± 0.06
18.75	0.38 ± 0.02	1.26 ± 0.10*
37.50	0.41 ± 0.00	1.42 ± 0.05
75.00	0.39 ± 0.02	1.56 ± 0.08
150.00	0.41 ± 0.00	1.32 ± 0.02
CYP	0.39 ± 0.01	2.22 ± 0.16*
Mixture		
NC	0.42 ± 0.01	1.78 ± 0.04
9.38	0.38± 0.02	1.44 ± 0.06
18.75	0.38 ± 0.03	1.33 ± 0.12*
37.50	0.37 ± 0.03	1.38 ± 0.11
75.00	0.42 ± 0.01	1.47 ± 0.05
150.00	0.41 ± 0.02	1.39 ± 0.09
CYP	0.39 ± 0.01	2.22 ± 0.16*

Data represent Mean ± SEM (n=5). * $p < 0.05$ in comparison with the mice treated with distilled water. Negative control (NC) = distilled water, CYP = cyclophosphamide (positive control).

Table 4. 13: Absolute and percentage relative heart weight in mice treated with titanium dioxide, zinc oxide nanoparticles and mixture for 10 days.

TiO_2 NPs		
Doses ($mgkg^{-1}$)	**Absolute heart weight (g)**	**Relative heart weight (%)**
NC	0.13 ± 0.01	0.56 ± 0.03
9.38	0.11 ± 0.01	0.47 ± 0.02
18.75	0.13 ± 0.00	0.54 ± 0.03
37.50	0.11 ± 0.01	0.56 ± 0.02
75.00	0.12 ± 0.00	0.48 ± 0.01
150.00	0.14 ± 0.01	0.53 ± 0.03
CYP	0.10 ± 0.01	0.54 ± 0.02
ZnO NPs		
NC	0.13 ± 0.01	0.56 ± 0.03
9.38	0.13 ± 0.00	0.48 ± 0.01
18.75	0.15 ± 0.02	0.50 ± 0.05
37.50	0.16 ± 0.01	0.56 ± 0.01
75.00	0.12 ± 0.02	0.48 ± 0.03
150.00	0.15 ± 0.01	0.48 ± 0.02
CYP	0.10 ± 0.01	0.54 ± 0.02
Mixture		
NC	0.13 ± 0.01	0.56 ± 0.03
9.38	0.14 ± 0.01	0.53 ± 0.03
18.75	0.14 ± 0.01	0.49 ± 0.02
37.50	0.15 ± 0.01	0.55 ± 0.04
75.00	0.16 ± 0.01	0.57 ± 0.02
150.00	0.15 ± 0.01	0.50 ± 0.03
CYP	0.10 ± 0.01	0.54 ± 0.02

Data represent Mean ± SEM (n=5). Negative control (NC) = distilled water, CYP = cyclophosphamide (positive control).

4.4.3 Haematological effects induced by titanium dioxide, zinc oxide nanoparticles and their mixture in mice for 5 and 10 days

The erythrocytes and their indices in the treated mice for 5 and 10 days are presented in Figures 4.14 – 4.34. For the 5- day exposure period, mice treated with TiO_2 NPs did not induce any significant ($p > 0.05$) decrease in the PCV (Figure 4.14), Hb (Figure 4.15) and RBC (Figure 4.16) at tested doses in comparison with the mice treated with distilled water. However, a significant ($p < 0.001$) decrease in MCHC (Figure 4.17) was observed at tested doses; and a significant increase ($p < 0.05$) in MCV (Figure 4.18) at tested doses except at the 75.00 $mgkg^{-1}$ of TiO_2 NPs in comparison with the mice treated with distilled water. In addition, no significant ($p > 0.05$) reduction in MCH (Figure 4.19) was observed at the 9.38, 75.00 and 150.00 $mgkg^{-1}$, and no significant ($p > 0.05$) increase at the 18.75 and 37.50 $mgkg^{-1}$ of TiO_2 NPs in comparison with the mice treated with distilled water. Likewise, platelets were not significantly ($p > 0.05$) decreased at the 9.38 and 18.75 $mgkg^{-1}$ and significantly increased at the 37.50, 75.00 and 150.00 $mgkg^{-1}$ of TiO_2 NPs in comparison with the mice treated with distilled water.

For the 10- day exposure period, mice treated with TiO_2 NPs exhibited no significant ($p > 0.05$) increase in the PCV (Figure 4.14), Hb (Figure 4.15) and MCHC (Figure 4.17) at tested doses. Subsequently, there was a significant ($p < 0.001$) increase in the RBC (Figure 4.16) at the 9.38 and 18.75 $mgkg^{-1}$; a significant ($p < 0.001$) decrease in the MCV (Figure 4.18); decrease in the MCH (Figure 4.19) at the 9.38 and 18.75 $mgkg^{-1}$ and a decrease in platelets (Figure 4.20) at the 150.00 $mgkg^{-1}$ of TiO_2 NPs in comparison with the mice treated with distilled water. Consequently, significant difference between the 5- and 10-day exposure periods for mice treated with TiO_2 NPs was observed at 37.50 $mgkg^{-1}$ ($p < 0.05$) for PCV; 37.50 ($p < 0.05$) and 150.00 $mgkg^{-1}$ ($p < 0.05$) for Hb; 9.38 ($p < 0.001$) and 18.75 $mgkg^{-1}$ ($p < 0.001$) for RBC; 150 $mgkg^{-1}$ ($p < 0.01$) for MCHC; 9.38 ($p < 0.001$) and 18.75 $mgkg^{-1}$ ($p < 0.001$) for MCV and MCH; and 37.50 ($p < 0.05$) and 150 $mgkg^{-1}$ ($p < 0.001$) for platelets.

For the 5- day exposure period, ZnO NPs did not induce a significant ($p > 0.05$) increase in the PCV (Figure 4.21), Hb (Figure 4.22), and RBC (Figure 4.23) at tested doses. A significant ($p < 0.01$) decrease was recorded in the MCHC (Figure 4.24) at tested doses;

and a significant decrease in the MCV (Figure 4.25) at the 18.75 and 150.00 $mgkg^{-1}$ of ZnO NPs in comparison with the mice treated with distilled water was observed. In addition, MCH (Figure 4.26) was not significantly ($p > 0.05$) decreased at the 9.38 and 75.00 $mgkg^{-1}$; increased at the 18.75, 37.50 and 150.00 $mgkg^{-1}$ while the platelets (Figure 4.27) decreased at tested doses except at the 9.38 and 150.00 $mgkg^{-1}$ of ZnO NPs in comparison with the mice treated with distilled water. For the 10- day exposure period, mice treated with ZnO NPs exhibited a significant ($p < 0.05$) increase in the PCV (Figure 4.21), Hb (Figure 4.22) and RBC (Figure 4.23) only at 9.38 $mgkg^{-1}$ in comparison with the mice treated with distilled water. Consequently, a significant difference between the 5- and 10- day exposure periods for mice treated with ZnO NPs was observed only at 75.00 $mgkg^{-1}$ ($p < 0.01$) for platelets.

For the 5- day exposure period, the mixture did not induce a significance ($p > 0.05$) in the PCV (Figure 4.28), Hb (Figure 4.29), RBC (Figure 4.30), MCH (Figure 4.33) and platelets (Figure 4.34) at tested doses. A significant ($p < 0.01$) decrease in the MCHC (Figure 4.31) at tested doses; and a significant ($p < 0.05$) increase in MCV (Figure 4.32) at the 75.00 and 150.00 $mgkg^{-1}$ of their mixture in comparison with the mice treated with distilled water were observed. For the 10- day exposure period, there was a significant ($p < 0.05$) increase in PCV (Figure 4.28), Hb (Figure 4.29) and RBC (Figure 4.30) at the 75.00 $mgkg^{-1}$ of their mixture in comparison with the mice treated with distilled water. Consequently, a significant difference between the 5- and 10- day exposure periods for mice treated with their mixture was observed only at 75.00 $mgkg^{-1}$ ($p < 0.01$) for platelets.

The WBC and their differentials in the treated mice for 5 and 10 days are presented in Figures 4.35 – 4.52. For the 5- day exposure period, mice treated with TiO_2 NPs did not show any significant ($p > 0.05$) increase in the WBC count (Figure 4.35), monocytes (Figure 4.38) and lymphocytes (Figure 4.36) at tested doses while no significant ($p > 0.05$) decrease in the neutrophils (Figure 4.37), eosinophils (Figure 4.39) and the neutrophil to lymphocyte ratio (Figure 4.40) at tested doses in comparison with the mice treated with distilled water were observed. For the 10- day exposure period, TiO_2 NPs did not induce any significance ($p > 0.05$) in the WBC (Figure 4.35), lymphocytes (Figure 4.36), neutrophils (Figure 4.37), neutrophil to lymphocyte ratio (Figure 4.40), monocytes (Figure

4.38) and eosinophils (Figure 4.39) across all doses in comparison with the mice treated with distilled water. Consequently, a significant difference between the 5- and 10- day exposure periods for mice treated with TiO_2 NPs was observed only at 9.38 $mgkg^{-1}$ ($p < 0.05$) for lymphocytes, neutrophils and neutrophil to lymphocyte ratio.

For the 5- day exposure period, mice treated with ZnO NPs did not show any significance ($p > 0.05$) in the WBC count (Figure 4.41), lymphocytes (Figure 4.42), neutrophils (Figure 4.43), monocytes (Figure 4.44), eosinophils (Figure 4.45), and neutrophil to lymphocyte ratio (Figure 4.46) at tested doses in comparison with the mice treated with distilled water. However, for the 10- day exposure period, there was a significant decrease in the WBC count (Figure 4.41) only at the 37.50 ($p < 0.05$) and 75.00 ($p < 0.01$) $mgkg^{-1}$ of ZnO NPs in comparison with the mice treated with distilled water.

Mice treated with the mixture of the NPs for the 5- day exposure revealed significant ($p < 0.001$) decrease in the WBC count (Figure 4.47) only at the 37.50, 75.00 and 150.00 $mgkg^{-1}$ in comparison with the mice treated with distilled water while for the 10- day exposure, a significant ($p < 0.05$) decrease in the WBC count (Figure 4.47) was observed only at the 9.38 and 18.75 $mgkg^{-1}$ of their mixture in comparison with the mice treated with distilled water. For the 5 and 10 day periods, no significance ($p > 0.05$) was observed in the lymphocytes (Figure 4.48), neutrophils (Figure 4.49), monocytes (Figure 4.50), eosinophils (Figure 4.51) and neutrophil to lymphocyte ratio (Figure 4.52) of mice teated with the NP mixture compared with mice treated with distilled water. Consequently, a significant difference between the 5- and 10- day exposure periods for mice treated with the NP mixture was observed only at 9.38 ($p < 0.001$), 75.00 ($p < 0.05$) and 150.00 $mgkg^{-1}$ ($p < 0.01$) for the WBC count.

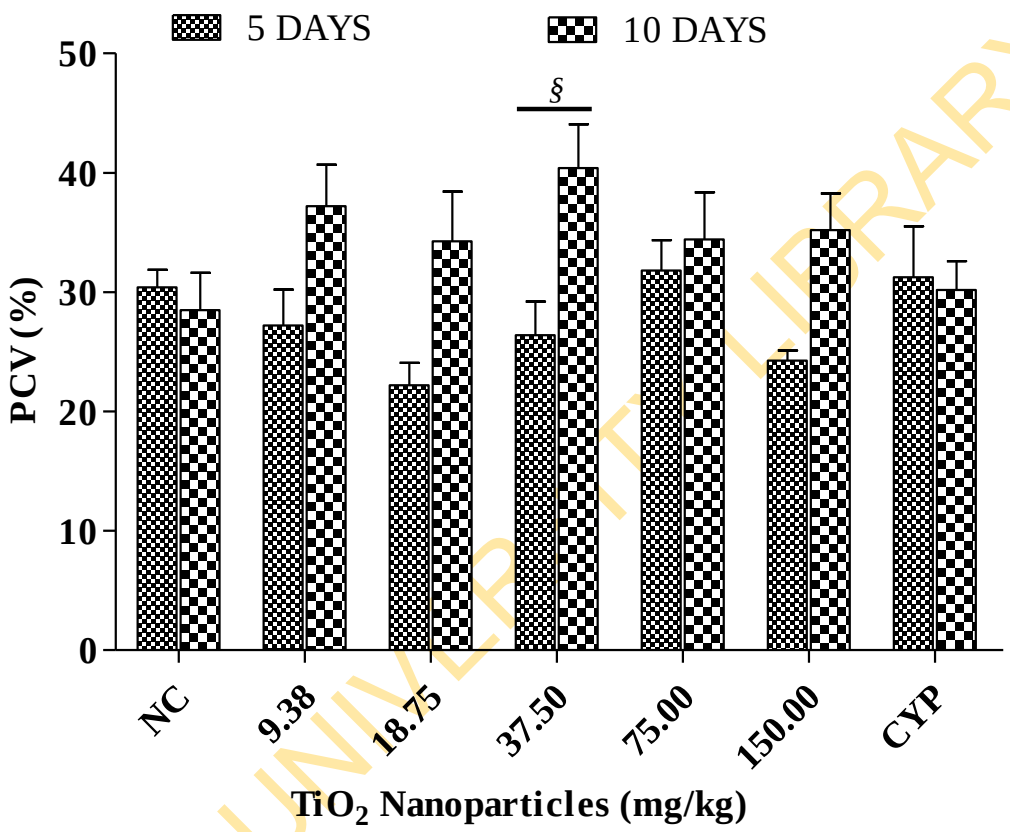

Figure 4. 13: Frequency of Packed Cell Volume (%) count in mice treated with TiO_2 NPs for 5- and 10- days.

Data represent mean ± SEM (n = 5). Negative control (NC) = distilled water, CYP = cyclophosphamide (positive control).

[§] $p < 0.05$ for the comparison between 5- and 10-day exposures

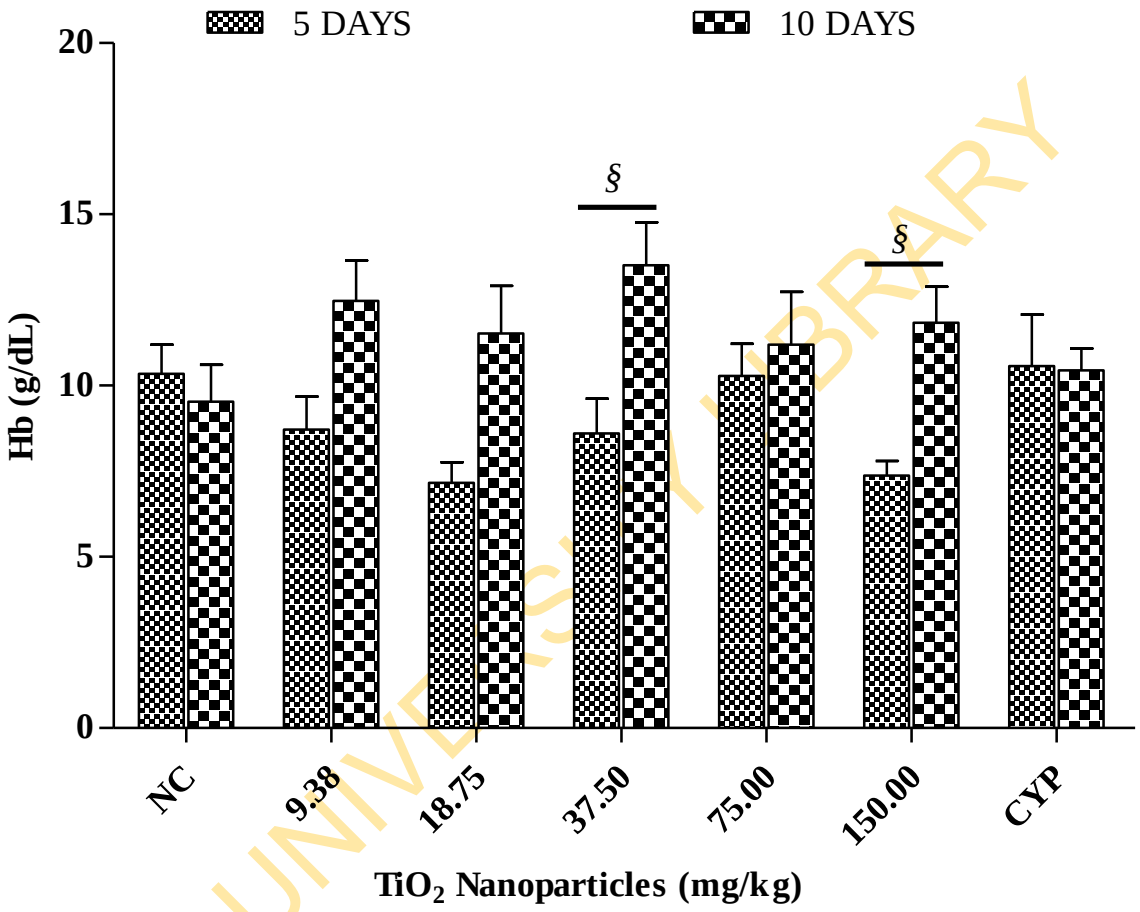

Figure 4. 14: Frequency of Haemoglobin (g/dL) concentration in mice treated with TiO_2 NPs for 5- and 10- days.

Data represent mean ± SEM (n = 5). Negative control (NC) = distilled water, CYP = cyclophosphamide (positive control).

[§] $p < 0.05$ for the comparison between 5- and 10-day exposures

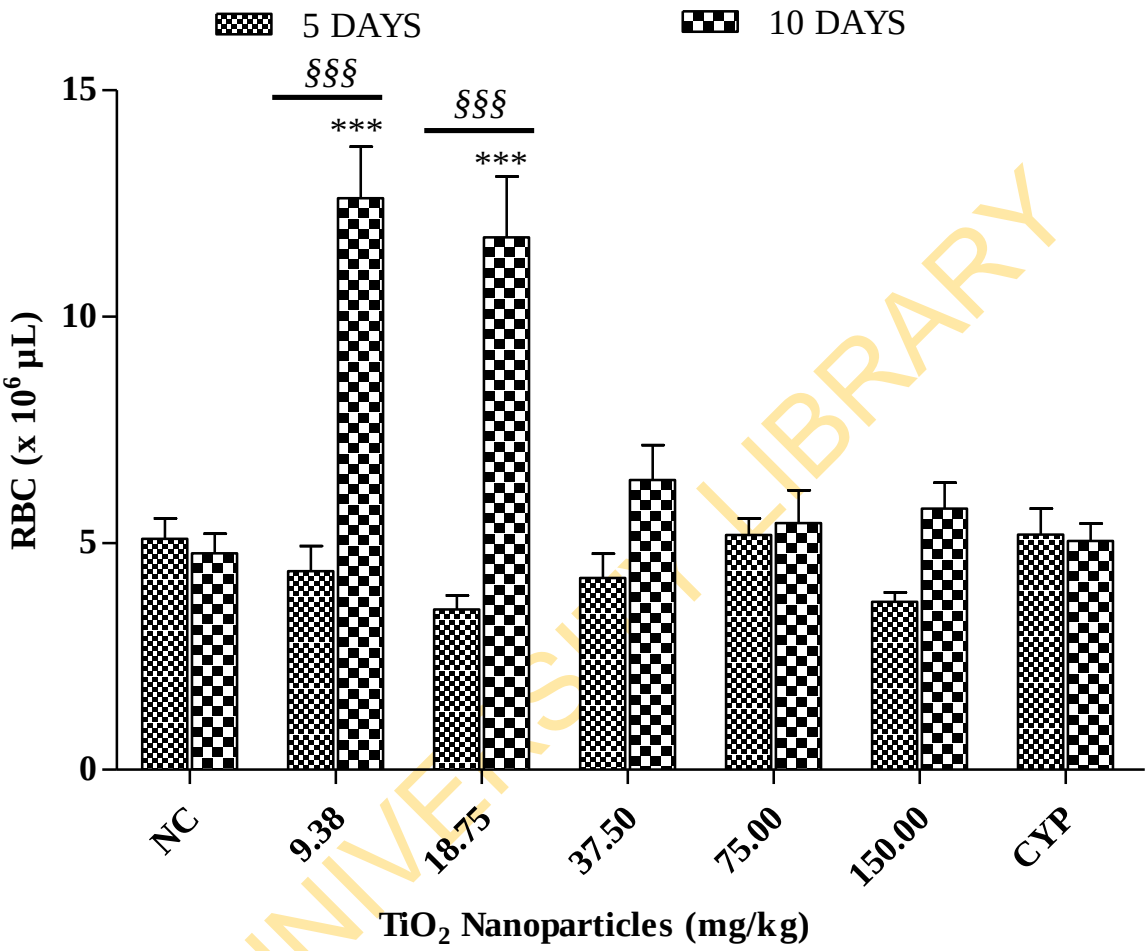

Figure 4. 15: Frequency of Red Blood Cells (x 10^6 µL) count in mice treated with TiO_2 NPs for 5- and 10- days.

Data represent mean ± SEM (n = 5). Negative control (NC) = distilled water, CYP = cyclophosphamide (positive control).

*** $p < 0.001$ in 10-days exposure

§§§ $p < 0.001$ for the comparison between 5- and 10-day exposures

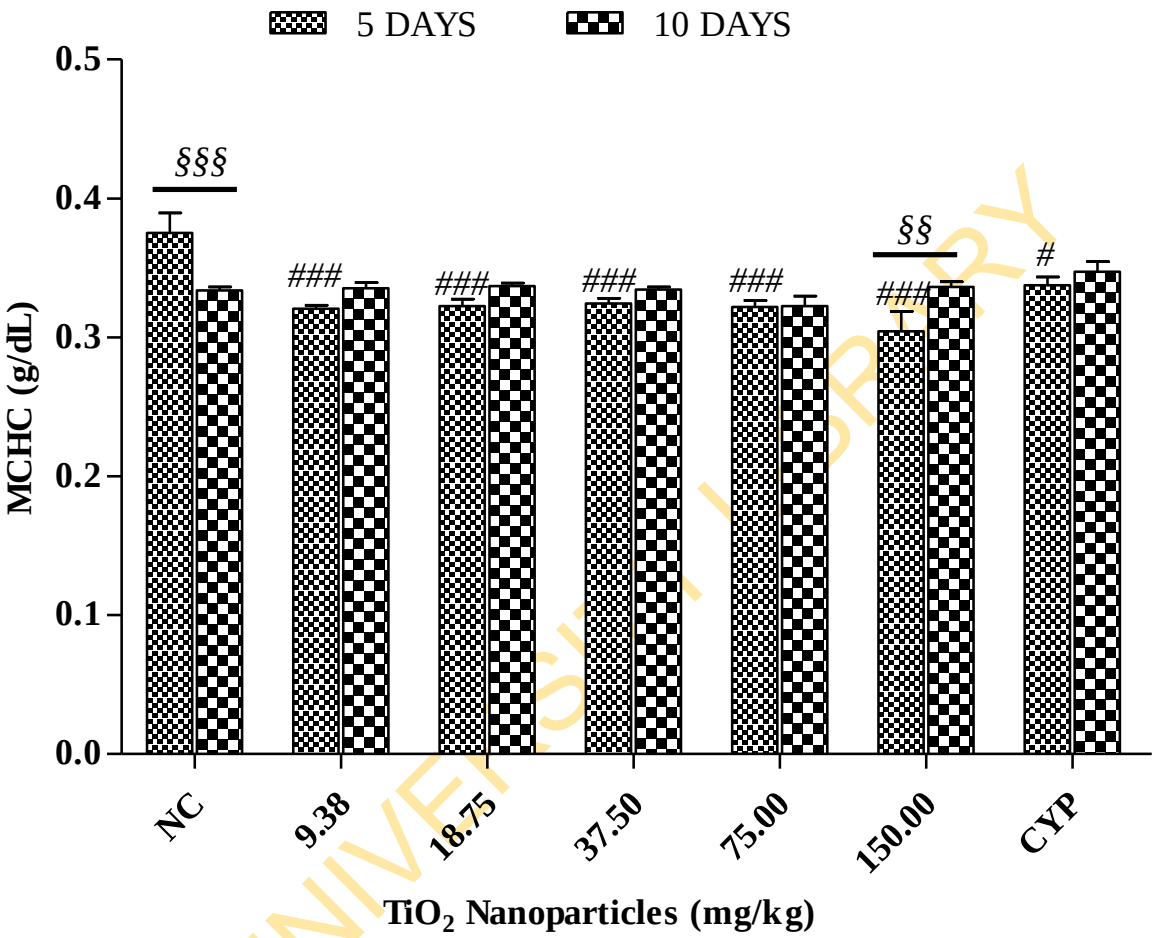

Figure 4. 16: Frequency of Mean Cell Haemoglobin Concentration (g/dL) in mice treated with TiO_2 NPs for 5- and 10- days.

Data represent mean ± SEM (n = 5). Negative control (NC) = distilled water, CYP = cyclophosphamide (positive control).

$^{\#}$ $p < 0.05$ and $^{\#\#\#}$ $p<0.001$ in 5-days exposure.

§§ $p < 0.01$ and §§§ $p < 0.001$ for the comparison between 5- and 10- day exposures

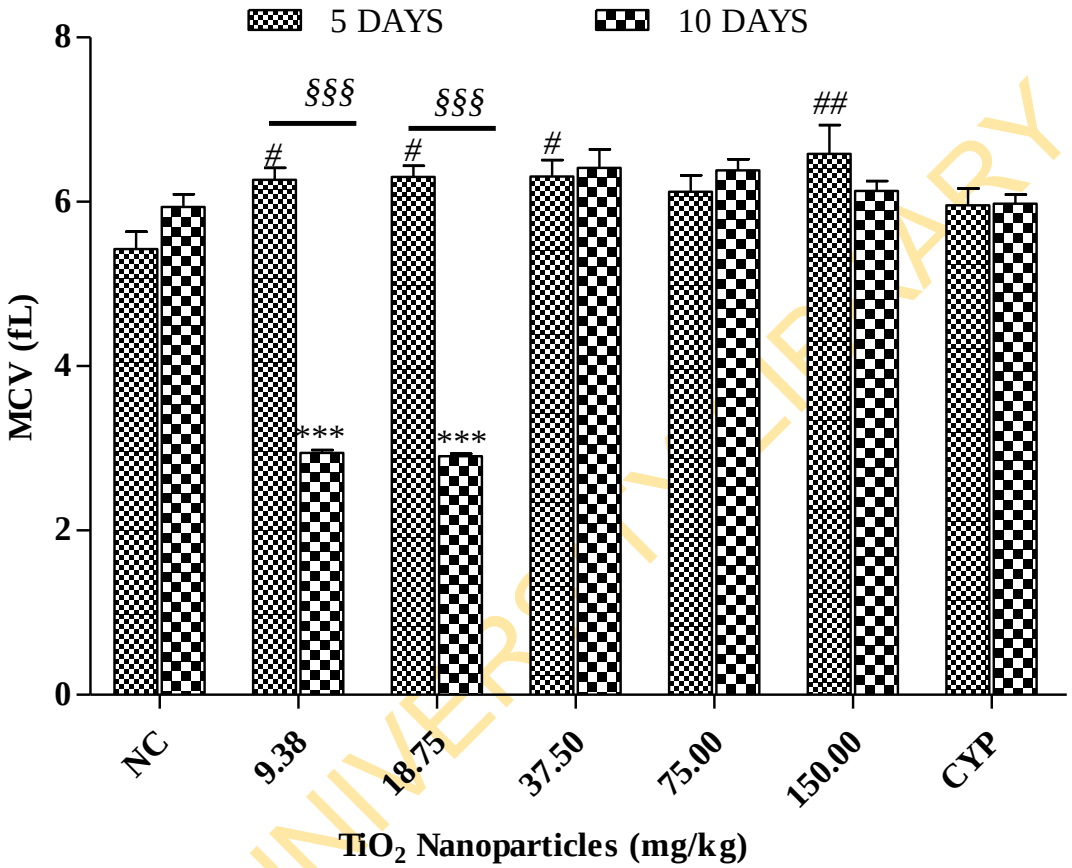

Figure 4. 17: Frequency of Mean Cell Volume (fL) in mice treated with TiO_2 NPs for 5- and 10- days.

Data represent mean ± SEM (n = 5). Negative control (NC) =distilled water, CYP = cyclophosphamide (positive control).

$^{\#}$ $p < 0.05$ and $^{\#\#}$ $p < 0.01$, in 5-days exposure.

*** $p < 0.001$ in 10- days exposure

§§§ $p < 0.001$ for the comparison between 5- and 10-day exposures

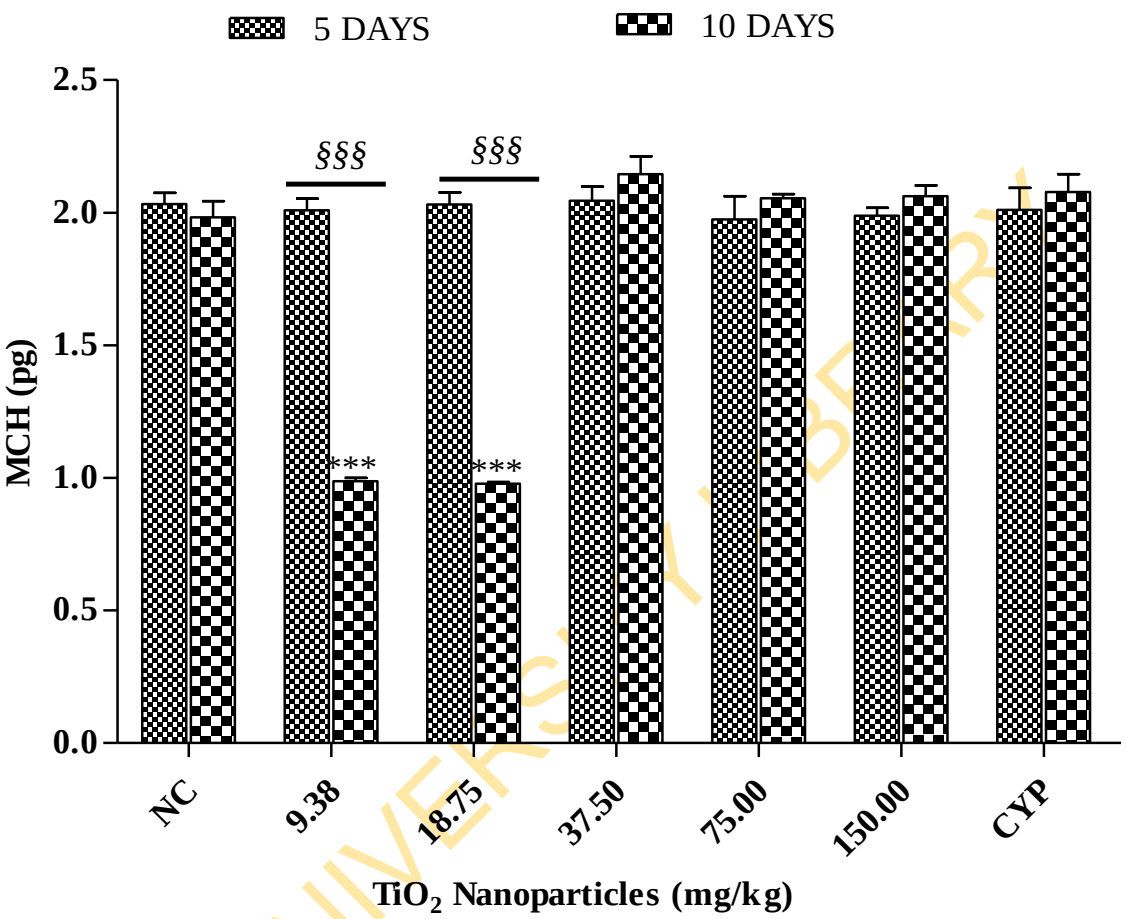

Figure 4. 18: Frequency of Mean Cell Haemoglobin (pg) in mice treated with TiO_2 NPs for 5- and 10- days.

Data represent mean ± SEM (n = 5). Negative control (NC) = distilled water, CYP = cyclophosphamide (positive control).

*** $p < 0.001$ in 10-days exposure

§§§ $p < 0.001$ for the comparison between 5- and 10-day exposures

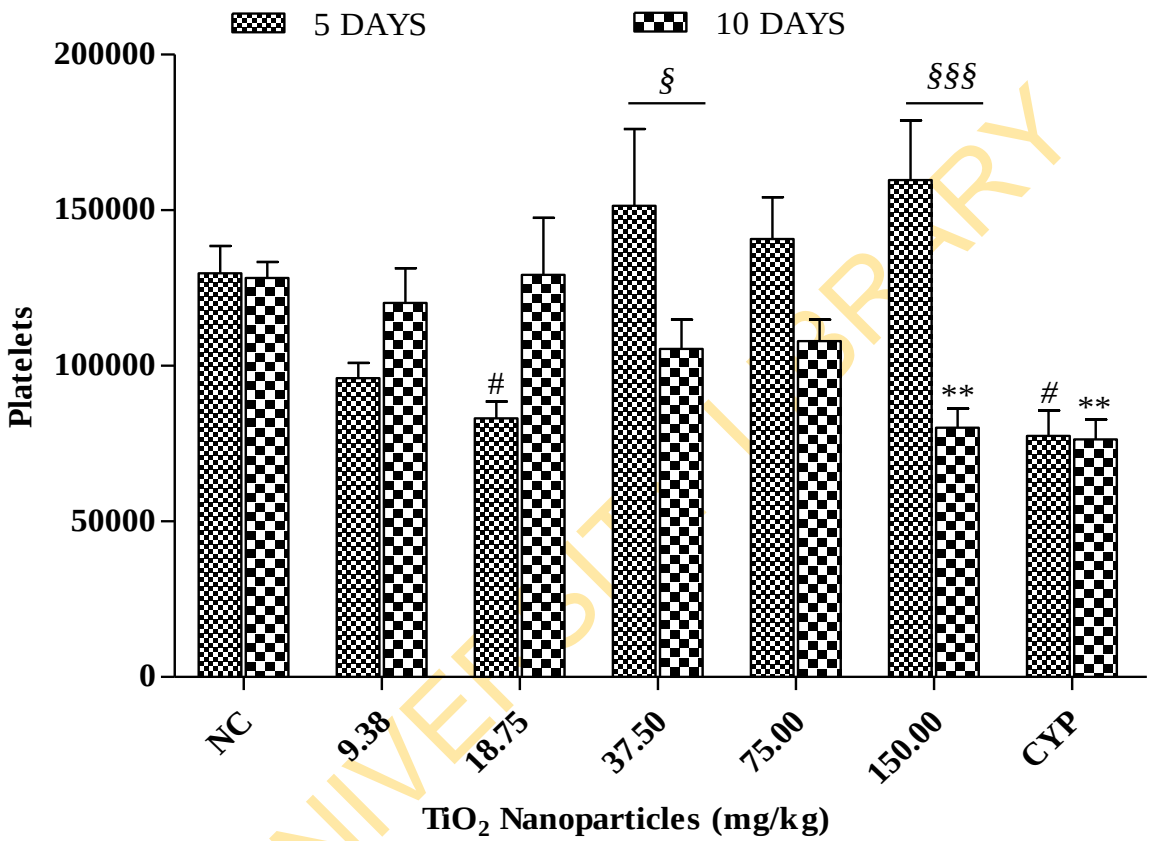

Figure 4. 19: Frequency of Platelet count in mice treated with TiO_2 NPs for 5- and 10-days.

Data represent mean ± SEM (n = 5). Negative control (NC) =distilled water, CYP = cyclophosphamide (positive control).

[#] $p < 0.05$ in 5-days exposure

[**] $p < 0.01$ in 10-days exposure

[§] $p < 0.05$ and [§§§] $p < 0.001$ for the comparison between 5- and 10-day exposures

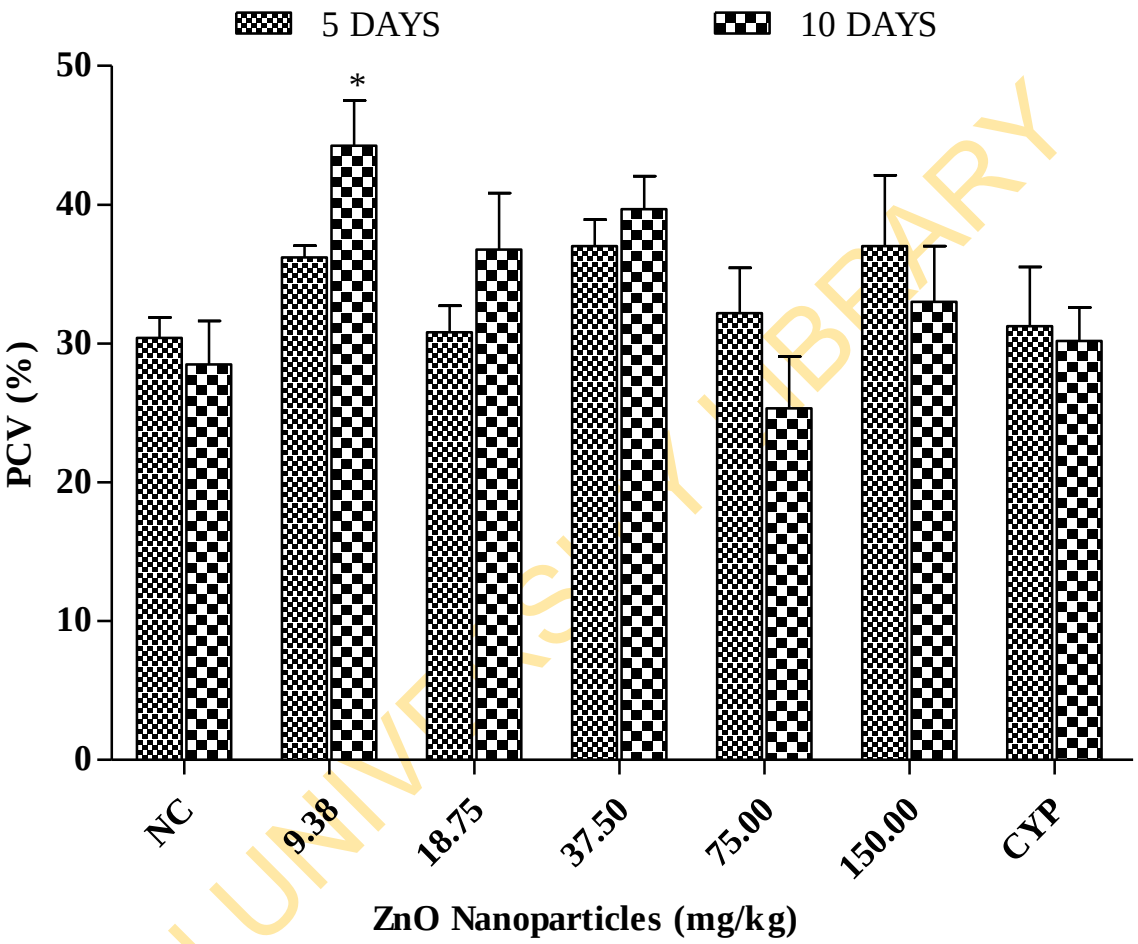

Figure 4. 20: Frequency of Packed Cell Volume (%) in mice treated with ZnO NPs for 5- and 10- days.

Data represent mean ± SEM (n = 5). Negative control (NC) =distilled water, CYP = cyclophosphamide (positive control).

* $p < 0.05$ in 10-days exposure

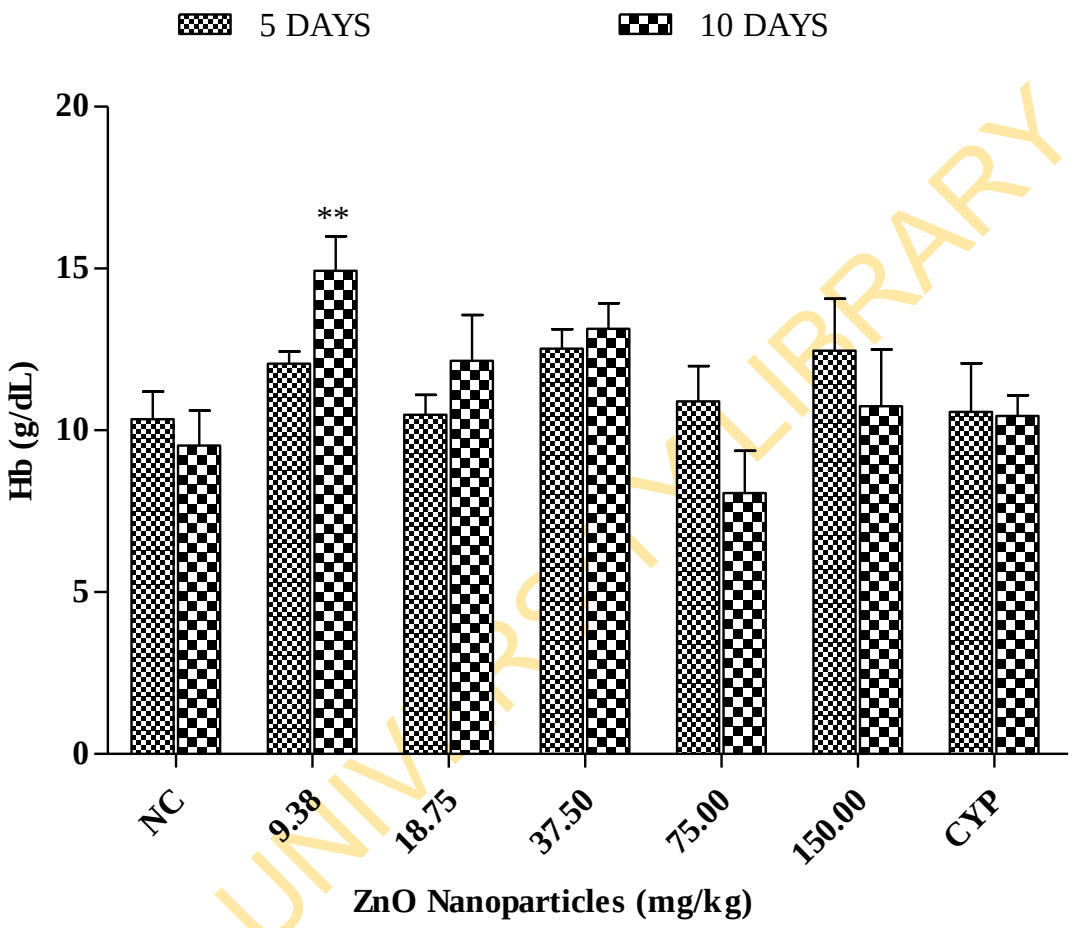

Figure 4. 21: Frequency of Haemoglobin concentration (g/dL) in mice treated with ZnO NPs for 5- and 10- days.

Data represent mean ± SEM (n = 5). Negative control (NC) =distilled water, CYP = cyclophosphamide (positive control).

** $p < 0.01$ in 10-days exposure

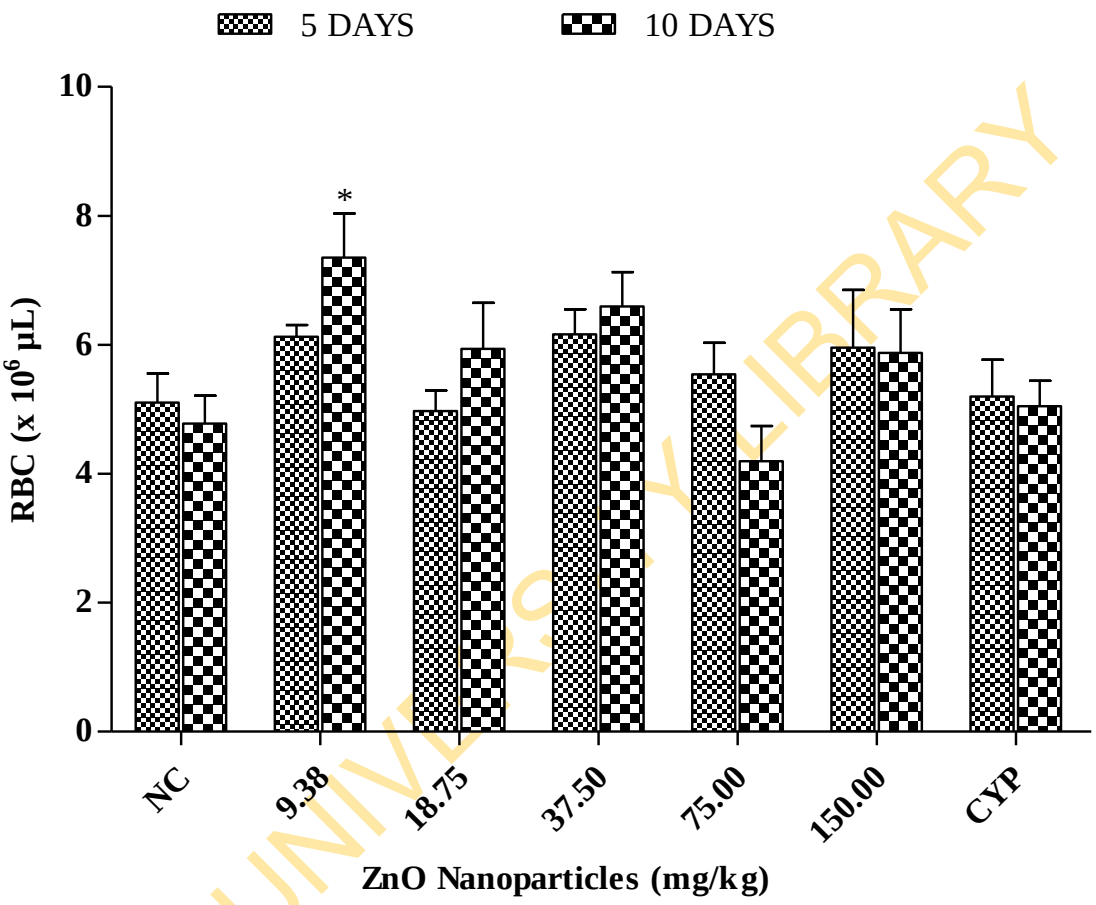

Figure 4. 22: Frequency of Red Blood Cell count (x 10^6 µL) in mice treated with ZnO NPs for 5- and 10- days.

Data represent mean ± SEM (n = 5). Negative control (NC) = distilled water, CYP = cyclophosphamide (positive control).

* $p < 0.05$ in 10- days exposure

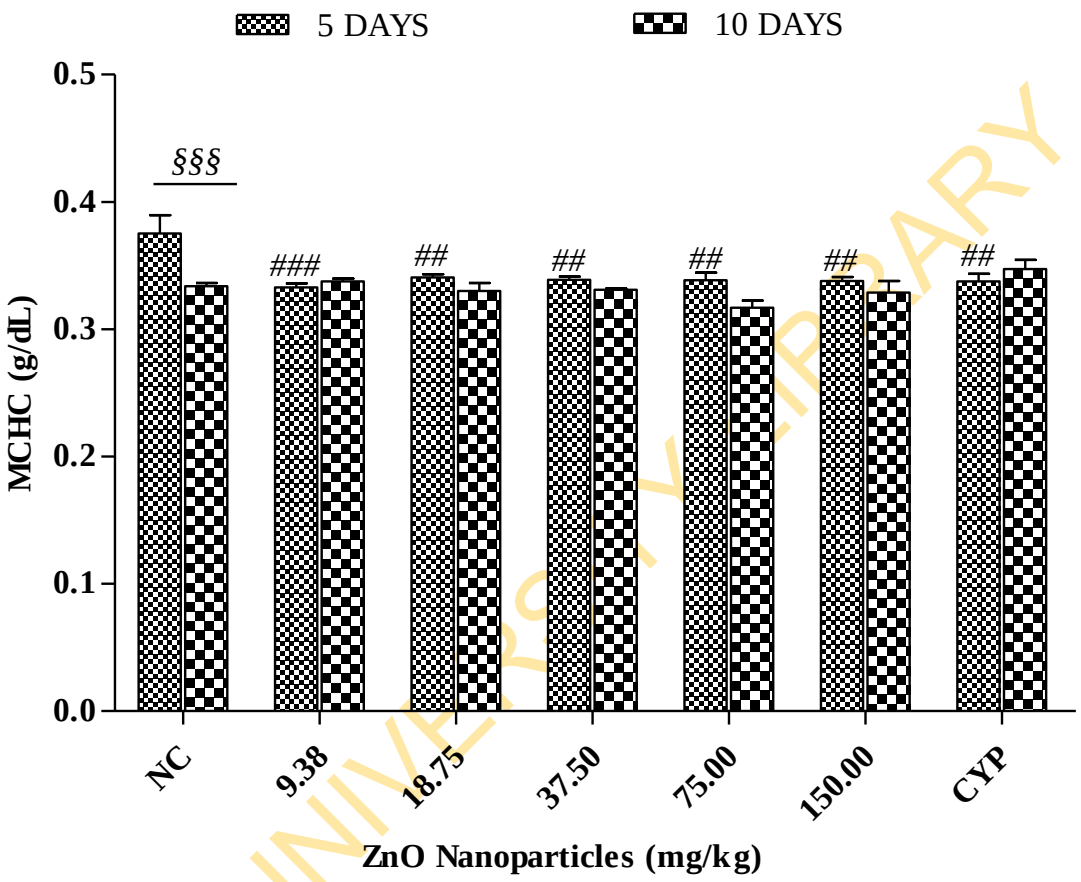

Figure 4. 23: Frequency of Mean Cell Haemoglobin Concentration (g/dL) in mice treated with ZnO NPs for 5- and 10- days.

Data represent mean ± SEM (n = 5). NC = distilled water, CYP = cyclophosphamide (positive control).

$^{##}p < 0.01$ and $^{###}p<0.001$ in 5-days exposure

§§§ $p < 0.001$ for the comparison between 5- and 10-day exposures

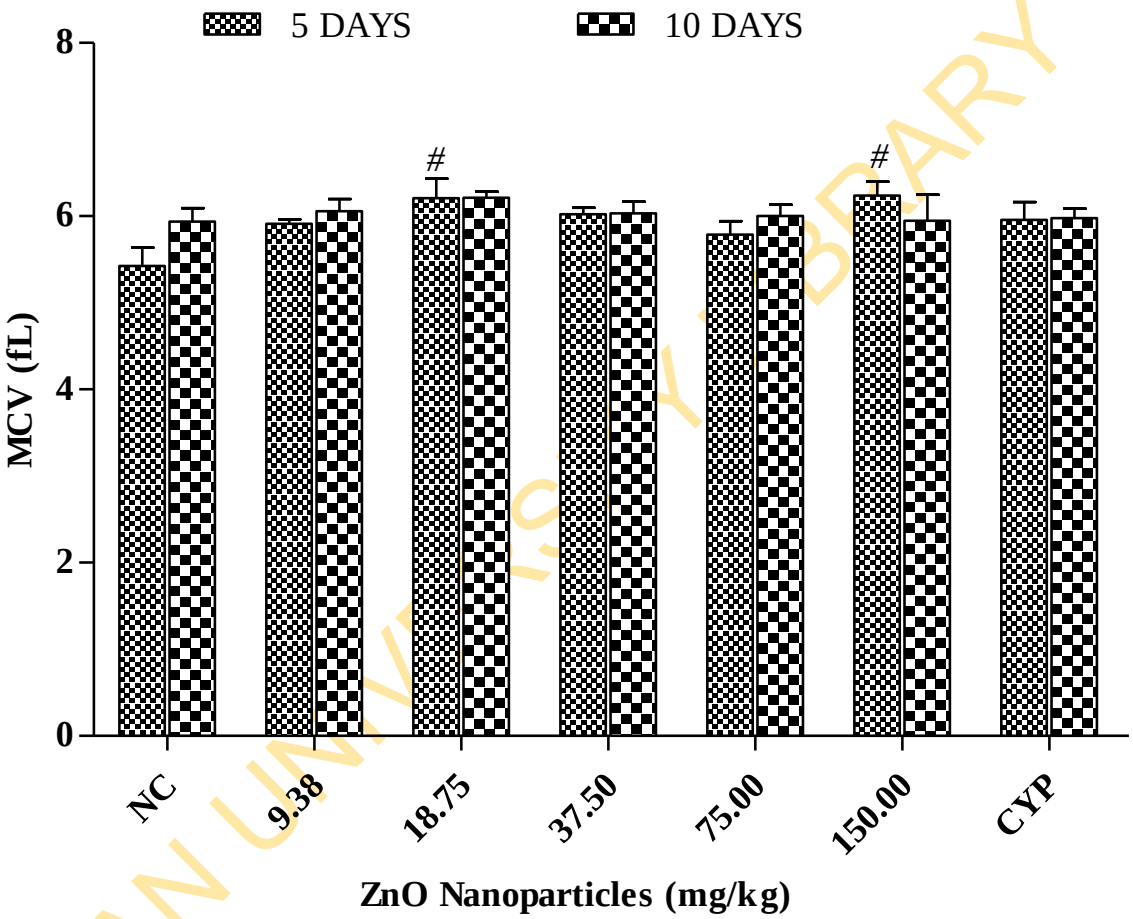

Figure 4. 24: Frequency of Mean Cell Volume (fL) in mice treated with ZnO NPs for 5- and 10- days.

Data represent mean ± SEM (n = 5). Negative control (NC) = distilled water, CYP = cyclophosphamide (positive control).

[#] $p < 0.05$ in 5-days exposure

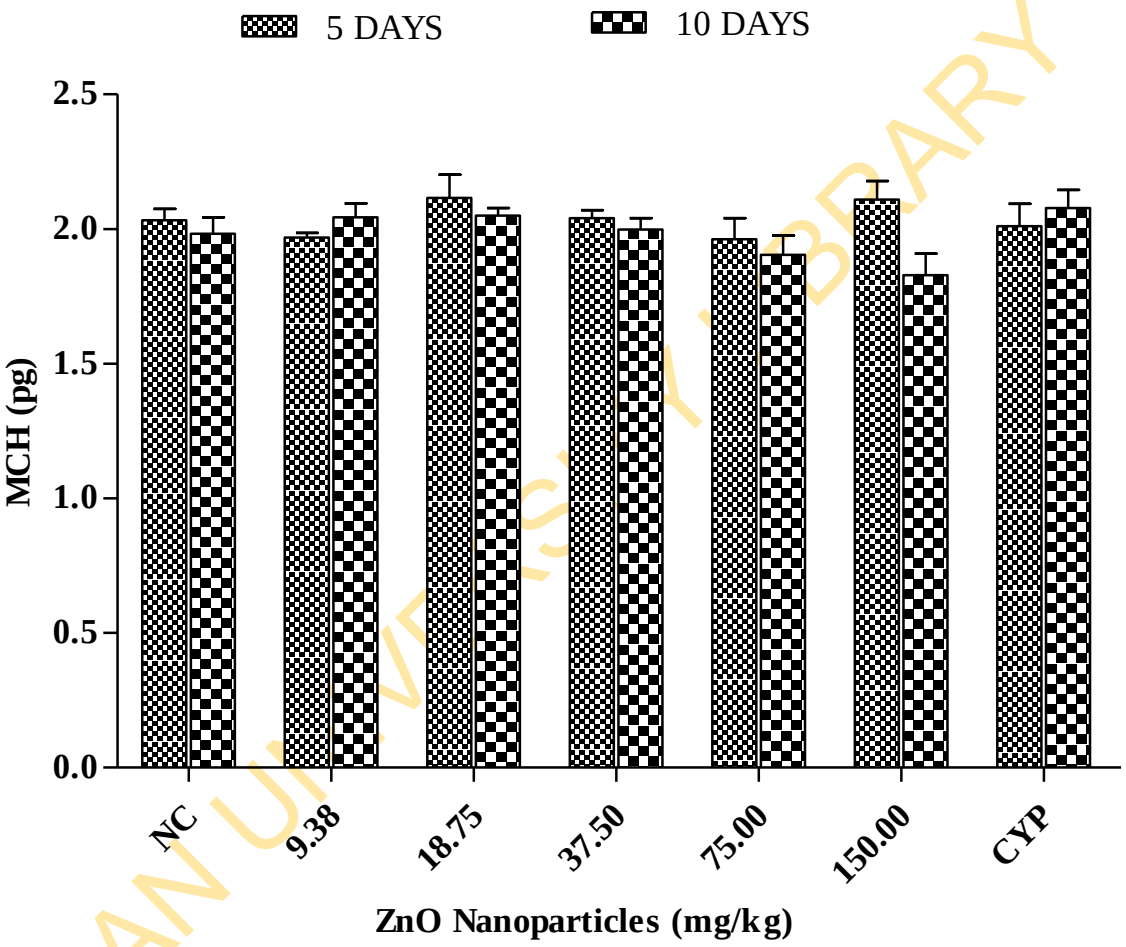

Figure 4. 25: Frequency of Mean Cell Haemoglobin (pg) in mice treated with ZnO NPs for 5- and 10- days.

Data represent mean ± SEM (n = 5). Negative control (NC) = distilled water, CYP = cyclophosphamide (positive control).

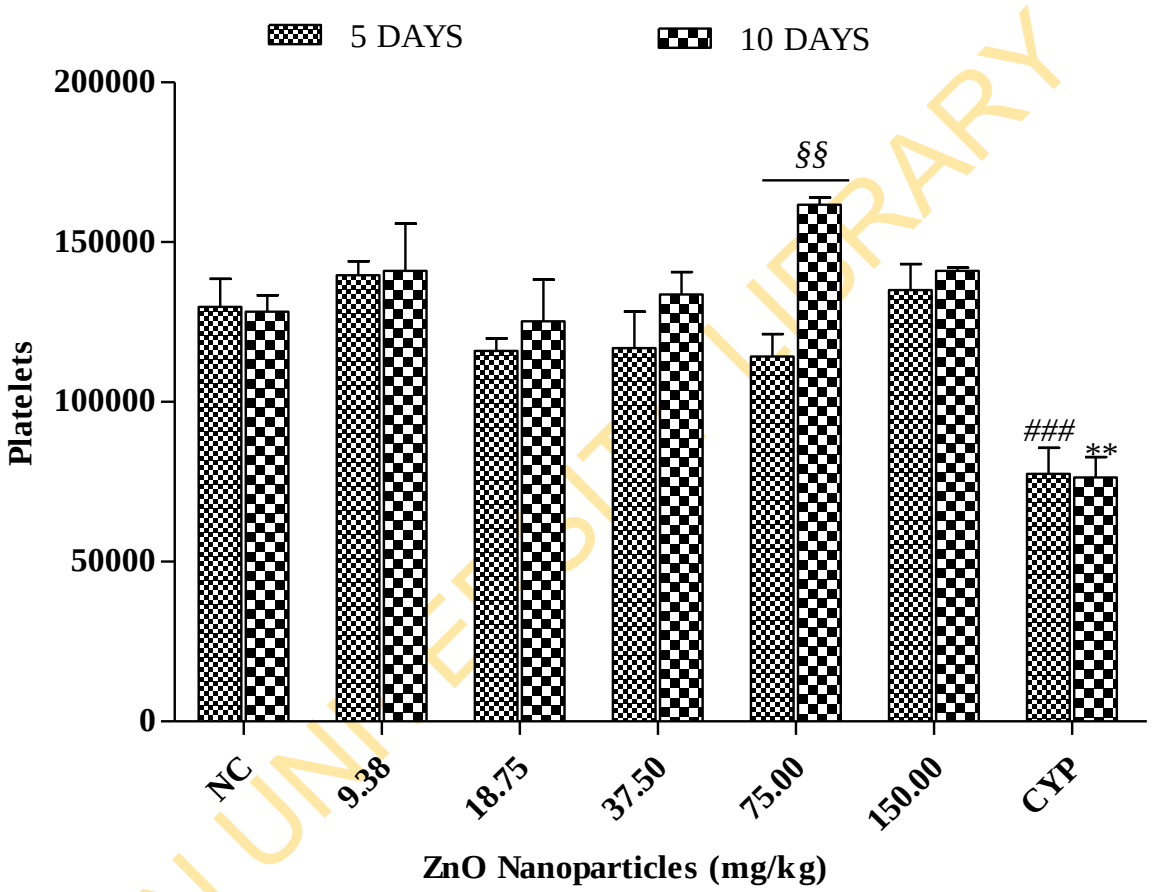

Figure 4. 26: Frequency of Platelets in mice treated with ZnO NPs for 5- and 10- days. Data represent mean ± SEM (n = 5). Negative control (NC) = distilled water, CYP = cyclophosphamide (positive control).

$p<0.001$ in 5- days exposure

** $p < 0.01$ in 10-days exposure

§§ $p < 0.01$ for the comparison between 5- and 10- day exposures

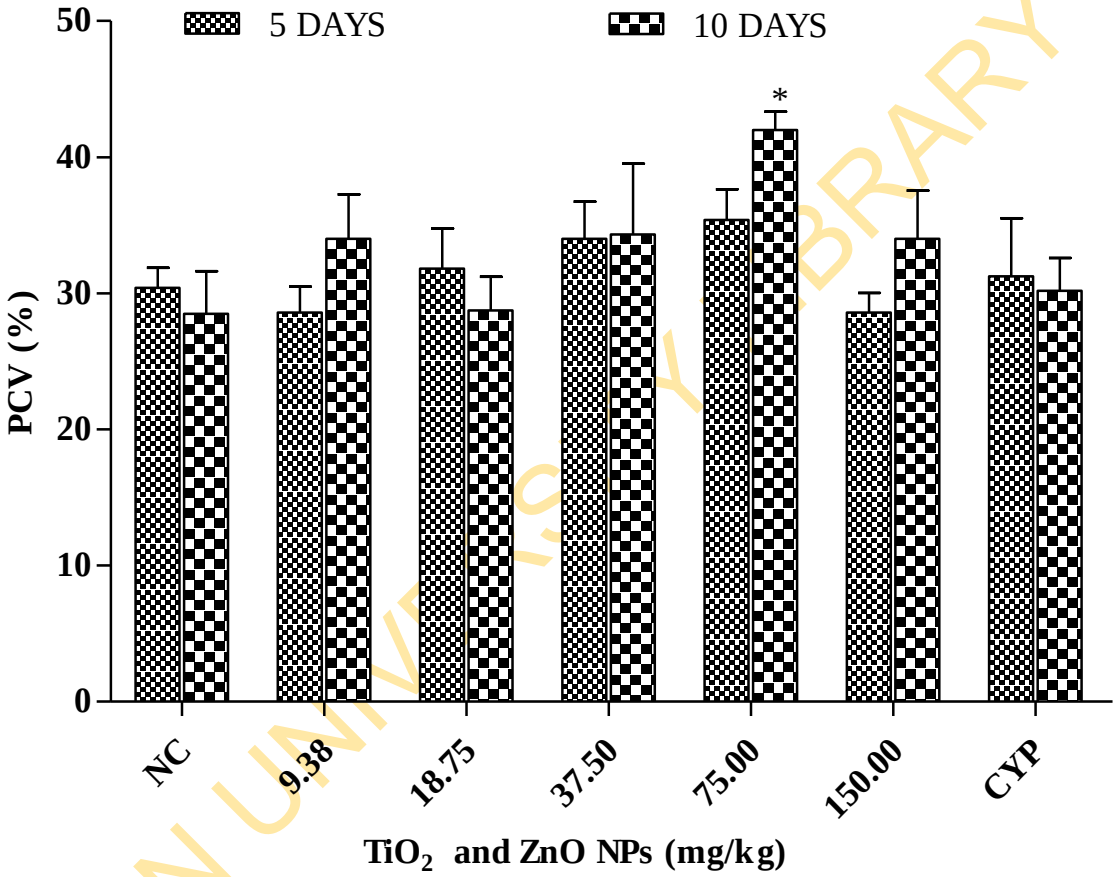

Figure 4. 27: Frequency of Packed Cell Volume (%) in mice treated with TiO_2 and ZnO NPs for 5- and 10- days.

Data represent mean ± SEM (n = 5). Negative control (NC) = distilled water, CYP = cyclophosphamide (positive control).

* $p < 0.05$ in 10-days exposure

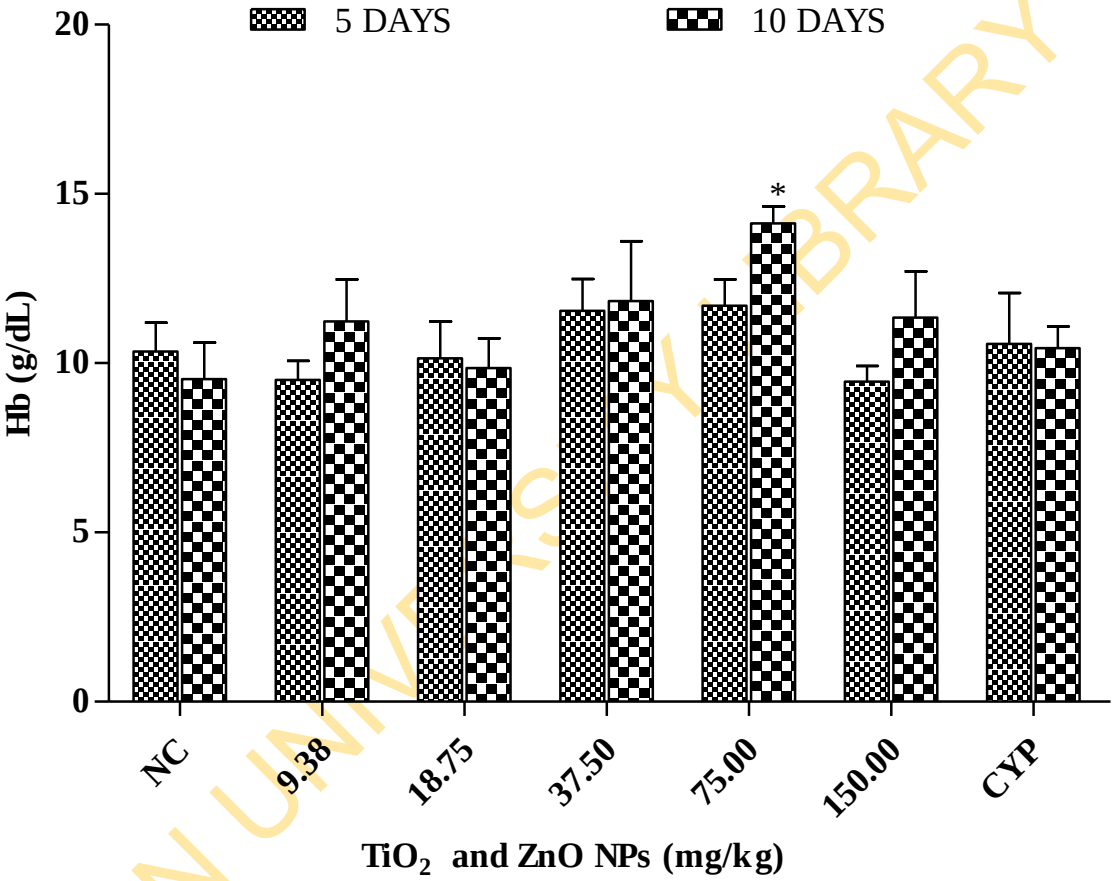

Figure 4. 28: Frequency of Haemoglobin concentration (g/dL) in mice treated with TiO_2 and ZnO NPs for 5- and 10- days.

Data represent mean ± SEM (n = 5). Negative control (NC) = distilled water, CYP = cyclophosphamide (positive control).

* $p < 0.05$ in 10-days exposure

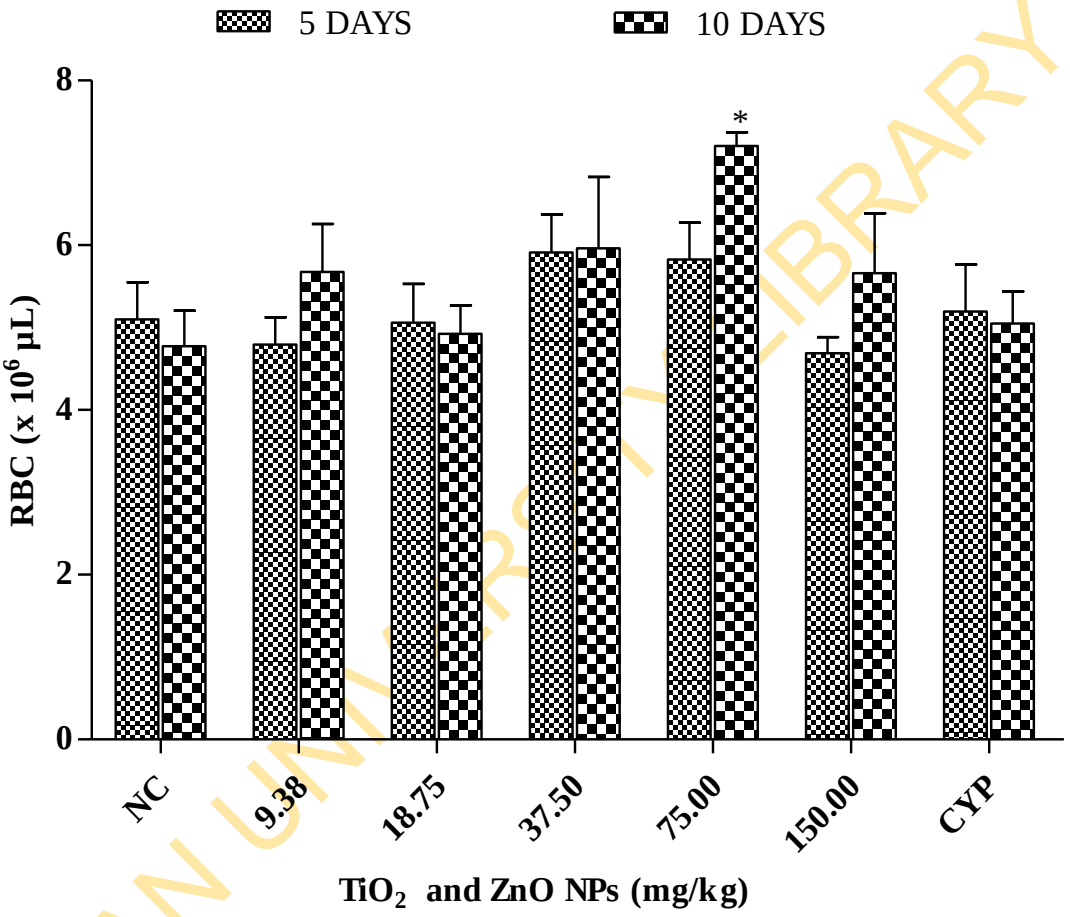

Figure 4. 29: Frequency of Red Blood Cell count (x 10^6 µL) in mice treated with TiO_2 and ZnO NPs for 5- and 10- days.

Data represent mean ± SEM (n = 5). Negative control (NC) = distilled water, CYP = cyclophosphamide (positive control).

* $p < 0.05$ in 10-days exposure

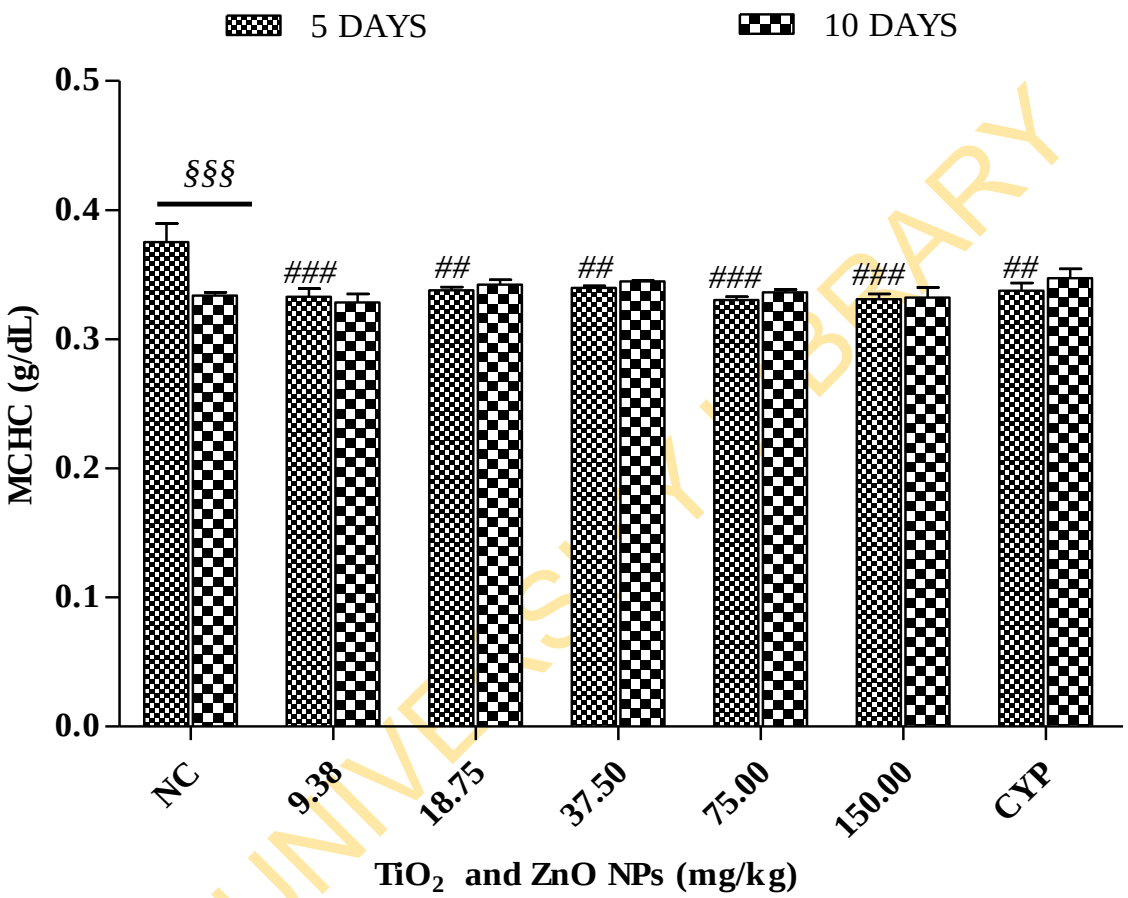

Figure 4. 30: Frequency of Mean Cell Haemoglobin Concentration (g/dL) in mice treated with TiO_2 and ZnO NPs for 5- and 10- days.

Data represent mean ± SEM (n = 5). Negative control (NC) =distilled water, CYP = cyclophosphamide (positive control).

$^{##}$ $p < 0.01$ and $^{###}$ $p<0.001$ in 5-days exposure

§§§ $p < 0.001$ for the comparison between 5- and 10-day exposures

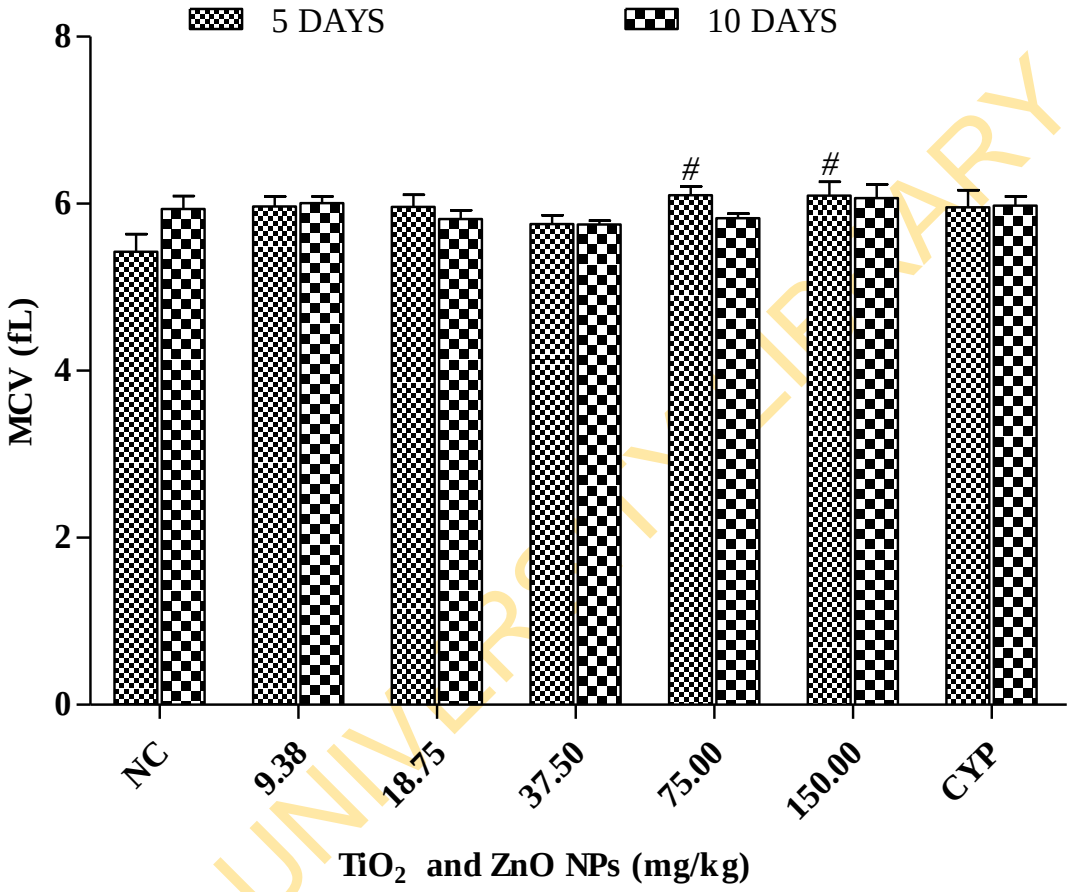

Figure 4. 31: Frequency of Mean Cell Volume (fL) in mice treated with TiO_2 and ZnO NPs for 5- and 10- days.

Data represent mean ± SEM (n = 5). Negative control (NC) = distilled water, CYP = cyclophosphamide (positive control).

[#] $p < 0.05$ in 5-days exposure

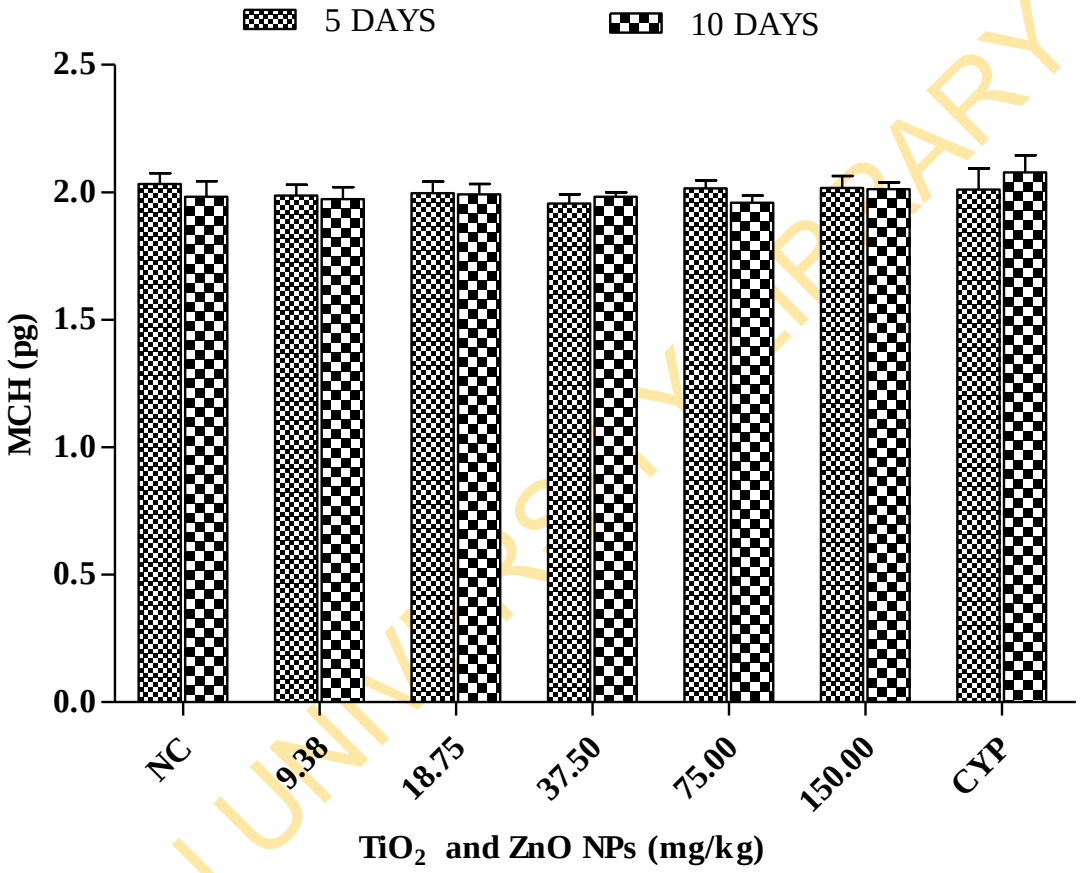

Figure 4. 32: Frequency of Mean Cell Haemoglobin (pg) in mice treated with TiO_2 and ZnO NPs for 5- and 10- days.

Data represent mean ± SEM (n = 5). Negative control (NC) = distilled water, CYP = cyclophosphamide (positive control).

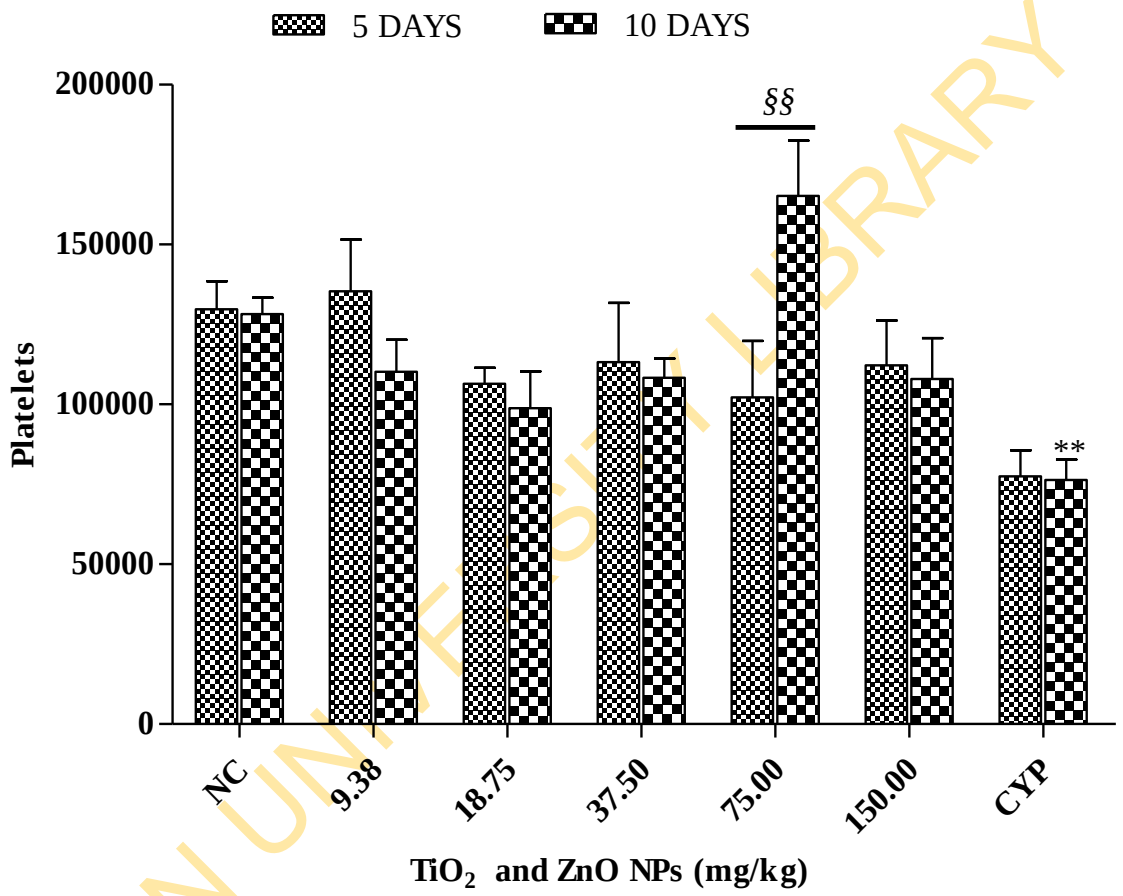

Figure 4. 33: Frequency of Platelets in mice treated with TiO_2 and ZnO NPs for 5- and 10- days.

Data represent mean ± SEM (n = 5). Negative control (NC) = distilled water, CYP = cyclophosphamide (positive control).

$p < 0.01$ in 5-days exposure

§§ $p < 0.01$ for the comparison between 5- and 10- day exposures

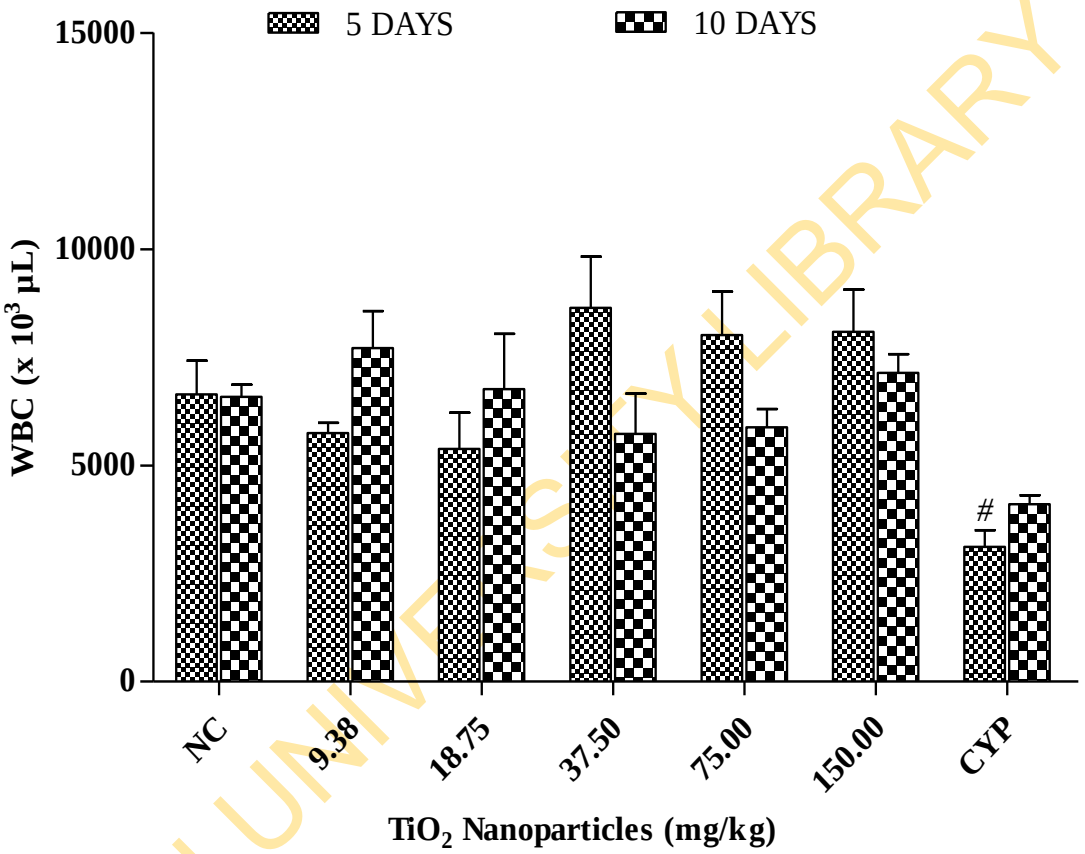

Figure 4. 34: Frequency of White Blood Cells count (x 10^3 µL) in mice treated with TiO_2 NPs for 5- and 10- days.

Data represent mean ± SEM (n = 5). Negative control (NC) = distilled water, CYP = cyclophosphamide (positive control).

[#] $p < 0.05$ in 5-days exposure

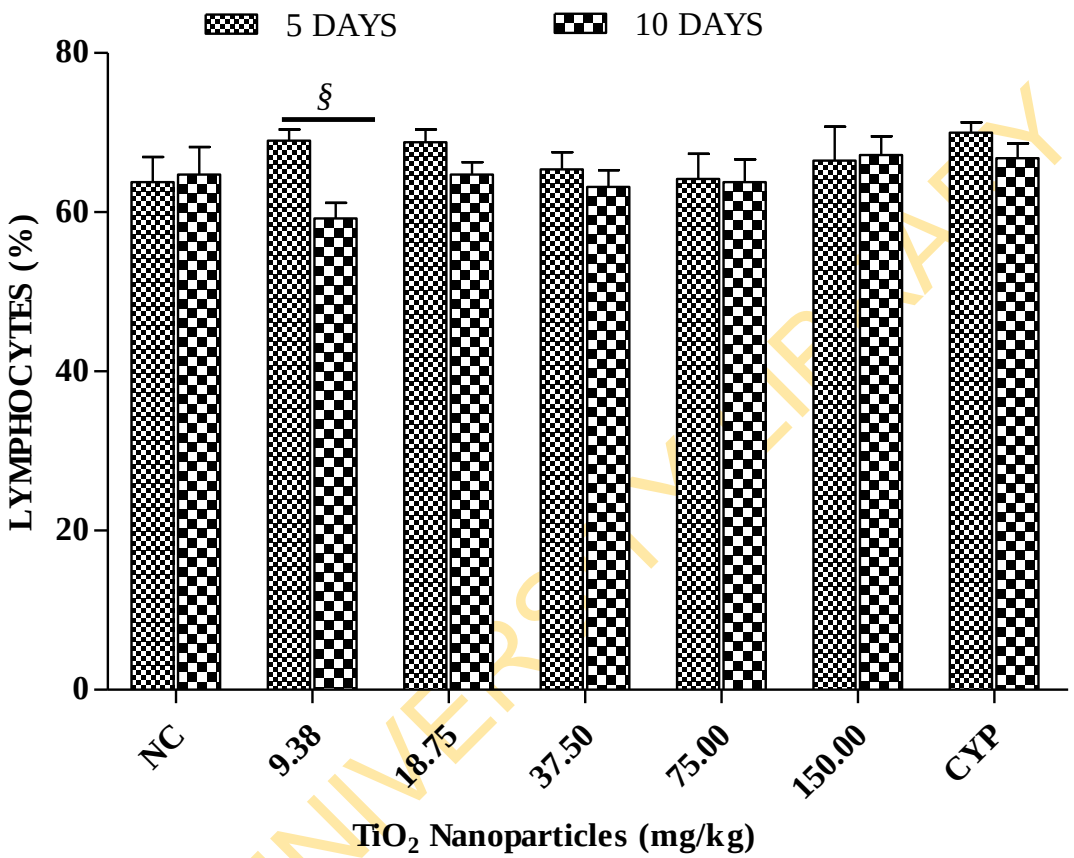

Figure 4. 35: Frequency of Lymphocytes (%) in mice treated with TiO_2 NPs for 5- and 10- days.

Data represent mean ± SEM (n = 5). Negative control (NC) = distilled water, CYP = cyclophosphamide (positive control).

§ $p < 0.05$ for the comparison between 5- and 10- day exposures

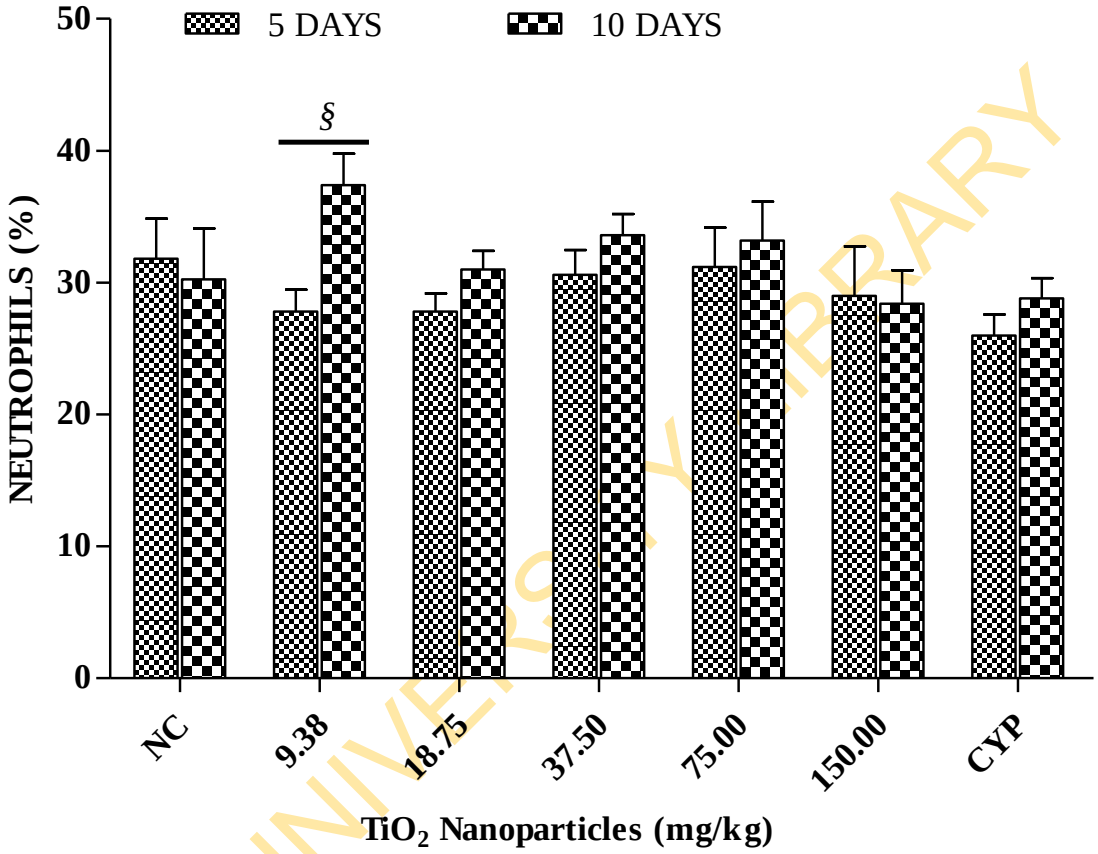

Figure 4. 36: Frequency of Neutrophils (%) in mice treated with TiO_2 NPs for 5- and 10-days.

Data represent mean ± SEM (n = 5). Negative control (NC) = distilled water, CYP = cyclophosphamide (positive control).

[1]$p < 0.05$ for the comparison between 5- and 10-days exposures

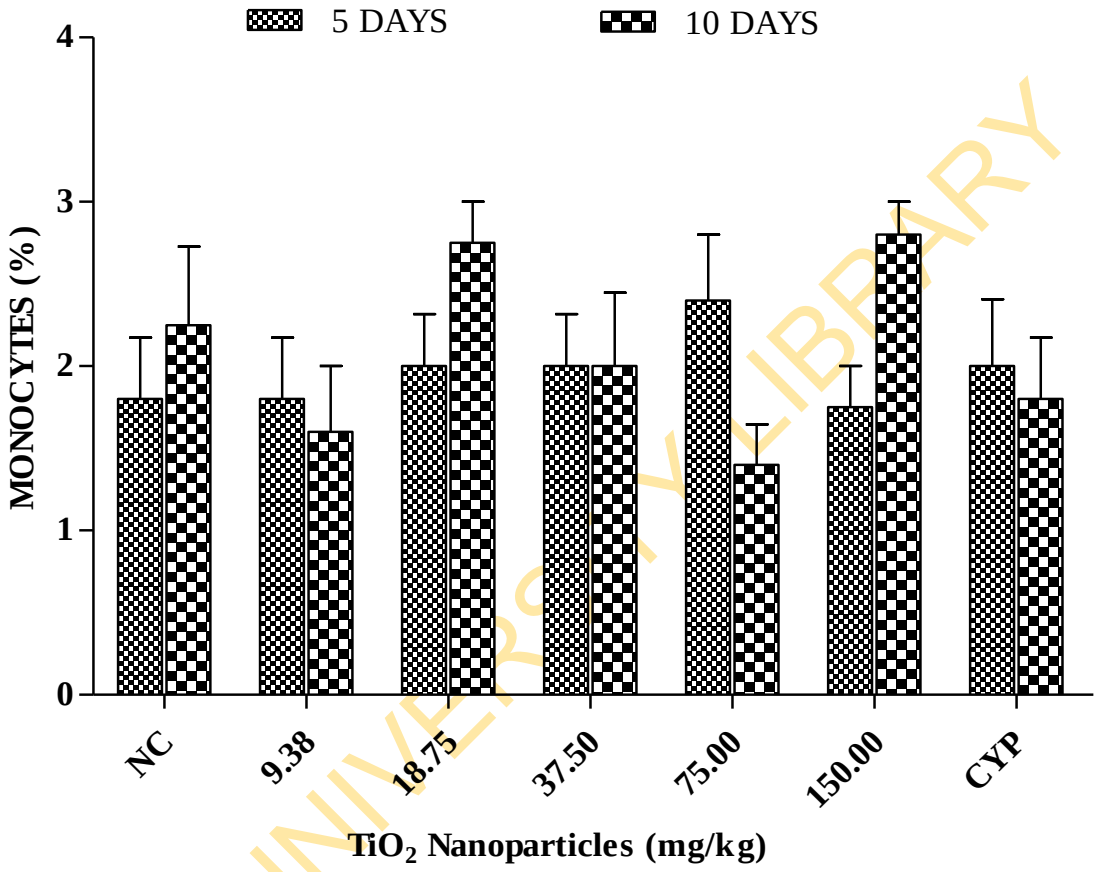

Figure 4. 37: Frequency of Monocytes (%) in mice treated with TiO_2 NPs for 5- and 10-days.

Data represent mean ± SEM (n = 5). Negative control (NC) = distilled water, CYP = cyclophosphamide (positive control).

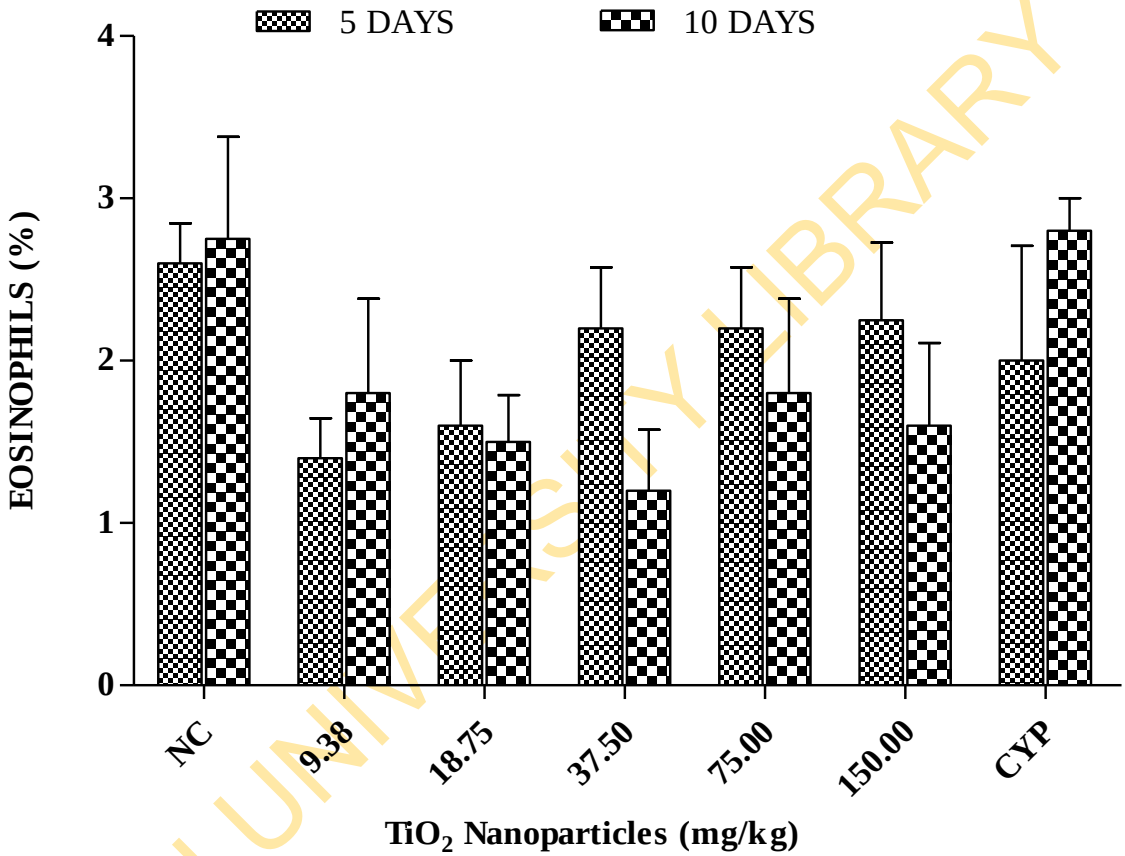

Figure 4. 38: Frequency of Eosinophils (%) in mice treated with TiO_2 NPs for 5- and 10-days.

Data represent mean ± SEM (n = 5). Negative control (NC) = distilled water, CYP = cyclophosphamide (positive control).

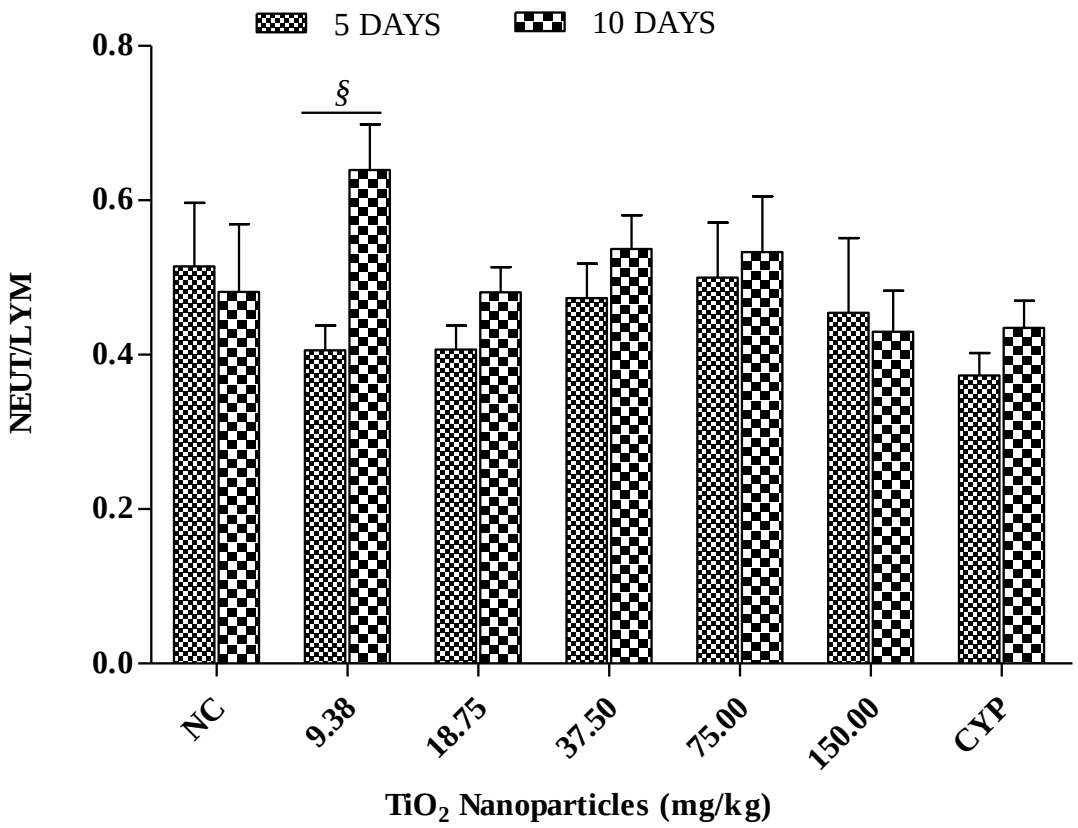

Figure 4. 39: Frequency of Neutrophil/Eosinophil in mice treated with TiO_2 NPs for 5- and 10- days.

Data represent mean ± SEM (n = 5). Negative control (NC) = distilled water, CYP = cyclophosphamide (positive control).

[§] $p < 0.05$ for the comparison between 5- and 10-days exposures

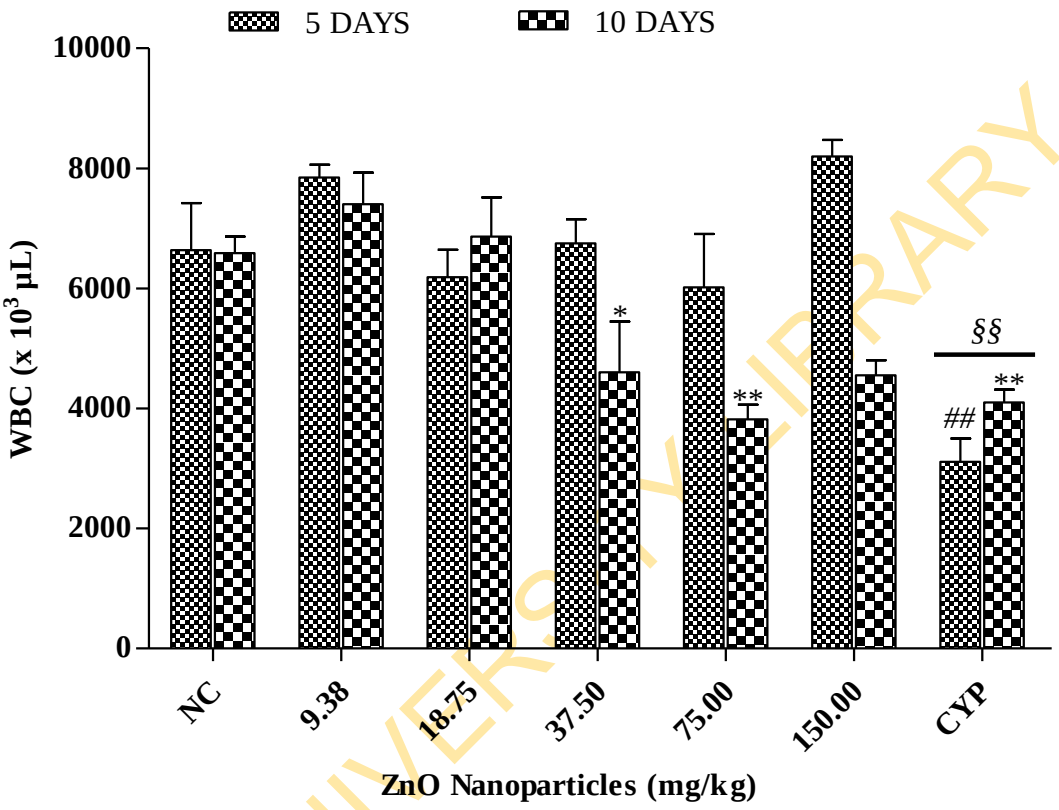

Figure 4. 40: Frequency of White Blood Cells count (x 10^3 µL) in mice treated with ZnO NPs for 5- and 10- days.

Data represent mean ± SEM (n = 5). Negative control (NC) = distilled water, CYP = cyclophosphamide (positive control).

$p < 0.01$ in 5-days exposure

* $p < 0.05$ and ** $p < 0.01$ in 10-days exposure.

§§ $p < 0.01$ for the comparison between 5- and 10- day exposures

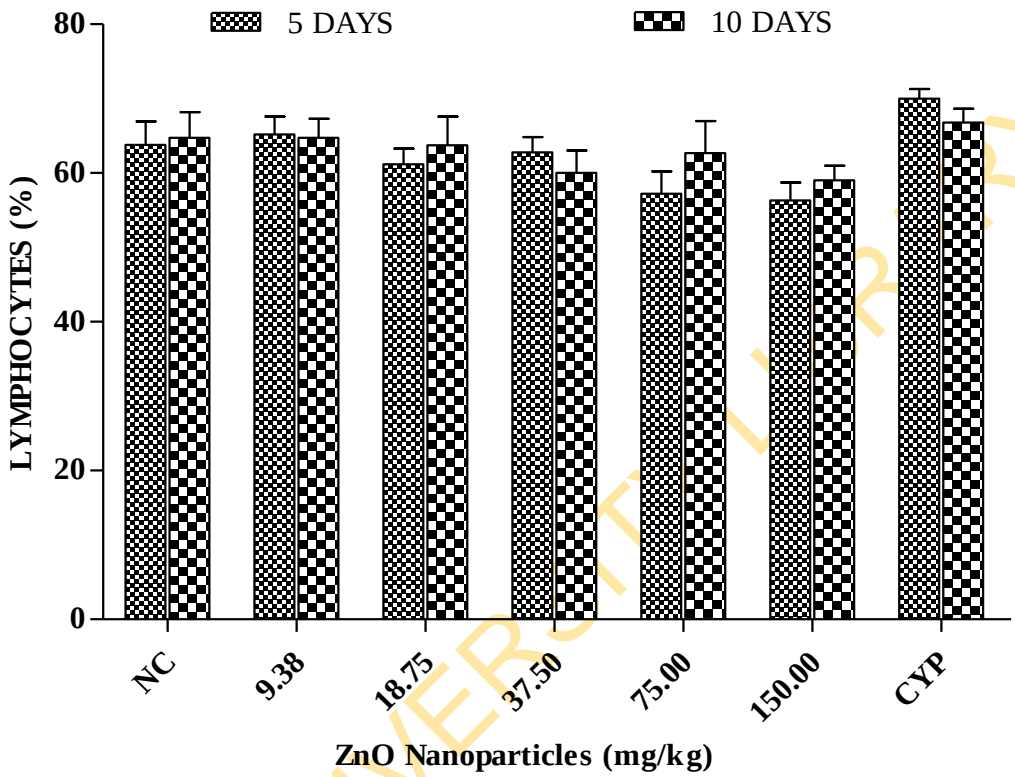

Figure 4. 41: Frequency of Lymphocytes (%) in mice treated with ZnO NPs for 5- and 10- days.

Data represent mean ± SEM (n = 5). Negative control (NC) = distilled water, CYP = cyclophosphamide (positive control).

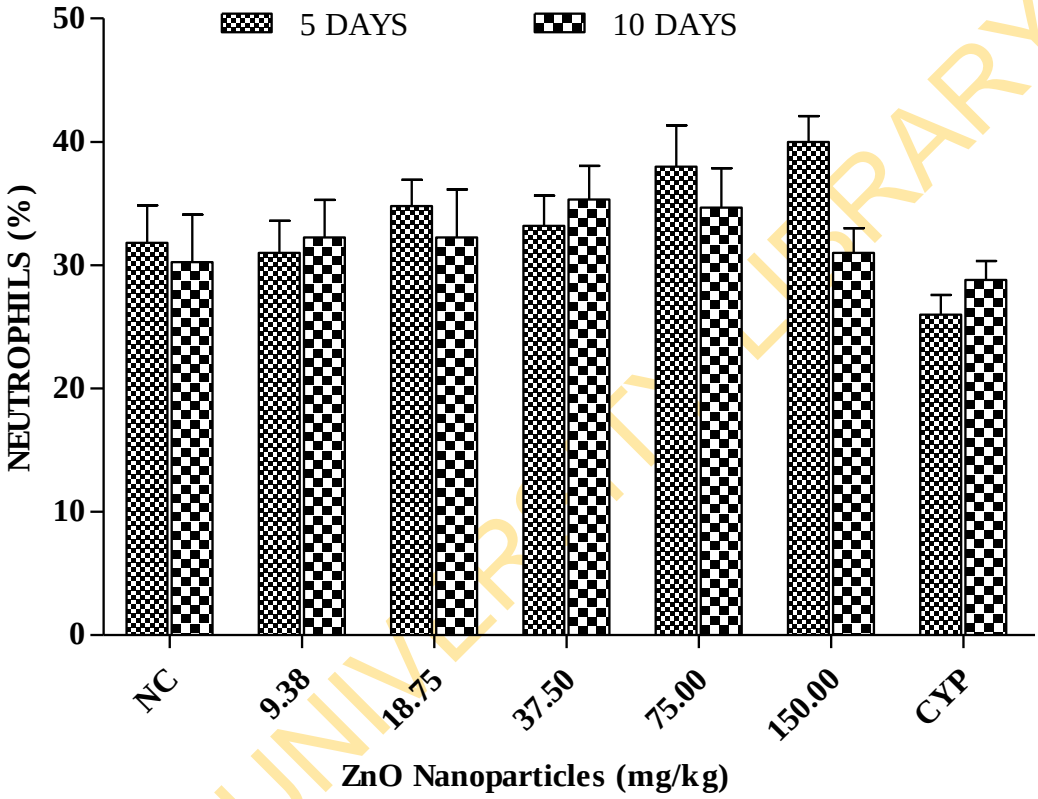

Figure 4. 42: Frequency of Neutrophils (%) in mice treated with ZnO NPs for 5- and 10-days.

Data represent mean ± SEM (n = 5). Negative control (NC) = distilled water, CYP = cyclophosphamide (positive control).

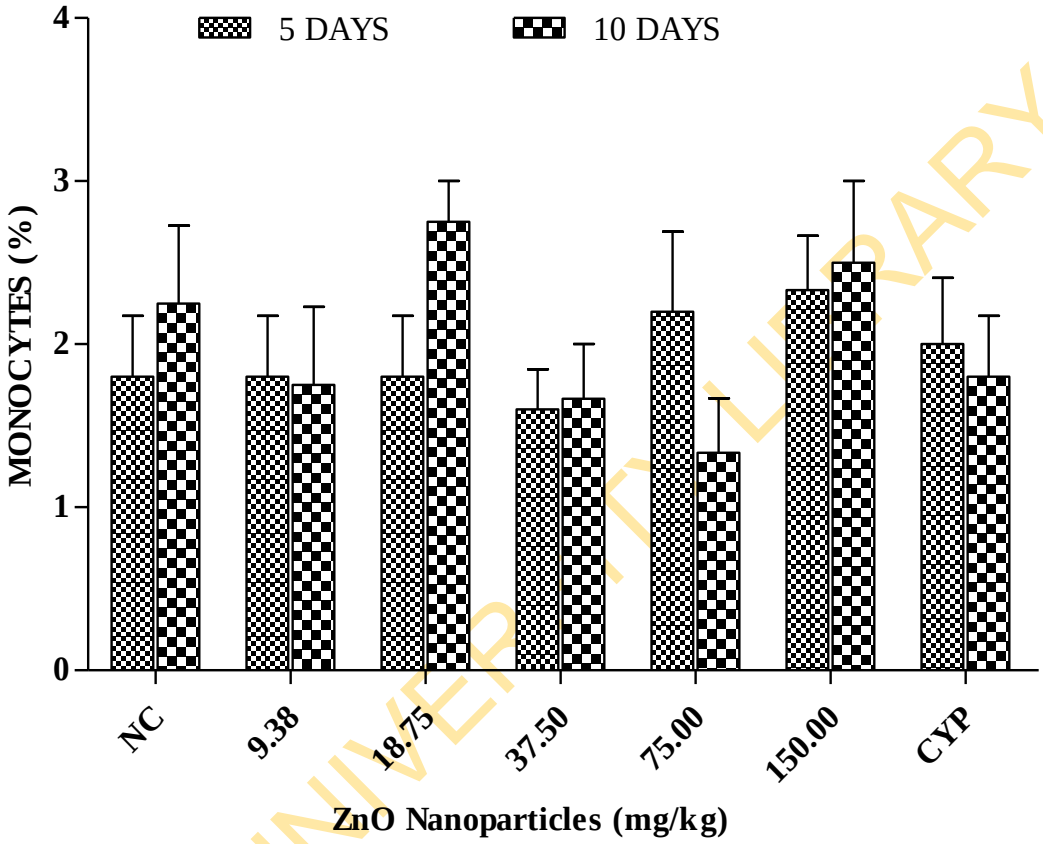

Figure 4. 43: Frequency of Monocytes (%) in mice treated with ZnO NPs for 5- and 10-days.

Data represent mean ± SEM (n = 5). Negative control (NC) = distilled water, CYP = cyclophosphamide (positive control).

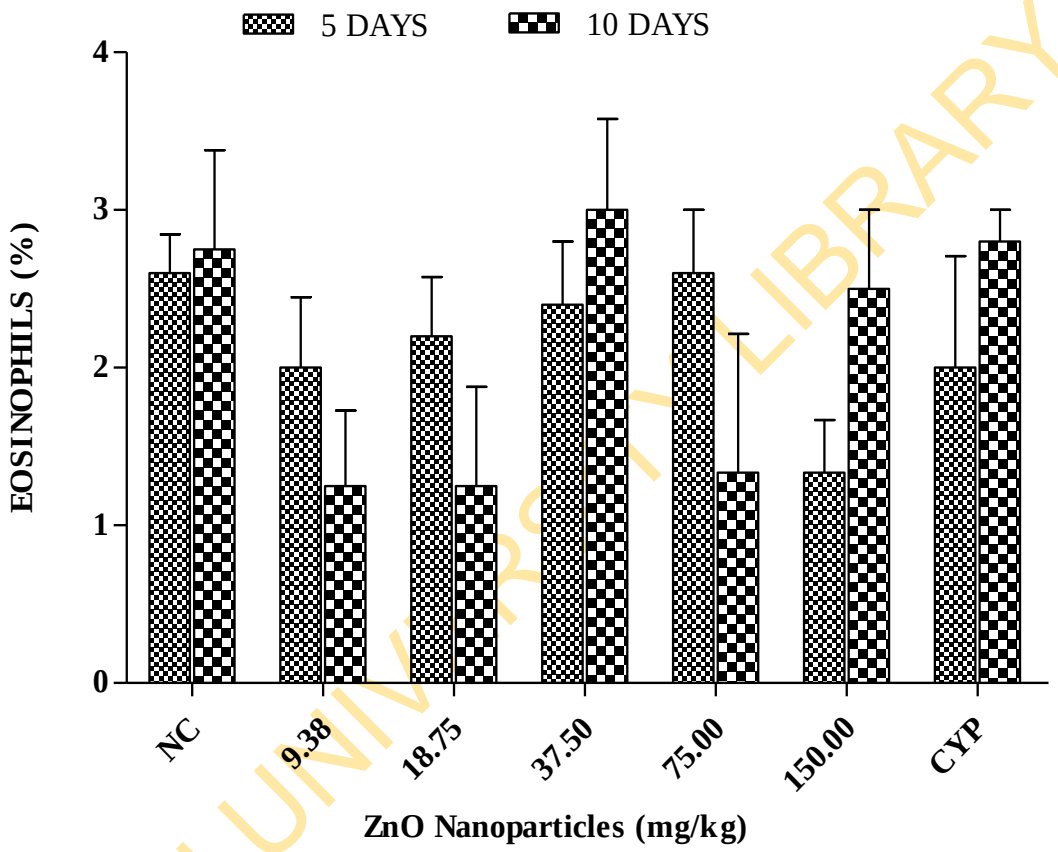

Figure 4. 44: Frequency of Eosinophils (%) in mice treated with ZnO NPs for 5- and 10-days.

Data represent mean ± SEM (n = 5). Negative control (NC) =distilled water, CYP = cyclophosphamide (positive control).

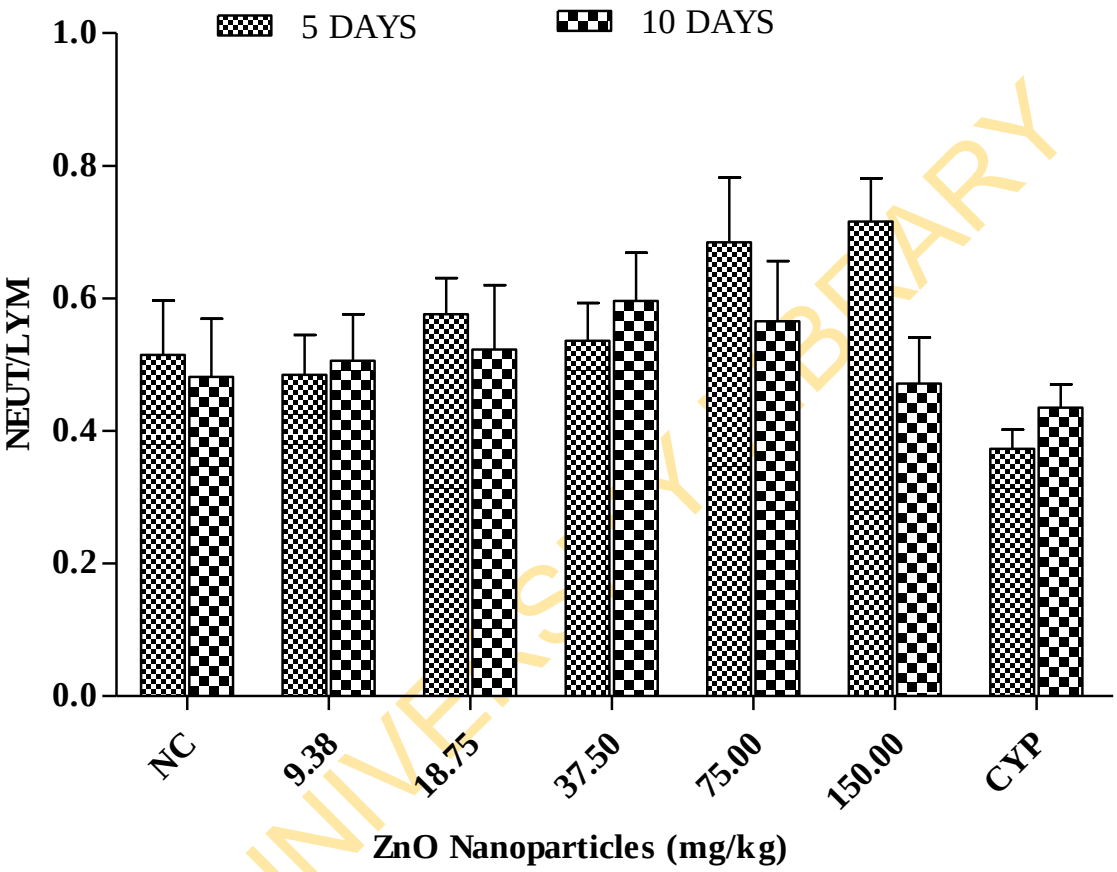

Figure 4. 45: Frequency of Neutrophil/Lymphocyte in mice treated with ZnO NPs for 5- and 10- days.

Data represent mean ± SEM (n = 5). Negative control (NC) = distilled water, CYP = cyclophosphamide (positive control).

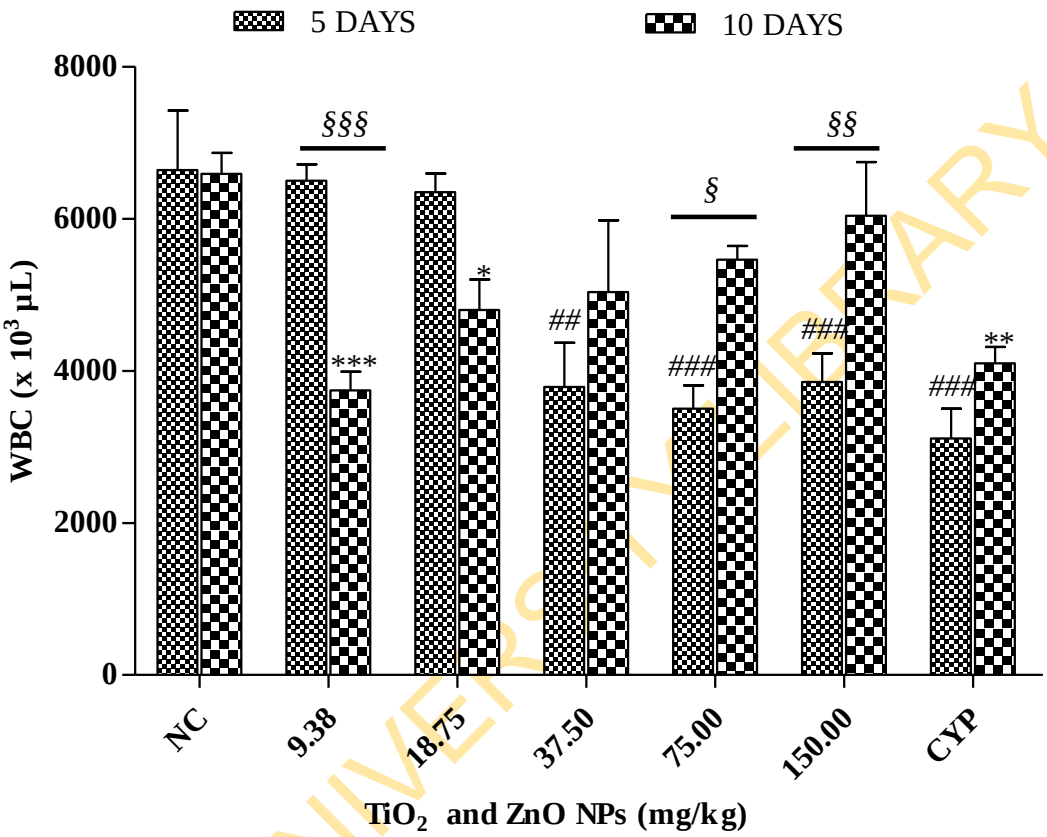

Figure 4. 46: Frequency of White Blood Cells count (x 10^3 µL) in mice treated with TiO_2 and ZnO NPs for 5- and 10- days.

Data represent mean ± SEM (n = 5). Negative control (NC) = distilled water, CYP = cyclophosphamide (positive control).

$^{\#\#}$ $p < 0.01$ and $^{\#\#\#}$ $p<0.001$ in 5-days exposure

* $p < 0.05$, ** $p < 0.01$ and *** $p < 0.001$ in 10-days exposure.

§ $p < 0.05$, §§ $p < 0.01$ and §§§ $p < 0.001$ for the comparison between 5- and 10-day exposures

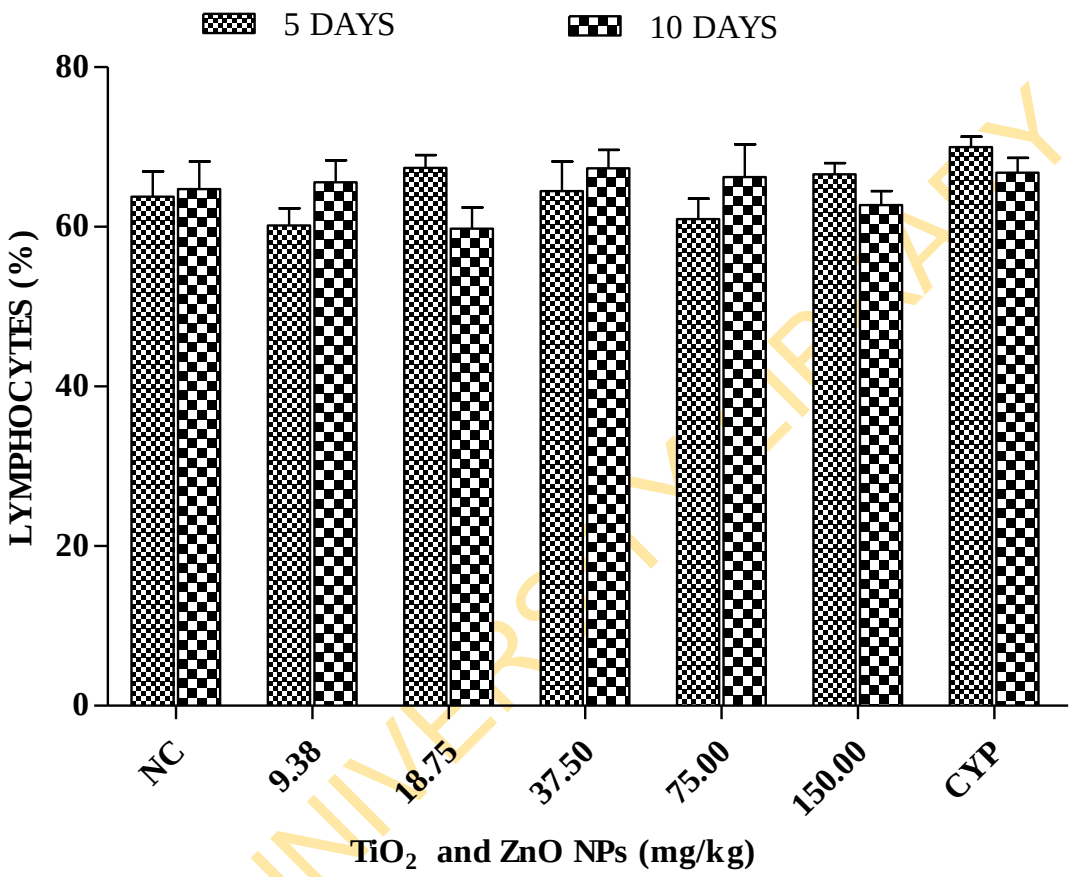

Figure 4. 47: Frequency of Lymphocytes (%) in mice treated with TiO_2 and ZnO NPs for 5- and 10- days.

Data represent mean ± SEM (n = 5). Negative control (NC) = distilled water, CYP = cyclophosphamide (positive control).

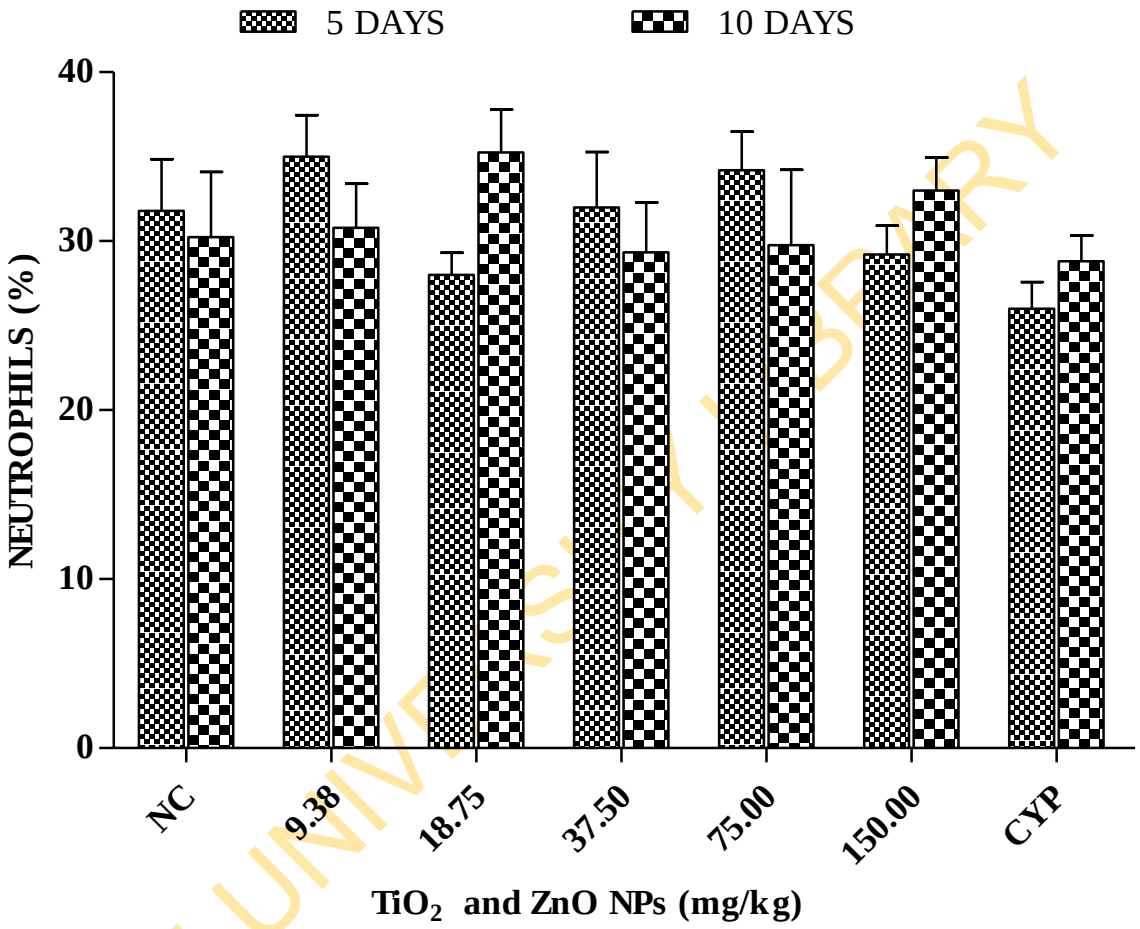

Figure 4. 48: Frequency of Neutrophils (%) in mice treated with TiO_2 and ZnO NPs for 5- and 10- days.

Data represent mean ± SEM (n = 5). Negative control (NC) = distilled water, CYP = cyclophosphamide (positive control).

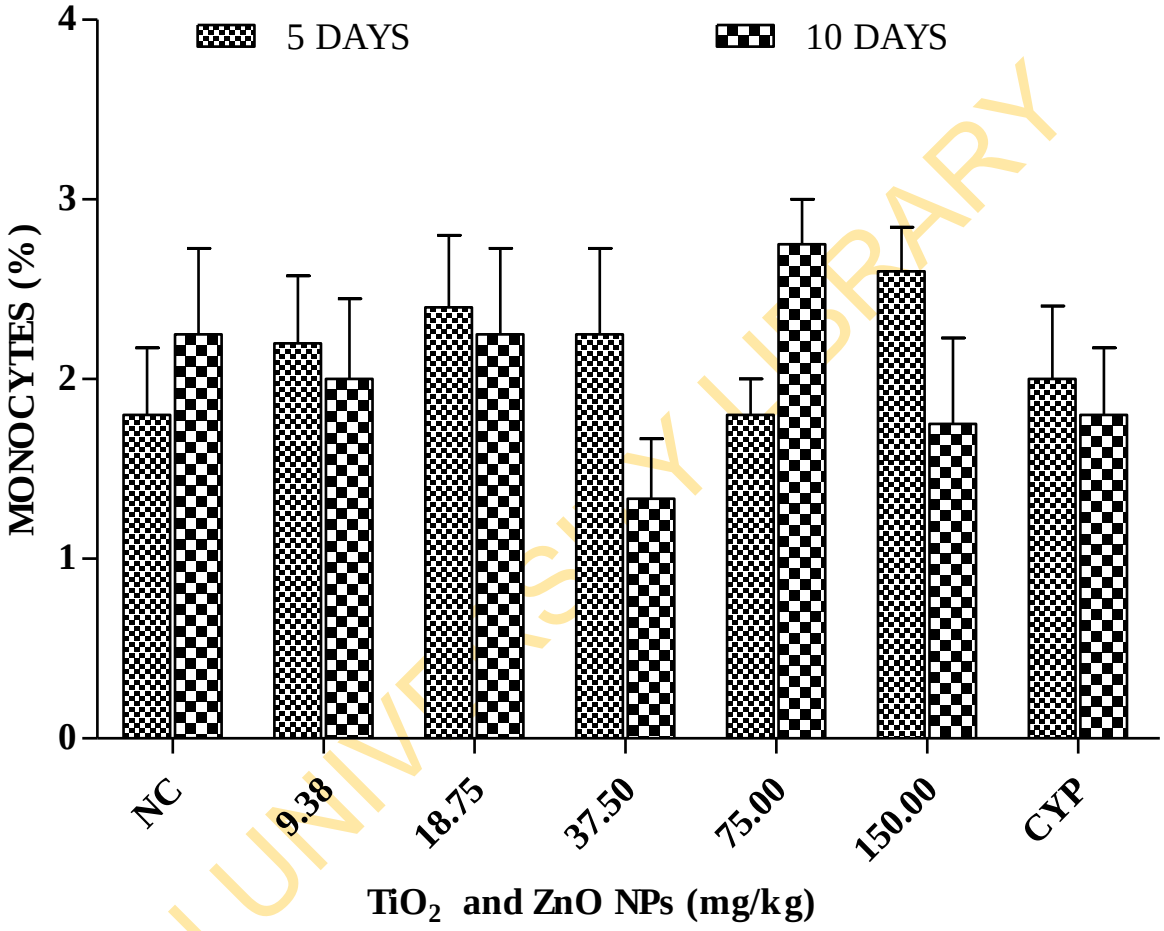

Figure 4. 49: Frequency of Monocytes (%) in mice treated with TiO_2 and ZnO NPs for 5- and 10- days.

Data represent mean ± SEM (n = 5). Negative control (NC) = distilled water, CYP = cyclophosphamide (positive control).

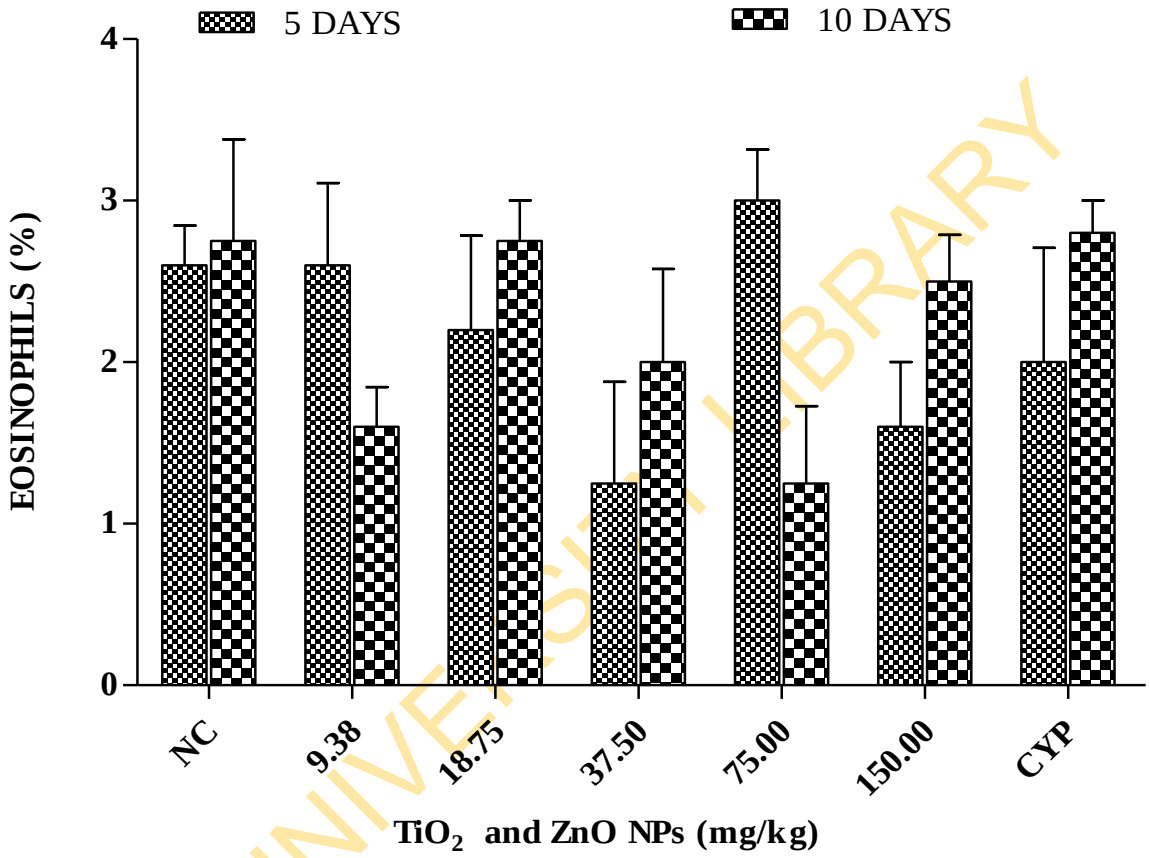

Figure 4. 50: Frequency of Eosinophils (%) in mice treated with TiO_2 and ZnO NPs for 5- and 10- days.

Data represent mean ± SEM (n = 5). Negative control (NC) = distilled water, CYP = cyclophosphamide (positive control).

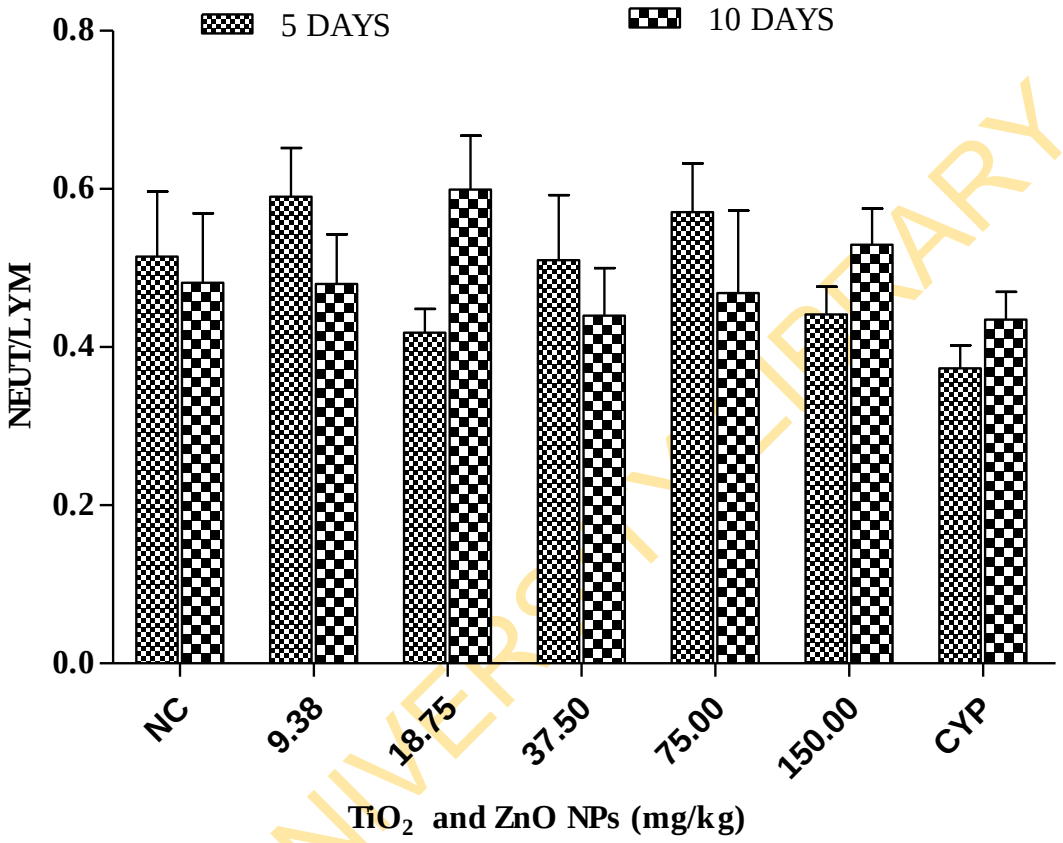

Figure 4. 51: Frequency of Neutrophils/Lymphocyes in mice treated with TiO_2 and ZnO NPs for 5- and 10- days.

Data represent mean ± SEM (n = 5). Negative control (NC) = distilled water, CYP = cyclophosphamide (positive control).

4.4.4 Histopathological alterations induced by titanium dioxide, zinc oxide nanoparticles and their mixture in the organs of mice

Histopathological alterations of the liver

The liver of the mice that received distilled water showed closely packed hepatic plates for 5 and 10 days exposure periods. However, the liver histopathology of mice treated with TiO_2, ZnO NPs and their mixture showed foci of vacuolar change of centrilobular hepatocytes and peri-portal hepatocytes, moderate to mild Kupffer cell hyperplasia with dark brown pigments, single cell hepatocellular necrosis, large megalocytes, multiple foci of mild thinning of hepatic plates, foci of dense aggregates of mononuclear inflammatory cells around the portal tracts, epitheloid macrophages and foci of mild thinning of hepatic cords resulting in dilated sinusoids (Figure 4.53).

Histopathological alterations of the kidney

The kidney histopathology of the mice that received distilled water for 5 and 10 days exposure periods indicated normal architecture of the glomeruli, tubules and renal interstitium. In contrast, the kidney histopathology of mice treated with TiO_2, ZnO NPs and their mixture at both 5- and 10- day exposure periods showed sloughing off of tubular epithelial cells, degeneration of the tubular epithelial cells, congestion of interstitial blood vessels, dilated tubules with increased luminal width and intraluminal casts (Figure 4.54).

Histopathological alterations of the spleen

The spleen histopathology of the mice that received distilled water for 5 and 10 days exposure periods showed distinct lymphoid follicles / closely-packed periarteriolar lymphoid sheath (PALS). Congestion of splenic sinuses and sinusoids, numerous foci of pigment-laden macrophages [haemosiderosis], antigenic stimulation and lymphoid proliferation, distinct mantle zones and atrophic spleen with wrinkled capsule were observed at the various doses of TiO_2, ZnO NPs and their mixture administered to mice (Figure 4.55).

Histopathological alterations of the heart

The histopathology of the heart of mice treated with distilled water evinced normal cardiomyocytes for 5 and 10 days exposure periods. Degeneration of cardiomyocytes with loss of striations, congestion of coronary blood vessels, necrotic cardiomyocytes (pyknotic nucleus and eosinophilic cytoplasm), vacuolar change, detachment of cardiomyocytes, increase in connective tissue (fibroblast nuclei), aggregates of inflammatory mononuclear cells especially around blood vessels and cytoplasmic vacuolations were observed in mice treated with TiO_2, ZnO NPs and their mixture (Figure 4.56).

Histopathological alterations of the brain

The Histopathology of the brain of mice treated with distilled water showed normal appearance of the neurons, glial cells and neuropil for 5 and 10 days exposure periods. However, multiple foci of aggregates of glial cells [gliosis] in the neuropil, foci of neuronal necrosis, accumulation of inflammatory cells around the meningeal blood vessels, swelling of the endothelial cells of the cerebral blood vessels, shrunken neurons with loss of nuclei, degenerate neurons with angular cell bodies, congestion of cerebral blood vessels, swollen endothelial cells lining the blood vessels, increased numbers of satellite cells (satelitosis), vacuolation of the neuropil and large neuronal bodies were observed mice treated with TiO_2, ZnO NPs and their mixture (Figure 4.57).

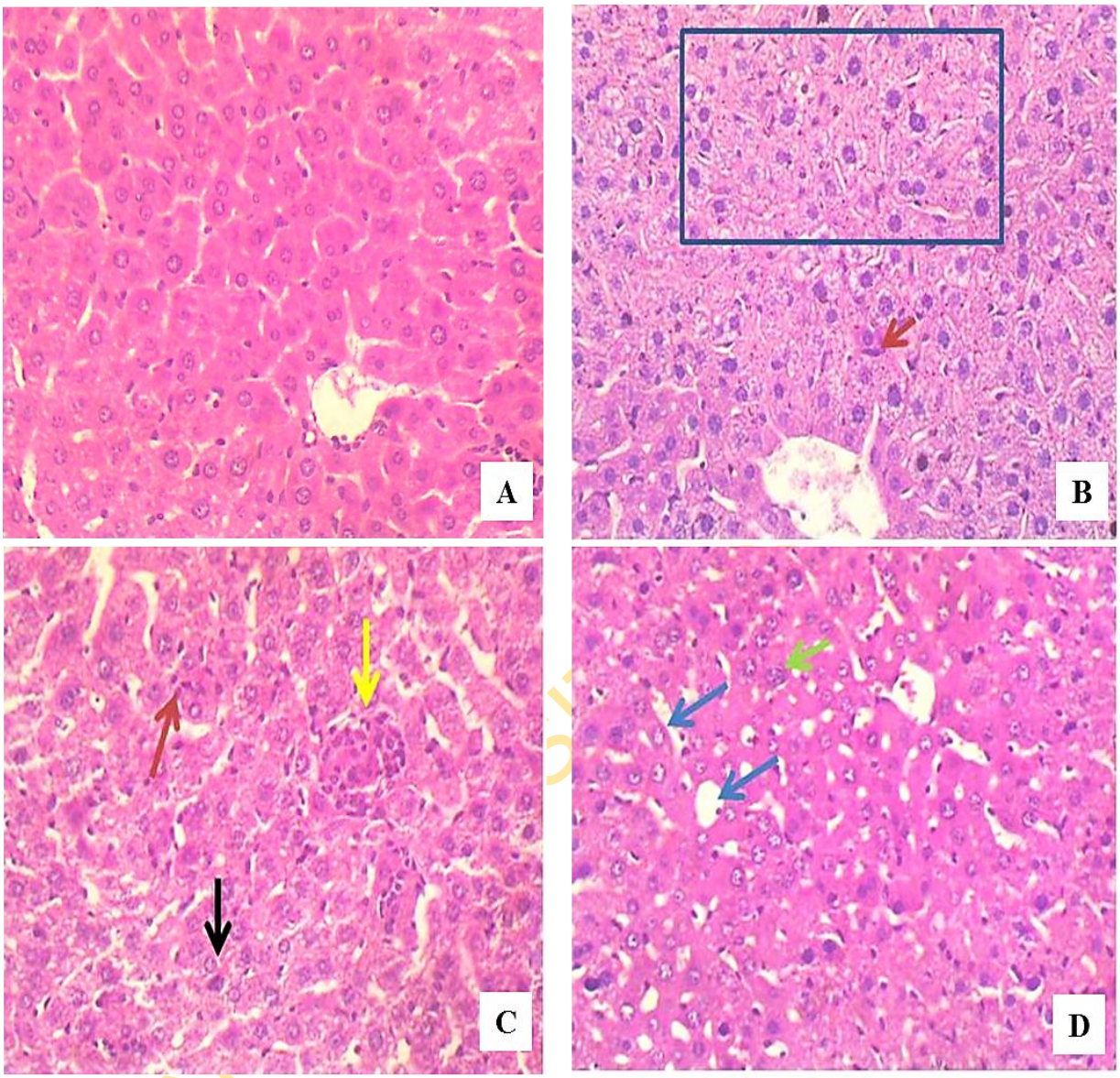

Figure 4. 52: Sections of the liver of mice treated with distilled water (A); 18.75 $mgkg^{-1}$ of the mixture for the 5- day exposure (B); 37.50 $mgkg^{-1}$ of TiO_2 NPs for the 5- day exposure (C); 37.50 $mgkg^{-1}$ of TiO_2 NPs for the 10- day exposure (D). Lesions observed are: aggregates of mononuclear inflammatory cells (yellow arrow), single-cell hepatocellular necrosis (black arrow), dilated sinusoids (blue arrow), kupffer cell hyperplasia (red arrow), large hepatocytes (megalocytes) (green arrow) and vacuolar change of the hepatocytes (blue box). Magnification: 400X.

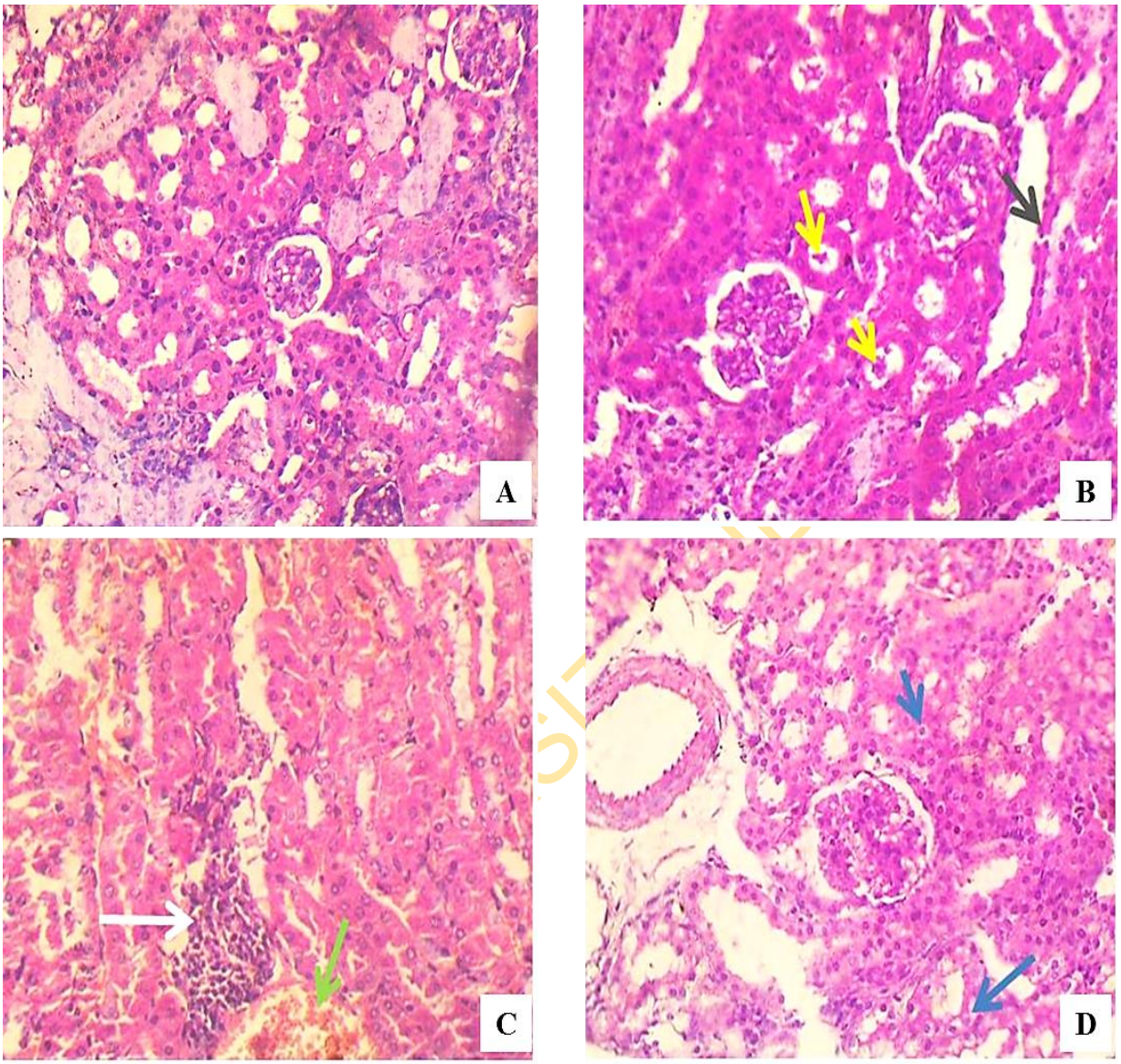

Figure 4. 53: Sections of the kidney of mice treated with distilled water (A); 150.00 $mgkg^{-1}$ of TiO_2 NPs for the 5- day exposure (B); 150.00 $mgkg^{-1}$ of TiO_2 NPs for the 10 day exposure (C); 75.00 $mgkg^{-1}$ of ZnO NPs for the 10 day exposure (D). Lesions observed are: moderate sloughing off of the tubular epithelial cells (black arrow), eosinophilic tubular casts (yellow arrow), congestion of interstitial blood vessels (green arrow), aggregates of mononuclear inflammatory cells (white arrow) and degeneration of tubular epithelial cells (blue arrow). Magnification: 400X.

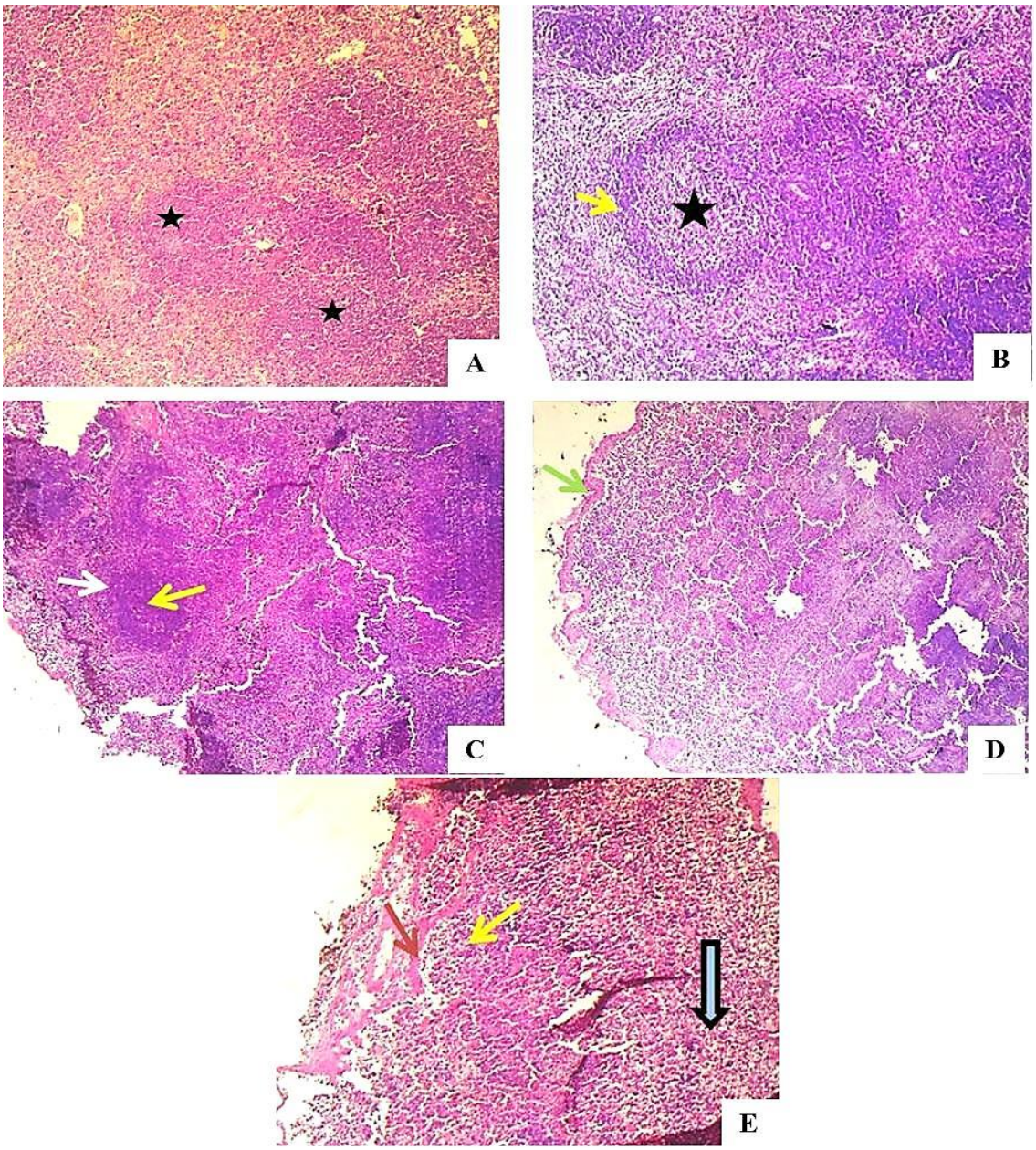

Figure 4. 54: Sections of the spleen of mice treated with distilled water (A); 75.00 $mgkg^{-1}$ of TiO_2 NPs for the 5- day exposure (B); 9.38 $mgkg^{-1}$ of ZnO NPs for the 5- day exposure (C); 75.00 $mgkg^{-1}$ of ZnO NPs for the 5- day exposure (D); 150.00 $mgkg^{-1}$ of TiO_2 NPs for the 10 day exposure (E). Lesions observed are: distinct lymphoid follicles/PALS (yellow arrow), prominent germinal centres (black stars), distinct mantle zones (white arrow), atrophic spleen with wrinkled capsule (green arrow), haemosiderosis (red arrow) and congestion of splenic cords and sinusoids (thick blue arrow). Magnification: 100X.

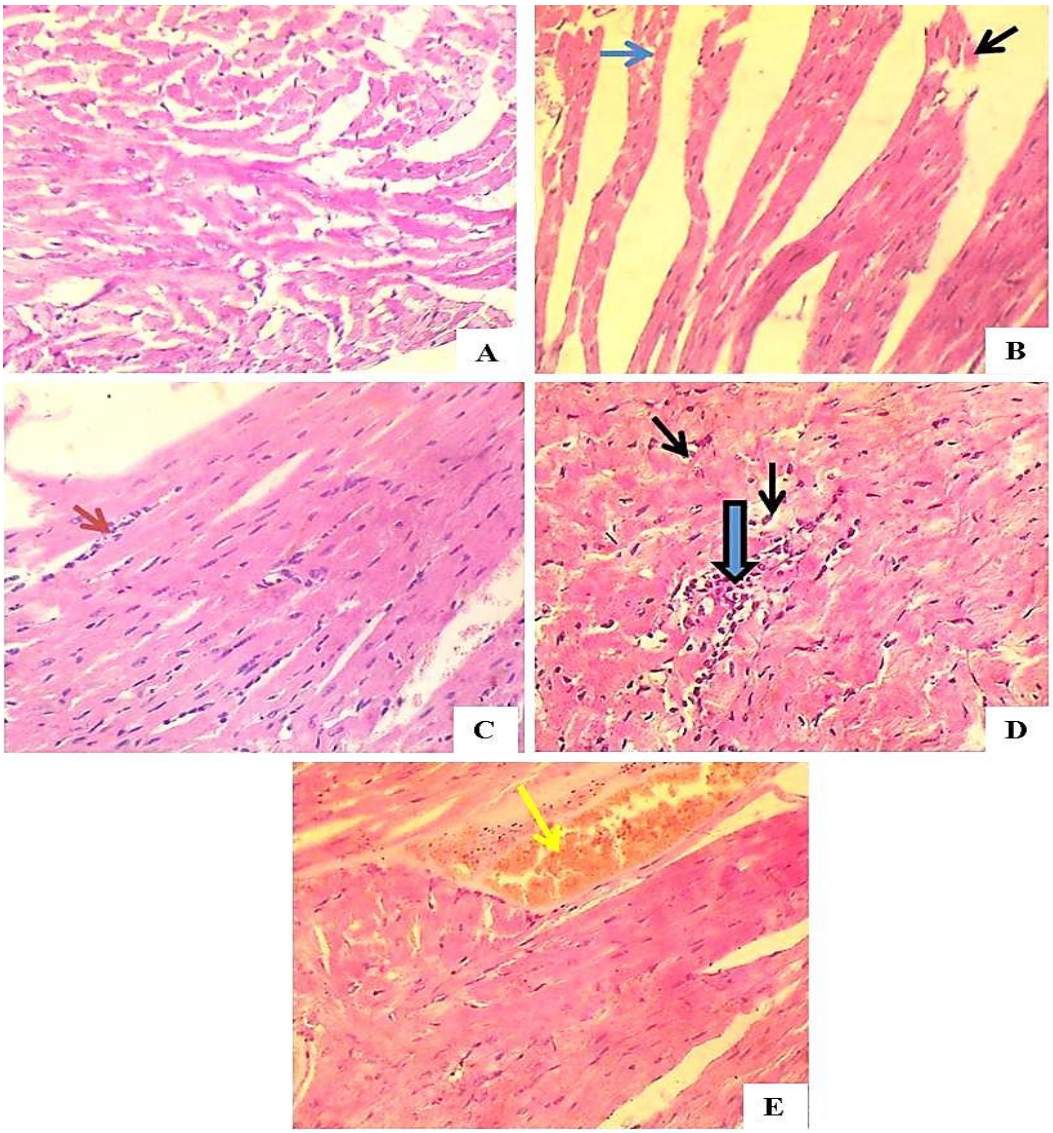

Figure 4. 55: Sections of the heart of mice treated with distilled water (A); 37.50 $mgkg^{-1}$ of ZnO NPs for the 5- day exposure (B); 37.50 $mgkg^{-1}$ of their mixture for the 10- day exposure (C); 37.50 $mgkg^{-1}$ of TiO_2 NPs for the 10- day exposure (D); 75.00 $mgkg^{-1}$ of their mixture for the 10- day exposure (E). Various lesions observed are: degeneration of cardiomyocytes with loss of striations and foci of vacuolar change (blue arrow), congestion of coronary blood vessels (yellow arrow), degenerate and necrotic cardiomyocytes (black arrow) with small pyknotic nucleus and eosinophilic cytoplasm, increase in the connective tissue (fibroblast nuceli) (red arrow) and loss of striations and aggregates of mononuclear inflammatory cells (thick blue arrow). Magnification: 400X.

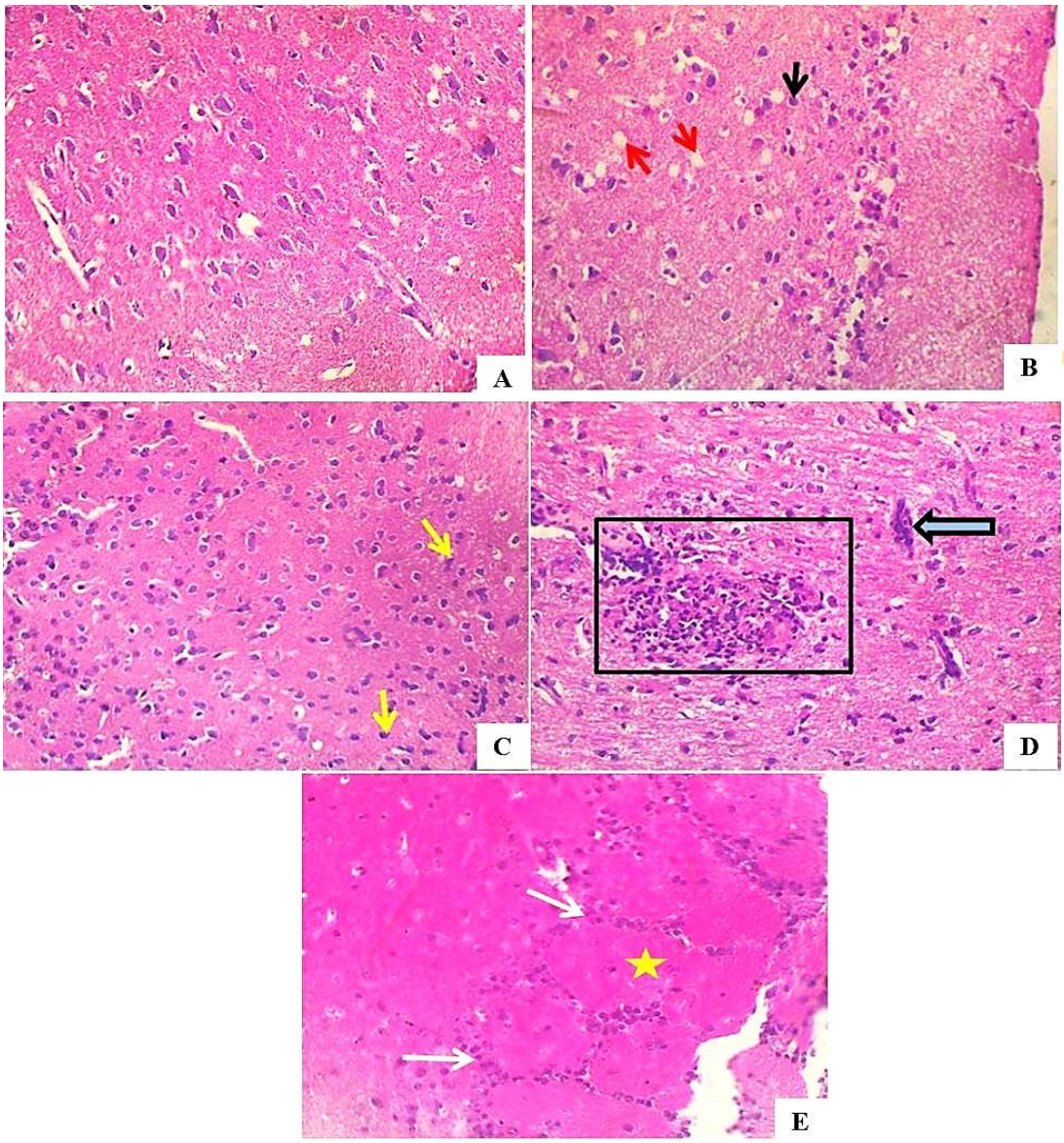

Figure 4. 56: Sections of the brain of mice treated with distilled water (A); 75.00 $mgkg^{-1}$ of ZnO NPs for the 5- day exposure (B); 75.00 $mgkg^{-1}$ of their mixture for the 5- day exposure (C); 150.00 $mgkg^{-1}$ of their mixture for the 5- day exposure (D); 75.00 $mgkg^{-1}$ of their mixture for the 10- day exposure (E). Various lesions observed are: necrotic and degenerated neurons (black arrow), accumulation of inflammatory cells (yellow arrow), swelling of the endothelial cells of the cerebral blood vessels (thick blue arrow) and aggregates of glial cells (box), vacuolation of neuropil (red arrows), numerous satellite cells (white arrows) surrounding the large neuronal bodies (yellow star). Magnification: 400X.

4.4.5 Biochemical alterations induced by titanium dioxide, zinc oxide nanoparticles and their mixture in the serum and urine of mice

Figures 4.58 – 4.60 show the results of the serum ALT activity in mice treated with TiO_2, ZnO NPs and their mixture for 5 and 10 days. For the 5- day exposure period, TiO_2 NPs administered to mice induced a significant ($p < 0.01$) increase in the serum ALT activity (Figure 4.58) at 18.75, 37.50, 75.00 and 150.00 $mgkg^{-1}$ in comparison with the mice treated with distilled water while at the 10-day exposure period, there was a significant ($p < 0.05$) reduction in the serum ALT activity (Figure 4.58) at tested doses in comparison with the mice treated with distilled water. Consequently, a significant difference between the 5- and 10- day exposure periods for mice treated with TiO_2 NPs was observed at 9.38 ($p < 0.001$), 18.75 ($p < 0.01$), 37.50 ($p < 0.001$), 75.00 ($p < 0.001$) and 150.00 $mgkg^{-1}$ ($p < 0.05$).

Similarly, mice treated with ZnO NPs for the 5- day exposure period exhibited a significant ($p < 0.001$) increase in the serum ALT activity (Figure 4.59) at tested doses in comparison with the mice treated with distilled water. For the 10- day exposure period, a significant ($p < 0.05$) reduction in the serum ALT activity (Figure 4.59) was observed at tested doses in comparison with the mice treated with distilled water. A significant difference between the 5- and 10- day exposure periods for mice treated with ZnO NPs was observed at 9.38 ($p < 0.001$), 18.75 ($p < 0.001$), 37.50 ($p < 0.001$), 75.00 ($p < 0.001$) and 150.00 $mgkg^{-1}$ ($p < 0.001$).

For the 5- day exposure period, mice treated with their mixture exhibited an increase in the serum ALT activity (Figure 4.60), which was significant ($p < 0.001$) only at the 18.75 and 75.00 $mgkg^{-1}$ in comparison with the mice treated with distilled water while for the 10- day exposure period, a significant ($p < 0.001$) reduction in the serum ALT activity (Figure 4.60) of the treated mice was observed at tested doses in comparison with the mice treated with distilled water.

Figures 4.61 – 4.63 show the results of the serum AST activity in mice treated with TiO_2, ZnO NPs and their mixture for 5 and 10 days. For the 5- day exposure period, TiO_2 NPs induced a significant ($p < 0.05$) increase in the serum AST activity (Figure 4.61) of the

treated mice across all doses in comparison with the mice treated with distilled water while for the 10- day exposure period, an increase in the serum AST activity (Figure 4.61) in the treated mice was observed at tested doses but significant ($p < 0.05$) only at the 9.38 and 18.75 $mgkg^{-1}$ of TiO_2 NPs in comparison with the mice treated with distilled water. Consequently, a significant difference between the 5- and 10- day exposure periods for mice treated with TiO_2 NPs was observed only at 150.00 $mgkg^{-1}$ ($p < 0.001$). Mice treated with ZnO NPs for both 5 and 10 days, exhibited a significant ($p < 0.05$) increase in the serum AST activity (Figure 4.62) at tested doses in comparison with the mice treated with distilled water. Consequently, a significant difference between the 5- and 10- day exposure periods for mice treated with ZnO NPs was observed at 18.75 ($p < 0.05$), 37.50 ($p < 0.05$), 75.00 ($p < 0.01$)and 150.00 $mgkg^{-1}$ ($p < 0.001$).

Similarly, their mixture administered to mice for the 5- day exposure period induced a significant ($p < 0.05$) increase in serum AST activity (Figure 4.63) at tested doses while for the 10- day exposure period, an increase in the serum AST activity (Figure 4.63) was observed at tested doses but significant ($p < 0.001$) only at the 9.38 $mgkg^{-1}$ of their mixture in comparison with the mice treated with distilled water. Consequently, a significant difference between the 5- and 10- day exposure periods for mice treated with the NP mixture was observed only at 150.00 $mgkg^{-1}$ ($p < 0.001$).

Figures 4.64 – 4.66 show the results of the ratio of the AST/ALT activity in mice treated with both NPs and their mixture for the 5 and 10 days. For the 5- and 10- day exposure periods, mice treated with TiO_2 NPs exhibited no significant ($p > 0.05$) increase in the AST/ALT activity (Figure 4.64) at tested doses in comparison with the mice treated distilled water. However, the treatment of mice with ZnO NPs for the 5- day exposure period induced no significant ($p > 0.05$) reduction in the AST/ALT activity (Figure 4.65) in comparison with the mice treated with distilled water. In contrast to the 10- day exposure period, a dose-dependent increase in the AST/ALT activity (Figure 4.65) was observed in the treated mice, which was significant ($p < 0.05$) only at the 150.00 $mgkg^{-1}$ of ZnO NPs in comparison with the mice treated with distilled water. Subsequently, a significant difference between the 5- and 10- day exposure periods was observed at the 18.75 ($p < 0.05$), 37.50 ($p < 0.05$) and 150.00 ($p < 0.01$) $mgkg^{-1}$ of ZnO NPs. For the 5-

day exposure period, the mixture of both NPs administered to mice induced an increase in the AST/ALT activity (Figure 4.66) at tested doses, which was significant only at the 9.38 ($p < 0.01$) and 75.00 ($p < 0.05$) $mgkg^{-1}$ while for the 10- day exposure, there was a significant ($p < 0.05$) increase in AST/ALT activity (Figure 4.66) at tested doses except at the 37.50 $mgkg^{-1}$ of their mixture in comparison with the mice treated with distilled water. Subsequently, a significant difference between the 5- and 10- day exposure periods was observed at only 9.38 ($p < 0.05$) $mgkg^{-1}$ of the NP mixture.

Figures 4.67 – 4.69 show the results of the serum GGT activity in mice treated with TiO_2, ZnO NPs and their mixture for 5 and 10 days. For the 5- day exposure period, mice treated with TiO_2 NPs exhibited a reduction in the serum GGT activity (Figure 4.67) at the 9.38 and 18.75 $mgkg^{-1}$, while an increase was observed at the 37.50, 75.00 and 150.00 $mgkg^{-1}$. Subsequently, a significant increase in the serum GGT activity was observed only at the 37.50 ($p < 0.01$) and 150.00 ($p < 0.05$) $mgkg^{-1}$ of TiO_2 NPs in comparison with the mice treated with distilled water. For the 10- day exposure period, TiO_2 NPs induced an increase in the serum GGT activity (Figure 4.67) at tested doses except at the 150.00 $mgkg^{-1}$, which was lower than the value of the mice treated with distilled water. In addition, significant ($p < 0.01$) increase was noted at the 18.75 $mgkg^{-1}$ of TiO_2 NPs in comparison with the mice treated with distilled water. A comparison between the 5- and 10- day exposure periods showed a significant difference only at the 18.75 ($p < 0.001$) $mgkg^{-1}$ of TiO_2 NPs.

Mice treated with ZnO NPs for the 5 days exhibited an increase in the serum GGT activity (Figure 4.68) at tested doses, which was significant only at the 37.50 ($p < 0.001$) and 75.00 ($p < 0.05$) $mgkg^{-1}$ of ZnO NPs in comparison with the mice treated with distilled water. The serum GGT activity showed a plateau at the 37.50 $mgkg^{-1}$ with a gradual decrease in the activity of GGT with increase in doses. For the 10- day exposure period, the serum GGT activity (Figure 4.68) in the experimental mice decreased at the 9.38 and 18.75 $mgkg^{-1}$; and increased at the 37.50, 75.00 and 150.00 $mgkg^{-1}$, which was only significant ($p < 0.05$) at the 37.50 $mgkg^{-1}$ of ZnO NPs in comparison with the mice treated with distilled water. A comparison between the 5- and 10- day exposure periods showed a significant difference only at the 150.00 ($p < 0.01$) $mgkg^{-1}$ of ZnO NPs.

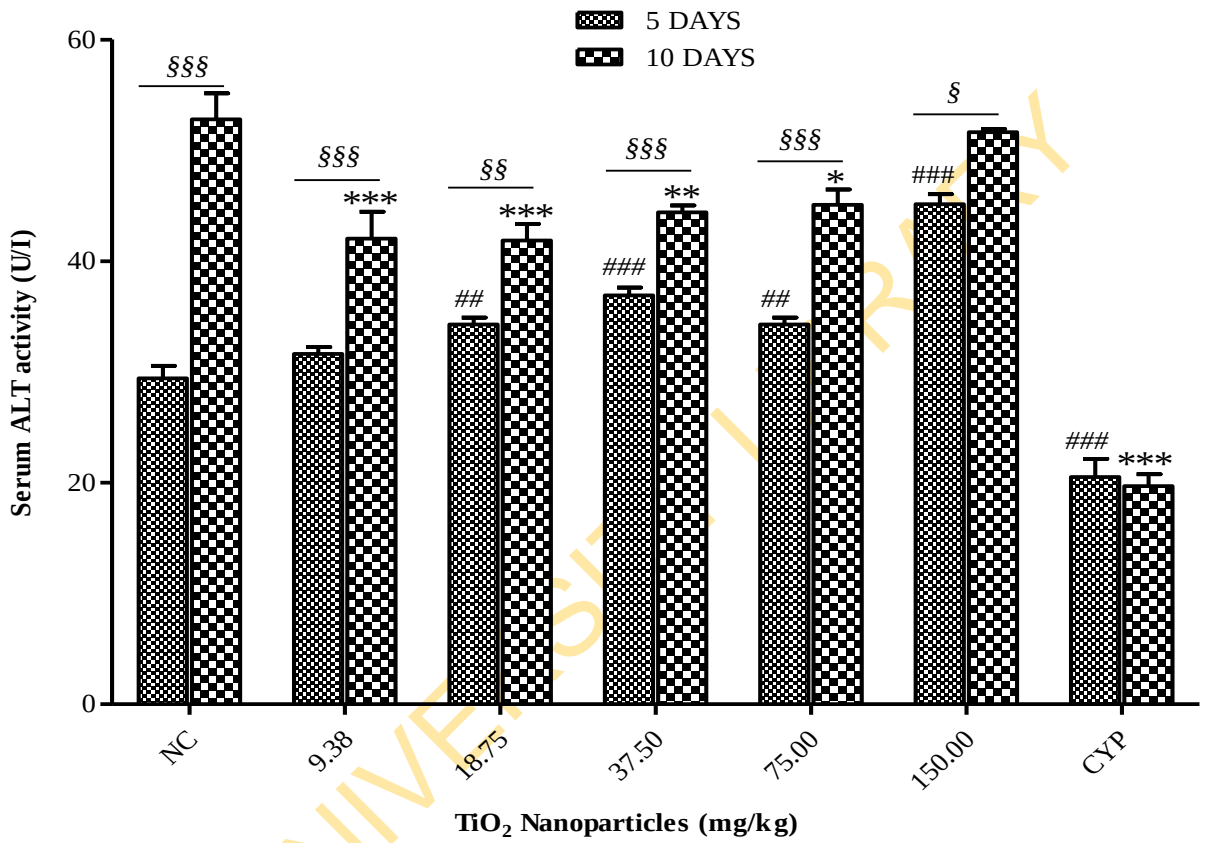

Figure 4. 57: Serum ALT activity in mice treated with TiO_2 NPs at the 5- and 10- day exposure periods.

Data represent mean ± SEM (n = 5). Negative control (NC) = distilled water, CYP = cyclophosphamide (positive control).

$^{\#\#}$ $p < 0.01$ and $^{\#\#\#}$ $p < 0.001$ in 5-days exposure

* $p < 0.05$, ** $p < 0.01$ and *** $p < 0.001$ in 10-days exposure

§ $p < 0.05$, §§ $p < 0.01$ and §§§ $p < 0.001$ for the comparison between the 5- and 10-day exposures

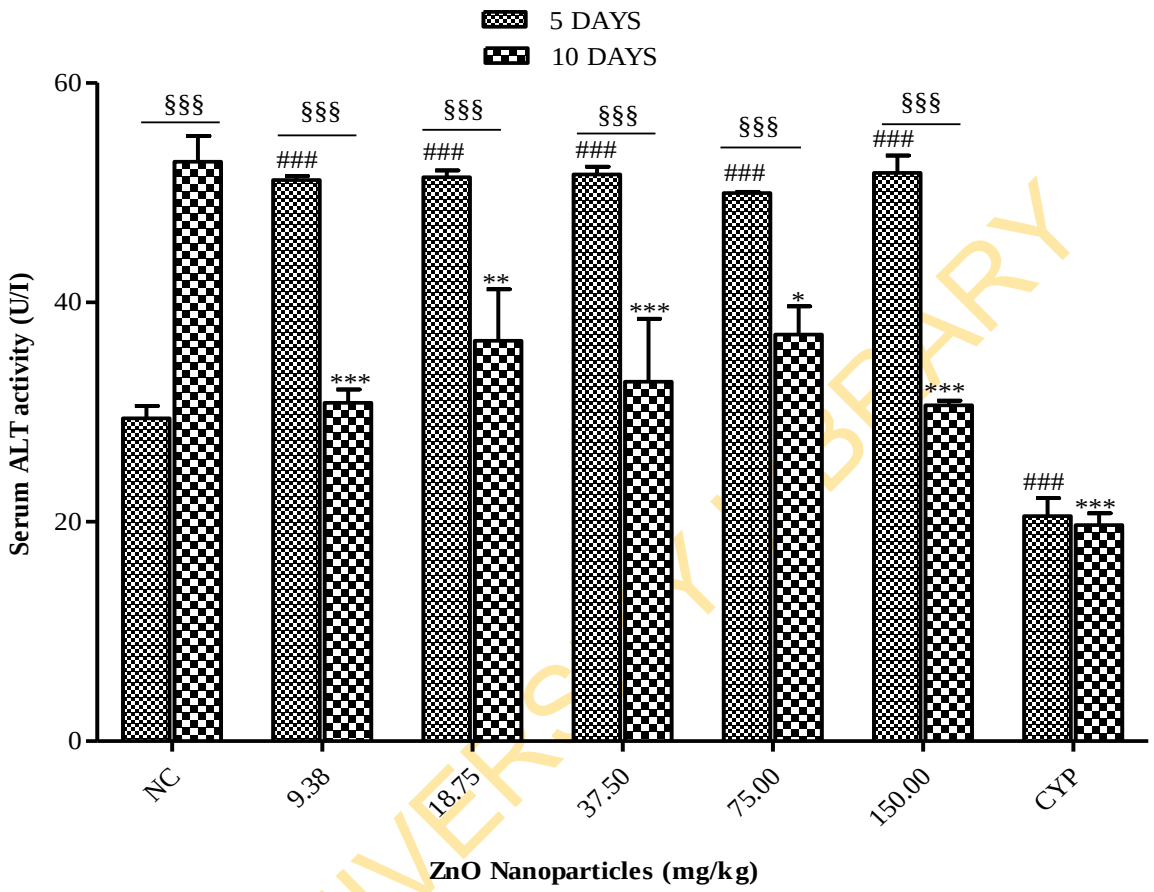

Figure 4. 58: Serum ALT activity in mice treated with ZnO NPs at the 5- and 10- day exposure periods.

Data represent mean ± SEM (n = 5). Negative control (NC) = distilled water, CYP = cyclophosphamide (positive control).

$^{###}$ $p < 0.001$ in 5-days exposure

* $p < 0.05$, ** $p < 0.01$ and *** $p < 0.001$ in 10-days exposure

§§§ $p < 0.001$ for the comparison between the 5- and 10-day exposures

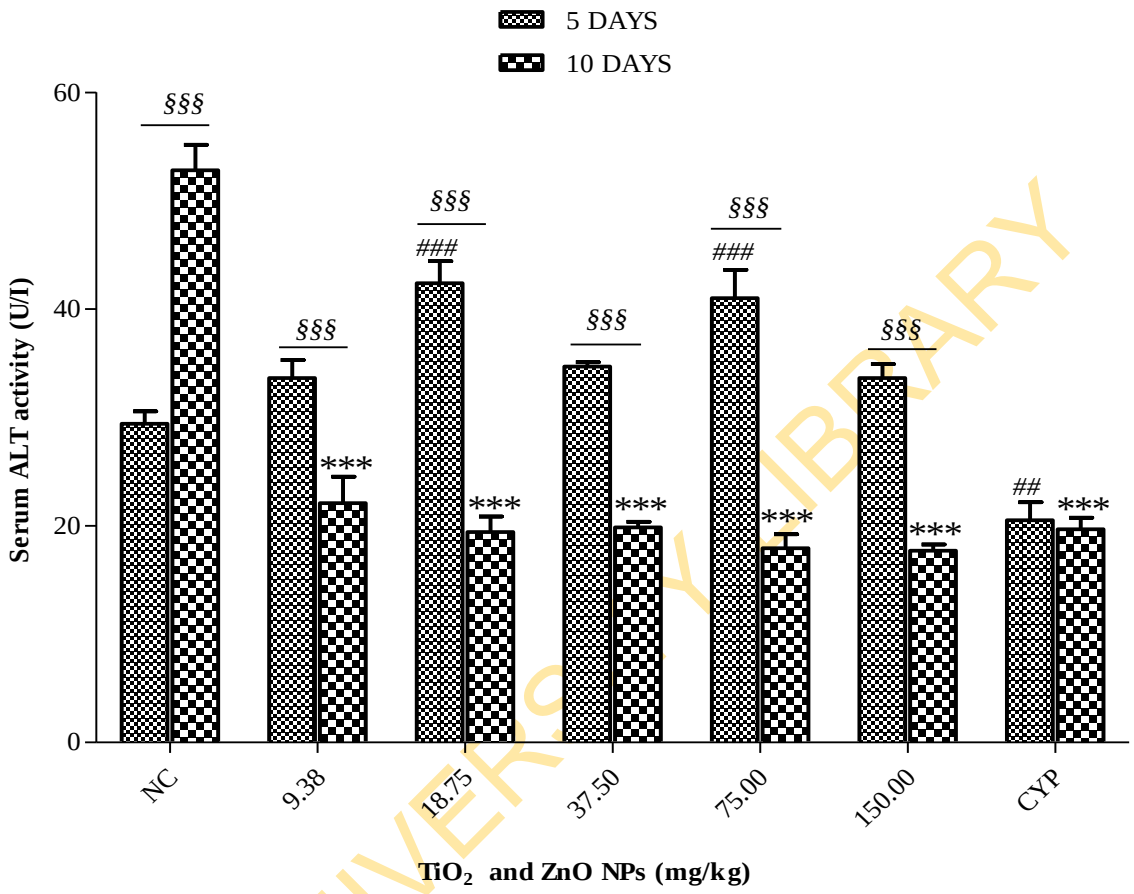

Figure 4. 59: Serum ALT activity in mice treated with TiO_2 and ZnO NPs at the 5- and 10- day exposure periods.

Data represent mean ± SEM (n = 5). Negative control (NC) = distilled water, CYP = cyclophosphamide (positive control).

$^{##}$ $p < 0.01$ and $^{###}$ $p < 0.001$ in 5-days exposure

*** $p < 0.001$ in 10-days exposure

§§§ $p < 0.001$ for the comparison between the 5- and 10-day exposures

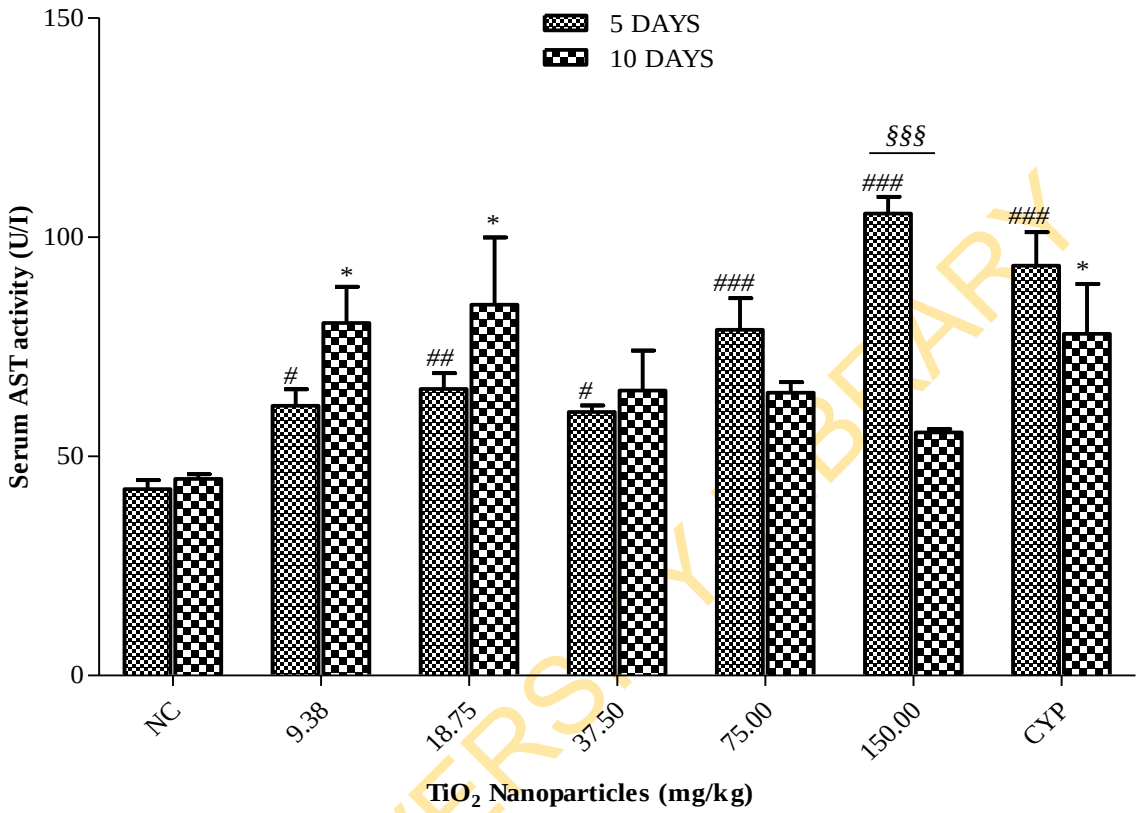

Figure 4. 60: Serum AST activity in mice treated with TiO_2 NPs at the 5- and 10- day exposure periods.

Data represent mean ± SEM (n = 5). Negative control (NC) = distilled water, CYP = cyclophosphamide (positive control).

$^{\#}$ $p < 0.05$, $^{\#\#}$ $p < 0.01$ and $^{\#\#\#}$ $p < 0.001$ in 5-days exposure

* $p < 0.05$ in 10-days exposure

§§§ $p < 0.001$ for the comparison between 5- and 10-days exposures

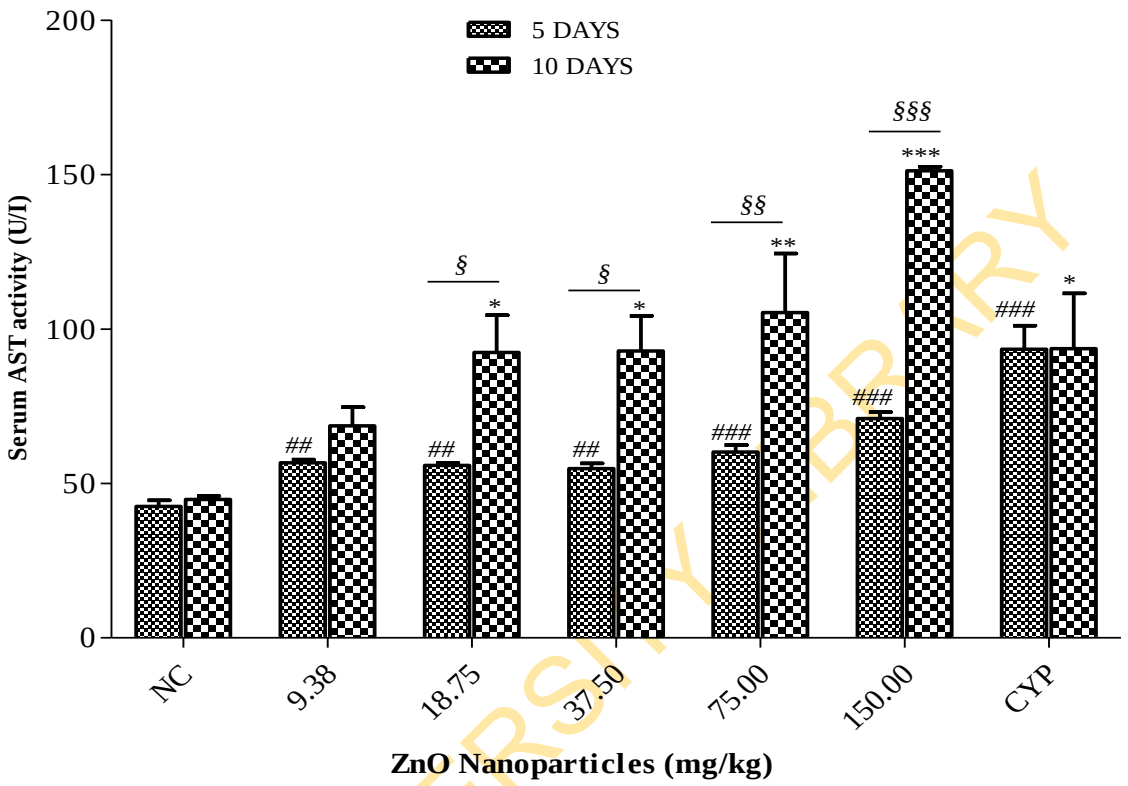

Figure 4. 61: Serum AST activity in mice treated with ZnO NPs at the 5- and 10- day exposure periods.

Data represent mean ± SEM (n = 5). Negative control (NC) = distilled water, CYP = cyclophosphamide (positive control).

$^{\#\#}$ $p < 0.01$ and $^{\#\#\#}$ $p < 0.001$ in 5- days exposure

* $p < 0.05$, ** $p < 0.01$ and *** $p < 0.001$ in 10- days exposure

§ $p < 0.05$, §§ $p < 0.01$ and §§§ $p < 0.001$ for the comparison between the 5- and 10- day exposures

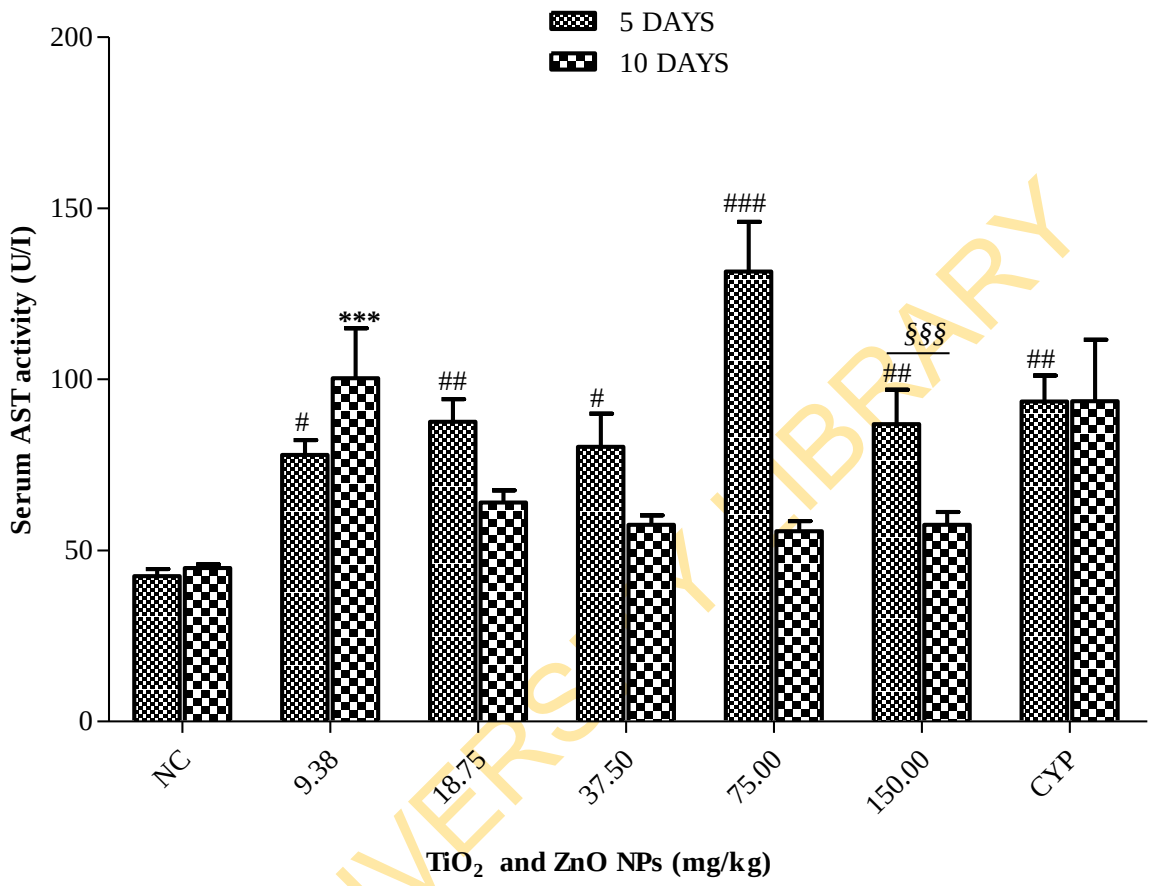

Figure 4. 62: Serum AST activity in mice treated with TiO_2 and ZnO NPs at the 5- and 10- day exposure periods.

Data represent mean ± SEM (n = 5). Negative control (NC) = distilled water, CYP = cyclophosphamide (positive control).

$^{\#}$ $p < 0.05$, $^{\#\#}$ $p < 0.01$ and $^{\#\#\#}$ $p < 0.001$ in 5-days exposure

*** $p < 0.001$ in 10-days exposure

§§§ $p < 0.001$ for the comparison between the 5- and 10- day exposures

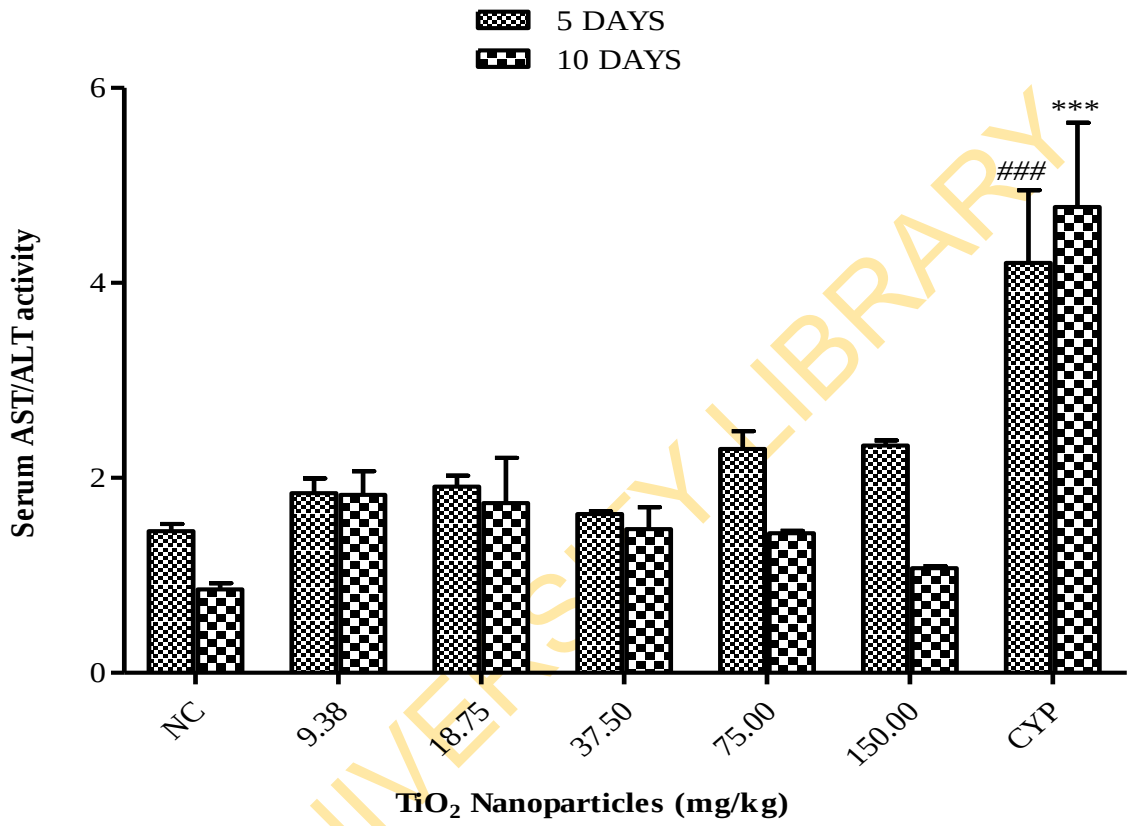

Figure 4. 63: Serum AST/ALT activity in mice treated with TiO_2 NPs at the 5- and 10-day exposure periods.

Data represent mean ± SEM (n = 5). Negative control (NC) = distilled water, CYP = cyclophosphamide (positive control).

$p < 0.001$ in 5-days exposure

*** $p < 0.001$ in 10-days exposure

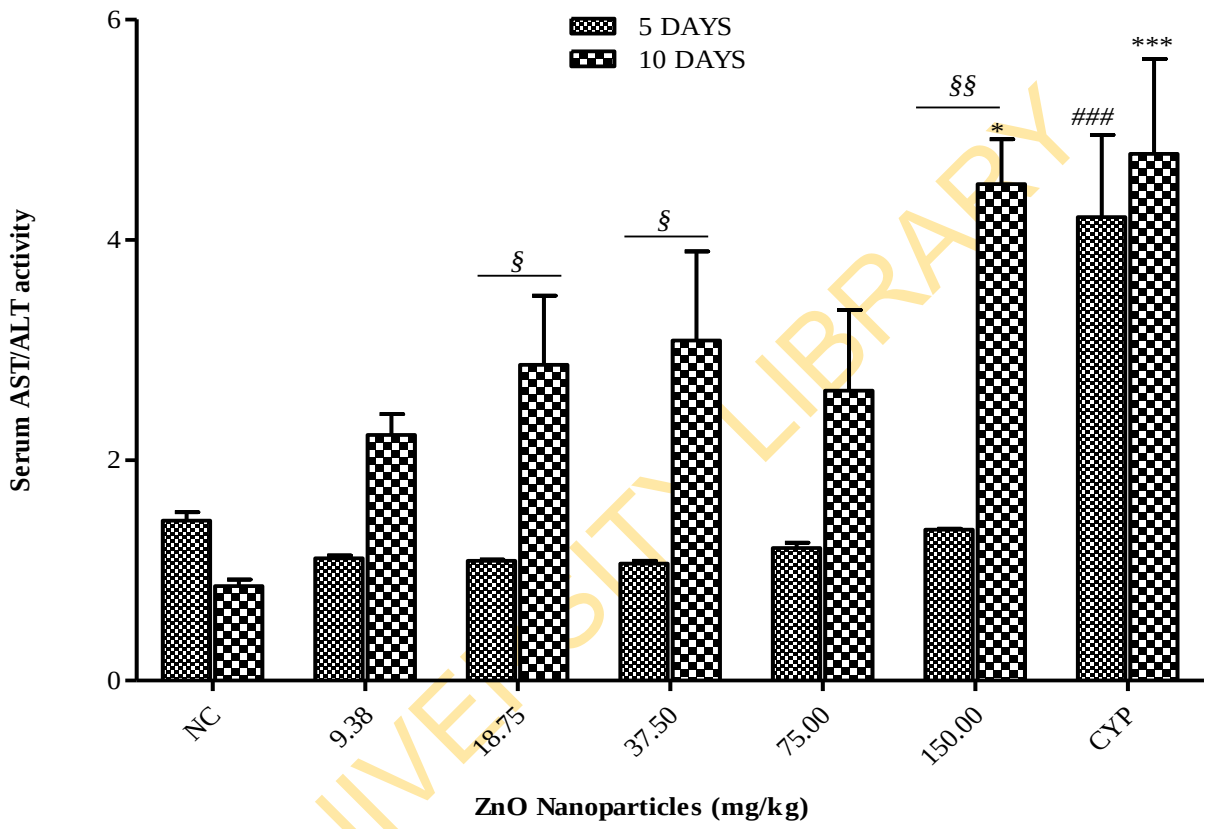

Figure 4. 64: Serum AST/ALT activity in mice treated with ZnO NPs at the 5- and 10-day exposure periods.

Data represent mean ± SEM (n = 5). Negative control (NC) = distilled water, CYP = cyclophosphamide (positive control).

$^{###}$ $p < 0.001$ in 5-days exposure

* $p < 0.05$ and *** $p < 0.001$ in 10-days exposure

§ $p < 0.05$ and §§ $p < 0.01$ for the comparison between the 5- and 10- day exposures

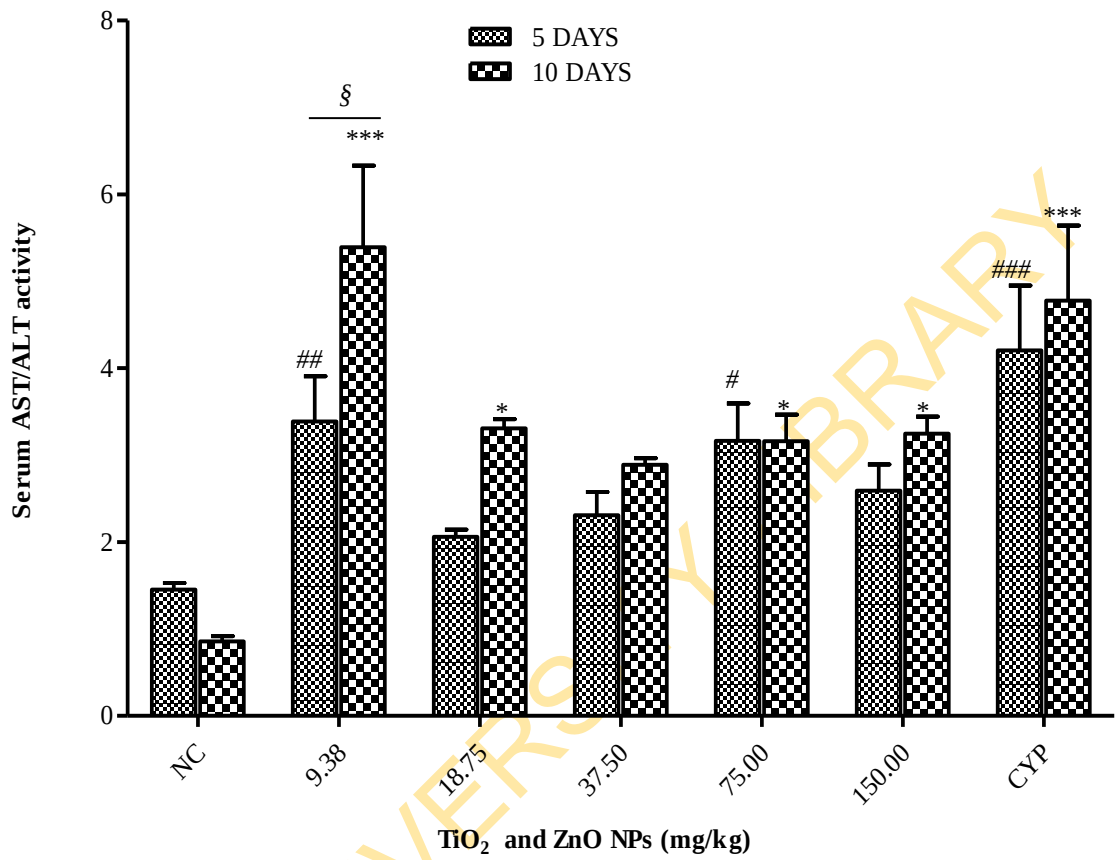

Figure 4. 65: Serum AST/ALT activity in mice treated with TiO_2 and ZnO NPs at the 5- and 10- day exposure periods.

Data represent mean ± SEM (n = 5). Negative control (NC) = distilled water, CYP = cyclophosphamide (positive control).

$^{\#}$ $p < 0.05$, $^{\#\#}$ $p < 0.01$ and $^{\#\#\#}$ $p<0.001$ in 5-days exposure

* $p < 0.05$ and *** $p < 0.001$ in 10-days exposure

§ $p < 0.05$ for the comparison between the 5- and 10- day exposures

The mixture of both NPs administered to mice for the 5- day exposure period induced a significant ($p < 0.01$) increase in the serum GGT activity (Figure 4.69) at tested doses while at the 10-day exposure period, a significant ($p < 0.05$) increase in the serum GGT activity (Figure 4.69) was also observed at the 9.38, 18.75 and 37.50 $mgkg^{-1}$ of their mixture in comparison with the mice treated with distilled water.

Figures 4.70 – 4.72 show the results of the serum total bilirubin concentration in mice treated with TiO_2, ZnO NPs and their mixture for 5 and 10 days. For the 5- day exposure period, mice treated with TiO_2 NPs exhibited an increase in the concentration of serum total bilirubin (Figure 4.70) at tested doses, which was significant ($p < 0.01$) only at the 150.00 $mgkg^{-1}$ in comparison with the mice treated with distilled water. For the 10- day exposure period, there was no significant ($p > 0.05$) reduction in the serum total bilirubin concentration (Figure 4.70) at the 18.75 and 150.00 $mgkg^{-1}$ while an increase at the 9.38, 37.50 and 75.00 $mgkg^{-1}$of TiO_2 NPs in comparison with the mice treated with distilled water.

For the 5- day exposure period, mice treated with ZnO NPs exhibited a significant reduction in the serum total bilirubin concentration (Figure 4.71) only at the 9.38 ($p < 0.001$) and increase at the 37.50 ($p < 0.01$) and 75.00 ($p < 0.05$) $mgkg^{-1}$ in comparison with the mice treated with distilled water. For the 10- day exposure period, mice treated with ZnO NPs exhibited a dose-dependent increase in the serum total bilirubin concentration (Figure 4.71) which was significant only at the 75.00 ($p < 0.05$) and 150.00 ($p < 0.01$) $mgkg^{-1}$ in comparison with the mice treated with distilled water. A significant ($p < 0.001$) difference between the two exposure periods for 5- and 10- days was noted at the 9.38, 18.75 and 150.00 $mgkg^{-1}$ of ZnO NPs. Mice treated with their mixture for 5 and 10 days exhibited a significant ($p < 0.001$) increase in the serum total bilirubin concentration (Figure 4.72) at tested doses in comparison with their corresponding groups of mice treated with distilled water. A comparison between the 5- and 10- day exposure periods showed a significant difference at the 9.38 ($p < 0.001$) and 18.75 ($p < 0.01$) $mgkg^{-1}$ of their mixture.

Figures 4.73 – 4.75 show the results of the serum direct bilirubin concentration in mice treated with TiO_2, ZnO NPs and their mixture for 5 and 10 days. For the 5- day exposure

period, mice treated with TiO_2 NPs exhibited a dose-dependent increase in the serum direct bilirubin concentration (Figure 4.73), which was significant ($p < 0.05$) only at the 37.50, 75.00 and 150.00 $mgkg^{-1}$ in comparison with the mice treated with distilled water. For the 10- day exposure period, TiO_2 NPs administered to mice induced an increase in the serum direct bilirubin concentration at tested doses with significance ($p < 0.05$) at the 18.75 $mgkg^{-1}$ in comparison with the mice treated with distilled water. A comparison between the 5- and 10- day exposure periods showed a significant ($p < 0.001$) difference only at the 150.00 $mgkg^{-1}$ of TiO_2 NPs. Mice treated with ZnO NPs for the 5- day exposure period exhibited no significant ($p > 0.05$) reduction of serum direct bilirubin concentration (Figure 4.74) at the 9.38 and 37.50 $mgkg^{-1}$ and an increase at the 18.75, 75.00 and 150.00 $mgkg^{-1}$ in comparison with the mice treated with distilled water.

In contrast, ZnO NPs administered to mice for the 10- day exposure period, induced a significant ($p < 0.001$) increase in the serum direct bilirubin concentration (Figure 4.74) at tested doses in comparison with the mice treated with distilled water. A comparison between the two exposure periods, 5- and 10- days showed a significant ($p < 0.001$) difference at tested doses of ZnO NPs. The mixture of both NPs administered to mice at the 5- and 10- day exposure periods induced a significant ($p < 0.001$) increase in the serum direct bilirubin concentration at tested doses in comparison with the mice treated with distilled water.

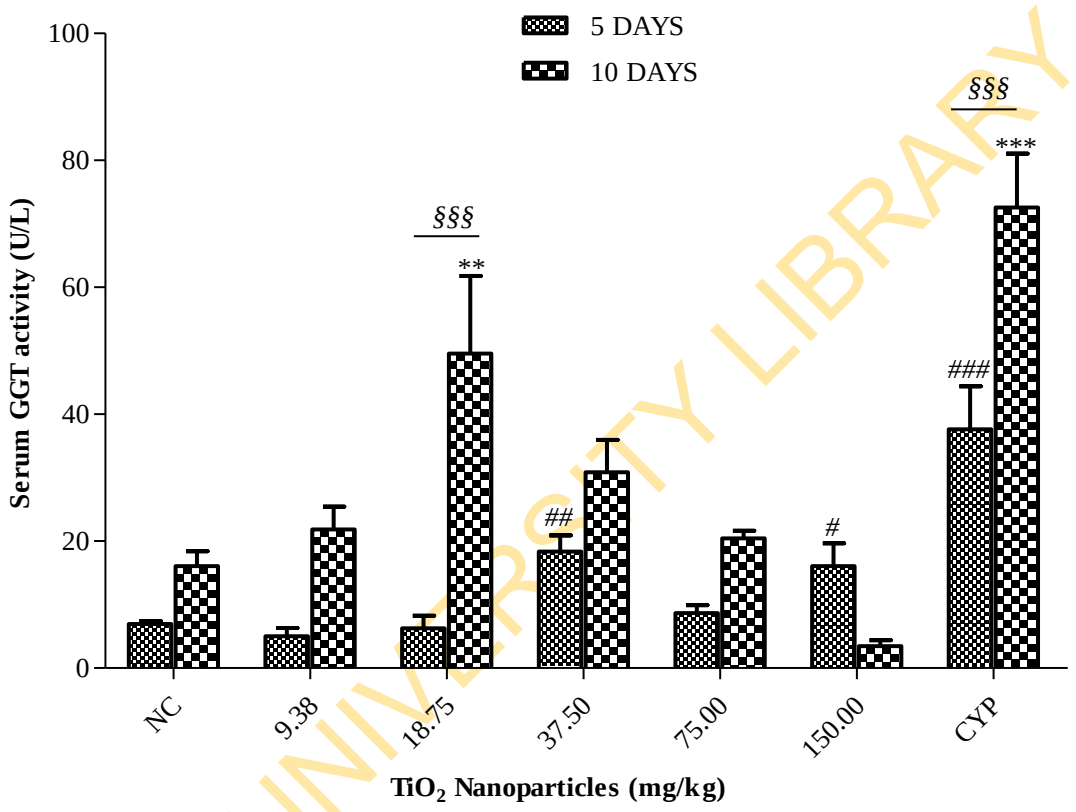

Figure 4. 66: Serum GGT activity in mice treated with TiO_2 NPs at the 5- and 10- day exposure periods.

Data represent mean ± SEM (n = 5). Negative control (NC) = distilled water, CYP = cyclophosphamide (positive control).

$^{\#}$ $p < 0.05$, $^{\#\#}$ $p < 0.01$ and $^{\#\#\#}$ $p < 0.001$ in 5-days exposure

** $p < 0.01$ and *** $p < 0.001$ in 10-days exposure

§§§ $p < 0.001$ for the comparison between the 5- and 10- day exposures

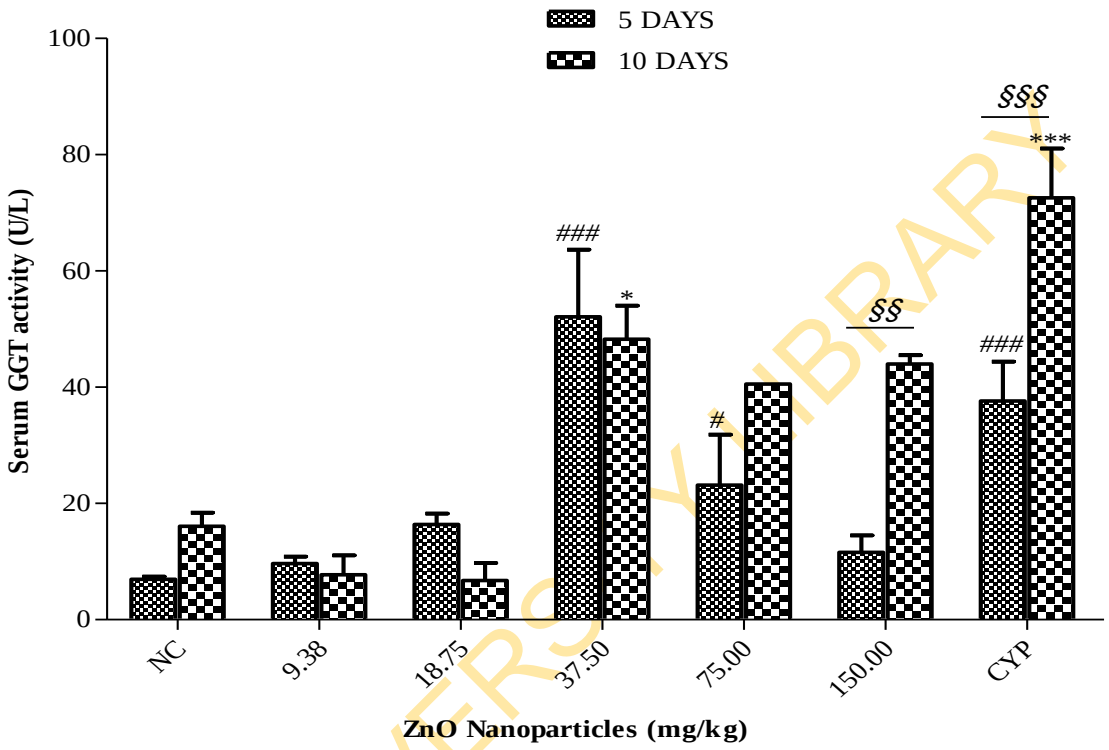

Figure 4. 67: Serum GGT activity in mice treated with ZnO NPs at the 5- and 10- day exposure periods.

Data represent mean ± SEM (n = 5). Negative control (NC) = distilled water, CYP = cyclophosphamide (positive control).

$^{\#}$ $p < 0.05$ and $^{\#\#\#}$ $p<0.001$ in 5-days exposure

* $p < 0.05$ and *** $p < 0.001$ in 10-days exposure

§§ $p < 0.01$ and §§§ $p < 0.001$ for the comparison between the 5- and 10- day exposures

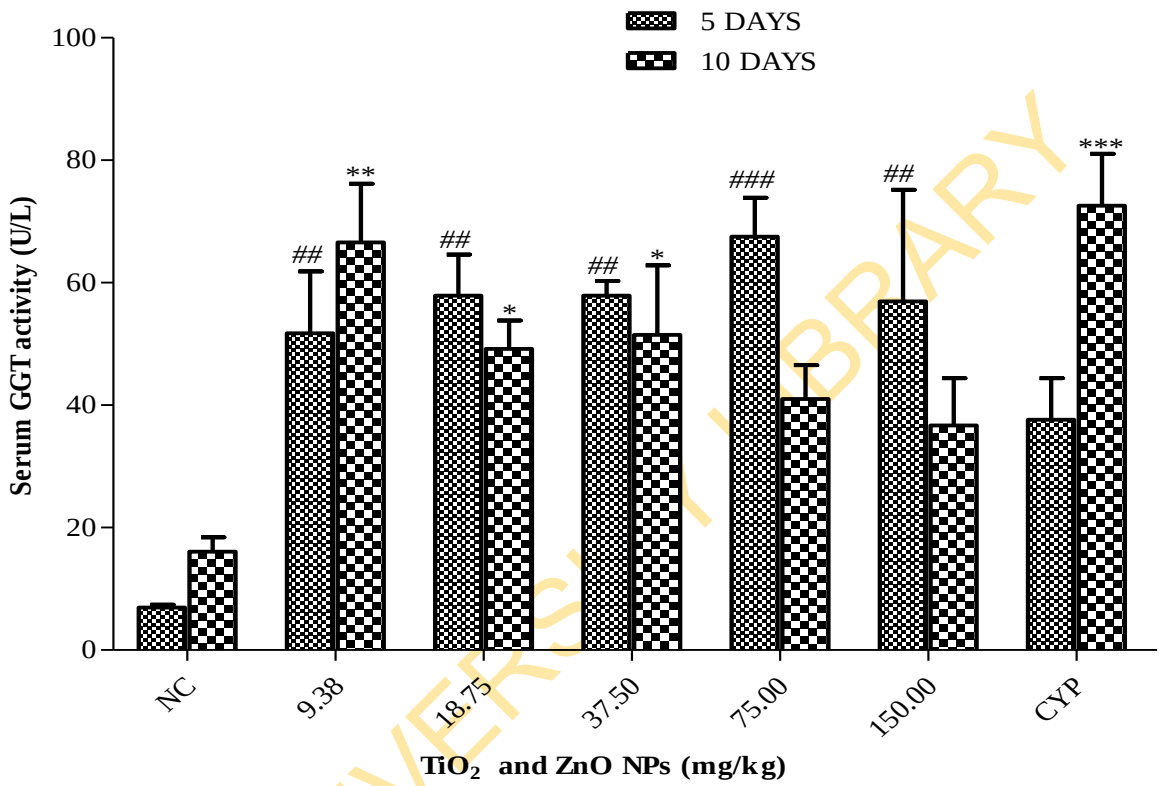

Figure 4. 68: Serum GGT activity in mice treated with TiO_2 and ZnO NPs at the 5- and 10- day exposure periods.

Data represent mean ± SEM (n = 5). Negative control (NC) = distilled water, CYP = cyclophosphamide (positive control).

$^{##}$ $p < 0.01$ and $^{###}$ $p < 0.001$ in 5-days exposure

* $p < 0.05$, ** $p < 0.01$ and *** $p < 0.001$ in 10-days exposure

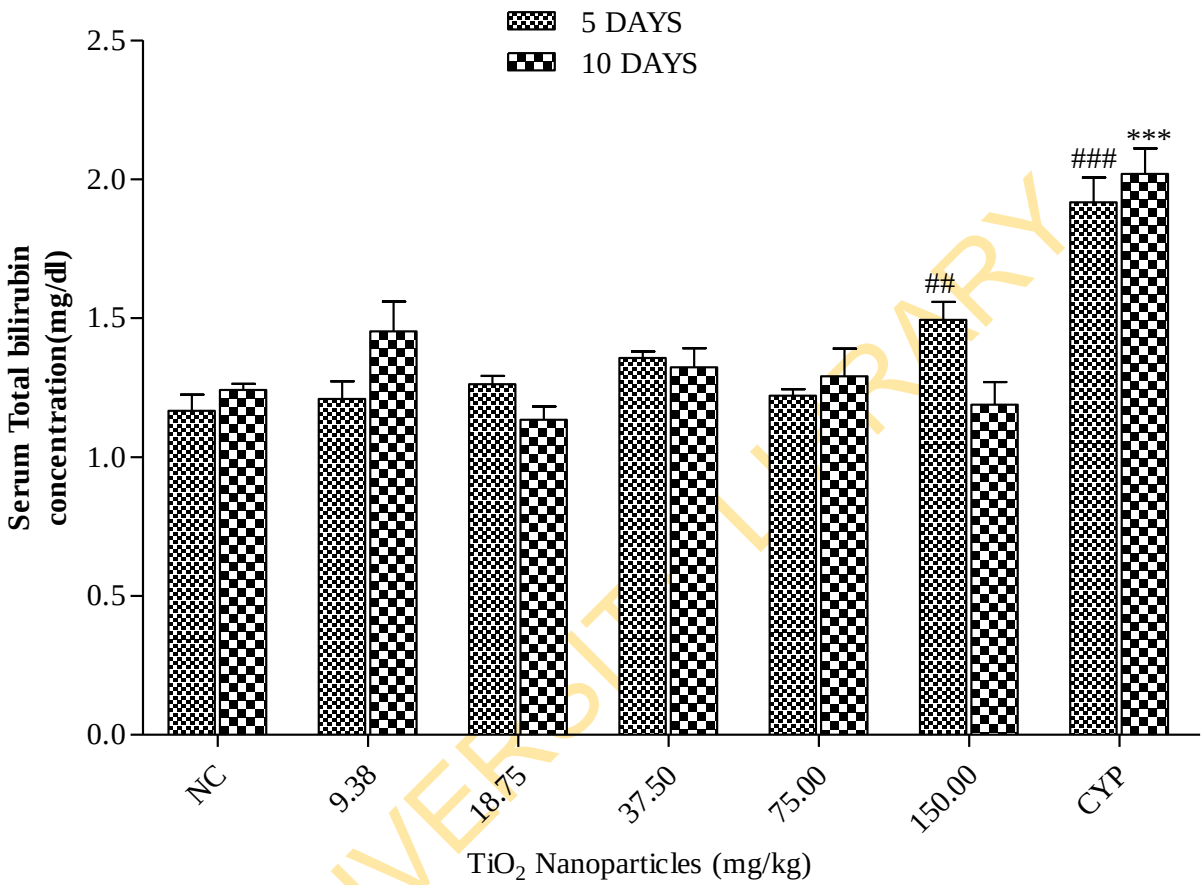

Figure 4. 69: Serum total bilirubin concentration in mice treated with TiO_2 NPs at the 5- and 10- day exposure periods.

Data represent mean ± SEM (n = 5). Negative control (NC) = distilled water, CYP = cyclophosphamide (positive control).

$^{##}$ $p < 0.01$ and $^{###}$ $p < 0.001$ in 5-days exposure

*** $p < 0.001$ in 10-days exposure

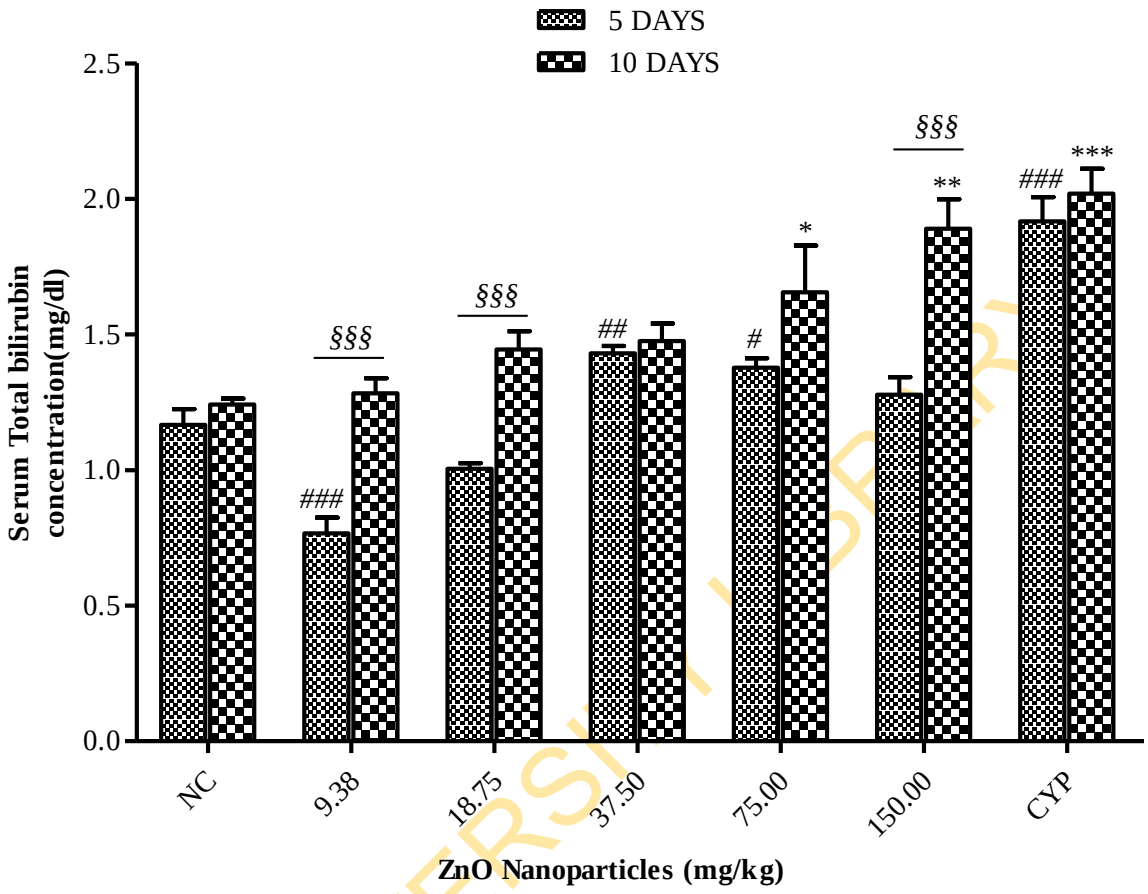

Figure 4. 70: Serum total bilirubin concentration in mice treated with ZnO NPs at the 5- and 10- day exposure periods.

Data represent mean ± SEM (n = 5). Negative control (NC) = distilled water, CYP = cyclophosphamide (positive control).

$^{\#}$ $p < 0.05$, $^{\#\#}$ $p < 0.01$ and $^{\#\#\#}$ $p < 0.001$ in 5-days exposure

* $p < 0.05$, ** $p < 0.01$ and *** $p < 0.001$ in 10-days exposure

§§§ $p < 0.001$ for the comparison between the 5- and 10-days exposures

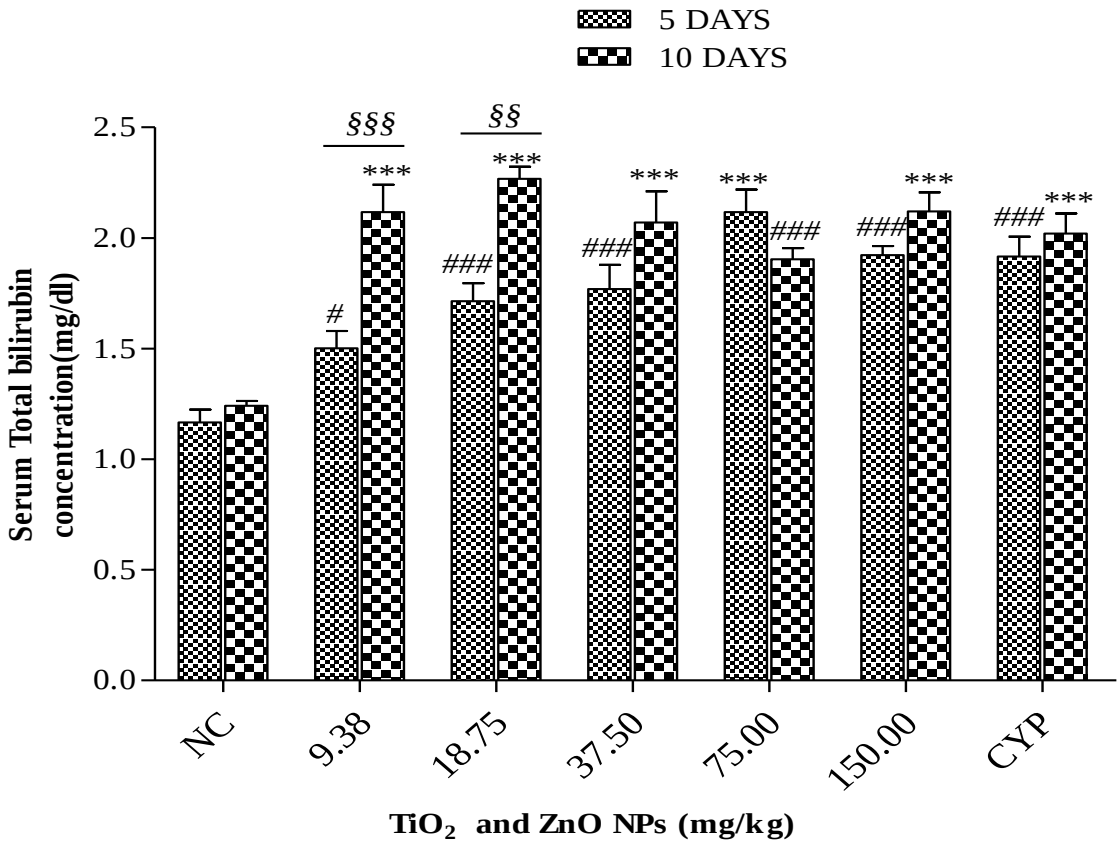

Figure 4. 71: Serum total bilirubin concentration in mice treated with TiO_2 and ZnO NPs at the 5- and 10- day exposure periods.

Data represent mean ± SEM (n = 5). Negative control (NC) = distilled water, CYP = cyclophosphamide (positive control).

$^{\#}$ $p < 0.05$ and $^{\#\#\#}$ $p < 0.001$ in 5-days exposure

* $p < 0.001$ in 10-days exposure

§§ $p < 0.01$ and §§§ $p < 0.001$ for the comparison between the 5- and 10- day exposures

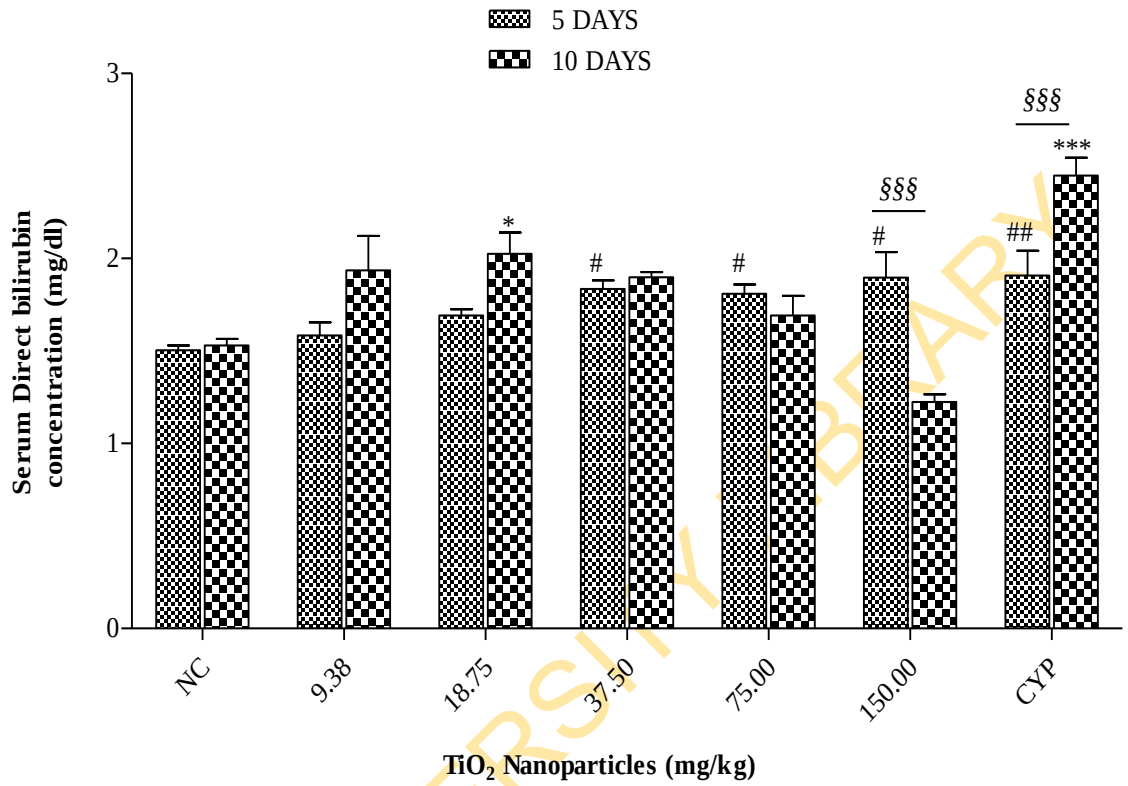

Figure 4. 72: Serum direct bilirubin concentration in mice treated with TiO_2 NPs at the 5- and 10- day exposure periods.

Data represent mean ± SEM (n = 5). Negative control (NC) = distilled water, CYP = cyclophosphamide (positive control).

$^{\#}$ $p < 0.05$ and $^{\#\#}$ $p < 0.01$ in 5-days exposure

* $p < 0.05$ and *** $p < 0.001$ in 10-days exposure

§§§ $p < 0.001$ for the comparison between the 5- and 10-day exposures

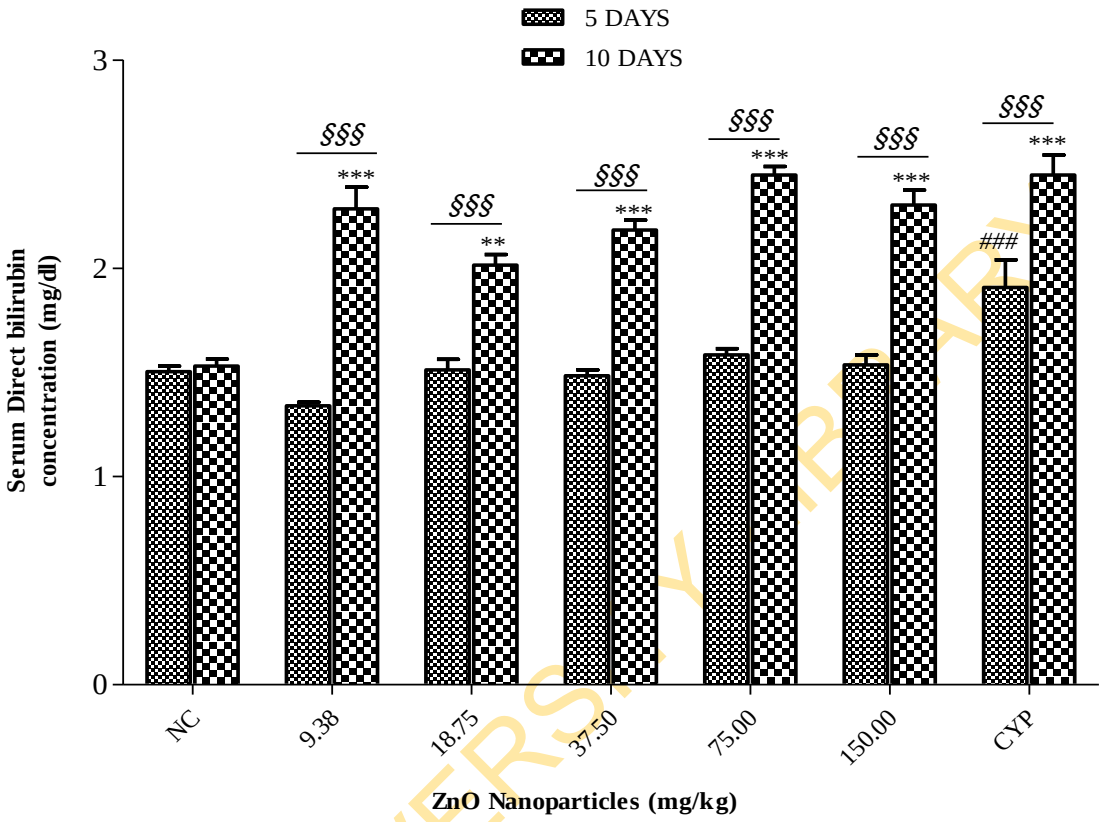

Figure 4. 73: Serum direct bilirubin concentration in mice treated with ZnO NPs at the 5- and 10- day exposure periods.

Data represent mean ± SEM (n = 5). Negative control (NC) = distilled water, CYP = cyclophosphamide (positive control).

$^{###}$ $p < 0.001$ in 5-days exposure

** $p < 0.01$ and *** $p < 0.001$ in 10-days exposure

§§§ $p < 0.001$ for the comparison between the 5- and 10-day exposures

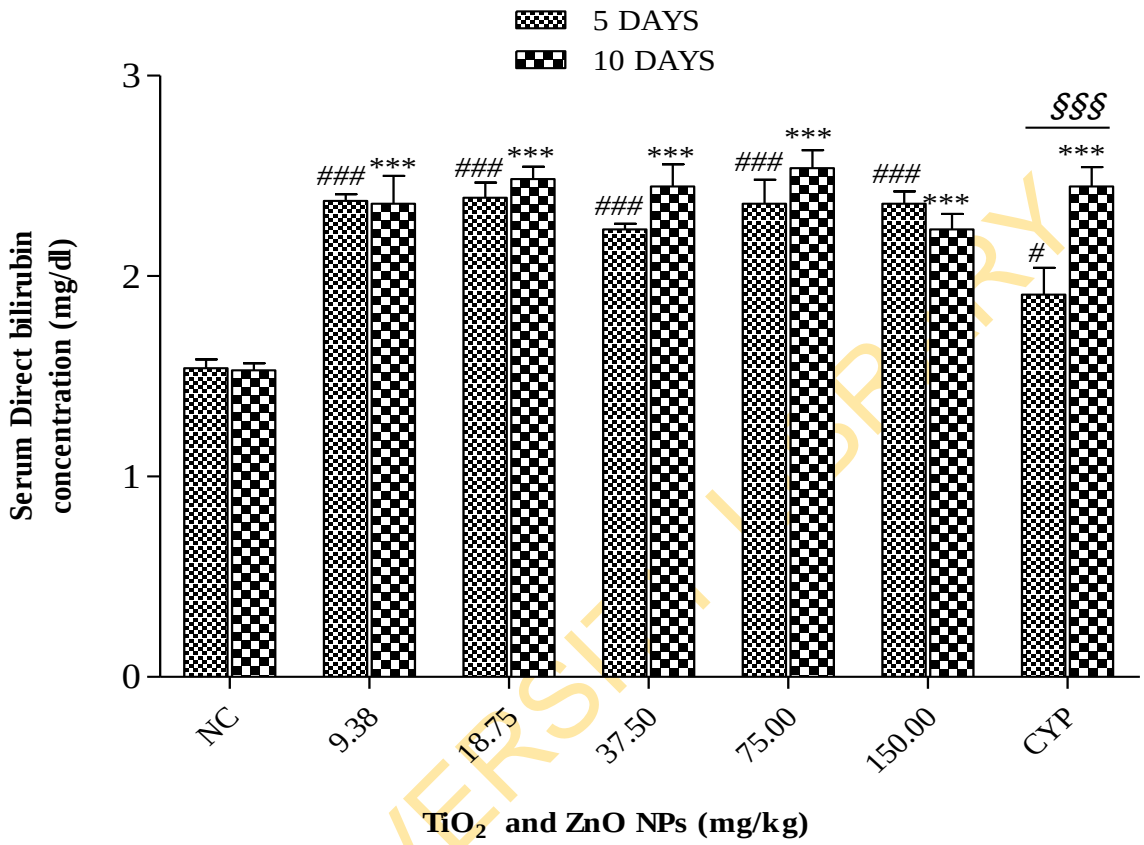

Figure 4. 74: Serum direct bilirubin concentration in mice treated with TiO_2 and ZnO NPs at the 5- and 10- day exposure periods.

Data represent mean ± SEM (n = 5). Negative control (NC) = distilled water, CYP = cyclophosphamide (positive control).

$^{\#}$ $p < 0.05$ and $^{\#\#\#}$ $p < 0.001$ in 5-days exposure

*** $p < 0.001$ in 10-days exposure

§§§ $p < 0.001$ for the comparison between the 5- and 10- day exposures

Figures 4.76 – 4.78 show the results of the serum albumin concentration in mice treated with TiO_2, ZnO NPs and their mixture for 5 and 10 days. For the 5- day exposure period, TiO_2 NPs administered to mice induced a reduction in the serum albumin concentration (Figure 4.76) at tested doses, which was significant at only the 18.75($p < 0.001$) and 37.50 ($p < 0.01$) $mgkg^{-1}$ in comparison with the mice treated with distilled water. For the 10- day exposure period, a reduction in the serum albumin concentration (Figure 4.76) was observed in the experimental mice at doses of 9.38, 18.75 and 37.50 $mgkg^{-1}$ and increased at the 75.00 and 150.00 $mgkg^{-1}$ of TiO_2 NPs. A significant ($p < 0.001$) decrease was only observed at the 37.50 $mgkg^{-1}$ in comparison with the mice treated with distilled water. A significant ($p < 0.001$) difference between the two exposure periods 5- and 10- days was observed only at the 18.75 $mgkg^{-1}$ of TiO_2 NPs.

For the 5- day exposure period, mice treated with ZnO NPs exhibited a significant increase in the serum albumin concentration (Figure 4.77) at the 9.38 ($p < 0.05$), 75.00 ($p < 0.01$) and 150.00 ($p < 0.05$) $mgkg^{-1}$ in comparison with the mice treated with distilled water while for the 10- day exposure period, there was an increase in the serum albumin concentration of the experimental mice at tested doses, which was significant at the 18.75 ($p < 0.05$), 75.00 ($p < 0.001$) and 150.00 ($p < 0.01$) $mgkg^{-1}$ in comparison with the mice treated with distilled water. The mixture of both NPs administered to mice for 5 and 10 days induced a significant ($p < 0.001$) decrease in the serum albumin concentration (Figure 4.78) only at the 37.50, 75.00 and 150.00 $mgkg^{-1}$ in comparison with the corresponding groups of mice treated with distilled water.

Figures 4.79 – 4.81 show the results of the serum urea concentration in mice treated with TiO_2, ZnO NPs and their mixture for 5 and 10 days. For the 5- day exposure period, mice treated with TiO_2 NPs exhibited an increase in the serum urea concentration (Figure 4.79) at the tested doses except at the 150.00 $mgkg^{-1}$ of TiO_2 NPs. A Significant ($p < 0.05$) increase in the serum urea concentration was observed only at the 9.38 and 18.75 $mgkg^{-1}$ of TiO_2 NPs in comparison with the mice treated with distilled water. For the 10- day exposure period, a significant ($p < 0.001$) decrease in the serum urea concentration (Figure 4.79) was observed only at the 9.38, 18.75 and 75.00 $mgkg^{-1}$ of TiO_2 NPs in comparison with the mice treated with distilled water. A comparison between the 5- and 10- day

exposure periods showed a significant difference at the 9.38 ($p < 0.01$), 18.75 ($p < 0.01$), 37.50 ($p < 0.01$) and 150.00 $mgkg^{-1}$ ($p < 0.05$) of TiO_2 NPs.

Similarly, mice treated with ZnO NPs exhibited an increase in the serum urea concentration (Figure 4.80) at tested doses except at the 150.00 $mgkg^{-1}$ of ZnO NPs which showed a decrease. A significant ($p < 0.001$) increase in the serum urea concentration was observed only at the 9.38 and 18.75 $mgkg^{-1}$ of ZnO NPs in comparison with the mice treated with distilled water. However, for the 10- day exposure period, ZnO NPs administered to mice induced a decrease in serum urea concentration (Figure 4.80) at tested doses, which was only significant ($p < 0.05$) at the 18.75 and 75.00 $mgkg^{-1}$ of ZnO NPs in comparison with the mice treated with distilled water. A significant difference between the two exposure period 5- and 10- days was observed at 9.38 ($p < 0.01$) and 18.75 ($p < 0.001$) $mgkg^{-1}$ of ZnO NPs.

For the 5- day exposure period, the mixture of both NPs administered to mice induced increased concentration of the serum urea (Figure 4.81) at tested doses but significant ($p < 0.001$) only at the 18.75, 37.50 and 150.00 $mgkg^{-1}$ of their mixture in comparison with the mice treated with distilled water. In contrast, for the 10-day exposure period (Figure 4.81), the treated mice exhibited a decrease at tested doses but significant ($p < 0.01$) only at the 150.00 $mgkg^{-1}$ of their mixture in comparison with the mice treated with distilled water. A significant difference between the 5- and 10- day exposure periods was observed at the 18.75 ($p < 0.01$) and 150.00 ($p < 0.001$) $mgkg^{-1}$ of their mixture.

Figures 4.82 – 4.84 show the results of the serum creatinine concentration in mice treated with TiO_2, ZnO NPs and their mixture for 5 and 10 days. For the 5- day exposure period, it was observed that mice treated with TiO_2 NPs had a no significant ($p > 0.05$) reduction of serum creatinine concentration (Figure 4.82) at the doses of 9.38 and 18.75 $mgkg^{-1}$ and an increase at 37.50, 75.00 and 150.00 $mgkg^{-1}$. A significant ($p < 0.05$) increase in the creatinine concentration was observed only at the 37.50 $mgkg^{-1}$ of TiO_2 NPs in comparison with the mice treated with distilled water. Similarly, at the 10-day exposure period, treated mice had a significant ($p < 0.05$) increase in the serum creatinine concentration (Figure 4.82) at the 18.75 and 37.50 $mgkg^{-1}$ of TiO_2 NPs in comparison with the mice treated with distilled water. A comparison between the 5- and 10- day exposure

periods showed a significant difference at the 37.00 ($p < 0.001$), 75.00 ($p < 0.01$) and 150.00 ($p < 0.001$) of TiO_2 NPs.

For the 5- day exposure period, ZnO NPs administered to mice induced a significant ($p < 0.05$) reduction in the serum creatinine concentration (Figure 4.83) at the 9.38, 18.75 and 37.50 $mgkg^{-1}$ of ZnO NPs in comparison with the mice treated with distilled water. While for the 10- day exposure period, treated mice had an increase in the serum creatinine concentration (Figure 4.83) at tested doses, but significant ($p < 0.05$) only at the 18.75 $mgkg^{-1}$ of ZnO NPs in comparison with the mice treated with distilled water. A significant difference between the 5- and 10- day exposure periods was observed at the 18.75 ($p < 0.01$) and 37.50 ($p < 0.05$) $mgkg^{-1}$ of ZnO NPs.

The mixture of both NPs administered to mice for the 5- day exposure period induced an increase in the serum creatinine concentration (Figure 4.84) at tested doses but was significant ($p < 0.05$) only at the 75.00 $mgkg^{-1}$ of their mixture in comparison with the mice treated with distilled water; while for the 10- day exposure, treated mice showed a significant increase in the serum creatinine concentration (Figure 4.84) at the 9.38 ($p < 0.05$), 18.75 ($p < 0.01$), 37.50 ($p < 0.05$) and 75.00 ($p < 0.001$) of their mixture in comparison with the mice treated with distilled water. A significant ($p < 0.01$) difference between the 5- and 10- day exposure periods was observed at the 150.00 $mgkg^{-1}$ of their mixture.

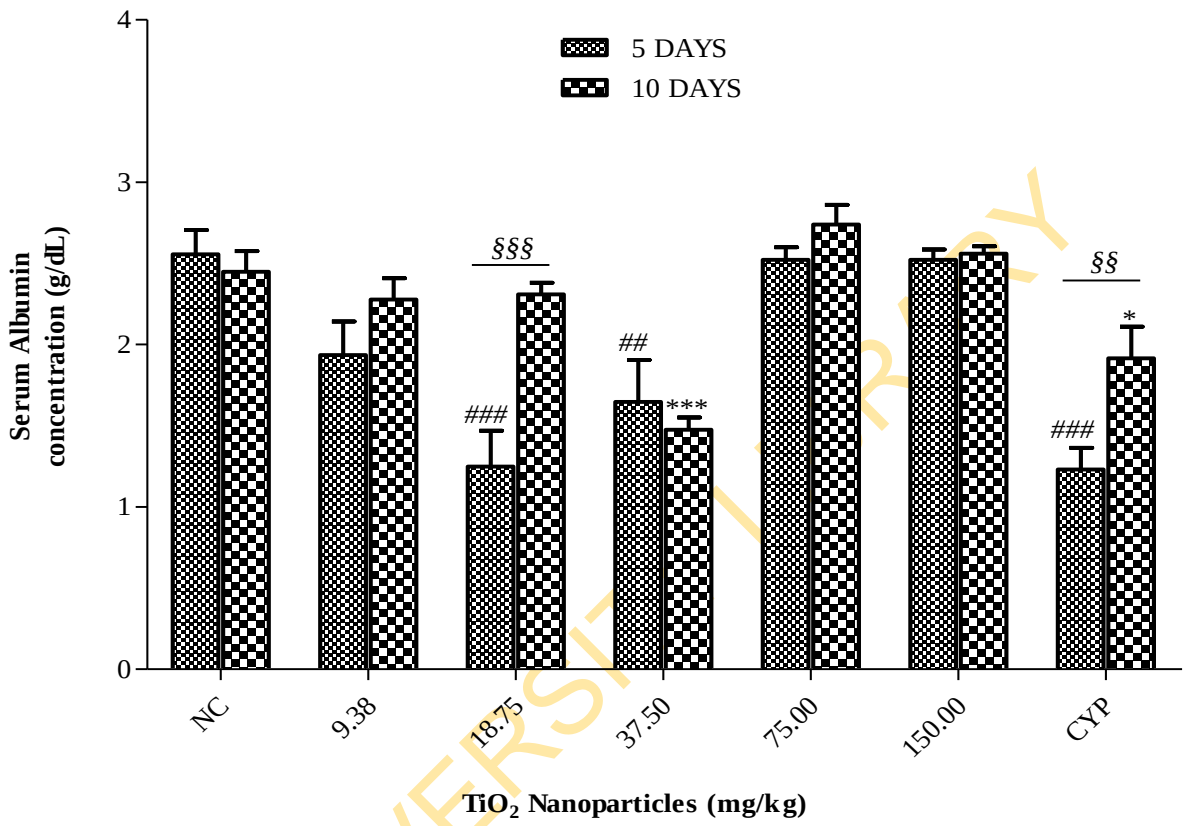

Figure 4. 75: Serum albumin concentration in mice treated with TiO_2 NPs at the 5- and 10- day exposure periods.

Data represent mean ± SEM (n = 5). Negative control (NC) = distilled water, CYP = cyclophosphamide (positive control).

$^{##}$ $p < 0.01$ and $^{###}$ $p < 0.001$ in 5-days exposure

* $p < 0.05$ and *** $p < 0.001$ in 10-days exposure

§§ $p < 0.01$ and §§§ $p < 0.001$ for the comparison between the 5- and 10-day exposures

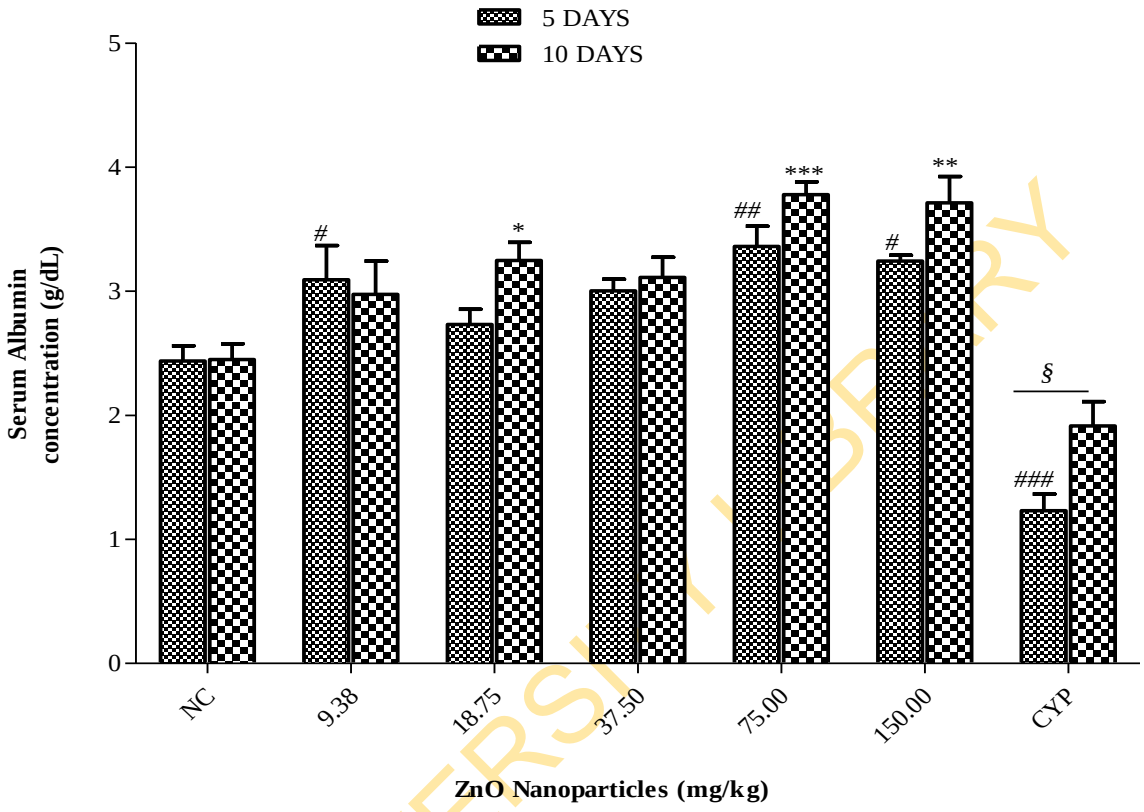

Figure 4. 76: Serum albumin concentration in mice treated with ZnO NPs at the 5- and 10- day exposure periods.

Data represent mean ± SEM (n = 5). Negative control (NC) = distilled water, CYP = cyclophosphamide (positive control).

$^{\#}$ $p < 0.05$, $^{\#\#}$ $p < 0.01$ and $^{\#\#\#}$ $p < 0.001$ in 5-days exposure

* $p < 0.05$, ** $p < 0.01$ and *** $p < 0.001$ in 10-days exposure

§ $p < 0.05$ for the comparison between the 5- and 10-day exposures

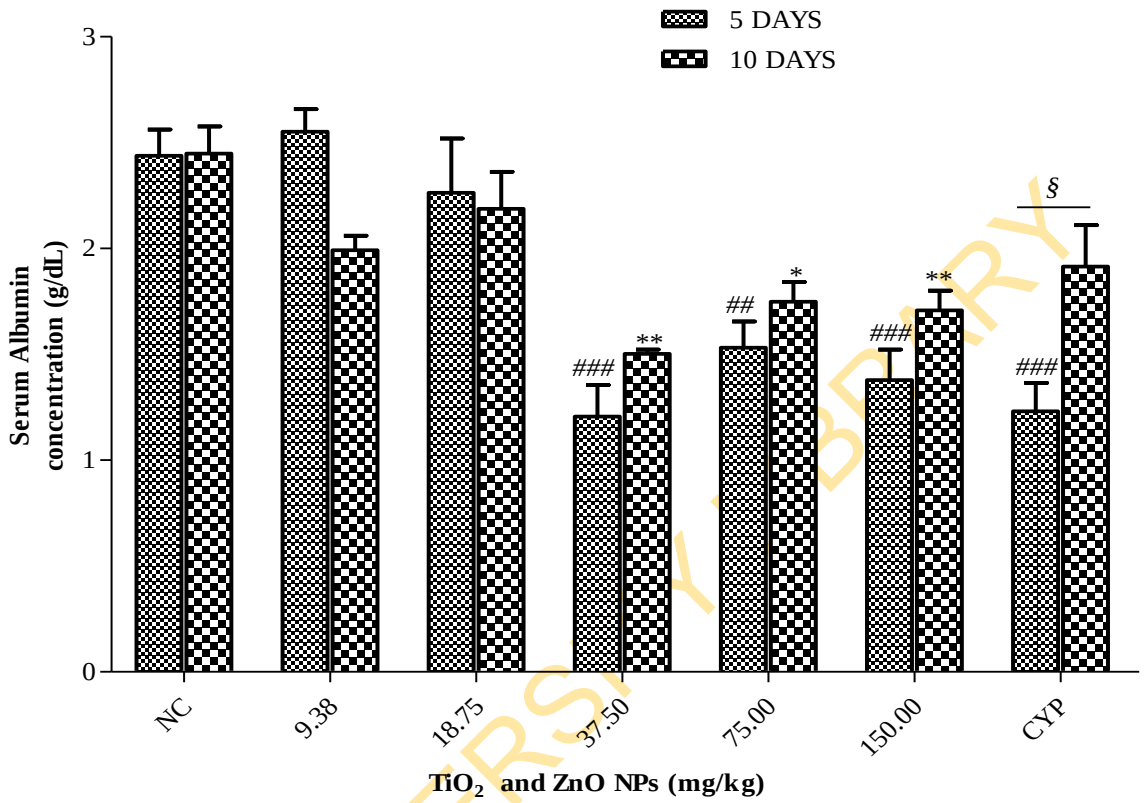

Figure 4. 77: Serum albumin concentration in mice treated with TiO_2 and ZnO NPs at the 5- and 10- day exposure periods.

Data represent mean ± SEM (n = 5). Negative control (NC) = distilled water, CYP = cyclophosphamide (positive control).

$^{##}$ $p < 0.01$ and $^{###}$ $p < 0.001$ in 5-days exposure

* $p < 0.05$ and ** $p < 0.01$ in 10-days exposure

§ $p < 0.05$ for the comparison between the 5- and 10-day exposures

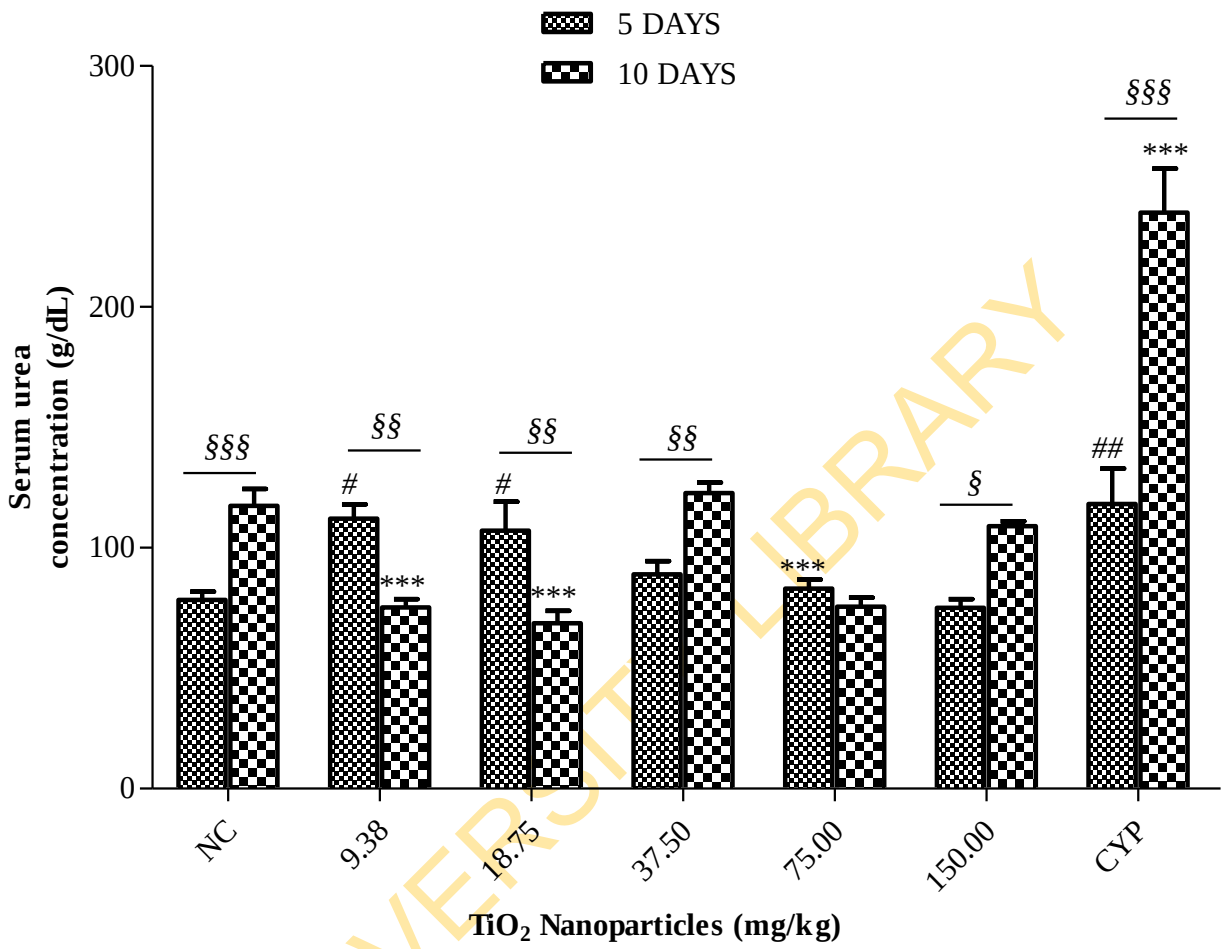

Figure 4. 78: Serum urea concentration in mice treated with TiO_2 NPs at the 5- and 10-day exposure periods.

Data represent mean ± SEM (n = 5). Negative control (NC) = distilled water, CYP = cyclophosphamide (positive control).

$^{\#}$ $p < 0.05$ and $^{\#\#}$ $p < 0.01$ in 5-days exposure

*** $p < 0.001$ in 10-days exposure

§ $p < 0.05$, §§ $p < 0.01$ and §§§ $p < 0.001$ for the comparison between the 5- and 10-day exposures

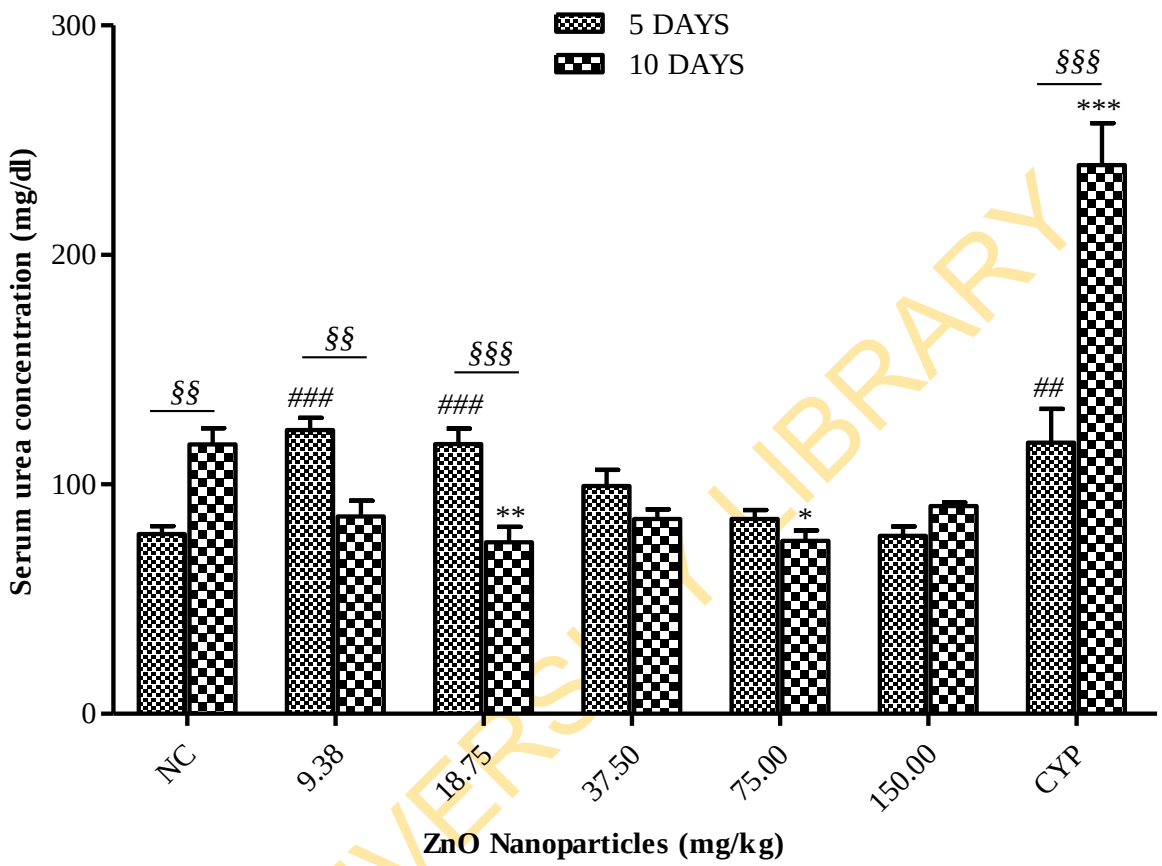

Figure 4. 79: Serum urea concentration in mice treated with ZnO NPs at the 5- and 10-day exposure periods.

Data represent mean ± SEM (n = 5). Negative control (NC) = distilled water, CYP = cyclophosphamide (positive control).

$^{\#\#}$ $p < 0.01$ and $^{\#\#\#}$ $p < 0.001$ in 5-days exposure

* $p < 0.05$, ** $p < 0.01$ and *** $p < 0.001$ in 10-days exposure

§§ $p < 0.01$ and §§§ $p < 0.001$ for the comparison between the 5- and 10-day exposures

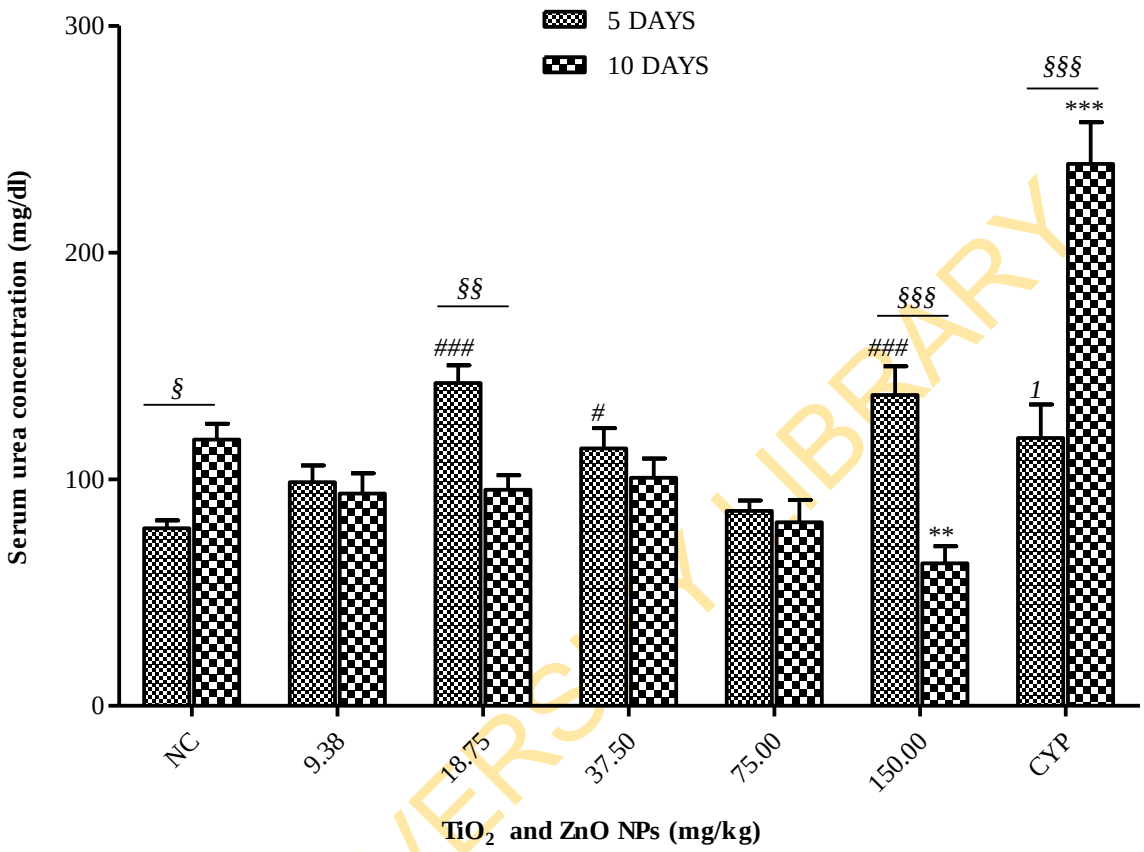

Figure 4. 80: Serum urea concentration in mice treated with TiO_2 and ZnO NPs at the 5- and 10- day exposure periods.

Data represent mean ± SEM (n = 5). Negative control (NC) = distilled water, CYP = cyclophosphamide (positive control).

$^{\#}$ $p < 0.05$ and $^{\#\#\#}$ $p < 0.001$ in 5-days exposure

** $p < 0.01$ and *** $p < 0.001$ in 10-days exposure

§ $p < 0.05$, §§ $p < 0.01$ and §§§ $p < 0.001$ for the comparison between the 5- and 10-day exposures

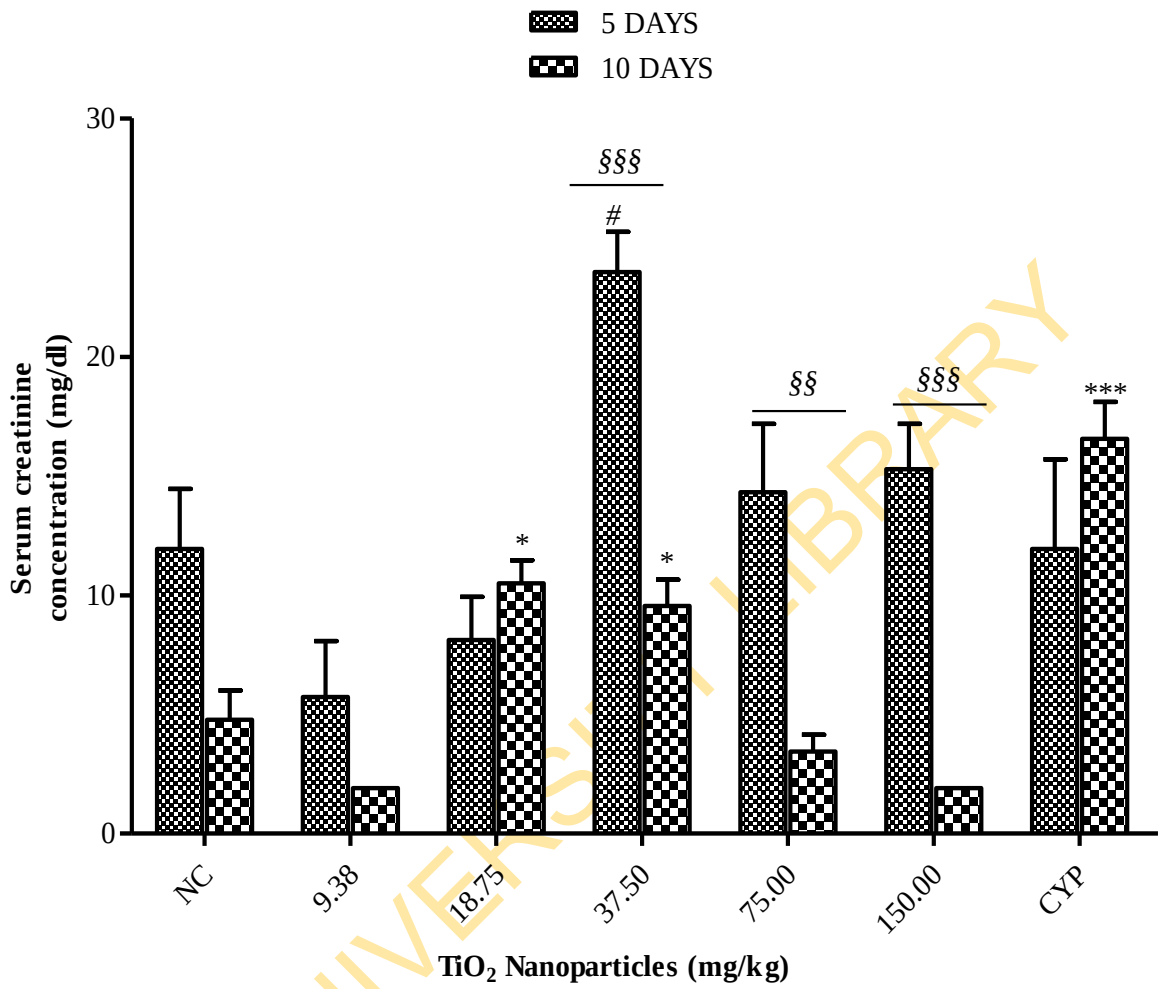

Figure 4. 81: Serum creatinine concentration in mice treated with TiO_2 NPs at the 5- and 10- day exposure periods.

Data represent mean ± SEM (n = 5). Negative control (NC) = distilled water, CYP = cyclophosphamide (positive control).

$^{\#}$ $p < 0.05$ in 5-days exposure

* $p < 0.05$ and *** $p < 0.001$ in 10-days exposure

§§ $p < 0.01$ and §§§ $p < 0.001$ for the comparison between the 5- and 10-day exposures

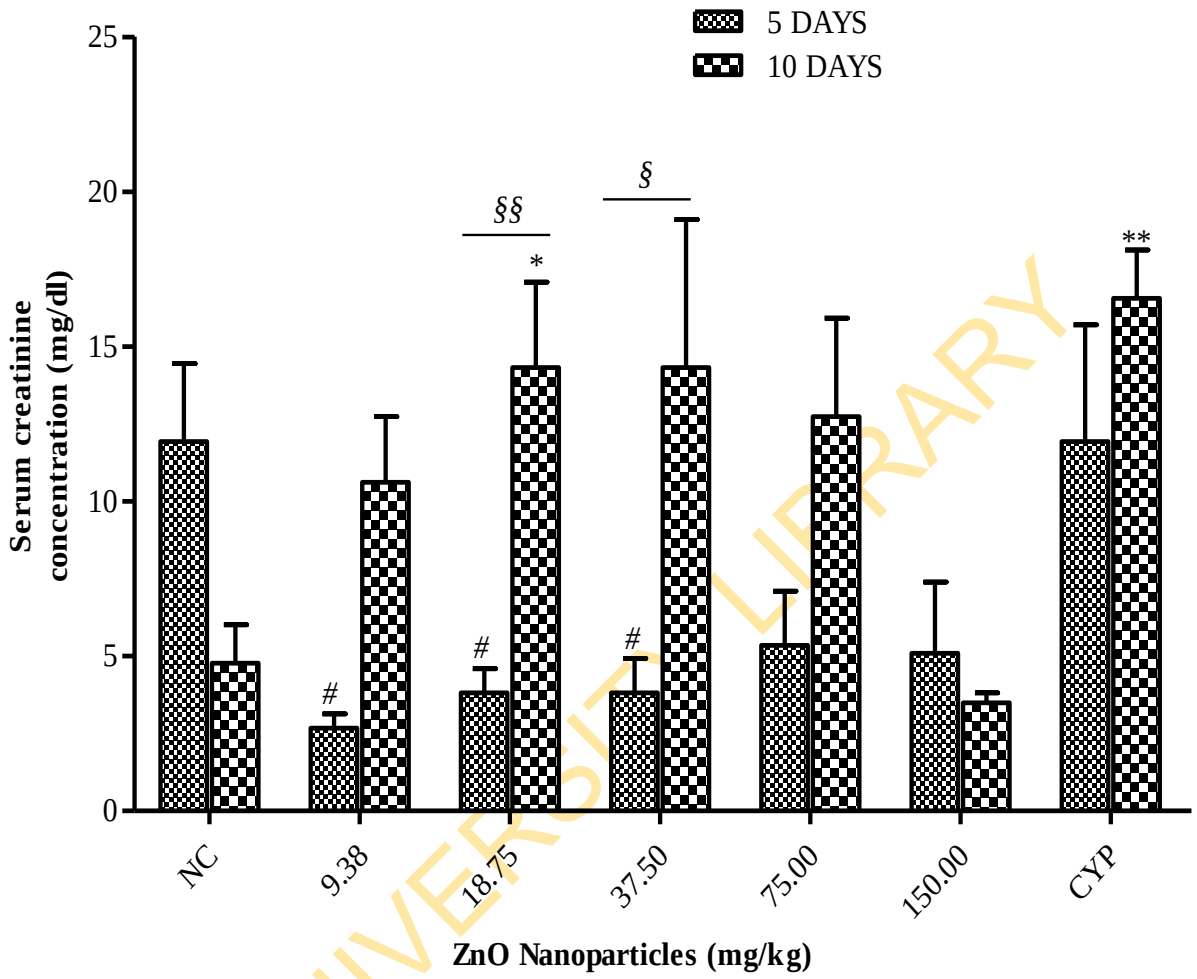

Figure 4. 82: Serum creatinine concentration in mice treated with ZnO NPs at the 5- and 10- day exposure periods.

Data represent mean ± SEM (n = 5). Negative control (NC) = distilled water, CYP = cyclophosphamide (positive control).

[#] $p < 0.05$ in 5-days exposure

[*] $p < 0.05$ and [**] $p < 0.01$ in 10-days exposure

[§] $p < 0.05$ and [§§] $p < 0.01$ for the comparison between the 5- and 10-day exposures

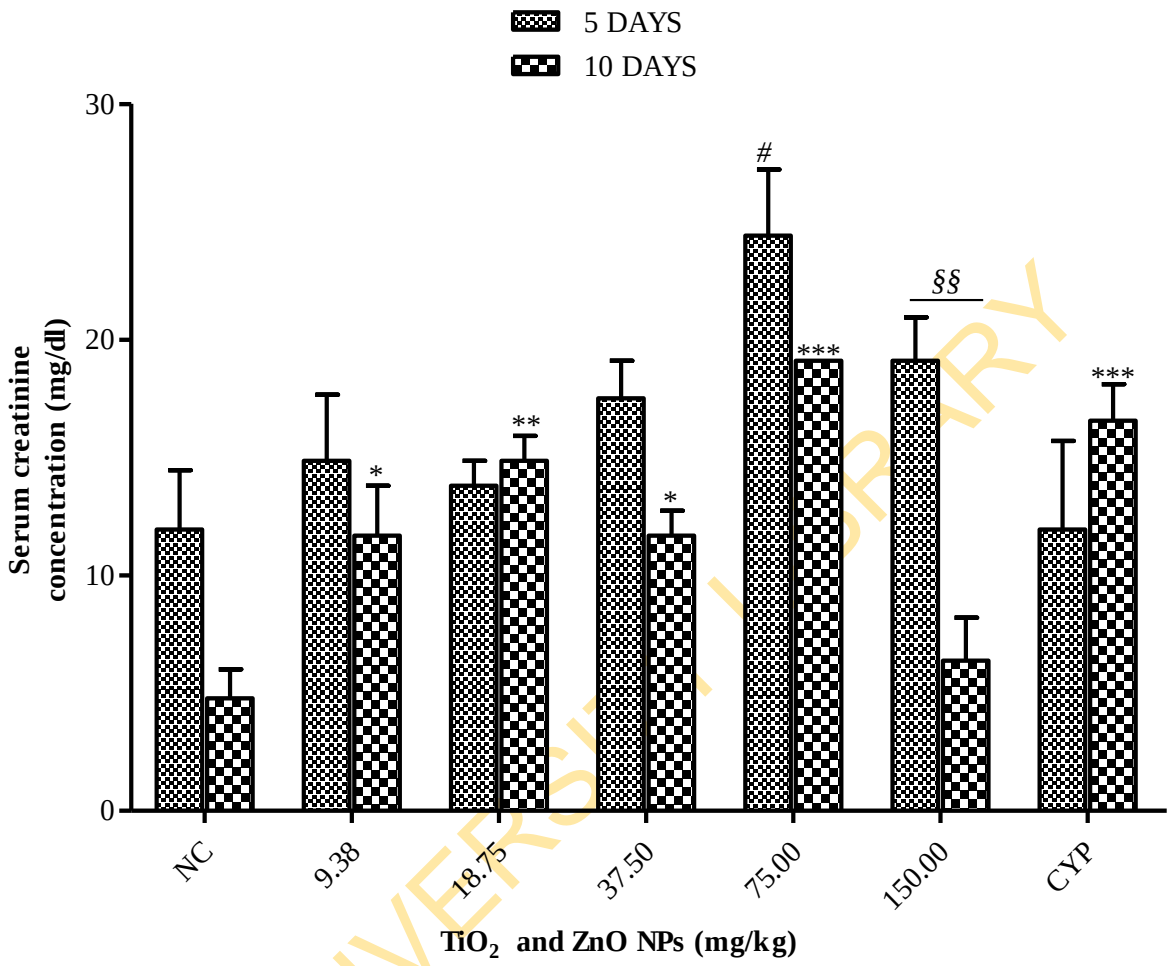

Figure 4. 83: Serum creatinine concentration in mice treated with TiO_2 and ZnO NPs at the 5- and 10- day exposure periods.

Data represent mean ± SEM (n = 5). Negative control (NC) = distilled water, CYP = cyclophosphamide (positive control).

$^{\#}$ $p < 0.05$ in 5-days exposure

* $p < 0.05$, ** $p < 0.01$ and *** $p < 0.001$ in 10-days exposure

§§ $p < 0.01$ for the comparison between the 5- and 10-day exposures

Figures 4.85 – 4.87 show the results of the serum total cholesterol levels in mice treated with TiO_2, ZnO NPs and their mixture for 5 and 10 days. For the 5- day exposure period, mice treated with TiO_2 NPs exhibited a reduction in the levels of the serum total cholesterol (Figure 4.85), which was significant at the 9.38 ($p < 0.001$), 18.75 ($p < 0.05$), 37.50 ($p < 0.01$) and 75.00 ($p < 0.001$) $mgkg^{-1}$ in comparison with the mice treated with distilled water while for the 10- day exposure period, a significant increase in the serum total cholesterol level (Figure 4.85) was observed in mice treated at the 9.38 ($p < 0.001$), 18.75 ($p < 0.001$), 37.50 ($p < 0.05$), 75.00 ($p < 0.01$) and 150.00 ($p < 0.001$) $mgkg^{-1}$ of TiO_2 NPs in comparison with the mice treated with distilled water. A comparison between the two exposure periods 5- and 10- days showed a significant difference at the 9.38 ($p < 0.001$) and 18.75 ($p < 0.01$) of TiO_2 NPs.

Mice treated with ZnO NPs for the 5- day exposure period exhibited a significant ($p < 0.001$) reduction in the serum total cholesterol level (Figure 4.86) at tested doses in comparison with the mice treated with distilled water. For the 10- day exposure period, the treated mice evinced significant increase in the serum total cholesterol level (Figure 4.86) at the 18.75 ($p < 0.05$), 75.00 ($p < 0.01$) and 150.00 ($p < 0.01$) $mgkg^{-1}$ of ZnO NPs in comparison with the mice treated with distilled water. A comparison between the 5- and 10- day exposure period revealed a significant ($p < 0.001$) difference at the 18.75, 75.00 and 150.00 $mgkg^{-1}$ of ZnO NPs. The mixture of both NPs administered to mice for the 5- day exposure period induced no significant increase ($p > 0.05$) in the level of serum total cholesterol (Figure 4.87) at the 9.38 and 18.75 $mgkg^{-1}$ and a decrease at the 37.50, 75.00 and 150.00 $mgkg^{-1}$ in comparison with the mice treated with distilled water. In contrast, for the 10- day exposure period, mice treated with their mixture exhibited a significant ($p < 0.05$) increase in the levels of serum total cholesterol (Figure 4.87) at the 9.38, 18.75 and 150.00 $mgkg^{-1}$ of their mixture compared with the control group treated with distilled water. A significant ($p < 0.001$) difference between the 5- and 10- day exposure periods was observed at 150.00 $mgkg^{-1}$ of their mixture.

Figures 4.88 – 4.90 show the results of the serum HDL levels in mice treated with TiO_2, ZnO NPs and their mixture for 5 and 10 days. For the 5- day exposure period, TiO_2 NPs administered to mice induced a significant reduction in the serum HDL levels (Figure

4.88) at the 9.38 ($p < 0.001$), 18.75 ($p < 0.05$) and 37.50 ($p < 0.05$) $mgkg^{-1}$ of TiO_2 NPs in comparison with the mice treated with distilled water. Similarly, mice treated with TiO_2 NPs for the 10- day exposure period exhibited a significant ($p < 0.001$) reduction in the serum HDL level (Figure 4.88) at tested doses. A comparison between the 5- and 10- day exposures showed a significant difference at the 9.38 ($p < 0.001$) and 18.75 ($p < 0.01$) of TiO_2 NPs.

For the 5- day exposure period, mice treated with ZnO NPs exhibited a significant ($p < 0.001$) increase in the level of serum HDL (Figure 4.89) at tested doses in comparison with the mice treated with distilled water. In contrast, for the 10- day exposure period mice treated with ZnO NPs exhibited a significant ($p < 0.001$) reduction in the serum HDL level (Figure 4.89) only at the 150.00 $mgkg^{-1}$ of ZnO NPs when in comparison with the mice treated with distilled water. A significant difference between the 5- and 10- day exposure periods was observed at the 9.38 ($p < 0.01$), 18.75 ($p < 0.001$), 75.00 ($p < 0.05$) and 150.00 ($p < 0.01$) $mgkg^{-1}$ of ZnO NPs. For the 5- day exposure period, mice treated with their mixture exhibited an increase in the level of serum HDL (Figure 4.90) at tested doses but significant only at the 9.38 ($p < 0.05$), 75.00 ($p < 0.001$) and 150.00 ($p < 0.05$) $mgkg^{-1}$ of their mixture in comparison with the mice treated with distilled water. Subsequently, treatment of mice to their mixture for the 10- day exposure period induced a significant ($p < 0.001$) reduction in the serum HDL level at tested doses in comparison with the mice treated with distilled water.

Figures 4.91 – 4.93 show the results of the serum triglycerides concentration in mice treated with TiO_2, ZnO NPs and their mixture for 5 and 10 days. For the 5- day exposure period, TiO_2 NPs administered to mice induced a significant reduction in the concentration of serum triglycerides (Figure 4.91) at the 9.38 ($p < 0.05$), 18.75 ($p < 0.01$) and 37.50 ($p < 0.001$) of TiO_2 NPs in comparison with the mice treated with distilled water. In contrast, for the 10- day exposure period, mice treated with TiO_2 NPs exhibited no significant reduction ($p > 0.05$) in the concentration of the serum triglycerides (Figure 4.91) at tested doses in comparison with the mice treated with distilled water. ZnO NPs administered to mice for the 5- day exposure period induced a significant ($p < 0.001$) reduction in the concentration of serum triglycerides (Figure 4.92) at the 9.38, 18.75 and 37.50 $mgkg^{-1}$ of

ZnO NPs in comparison with the mice treated with distilled water. In addition, for the 10-day exposure period, a significant reduction in the concentration of serum triglycerides (Figure 4.92) was observed at the 9.38 ($p < 0.01$), 18.75 ($p < 0.05$) and 75.00 ($p < 0.01$) of ZnO NPs in comparison with the mice treated with distilled water. A significant difference between the 5- and 10- day exposure period was observed at the 150.00 ($p < 0.001$) of ZnO NPs.

For the 5- day exposure period, mice treated with their mixture of both NPs exhibited a significant ($p < 0.01$) reduction in the concentration of serum triglycerides (Figure 4.93) at tested doses in comparison with the mice treated with distilled water while for the 10- day exposure period, the treated mice exhibited a significant reduction in the concentration of serum triglycerides (Figure 4.93) at the 9.38 ($p < 0.05$) and 37.50 ($p < 0.01$) $mgkg^{-1}$ of their miture. A comparison between the two exposure periods, 5- and 10- days showed a significant difference at the 18.75 ($p < 0.001$) and 150.00 ($p < 0.01$) of their mixture.

Figures 4.94 – 4.96 show the results of the urine creatinine concentration in mice treated with TiO_2, ZnO NPs and their mixture for 5 and 10 days. For the 5- day exposure period, mice treated with TiO_2 NPs exhibited a significant increase in the urine creatinine concentration (Figure 4.94) only at the 9.38 ($p < 0.01$) and 18.75 ($p < 0.05$) $mgkg^{-1}$ of TiO_2 NPs in comparison with the mice treated with distilled water. For the 10- day exposure period, there was a significant ($p < 0.05$) increase in the urine creatinine concentration (Figure 4.94) only at the 18.75 $mgkg^{-1}$ of TiO_2 NPs in the treated mice in comparison with the mice treated with distilled water. A significant ($p < 0.001$) difference between the 5- and 10- day exposure period was observed at the 9.38 $mgkg^{-1}$ of TiO_2 NPs.

ZnO NPs administered to mice for the 5- day exposure period induced no significant ($p > 0.05$) increase in the urine creatinine concentration (Figure 4.95) at the 9.38 and 18.75 $mgkg^{-1}$ and no significant ($p > 0.05$) reduction at the 37.50, 75.00 and 150.00 $mgkg^{-1}$ of ZnO NPs in comparison with mice treated with distilled water. For the 10- day exposure period, mice treated with ZnO NPs exhibited a significant ($p < 0.05$) increase in the urine creatinine concentration (Figure 4.95) at the 9.38 and 18.75 $mgkg^{-1}$ in comparison with the mice treated with distilled water.

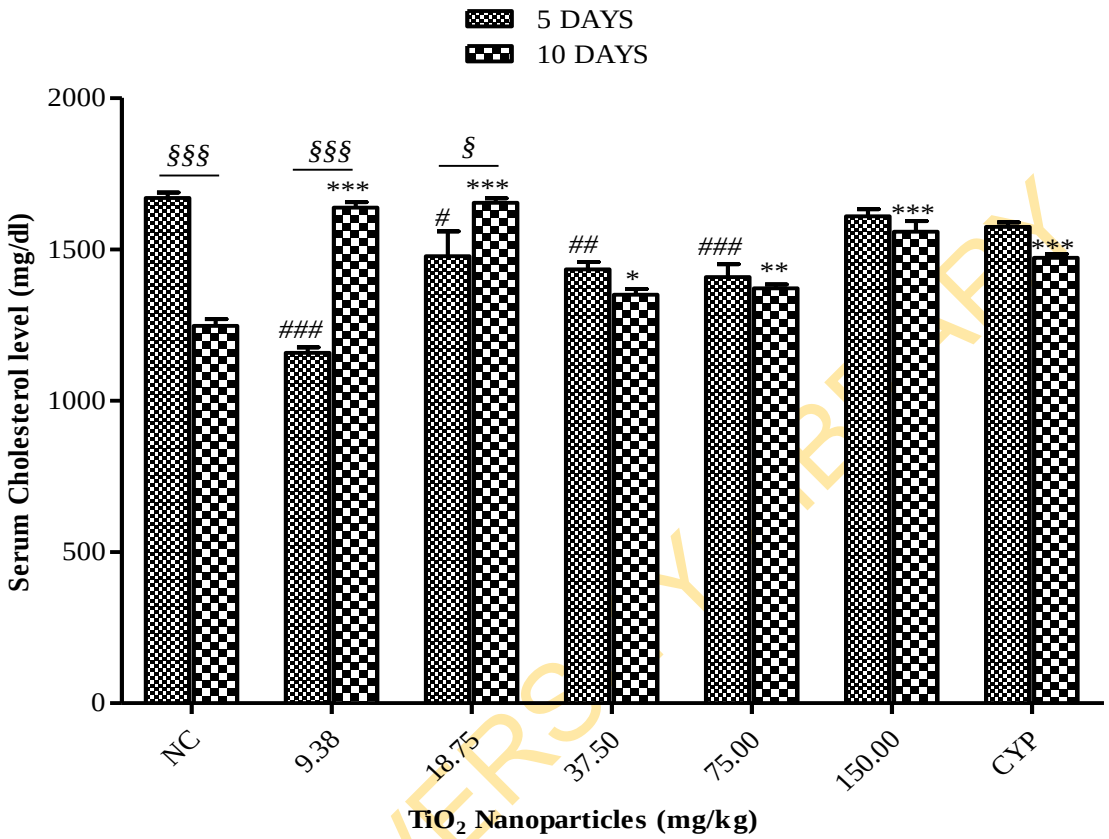

Figure 4. 84: Serum cholesterol levels in mice treated with TiO_2 NPs at the 5- and 10- day exposure periods.

Data represent mean ± SEM (n = 5). Negative control (NC) = distilled water, CYP = cyclophosphamide (positive control).

$^{\#}$ $p < 0.05$, $^{\#\#}$ $p < 0.01$ and $^{\#\#\#}$ $p < 0.001$ in 5-days exposure

* $p < 0.05$, ** $p < 0.01$ and *** $p < 0.001$ in 10-days exposure

§ $p < 0.05$ and §§§ $p < 0.001$ for the comparison between the 5- and 10-day exposures

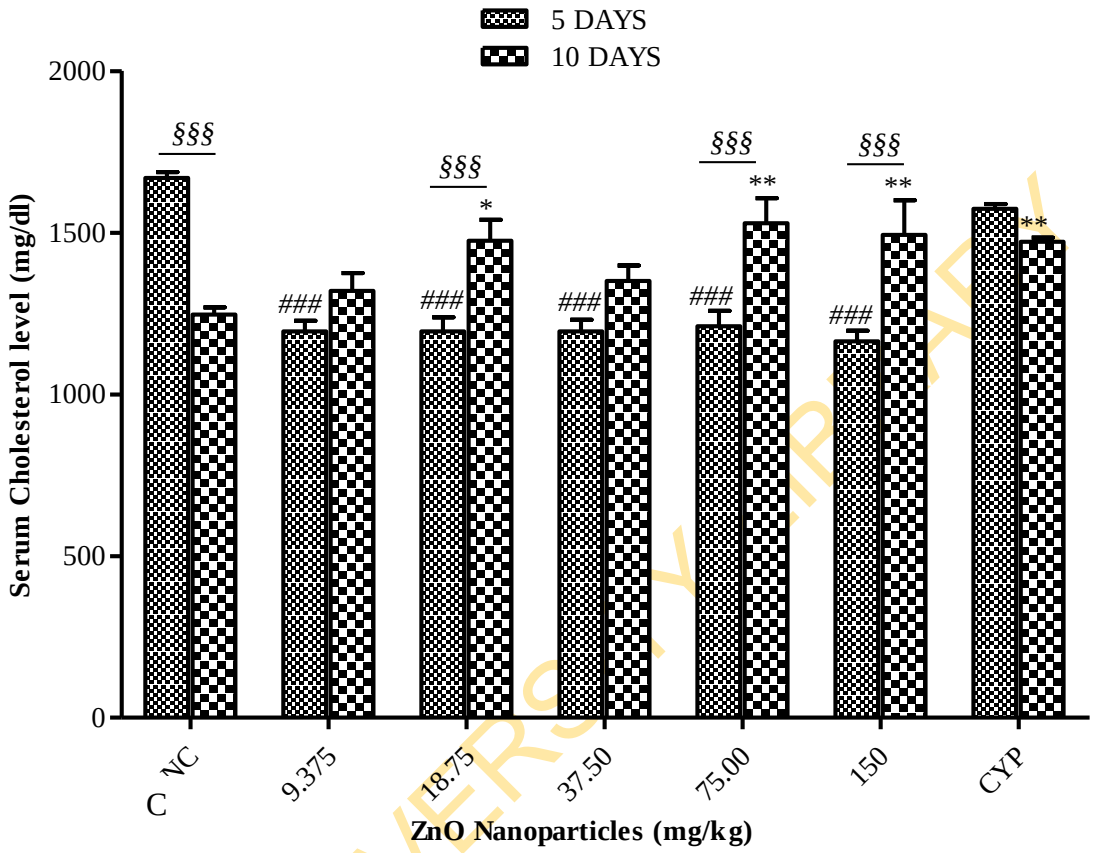

Figure 4. 85: Serum cholesterol levels in mice treated with ZnO NPs at the 5- and 10- day exposure periods.

Data represent mean ± SEM (n = 5). Negative control (NC) = distilled water, CYP = cyclophosphamide (positive control).

$^{###}$ $p < 0.001$ in 5-days exposure

* $p < 0.05$ and ** $p < 0.01$ in 10-days exposure

§§§ $p < 0.001$ for the comparison between the 5- and 10-day exposures

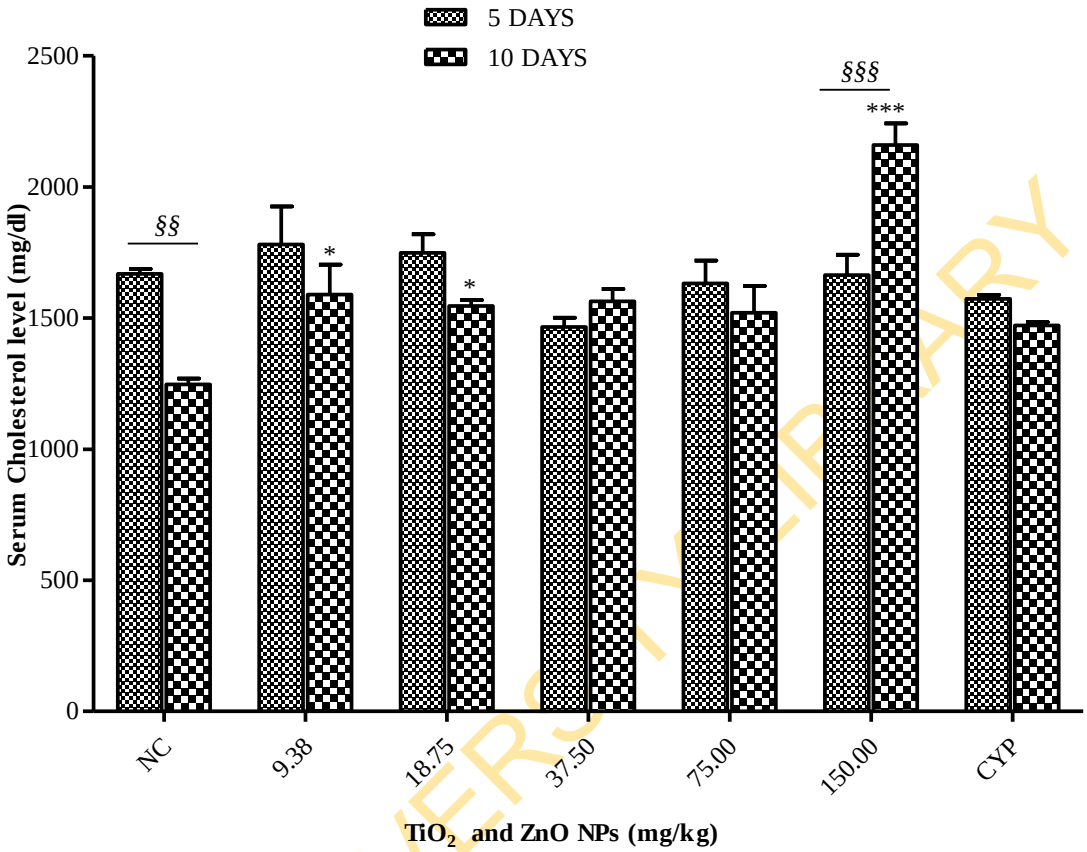

Figure 4. 86: Serum cholesterol levels in mice treated with TiO_2 and ZnO NPs at the 5- and 10- day exposure periods.

Data represent mean ± SEM (n = 5). Negative control (NC) = distilled water, CYP = cyclophosphamide (positive control).

* $p < 0.05$ and *** $p < 0.001$ in 10-days exposure

§§ $p < 0.01$ and §§§ $p < 0.001$ for the comparison between the 5- and 10-day exposures

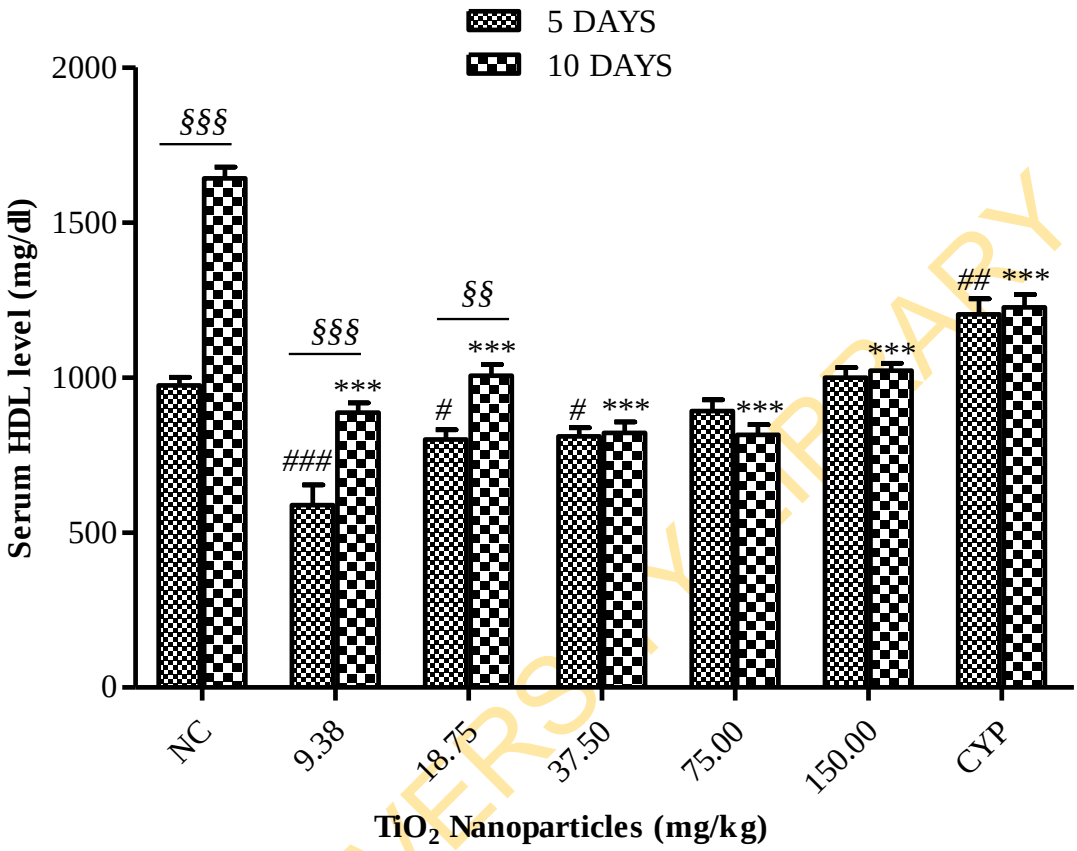

Figure 4. 87: Serum HDL levels in mice treated with TiO_2 NPs at the 5- and 10- day exposure periods.

Data represent mean ± SEM (n = 5). Negative control (NC) = distilled water, CYP = cyclophosphamide (positive control).

$^{\#}$ $p < 0.05$, $^{\#\#}$ $p < 0.01$ and $^{\#\#\#}$ $p < 0.001$ in 5-days exposure

*** $p < 0.001$ in 10-days exposure

§§ $p < 0.01$ and §§§ $p < 0.001$ for the comparison between the 5- and 10-day exposures

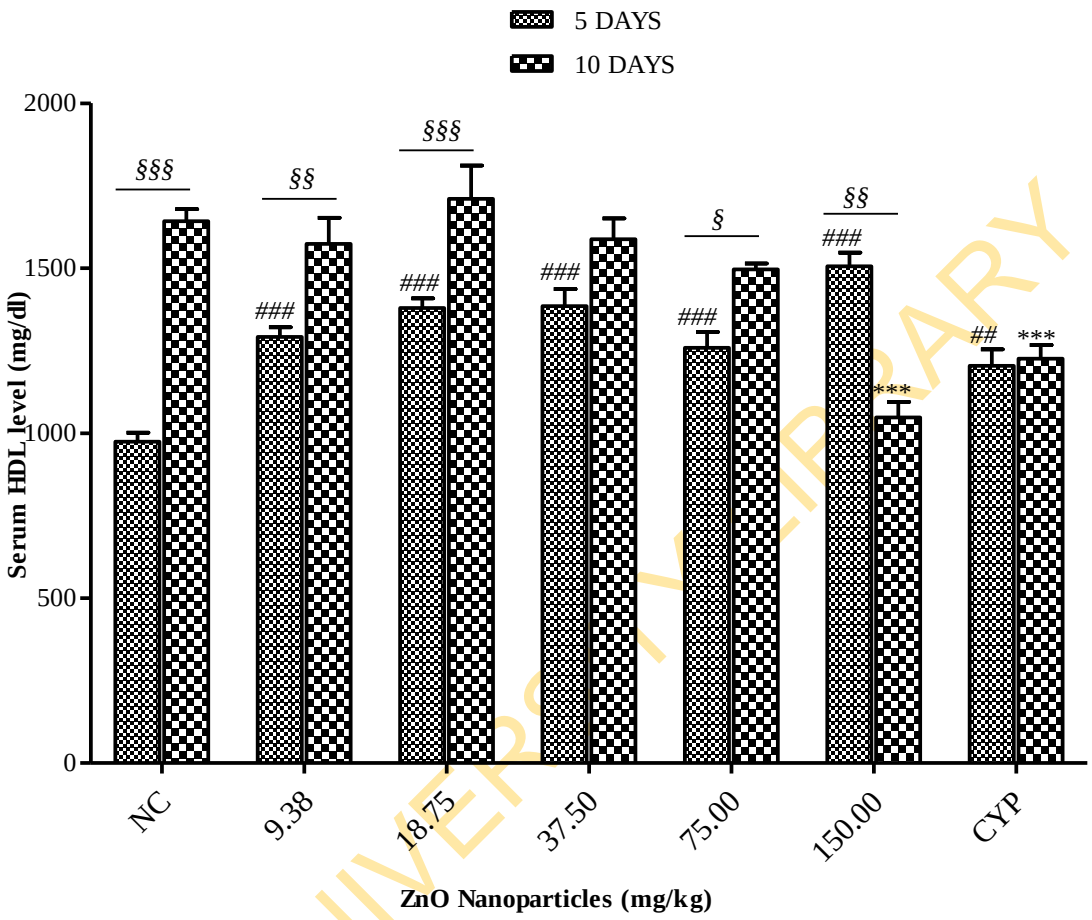

Figure 4. 88: Serum HDL levels in mice treated with ZnO NPs at the 5- and 10- day exposure periods.

Data represent mean ± SEM (n = 5). Negative control (NC) = distilled water, CYP = cyclophosphamide (positive control).

$^{\#\#}$ $p < 0.01$ and $^{\#\#\#}$ $p < 0.001$ in 5-days exposure

*** $p < 0.001$ in 10-days exposure

§ $p < 0.05$, §§ $p < 0.01$ and §§§ $p < 0.001$ for the comparison between the 5- and 10-days exposures

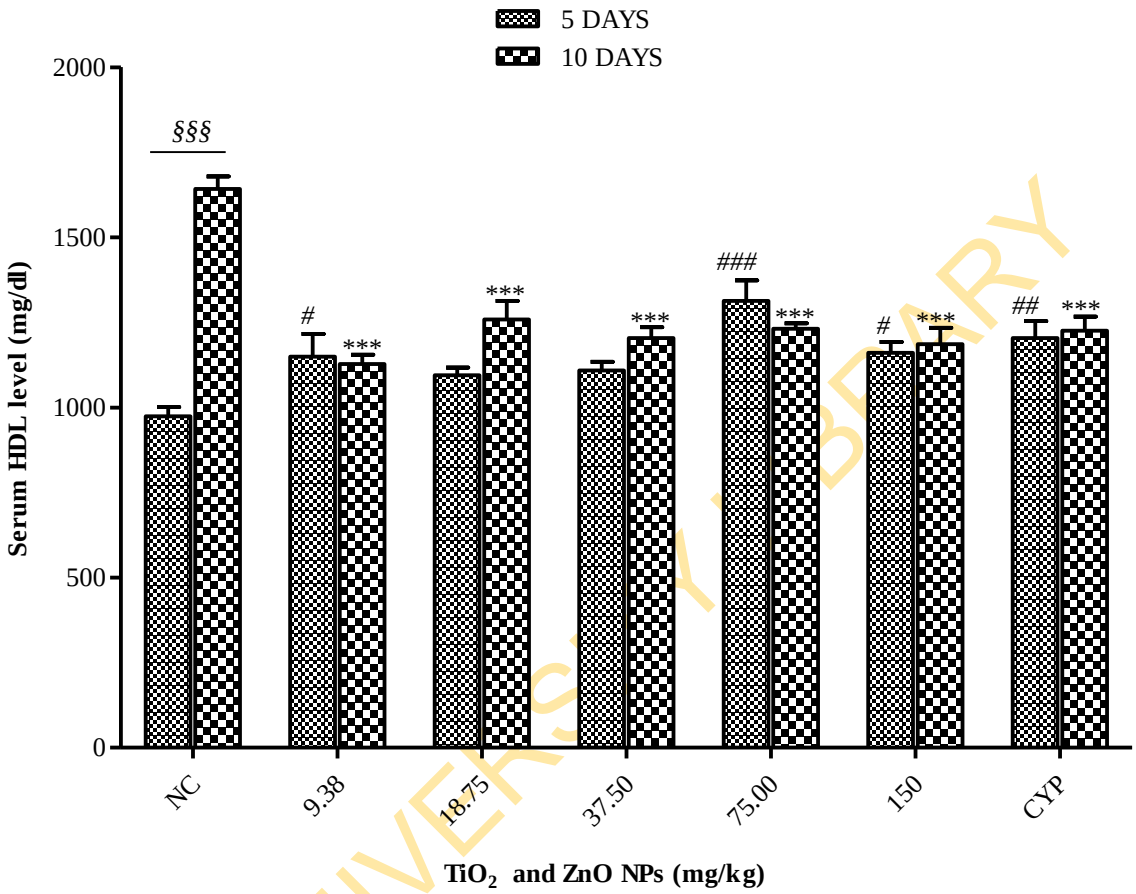

Figure 4. 89: Serum HDL levels in mice treated with TiO_2 and ZnO NPs at the 5- and 10-day exposure periods.

Data represent mean ± SEM (n = 5). Negative control (NC) = distilled water, CYP = cyclophosphamide (positive control).

$^{\#}$ $p < 0.05$, $^{\#\#}$ $p < 0.01$ and $^{\#\#\#}$ $p < 0.001$ in 5-days exposure

*** $p < 0.001$ in 10-days exposure

§§§ $p < 0.001$ for the comparison between the 5- and 10-day exposures

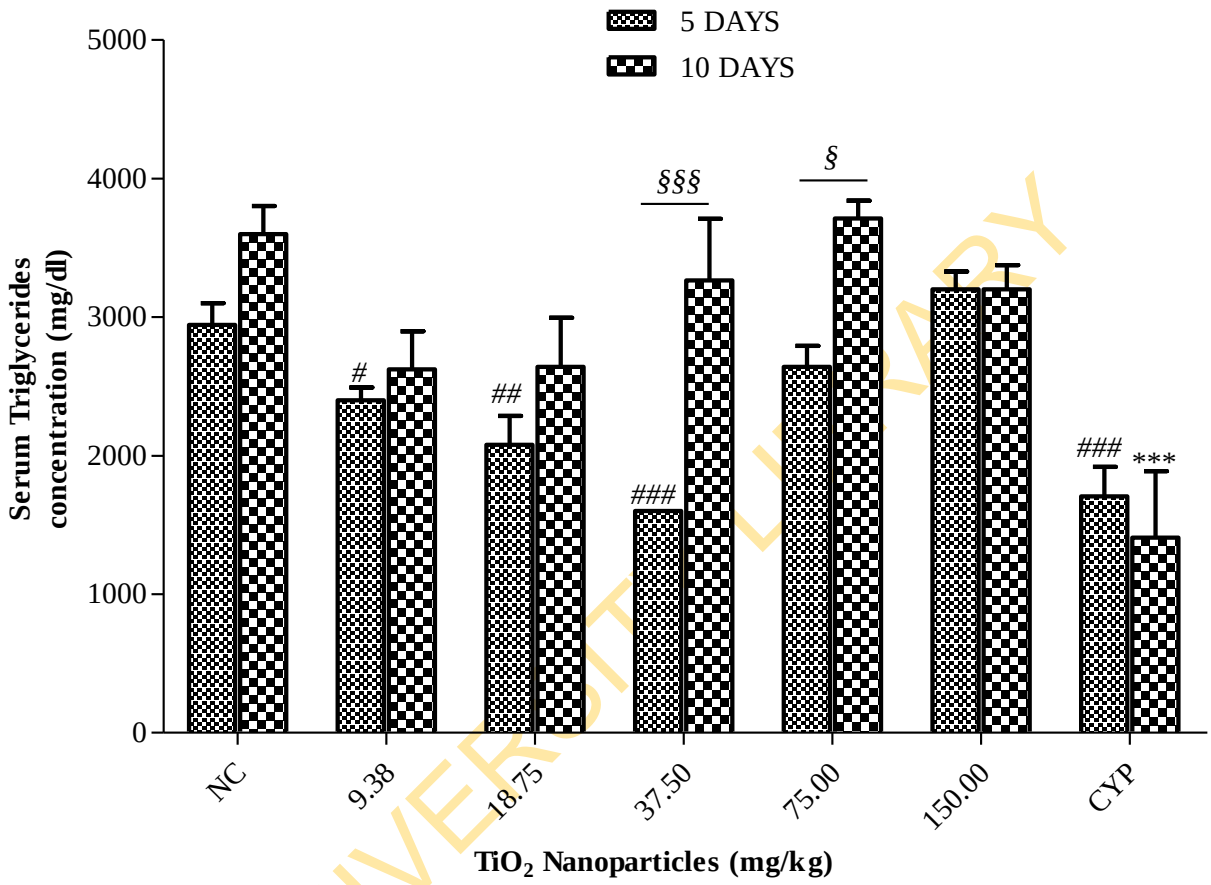

Figure 4. 90: Serum triglycerides concentration in mice treated with TiO_2 NPs at the 5- and 10- day exposure periods.

Data represent mean ± SEM (n = 5). Negative control (NC) = distilled water, CYP = cyclophosphamide (positive control).

$^{\#}$ $p < 0.05$, $^{\#\#}$ $p < 0.01$ and $^{\#\#\#}$ $p < 0.001$ in 5-days exposure

*** $p < 0.001$ in 10-days exposure

§ $p < 0.05$ and §§§ $p < 0.001$ for the comparison between the 5- and 10-day exposures

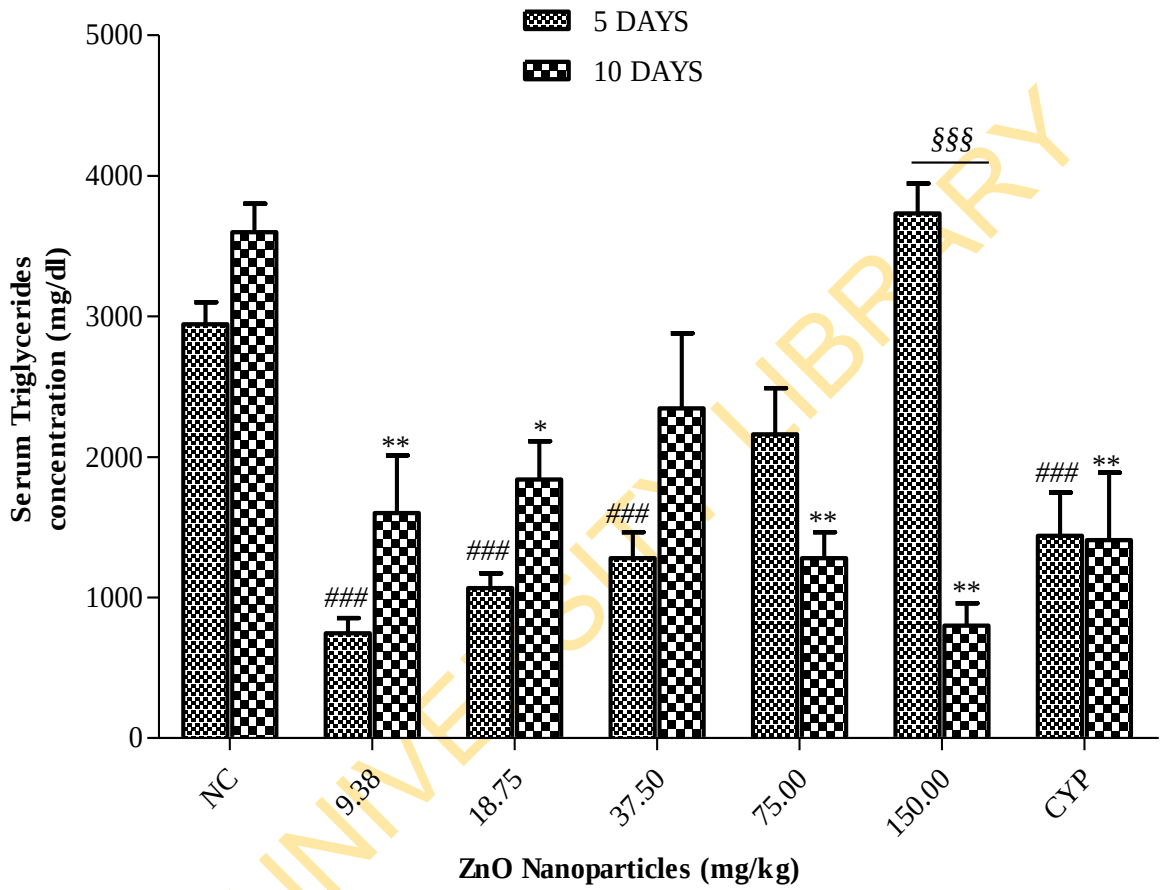

Figure 4. 91: Serum triglyceride levels in mice treated with ZnO NPs at the 5- and 10-day exposure periods.

Data represent mean ± SEM (n = 5). Negative control (NC) = distilled water, CYP = cyclophosphamide (positive control).

$^{###}$ $p < 0.001$ in 5-days exposure

* $p < 0.05$ and ** $p < 0.01$ in 10-days exposure

§§§ $p < 0.001$ for the comparison between the 5- and 10-day exposures

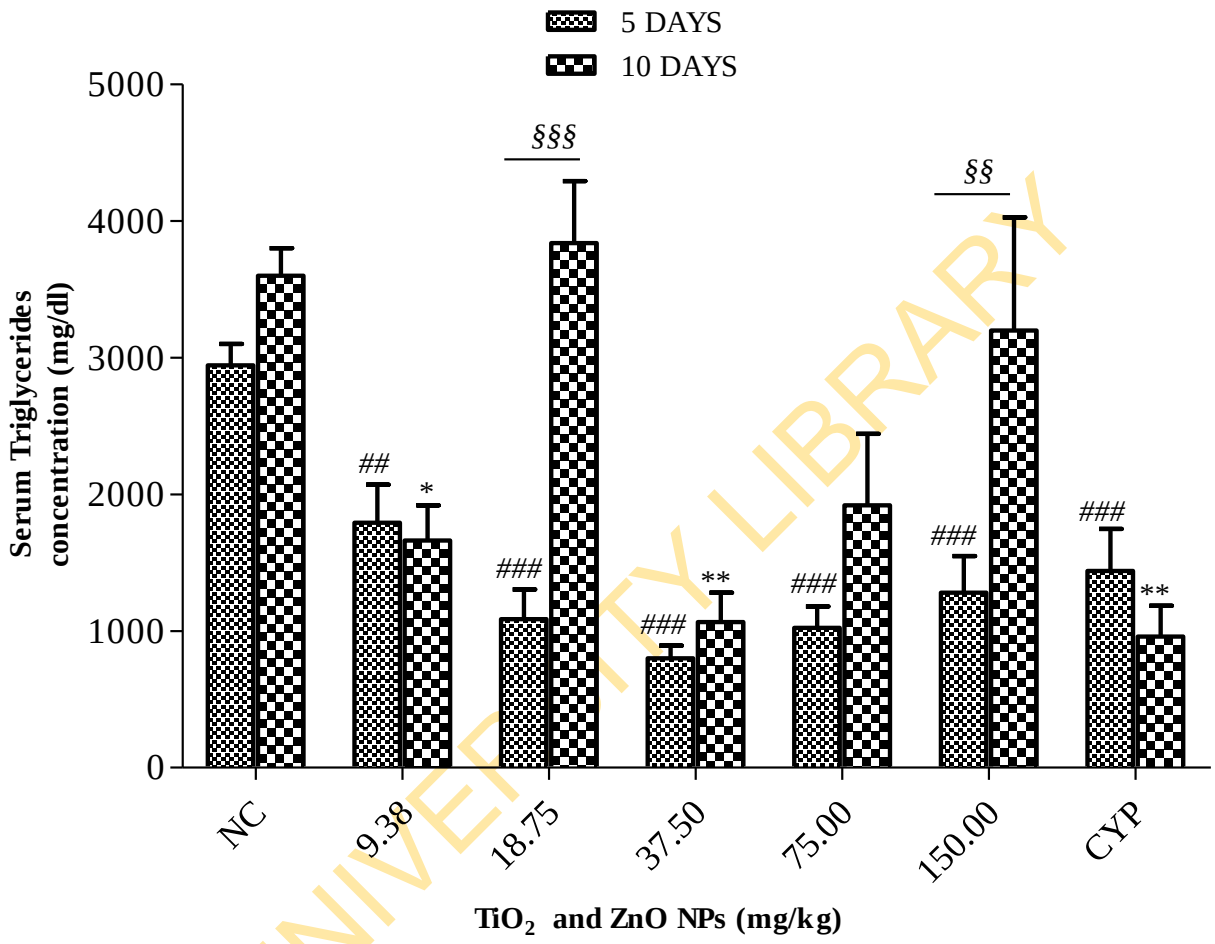

Figure 4. 92: Serum triglyceride levels in mice treated with TiO_2 and ZnO NPs at the 5- and 10- day exposure periods.

Data represent mean ± SEM (n = 5). Negative control (NC) = distilled water, CYP = cyclophosphamide (positive control).

$^{\#\#}$ $p < 0.01$ and $^{\#\#\#}$ $p < 0.001$ in 5-days exposure

* $p < 0.05$ and ** $p < 0.01$ in 10-days exposure

§§ $p < 0.01$ and §§§ $p < 0.001$ for the comparison between the 5- and 10-day exposures

A comparison between the 5- and 10- day exposures showed a significant difference at the 9.38 ($p < 0.010$ and 18.75 ($p < 0.05$) $mgkg^{-1}$ of ZnO NPs. For the 5- day exposure period, mice treated with their mixture of the NPs exhibited a significant increase in the urine creatinine concentration (Figure 4.96) only at 9.38 ($p < 0.05$), 18.75 ($p < 0.05$) and 37.50 ($p < 0.001$) $mgkg^{-1}$ in comparison with the mice treated with distilled water while for the 10-day exposure period, their mixture administered to mice induced a significant increase in the urine creatinine concentration (Figure 4.96) at 18.75 ($p < 0.001$), 37.50 ($p < 0.05$), 75.00 ($p < 0.001$) and 150.00 ($p < 0.01$) $mgkg^{-1}$ in comparison with the mice treated with distilled water. A significant difference between the 5- and 10- day exposure period was observed at the 9.38 ($p < 0.01$), 18.75 ($p < 0.01$) and 75.00 ($p < 0.001$) of the mixture.

Figures 4.97 – 4.99 show the results of the urine albumin concentration in mice treated with TiO_2, ZnO NPs and their mixture for 5 and 10 days. Generally, TiO_2 NPs administered to mice for the 5- day exposure period induced a reduction in the urine albumin concentration (Figure 4.97) at tested doses, which was significant ($p < 0.05$) only at the 37.50 $mgkg^{-1}$ of TiO_2 NPs in comparison with the mice treated with distilled water while for the 10- day exposure period, a significant ($p < 0.001$) reduction in the urine albumin concentration (Figure 4.97) was observed at tested doses of the treated mice in comparison with those treated with distilled water. Similarly, mice treated with ZnO NPs for the 5- day exposure period exhibited a significant ($p < 0.001$) increase in the urine albumin concentration (Figure 4.98) at tested doses of ZnO NPs in comparison with the mice treated with distilled water while for the 10- day exposure period, the treated mice exhibited no significant ($p > 0.05$) reduction in the urine albumin concentration at tested doses (Figure 4.98). For the 5- day exposure period, mice treated with their mixture of the NPs exhibited a significant ($p < 0.001$) increase in the urine albumin concentration (Figure 4.99) at tested doses in comparison with the mice treated with distilled water while for the 10-day exposure, treated mice exhibited a reduction in the urine albumin concentration (Figure 4.99) at tested doses, but was significant ($p < 0.05$) only at the 9.38 $mgkg^{-1}$ of their mixture in comparison with those treated with distilled water.

4.4.6 Oxidative stress induced by titanium dioxide, zinc oxide nanoparticles and their mixture in the liver, kidney and testes of mice

Oxidative stress parameters in the liver of mice treated with TiO_2, ZnO NPs and their mixture for 5 and 10 days are presented in Figures 4.100 – 4.111. For the 5- day exposure period, TiO_2 (Figure 4.100), ZnO NPs (Figure 4.101) and their mixture (Figure 4.102) significantly ($p < 0.001$) reduced SOD activity in the liver of the treated mice at tested doses in comparison with the mice treated with distilled water. For the 10- day exposure period, the activity of SOD significantly increased only at the 37.50 $mgkg^{-1}$ ($p < 0.05$) of TiO_2 NPs (Figure 4. 100); and at the 18.75 ($p < 0.01$), 75.00 ($p < 0.05$) and 150.00 $mgkg^{-1}$ ($p < 0.001$) of their mixture (Figure 4.102) in comparison with the mice treated with distilled water. A significant ($p < 0.05$) difference between the 5- and 10- day exposure periods was observed at the 9.38 and 150.00 $mgkg^{-1}$ of ZnO NPs and at tested doses of their mixture (except at 37.50 $mgkg^{-1}$).

For the 5- day exposure period, CAT activity in the liver of the treated mice was significantly ($p < 0.001$) decreased at the 9.38, 18.75 and 150.00 $mgkg^{-1}$ of TiO_2 NPs (Figure 4.103); 37.50, 75.00 and 150.00 $mgkg^{-1}$ of ZnO NPs (Figure 4.104); and at tested doses of their mixture (Figure 4.105) in comparison with the mice treated with distilled water. For the 10- day exposure period, CAT activity significantly ($p < 0.001$) increased at tested doses of TiO_2 NPs (Figure 4.103); significantly ($p < 0.001$) decreased at the 37.50, 75.00 and 150.00 $mgkg^{-1}$ of ZnO NPs (Figure 4.104); and at the 18.75 and 150.00 $mgkg^{-1}$ of their mixture (Figure 4.105) in comparison with the mice treated with distilled water. A significant difference ($p < 0.001$) between the 5- and 10- day exposure periods was observed at tested doses of TiO_2 NPs; at the 9.38 and 18.75 $mgkg^{-1}$ of ZnO NPs and at tested doses of their mixture (except at 18.75 $mgkg^{-1}$). For the 5- day exposure period, the GSH level in the liver of the treated mice was significantly ($p < 0.001$) decreased at tested doses of TiO_2 NPs (Figure 4.106); increased at tested doses of ZnO NPs (Figure 4.107) and their mixture (Figure 4.108) respectively in comparison with the mice treated with distilled water.

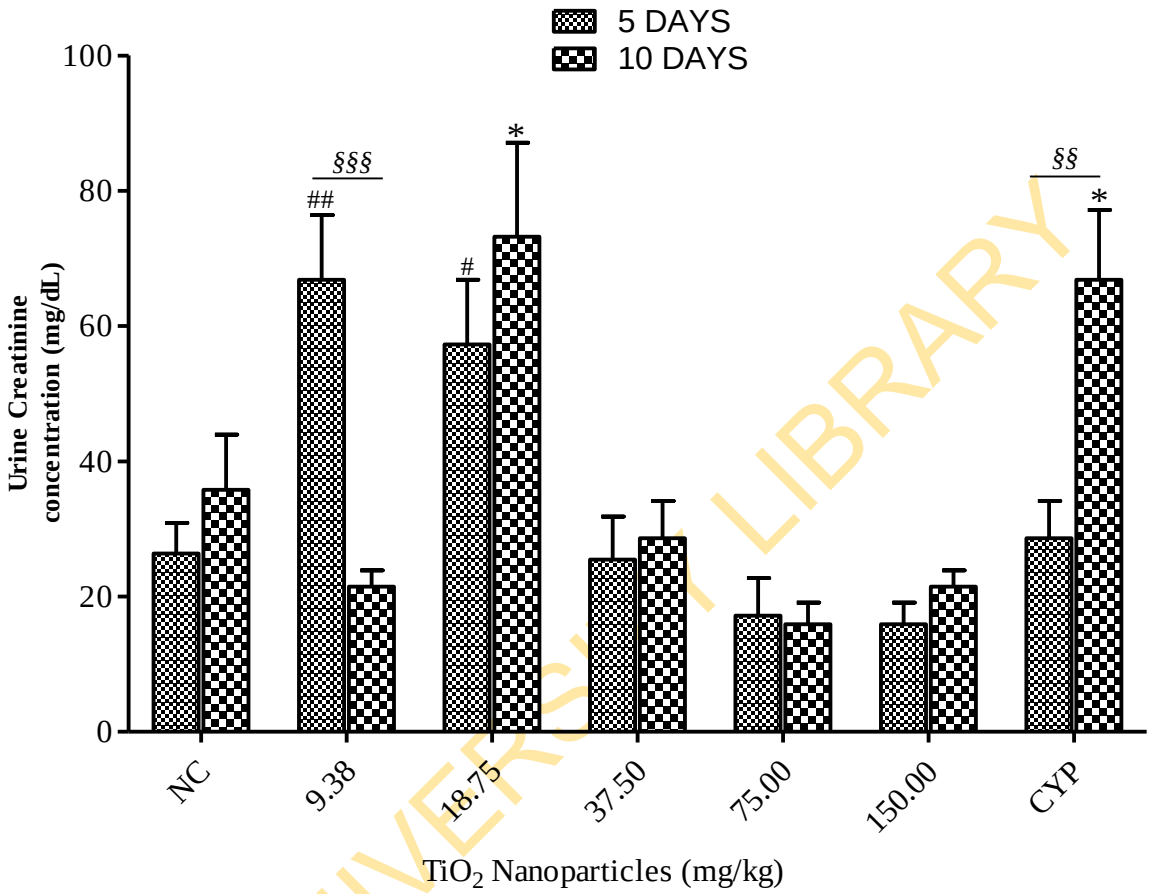

Figure 4. 93: Urine creatinine concentration in mice treated with TiO_2 NPs at the 5- and 10- day exposure periods.

Data represent mean ± SEM (n = 5). Negative control (NC) = distilled water, CYP = cyclophosphamide (positive control).

$^{\#}p < 0.05$ and $^{\#\#}p < 0.01$ in 5-days exposure

$^{*}p < 0.05$ in 10-days exposure

$^{\S\S}p < 0.01$ and $^{\S\S\S}p < 0.001$ for the comparison between the 5- and 10-day exposures

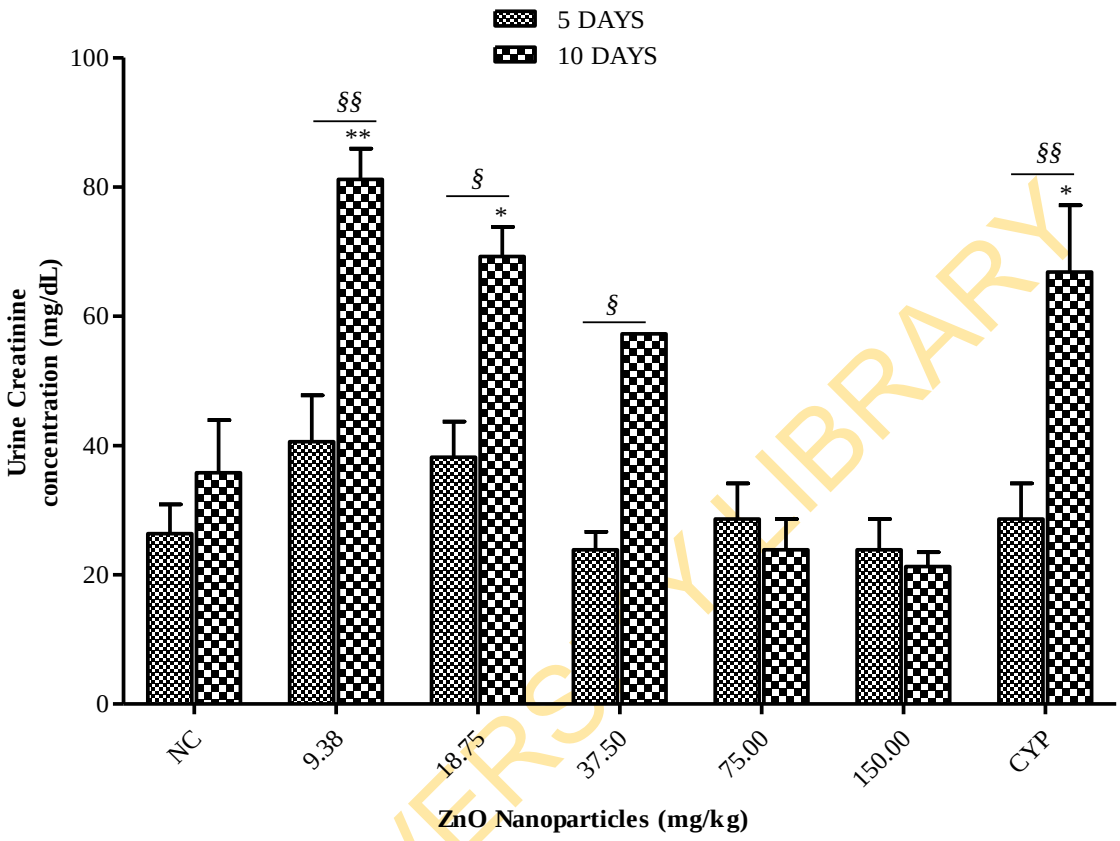

Figure 4. 94: Urine creatinine concentration in mice treated with ZnO NPs at the 5- and 10- day exposure periods.

Data represent mean ± SEM (n = 5). Negative control (NC) = distilled water, CYP = cyclophosphamide (positive control).

$^{*}p < 0.05$ and $^{**}p < 0.01$ in 10-days exposure

$^{\S}p < 0.05$ and $^{\S\S}p < 0.01$ for the comparison between the 5- and 10-day exposures

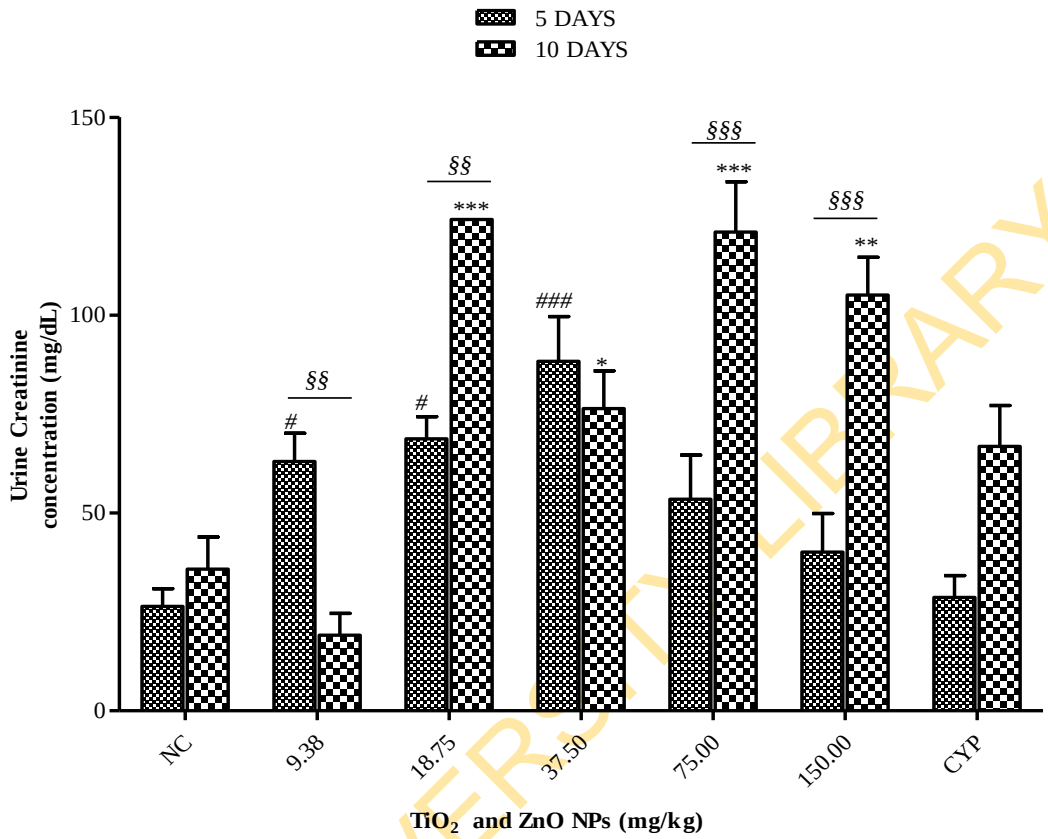

Figure 4. 95: Urine creatinine concentration in mice treated with TiO_2 and ZnO NPs at the 5- and 10- day exposure periods.

Data represent mean ± SEM (n = 5). Negative control (NC) = distilled water, CYP = cyclophosphamide (positive control).

$^{\#}$ $p < 0.05$and $^{\#\#\#}$ $p < 0.001$ in 5-days exposure

** $p < 0.01$ and *** $p < 0.001$ in 10-days exposure

§§ $p < 0.01$ and §§§ $p < 0.001$ for the comparison between the 5- and 10-day exposures

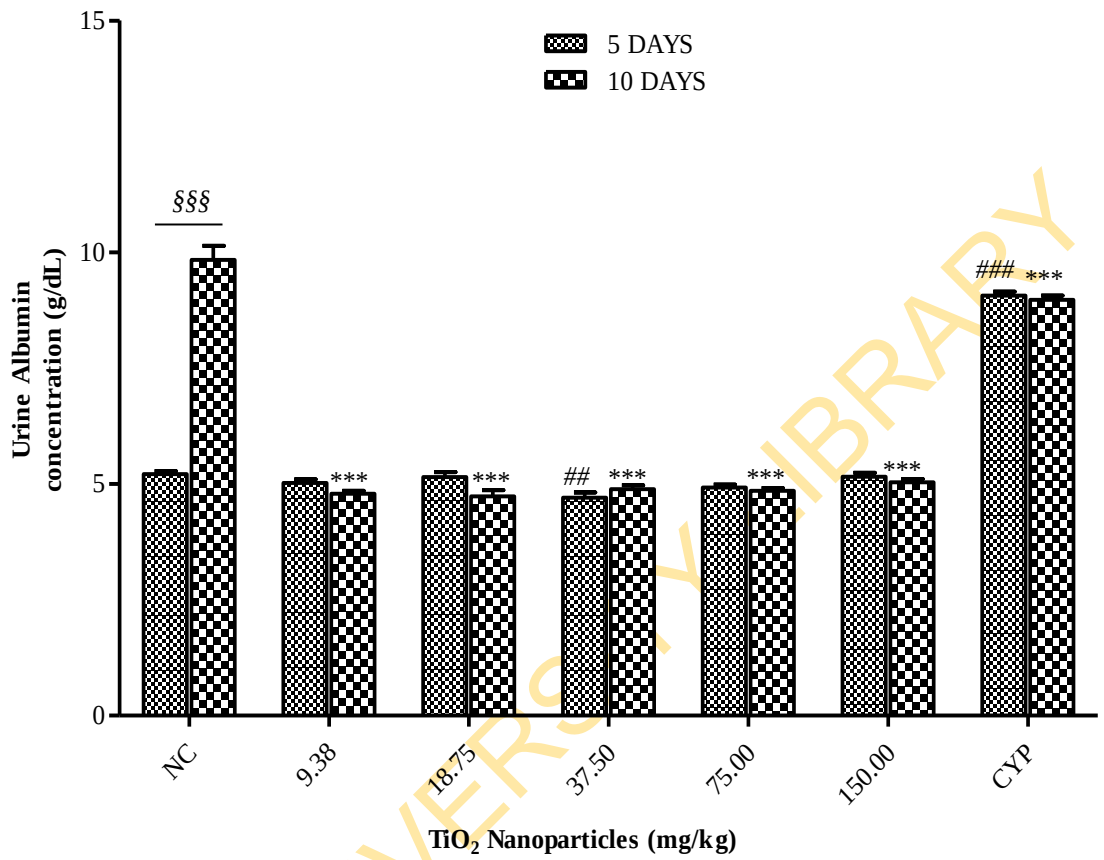

Figure 4. 96: Urine albumin concentration in mice treated with TiO_2 NPs at the 5- and 10-day exposure periods.

Data represent mean ± SEM (n = 5). Negative control (NC) = distilled water, CYP = cyclophosphamide (positive control).

$^{##}$ $p < 0.01$ and $^{###}$ $p < 0.001$ in 5-days exposure

*** $p < 0.001$ in 10-days exposure

§§§ $p < 0.001$ for the comparison between the 5- and 10-day exposures

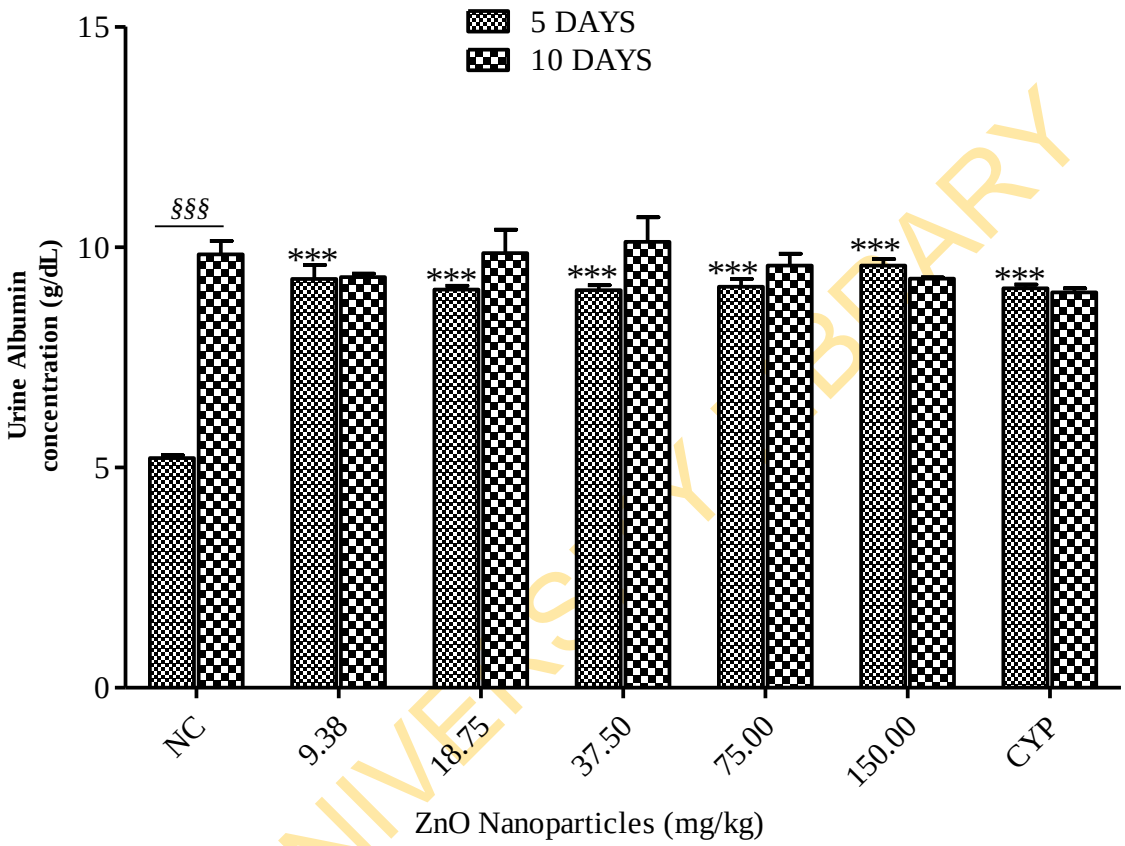

Figure 4. 97: Urine albumin concentration in mice treated with ZnO NPs at the 5- and 10-day exposure periods.

Data represent mean ± SEM (n = 5). Negative control (NC) = distilled water, CYP = cyclophosphamide (positive control).

$p < 0.001$ in 5-days exposure

§§§ $p < 0.001$ for the comparison between the 5- and 10-day exposures

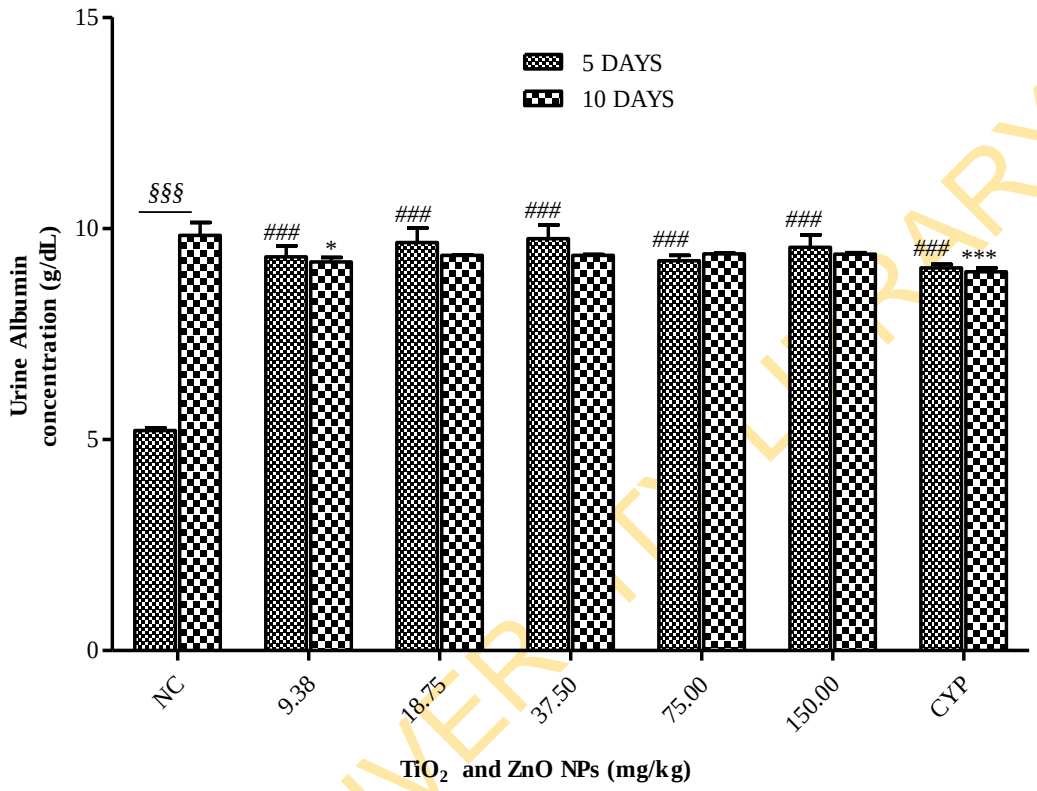

Figure 4. 98: Urine albumin concentration in mice treated with TiO_2 and ZnO NPs at the 5- and 10- day exposure periods.

Data represent mean ± SEM (n = 5). Negative control (NC) = distilled water, CYP = cyclophosphamide (positive control).

$^{\#}$ $p < 0.05$ and $^{\#\#\#}$ $p < 0.001$ in 5-days exposure

*** $p < 0.001$ in 10-days exposure

§§§ $p < 0.001$ for the comparison between the 5- and 10-day exposures

For the 10- day exposure period, TiO_2 NPs significantly ($p < 0.001$) decreased GSH level (Figure 4.106) in the liver of the treated mice, while an increase was induced by their mixture (Figure 4.108) at tested doses in comparison with the mice treated with distilled water. A comparison between the 5- and 10- day exposure periods showed a significant ($p < 0.001$) difference at tested doses of TiO_2, ZnO NPs (except at 150.00 $mgkg^{-1}$) and their mixture (except at 150.00 $mgkg^{-1}$). For the 5- day exposure period, the MDA level in the liver of the treated mice was significantly ($p < 0.001$) increased at tested doses of TiO_2 NPs (except at 9.38 $mgkg^{-1}$) (Figure 4.109), ZnO NPs (Figure 4.110) and their mixture (Figure 4.111) respectively. For the 10- day exposure period, the MDA level was significantly ($p < 0.001$) increased at tested doses of TiO_2 (Figure 4.109), ZnO NPs (Figure 4.110) and their mixture (Figure 4.111) respectively. A significant ($p < 0.05$) difference between the 5- and 10- day exposure periods was observed only at the 9.38 and 37.50 $mgkg^{-1}$ of TiO_2 NPs, and at the 75.00 $mgkg^{-1}$ of ZnO NPs.

Oxidative stress parameters in the kidney of mice treated with TiO_2, ZnO NPs and their mixture for 5 and 10 days are presented in Figures 4.112 – 4.123. For the 5- day exposure period, SOD activity in the kidney of the treated mice was significantly ($p < 0.01$) reduced at tested doses of TiO_2 NPs (except at 37.50 $mgkg^{-1}$) (Figure 4.112), ZnO NPs (except at 37.50, 75.00 and 150.00 $mgkg^{-1}$) (Figure 4. 113) and was significantly ($p < 0.001$) increased at tested doses of the mixture (except at 37.50 $mgkg^{-1}$) (Figure 4. 114) in comparison with the mice treated with distilled water. For the 10- day exposure period, SOD activity in the kidney of the treated mice was significantly ($p < 0.001$) increased at tested doses of TiO_2 NPs (except at 18.75 and 75.00 $mgkg^{-1}$) (Figure 4.112), ZnO NPs (Figure 4.113) and their mixture (Figure 4.114) respectively in comparison with the mice treated with distilled water. A significant ($p < 0.05$) difference between the 5- and 10- day exposure periods was observed at the 37.50 and 150.00 $mgkg^{-1}$ of TiO_2 NPs; at tested doses of ZnO NPs (except 150.00 $mgkg^{-1}$); and at the 18.75, 37.50 and 75.00 $mgkg^{-1}$ of their mixture.

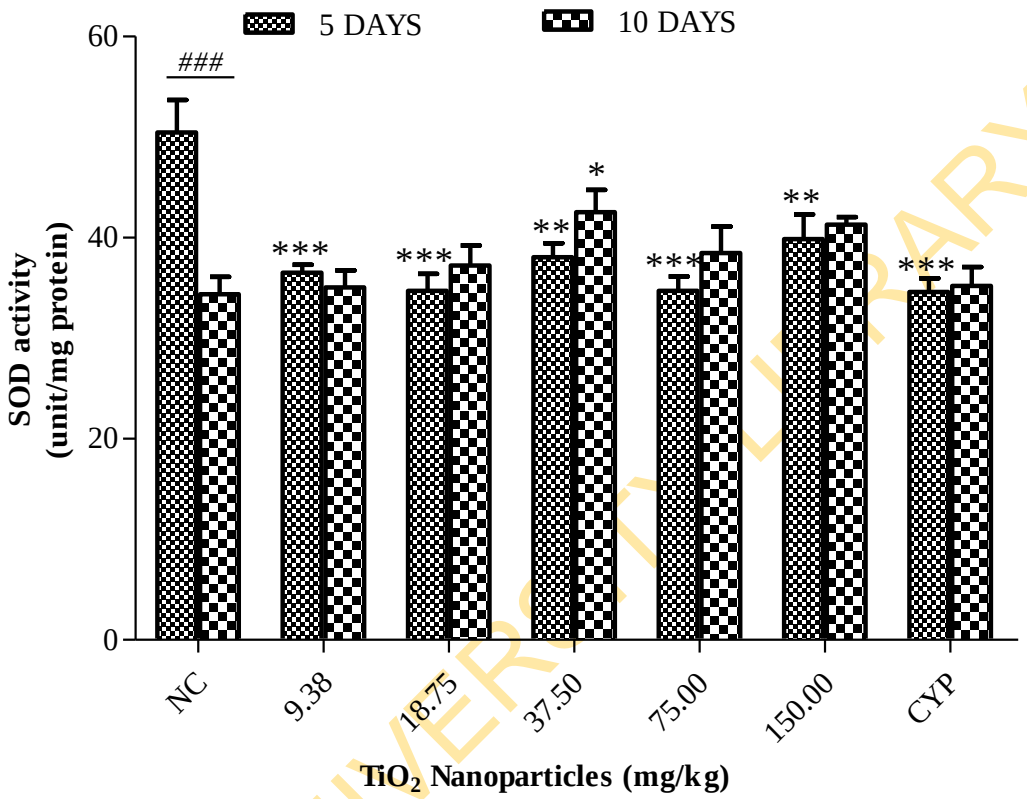

Figure 4. 99: SOD activity in the liver of mice treated with TiO_2 NPs at the 5- and 10-day exposure periods.

Data represent mean ± SE (n = 5). $^{*}p < 0.05$, $^{**}p < 0.01$ and $^{***}p < 0.001$ for 5- days and 10- days exposure in comparison with their corresponding negative controls (NC) = distilled water; CYP = cyclophosphamide (positive control).

$^{###}p < 0.001$ for the comparison between the 5- and 10-day exposures

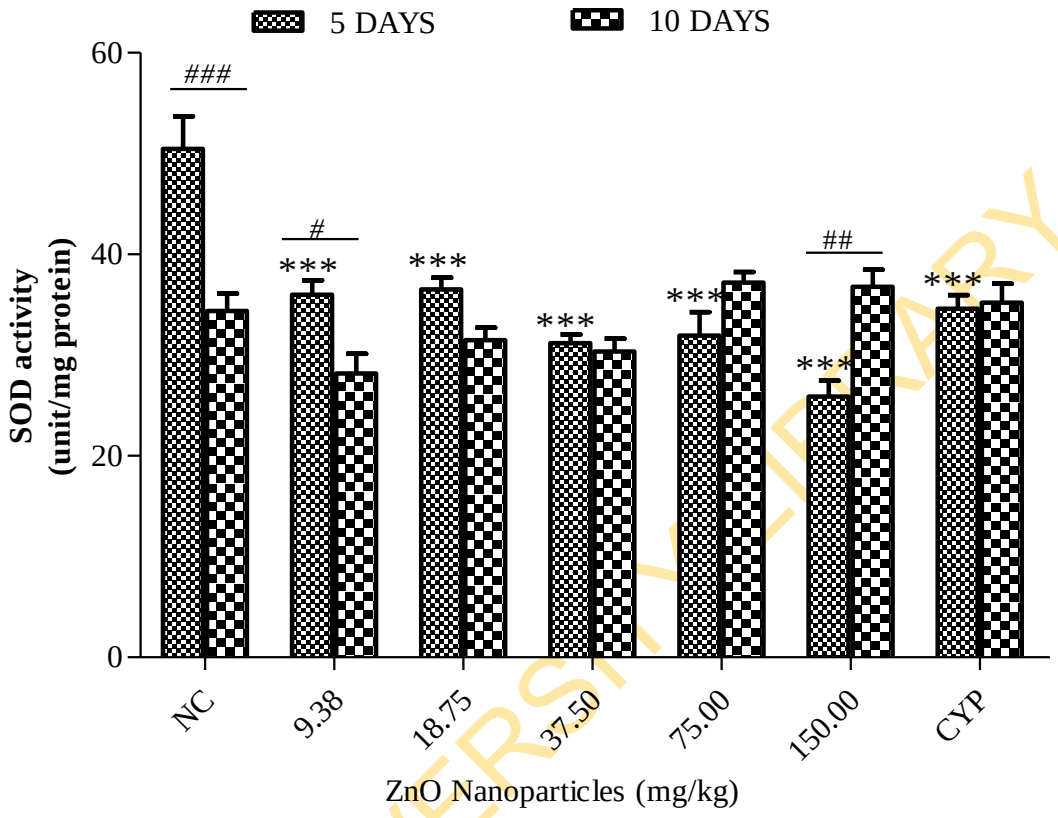

Figure 4. 100: SOD activity in the liver of mice treated with ZnO NPs at the 5- and 10-day exposure periods.

Data represent mean ± SE (n = 5).

*** $p < 0.001$ for 5- days and 10- days exposure in comparison with their corresponding negative controls (NC) = distilled water; CYP = cyclophosphamide (positive control).

# $p < 0.05$, # # $p < 0.01$ and # # # $p < 0.001$ for the comparison between the 5- and 10-day exposures

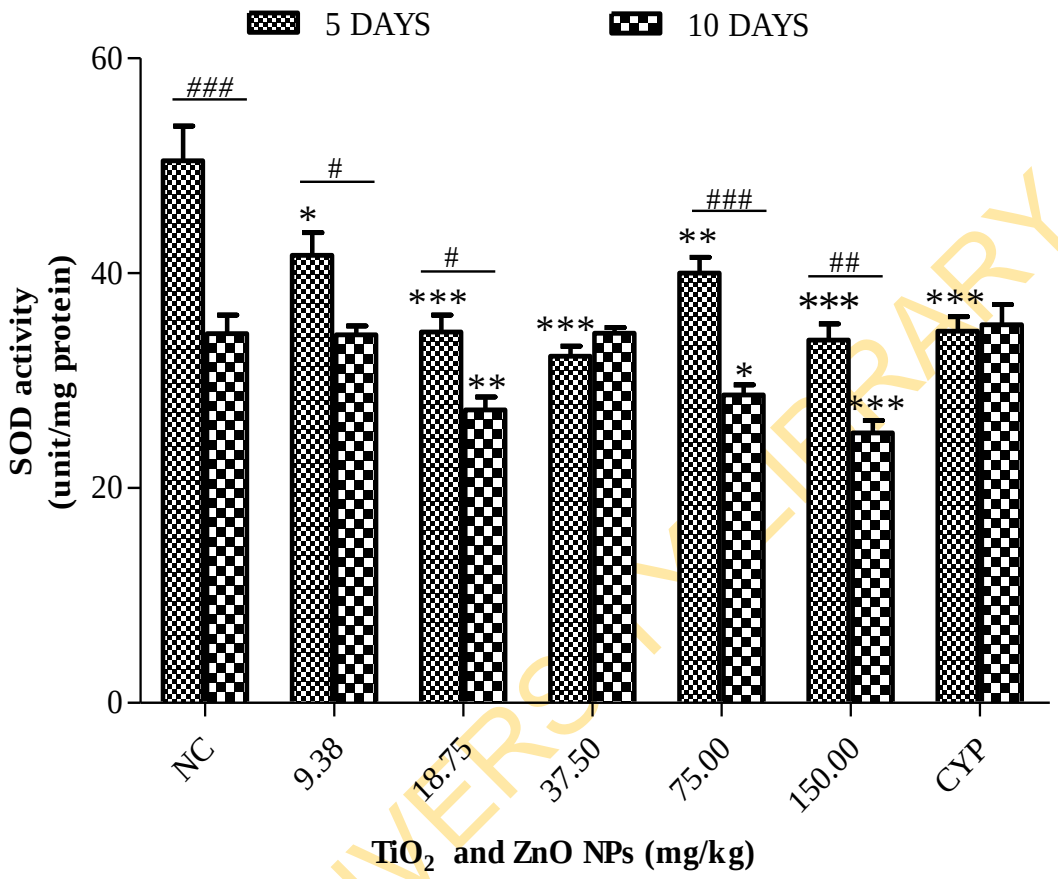

Figure 4. 101: SOD activity in the liver of mice treated with TiO_2 and ZnO NPs at the 5- and 10- day exposure periods.

Data represent mean ± SE (n = 5). * $p < 0.05$, ** $p < 0.01$ and *** $p < 0.001$ for 5- days and 10- days exposure in comparison with their corresponding negative controls (NC) = distilled water; CYP = cyclophosphamide (positive control).

$^{\#}$ $p < 0.05$, $^{\#\#}$ $p < 0.01$ and $^{\#\#\#}$ $p < 0.001$ for the comparison between the 5- and 10-day exposures

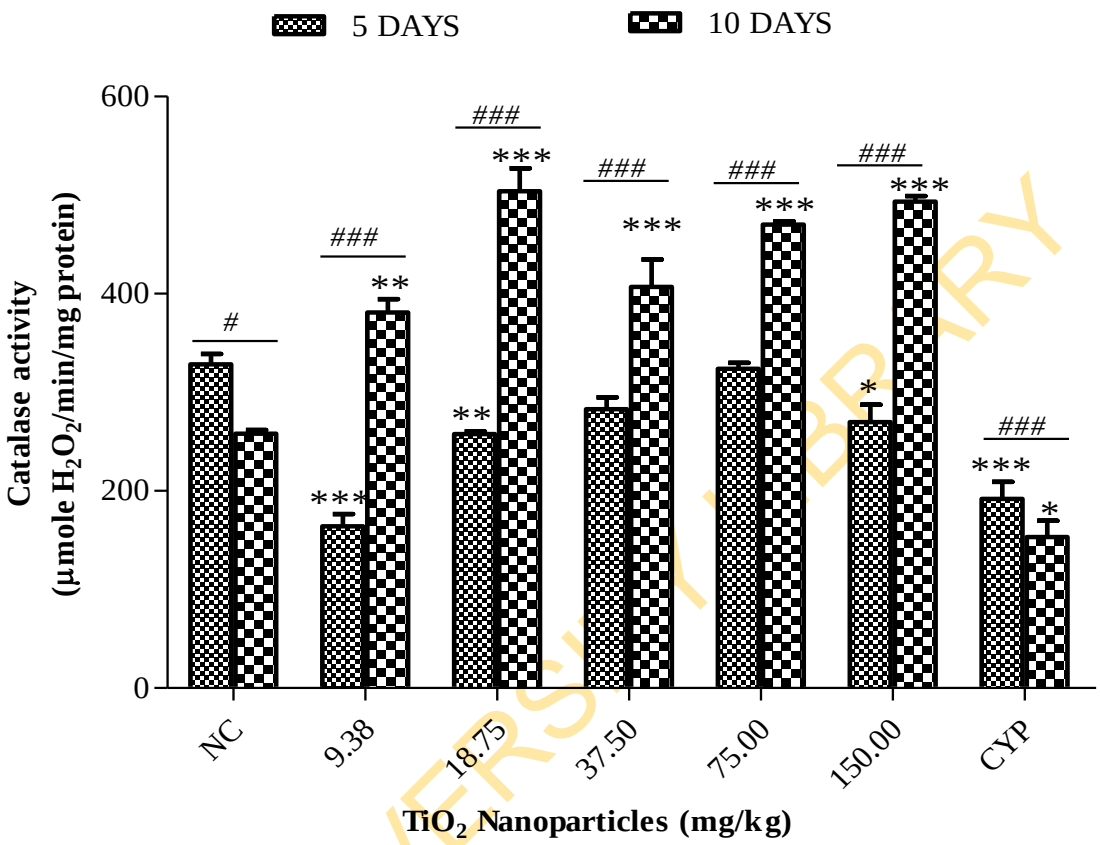

Figure 4. 102: CAT activity in the liver of mice treated with TiO_2 NPs at the 5- and 10-day exposure periods.

Data represent mean ± SE (n = 5). * $p < 0.05$, ** $p < 0.01$ and *** $p < 0.001$ for 5- days and 10- days exposure in comparison with their corresponding negative controls (NC) = distilled water; CYP = cyclophosphamide (positive control).

$^{\#}$ $p < 0.05$ and $^{\#\#\#}$ $p < 0.001$ for the comparison between the 5- and 10-day exposures

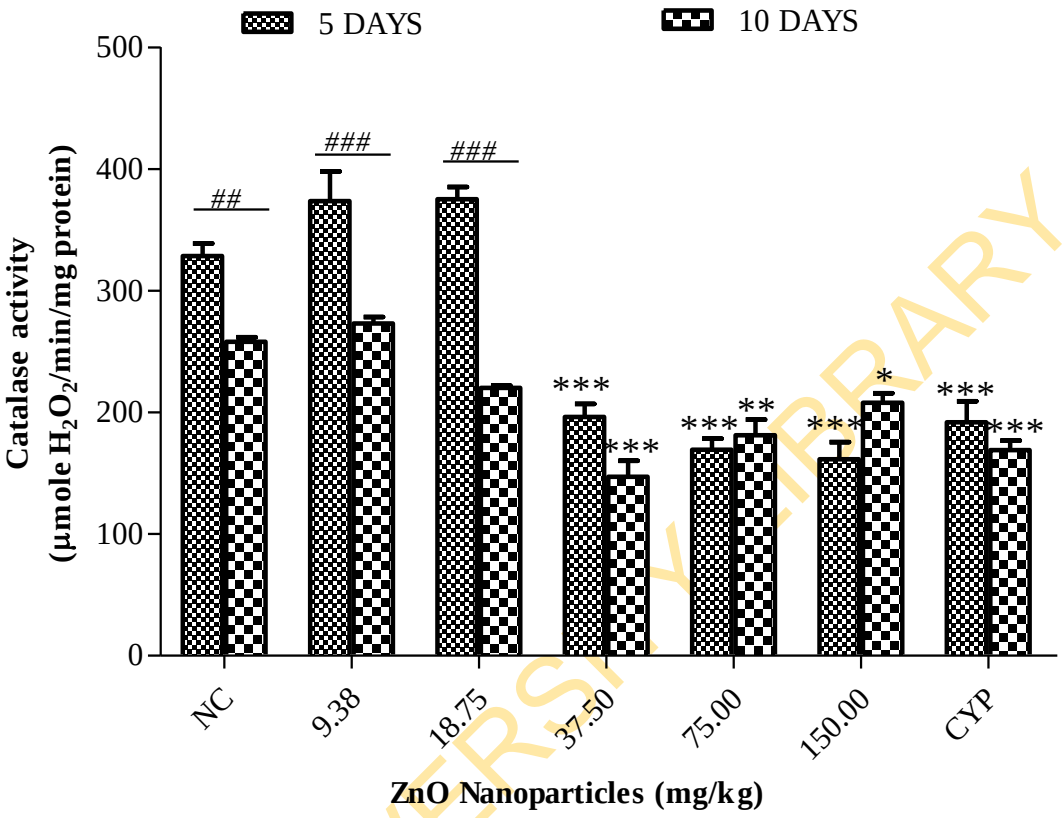

Figure 4. 103: CAT activity in the liver of mice treated with ZnO NPs at the 5- and 10-day exposure periods.

Data represent mean ± SE (n = 5). * $p < 0.05$, ** $p < 0.01$ and *** $p < 0.001$ for 5- days and 10- days exposure in comparison with their corresponding negative controls (NC) = distilled water; CYP = cyclophosphamide (positive control).

$^{\#\#}$ $p < 0.01$ and $^{\#\#\#}$ $p < 0.001$ for the comparison between the 5- and 10-day exposures

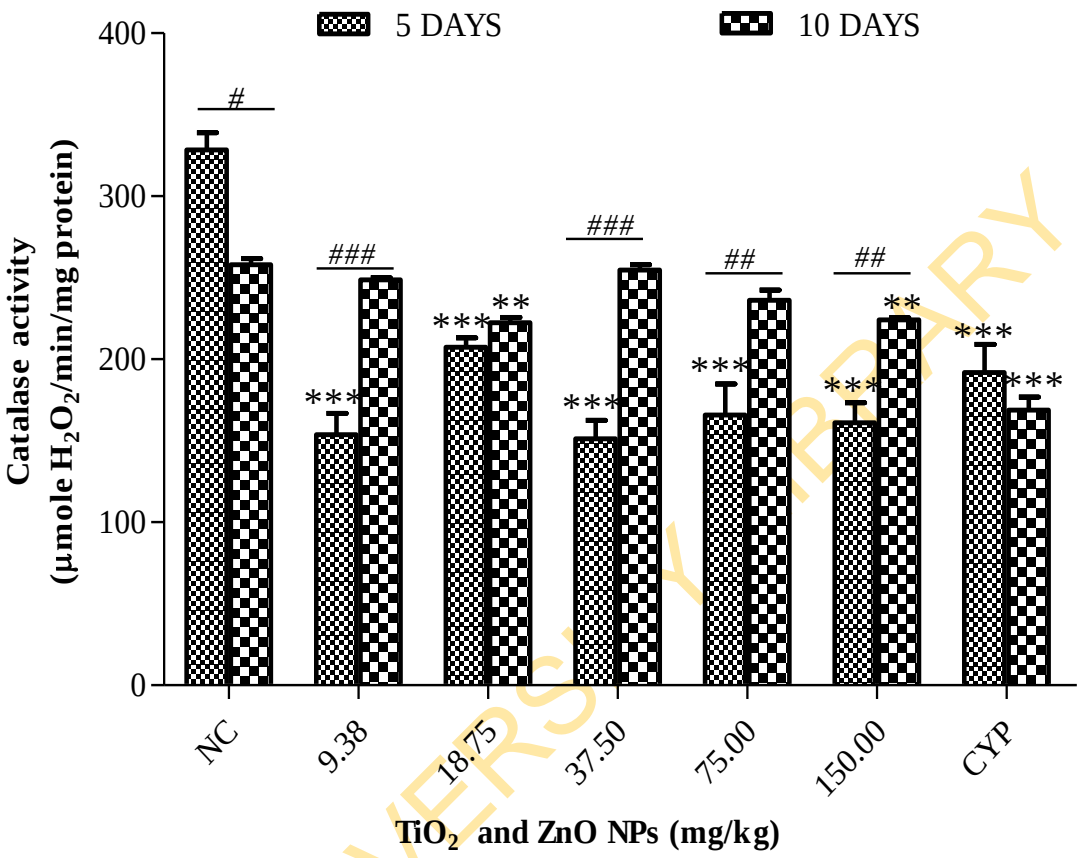

Figure 4. 104: CAT activity in the liver of mice treated with TiO_2 and ZnO NPs at the 5- and 10- day exposure periods.

Data represent mean ± SE (n = 5). ** $p < 0.01$ and *** $p < 0.001$ for 5- days and 10- days exposure in comparison with their corresponding negative controls (NC) = distilled water; CYP = cyclophosphamide (positive control).

$^{\#}$ $p < 0.05$, $^{\#\#}$ $p < 0.01$ and $^{\#\#\#}$ $p < 0.001$ for the comparison the between 5- and 10-day exposure

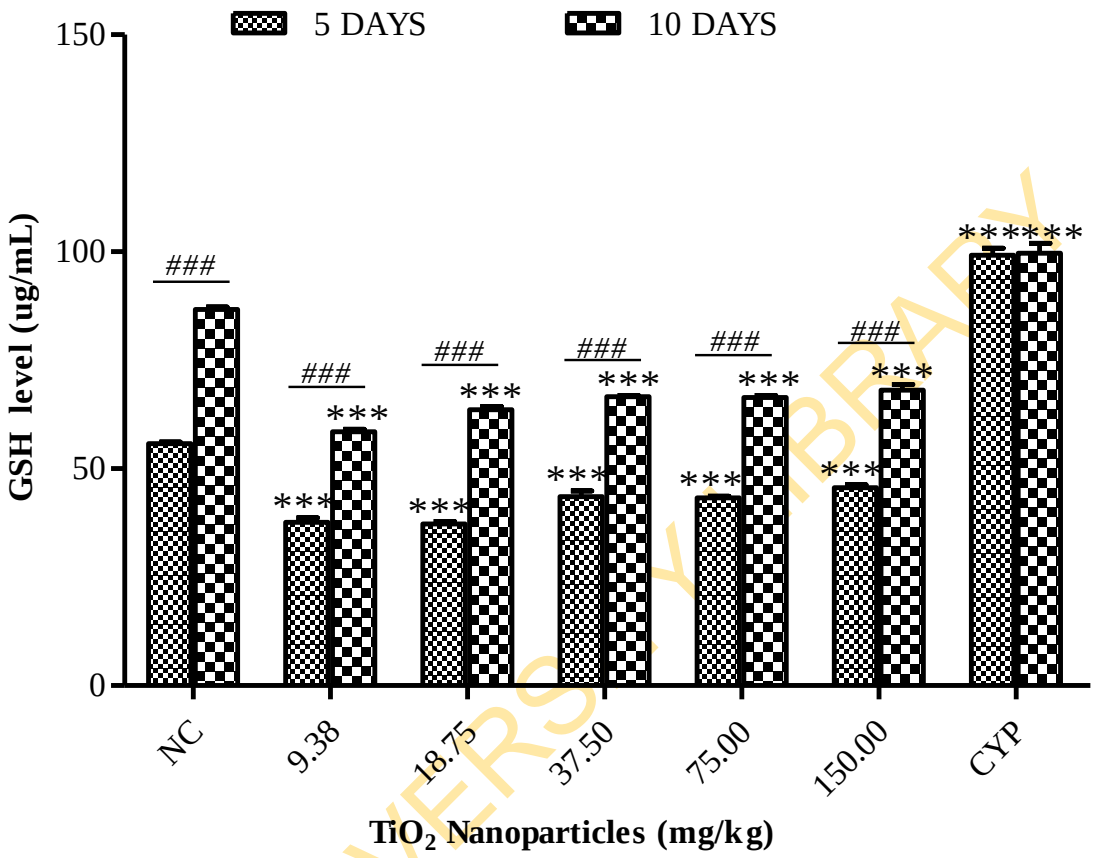

Figure 4. 105: GSH level in the liver of mice treated with TiO_2 NPs at the 5- and 10- day exposure periods.

Data represent mean ± SE (n = 5). *** $p < 0.001$ for 5- days and 10- days exposure in comparison with their corresponding negative controls (NC) = distilled water; CYP = cyclophosphamide (positive control).

$p < 0.001$ for the comparison between the 5- and 10-day exposures

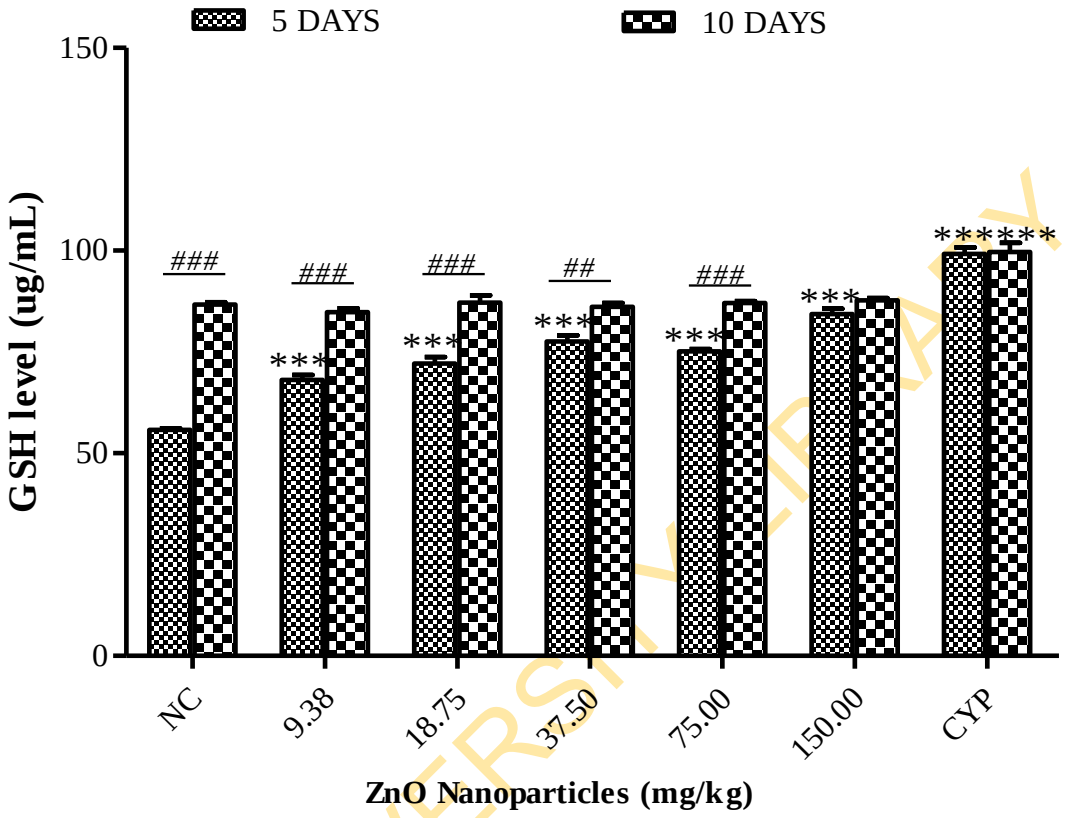

Figure 4. 106: GSH level in the liver of mice treated with ZnO NPs at the 5- and 10- day exposure periods.

Data represent mean ± SE (n = 5). *** $p < 0.001$ for 5- days and 10- days exposure in comparison with their corresponding negative controls (NC) = distilled water; CYP = cyclophosphamide (positive control).

$p < 0.01$ and ### $p < 0.001$ for the comparison between the 5- and 10-day exposures

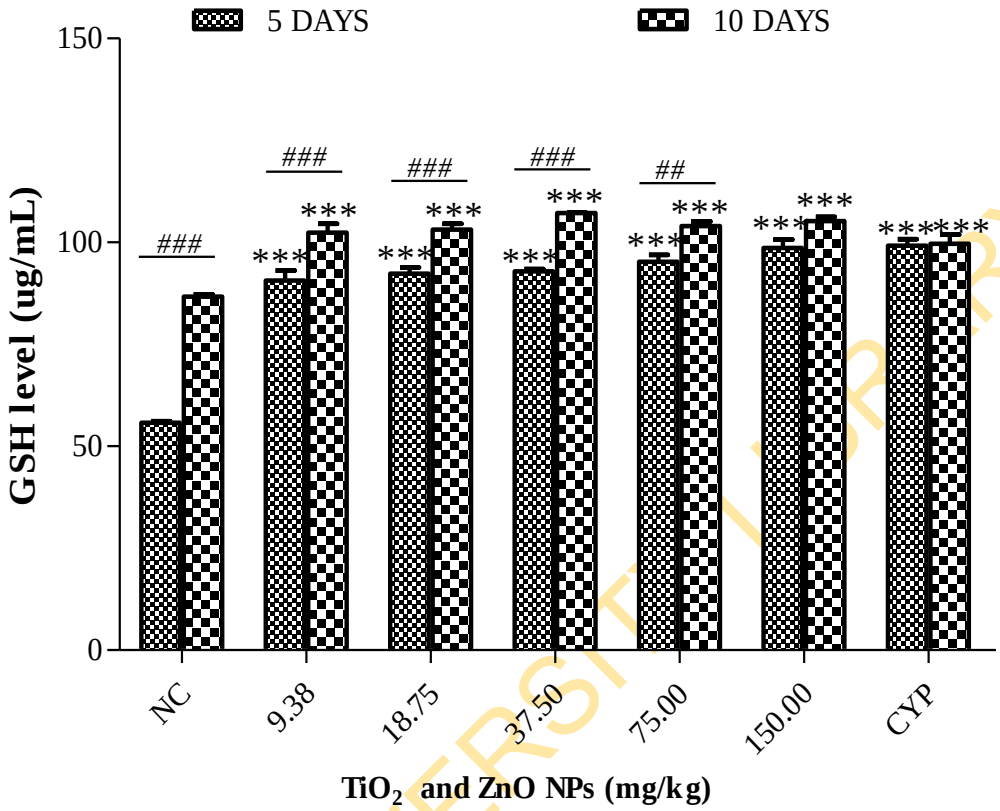

Figure 4. 107: GSH level in the liver of mice treated with TiO_2 and ZnO NPs at the 5- and 10- day exposure periods.

Data represent mean ± SE (n = 5). *** $p < 0.001$ for 5- days and 10- days exposure in comparison with their corresponding negative controls (NC) = distilled water; CYP = cyclophosphamide (positive control).

$^{\#\#}$ $p < 0.01$ and $^{\#\#\#}$ $p < 0.001$ for the comparison between the 5- and 10-day exposure

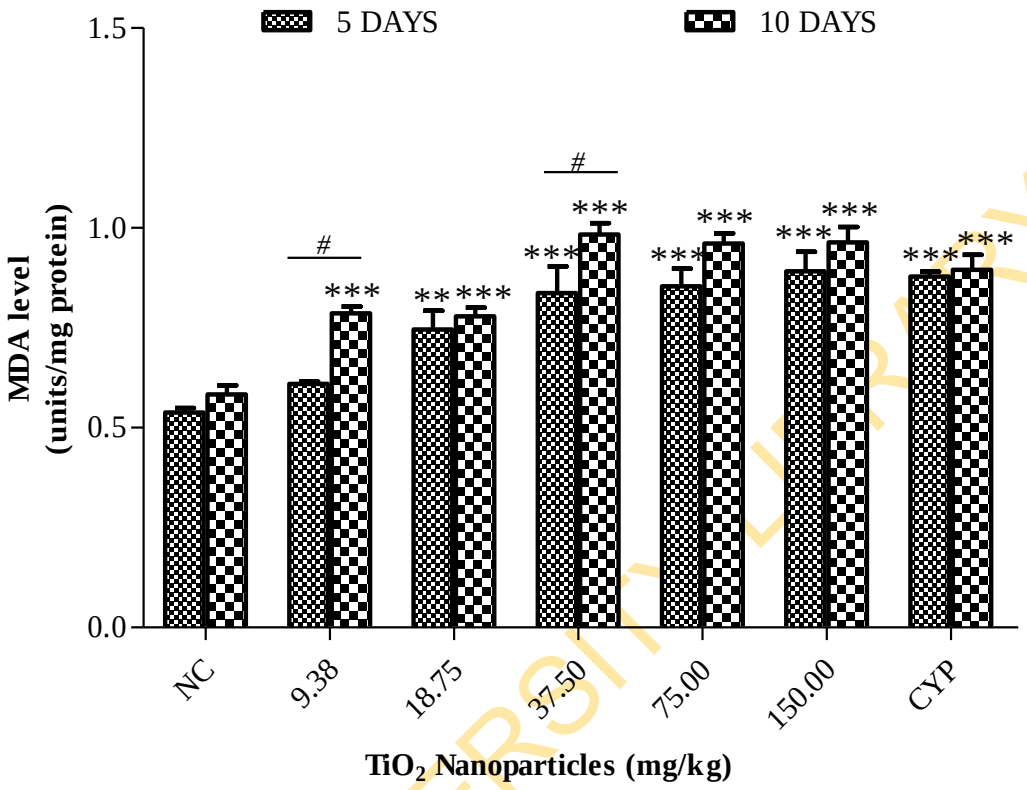

Figure 4. 108: MDA level in the liver of mice treated with TiO_2 NPs at the 5- and 10- day exposure periods.

Data represent mean ± SE (n = 5). ** $p < 0.01$ and *** $p < 0.001$ for 5- days and 10- days exposure in comparison with their corresponding negative controls (NC) = distilled water; CYP = cyclophosphamide (positive control).

$^{\#}$ $p < 0.05$ for the comparison between the 5- and 10-day exposures

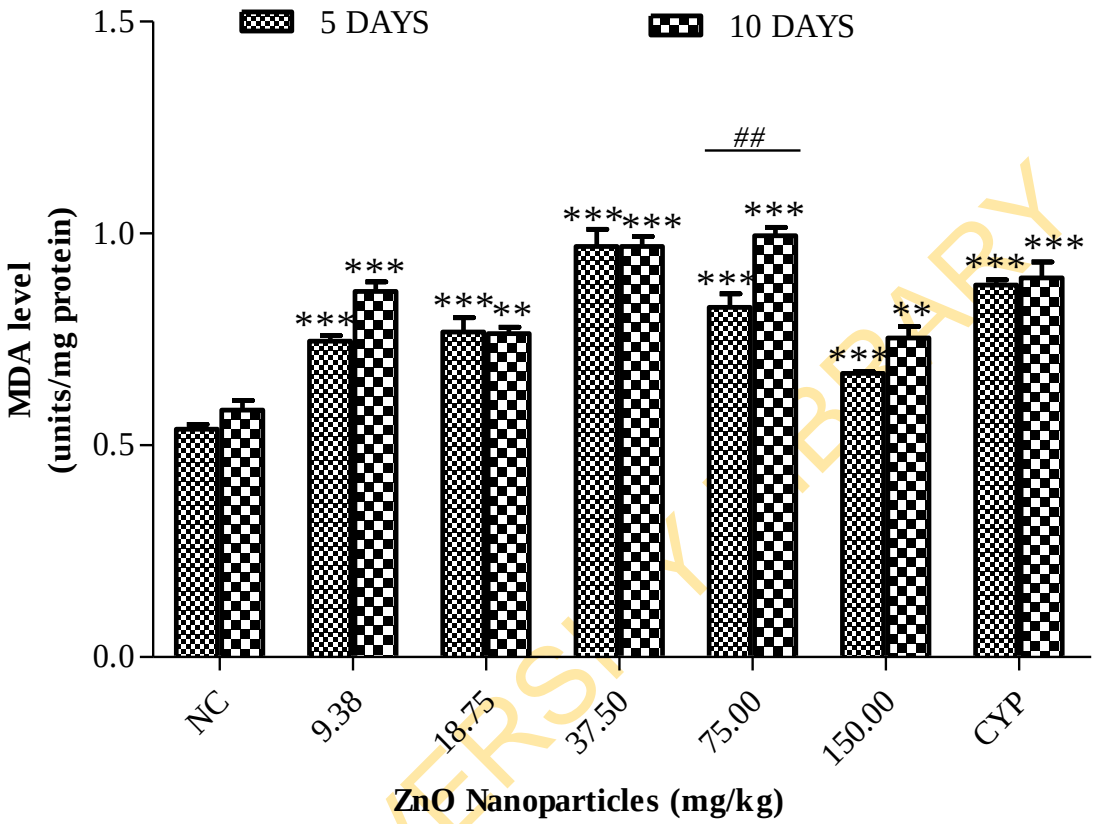

Figure 4. 109: MDA level in the liver of mice treated with ZnO NPs at the 5- and 10- day exposure periods.

Data represent mean ± SE (n = 5). ** $p < 0.01$ and *** $p < 0.001$ for 5- days and 10- days exposure in comparison with their corresponding negative controls (NC) = distilled water; CYP = cyclophosphamide (positive control).

$^{\#\#}$ $p < 0.01$ for the comparison between the 5- and 10-day exposures

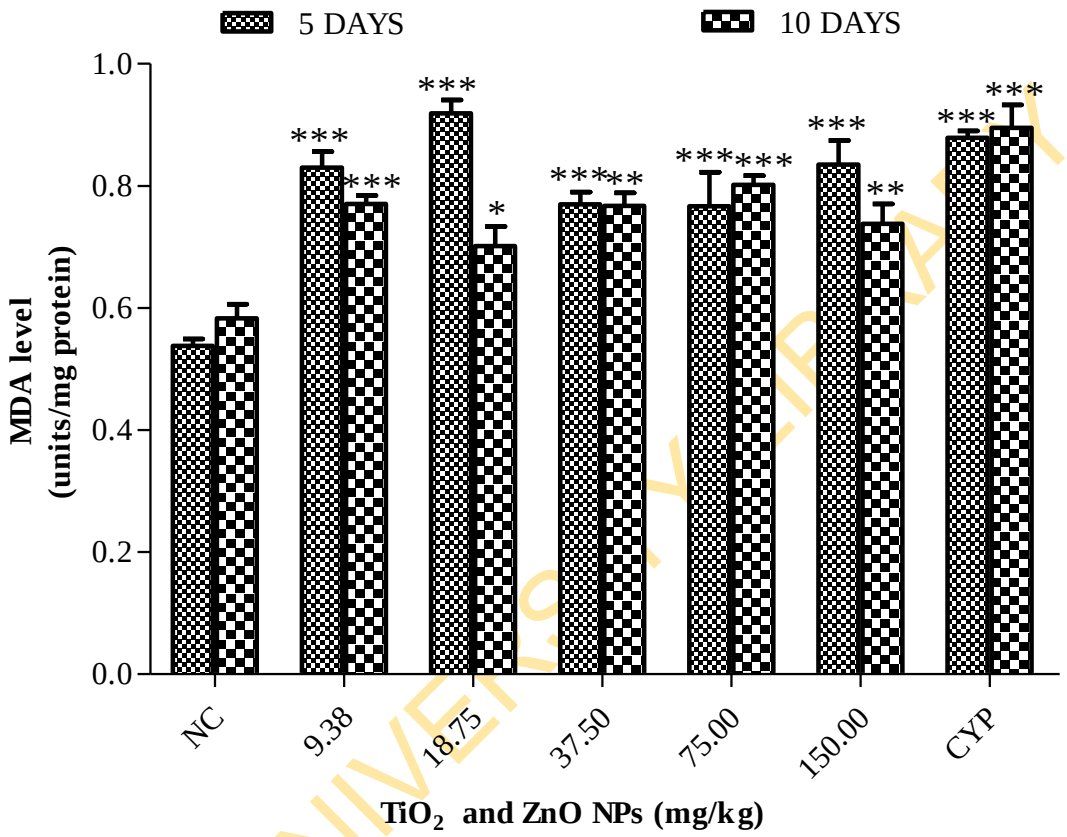

Figure 4. 110: MDA level in the liver of mice treated with TiO_2 and ZnO NPs at the 5- and 10- day exposure periods.

Data represent mean ± SE (n = 5). * $p < 0.05$, ** $p < 0.01$ and *** $p < 0.001$ for 5- days and 10- days exposure in comparison with their corresponding negative controls (NC) = distilled water; CYP = cyclophosphamide (positive control).

For the 5- day exposure, CAT activity in the kidney of the treated mice significantly ($p < 0.001$) increased at tested doses of TiO_2 NPs (except at 9.39 and 18.75 $mgkg^{-1}$) (Figure 4.115), ZnO NPs (except at 18.75 and 150.00 $mgkg^{-1}$) (Figure 4.116) and their mixture (Figure 4.117) respectively in comparison with the mice treated with distilled water. While for the 10- day exposure period, CAT activity significantly ($p < 0.001$) reduced at tested doses of TiO_2 NPs (Figure 4.115); significantly increased ($p < 0.05$) only at the 18.75 $mgkg^{-1}$ of ZnO NPs (Figure 4.116); and significantly ($p < 0.05$) increased at the 9.38 $mgkg^{-1}$ and reduced at the 18.75 and 150.00 $mgkg^{-1}$of their mixture (Figure 4.117) in comparison with the mice treated with distilled water. A significant ($p <0.001$) difference between the 5- and 10- day exposure periods was observed at tested doses of TiO_2 NPs (except at 9.38 $mgkg^{-1}$), ZnO NPs and their mixture (except at 37.50 and 150.00 $mgkg^{-1}$).

For the 5- day exposure, GSH level in the kidney of the treated mice was significantly ($p < 0.001$) decreased at tested doses of TiO_2 NPs (Figure 4.118); increased only at the 150.00 $mgkg^{-1}$ of ZnO NPs (Figure 4.119); and at tested doses of their mixture (Figure 4.120) in comparison with those treated with distilled water. For the 10- day exposure period, GSH level was significantly ($p < 0.001$) reduced at tested doses of TiO_2 NPs (Figure 4.118); and significantly ($p < 0.01$) increased only at the 18.75 $mgkg^{-1}$ of their mixture (Figure 4.120). A significant ($p < 0.001$) difference between the 5- and 10- day exposure periods was observed at tested doses of TiO_2, ZnO NPs (except at 150.00 $mgkg^{-1}$) and their mixture (except at 37.50 and 75.00 $mgkg^{-1}$) respectively.

For the 5- and 10- day exposure periods, MDA level in the kidney of the treated mice was significantly ($p < 0.001$) increased at tested doses of TiO_2 (Figure 4.121), ZnO NPs (Figure 4.122) and their mixture (Figure 4.123), respectively in comparison with the mice treated with distilled water. A significant difference ($p < 0.001$) between the 5- and 10- day exposure periods was observed only at the 9.38 $mgkg^{-1}$ of ZnO NPs and at tested doses of their mixture.

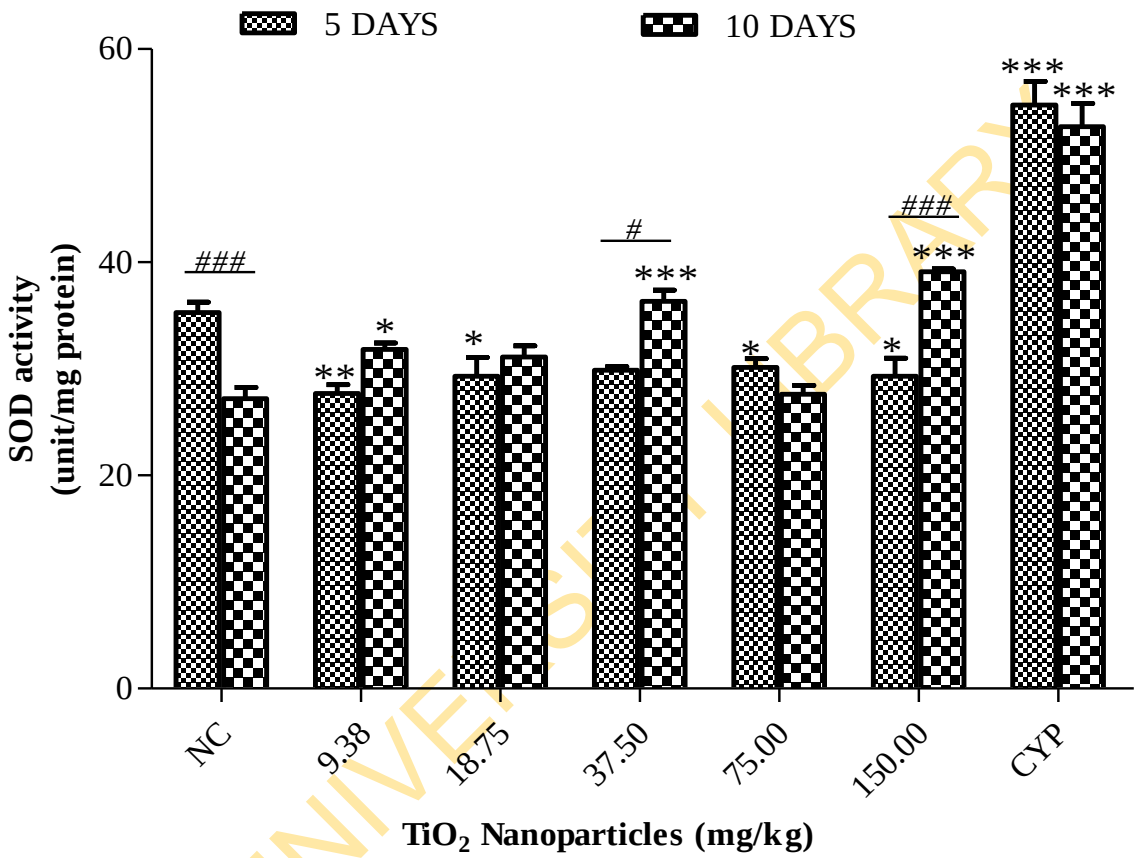

Figure 4. 111: SOD activity in the kidney of mice treated with TiO_2 NPs at the 5- and 10-day exposure periods.

Data represent mean ± SE (n = 5). * $p < 0.05$, ** $p < 0.01$ and *** $p < 0.001$ for 5- days and 10- days exposure in comparison with their corresponding negative controls (NC) = distilled water; CYP = cyclophosphamide (positive control).

$^{\#}$ $p < 0.05$ and $^{\#\#\#}$ $p < 0.001$ for the comparison between the 5- and 10-day exposures

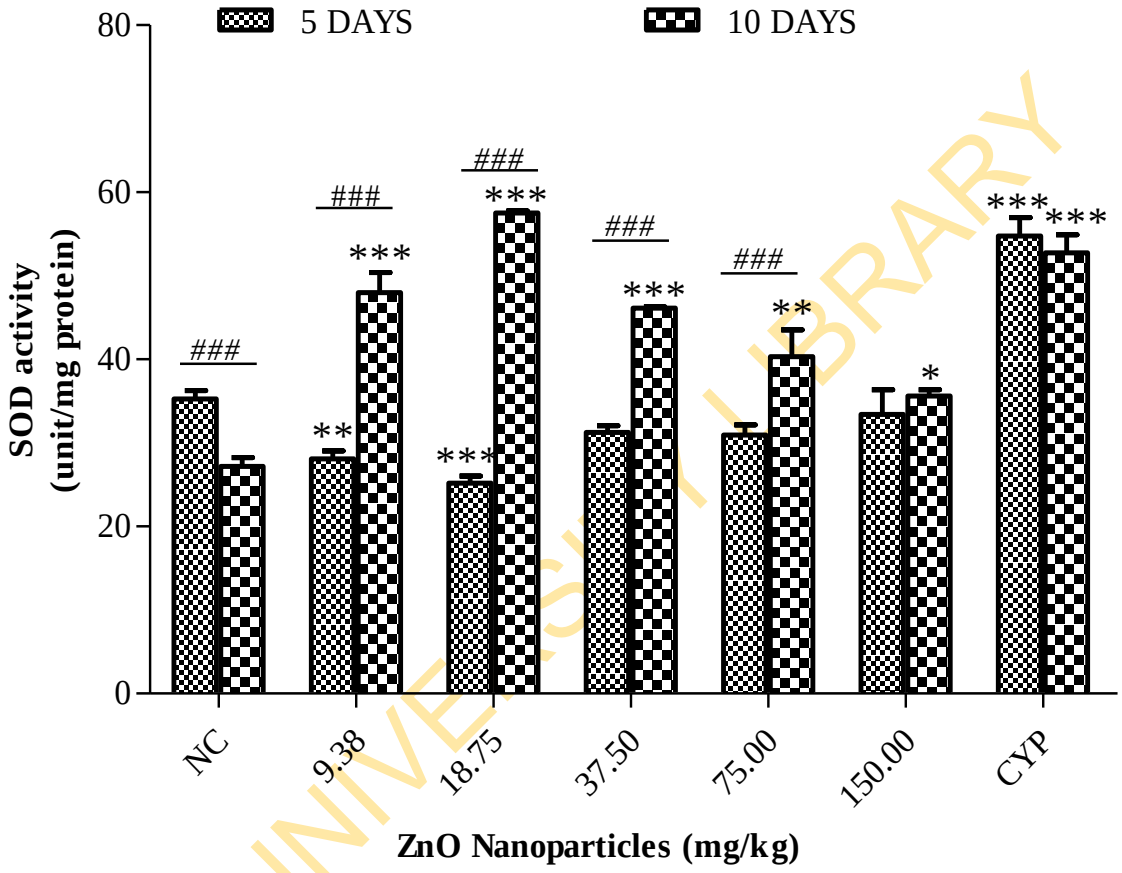

Figure 4. 112: SOD activity in the kidney of mice treated with ZnO NPs at the 5- and 10-day exposure periods.

Data represent mean ± SE (n = 5). * $p < 0.05$, ** $p < 0.01$ and *** $p < 0.001$ for 5- days and 10- days exposure in comparison with their corresponding negative controls (NC) = distilled water; CYP = cyclophosphamide (positive control).

$^{\#\#\#}$ $p < 0.001$ for the comparison between the 5- and 10-day exposures

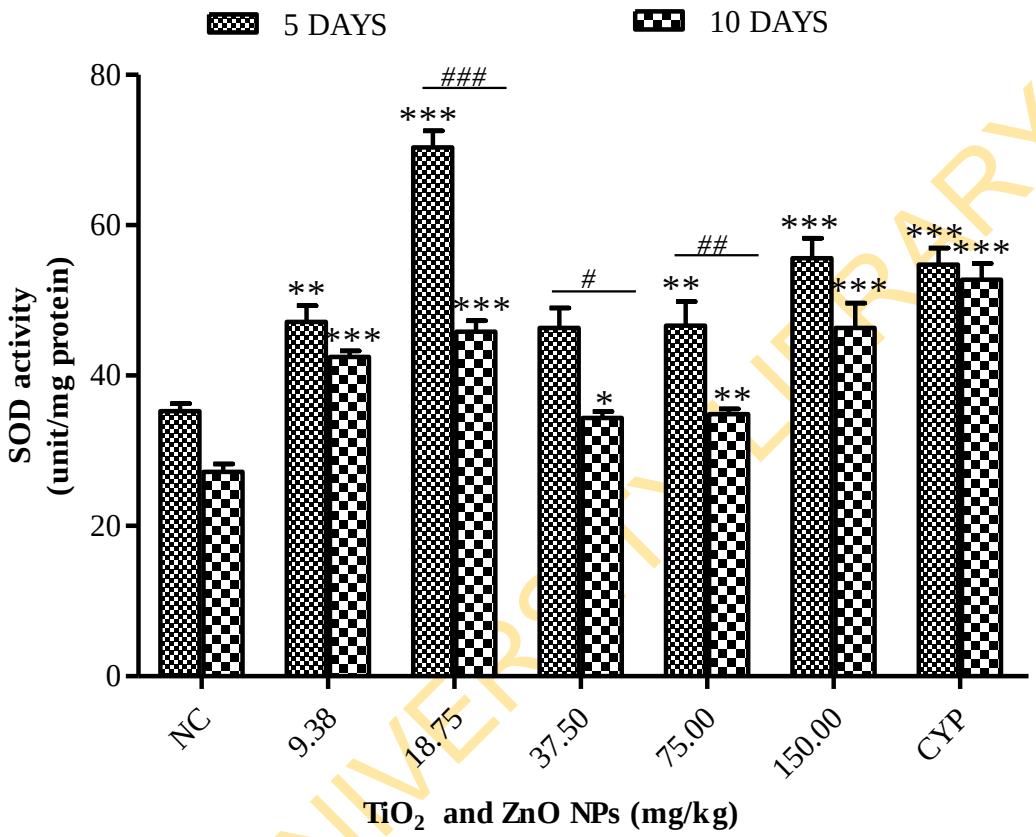

Figure 4. 113: SOD activity in the kidney of mice treated with TiO_2 and ZnO NPs at the 5- and 10- day exposure periods.

Data represent mean ± SE (n = 5). * $p < 0.05$, ** $p < 0.01$ and *** $p < 0.001$ for 5- days and 10- days exposure in comparison with their corresponding negative controls (NC) = distilled water; CYP = cyclophosphamide (positive control).

$^{\#}$ $p < 0.05$, $^{\#\#}$ $p < 0.01$ and $^{\#\#\#}$ $p < 0.001$ for the comparison between the 5- and 10-day exposures

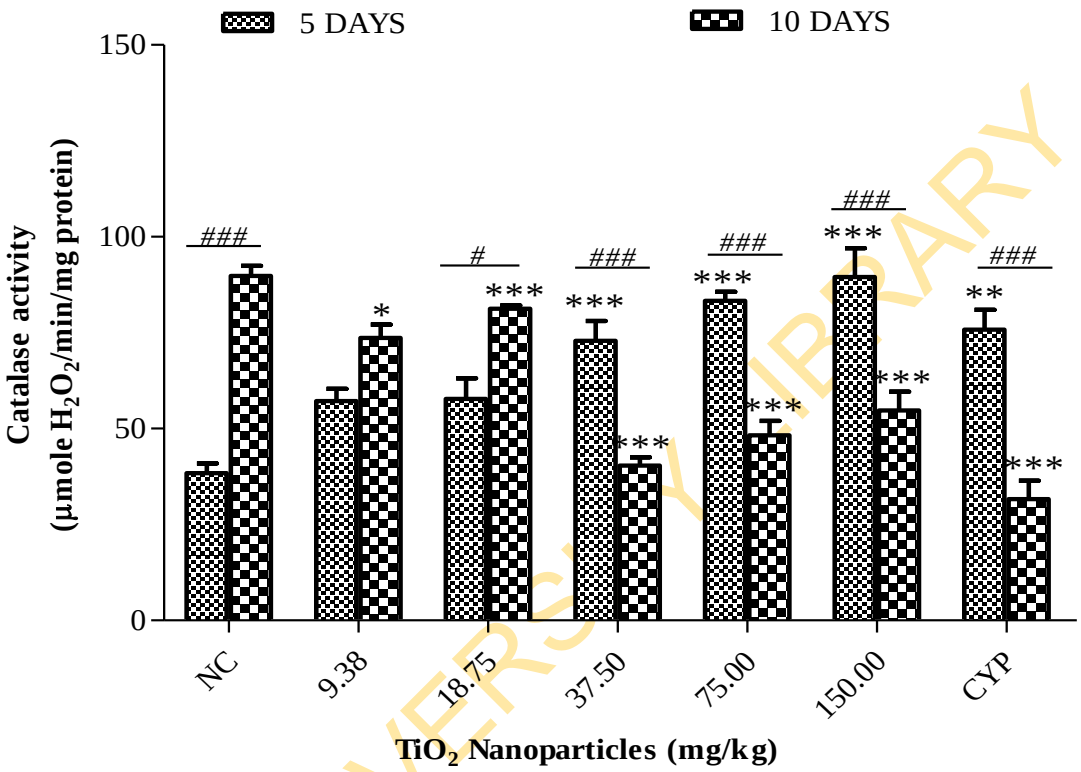

Figure 4. 114: CAT activity in the kidney of mice treated with TiO_2 NPs at the 5- and 10-day exposure periods.

Data represent mean ± SE (n = 5). * $p < 0.05$, ** $p < 0.01$ and *** $p < 0.001$ for 5- days and 10- days exposure in comparison with their corresponding negative controls (NC) = distilled water; CYP = cyclophosphamide (positive control).

$^{\#}$ $p < 0.05$ and $^{\#\#\#}$ $p < 0.001$ for the comparison between the 5- and 10-day exposures

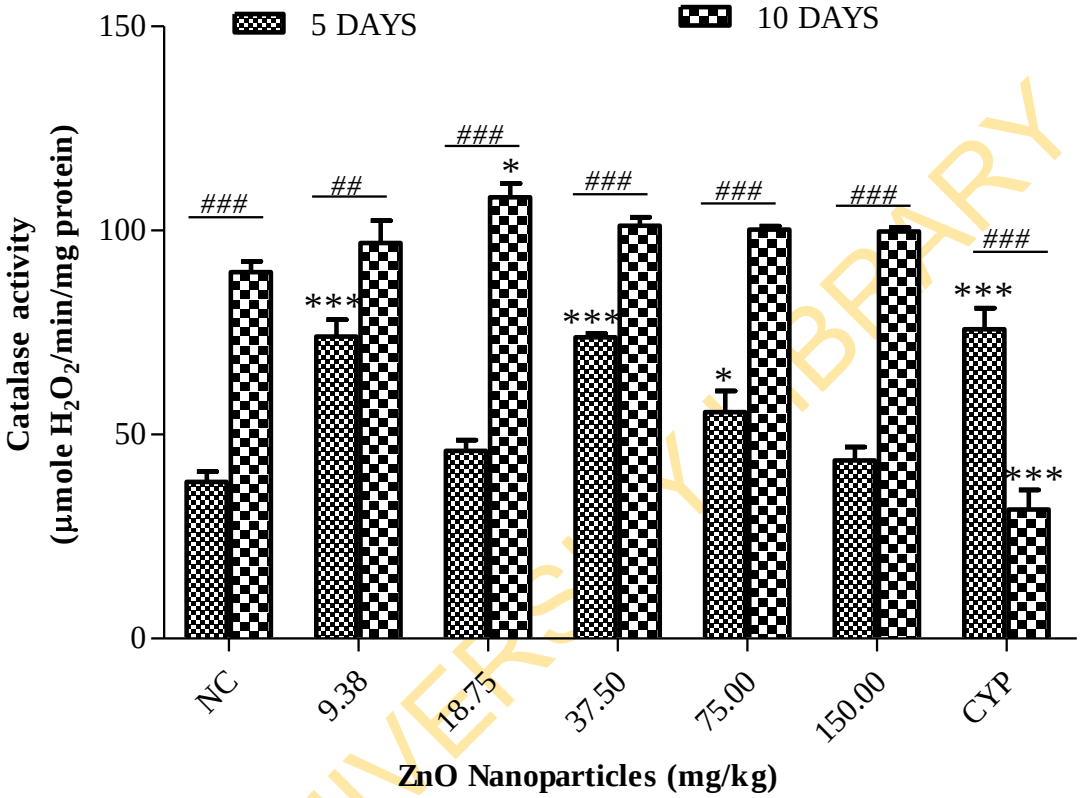

Figure 4. 115: CAT activity in the kidney of mice treated with ZnO NPs at the 5- and 10-day exposure periods.

Data represent mean ± SE (n = 5). * $p < 0.05$ and *** $p < 0.001$ for 5- days and 10- days exposure in comparison with their corresponding negative controls (NC) = distilled water; CYP = cyclophosphamide (positive control).

$^{\#\#}$ $p < 0.01$ and $^{\#\#\#}$ $p < 0.001$ for the comparison between the 5- and 10-day exposures

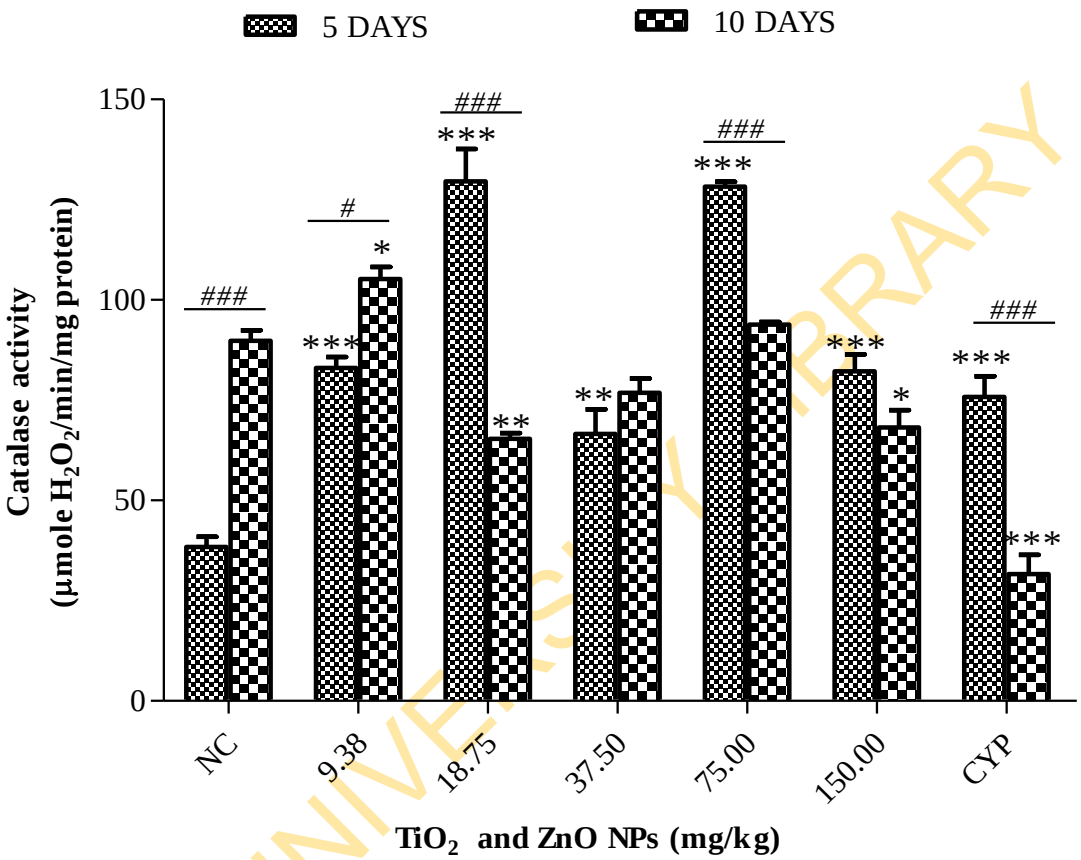

Figure 4. 116: CAT activity in the kidney of mice treated with TiO_2 and ZnO NPs at the 5- and 10- day exposure periods.

Data represent mean ± SE (n = 5). * $p < 0.05$, ** $p < 0.01$ and *** $p < 0.001$ for 5- days and 10- days exposure in comparison with their corresponding negative controls (NC) = distilled water; CYP = cyclophosphamide (positive control).

$^{\#}$ $p < 0.05$ and $^{\#\#\#}$ $p < 0.001$ for the comparison between the 5- and 10-days exposures

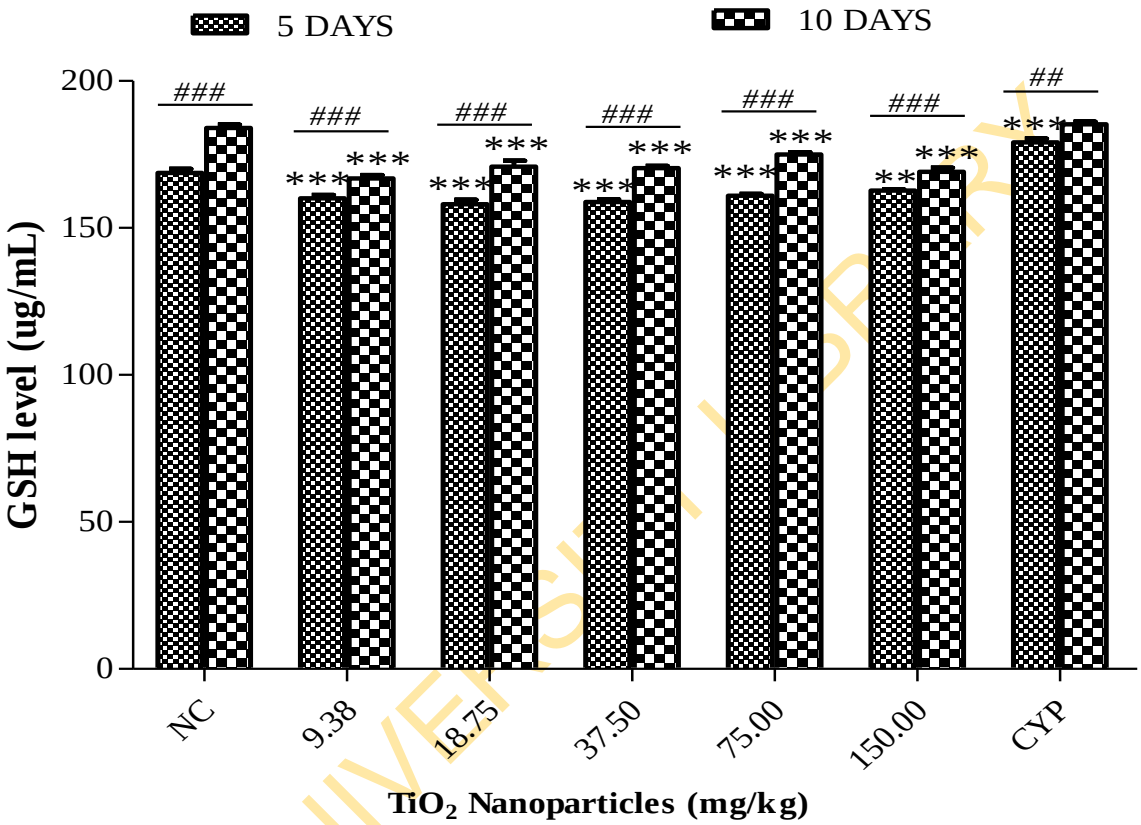

Figure 4. 117: GSH level in the kidney of mice treated with TiO_2 NPs at the 5- and 10-day exposure periods.

Data represent mean ± SE (n = 5). ** $p < 0.01$ and *** $p < 0.001$ for 5- days and 10- days exposure in comparison with their corresponding negative controls (NC) = distilled water; CYP = cyclophosphamide (positive control).

$^{\#\#}$ $p < 0.01$ and $^{\#\#\#}$ $p < 0.001$ for the comparison between the 5- and 10-days exposures

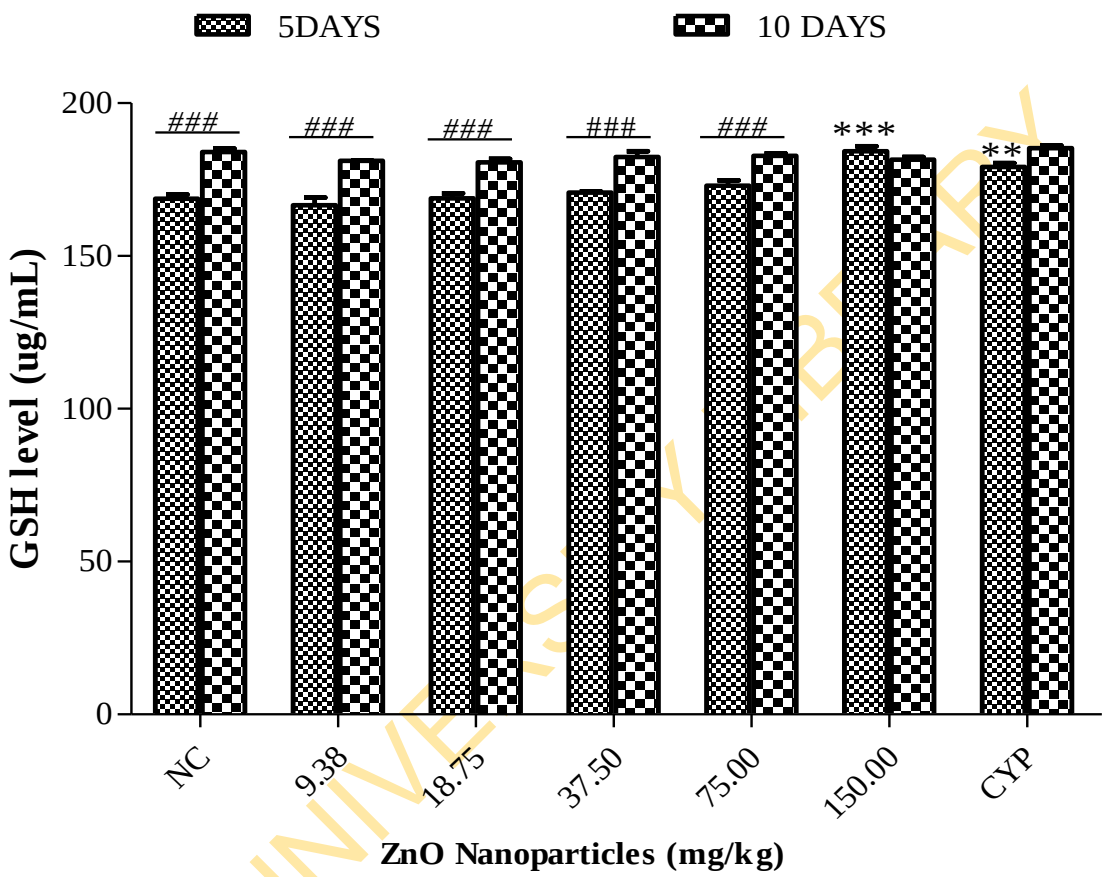

Figure 4. 118: GSH level in the kidney of mice treated with ZnO NPs at the 5- and 10-day exposure periods.

Data represent mean ± SE (n = 5). ** $p < 0.01$ and *** $p < 0.001$ for 5- days and 10- days exposure in comparison with their corresponding negative controls (NC) = distilled water; CYP = cyclophosphamide (positive control).

$^{\#\#\#}$ $p < 0.001$ for the comparison between the 5- and 10-day exposures

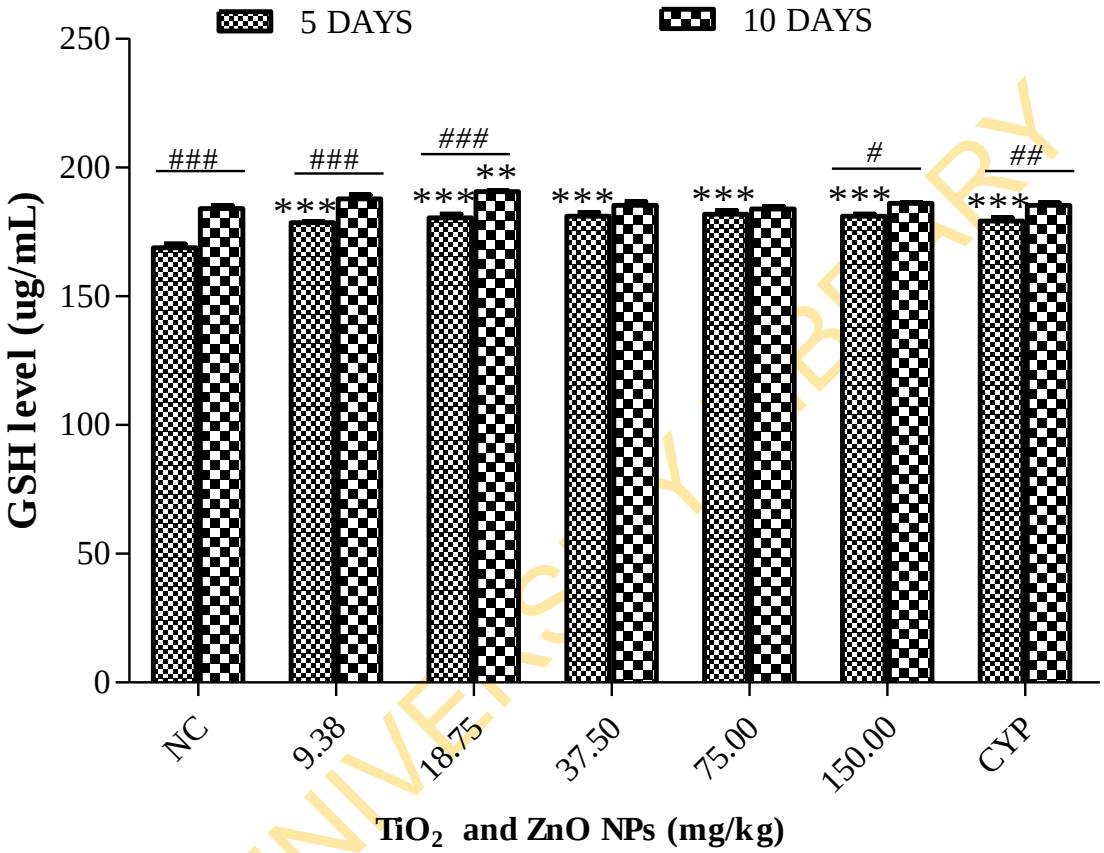

Figure 4. 119: GSH level in the kidney of mice treated with TiO_2 and ZnO NPs at the 5- and 10- day exposure periods.

Data represent mean ± SE (n = 5). ** $p < 0.01$ and *** $p < 0.001$ for 5- days and 10- days exposure in comparison with their corresponding negative controls (NC) = distilled water; CYP = cyclophosphamide (positive control).

$^{\#}$ $p < 0.05$, $^{\#\#}$ $p < 0.01$ and $^{\#\#\#}$ $p < 0.001$ for the comparison between the5- and 10-day exposures

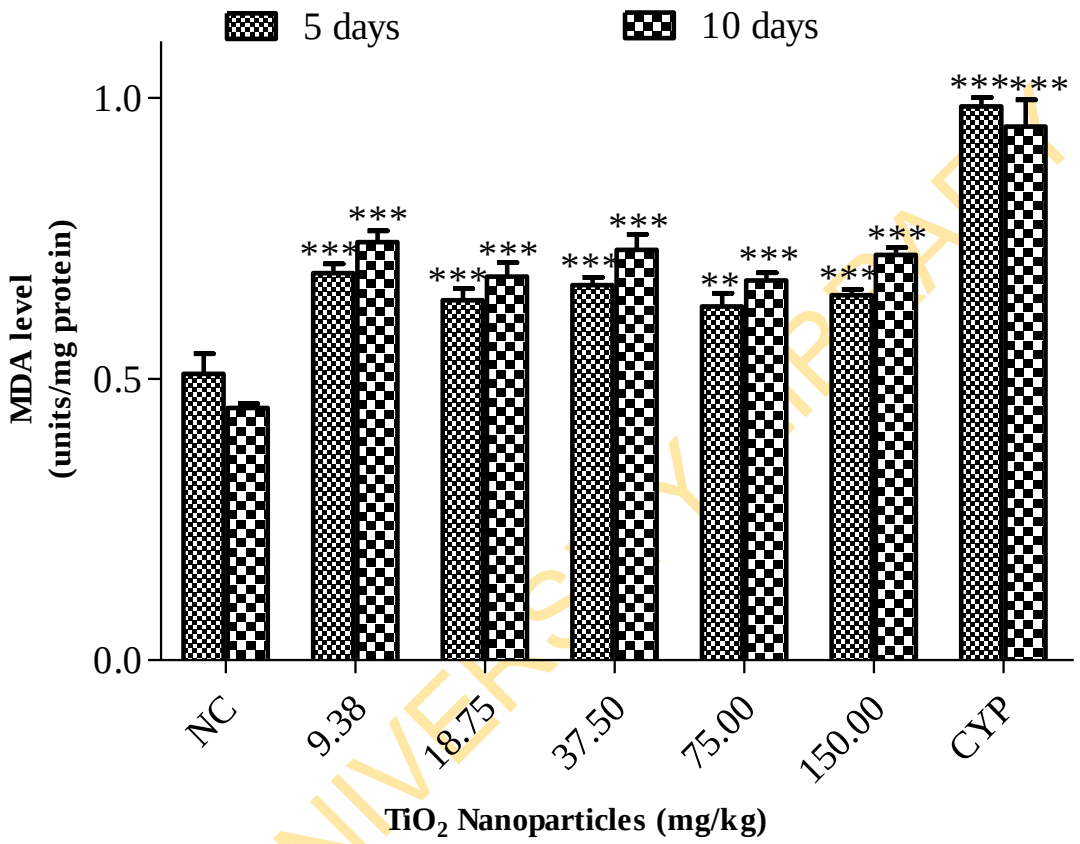

Figure 4. 120: MDA level in the kidney of mice treated with TiO_2 NPs at the 5- and 10-day exposure periods.

Data represent mean ± SE (n = 5). ** $p < 0.01$ and *** $p < 0.001$ for 5- days and 10- days exposure in comparison with their corresponding negative controls (NC) = distilled water; CYP = cyclophosphamide (positive control).

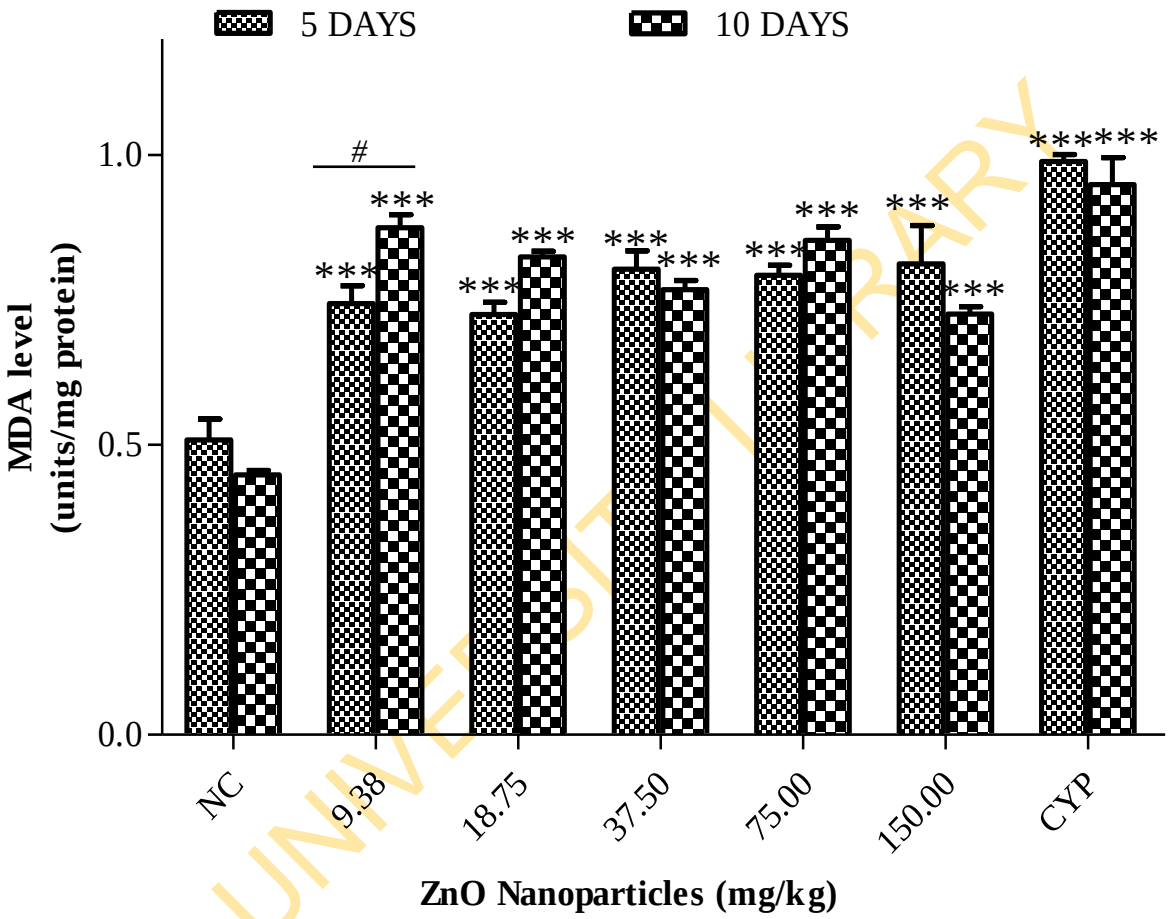

Figure 4. 121: MDA level in the kidney of mice treated with ZnO NPs at the 5- and 10-day exposure periods.

Data represent mean ± SE (n = 5). *** $p < 0.001$ for 5- days and 10- days exposure in comparison with their corresponding negative controls (NC) = distilled water; CYP = cyclophosphamide (positive control).

# $p < 0.05$ for the comparison between the 5- and 10-day exposures

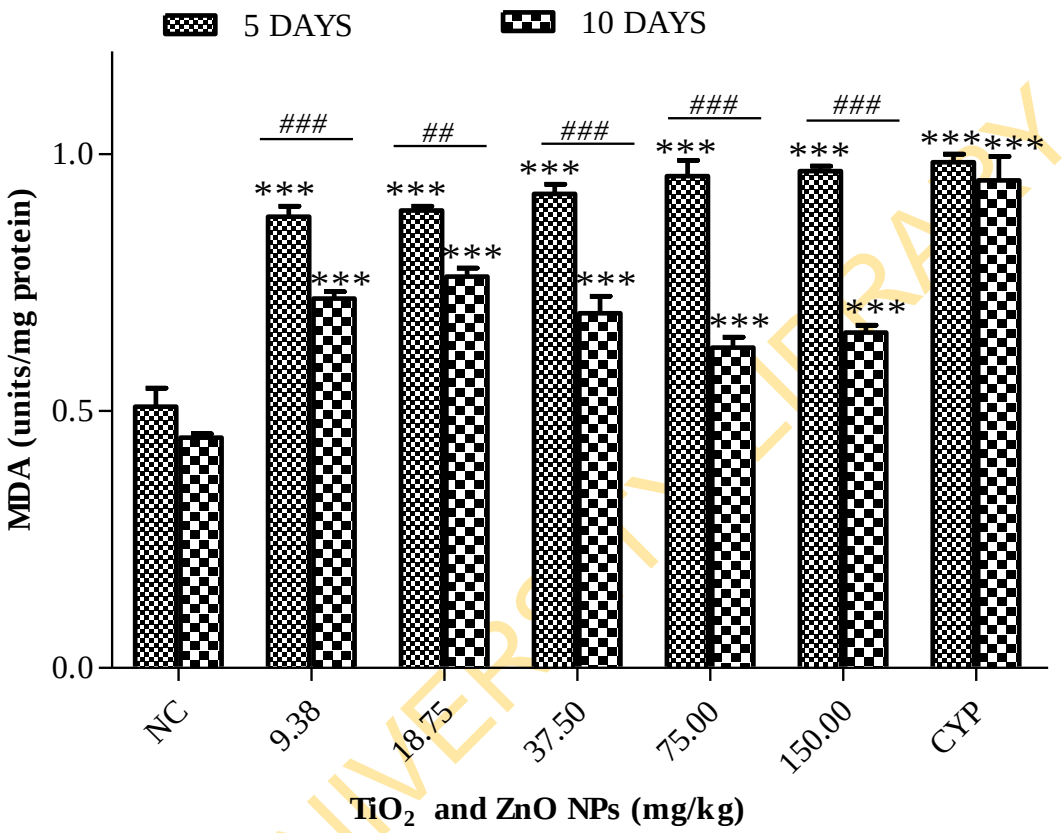

Figure 4. 122: MDA level in the kidney of mice treated with TiO_2 and ZnO NPs at the 5- and 10- day exposure periods.

Data represent mean ± SE (n = 5). *** $p < 0.001$ for 5- days and 10- days exposure in comparison with their negative controls (NC) = distilled water; CYP = cyclophosphamide (positive control).

$^{\#\#}$ $p < 0.01$ and $^{\#\#\#}$ $p < 0.001$ for the comparison between the 5- and 10-day exposures

Oxidative stress parameters in the testis of mice treated with TiO_2, ZnO NPs and their mixture for 5 and 10 days are presented in Figures 4.124 – 4.135. For the 5- day exposure period, SOD activity in the testes of the treated mice was significantly ($p < 0.001$) reduced at tested doses of TiO_2 NPs (except at 75.00 $mgkg^{-1}$) (Figure 4.124), ZnO NPs (Figure 4.125) and their mixture (Figure 4.126) respectively in comparison with the mice treated with distilled water. In contrast, for the 10- day exposure period, there was a significant ($p < 0.001$) increase only at the 37.50 and 150.00 $mgkg^{-1}$ of TiO_2 NPs (Figure 4.124); at tested doses of ZnO NPs (Figure 4.125) and their mixture (Figure 4.126) respectively in comparison with the mice treated with distilled water. Comparison between the 5- and 10- day exposure periods showed a significant ($p < 0.01$) difference at the 75.00 and 150.00 $mgkg^{-1}$ of TiO_2 NPs; at all tested doses of ZnO NPs (except at 150.00 $mgkg^{-1}$) and their mixture (except at 18.75 $mgkg^{-1}$) respectively.

The CAT activity in the testes of the treated mice was significantly ($p < 0.001$) reduced across all tested doses of TiO_2 (Figure 4.127), ZnO NPs (except at 150 $mgkg^{-1}$) (Figure 4.128) and their mixture (Figure 4.129) respectively in comparison with the mice treated with distilled water for the 5- day exposure period. Similarly, for the 10- day exposure period, there was a significant ($p < 0.001$) reduction at tested doses of TiO_2 NPs (except at 75.00 $mgkg^{-1}$) (Figure 4.127), ZnO NPs (Figure 4.128) and their mixture (Figure 4.129) respectively in comparison with the mice treated with distilled water. Comparison between the 5- and 10- day exposure periods showed a significant ($p < 0.001$) difference only at the 75.00 $mgkg^{-1}$ of TiO_2 NPs, and 75.00 and 150.00 $mgkg^{-1}$ of ZnO NPs.

For the 5- day exposure, the GSH level in the testes of the treated mice was significantly ($p < 0.001$) reduced only at the 9.38 $mgkg^{-1}$ of TiO_2 NPs (Figure 4.130); no significance ($p > 0.05$) in all the doses of ZnO NPs (Figure 4.131) and their mixture (Figure 4.132) were respectively observed in comparison with the mice treated with distilled water. In addition, for the 10- day exposure period, no significance ($p > 0.05$) was observed at tested doses of TiO_2 (Figure 4.130), ZnO NPs (Figure 4.131) and their mixture (Figure 4.132). The comparison between the 5- and 10- day exposure periods showed a significant ($p < 0.05$) difference only at the 18.75 $mgkg^{-1}$ of ZnO NPs.

The MDA level in the testis of treated mice for the 5- day exposure period showed a significant ($p < 0.001$) increase at tested doses of TiO_2 NPs (except at 9.38 $mgkg^{-1}$) (Figure 4.133), ZnO NPs (Figure 4.134) and their mixture (Figure 4.135) respectively in comparison with the mice treated with distilled water. Subsequently, for the 10- day exposure period, a significant ($p < 0.001$) increase was observed at tested doses of TiO_2 (Figure 4.133), ZnO NPs (Figure 4.134) and their mixture (Figure 4.135) respectively in comparison with the mice treated with distilled water. Comparison between the 5- and 10-day exposure periods revealed a significant ($p < 0.001$) difference at the 9.38, 18.75 and 37.50 $mgkg^{-1}$ of TiO_2NPs; and at the 75.00 and 150.00 $mgkg^{-1}$ of ZnO NPs.

4.5 Germ cell toxicity induced by titanium dioxide, zinc oxide nanoparticles and their mixture in mice

4.5.1 Effects of titanium dioxide, zinc oxide nanoparticles and their mixture on the body and testicular weights of mice

The percentage net body weights of mice treated with TiO_2, ZnO NPs and their mixture for 35 days are presented in Table 4.14. There was a significant ($p < 0.05$) reduction in the net body weights of the mice treated with NPs and their mixture during the 35- day exposure period. The net body weights of the treated mice varied in a non-specific pattern across the five week exposure period. Subsequently, TiO_2, ZnO NPs and their mixture were able to penetrate and accumulate in the testicular region of the treated mice (Figure 4.136). Additionally, testicular weights of the treated mice showed no significant ($p > 0.05$) decrease at the 9.38, 37.5, 75.0 and 150 $mgkg^{-1}$ of TiO_2 NPs, and at tested doses of their mixture in comparison with the mice treated with distilled water. In contrast, testicular weight of the mice treated with ZnO NPs for 35 days showed no significant increase at 37.5 and 75.0 $mgkg^{-1}$ in comparison with the mice treated distilled water (Table 4.15).

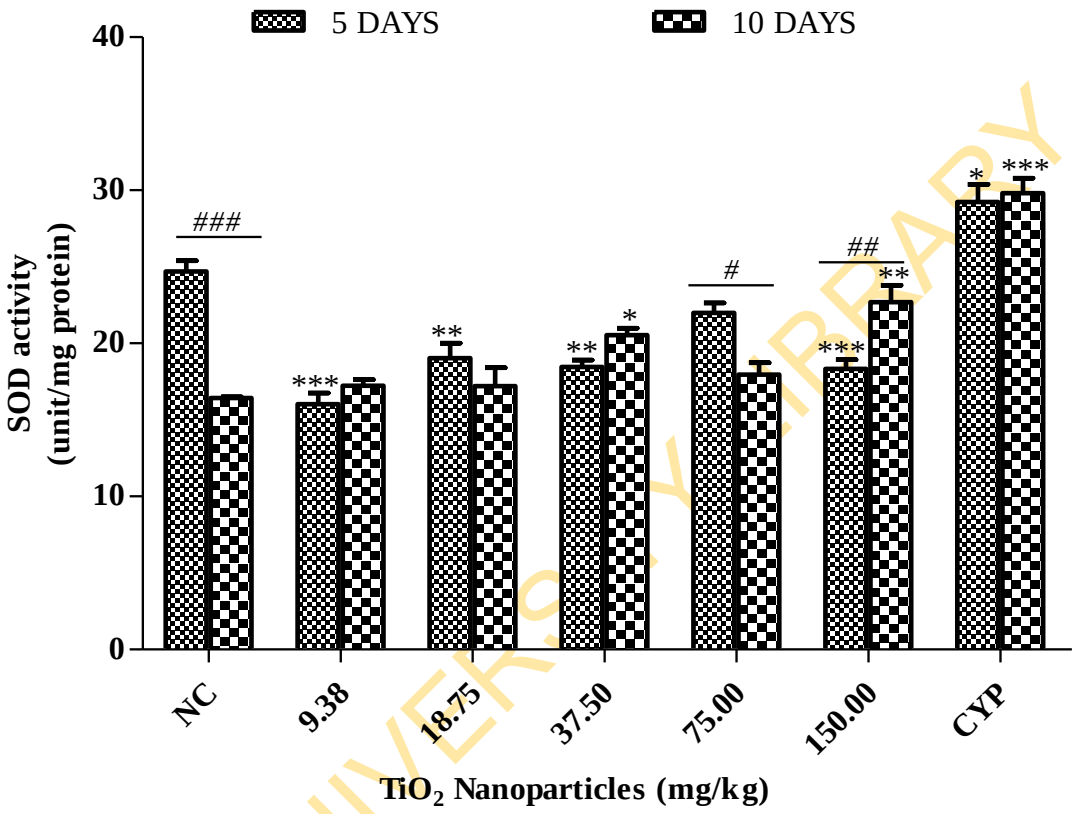

Figure 4. 123: SOD activity in the testes of mice treated with TiO_2 NPs at the 5- and 10-day exposure periods.

Data represent mean ± SE (n = 5). * $p < 0.05$, ** $p < 0.01$ and *** $p < 0.001$ for 5- days and 10- days exposure in comparison with their corresponding negative controls (NC) = distilled water; CYP = cyclophosphamide (positive control).

$^{\#}$ $p < 0.05$, $^{\#\#}$ $p < 0.01$ and $^{\#\#\#}$ $p < 0.001$ for the comparison between the 5- and 10-day exposures

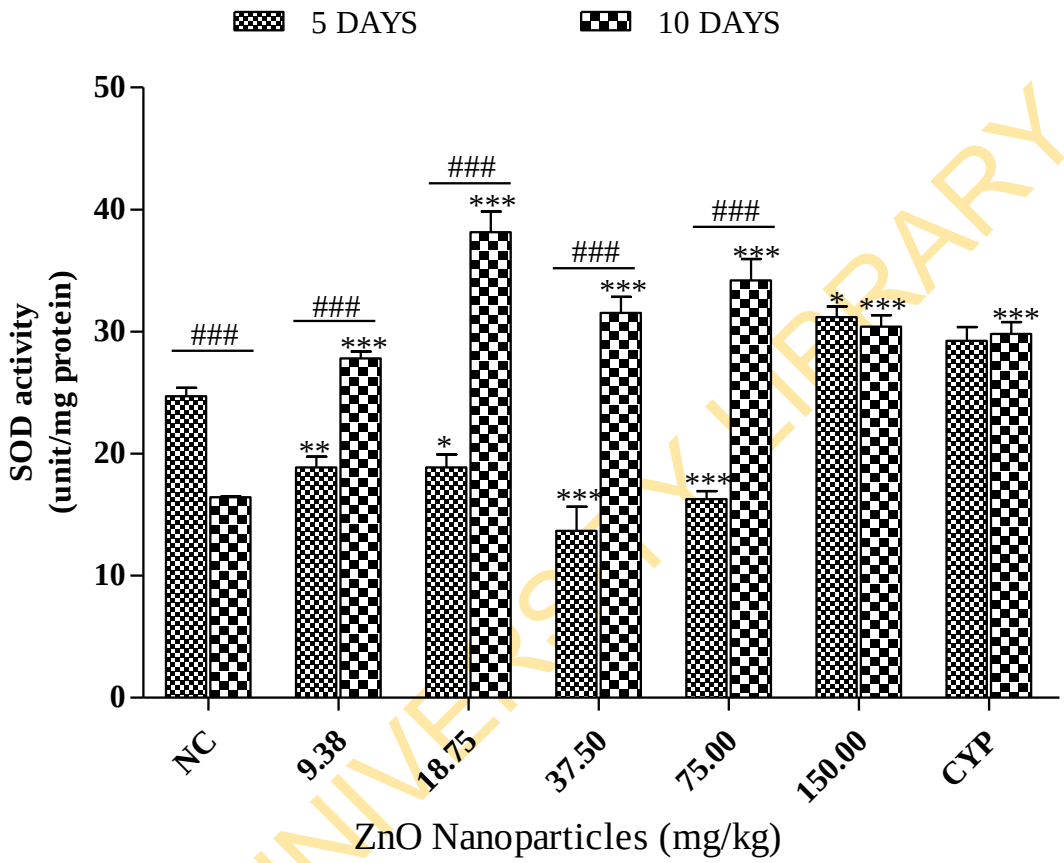

Figure 4. 124: SOD activity in the testes of mice treated with ZnO NPs at the 5- and 10-day exposure periods.

Data represent mean ± SE (n = 5). * $p < 0.05$, ** $p < 0.01$ and *** $p < 0.001$ for 5- days and 10- days exposure in comparison with their corresponding negative controls (NC) = distilled water; CYP = cyclophosphamide (positive control).

$^{\#\#\#}$ $p < 0.001$ for the comparison between the 5- and 10-day exposures

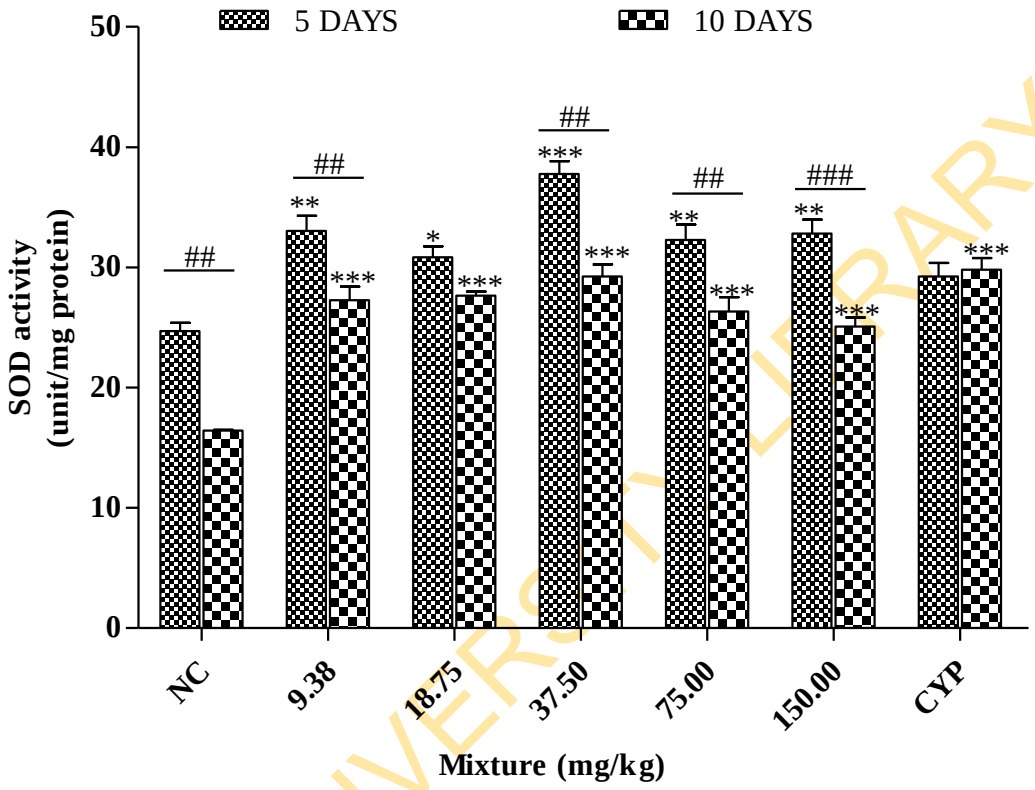

Figure 4. 125: SOD activity in the testes of mice treated with TiO_2 and ZnO NPs at the 5- and 10- day exposure periods.

Data represent mean ± SE (n = 5). * $p < 0.05$, ** $p < 0.01$ and *** $p < 0.001$ for 5- days and 10- days exposure in comparison with their corresponding negative controls (NC) = distilled water; CYP = cyclophosphamide (positive control).

$^{\#\#}$ $p < 0.01$ and $^{\#\#\#}$ $p < 0.001$ for the comparison between the 5- and 10-day exposures

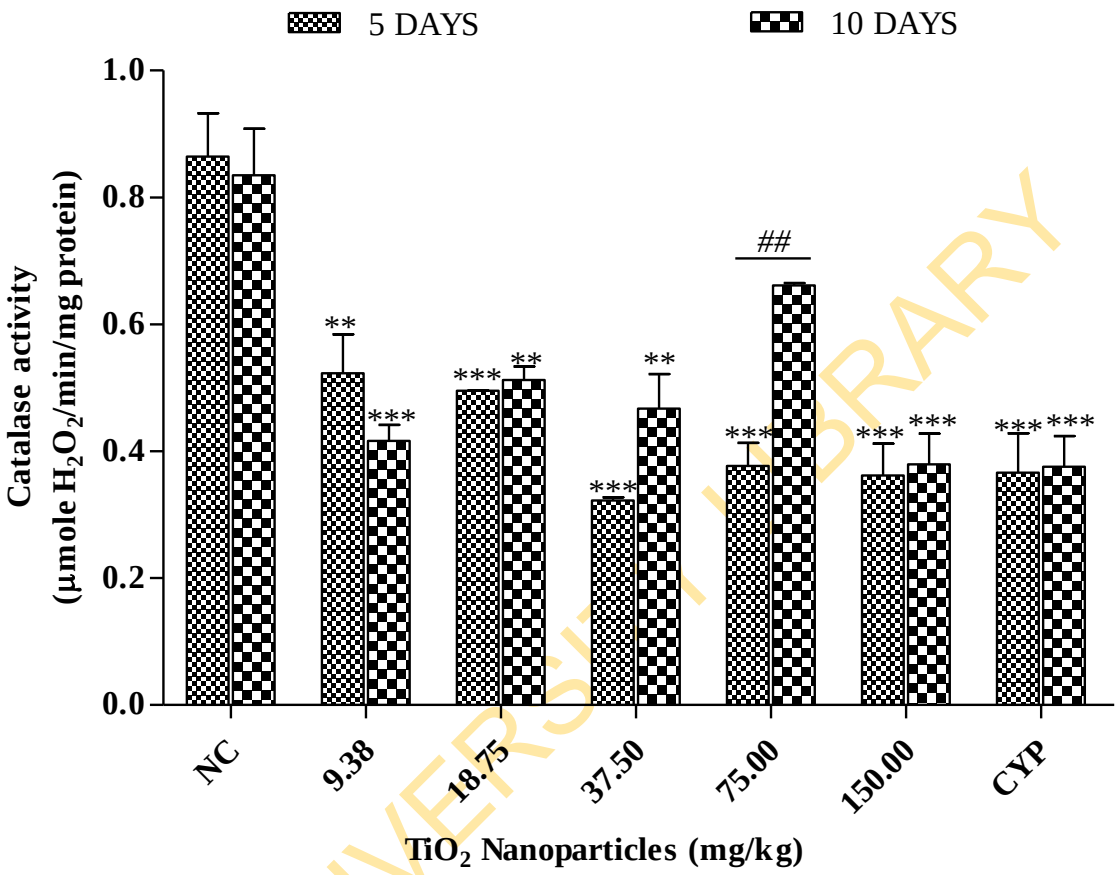

Figure 4. 126: CAT activity in the testes of mice treated with TiO_2 NPs at the 5- and 10-day exposure periods.

Data represent mean ± SE (n = 5). ** $p < 0.01$ and *** $p < 0.001$ for 5- days and 10- days exposure in comparison with their corresponding negative controls (NC) = distilled water; CYP = cyclophosphamide (positive control).

$^{\#\#}$ $p < 0.01$ for the comparison between the 5- and 10-day exposures

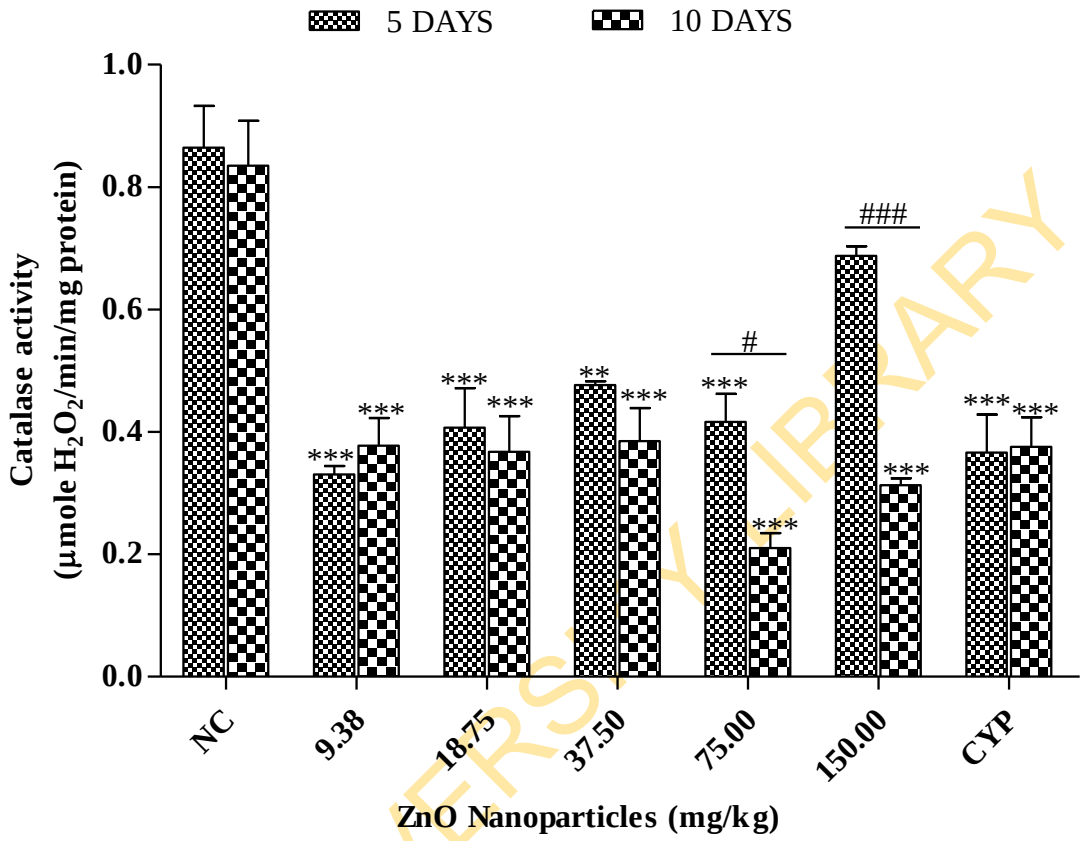

Figure 4. 127: CAT activity in the testes of mice treated with ZnO NPs at the 5- and 10-day exposure periods.

Data represent mean ± SE (n = 5). $^{**}p < 0.01$ and $^{***}p < 0.001$ for 5- days and 10- days exposure in comparison with their corresponding negative controls (NC) = distilled water; CYP = cyclophosphamide (positive control). $^{\#}$ $p < 0.05$ and $^{\#\#\#}$ $p < 0.001$ for the comparison between the 5- and 10-day exposures

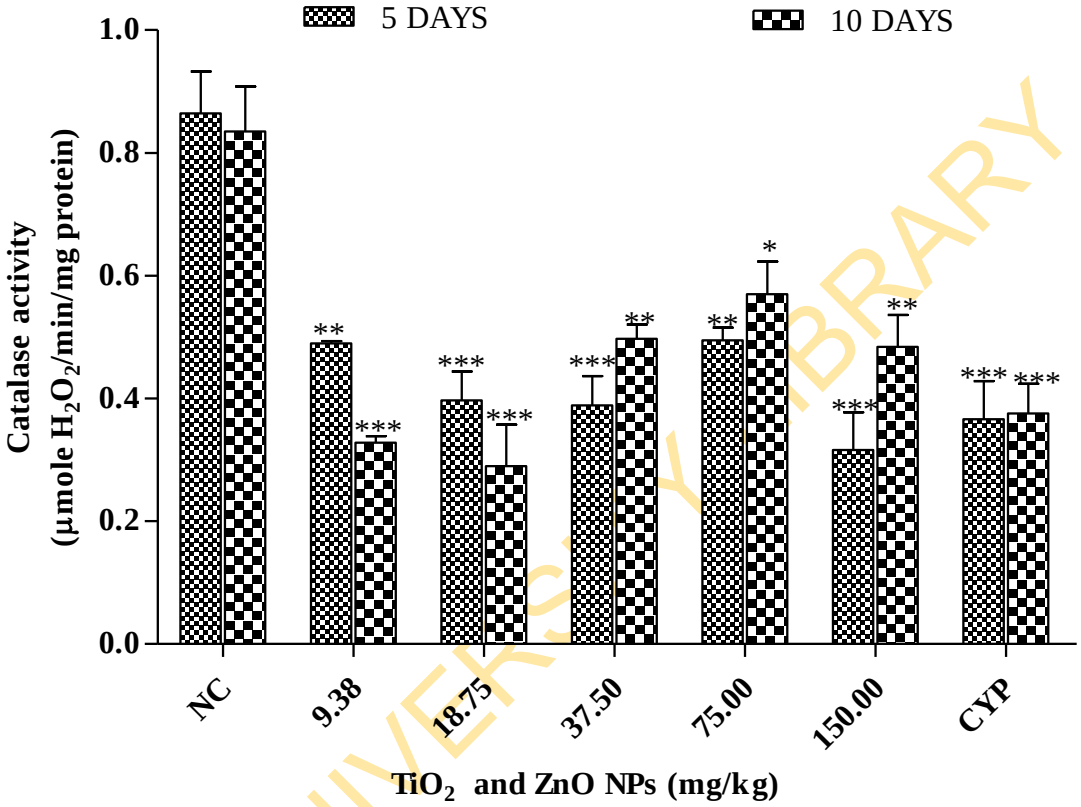

Figure 4. 128: CAT activity in the testes of mice treated with TiO_2 and ZnO NPs at the 5- and 10- day exposure periods.

Data represent mean ± SE (n = 5). * $p < 0.05$, ** $p < 0.01$ and *** $p < 0.001$ for 5- days and 10- days exposure in comparison with their corresponding negative controls (NC) = distilled water; CYP = cyclophosphamide (positive control).

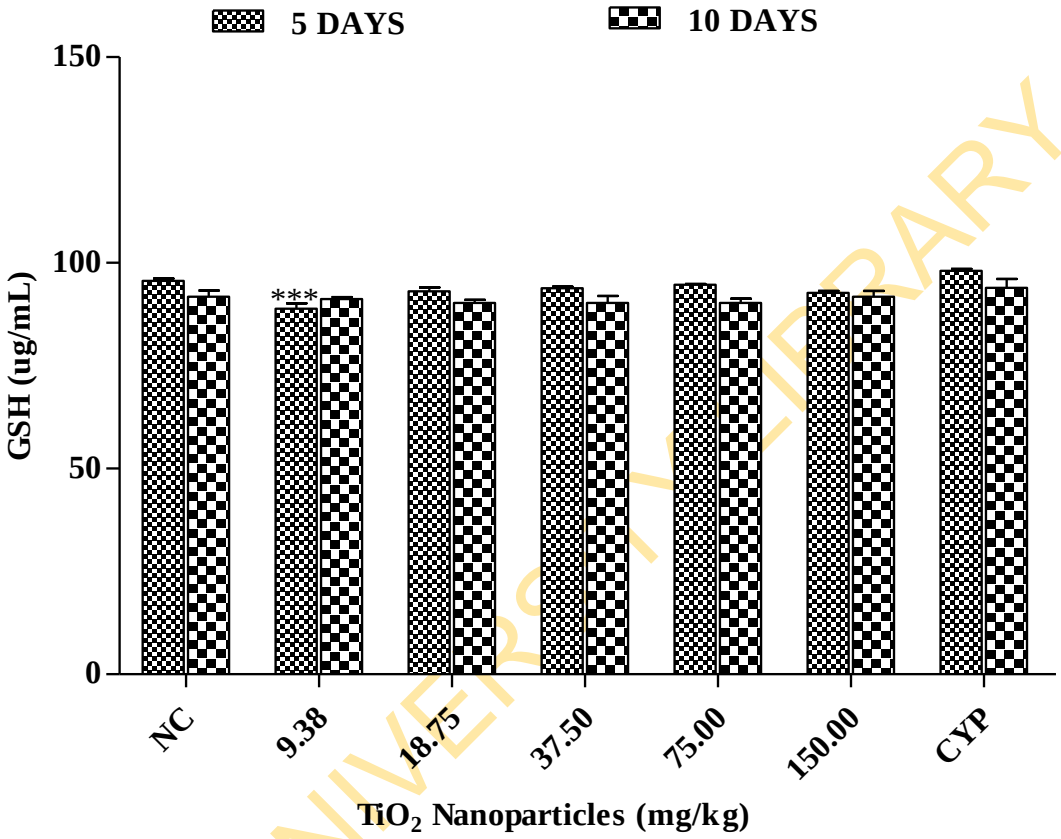

Figure 4. 129: GSH level in the testes of mice treated with TiO_2 NPs at the 5- and 10- day exposure periods.

Data represent mean ± SE (n = 5). *** $p < 0.001$ for 5- days exposure in comparison with distilled water (NC) = distilled water; CYP = cyclophosphamide (positive control).

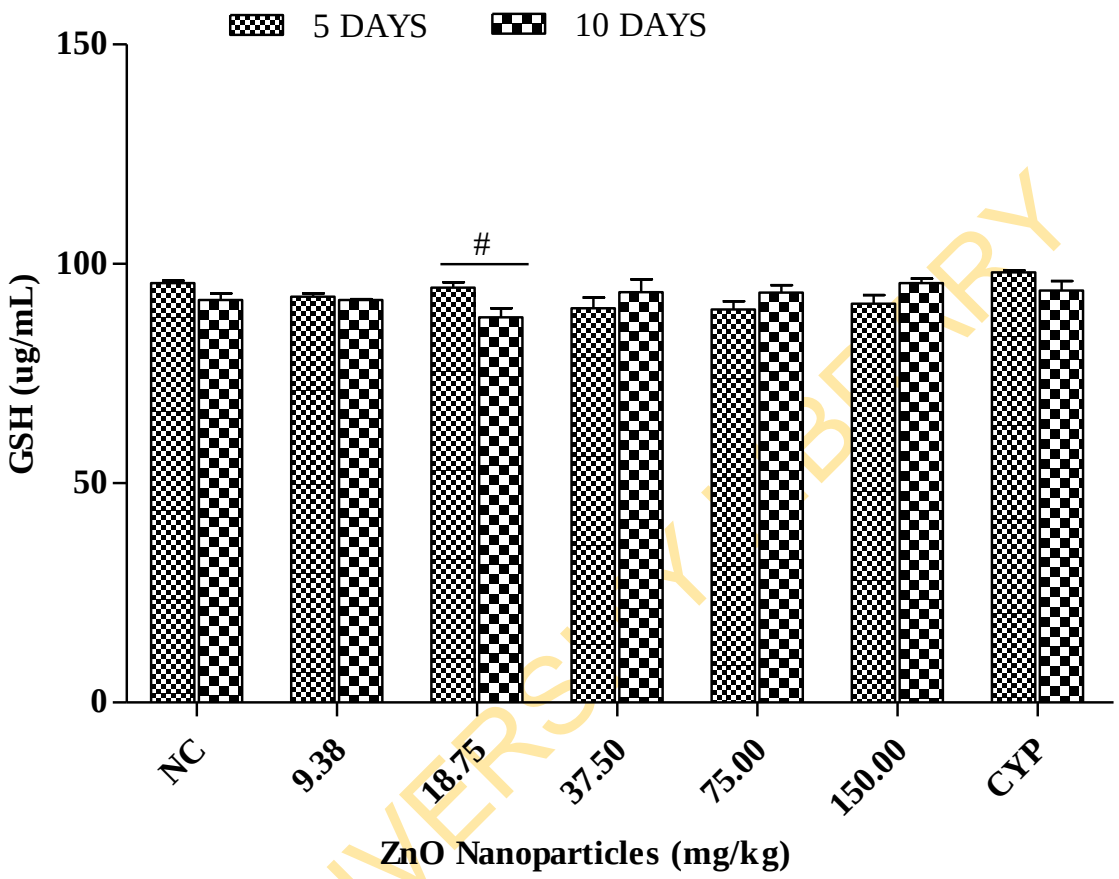

Figure 4. 130: GSH level in the testes of mice treated with ZnO NPs at the 5- and 10- day exposure periods.

Data represent mean ± SE (n = 5). Negative controls (NC) = distilled water; CYP = cyclophosphamide (positive control). # $p < 0.05$ for the comparison between the 5- and 10-day exposures

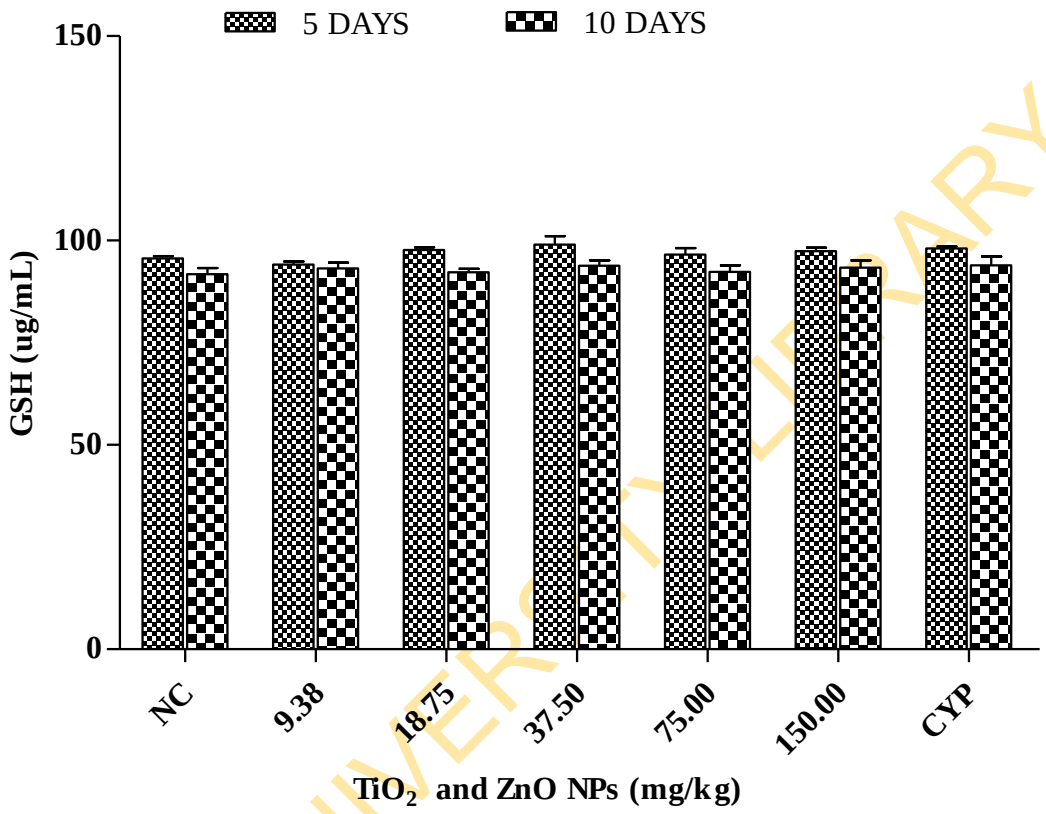

Figure 4. 131: GSH level in the testes of mice treated with TiO_2 and ZnO NPs at the 5- and 10- day exposure periods.

Data represent mean ± SE (n = 5). Negative controls (NC) = distilled water; CYP = cyclophosphamide (positive control).

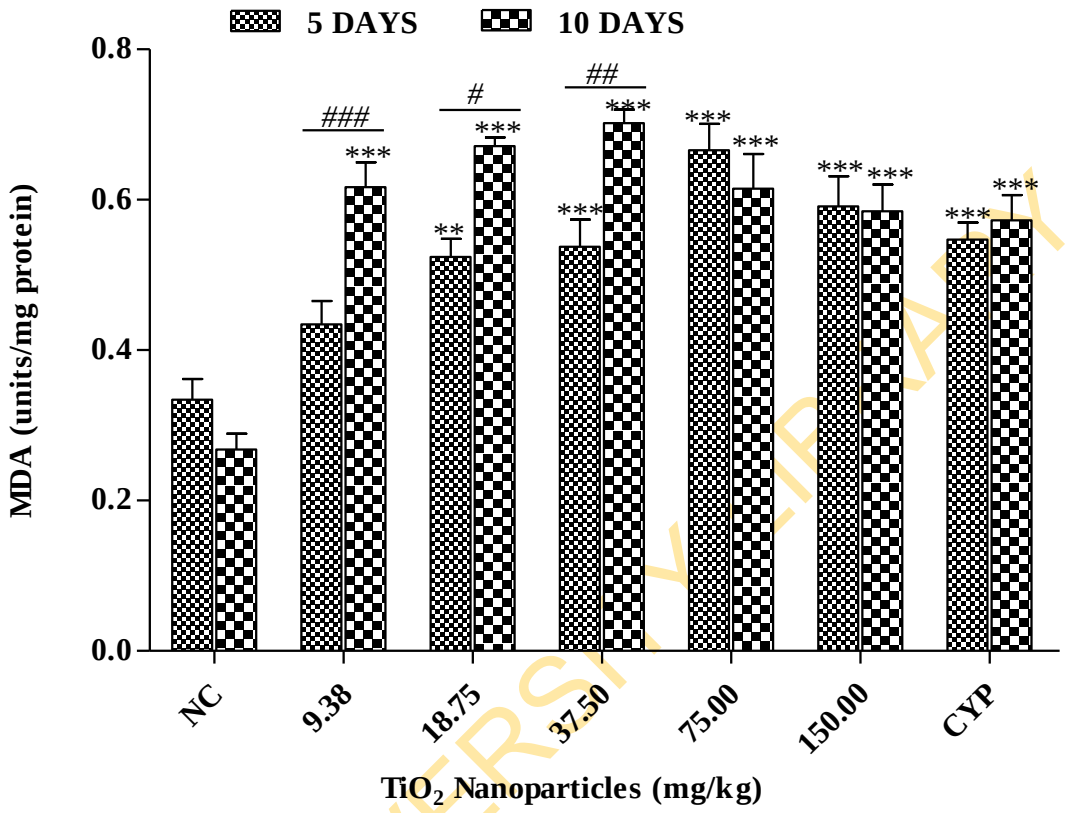

Figure 4. 132: MDA level in the testes of mice treated with TiO_2 NPs at the 5- and 10-day exposure periods.

Data represent mean ± SE (n = 5). ** $p < 0.01$ and *** $p < 0.001$ for 5- days and 10- days exposure in comparison with their corresponding negative controls (NC) = distilled water; CYP = cyclophosphamide (positive control). $^{\#}$ $p < 0.05$, $^{\#\#}$ $p < 0.01$ and $^{\#\#\#}$ $p < 0.001$ for the comparison between 5- and 10-days exposure.

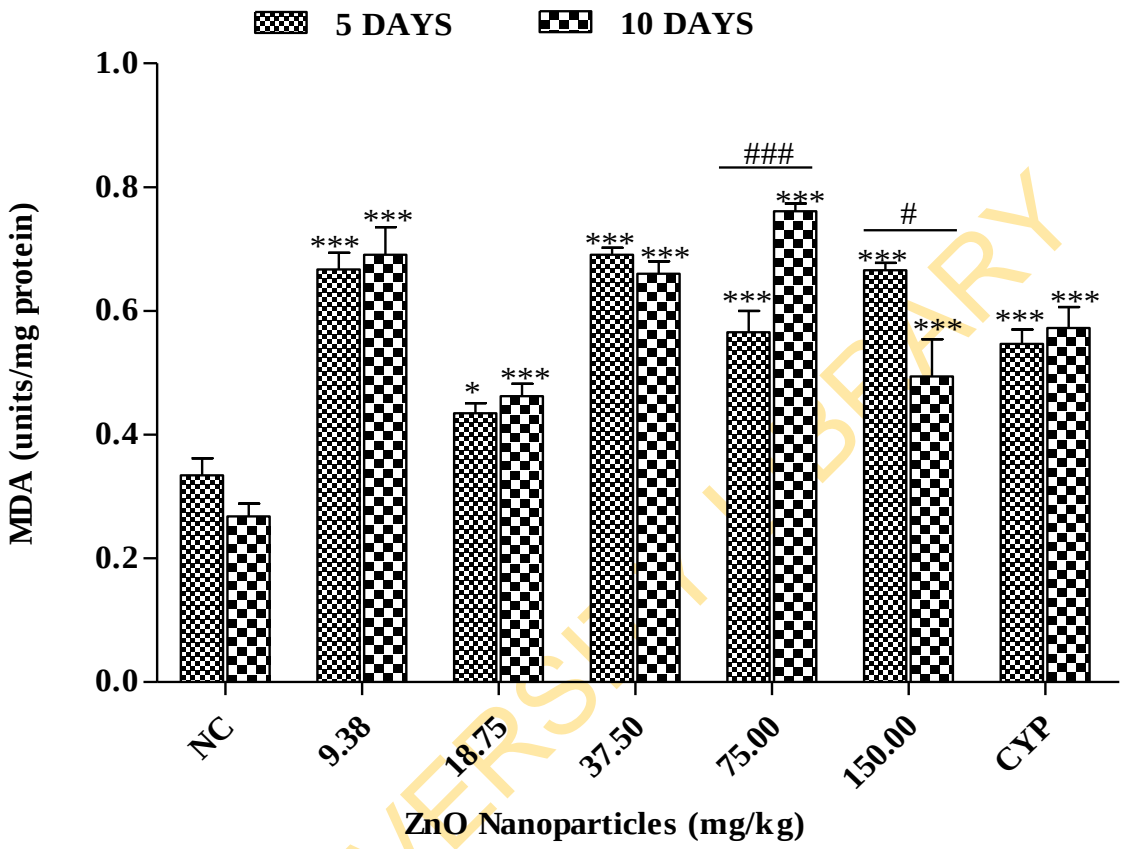

Figure 4. 133: MDA level in the testes of mice treated with ZnO NPs at the 5- and 10-day exposure periods.

Data represent mean ± SE (n = 5). * $p < 0.05$ and *** $p < 0.001$ for 5- days and 10- days exposure in comparison with their corresponding negative controls (NC) = distilled water; CYP = cyclophosphamide (positive control).

$^{\#}$ $p < 0.05$ and $^{\#\#\#}$ $p < 0.001$ for the comparison between the 5- and 10-day exposures

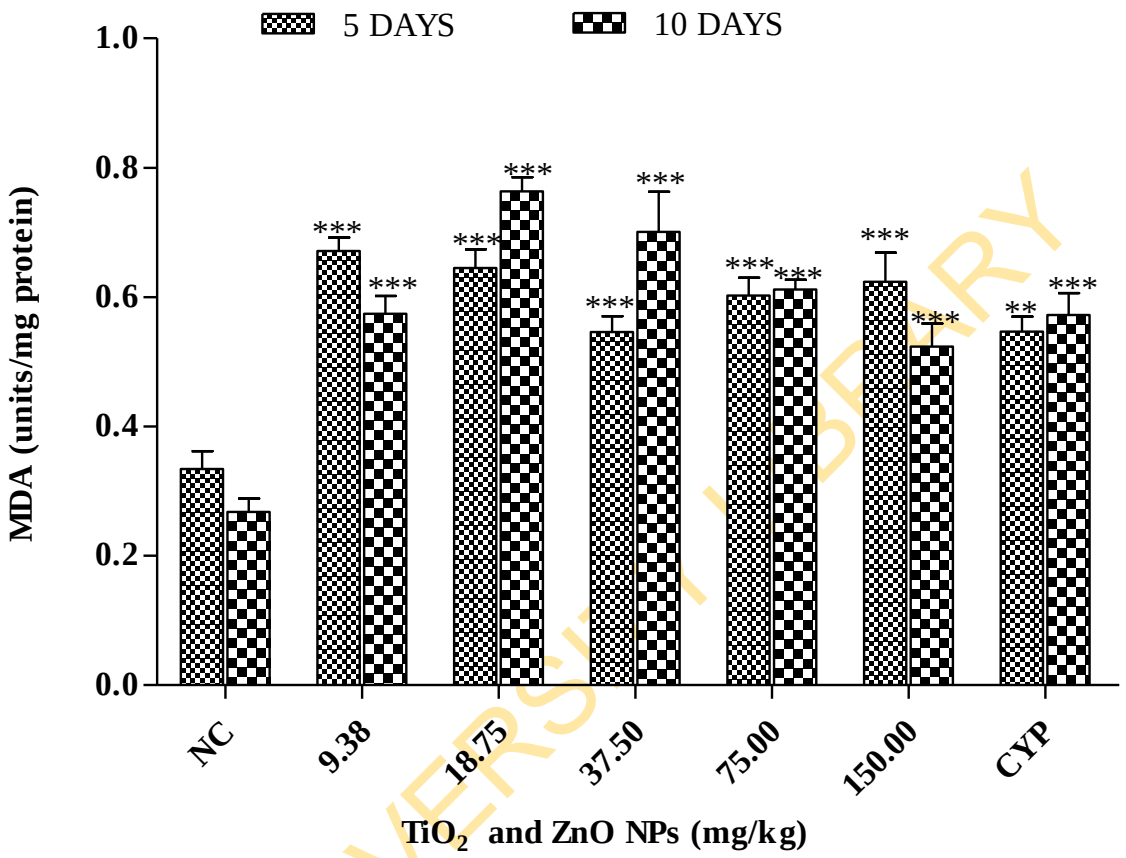

Figure 4. 134: MDA level in the testes of mice treated with TiO_2 and ZnO NPs at the 5- and 10- day exposure periods.

Data represent mean ± SE (n = 5). ** $p < 0.01$ and *** $p < 0.001$ for 5- days and 10- days exposure in comparison with their corresponding negative controls (NC) = distilled water; CYP = cyclophosphamide (positive control).

4.5.2 Epididymal sperm parameters in mice treated with titanium dioxide, zinc oxide nanoparticles and their mixture

The effect of the NPs and their mixture on the sperm motility in cauda epididymis of treated mice is presented in Figures 4.137- 4.139. After the 35- day exposure period, TiO_2 NPs (Figure 4.137) induced a significant ($p < 0.001$) reduction in the percentage means of the motile spermatozoa in comparison with the mice treated with distilled water. In contrast, a significant ($p < 0.001$) increase in the immotile spermatozoa of the treated mice was observed at tested doses of TiO_2 NPs in comparison with those treated with distilled water. The rapidly progressive, slow progressive, non progressive and immotile spermatozoa of the mice treated with distilled water were 29.40, 1.25, 13.80 and 55.55 % respectively. The rapidly progressive motile spermatozoa showed means of 9.0, 1.8, 0.4, 2.2 and 2.4 %; the slow progressive motility showed means of 0.5, 0.5, 0.5, 0.6 and 1.7 %; the non-progressive spermatozoa showed means of 9.6, 4.4, 10.4, 7.9 and 4.3 % while the immotile spermatozoa showed means of 81.0, 93.4, 88.8, 89.3 and 91.7 % corresponding to the doses at the 9.35, 18.75. 37.50, 75.00 and 150.00 $mgkg^{-1}$ of TiO_2 NPs, respectively.

In addition, mice treated with ZnO NPs (Figure 4.138) for 35 days exhibited a significant ($p < 0.001$) reduction in the percentage means of the motile spermatozoa in comparison with the mice treated with distilled water. In contrast, a significant ($p < 0.001$) increase in the immotile spermatozoa was induced at tested doses in the mice treated with ZnO NPs in comparison with those treated with distilled water. The rapidly progressive motile showed means of 7.4, 7.4, 6.9 and 11.4 %; the slow progressive spermatozoa showed means of 0.6, 0.9, 0.5 and 0.6 %; the non-progressive spermatozoa showed means of 10.3, 9.8, 12.7 and 10.9 % while the immotile spermatozoa showed means of 81.8, 82.1, 80.1 and 77.3 % corresponding to the doses at the 9.38, 18.75, 37.50 and 75.00 $mgkg^{-1}$ of ZnO NPs respectively.

Similarly, mice treated with the mixture of NPs (Figure 4.139) exhibited a significant ($p< 0.001$) reduction in the percentage means of the motile spermatozoa in comparison with the mice treated with distilled water. The rapidly progressive motile spermatozoa showed means of 8.1, 8.4, 7.6, 5.8 and 7.6%; the slow progressive motile spermatozoa showed means of 0.8, 0.4, 1.0, 0.6 and 0.6%; the non-progressive motile spermatozoa showed

means of 8.2, 8.9, 9.2, 9.8 and 8.7% while the immotile spermatozoa showed means of 82.9, 82.4, 82.3, 83.8 and 83.2% corresponding to the doses at the 9.38, 18.75, 37.50, 75.00 and 150.00 $mgkg^{-1}$ of their mixture respectively.

The epididymal sperm count of mice treated with TiO_2, ZnO NPs and their mixture is presented in Figure 4. 140. A significant ($p < 0.001$) decrease in the sperm count was revealed in the cauda epididymis of mice treated with TiO_2, ZnO NPs and their mixture at tested doses respectively in comparison with those treated with distilled water. A 1.6-, 2.4-, 3.1-, 4.0- and 4.0- fold decrease of epididymal sperm count for TiO_2 NPs; 2.2-, 2.1-, 6.4- and 5.8 fold decrease of epididymal sperm count for ZnO NPs; 2.8-, 2.3-, 3.0-, 11.2- and 2.8-fold decrease of epididymal sperm count for their mixture corresponding to doses at 9.38, 18.75, 37.50, 75.00 and 150.00 $mgkg^{-1}$ were observed.

The frequency of abnormal spermatozoa in the cauda epididymis of the mice treated with TiO_2, ZnO NPs and their mixture are presented in Figure 4.141. At the 35- day exposure period, the frequency of sperm abnormalities in the cauda epididymis of the treated mice showed a significant ($p < 0.001$) increase only at the 75.00 and 150.00 $mgkg^{-1}$ of TiO_2 NPs; only at the 18.75 and 37.50 $mgkg^{-1}$ of ZnO NPs; and at tested doses of their mixture in comparison with the mice treated with distilled water. The frequencies of sperm abnormalities at the tested doses of TiO_2 NPs were higher than distilled water by a 1.3-, 2.1-, 2.6-, 5.9- and 8.0 fold increase; a 2.6- and 1.9- fold increase for ZnO NPs; and their combination by a 12.1-, 8.1-, 5.3-, 4.6- and 6.3 fold increase corresponding to the doses at 9.38, 18.75, 37.50, 75.00 and 150.00 $mgkg^{-1}$.

The order of frequency of abnormal spermatozoa (Figures 4.142 - 4.149) in the cauda epididymis of the mice treated with TiO_2 NPs was the spermatozoa with no hook > short hook > wrong angled hook > amorphous head > banana shape head > pin head > knobbed > wrong tail attachment > folded spermatozoa > long and sickled hook > double tails > abnormal mid piece > double heads. Other abnormalities observed ($p > 0.05$) included the pin head and triple tails, massive head and double hooks. Similarly, the order of frequency of abnormal spermatozoa in the cauda epididymis of the mice treated with ZnO NPs was the spermatozoa with amorphous head, followed in a descending order the pin head > no hook > folded spermatozoa > short hook > wrong angled hook > banana > knobbed head

> long and sickled > wrong tail attachment > abnormal mid piece > double tails. Other abnormalities observed ($p > 0.05$) included double tails and amorphous head, pin head and double tails, amorphous head and triple tails, amorphous head and double tails, massive head and pin head and triple tails. Finally, the mixture of the NPs administered to mice induced abnormal spermatozoa in the following order of frequency: amorphous head > pin head > no hook > wrong angle hook > knobbed head > short hook > wrong tail attachment > folded > banana head > double tails > long and sickled hook > abnormal mid piece > double heads. Other spermatozoa abnormalities ($p > 0.05$) included the massive head and double hook (Figure 4.142).

The interaction factor (IF) for the frequency of sperm count and sperm abnormality are presented in Table 4.16. A synergistic effect between TiO_2 NPs and ZnO NPs was observed in the sperm count and abnormalities at all doses except at the 75.00 mg/kg for the sperm abnormalities that showed antagonism.

Table 4. 14: Percentage net bodyweights of mice treated with titanium dioxide, zinc oxide nanoparticles and their mixture after 35 days exposure period

TiO_2 NPs	Week 1	Week 2	Week 3	Week 4	Week 5
Doses ($mgkg^{-1}$)					
NC	2.03 ± 0.36	3.57 ± 0.97	7.73 ± 0.88	-7.43 ±2.37	1.09 ± 1.44
9.38	3.23 ± 4.02	-1.80 ± 4.41	3.12 ± 2.47	0.28 ± 2.74	2.51 ± 1.40
18.75	-1.49 ± 0.82	-0.56 ± 0.37	-0.96 ± 0.56[a]	-0.12 ± 0.66	-7.54 ± 0.45[b]
37.50	12.42 ± 1.53[b]	5.72 ± 0.58	5.97 ± 0.99	-3.37 ± 2.90	-0.52 ± 1.30
75.00	1.18 ± 2.18	-13.77 ± 1.16[c]	24.84 ± 4.44[c]	-2.46 ± 2.09	11.43 ± 1.86[b]
150.00	-2.02 ± 1.24	-5.55 ± 1.73[a]	0.67 ± 0.97	-12.51 ± 1.80	22.72 ± 3.44[c]
CYP	-2.73 ± 0.75	0.73 ± 0.21	10.67 ± 1.31	1.53 ± 2.97	1.58 ± 0.86
ZnO NPs					
Doses ($mgkg^{-1}$)					
9.38	-3.90 ± 1.48	7.98 ± 0.72	-12.57 ± 2.00[c]	13.58 ± 2.37[c]	-0.63 ± 1.82
18.75	-13.82 ± 0.95[c]	3.60 ± 2.17	16.80 ± 3.53	-3.92 ± 1.02	8.79 ± 1.03[b]
37.50	-5.71 ± 4.99	20.68 ± 13.72	-8.17 ± 4.67[b]	8.71 ± 3.72[c]	-0.43 ± 1.47
75.00	-3.92 ± 3.08	9.34 ± 3.01	7.92 ± 4.09	-0.68± 0.64	-0.33 ± 1.26
CYP	-2.73 ± 0.75	0.73 ± 0.21	10.67 ± 1.31	1.53 ±2.97	1.58 ± 0.85
Mixture					
Doses ($mgkg^{-1}$)					
9.38	-2.02 ± 3.42	0.90 ± 2.43	-0.04 ± 1.55[b]	-16.51 ± 0.62[b]	16.49 ± 2.63[c]
18.75	9.62 ± 2.06	9.39 ± 0.98[a]	1.45 ± 0.72[b]	-3.42 ± 0.77	-7.23 ± 1.39[b]
37.50	8.94 ± 2.37	4.84 ± 1.37	4.99 ± 2.01	2.34 ± 1.20[b]	11.17 ± 1.12[b]
75.00	-4.72 ± 3.88	-4.41 ± 1.32[b]	3.31 ± 1.48	-2.46 ± 0.97	-1.69 ± 1.81
150.00	-7.87 ± 5.93	-3.37 ± 0.91[b]	3.50 ± 1.19	-9.60 ± 0.97[b]	10.34 ± 1.27[b]
CYP	-2.73 ± 0.75	0.73 ± 0.21	10.67 ± 1.31	1.53 ± 2.97	1.58 ± 0.85

Data represent Mean (n=5) ± SE. [a] $p < 0.05$, [b] $p < 0.01$ and [c] $p < 0.001$ for the comparison between the treatment groups and the negative control (NC) = distilled water; CYP = cyclophosphamide (positive control).

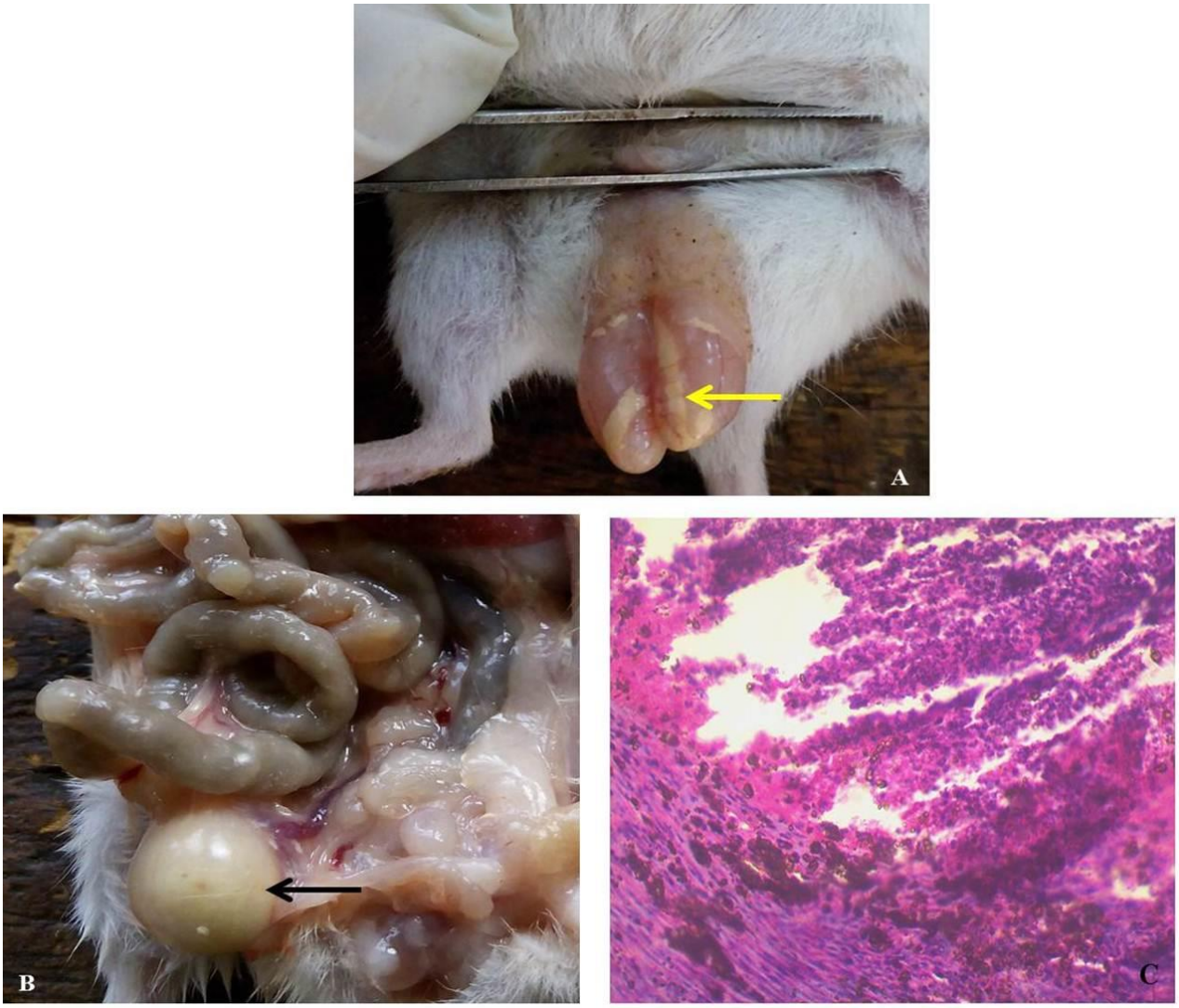

Figure 4. 135: Mouse showing agglomerates of TiO_2 and ZnO NPs in the testes after 35 days exposure (A). Mouse treated with ZnO NPs showing a tumour in the testicular region (B). The histopathology of the tumour in (B) revealed severely necrotic, deeply eosinophilic with basophilic debris. Likewise, there were numerous degenerate neutrophils, with dense fibrous connective tissue invaded by different inflammatory cells (macrophages, lymphocytes) (C) Magnification: 400X.

Table 4. 15: Absolute and relative testicular weights of mice treated with titanium dioxide, zinc oxide nanoparticles and their mixture at 35- day exposure period

Doses ($mgkg^{-1}$)	Absolute Testicular weight (g)	Relative Testicular weight (%)
TiO_2 NPs		
NC	0.18 ± 0.01	0.61 ± 0.04
9.38	0.18 ± 0.14	0.60 ± 0.02
18.75	0.19 ± 0.01	0.67 ± 0.03
37.50	0.17 ± 0.00	0.53 ± 0.01
75.00	0.18 ± 0.00	0.54 ± 0.02
150.00	0.17 ± 0.01	0.55 ± 0.02
CYP	0.17 ± 0.01	0.54 ± 0.02
ZnO NPs		
NC	0.18 ± 0.01	0.61 ± 0.04
9.38	0.18 ± 0.01	0.61 ± 0.06
18.75	0.18 ± 0.02	0.54 ± 0.04
37.50	0.20 ± 0.02	0.66 ± 0.05
75.00	0.19 ± 0.01	0.57 ±0.06
150.00	Mortality (100%)	Mortality (100%)
CYP	0.17 ± 0.01	0.54 ± 0.02
Mixture		
NC	0.18 ± 0.01	0.61 ± 0.04
9.38	0.16 ± 0.01	0.51 ± 0.03
18.75	0.17 ± 0.00	0.63 ± 0.05
37.50	0.17 ± 0.00	0.66 ± 0.04
75.00	0.17 ± 0.02	0.63 ± 0.05
150.00	0.17 ± 0.02	0.59 ± 0.05
CYP	0.17 ± 0.01	0.54 ± 0.02

Data represent Mean (n=5) ± SE for the comparison between the treatment groups and the negative control (NC) = distilled water; CYP = cyclophosphamide (positive control).

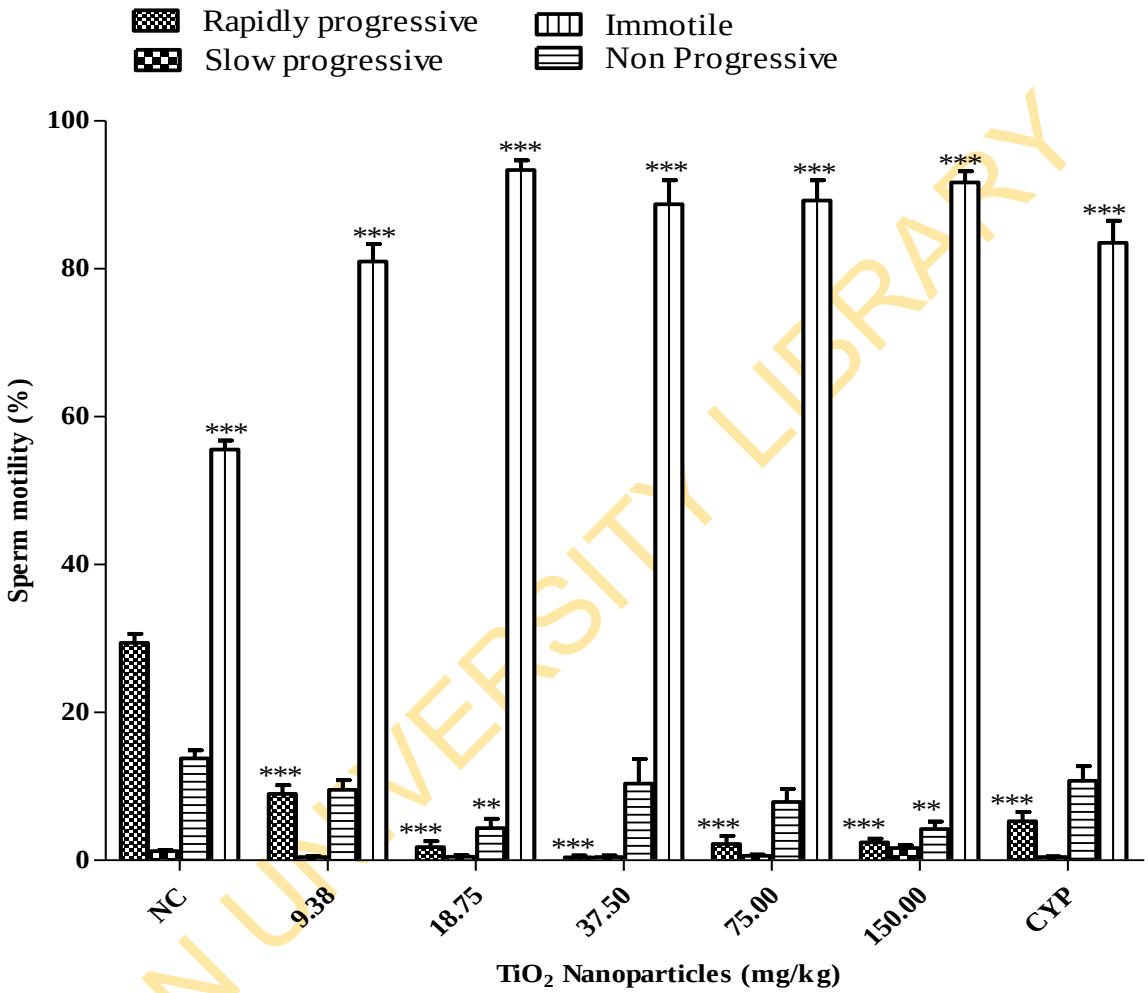

Figure 4. 136: Sperm motility in the cauda epididymis of mice treated with TiO_2 NPs after 35 days.

Data represent Mean (n=5) ± SE. ** $p < 0.01$ and *** $p < 0.001$ in comparison with the mice expose to distilled water. Negative control (NC) = distilled water; CYP =cyclophosphamide (positive control).

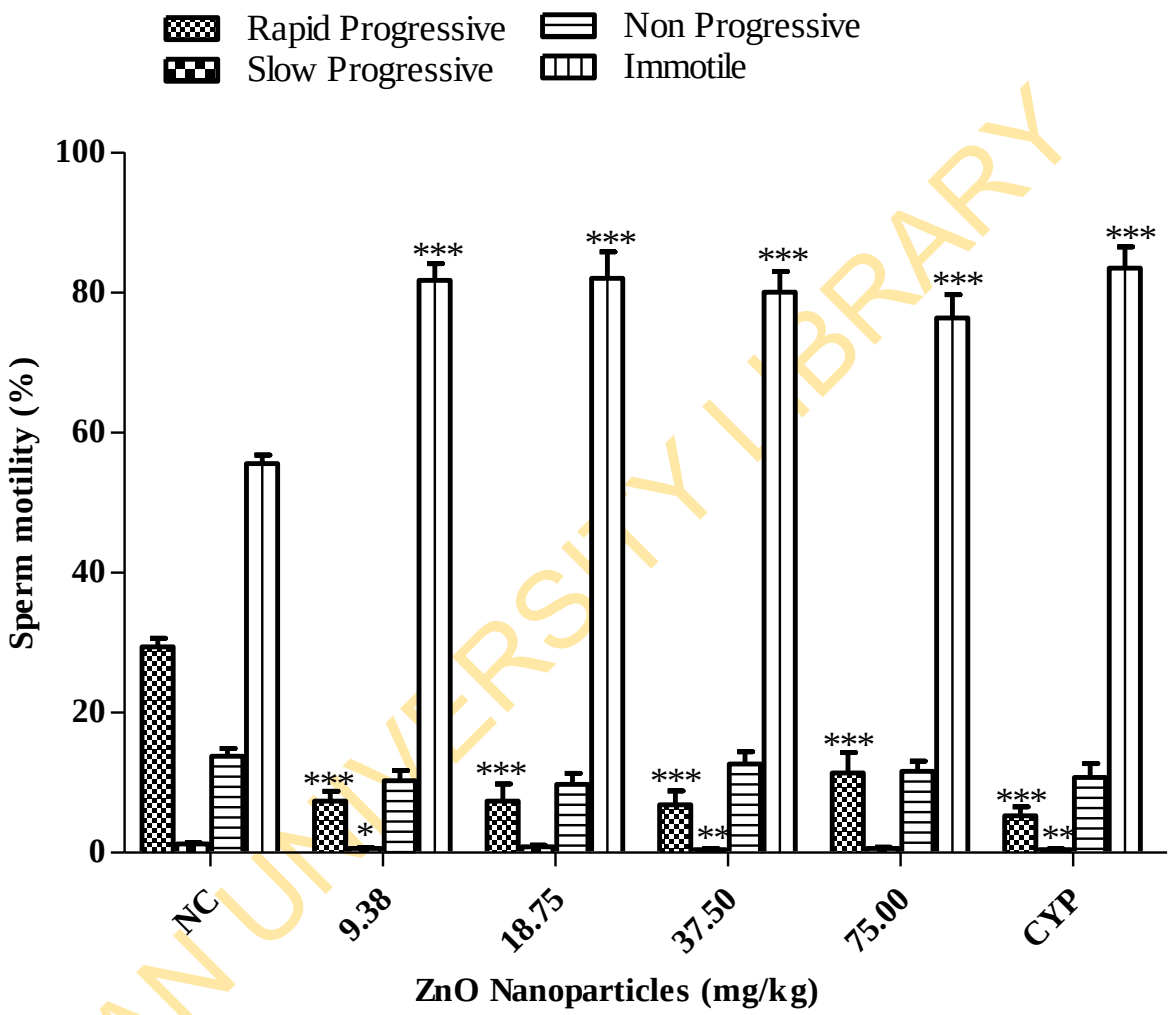

Figure 4. 137: Sperm motility in the cauda epididymis of mice treated with ZnO NPs after 35 days.

Data represent Mean (n=5) ± SE. * $p < 0.05$, ** $p < 0.01$ and *** $p < 0.001$ in comparison with the mice treated with distilled water. Negative control (NC) = distilled water; CYP =cyclophosphamide (positive control).

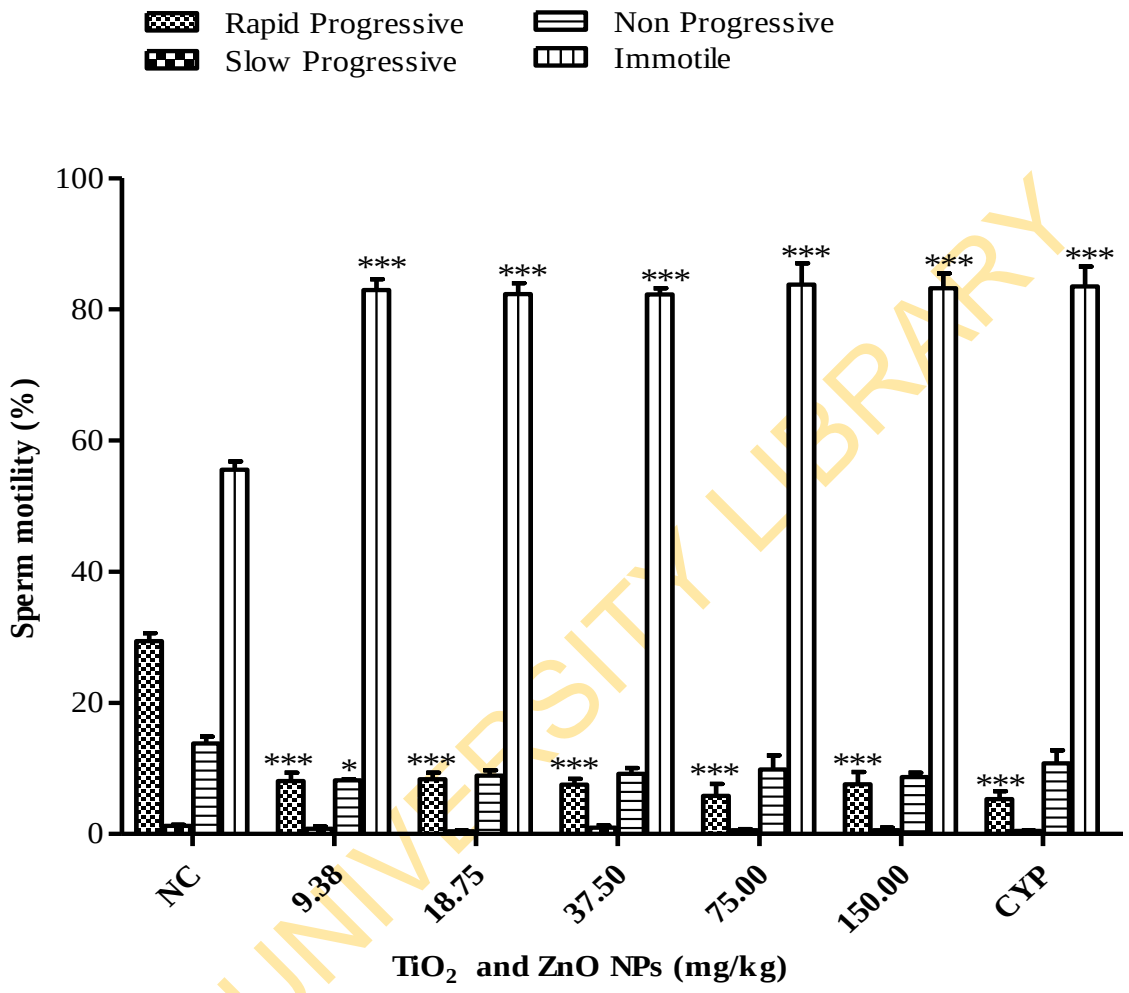

Figure 4. 138: Sperm motility in the cauda epididymis of mice treated with TiO_2 and ZnO NPs after 35 day.

Data represent Mean (n=5) ± SE. * $p < 0.05$ and *** $p < 0.001$ in comparison with the mice treated with distilled water. Negative control (NC) = distilled water; CYP =cyclophosphamide (positive control).

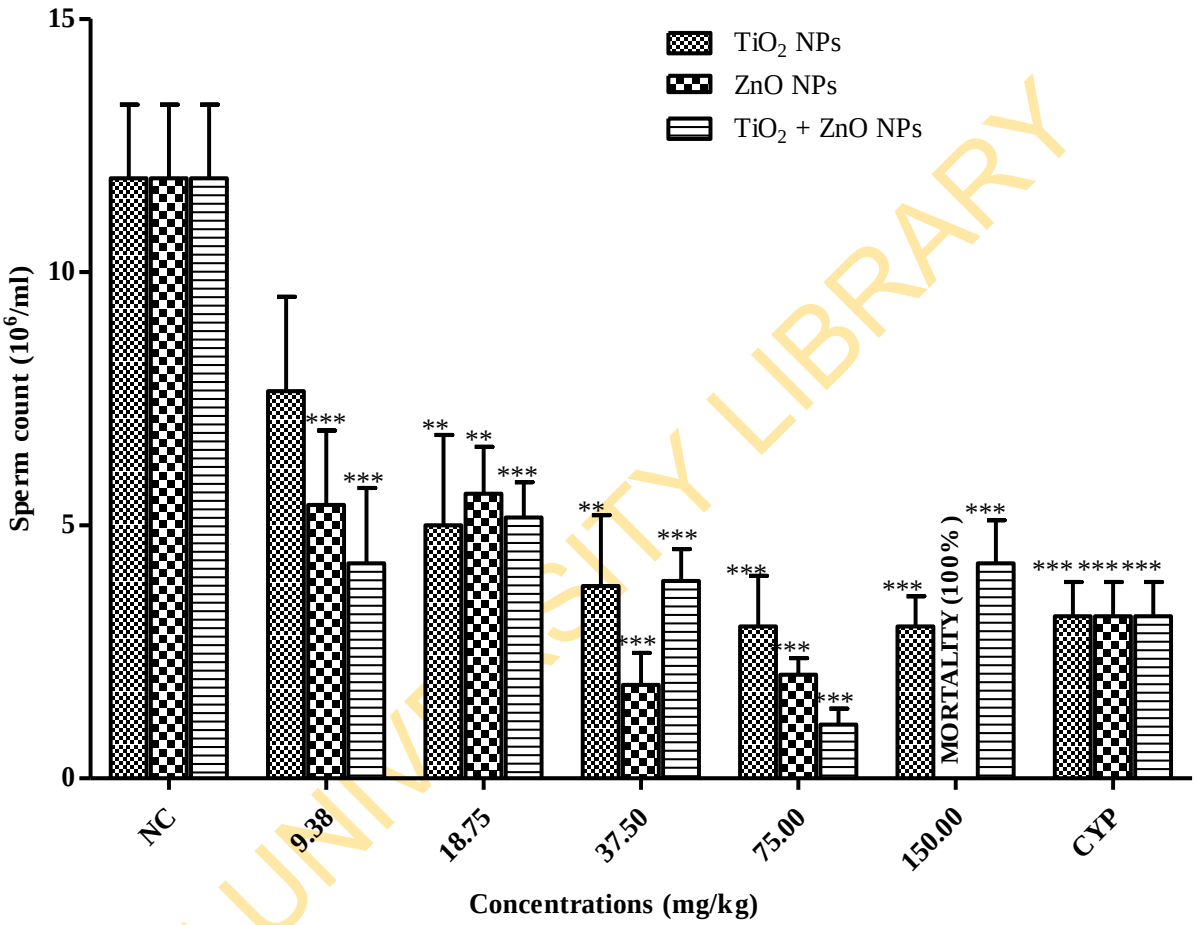

Figure 4. 139: Epididymal sperm count in the cauda epididymis of mice treated with TiO_2, ZnO NPs and TiO_2 and ZnO NPs after 35 days.

Data are represented in Mean ± SEM (n=5); ** $p < 0.01$ and *** $p < 0.01$ in comparison with the mice treated with distilled water. Negative control (NC) = distilled water; CYP = cyclophosphamide (positive control).

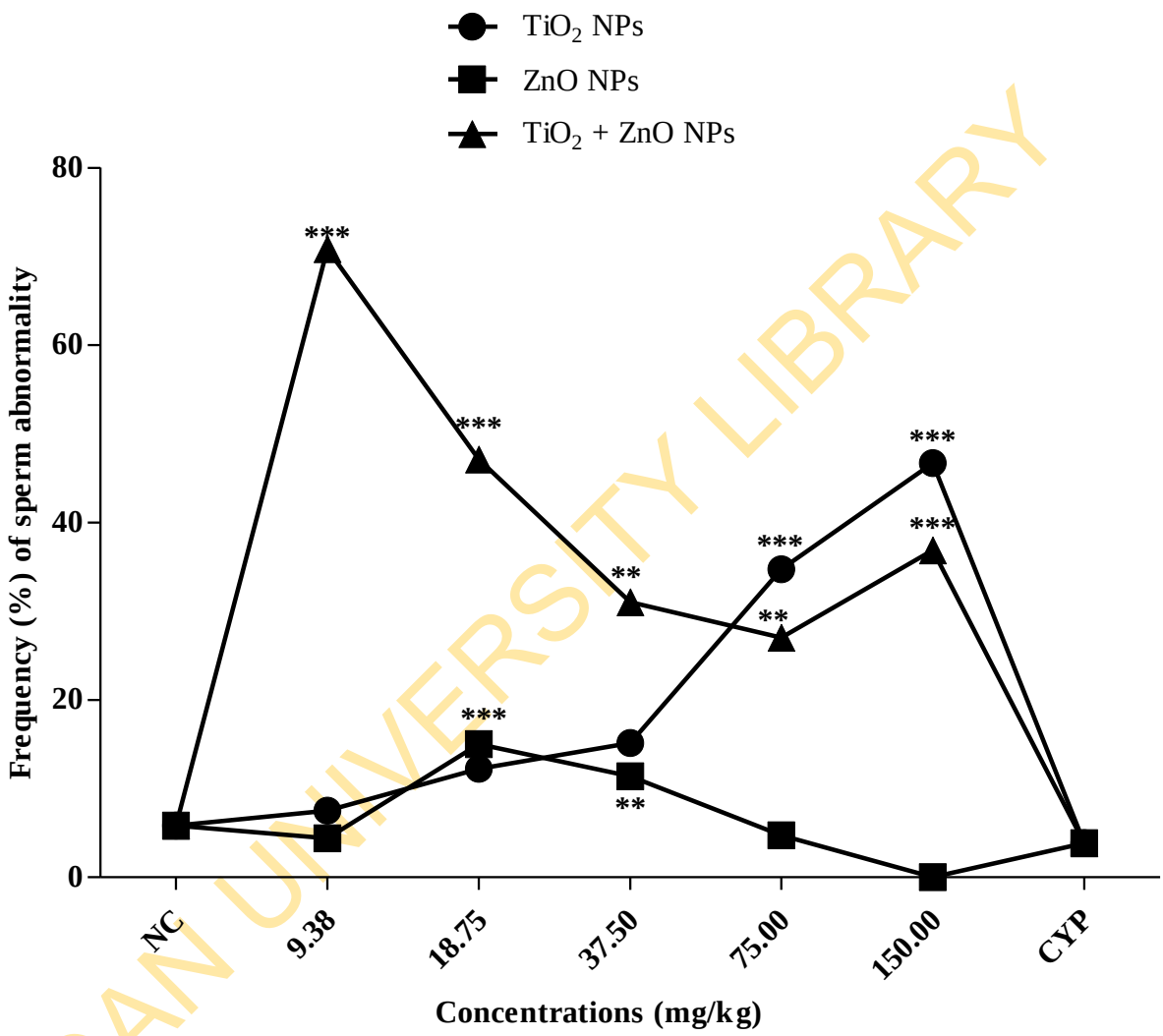

Figure 4. 140: Frequency of the sperm abnormality in the cauda epididymis of mice treated with TiO_2, ZnO NPs and TiO_2 and ZnO NPs after 35 days.

Data represent Mean (n=5) ± SE. * $p < 0.05$, ** $p < 0.01$ and *** $p < 0.001$ in comparison with the mice treated with distilled water (NC) = distilled water; CYP = cyclophosphamide (positive control).

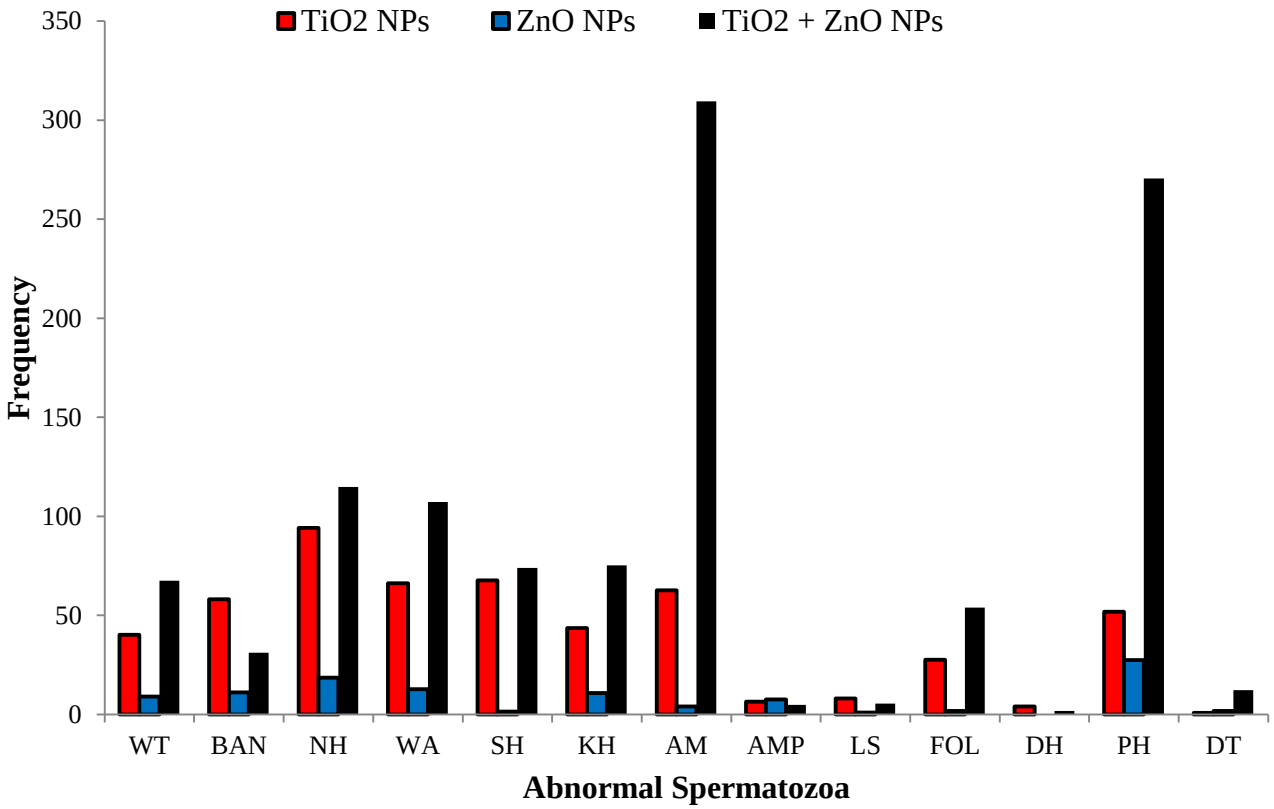

Figure 4. 141: Frequency of abnormal spermatozoa in mice treated with TiO_2, ZnO NPs and TiO_2 and ZnO NPs.

WT: wrong tail attachment; BAN: banana; NH: no hook; WA: wrong angled hook; SH: short hook; KH: knobbed head; AM: Amorphous head; AMP: abnormal mid piece; LS: long and sickled hook; FOL: folded; DH: double heads; PH: pin head; and DT: double tails.

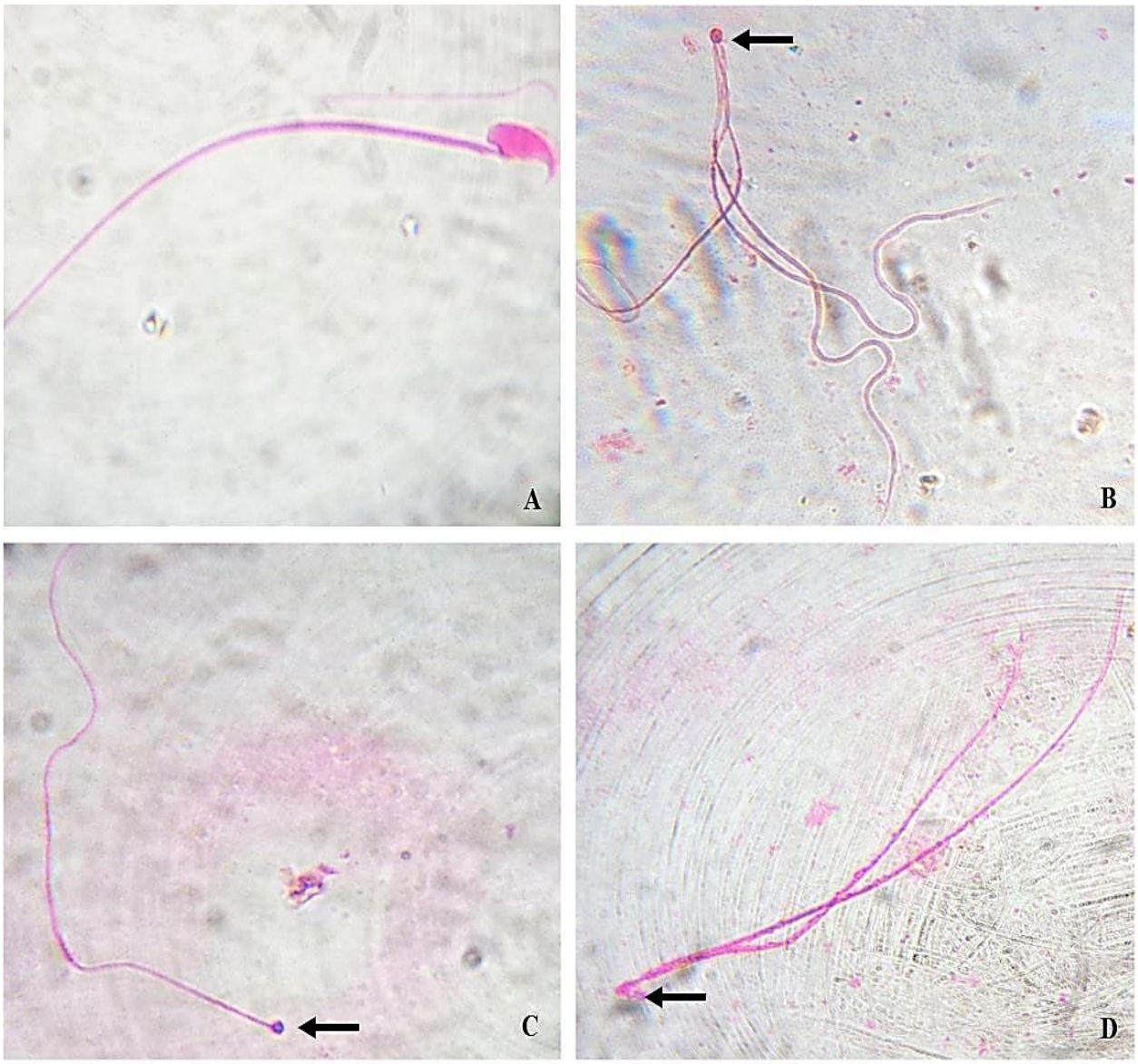

Figure 4. 142: Normal spermatozoon from a mouse treated with distilled water, having its head with the hook (almost 90°) and tail rightly attached to the mid piece (A). Spermatozoon having a pin head with triple tails from mouse treated with 18.75 mgkg^{-1} of ZnO NPs (B); single tail from mouse treated with 9.38 mgkg^{-1} of their mixture (C); and double tails from mouse treated with 150.00 mgkg^{-1} of TiO_2 NPs (D). Magnification: 1000X

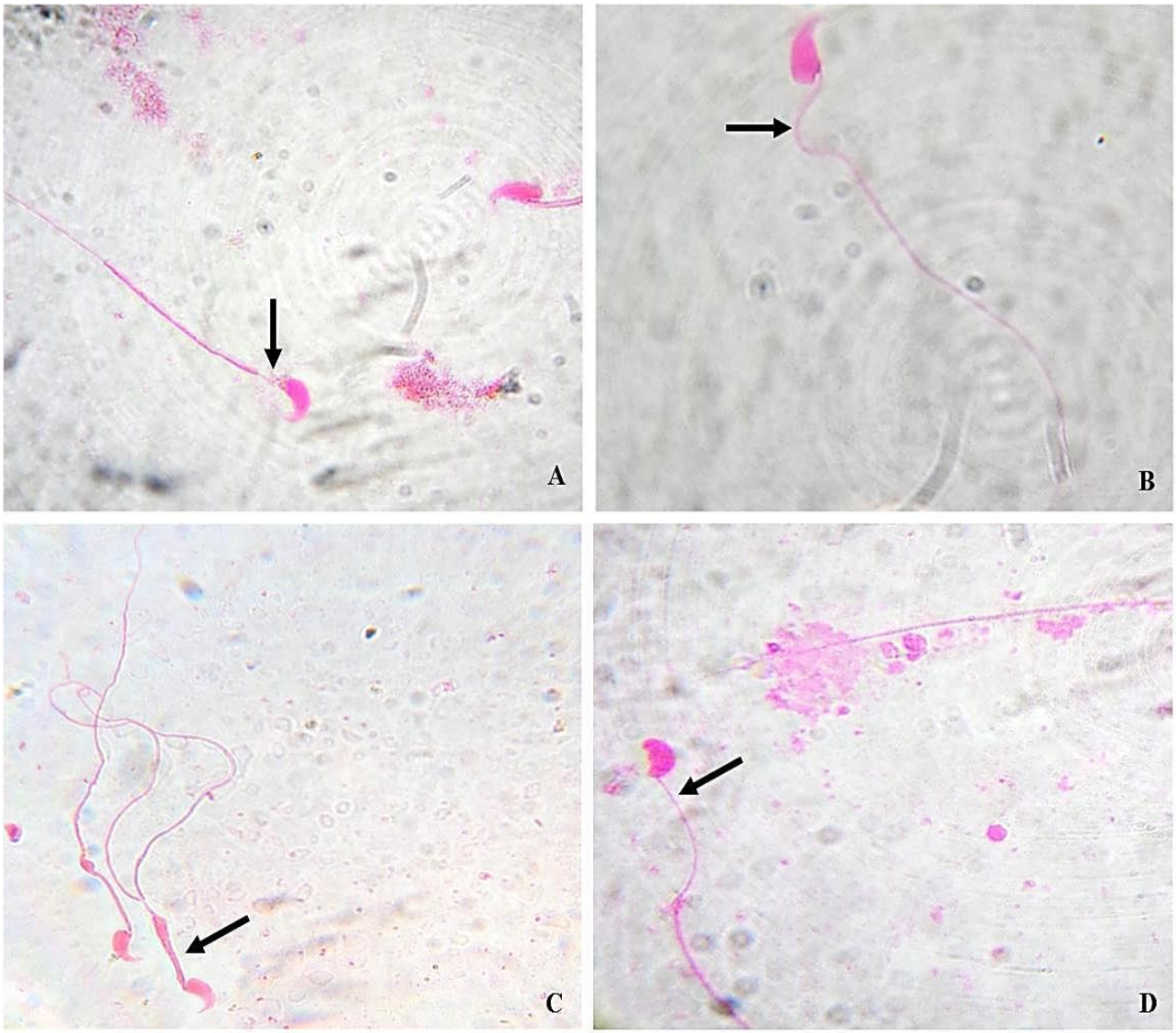

Figure 4. 143: Spermatozoa with abnormal mid-pieces from mouse treated with 18.75 $mgkg^{-1}$ of ZnO NPs (A-B); spermatozoon with abnormal mid piece and double tails from mouse treated with 150.00 $mgkg^{-1}$ of their mixture (C); and no hook from mouse treated with 150.00 $mgkg^{-1}$ of TiO_2 NPs (D). Magnification: 1000X

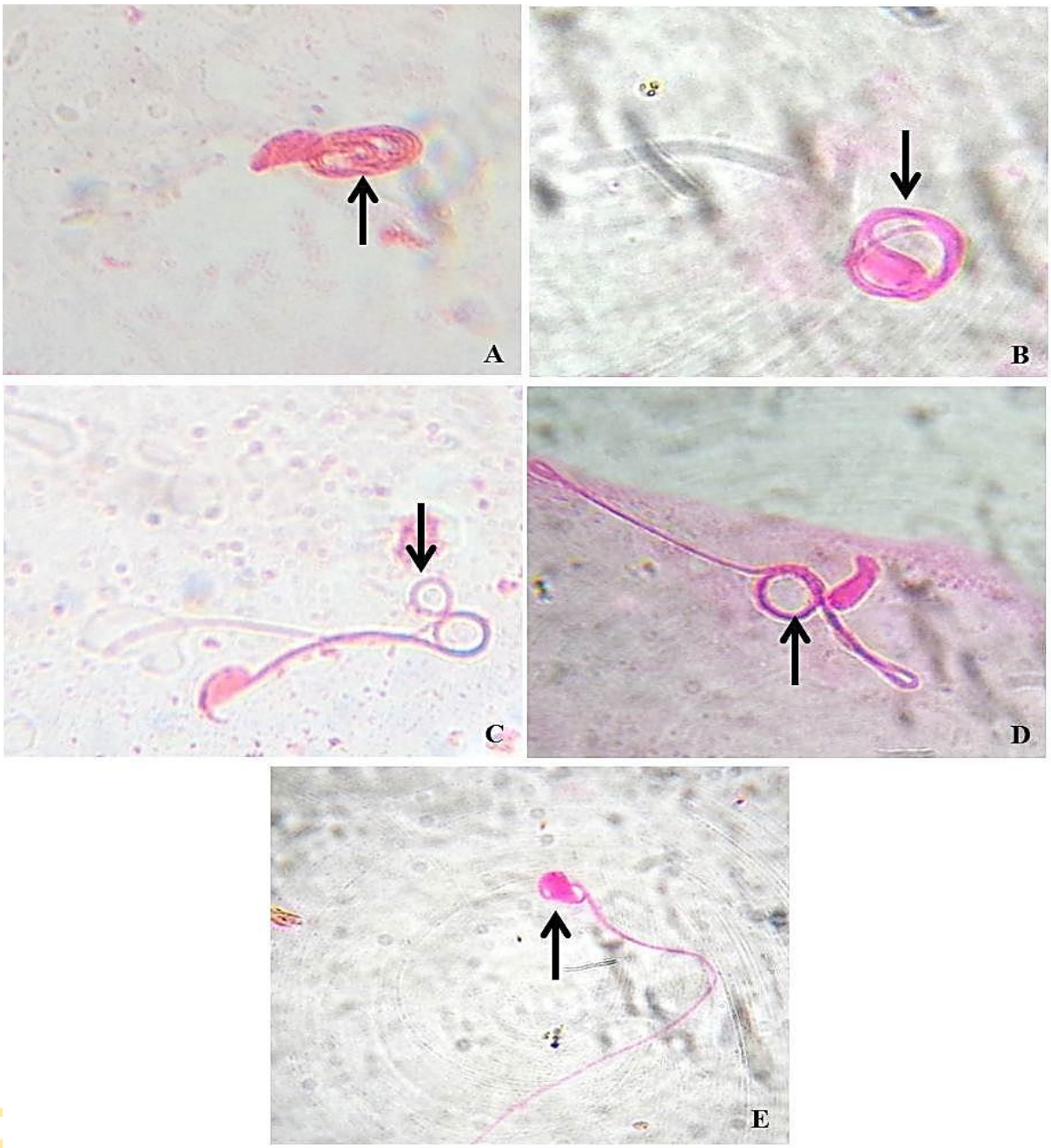

Figure 4. 144: Folded spermatozoa from mouse treated with 75.00 $mgkg^{-1}$ of their mixture (A – C); 150.00 $mgkg^{-1}$ of TiO_2 NPs (D) and 18.75 $mgkg^{-1}$ of ZnO NPs (E). Magnification: 1000X.

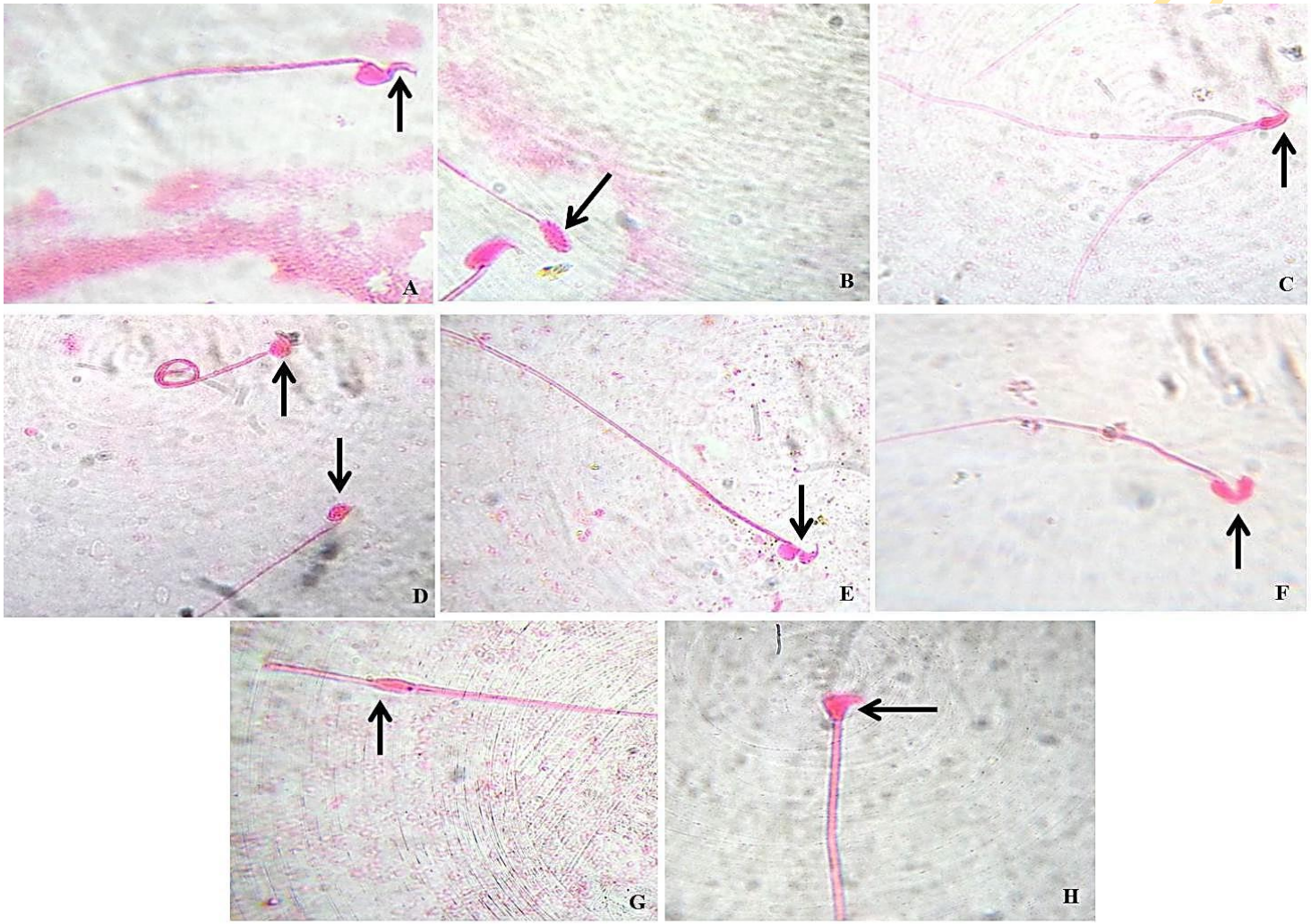

Figure 4. 145: Spermatozoa with amorphous heads from mouse treated with 150.00 $mgkg^{-1}$ of TiO_2 NPs (A – B); mouse treated with 37.50 $mgkg^{-1}$ of ZnO NPs (C – D); mouse treated with 9.38 $mgkg^{-1}$ (E – F); and 150.00 $mgkg^{-1}$ of their mixture (G – H) Magnification: 1000X.

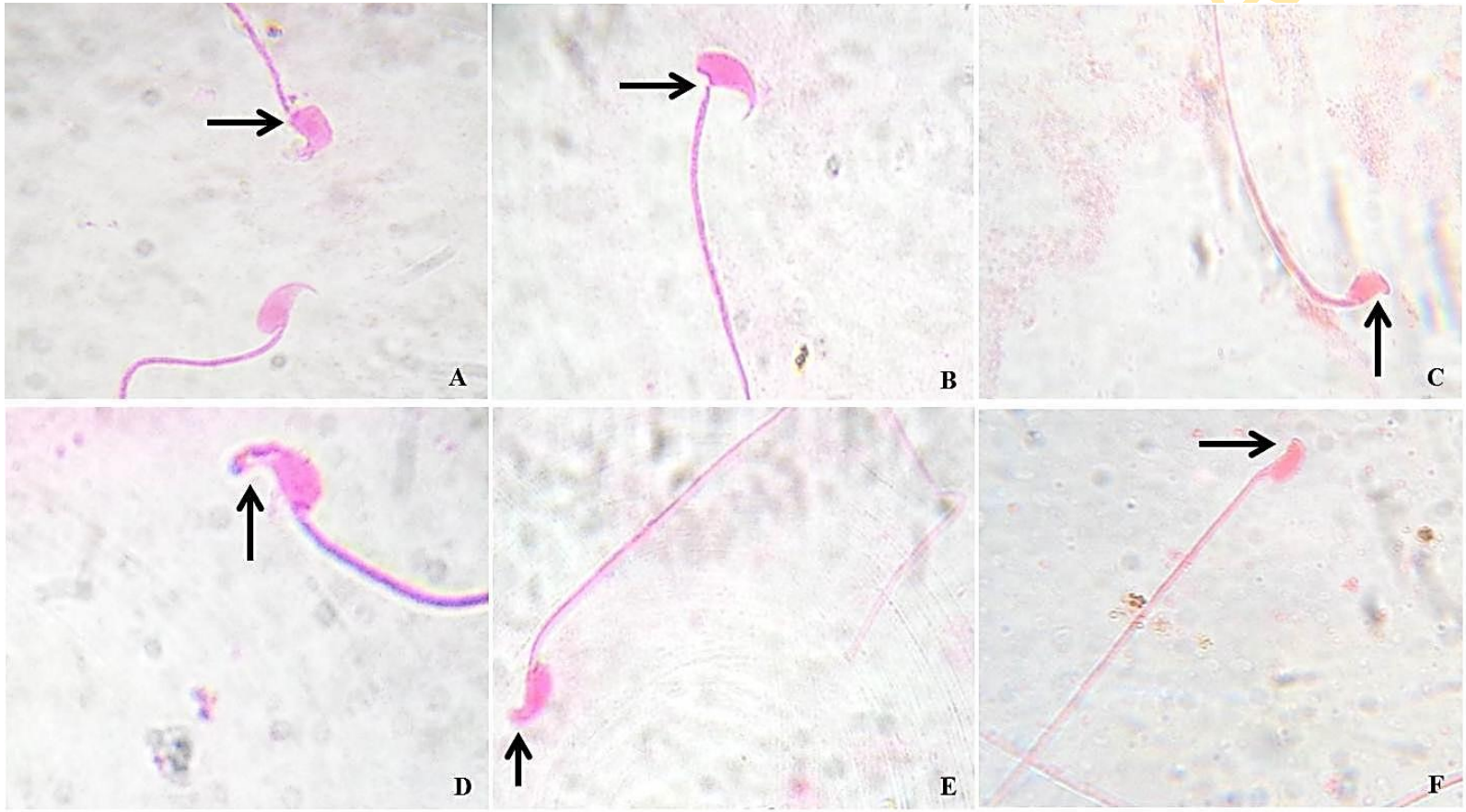

Figure 4. 146: Spermatozoa with wrong tail attachments from mouse treated with 37.50 $mgkg^{-1}$ of their mixture (A – B); Spermatozoon with short hook from mouse treated with 75.00 $mgkg^{-1}$ of TiO_2 NPs (C); Spermatozoa with banana heads (D – E) and no hook (F) from mouse treated with 9.38 $mgkg^{-1}$of their mixture. Magnification: 1000X.

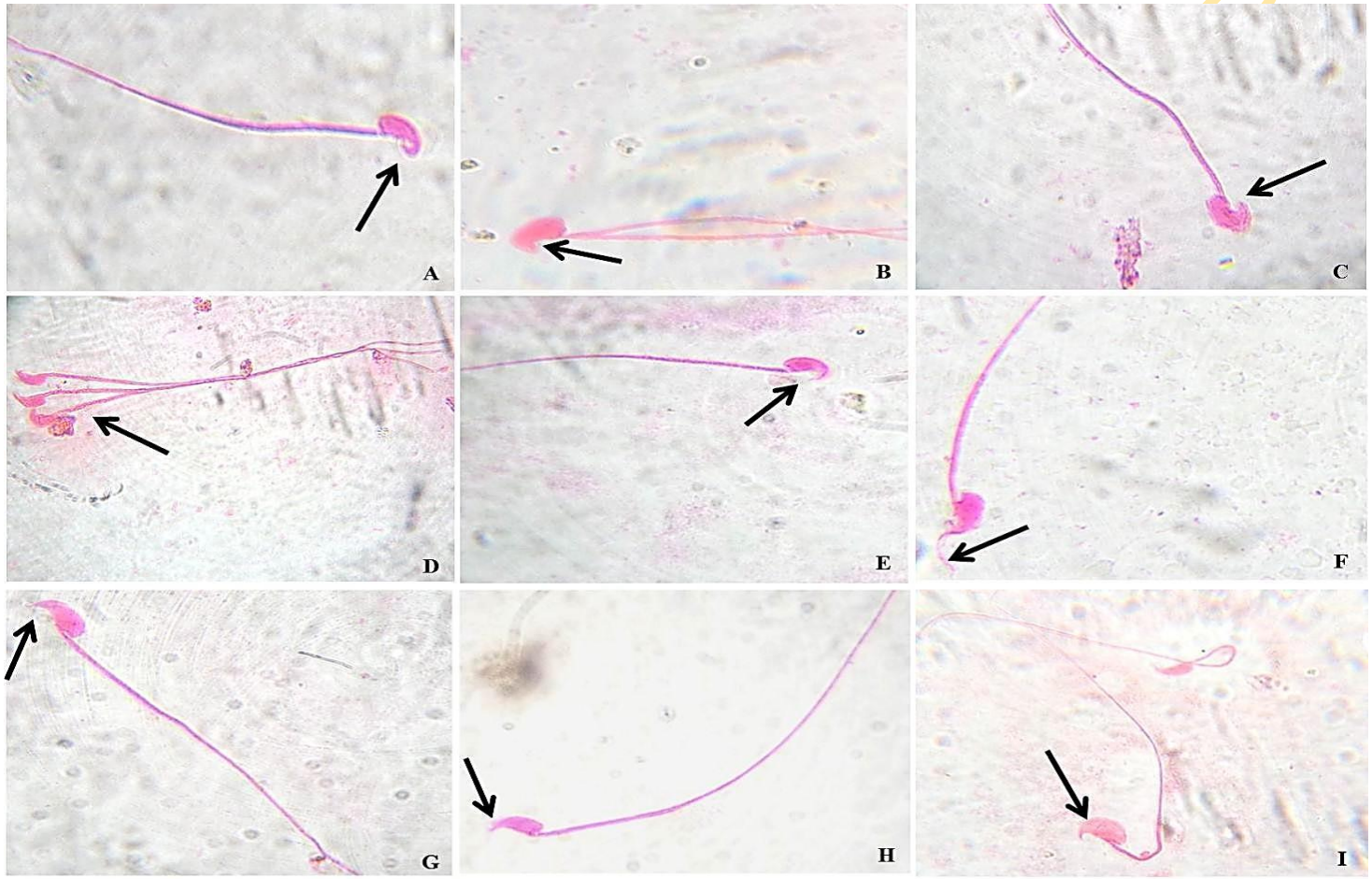

Figure 4. 147: Spermatozoa with knobbed hook from mouse treated with 150.00 $mgkg^{-1}$ of TiO_2 NPs (A – C); Spermatozoon with triple heads and fused tail from mouse treated with 18.75 $mgkg^{-1}$ of ZnO NPs (D); Spermatozoon with sickle-like hook from mouse treated with 37.50 $mgkg^{-1}$ of ZnO NPs (E); Spermatozoa with wrong angled hook from mouse treated with 9.38 $mgkg^{-1}$ of their mixture (F – H); and Spermatozoon with a massive head from mouse treated with 37.50 $mgkg^{-1}$ of ZnO NPs (I). Magnification: 1000X.

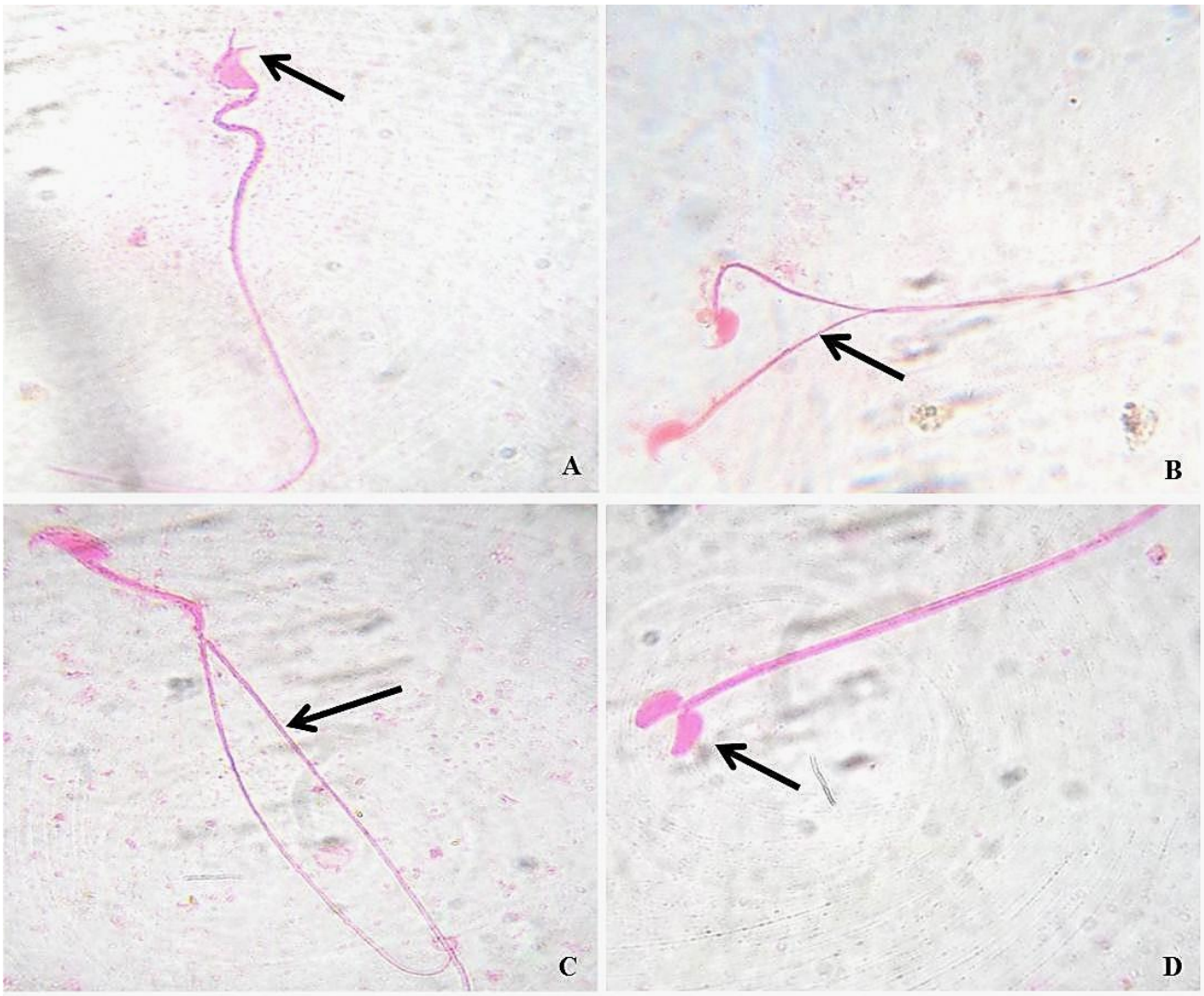

Figure 4. 148: Spermatozoa with double hooks (A) and double heads (B) from mouse treated with 150.00 $mgkg^{-1}$ of TiO_2 NPs; double tails (C) and double heads and fused mid pieces (D) form mouse treated with 18.75 $mgkg^{-1}$ of their mixture. Magnification: 1000X.

Table 4. 16: Interaction factor (IF) of titanium dioxide and zinc oxide nanoparticles using the sperm count and abnormalities

Conc. ($mgkg^{-1}$)	Sperm count IF ± SE_{IF}	Sperm abnormalities IF ± SE_{IF}
9.38	3.05 ± 3.15	64.69 ± 6.47
18.75	6.37 ± 2.58	25.78 ± 7.89
37.50	10.10 ± 2.21	10.41 ± 2.96
75.00	7.86 ± 1.82	-6.58 ± 1.27

4.5.3 Serum reproductive hormone in mice treated with titanium dioxide, zinc oxide nanoparticles and their mixture after 35 days

The serum concentrations of LH, FSH and testosterone in mice treated with TiO_2, ZnO NPs and their mixture for 35 days are presented in Figures 4.150 – 4.152. TiO_2, ZnO NPs and their mixture induced a significant ($p < 0.05$) reduction in the serum concentrations of LH in the mice. The serum concentrations of LH in the mice treated with 9.38, 18.75, 37.50, 75.00 and 150.00 $mgkg^{-1}$ of TiO_2, ZnO NPs and their mixture were lower than those treated with distilled water by a 11.0-, 3.6-, 1.9-, 4.3- and 2.4- fold decrease; a 2.6-, 2.9-, 1.5- and 6.2- fold decrease; a 2.2-, 3.4-, 4.1, 4.5- and 4.0 fold decrease respectively (Figure 4.150).

The serum concentrations of FSH in the mice treated with TiO_2 NPs showed a significant ($p < 0.01$) increase at the 75.00 and 150.00 $mgkg^{-1}$ in comparison with the mice treated with distilled water. In contrast, mice treated with ZnO NPs and their mixture respectively showed no significant ($p > 0.05$) increase at the doses of 9.38, 18.75, 37.50, 75.00 and 150.00 $mgkg^{-1}$ in comparison with those treated with distilled water (Figures 4.151). The concentrations of FSH in the treated mice were higher by a 1.5-, 1.6-, 1.9-, 4.1- and 3.0-fold increase; a 1.4-, 1.6-, 0.6-, and 0.5- fold increase; and 1.5-, 1.3-, 1.6-, 1.4- and 1.6-fold increase corresponding to the doses of the 9.38, 18.75, 37.50, 75.00 and 150.00 $mgkg^{-1}$ of TiO_2, ZnO NPs and their mixture.

The serum testosterone concentration in the treated mice showed a dose-dependent increase at 9.38, 18.75, 37.50, 75.00 and 150.00 $mgkg^{-1}$ but was significant ($p < 0.001$) only at the 150.00 $mgkg^{-1}$ of TiO_2 NPs in comparison with the mice treated with distilled water. ZnO NPs treated mice showed a significant ($p < 0.001$) increase in the serum testosterone at tested doses in comparison with the mice treated with distilled water. Likewise, the mixture of the NPs was able to induce a significant ($p < 0.05$) increase in the serum testosterone concentrations at doses of 9.38, 18.75 and 37.50 $mgkg^{-1}$ in comparison with those treated with distilled water. The serum concentrations of Testosterone in the mice treated with 9.38, 18.75, 37.50, 75.00 and 150.00 $mgkg^{-1}$ of TiO_2, ZnO NPs and their mixture were higher than those treated with distilled water by a 1.0-, 1.3-, 1.4-, 1.5- and

2.5- fold increase; a 2.3-, 2.3-, 2.0- and 2.6- fold decrease; a 2.1-, 2.0-, 1.9, 1.4- and 1.3 fold increase respectively (Figure 4.152)

4.5.4 Histopathological alterations induced by titanium dioxide, zinc oxide nanoparticles and their mixture in the testis of mice

The histopathology of the testes of the mice treated with distilled water showed numerous uniformly-sized seminiferous tubules which were closely packed with regular outlines, and contained numerous spermatogenic cells with spermatocytes and round spermatids. However, severe depletion of spermatogenic cells with irregular outlines, necrosis of spermatogenic cells, distended and void appearance of seminiferous tubules, loss of basal germinal epithelial cells, increase in luminal width, exfoliation of germinal cells from the basal compartment into the luminal compartment and congestion of testicular interstitial blood vessels were present in testes of mice treated with various doses of TiO_2, ZnO NPs and their mixture (Figure 4.153).

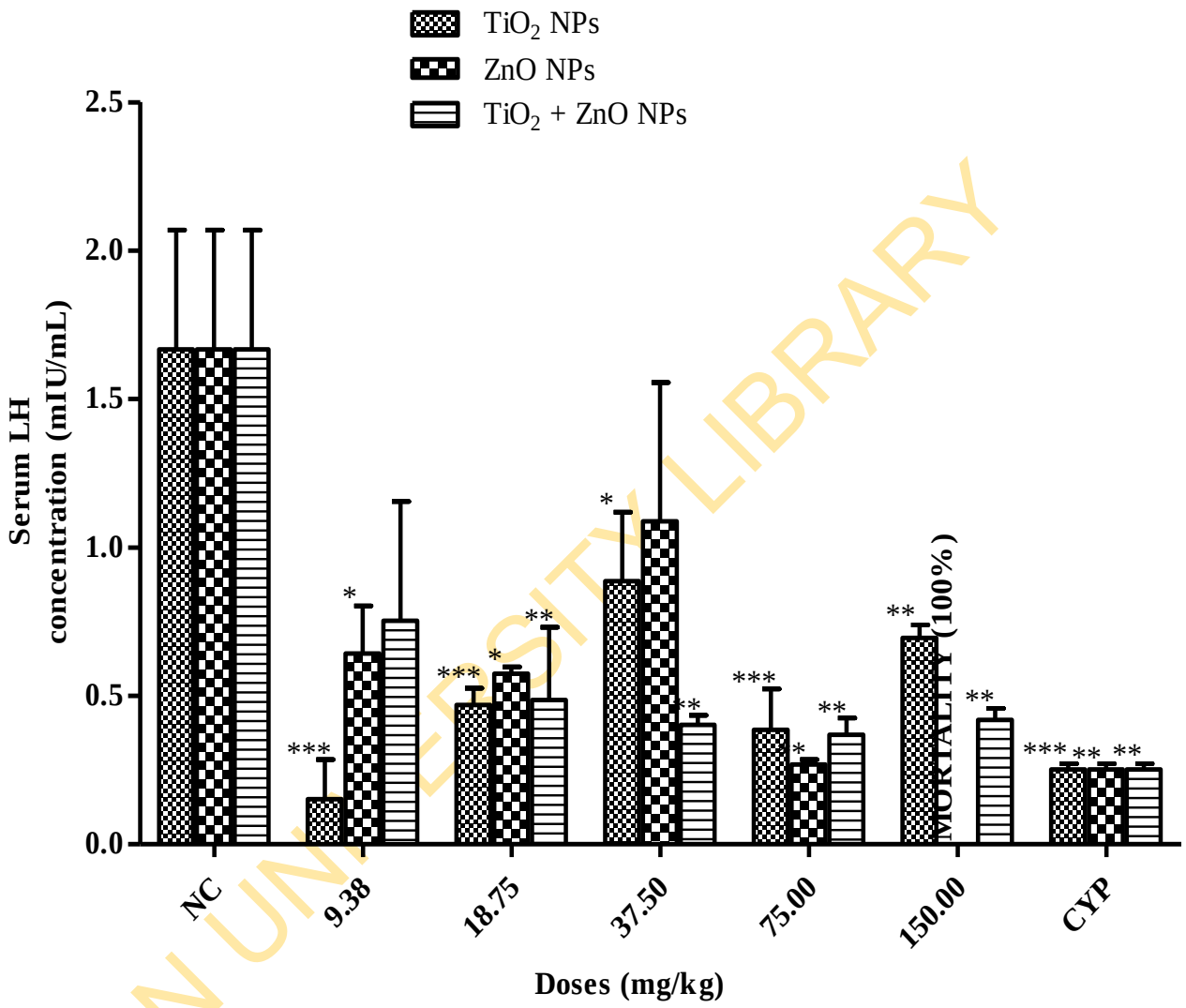

Figure 4. 149: Serum LH concentration in mice treated with TiO_2, ZnO NPs and TiO_2 and ZnO NPs at 35 days.

Data represent Mean ± SEM (n=4); * $p < 0.05$, ** $p < 0.01$ and *** $p < 0.001$ in comparison with the mice treated with distilled water. Negative control (NC) = distilled water; CYP = cyclophosphamide (positive control).

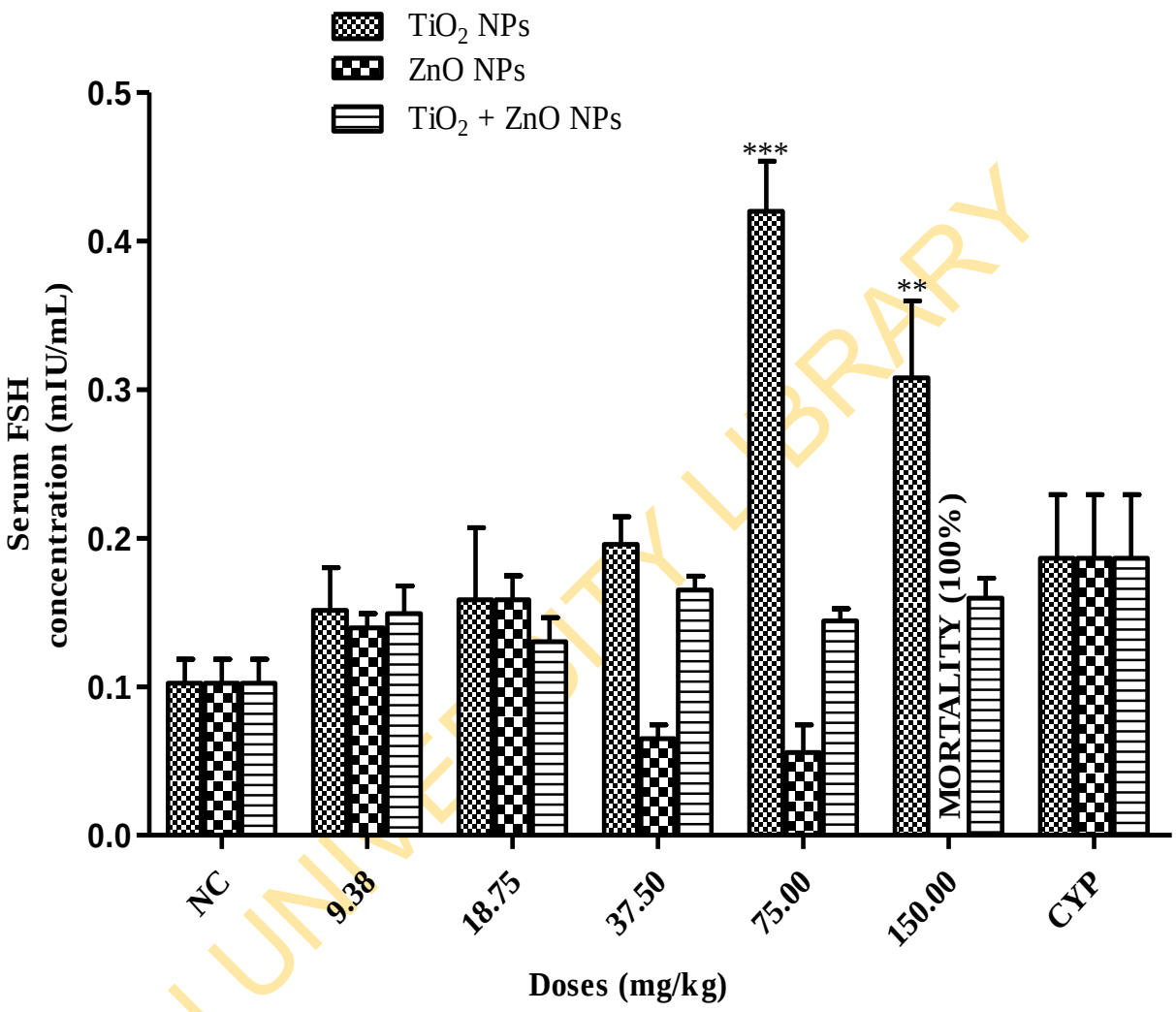

Figure 4. 150: Serum FSH concentration in mice induced treated with TiO_2, ZnO NPs and TiO_2 and ZnO NPs at 35 days.

Data represent Mean ± SEM (n=4); ** $p < 0.01$ and *** $p < 0.001$ in comparison with the mice treated with distilled water (NC) = distilled water; CYP = cyclophosphamide (positive control).

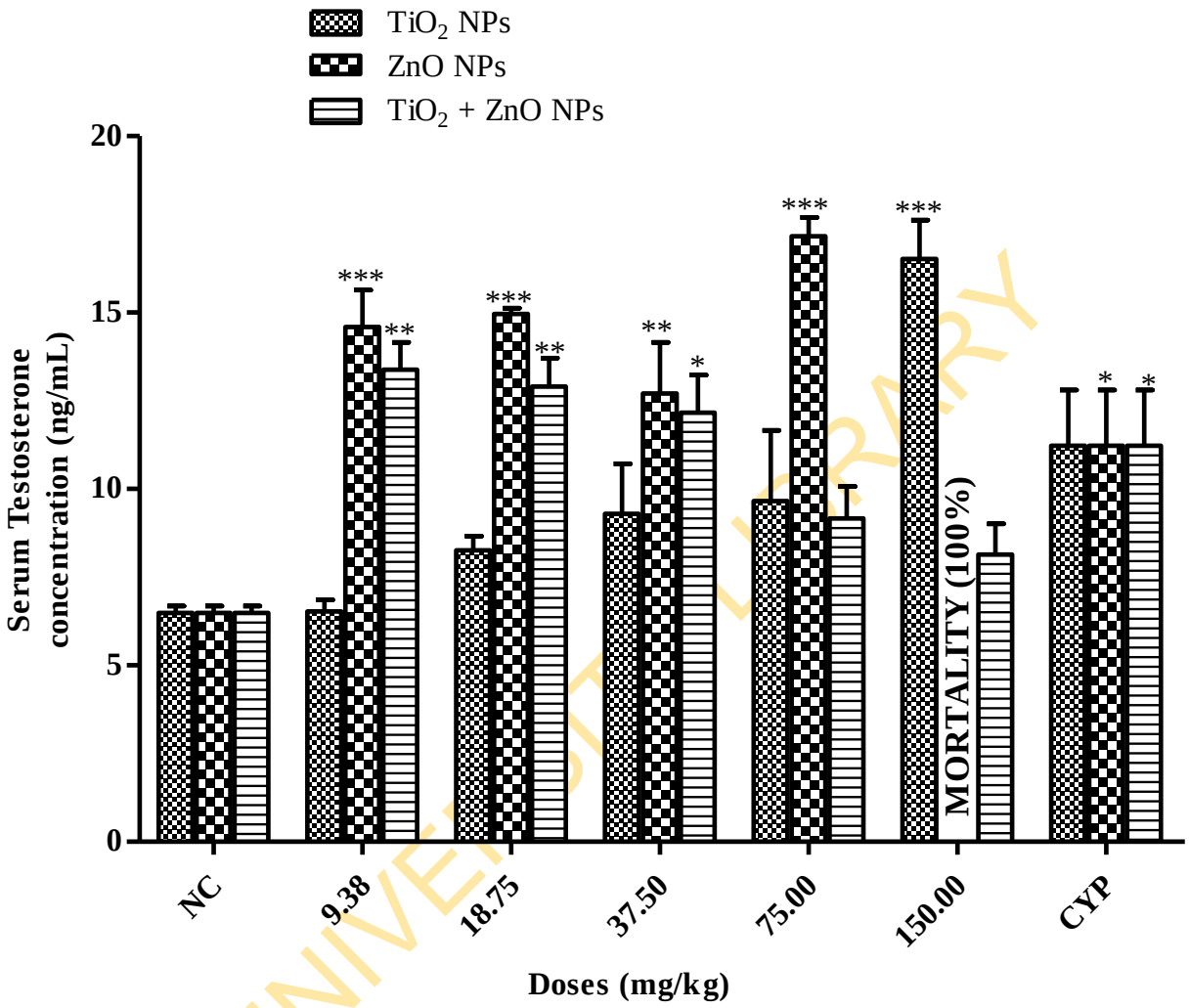

Figure 4. 151: Serum Testosterone concentration in mice treated with TiO_2, ZnO NPs and TiO_2 and ZnO NPs at 35 days.

Data represent Mean ± SEM (n=4); * $p < 0.05$, ** $p < 0.01$ and *** $p < 0.001$ in comparison with the mice treated with distilled water (NC) = distilled water; CYP = cyclophosphamide (positive control).

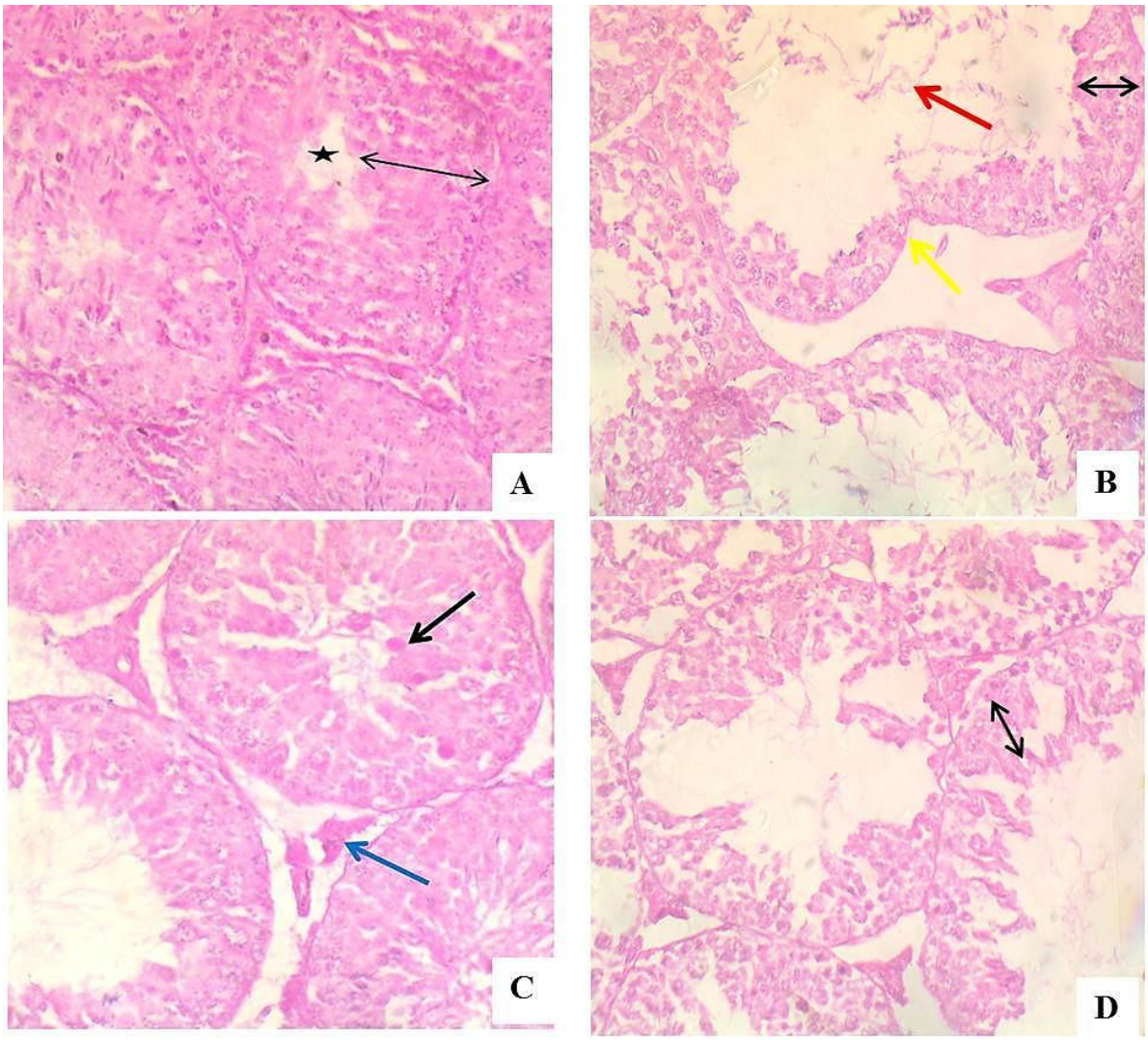

Figure 4. 152: Sections of the testes of treated mice. Mouse treated with distilled water shows closely packed seminiferous tubules with reduced lumen (black star) and high germinal epithelium (double end arrows) (A); 37.50 $mgkg^{-1}$ of TiO_2 NPs (B); 75.00 $mgkg^{-1}$ of TiO_2 NPs (C); and 37.50 $mgkg^{-1}$ of their mixture (D). Lesions observed include: loss of basal germinal epithelial cell (yellow arrow), decreased germinal epithelium (double ended arrow), increased luminal width (red arrow), congestion of testicular interstitial blood vessels (blue arrow), necrotic spermatogenic cells (black arrow) and severe loss and necrosis of basal germinal epithelial cells.

CHAPTER FIVE

DISCUSSION

The industrial and biomedical applications of nanoparticles are tremendously increasing and consequently leading to persistent increase in human exposure via oral, dermal, inhalation and injection (Pourhamzeh *et al*., 2016). Therefore, it has become imperative and of a growing concern to evaluate the potential of nanoparticles to bioaccumulate and cause undesirable health effects (Ferreira *et al*., 2015). So far, manufacturers, researchers and other end users are highly exposed to NPs either intentionally or unintentionally (Reshma and Mohanan, 2016). This has led to extensive investigation of various NPs on the respiratory system (Liang *et al*., 2009) and gastrointestinal tracts (Strojny *et al*., 2015; Patlolla *et al*., 2016; Bollu *et al*., 2016b; Srivastav *et al*., 2016), through intravenous (Gaharwar and Paulraj, 2015; Silva *et al*., 2017) and intraperitoneal exposure (Abdelhalim *et al*., 2015; Ferreira *et al*., 2015; Afifi *et al*., 2015). Thus, the present study focused on the exposure of TiO_2, ZnO NPs and their mixture on the somatic and germ cells. Based on our knowledge, this is likely to be the first major study of evaluating *in vivo* genotoxicity, systemic toxicity and possible mechanism of toxicity in mice treated with their mixture of TiO_2 and ZnO NPs.

The administration of NPs intraperitoneally allows rapid testing of their toxicity within a short period of time in the test animal (Silva *et al*., 2017). The peritoneal cavity is rich in blood vessels and thus increases the absorption of the tested material, mimicking the intravenous administration (Silva *et al*., 2017). In addition, this route of administration is usually employed to test animals and ensure that the accurate amount of the test material is adequately treated. Most importantly, NPs are treated via this exposure route because of the colloidal suspension that is formed in distilled water (Strojny *et al*., 2015).

5.1 Physicochemical characterisation of titanium dioxide, zinc oxide nanoparticles and their mixture using transmission electron microscopy and dynamic light scattering

One of the crucial steps in nanotoxicology studies is the physicochemical characterisation of NPs (Akhtar *et al*., 2012; Srivastav *et al*., 2016; Silva *et al*., 2017). The properties and the biological functions of NPs are highly dependent on the size, shape, surface area, surface charge and crystallinity (Shukla *et al*., 2014; Kansara *et al*., 2015; Srivastav *et al*., 2016). TiO_2, ZnO NPs and their mixture were characterised using two different methods: TEM and DLS. The TEM showed that TiO_2 NPs were spherical with a narrow distribution (Catalan *et al*., 2012; Zhang *et al*., 2013; Demir *et al*., 2015; Uboldi *et al*., 2016) while ZnO NPs were irregular with a wider distribution (Cho *et al*., 2013; Srivastav *et al*., 2016). The internalisation of NPs into the cell is determined by their shape (Magdolenova *et al*., 2014; Setyawati *et al*., 2016). It may be assumed that the spherical shape of TiO_2 NPs may have induced a higher diffusion coefficient, thus, penetrating faster while the irregular shape of ZnO NPs may have resulted into a lower diffusion coefficient, thereby prolonging penetration into the cells.

The size distribution, surface charge and polydispersity index were obtained by DLS. The DLS gives the hydrodynamic diameter by measuring the size distribution and Brownian motion of clustered particles (Akhtar *et al*., 2012; Sharma *et al*., 2012b; Shukla *et al*., 2014; Kansara *et al*., 2015). The larger hydrodynamic sizes of TiO_2, ZnO NPs and their mixture in sterile MilliQ water in comparison to their primary sizes provided by the manufacturer may have been due to the tendency of both NPs and their mixture to have agglomerated (Setyawati *et al*., 2016). The divalent ion and low zeta potential values may be factors that induced aggregation of TiO_2 and ZnO NPs in the sterile MilliQ water (Srivastav *et al*., 2016). These results are supported by the findings of Akhtar *et al*., 2012; Sharma *et al*., 2012b and Shukla *et al*., 2014.

The surface charge of NPs strongly determines the tendency of NPs to aggregate or disperse. The charge accumulation around the surface of NPs in a solution, given them their stability in a colloidal system, is defined as the zeta potential (Pasupuleti *et al*.,

2012a). The zeta potential values suggest that ZnO NPs were fairly stable while TiO_2 NPs and their mixture were less stable in the MilliQ water.

5.2 Acute toxicity induced by titanium dioxide, zinc oxide nanoparticles and their mixture in mice

The determination of the doses of TiO_2, ZnO NPs and their mixture was carried out using acute toxicity, which could induce mortality within 24 hours *vis a vis* displaying clinical signs of toxicity. The individual responses of the mice to the doses of TiO_2, ZnO NPs and their mixture observed in the exhibition of the various clinical signs of toxicity may be due to their immune systems that acted as defense mechanisms against the NPs. Mice treated with 150 and 300 $mgkg^{-1}$ of TiO_2 NPs did not show any mortality or abnormal changes within 24 hours. This finding supports Li *et al*. (2010c) where mice were intraperitoneally treated for 14 days consecutively with TiO_2 NPs (5 nm; 5 – 150 $mgkg^{-1}$), and no death was recorded; feeding and drinking of treated mice were normal. Also, Silva *et al*. (2017) treated mice intraperitoneally with TiO_2 NPs (100 nm; 2 $mgkg^{-1}$) for 10 days and observed no death and abnormal behaviour. However, the body weight of the treated mice was significantly reduced. In contrast, mice treated with 150 and 300 $mgkg^{-1}$ of ZnO NPs showed severe toxicity and mortality within 24 hours. Our result is also in consonance with Esmaeillou *et al*. (2013) where 20 – 30 nm of ZnO NPs (333 $mgkg^{-1}$) was administered via oral gavage to mice. The researchers observed loss of appetite, severe lethargy and vomiting. On the third day after administration, one mouse died. The induction of 25 nm, 80 nm and 155 nm of ZnO NPs (5 g/kg) to ICR mice via single oral exposure showed that some female mice treated with 155 nm, 80 nm and 25 nm were inactive, anorectic and spiritless, and died within 2 days (Wang *et al*., 2007). Conversely, Li *et al*. (2012) treated ICR mice (males and females) to 50 nm of ZnO NPs (1.25, 2.5 and 5 g/kg bw) or > 100 nm ZnO MPs (1.25, 2.5 and 5 g/kg bw) orally for 14 days. All mice survived throughout the testing period without exhibiting any abnormalities. Likewise, Baek *et al*. (2012) treated rats for 14 days to 20 nm and 70 nm of ZnO NPs (50 $mgkg^{-1}$, 300 $mgkg^{-1}$ and 2000 $mgkg^{-1}$). The rats treated 50 and 300 $mgkg^{-1}$ showed no mortality, body weight changes or abnormal behaviour when in comparison with the mice treated

with distilled water. Contrastingly, diarrhoea and slight body weight reduction were revealed in some rats that received 2000 $mgkg^{-1}$.

The discrepancy between the results obtained in comparison with others is most likely attributed to their solubility properties. ZnO NPs are soluble in acidic environments (such as the stomach, pH 5.5), thereby dissociating to produce Zn^{2+} ions that absorb into the circulatory system, thereby contributing to their toxicity (Cho *et al*., 2013; Srivastav *et al*., 2016). In contrast, TiO_2 NPs are highly insoluble (Falck *et al*., 2009) and stable (Choi *et al*., 2013), which may make them less toxic than ZnO NPs. The exposure route (oral, intraperitoneal, and intravenous), experimental animals (rats, mice, strain, and gender), exposure dose, duration, solvent used in dissolving the NPs and preparation of the NPs may all be contributing factors to the different results obtained.

5.3 Cytogenotoxic effects of titanium dioxide, zinc oxide nanoparticles and their mixture in the bone marrow cells of mice

To emphasise the role of genetic damage in human health, genotoxicity of TiO_2, ZnO NPs and their mixture were evaluated. The MN assay is one of the genotoxicity screening tests for chemicals, which detects chromatid and chromosome breakage (clastogenicity), and chromosome lagging and loss (aneugenicity) (Savage, 1988). The frequency of micronuclei in the PCE, as evaluated by the MN assay, increased in a dose-dependent manner in mice treated with TiO_2 NPs for 5 days. The induction of MN in mice treated with TiO_2 NPs is an indication that they have clastogenic and aneugenic effects on the bone marrow cells.

The MN induction by TiO_2 NPs may be due to their physicochemical properties of small primary particle size and large surface area to mass ratio. Nanoparticles with a small size and large surface area to mass ratio have larger amount of atoms on their surfaces, leading to high reactivity potential with biological materials (Magdolenova *et al*., 2012; 2014). In order words, TiO_2 NPs owing to their small size may have penetrated the cell membrane and the nuclear pore complex where they probably interacted directly with the DNA or proteins involved in spindle formation, cell division and chromosome segregation (AshaRani *et al*., 2009; Barillet *et al*., 2010).

The MN induction for the 10- day exposure period showed a reduction of micronuclei across tested doses in comparison with the 5- day exposure period, indicating a reduction of DNA damage with time in the bone marrow cells. This shows that protective pathways and DNA repair processes may have occurred (Balasubramanyam *et al*., 2009b). Previous studies have shown that NPs are transported to the blood (Balasubramanyam *et al*., 2009b) and accumulate in the spleen and liver (Singh *et al*., 2013). The liver, bone marrow and spleen, which make up the mononuclear phagocytic system consist of monocytes and macrophages, and specialised endothelial cells, which remove and neutralise pathogens that enter the body. These cells may have the capacity to take up TiO_2 NPs through phagocytosis, thereby significantly reducing them over time (Sycheva *et al*., 2011; Singh *et al*., 2013).

The non-significant induction of micronuclei in the cells of the bone marrow of mice induced by ZnO NPs for 5- and 10- days implies that they may not be genotoxic. The effect may be due to the larger particle size, surface area and agglomeration of ZnO NPs. ZnO NPs (< 100 nm) used in the study agglomerated excessively in MilliQ water, thereby resulting in larger diameter as indicated by the hydrodynamic diameter and polydispersity index preventing their penetration in the nuclear membrane. Generally, NPs have the tendency to agglomerate in different surrounding media (e.g. distilled water, phosphate buffered saline and culture medium among others) due to the Van der Waals' forces they exhibit at the nanoscale. Agglomeration occurs because of the interaction between the surface charge of the NPs and their surrounding medium. However, when agglomeration occurs, it may change the physicochemical properties of ZnO NPs (Kumar and Dhawan, 2013) and reduce the bioavailability and toxicity of ZnO NPs in the bone marrow cells of the treated mice. The micronuclei induced by ZnO NPs in the present study may be due to their solubility, in comparison with extremely less soluble metal oxide NPs, such as TiO_2 NPs (Cho *et al*., 2013). In addition, ZnO NPs may also have been retained in the cytoplasm of the cell and gain access into the nuclear DNA when the nuclear membrane disintegrated during cell division (Magdolenova *et al*., 2014).

Similarities have been reported by Li *et al*. (2012) and Bollu *et al*. (2016b). However, other studies have shown the ability of ZnO NPs to induce genotoxicity (Sharma *et al*.,

2012a; Choi *et al*., 2015, Ghosh *et al*., 2016). Differences observed may be as a result of the preparation and size of ZnO NPs, duration of exposure and the concentrations employed. In comparison to the 10-day exposure of TiO_2 NPs, no reduction of MN was observed for the ZnO NPs exposure condition. This may be due to the persistence of ZnO NPs in the circulatory system of the treated mice (Cho *et al*., 2013). Zinc oxide nanoparticles intraperitoneally administered to mice take a longer time to be eliminated from the system in comparison to mice orally treated with ZnO NPs (Li *et al*., 2012).

The PCE: NCE ratio for any test-treated animal gives the cytotoxicity index as well as the rate of cell proliferation (Suzuki *et al*., 1989; Krishna and Hayashi, 2000). There were significantly increased levels of NCE in comparison with PCE in mice treated with TiO_2 NPs during the 5- and 10- day exposure periods. In contrast, percentage PCE: NCE in mice treated with ZnO NPs significantly increased only at the highest concentration for the 5- day exposure period. This indicates that both NPs have the ability to induce rapid proliferation and differentiation of PCE to NCE within the bone marrow resulting to bone marrow toxicity, cell depression, aging and reduction of the normal life span (Balasubramanyam *et al*., 2009; Singh *et al*., 2013; Lozovska *et al*., 2015).

TiO_2 NPs showed a higher genotoxicity than ZnO NPs. This may be due to the assumption that titanium is a transition metal, capable of inducing oxidative stress from DNA damaging groups like the hydroxyl radicals produced from hydrogen peroxide and superoxide anions, which are cellular oxygen metabolic products (Manke *et al*., 2013). Also, it may be due to the penetration of TiO_2 NPs via the mitochondrial membrane by passive diffusion (Zhang *et al*., 2012), leading to ROS production, opening of the transition pores and the loss of the mitochondrial membrane potential (MMP) (Manke *et al*., 2013; Magdolenova *et al*., 2014; Dobrzynska *et al*., 2014).

The extensive usage of TiO_2 and ZnO NPs individually can increase the risk of their co-existence causing health risks to the environment and humans. Their mixture showed a reduction of MNPCE below the negative control and an antagonistic effect during the 5-day exposure period. The antagonistic effect may be due to the agglomeration of their mixture in MilliQ water as revealed by the polydispersity index preventing their immediate genotoxic effect to the bone marrow cells. The MNPCE frequency and

percentage PCE: NCE during the 10- and 5- day exposure periods respectively were higher at lower dose (18.75 $mgkg^{-1}$), with a gradual decline with increasing doses. This may have been due to the number of particles present in distilled water. Lower doses tend to have lower particle number, thereby resulting into less agglomeration while higher doses tend to have higher particle number resulting into increased agglomeration. Kurzawa-Zegota *et al*. (2017) stated that increase in agglomeration may most likely be due to the increase in the chances of interparticle interaction as doses increase. The degree of agglomeration occurs as a result of the higher chances of particles interacting due to the surface charges.

The synergistic effect of the mixture of TiO_2 and ZnO NPs resulting in an increase in the MNPCE during the 10- day exposure period is an indication that the mixture is more genotoxic through the induction of more micronuclei than the individual forms of TiO_2 or ZnO NPs. The synergism observed may be explained by the following: Firstly, the behaviour of NPs is governed by the unique characteristic of diffusion; and as the particle size decreases, with increase in surface area, their diffusion increases making them behave similar to a gas (Kumar and Dhawan, 2013). TiO_2 NPs used in this study may have a high diffusion coefficient due to the large surface area, thereby migrating faster into the cell membrane first while ZnO NPs may have a smaller diffusion coefficient migrating with time, and working synergistically with TiO_2 NPs (Kumar and Dhawan, 2013).

Secondly, it is well known that both NPs have photocatalytic properties; hence they are used in the adsorption and degradation of other environmental pollutants. With the large surface area, TiO_2 NPs may have served as a platform for an effective adsorption rate to take up large amounts of ZnO NPs through electrostatic interaction and cross the cell membrane thereby increasing the intracellular concentration that optimised the synergistic interaction increasing DNA damage (Liu *et al*., 2013). Thirdly, exposure to their mixture may indicate enhanced accumulation of TiO_2 and ZnO NPs, which might depend on the bad excretion capability of the mice. Lastly, the molar ratio (1:1) of their mixture has been shown to be the highest photocatalytic activity in degrading and adsorbing pollutants by producing hydroxyl radicals (Jiang *et al*., 2008). Their mixture may have increased the concentration of hydroxyl radicals intracellularly. It is obvious that when excess hydroxyl

radicals are produced intracellularly, they interact with lipids causing lipid peroxidation, which can in turn, damage DNA, proteins and other lipids (Jiang *et al*., 2008).

It hypothesised that TiO_2 NPs can cross biological barriers without a specific transporter or through paracellular transport and be distributed across the cell membrane and cytoplasm. This suggests that ZnO NPs adsorbed into TiO_2 NPs could enter the bone marrow cells. Once in the nucleus, ZnO NPs may dissociate to Zn^{2+} and induce DNA damage. Moreover, adsorption of ZnO NPs by TiO_2 NPs, combined with the capability of TiO_2 NPs to penetrate the membranes of cells is critical to increasing intracellular concentration of both ZnO and TiO_2 NPs (Zheng *et al*., 2012). Overall, TiO_2, ZnO NPs and their mixture were able to induce both clastogenic (chromosome breakage) and aneugenic effects (inhibition of mitotic spindle) attributed to primary and secondary genotoxicity. Clastogenicity of both NPs and their mixture may be due to the continuous contact of the NPs with the DNA. The direct or indirect involvement of proteins involved in chromosome segregation, and the mitotic spindle components in cell division may have a physical interaction with the NPs resulting in aneugenicity (Muller *et al*., 2008; Patlolla *et al*., 2016).

The safety of TiO_2 and ZnO NPs has been raised through several cytotoxic and genotoxic studies as they generate ROS resulting to oxidative stress. ROS has revealed a strong relationship between oxidative stress and NPs (Rahman *et al*., 2002; Osman *et al*., 2010; Akhtar *et al*., 2012). Accordingly, excessive ROS production may be one of the mechanisms through which both NPs and their mixture induced micronucleus, as they can react with the cell membrane inducing a breakdown of the membrane lipids resulting into lipid peroxidation (Manke *et al*., 2013), imbalance of intracellular calcium homeostasis (Zhang *et al*., 2012) and alterations in several metabolic pathways. Chromatin fragmentation, which is a key feature of apoptosis, can be initiated through the calcium-dependent endonuclease activation occurring from the imbalance of calcium homeostasis (Rahman *et al*., 2002). Our findings are in accordance with Kang *et al*. (2008), Trouiller *et al*. (2009), Sycheva *et al*. (2011), Song *et al*. (2012), Tavares *et al*. (2014), Dobrzynska *et al*. (2014) and Demir *et al*. (2015). In contrast, no genotoxicity was found in studies of Sadiq *et al*. (2012), Lindberg *et al*. (2012), Li *et al*. (2012), Ramesh *et al*. (2014),

Browning *et al*. (2014) and Bollu *et al*. (2016b). Moreover, the existing results of genotoxicity studies of TiO_2 and ZnO NPs are conflicting due to the cellular responses, which may depend among others on the particle size, degree of agglomeration, doses, and preparation method.

The toxicity of TiO_2 NPs and ZnO NPs are well known and their simultaneous presence might induce an overlapping effect. From this study, it may be assumed that TiO_2 NPs or ZnO NPs exhibit a synergistic property regardless of the inorganic compound utilised as a mixture with them. This has been indicated through several experimental studies that TiO_2 NPs interacted with lead acetate (Zhang *et al*., 2010; Du *et al*., 2012), bisphenol A (Zheng *et al*., 2012), arsenic (Wang *et al*., 2011), cadmium chloride (Xia *et al*., 2011), p, p' – DDT (Shi *et al*., 2010), and ZnO NPs combined with paclitaxel or cisplatin (Hackenberg *et al*., 2012) to synergistically induce cytogenotoxicity in different cell lines. Furthermore, Jiang *et al*. (2008) showed that the mixture of TiO_2 and ZnO NPs in the molar ratio1:1 decolourised CI Basic Blue 41 dye effectively with time, pH and catalyst amount.

Morphological changes observed in the bone marrow haemopoietic stem cells across all the doses of TiO_2, ZnO NPs and their mixture, will be one of the very few studies to report cytomorphological characteristics in assessing nanotoxicity. A normal red blood cell has a diameter of 8 µm with a central pallor as a result of its biconcavity. However, an abnormal red blood cell occurs as a result of its deviation from the normal size, shape and colour. Normal red blood cells are referred to as normocytic (normal sized red cells) and normochromic (normal staining of red cells seen because of adequate haemoglobinisation) (Cheesbrough, 2005). Aetiological processes give rise to different red blood cell abnormalities and the interpretation of red blood cell pathology with other laboratory and clinical information provide the necessary information on disease diagnosis.

The microcytic (smaller than normal red cells) hypochromic (pale staining of red cells) red blood cells induced by both NPs and their mixture is an indication that they may cause chronic anaemia. This may be as a result of the deficiency of haemoglobin synthesis due to Fe^{2+} replacement to either Ti^{4+} or Zn^{2+}. Macrocytic (larger than normal cells) hyperchromic (excess haemoglobinisation) red cells induced by the NPs implies that they may have the capability of altering erythropoiesis and haemoglobin synthesis. This may

occur due to folate deficiency, oxidative stress erythropoiesis and impairment of DNA synthesis in the bone marrow. In addition, the presence of target cells (codocytes) (hypochromic cells with a round pigmentation at the central area) may be an indication of the NPs inducing severe liver disease and iron deficiency anaemia. Large amount of blebbing of the cytoplasmic membrane of cells were mostly observed in the two higher doses of both NPs and their mixture. Blebbing of the cytoplasmic membrane is one of the stages through which apoptosis occur. This may occur through the damage of the mitochondrial membrane potential (MMP) resulting in the destruction of intracellular signal transduction and release of proteins that will activate apoptosis (Rahman *et al*., 2002). Lozovska *et al*. (2015) showed that cells with increased MN frequency have a fall in the MMP.

5.4 Effects of titanium dioxide, zinc oxide nanoparticles and their mixture on organ weights of mice

One of the most important indicators in toxicology is the organ weight; it reflects the impact of a test agent on the metabolism due to the immunological and health status of the body (Bailey *et al*., 2004; Almansour *et al*., 2015). Generally, both NPs and their mixture induced atrophy in the liver, spleen and brain while hypertrophy was induced in the kidneys, heart and testes of the treated mice during the 5- and 10- day exposure periods. A possible explanation for liver, spleen and brain atrophies induced by the NPs and their mixture may be due to the degeneration of the hepatocytes, splenocytes and neurons, respectively. Subsequently, kidney enlargement may be due to agglomerated NPs blocking the glomeruli and preventing proper filtration. This study is similar to Choi *et al*. (2015) who observed significant reduction in the coefficient of the liver and increase in the coefficient of the kidneys in rats intravenously treated with 30 $mgkg^{-1}$ of ZnO NPs after 24 hours. Similarly, a reduction which was significant in the relative weights of the brain and increased significantly in the kidneys during the 5- day exposure period conformed to the study of Liu *et al*. (2009a).

In contrast to our results obtained, a significant increase in the liver and slight changes in the kidneys and spleen of mice was observed after oral exposure once to TiO_2 NPs (25 and 80 nm) for 2 weeks (Wang *et al*., 2007). Also, a significant increase in the coefficients of

liver, kidney and spleen after a 14-day exposure were observed by Liu *et al*. (2009a). Similarly, Li *et al*. (2010c) revealed a considerable gain in the coefficient of spleen of female mice treated intraperitoneally with 5 - 150 $mgkg^{-1}$ of TiO_2 NPs for 45 consecutive days. Silva *et al*. (2017) revealed a significant reduction in the kidneys and increase in the spleen of mice treated intrapritoneally with 2 $mgkg^{-1}$ of TiO_2 NPs for 10 days. The discrepancy between the present study and previous once might be attributed to the variations in sizes of the NPs, doses, and exposure duration and routes. Nonetheless, all the studies showed that NPs are able to target the liver, kidneys, spleen and brain regardless of the NP type and experimental variations employed.

5.5 Effects of titanium dioxide, zinc oxide nanoparticles and their mixture on the haematological parameters in mice

As nanoparticles are transported through the circulatory system, they interact directly with the blood components (WBC, RBC, dissolved nutrients, bioactive factors, platelets, coagulation factors and serum proteins) to induce inflammatory responses and haematological changes (Lovric *et al*., 2005; Choi *et al*., 2013; Shi *et al*., 2013; Gaharwar and Paulraj, 2015; Setyawati *et al*., 2015; Silva *et al*., 2017). An effective and sensitive index to the physiological and pathological changes in animals and humans is the haematological characteristics (Grissa *et al*., 2015). Haematological parameters observed during the 5- day exposure period showed a decrease in RBC, Hb and PCV count in mice treated with TiO_2 NPs in comparison with those treated with distilled water. The decreased level of RBC, Hb and PCV in blood might be due to the hemolytic condition, reduced red cell production and toxicity to the bone marrow induced by TiO_2 NPs, eventually leading to anaemia. The NPs may have affected heme biosynthesis through metal ion exchange as Ti^{4+} may replace ferric ion utilised in haemoglobin synthesis, reducing erythropoiesis and haemoglobin production and increasing the rate of destruction of the erythrocytes in the haemopoietic organs (Grissa *et al*., 2015; Srivastav *et al*., 2016). This is similar to the observations of Grissa *et al*. (2015) who reported significant reduction in RBC, HCT and Hb and a significant increase in MCV, PLT, MPV and WBC in rats treated with TiO_2 NPs (5 - 12 nm; 50, 100 and 200 $mgkg^{-1}$) orally for 60 days.

Similarly, Srivastav *et al*. (2016) reported decreased levels of RBC, Hb, HCT and platelets in rats treated with 2000 $mgkg^{-1}$ of ZnO NPs 48 hours post administration.

Our study also revealed increased levels of RBC, Hb and PCV after 10- day exposure to TiO_2 NPs, and also after both 5- and 10- day exposure to ZnO NPs and their mixture. This is an indication that both NPs and their mixture induced polycythaemia compared to the low levels of RBC for the 5- day exposure period. Reports have shown that dehydration or hypoxia may induce elevated RBC, PCV and Hb (Nitsche, 2004). Excessive release of erythropoietin due to renal damage may stimulate production of red cells (Cheesbrough, 2005). This result is in accordance with Wang *et al*. (2008a) where it was demonstrated that 20 nm and 120 nm of ZnO NPs administered to mice induced increased levels of RBC and HCT. Furthermore, decreased levels of MCH and MCHC were found in TiO_2 NPs during both 5- and 10- day exposure periods and 5- day exposure period of both ZnO NPs and their mixture, which is associated with mitotic period delay (Cheraghi *et al*., 2013).

Previous studies have shown that growth retardation and anaemia resulting from deficiencies in copper and iron may be due to excessive dietary zinc in animals (Hein, 2003). Srivastav *et al*. (2016) showed that excess ZnO NPs were able to induce copper deficiency, in which copper is an essential co-factor for ferrooxidase. Ferroxidase reduction leads to the immobilisation of liver iron and iron recycling of the erythrocytes by the Kupffer cells (Chen *et al*., 2006). Also in this study, WBC counts levels were significantly decreased during the 10- day exposure period of ZnO NPs and both 5- and 10- day exposures of the mixture. The decreased WBC counts may be related to the immunosuppressive effect of TiO_2 and ZnO NPs on pluripotent stem cells in the bone marrow (Cheraghi *et al*., 2013).

Due to the higher surface area to mass ratio and more influence on the cell membrane, TiO_2 and ZnO NPs may have influenced the WBC mitochondria and altered their enzyme activity. It was also reported by Sriram *et al*. (2010) that apoptosis occurred through the activation of mitochondrial enzyme caspase 3 in lymphoid cancerous cells treated with Ag NPs. For this reason, TiO_2 and ZnO NPs perhaps may have induced oxidative stress and adversely affected the structure and physiology of the cells, oxidative metabolism, fat membrane structure and function that may induce red and white blood cells to be

destroyed when they pass the reticuloendothelial system of spleen and liver (Iwagami, 1996; Sharma *et al*., 2009).

5.6 Effects of titanium dioxide, zinc oxide nanoparticles and their mixture on the biochemical parameters evaluated in mice

The detoxifying organ in humans is the liver; making it susceptible to NP-induced damage (Awasthi *et al*., 2015; Ferreira *et al*., 2015; Silva *et al*., 2017). Assessment of liver functions takes into considerations hepatocellular integrity (aminotransferases), formation and subsequent free flow of bile (bilirubin and transpeptidase) and protein synthesis (albumin and globulin). The most frequently used indicators for hepatocellular injury are the alanine aminotransferases (ALT) and aspartate aminotransferase (AST). Their activities are rapidly increased when the liver is damaged by any cause, including hepatitis or hepatic cirrhosis (Sheth *et al*., 1998) and inflammatory condition (Pasupuleti *et al*., 2012a). The serum AST activity was significantly elevated after both 5- and 10- day exposure periods of TiO_2, ZnO NPs and their mixture. Subsequently, serum ALT activity was significantly elevated after the 5- day exposure period of both NPs and their mixture. This may be an indication that both NPs and their mixture altered the hepatocellular membrane permeability through ionisation of TiO_2 and ZnO NPs possibly resulting into liver damage. Our findings agree with Wang *et al*. (2007), Liu *et al*. (2009a), Pasupuleti *et al*. (2012a), Li *et al*. (2012), Sharma *et al*. (2012a), Singh *et al*. (2013), Shukla *et al*. (2014), Choi *et al*. (2015), Srivastav *et al*. (2016) and Silva *et al*. (2017).

Interestingly, this study indicated that TiO_2, ZnO NPs and their mixture induced significant reduction in serum ALT activity across all the doses after the 10- day exposure period. This study may be the first to report significant low ALT activity in nanotoxicity. Increased risks of mortality, end-stage renal disease and increased frailty have been associated with low ALT activity (Ono *et al*., 1995; Yasuda *et al*., 1995). Reduced ALT activity is used as a marker for detecting 'early aging syndrome' and sarcopenia (Ramaty *et al*., 2014). Decreased activity of ALT does not indicate a sign of recovery but cell destruction, which results in the inadequacy of the remaining hepatocytes to support life (Reichling and Kaplan, 1988). This corroborates our earlier finding where there was

mortality from the sixth day in mice treated with ZnO NPs and their mixture during the 10- day exposure period.

Reports have shown that there are more clinical significance in the ratio of AST to ALT than their individual activities. Patients with liver impairment such as liver fibrosis and chronic hepatitis C (Gowda *et al*., 2009) usually have an increased ratio of AST to ALT greater than 1 (Giannini *et al*., 2003). In the study, TiO_2, ZnO NPs and their mixture induced an elevated ratio greater than 1, which suggests that both NPs and their mixture may have induced liver cirrhosis in the treated mice. Another clinical biomarker assessed for liver functionality is Gamma Glutamyl Transferases (GGT). GGT activity is used primarily for hepatobiliary and pancreatic disease evaluation and are abnormally increased in cholestasis (decrease in bile flow due to impaired secretion by the hepatocytes) (Lee *et al*., 2005). In this study, a significant increase in GGT activity was induced, indicating that TiO_2, ZnO NPs and their mixture may have induced biliary obstruction.

An important biomarker for bile flow obstruction is bilirubin concentration, which is formed from the breakdown of haemoglobin in the reticuloendothelial system (Gowda *et al*., 2009). Damaged hepatocytes are unable to excrete bilirubin normally thereby causing bilirubin build up in the blood. Our results showed an elevation of both total and direct bilirubin induced by TiO_2, ZnO NPs and their mixture after the 5- and 10- day exposure periods. This might indicate hepatocellular damage, haemolysis, defects in biliary metabolism and obstruction of the bile ducts. One of the most predominant serum-binding proteins in the body is albumin, which is synthesised in the liver (Ballmer, 2001). It is involved in the maintenance of osmotic pressure, metal ions, bilirubin, drugs, amino acids and transportation of thyroid hormones. Hepatic cirrhosis, nephrotic syndrome and malnutrition are a few conditions that occur as a result of low levels of albumin (Hypoalbuminemia). In addition, acute and chronic inflammatory responses also induce hypoalbuminemia (Don and Kaysen, 2004; Kaysen *et al*., 2004).

For the urine albumin concentration, TiO_2 NPs induced microalbuminuria in the mice after both 5- and 10- day exposure periods. Adverse renal expression of vascular damage is predicted through albuminuria (Dabla, 2010). However, ZnO NPs after the 5- and 10- day exposure period and their mixture after the 5- day exposure period induced

macroalbuminuria or proteinuria. Proximal tubular damage, glomerular filtration disease that prevents the ability of the tubular cells' to reabsorb or combinations of both are suggestive of the excessive excretion of albumin (Dabla, 2010).

Serum hypoalbuminemia (low levels of albumin) was induced by TiO_2 NPs and their mixture after both 5- and 10- day exposure periods, indicating that the NPs and their mixture may have induced liver disease (cirrhosis or hepatitis), renal dysfunction and chronic inflammation, among others. Subsequently, significant increases of serum albumin concentration (hyperalbuminemia) were induced by ZnO NPs after the 5- and 10-day exposure periods. A possible explanation for hyperalbumnemia may be due to chronic dehydration, severe infections, hepatitis, chronic inflammatory disease and kidney disease.

Maintenance of physiological homeostasis is important for a healthy renal function. Serum urea and creatinine are good indicators for renal function and their increased levels in serum indicate kidney dysfunction. The major end product of nitrogen-containing substances is urea, which is mainly excreted by the kidneys. The present study indicated increased levels of urea after 5- day exposure period and a decrease after the 10- day exposure period in mice treated with TiO_2, ZnO NPs and their mixture. Both NPs and their mixture may have the capability of inducing acute or chronic kidney damage or failure. In addition, excessive breakdown of tissue protein from wasting diseases may also increase urea concentration. Severe hepatic dysfunction may lead to decreased BUN, since urea is synthesised the liver (Baum *et al*., 1975).

Creatinine is a by-product of muscle metabolism, which is released into the blood and excreted by the kidneys into the urine. Basically, the function of the glomerular filtration rate (GFR) determines the concentration of serum creatinine. When the GFR significantly decreases due to kidney dysfunction, the serum creatinine concentration rapidly increase. TiO_2 NPs and their mixture significantly increased the levels of serum creatinine in treated mice after the 5- and 10- day exposure periods. The possible explanation for this may be due to the fact that both NPs and their mixture have the capacity of inducing a poor GFR of the kidney (Jurado and Mattix, 1998; Dalton *et al*., 2010). The levels of serum creatinine were found to be lower than the control in mice treated with ZnO NPs after the 5- day exposure period. This may possibly be due to muscle mass deterioration and/or

kidney impairment, since creatinine is produced from muscle metabolism and excreted by the kidneys.

One of the most common metabolic dysfunctions is the lipid abnormalities. They have been employed in determining the development of atherosclerosis or any heart-related diseases (Siemianowicz *et al*., 2000). Our study revealed that TiO_2 and ZnO NPs induced a significant reduction in the level of serum cholesterol after 5- and 10- day exposure periods while both NPs and their mixture induced an increase in serum cholesterol after 10- day exposure period respectively. Subsequently, significant reductions in serum triglyceride levels were induced by both NPs and their mixture. Additionally, HDL-cholesterol levels were significantly low in mice treated with TiO_2 NPs after 5- day exposure period while ZnO NPs and their mixture induced a significant increase after 5-day exposure period. However after the 10- day exposure period, both NPs and their mixture induced a significant reduction in serum HDL-cholesterol levels.

Low plasma cholesterol levels (hypocholesterolemia) have been generally accepted to be a marker for cancer. It is considered an effect for a neoplastic process, where they produce the pro-inflammatory marker and the tumour necrosis factor that lowers serum cholesterol levels (Siemianowicz *et al*., 2000). For example, reduced plasma cholesterol levels are found in patients who often exhibit liver cancer (Iso *et al*., 2009), breast cancer (Touvier *et al*., 2015) and lung cancer (Siemianowicz *et al*., 2000). The most frequent lipoprotein abnormality is the low HDL-cholesterol (hypoalphalipoproteinemia), correlated with coronary heart disease risk (Van der Steeg *et al*., 2008; Bitzur *et al*., 2009). In our study, TiO_2, ZnO NPs and their mixture showed to be quite effective in lipid metabolism by the significant decrease in HDL fraction and the increased serum cholesterol with a concomitant significant decrease in triglycerides, respectively.

In comparison to the negative control, mice treated with TiO_2, ZnO NPs and their mixture displayed lower HDL-cholesterol concentrations in the sera after 10-day exposure period. Interestingly, this study appear to be the first to examine the consequence of the mixture of both NPs on the lipid profile. Cholesterol is carried from the arteries to the liver with the help of HDL-cholesterol. Therefore, high levels of serum cholesterol may occur due to hepatic dysfunction (Toth, 2005; Le and Walter, 2007; Mousavi *et al*., 2016). This study is

in accordance with those of Soliman *et al*. (2013), Esmaeillou *et al*. (2013), Mousavi *et al*. (2016) and Wei *et al*. (2016) which showed that various NPs injected via different exposure routes induced significant increase in serum cholesterol, triglyceride and reduced HDL levels in treated rodents. An important biomarker of cardiovascular disease (CVD) risk is the triglycerides. However, with hypotriglyceridemia induced by both NPs and their mixture, it can be hypothesised that they do not have the ability of inducing coronary artery and cardiovascular diseases.

5.7 Histopathological changes in organs treated with titanium dioxide, zinc oxide nanoparticles and their mixture in mice

The liver is easily predisposed more than other organs to lipid peroxidation and oxidative stress, since it contains kupffer cells (macrophages) that are responsible for the uptake of NPs (Abdelhalim *et al*., 2015; Ferreira *et al*., 2015). In the kidneys, the glomerular filtration of NPs is majorly dependent on the size of the NPs (Sharma *et al*., 2012a). Nanoparticles with a hydrodynamic size of ≤ 5.5 nm are easily excreted by the kidneys because of the glomerular pore that measures 5.5 nm. Thus, NPs having a bigger size than 5.5 nm are eliminated by the reticuloendothelial system such as the hepatobilliary mechanism. Therefore, bioaccumulation as a result of 'long term retention' of the NPs make the liver and kidney more susceptible to ROS attacks (Li *et al*., 2012; Sharma *et al*., 2012a; Abdelhalim *et al*., 2015; Ferreira *et al*., 2015). Accumulation of TiO_2 and ZnO NPs are usually in the liver and kidney, thus making them potential target organs (Wang *et al*., 2007; Fabian *et al*., 2008; Liang *et al*., 2009; Ma *et al*., 2009; Xie *et al*., 2011; Baek *et al*., 2012; Li *et al*., 2012; Akhtar *et al*., 2012; Sharma *et al*., 2012a; Cho *et al*., 2013).

Histopathological examinations of the tissues in this study revealed hepatotoxicity of both NPs and their mixture through hepatocellular necrosis, kupffer cell hyperplasia, aggregation of inflammatory cells, thinning of hepatic cords, dilated sinusoids and dense aggregates of mononuclear cells. Similarly, nephrotoxicity revealed sloughing off of the tubular epithelial cells, dilated glomerular tubules, congestion of the interstitial vessels, swelling and degeneration of tubular epithelial cells. Also, there were numerous foci of pigment-laden macrophages, antigenic stimulation and lymphoid proliferation, distinct mantle zones and atrophic spleen with wrinkled capsule in the spleen tissues. The lesions

observed in the liver and kidney correlate with the serum hepatic and renal function biochemical tests and oxidative stress induction, which may suggest the localisation and accumulation of TiO_2 and ZnO NPs in these organs. This is in accordance with Wang *et al*. (2007; 2008a), Fabian *et al*. (2008), Li *et al*. (2010c), Pasupuleti *et al*. (2012a), Shukla *et al*. (2013), Najafzadeh *et al*. (2013), Esmaeillou *et al*. (2013), Soliman *et al*. (2013), Noori *et al*. (2014), Reddy *et al*. (2015), Srivastav *et al*. (2016) and Silva *et al*. (2017).

A limitation of this study was the inability to assess the bioaccumulation of TiO_2 and ZnO NPs in the kidney, heart, liver, spleen and brain tissues of the treated mice using inductively coupled plasma mass spectrophotometer. Nonetheless, *in vivo* studies did show TiO_2 and ZnO NPs accumulation in the spleen, heart, liver, brain and kidney, which elicited various severities of histopathological alterations (Li *et al*., 2010c; Baek *et al*., 2012; Cho *et al*., 2013). Recently, investigations on the potential hepatic and renal toxicity have demonstrated the impact of TiO_2 and ZnO NPs on the liver and kidneys. Chen *et al*. (2009) demonstrated that intraperitoneal exposure of TiO_2 NPs to mice accumulated in the liver, kidney, spleen and lungs causing hepatic fibrosis, necrosis and apoptosis of the hepatocytes, spleen lesions, interstitial pneumonia and renal glomerulus swelling It was also reported by Sharma *et al*. (2012b) that Zn accumulated in the human liver cells treated with ZnO NPs. Bioaccumulation was significantly present in the liver and kidney after 72 hours following administration of ZnO NPs (Baek *et al*., 2012) and in the kidney of rainbow trout treated with TiO_2 NPs (Scown *et al*., 2009). Ma *et al*. (2009, 2010) reported elevated sizes of the spleen, kidney, thymus, liver, inflammatory cascade, altered liver function and histopathological changes of the liver and brain as a result of the intraperitoneal or intragastric administration of TiO_2 NPs to mice for 14 days or 30 days.

Several studies have also demonstrated that other NPs are distributed in the liver and spleen. Lankveld *et al*. (2010) reported the accumulation of 20 nm Ag NPs primarily in the liver, kidney and spleen while 110 nm and 80 nm were found in the lungs, spleen, and liver. Similarly, Zhang *et al*. (2011b) revealed the accumulation of PEG-coated gold NPs (5 nm and 10 nm) in the liver and 30 nm of of PEG-coated gold NPs in the spleen. Toblli *et al*. (2011) demonstrated that iron dextran and ferumoxytol induced renal and hepatic damage in rats through proteinuria and increased hepatic enzymes. In another study, Feng

et al. (2011) reported renal, hepatic and spleen alterations through changes in the metabolic pathways participating in lipid, glucose, energy and amino acid breakdown after the intraperitoneal exposure of superparamagnetic particles of iron oxide. Nonetheless, it is suggestive that the spleen, kidney and liver are the significant viscera for NPs accumulation irrespective of the exposure route and duration (Sharma *et al*., 2012a; Li *et al*., 2012).

5.8 Mechanism of toxicity induced by titanium dioxide, zinc oxide nanoparticles and their mixture in mice

Nanoparticles of various sizes, chemical composition and surface properties have been reported to attack the mitochondria, which are the organelles where redox reactions take place (Alarifi *et al*., 2014). NPs may alter the production of ROS and antioxidants, resulting into oxidative stress. Hence, to determine the mechanism of toxicity induced by TiO_2, ZnO NPs and their mixture, the activities of SOD, CAT and the levels of GSH and MDA were evaluated in the kidney and liver tissues. The mechanism of NP-induced toxicity is not clearly understood but it is presumed that oxidative stress is one of the ways of inducing toxicity (Syama *et al*., 2014; Reddy *et al*., 2015; Niska *et al*., 2015; Ferreira *et al*., 2015).

An imbalance between the levels of antioxidants and the excessive production of free radicals leads to oxidative stress (Syama *et al*., 2014; Reddy *et al*., 2015). ROS are produced in the inner mitochondria membrane during oxidative metabolism (Syama *et al*., 2014; Niska *et al*., 2015) and are eliminated by both endogenous and exogenous antioxidants (Pourhamzeh *et al*., 2016). Alterations of metabolic pathways, imbalance of intracellular calcium homeostasis and breakdown of membrane lipids are induced through the generation of oxidative stress, which may result in apoptosis (Xue *et al*., 2011; Zhang *et al*., 2012). ROS can also be generated through NADPH (nicotinamide adenine dinucleotide phosphate) oxidase in the mitochondria (Manke *et al*., 2013; Sharma *et al*., 2012b; Ryu *et al*., 2014). Damage is induced in the inner mitochondrial membrane through elevated ROS leading to the loss of MMP. Thus, cytochrome C is released in the intermembrane space due to diminished MMP, which activates other caspase proteins and apoptotic genes and eventually leading to cell death.

Antioxidants (enzymatic and non-enzymatic) play important roles in cellular maintenance (Huang *et al*., 2010; Niska *et al*., 2015). SOD, CAT and GPx are the primary antioxidant defense enzymes (Syama *et al*., 2014; Gaharwar and Paulraj, 2015). The first line of enzyme against free radicals is the SOD. Hydrogen peroxide (H_2O_2) and molecular oxygen (O_2) are generated through the catalytic dismutation of superoxide radical (O_2^-) by SOD (Abdelhalim *et al*., 2015), while CAT metabolises H_2O_2 to O_2 and water (H_2O). However, increased SOD and CAT activities are indications of increased H_2O_2 production that would cause more damage to the DNA, protein and lipids (Sarkar and Sil, 2014; Ferreira *et al*., 2015). Emphasis must be made on the interactions of some antioxidants with one another forming the 'antioxidant network' (Sies *et al*., 2005). As a result, more relevant biological information is provided by not only measuring a single antioxidant but several antioxidants that are involved in the cellular defense mechanism (Niska *et al*., 2015).

Among the antioxidants, GSH is the main antioxidant that is involved in scavenging ROS and electrophiles (Syama *et al*., 2014; Strojny *et al*., 2015). GSH contains the thiol group (-SH) which plays a critical role in cellular defense. It serves as a substrate for glutathione peroxidase, where it is oxidised to glutathione disulfide (GSSG). Glutathione reductase (GR) reduces the formed GSSG to GSH in a nicotinamide adenine dinucleotide phosphate (NADPH) dependent manner establishing a balance between GSH and GSSG, where 98% of the thiol group accounts for reduced GSH (Abdelhalim *et al*., 2015; Strojny *et al*., 2015). In addition, lipids are also major targets of ROS generation eventually leading to peroxides. Peroxidation of lipids is a chain initiation reaction that involves the removal of hydrogen atoms from unsaturated fatty acids (membrane phospholipids) (Syama *et al*., 2014; Reshma and Mohanan, 2016). ROS continually attack phospholipids and fatty acid hydroperoxides and MDA, which is an aldehydic secondary product of lipid peroxidation, is an accepted marker for oxidative stress.

Evaluation of the oxidative stress parameters in this study showed a significant decrease in the SOD and CAT activities and GSH level except for the treated mice of ZnO NPs that revealed a significant increase of GSH level in the liver after the 5- day exposure period. Lipid peroxidation levels increased across all the doses for both NPs and their mixture.

Decrease in SOD and CAT activities may be due to the increased formation of H_2O_2 production and consequently hydroxyl radicals ($^{\cdot}OH$) overwhelming the expression activities of SOD and CAT respectively. These findings also support the increased MDA level indicating that excess $^{\cdot}OH$ may have interacted with the lipids causing lipid peroxidation. Subsequently, the increased GSH level observed may be as a result of cells treated with ZnO NPs trying to overwhelm the effects of ROS. Another possible explanation for the significant increase in GSH may be due to the increased levels of MDA, which may serve as a protective measure in the liver. After the 10 – day exposure period, TiO_2 NPs induced increased SOD and CAT activities, ZnO NPs and their mixture induced decreased SOD and CAT activities while the GSH level was decreased and increased in TiO_2 NPs and their mixture respectively in the treated mice. Increased SOD activities in the liver may have induced increased levels of superoxide radical (O_2^-) formation, which subsequently led to the elevation of CAT activity against the excess H_2O_2. This study agree with that of Reddy *et al*. (2015) which reported increased CAT activity in the liver, kidney and brain of female rats orally treated with Fe_2O_3 NPs (30, 300 and 1000 $mgkg^{-1}$) for 28 days.

TiO_2 and ZnO NPs induced a decrease in SOD activity while their mixture induced an increase in the kidney of the treated mice after the 5- day exposure period, which led to an increase in the formation of H_2O_2. The CAT activity increased in the mice treated with both NPs and their mixture.This may be explained by the catalytic adaptation of the kidney cells to withstand transient levels of hydroxyl radicals produced. This is supported by the increased MDA level, indicating that hydroxyl radicals produced may have interacted with the lipid membrane. Accordingly, adaptation or injury can occur to cells treated with oxidative stress. Transient levels of oxidative stress parameters usually results in adaptation of the cells leading to an up regulation of antioxidants (Ferreira *et al*., 2015). However, oxidative damage to the macromolecules may lead to cell injury depending on their severity.

After the 10- day exposure period, the kidney of the treated mice showed increased SOD activity in both NPs and their mixture, along with a decrease in CAT activity in TiO_2 NPs and their mixture, and an increase in the ZnO NPs treated mice. It has been previously

demonstrated by Niska *et al*. (2015) that TiO_2 NPs significantly increased O_2^- radical in a dose-dependent manner. Superoxide radical is produced from the reduction of oxygen by one electron and it is the precursor of other oxidizing species such as $^{\cdot}OH$, H_2O_2 and peroxynitrite ($ONOO^{\cdot}$). Thus, it can be concluded that both NPs and their mixture have strong inhibitory effects on the defense systems. Zhu *et al*. (2011) reported a significant increase in SOD activity in *Haliotis diversicolor supertexta* treated with TiO_2 NPs (1.0 mg/L). Rapid increase in ROS generation can bring about the increased utilisation of antioxidant activities in the cell (Niska *et al*., 2015). TiO_2, ZnO NPs and their mixture caused the excess production of O_2^- radical, which led to the alternation of the antioxidant defense and lipid peroxidation through the cell membrane as indicated by increased MDA level. These findings agree with that of Ahamed *et al*. (2016) which reported that Zn-doped TiO_2 NPs induced ROS generation and GSH and depleted SOD in human breast cancer (MCF-7) cells. It was also demonstrated by Haseeb *et al*. (2012) that MDA level was significantly increased in the rat's liver while no significance were observed in its heart and lung. Sahu *et al*. (2013) reported similar findings where human lung epithelial (L-132) cell treated with ZnO NPs (50.24 ± 8.19 nm) at 5 – 100 µg/mL showed significant increase in ROS generation and a depletion of reduced GSH.

DNA damage, oxidative stress, and apoptosis have displayed a strong positive correlation in several nanotoxicological studies that have utilised cultured cells and animal models (Akhtar *et al*., 2012). In healthy cells, the genomic DNA is continually under attack, and incomplete or excessive DNA repair can result in the accumulation of mutations, leading to the formation of oncogenesis. Single- and double-strand breaks, DNA-protein crosslinks and oxidation of purines are generated through oxygen radicals by damaging the nitrogen bases or DNA sugar-phosphate back bone (Osman *et al*., 2010; Sharma *et al*., 2012a; 2012b). The present study has been able to establish that TiO_2 and ZnO NPs induced oxidative stress via generation of ROS. These ROS have the potential of interacting with the DNA and inducing DNA damage via oxidative stress induction as the main molecular mechanism of genotoxicity. Cell cycle checkpoints and DNA repair processes are activated through a complete signaling network triggered by DNA damage (Awasthi *et al*., 2015). These signalling networks occur in a synchronous manner leading to the activation of tumour protein 53 (p53). p53 plays a major role in reacting to several

environmental toxicants that induce cellular DNA damage, most importantly as phosphorylation modulates the stability of p53 (Morsy *et al*., 2016). The possible mechanism of the DNA damage induction through hepatic and renal oxidative stress is in concert with the study of Li *et al*. (2008b) which showed that TiO_2 NPs directly interacted with the DNA through the DNA phosphate group. Similarly, Federici *et al*. (2007) has also reported the indirect binding of TiO_2 NPs to the DNA through the generation of ROS and inflammation.

Accordingly, Mroz *et al*. (2008) reported that NPs have the capability of inducing DNA damage via ROS leading to carcinogenesis, p53 activation and proteins involved in DNA repair. In addition, Song *et al*. (2012) reported the production of MN and DNA damage via oxidative stress, which was the major mechanism of cell death by several metal NPs. Studies have demonstrated that exposure of ZnO NPs can alter the gene expression levels of various receptor protein kinases, signalling molecules, nuclear transcription factors and growth factors through ROS induction. In particular, p53 activation (Ng *et al*., 2011) and tyrosine phosphorylation alternations (Osman *et al*., 2010) involved in differentiation, metabolic regulation, host defence and cell growth (Hubbard *et al*., 1998) are reported to occur in the exposure to ZnO NPs.

Bhattacharya *et al*. (2009) reported high levels of DNA adduct formation (8-hydroxy-2-deoxyguanosine), which was probably due to the formation of intra- and acellular ROS generation in human lung cells treated with TiO_2 NPs. In another study, Gurr *et al*. (2005) reported oxidative DNA damage and lipid peroxidation due to H_2O_2 and nitric oxide generation in the lung epithelial cells treated with TiO_2 NPs. Also, Kang *et al*. (2008) reported that ROS generation induced DNA damage as well as activation of DNA damage checkpoints and p53 up-regulation in peripheral blood lymphocytes treated with TiO_2 NPs. Similarly, Shukla *et al*. (2011) reported increased DNA oxidation damage and MN induction in human epidermal cells (A431) treated with TiO_2 NPs. It was suggested that ROS has a strong correlation with DNA oxidation damage and may be a likely mechanism of genotoxicity. Likewise, Sharma *et al*. (2012b) equally reported that DNA damage and apoptosis occurred due to the induction of oxidative stress in the liver cell treated with ZnO NPs. Evidences indicate that the formation of ROS resulting to oxidative stress is the

major mechanism of TiO_2 and ZnO NPs toxicity. It can be postulated from this study, therefore, that genomic damage and systemic toxicity might have been induced through the ROS-mediated pathway from the inner membrane of the mitochondria. This complex pathway involves a cascade of events that may eventually lead to cell death (Figure 5.1).

5.9 DNA damage induced by titanium dioxide, zinc oxide nanoparticles and their mixture in the germ cells of mice

An important part of nanotoxicity that has become increasingly recognised is the germ cell toxicity (Ema *et al*., 2010). In this study, sperm count, motility and abnormality in mice treated with TiO_2, ZnO NPs and their mixture were evaluated. In addition, the endocrine-disrupting effects of TiO_2, ZnO NPs and their mixture were investigated through the evaluation of serum LH, FSH and testosterone levels. In experimental studies, useful reproductive risk assessments are provided through the weight of the male reproductive organ. During spermatogenesis, the primary assessment is the testicular size, as approximately 98 % of the testicular mass consists of both tubules and germinal elements. A normal testicle consists of two types of cells: germ cells and leydig cells in equal proportions, thereby making the testicle round, firm and full. The function of the leydig cells and germ cells is to produce testosterone and spermatozoa, respectively.

Our results revealed that mice intraperitoneally administered to TiO_2, ZnO NPs and their mixture induced no significant changes in their testicular weight in comparison with those treated with distilled water. However, TiO_2 NPs and their mixture induced testicular atrophy while ZnO NPs induced testicular hypertrophy in the mice. Testicular atrophy may occur due to the apoptosis of either the leydig cells or germ cells or both resulting in the alterations such as fluid level fluctuations, shrinking of the testicles, making them loose and soft. Most importantly, hormonal imbalance is reported to be a major cause of testicular atrophy. This is an indication that both NPs and their mixture have the ability to significantly affect germ cell physiology. A possible explanation of testicular atrophy or hypertrophy induced by TiO_2 and their mixture, and ZnO NPs respectively may be due to their particle sizes. This implies that the TiO_2 NPs and their mixture have the ability of damaging the testicular architecture, thus reducing spermatozoa production while ZnO NPs may have a longer half life in the circulatory system of the treated mice eventually

affecting the testicular size. It may likely suggests that ZnO NPs (< 100 nm) accumulation led to changes in the epithelium morphology and 'swelling up' of the seminiferous tubules since they are less prone to germinal cell penetration and would rather accumulate and aggregate in the extracellular space of the spermatocyte (Jang *et al*., 2010). On the other hand, TiO_2 NPs (< 25 nm) may have easily entered the seminiferous tubules and penetrated into the germ cells directly without the accumulation in the extracellular space (Singh and Lillard, 2009). Another possible explanation for testicular atrophy may be due to the inhibition of the microtubules and intermediate filaments of the Sertoli cells, thus affecting germ cell division (Attia, 2014). It was also observed that TiO_2, ZnO NPs and their mixture could cross the blood-testis barrier forming agglomerates within the testes (Figure 4.136A). The bioaccumulation of NPs in the testes is in line with other studies such as Chen *et al*. (2003), Liu *et al*. (2010b), Kim *et al*. (2011), Morishita *et al*. (2012), Li *et al*. (2013), Gromadzka-Ostrowska *et al*. (2012), Thakur *et al*. (2014), Smith *et al*. (2015) and Yoisungern *et al*. (2015)

The fertilisation of the ovum by the sperm cell is determined by the integrity (viability) of the sperm membrane (Sleiman *et al*., 2013; Mathias *et al*., 2015; Yoisungern *et al*., 2015). Several *in vitro* studies have shown plasma membrane toxicity in various germ cell lines such as mammalian germline stem cells, mouse testis leydig cell line (Komatsu *et al*., 2008), spermatogonial stem cells (Zhang *et al*., 2015) and human spermatozoa (Gopalan *et al*., 2009; Barkhordari *et al*., 2013; Moretti *et al*., 2013; Wang *et al*., 2017b). In agreement with what has been previously reported, TiO_2, ZnO NPs and their mixture may have significantly altered the plasma membrane of the spermatozoa. A possible hypothesis may be that both NPs and their mixture were phagocytosed by the spermatogonial stem cells during the dissolution of the NPs by the Trojan horse-type mechanism (Park *et al*., 2010).

One of the most important biomarkers used in determining the testicular toxicity of chemicals is the sperm motility. In the spermatozoa, the mitochondria located in the midpiece promote sperm movement through the generation of energy to the flagella (Mathias *et al*., 2015). Reduction of sperm motility induced by TiO_2, ZnO NPs and their mixture is an indication that they affected energy production in the sperm cells. This may likely be as a result of the reduced mitochondrial activity of the spermatozoa causing

‘opening of the permeability transition pore in the inner mitochondrial membrane’, thus reducing the mitochondrial membrane potential and affecting ATP production (Almofti *et al*., 2003; Mathias *et al*., 2015; Smith *et al*., 2015; Yoisungern *et al*., 2015). In addition, it is possible to assume that the membrane receptors or cells signaling involved in motility maintenance were affected by TiO_2, ZnO NPs and their mixture (Moretti *et al*., 2013). This result agree with Smith *et al*. (2015) which reported a significant reduction in the progressive motility of mice spermatozoa treated with TiO_2 NPs for 120 hours. Likewise, Moretti *et al*. (2013) reported human spermatozoa treated with gold and silver nanoparticles respectively, and observed a dose-dependent significant decrease. Yoisungern *et al*. (2015) observed abnormal mitochondrial architecture and increased mitochondrial DNA copy number in the spermatozoa of mice treated with Ag NPs.

An important factor that is used for assessing fertility is the sperm count (Bebb *et al*., 1996). Reduction in epididymal sperm count is an indication that both NPs and their mixture have the ability of altering the testicular architecture such as decreased epididymal sperm count, increased number of damaged seminiferous tubules, leydig cell degeneration (Yoshida *et al*., 2009b; Talebi *et al*., 2013; Attia, 2014), and apoptosis of germ and sertoli cells (Gao *et al*., 2013). Sperm count reduction may also be attributed to a decrease in the diameter of the seminiferous tubules epithelial cells, increased lumen volume, reduction in spermatogonia, spermatocytes and spermatids (Ono *et al*., 2007). Excess ROS generated may have contributed to the degeneration of the seminiferous tubules and loss of the spermatogonia, spermatocytes, spermatids and the production of the spermatozoa. A reduction in sperm count may also be due to the inhibitory effects of TiO_2, ZnO NPs and their mixture on the spermatogonia proliferation and reduction in sperm cell precursors (Attia, 2014). Therefore, it may be concluded that the spermatogonial stem cells (SSC) are susceptible to damage by TiO_2, ZnO NPs and their mixture since spermatogenesis involves the renewal and proliferation of SSC that will give rise to highly differentiated spermatozoa (Garcia *et al*., 2014). This finding agree with the studies of Gromadzka-Ostrowska *et al*. (2012) and Attia (2014).

Synchronous morphological and biochemical steps such as the manchette formations and the replacement of histones with protamine are involved in the formation of the normal

sperm head (Bruce *et al*., 1974). The nuclei present in the sperm heads are homogeneous with specific structural definition (Beatty, 1970). An important endpoint that is very sensitive and reliable in identifying germ cell mutagens is the sperm head abnormality assay (Giri *et al*., 2002). Usually, autosomes carry the characteristics controlling sperm head shape (Tophan, 1980a; 1980b); however, accumulation of exogenous toxicants in the germ cell pool may induce alterations such as point mutations in the testicular DNA (Giri *et al*., 2002) or partial deletion on the Y chromosome (Styrna *et al*., 1991). In this study, the mechanism of sperm head abnormality induced by TiO_2, ZnO NPs and their mixture may not be clearly known. However, it may be due to the mistakes that naturally occur at the differentiation process (Bruce *et al*., 1974). In addition, both NPs and their mixture may also have increased the frequency of the sperm head abnormality. Packaging of the genetic material may result in few mistakes that will lead to the abnormal sperm heads.

An important pathway that may also have induced high frequency of sperm head abnormality in this study is the association between the ubiquitin-dependent pathway of protein degradation and spermatogenesis (Bebington *et al*., 2001). Testes of mammals that contain haploid spermatids usually have an increased level of ubiquitination (Rajapurohitam *et al*., 1999; 2002). The *Ube2b* is an important autosomal gene that encodes mHR6B, which is a murine ubiquitin conjugating enzyme highly predominant in mammalian testis (Koken *et al*., 1996). The formation of an abnormal sperm head during spermatid nuclear condensation usually results in infertility and spermatogenesis impairment in male mice that have a deficiency of *Ube2b* (Roest *et al*., 1996). In addition, mice deficient of this gene exhibit irregular diameter of the sperm flagella, impairment of sperm motility, apoptosis of the germ cells and depletion of the testis (Roest *et al*., 1996). Therefore, both NPs and their mixture may have led to the complete or partial loss of *Ube2b* leading to a loss of function of the *Ube2b* protein expression in the testes of the treated mice. Remodeling of the postmeiotic chromatin in the mouse testis requires histone degradation and subsequently replacing the transition proteins with protamines. Ubiquitinated nuclear proteins and histones are clearly seen in the nucleus of the mouse testis (Baarends *et al*., 1999). However, it is strongly assumed that both NPs and their mixture may have altered the histone ubiquitination process and replacement of histones with protamines as seen in the various sperm head abnormalities.

Another important structure that is essential for the sperm head shaping and condensation is the manchette development, which is primarily formed by the microtubules and its associated proteins (Rattner and Brinkley, 1972). During the beginning of the nuclear shaping, the microtubules assemble; thereafter dissemble when the nucleus reaches a compressed state (Meistrich *et al*., 1990; Russell *et al*., 1991). Microtubule-associated protein, Spnr (for spermatid perinuclear RNA binding protein) (Schumacher *et al*., 1998), and Ran-GTPase (Kierszenbaum *et al*., 2002a) are sperm components stored in the manchette (Escalier *et al*., 2003). On the other hand, TBP-1 (tat-binding protein-1), axonemal-binding protein Spag4 (Shao *et al*., 1999), periaxonemal cytoskeletal structures (Brohmann *et al*., 1997) and paraaxonemal mitochondria (Rivkin *et al*., 1997) are components of the manchette sorted secondarily into the developing sperm tail. Therefore, it can be assumed in this study that TiO_2, ZnO NPs and their mixture were able to alter the sperm components in the manchette and cytoskeletal proteins thereby affecting the structure of the sperm heads of the treated mice.

Mutation of the abnormal spermatozoon head shape (*azh*) located on chromosome 4 may be another possible explanation for the increased frequency of sperm head abnormality induced by both NPs and their mixture in the treated mice. Mutation of *azh* displays an autosomal mode of inheritance and the mutated *azh* spermatozoa often lead to tail detachment due to their sensitivity to mechanical forces (Mendoza-Lujambio *et al*., 2002). Likewise, the *Hook1* gene (predominantly expressed in the testis) mapped on the same region where the *azh* locus is, has been reported to be extensively involved in microtubular structure positioning within the haploid germ cells. The mutation of the *Hook1* gene by both NPs and their mixture may possibly lead to a total or incomplete loss of function of the protein in the treated mice, subsequently leading to the high frequency of abnormal sperm heads and reduced fertility. According to Mendoza-Lujambio *et al*. (2002), the microtubules bind to the murine Hook1 protein and also establish a contact between the nuclear envelope and the manchette (Walenta *et al*., 2001). Therefore, abnormal sperm head shape may be as a result of the wrong positioning of the microtubules due to the absence of the C-terminal domain of the Hook1 protein. This may often lead to the interference between the attachment of the nuclear envelope and manchette. In addition, the mixture of TiO_2 and ZnO NPs induced the highest frequency

of sperm abnormalities, mostly amorphous and pin heads, which may indicate that the mixture targeted the DNA located in the sperm head. However, alterations in the genetic material results in the damage to the structure and function of the spermatozoa. The significant increase in the frequency of sperm anomalies induced by the mixture may be due to their synergistic effect in the testes. The interaction factor of TiO_2 and ZnO NPs revealed synergism for sperm count and abnormalities, which confirms that either of the NPs has a synergistic property when co-administered in the biological system. Our result of this study agree with Gromadzka-Ostrowska *et al*. (2012), Attia (2014) and Yoisungern *et al*. (2015). Therefore, the consequences of TiO_2 and ZnO NPs - induced germ cell mutation include reduced fertility, cancer, numerical chromosome aberrations, and heritable abnormal structural germ cells (Allen *et al*., 1986; Tilly, 1998; Braydich-Stolle *et al*., 2005; Aitken and De Luliis, 2010). In addition, the implications of having mutation of germ cells in successive generations consist of genetic diseases with various severity of health implications, reduced fertility, congenital malformations and embryonic or perinatal death (Brinkworth, 2000; Braydich-Stolle *et al*., 2005).

Spermatogenesis is a multiple complex process where differentiated spermatozoa are produced from the spermatogonial stem cells within the seminiferous tubules of the testis (Li *et al*., 2013). This process is being controlled by a 'complex-regulation' of neuroendocrine hypothalamic-pituitary gonadal axes together with 'local testicular steroids' (Li *et al*., 2013). Male reproductive hormones such as LH, FSH and testosterone are essential for spermatogenesis. However, production and regulation of these hormones can be disrupted by endocrine disruptors or environmental toxicants (Iavicoli *et al*., 2012; Garcia *et al*., 2014). Therefore, alterations of these reproductive hormone concentrations may result in male infertility, testicular damage and malfunction of spermatogenesis (Li *et al*., 2013; Garcia *et al*., 2014). The study revealed a significant decline in LH, increased levels of FSH and testosterone indicating that TiO_2, ZnO NPs and their mixture might have a causative effect in the steroidogenic process in the testis and interfere with the hypothalamic-pituitary-gonadal axis as potential endocrine disruptors. As it is known, testosterone, an androgen hormone maintains spermatogenesis, pubertal development and also necessary for male sexual differentiation (Chandra *et al*., 2010). In addition, it is responsible for the maturation of the spermatids between stages VII – VIII in the

spermatogenic cycle (Chandra *et al*., 2007) and regulation of spermatogenesis by the Sertoli cells (Attia, 2014).

A possible explanation of elevated testosterone may be due to an adverse effect on the leydig cells and the upregulation of genes that are responsible for testosterone biosynthesis, which may have negative impacts on the spermatogenesis of the treated mice. Steroidogenic acute regulatory (StAR) protein, cytochrome P450 side chain cleavage (P450scc), 3β- Hydroxysteroid dehydrogenase (3β-HSD), P450-17α and 17β-HSD are genes involved in the synthesis of testosterone. In the mitochondria membrane, cholesterol is transported from the outer to the inner space with the help of StAR, which is a rate limiting step (Stocco, 2001). Also, P450scc catalyses the conversion of cholesterol to pregnenolone, which is a rate limiting step (Omura and Morohashi, 1995). The catalytic action of 3β-HSD converts pregnenolone to progesterone. P450-17α converts progesterone to androstenedione production (Payne and Hales, 2004). Finally, 17β-HSD converts androstenedione to testosterone (Payne and Youngblood, 1995).

The present study also corroborates the result of Garcia *et al*. (2014) which revealed that Ag NPs induced a significant increase in both serum and intratesticular testosterone and Cyp11a1 and Hsd3b1, two enzymes involved in the biosynthetic pathway of testosterone. Likewise, Ramdhan *et al*. (2009) reported increased expression levels of Cyp11a1 mRNA in the testes of animals treated with nanoparticle rich diesel exhaust. Similarly, Li *et al*. (2013) also reported high testosterone levels in mice treated with PEG-NH_2@AuNP. In addition, high testosterone levels may have occuured due to an impaired negative feedback mechanism on the hypothalamus and pituitary gland, resulting into leydig cell dysfunction and altering spermatogenesis (Yoshida *et al*., 1999; Ono *et al*., 2007). Similarly, a significant increase in FSH, in the absence of LH suggests a paracrine effect mediated by Sertoli cells (Ono *et al*., 2007).

The testicular histology of mice treated with distilled water showed the normal architecture of the seminiferous tubules. The tubules depicted an orderly arrangement of the germinal cells (spermatogonia, spermatocytes, spermatids of different stages and the spermatozoa) and sertoli cells. In addition, the interstitial tissue was found to have a well organised leydig cells, blood vessels, leukocytes, lymphatic vessels and fibroblasts.

However, the present study showed that TiO_2, ZnO NPs and their mixture induced necrotic spermatogenic cells, loss of basal germinal epithelial cells, increased luminal width and congestion of testicular interstitial blood. These histopathological findings corroborate the initial report of the penetration and accumulation of TiO_2, ZnO NPs and their mixture in the testicular tissues. Depletion of spermatogenic cells and increased luminal width support the significant reduction of low sperm counts. These present study agree with that of Thakur *et al*. (2014) which reported atrophy in seminiferous tubules, germinal epithelium disorganisation, basement membrane degeneration and apoptosis of different germinal cells in Wistar rats treated with Ag NPs (20 µg/kg) orally for 90 days.

Also, Smith *et al*. (2015) identified aggregates of TiO_2 NPs (anatase) in the scrotal adipose tissues surrounding the testis and epididymis, thus, leading to histopathological alterations such as enlarged interstitial spaces, increased apoptotic cells and disorganised seminiferous tubules. Similarly, Hong *et al*. (2016) reported necrosis, severe disorganisation of tissue and spermatolysis in the testes of mice treated with TiO_2 NPs. Attia (2014) reported degenerative seminiferous tubules, loss in spermatogenic epithelium height and sloughing of the seminiferous cellular components in the testes of mice treated with 500 and 1000 $mgkg^{-1}$ of Ag NPs. Likewise, Talebi *et al*. (2013) reported vacuolisation of the sertoli cells in ZnO NPs treated with NMRI mice. Yoshida *et al*. (2008) also reported degeneration and vacuolation of the seminiferous tubules in mice treated with carbon black particles. Gao *et al*. (2013) reported decreased germinative layer thickness, vacuolation and mesenchymal congestion among others in mice treated with TiO_2 NPs for 90 consecutive days.

The exact mechanism of spermatozoa dysfunction induced by TiO_2 and ZnO NPs is not clearly understood. However, the induction of oxidative stress and increase in intracellular ROS generation are one of the most importantly proposed mechanisms of DNA nanotoxicity due to the photocatalytic properties of both NPs. It is well established that the high concentration of polyunsaturated fatty acid (docosahexaenoic acid) and low expression levels of antioxidants make spermatozoa highly susceptible to ROS attack resulting in lipid peroxidation (Vernet *et al*., 2004; Gromadzka-Ostrowska *et al*., 2012; Chen *et al*., 2013). This study showed that TiO_2, ZnO NPs and their mixture significantly

altered the antioxidants (SOD, CAT and reduced GSH) and increased lipid peroxidation through increased MDA level indicating oxidative stress induction in the testes of the treated mice. This is in accordance with the work of Zhao *et al*. (2014) which reported reduced GSH depletion, oxidised glutathione levels, reduced SOD activity and increased CAT activity in the testes treated with TiO_2 NPs for 90 consecutive days. Similarly, Meena *et al*. (2015) reported decreased activities of CAT, GSH-Px and SOD and increased lipid peroxidation in the testes of animals treated with TiO_2 NPs. Several studies have shown the interaction between lipid peroxidation, ROS and DNA damage (Ema *et al*., 2010; Zhang *et al*., 2015). The possible induction of spermatotoxicity affecting the structure and function of the spermatozoa of the mice treated with both NPs and their mixture is depicted in Figure 5.2. Excess ROS as indicated by the oxidative stress induction may have affected the DNA, proteins and lipid actively involved in spermatogenesis of the treated mice.

In addition to the production of increased intracellular ROS, inflammatory responses may also weaken the integrity of the blood-testis barrier (BTB) through the expression of cytokines (Smith *et al*., 2015; Hong *et al*., 2016). Although inflammatory cytokines were not determined in this study but studies such as Smith *et al*. (2015) observed significantly increased levels of cytokines in the epididymal tissues of mice treated with TiO_2 NPs. Similarly, Hong *et al*. (2016) reported significant increase in macrophages, lymphocytes, neutrophils, eosinophils and Toll-like receptors indicating inflammation in the testis of TiO_2 NPs treated mice. The BTB is made up of adjacent Sertoli cells located at the basal compartment of the seminiferous epithelium (Li *et al*., 2013). The BTB prevents the penetration of exogenous and harmful toxicants from having access to developing and viable germ cells by serving as a 'fence' or 'gate keeper'. Tight junctions are composed of different proteins such as occludin, zonula occludens, N-cadherin and connexin 43 (Fiorini *et al*., 2004) and are found between Sertoli cells where they protect developing sperm cells during spermatogenesis (Li *et al*., 2013). The mechanism of how TiO_2, ZnO NPs and their mixture penetrated through the BTB was not investigated; however, some studies put forward an 'elevator door' hypothesis for the penetration of NPs (Lan and Wang, 2012). The extent of the inflammatory responses determines the scale of the gap of the BTB (Li *et al*., 2013). However, the size of the BTB intracellular gap might become larger as a

result of the severity of the inflammatory responses of the NP exposure. Such an assumption may explain the reason for the accumulation of TiO_2 NPs in the testis while ZnO NPs (< 100 nm) were kept out because their size is larger than the size of the BTB gaps. This conforms to our result as TiO_2 NPs induced more damage to the spermatogonial stem cells (Ema *et al*., 2010) than ZnO NPs that induced moderate toxicity (Barkhordari *et al*., 2013).

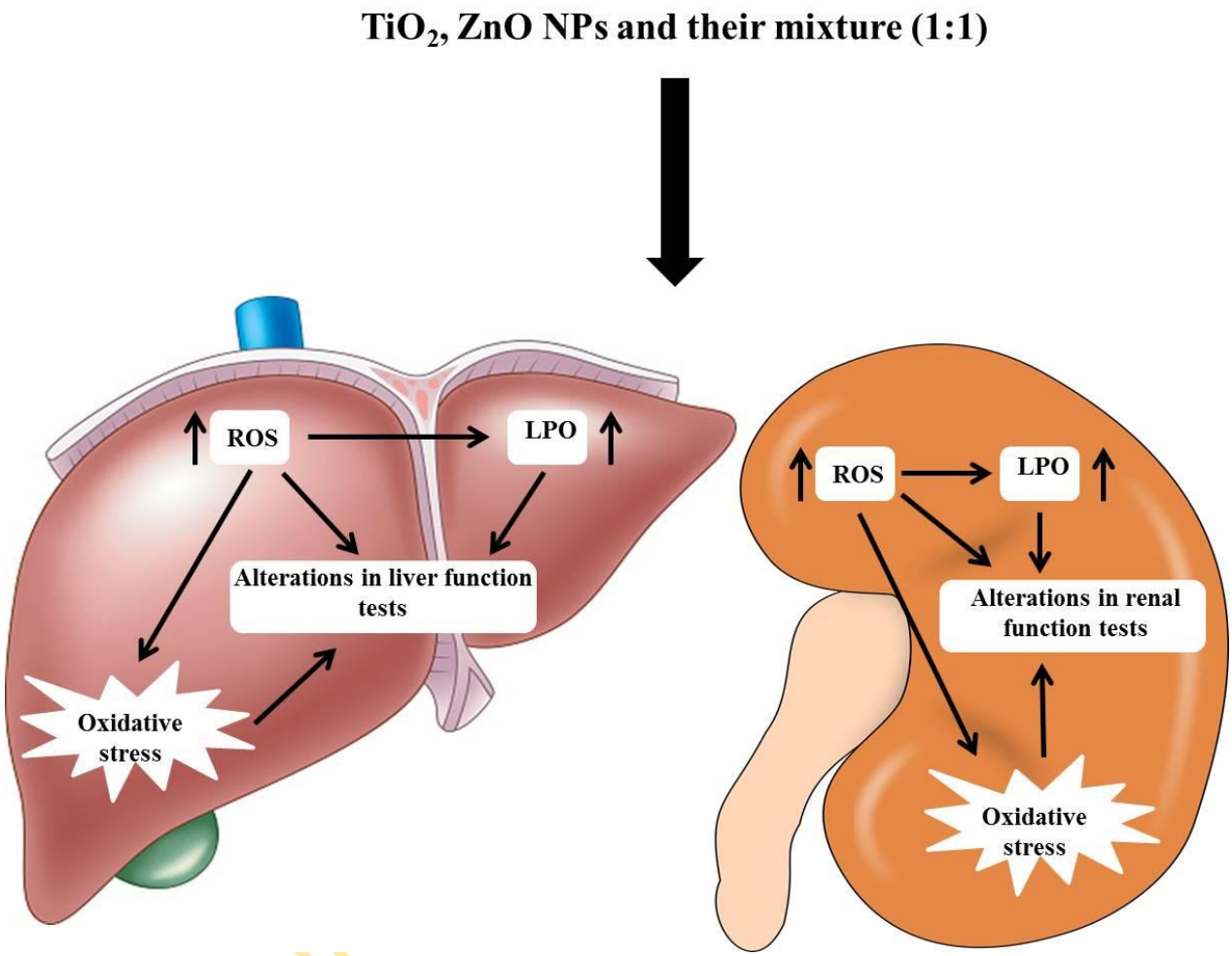

Figure 5. 1: Possible mechanism of DNA damage and systemic toxicity induced by TiO_2, ZnO NPs, and TiO_2 and ZnO NPs in the liver, kidney and bone marrow cells respectively in mice. ROS: reactive oxygen species; LPO: lipid peroxidation; MN: micronucleus induction.

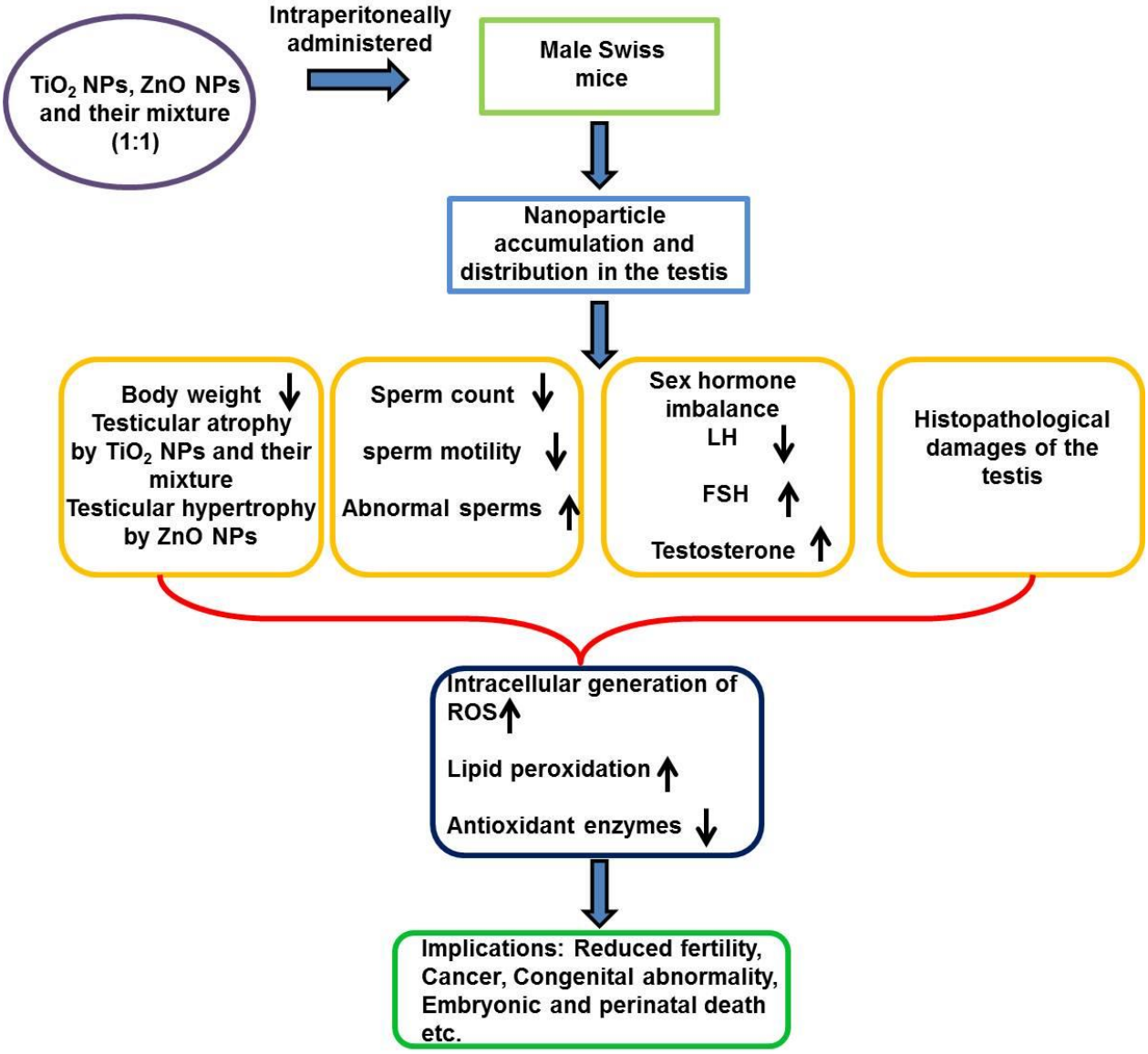

Figure 5. 2: A schematic diagram showing a summary of the possible mechanism of TiO_2, ZnO NPs and their mixture induced damage in mouse testis.

CHAPTER SIX

CONCLUSIONS AND RECOMMENDATIONS

The genetic and systemic damage of TiO_2, ZnO NPs and their mixture using somatic and germ organs in mice were investigated. The results showed that TiO_2, ZnO NPs and their mixture induced micronucleus in mice. TiO_2 NPs were more genotoxic at tested doses following the 5 day- exposure period, due to the smaller particle size and large surface area to volume ratio. However, ZnO NPs showed lower toxicity probably due to the larger particle size. For the 10- day exposure period, the bone marrow cells were not repaired indicating that ZnO NPs induced almost permanent genotoxic damage. Furthermore, their mixture induced significant MN after the 10- day exposure period because of the ZnO-bound TiO_2 NPs taken up into the cell membrane. Taken together, the present study suggests that TiO_2, ZnO NPs and their mixture caused cytogenotoxic effects through the induction of DNA damage. TiO_2, ZnO NPs and their mixture also induced various signs of systemic toxicity in *Mus musculus*. These changes include: changes in body and organ weights, alterations in haematologial parameters, clinical biochemical parameters and histopathology.

The study also revealed that TiO_2, ZnO NPs and their mixture can enter the testis via the blood-testis barrier, accumulate in the testis, which in turn, can affect testicular mass, sperm motility, sperm count and levels of male reproductive hormones. Most importantly, the sperm head abnormalities observed in the testes of the treated mice revealed that TiO_2, ZnO NPs and their mixture are potential germ cell mutagens, with the mixture able to induce highest frequency of DNA damage through the mutation of genes associated with sperm head formation. These mutations may even be hereditary in the progeny of the next generation. Furthermore, it may be indicated that TiO_2, ZnO NPs and their mixture effected testicular damage primarily on the germ cells and secondarily by disrupting LH,

FSH and Testosterone, which in turn affected spermatogonial stem cells.

It was also observed that TiO_2, ZnO NPs and their mixture induced oxidative stress and lipid peroxidation through alterations of SOD and CAT activities, GSH and MDA in the liver, kidney and testis. It is evident that the pathway for induction of DNA damage that brought about cytogenotoxicity in the haemopoietic stem cells and germ cells respectively; and systemic toxicity may possibly be through the excessive production of intracellular ROS.

The specific recommendations arising from this study include:

1. Full characterisation of the physicochemical properties (e.g. particle size, surface charge and surface reactivity) of NPs should be extensively assessed in both powder form and suspension before toxicity evaluation, to have an in-depth understanding on the behaviour of NPs in the biological system.
2. Due to the severe damage induced by TiO_2 and ZnO NPs in the study, there should be ways to facilitate safer synthesis and minimise the release of these NPs from the factories to the environment, as they are biopersistent and nondegradable and thus should be treated as hazardous.
3. Their photocatalytic property enables them to be utilised for bioremediation in polluted environments and it is recommended that they should be prohibited due to the adverse effects they induce on the environment and human health.
4. The health, safety and environmental risk of NPs from the air, water and soil should be properly investigated and should commensurate with the rate of their production.
5. Due to the MN induction and germ cell toxicity induced by TiO_2, ZnO NPs and their mixture, it is recommended that epidemiological studies be carried out to have an in-depth understanding of the health and safety of these NPs, most especially at the reproductive level.
6. Establishment of a public dialogue is essential to creating awareness on the benefits and adverse effects. Also it is pivotal in regulating the disposal of these NPs in order to protect the environment.

CONTRIBUTIONS TO CURRENT KNOWLEDGE

The following are the significant contributions to the current state of knowledge arising from the study:

1. TiO_2 NPs, and mixture of TiO_2 and ZnO NPs induced significant cytogenetic damage in the bone marrow cells of mice.

2. The mixture of TiO_2 and ZnO NPs in comparison to the individual NPs induced more abnormalities of sperm parameters and reproductive hormones in mice.

3. TiO_2, ZnO NPs and their mixture induced significant genetic and systemic damage via intracellular ROS production as the major mechanism.

4. The mixture of TiO_2 and ZnO NPs had a synergistic interactive effect on the cytogenotixicity and sperm parameters respectively in mice.

REFERENCES

Abdelhalim, M. A., Al-yed, M. S. and Moussa, S. A. 2015. The effects of intraperitoneal administration of gold nanoparticles size and exposure duration on oxidative and antioxidants levels in various rat organs. *Pakistan Journal of Pharmaceutical Sciences* 28: 705-712.

Abidi, P., Afaq, F., Arif, J. M., Lohani, M. and Rahman, Q. 1999. Chrysotile-mediated imbalance in the glutathione redox system in the development of pulmonary injury. *Toxicology Letters* 106.1: 31–39.

Adam, N., Schmitt, C., Galceran, J., Companys, E., Vakurov, A., Wallace, R., Knapen, D. and Blust, R. 2014. The chronic toxicity of ZnO nanoparticles and $ZnCl_2$ to *Daphnia magna* and the use of different methods to assess nanoparticle aggregation and dissolution. *Nanotechnology* 8.7: 709-717.

Adamcakova-Dodd, A., Stebounova, L. V., Kim, J. S., Vorrink, S. U., Ault, A. P., O'Shaughnessy, P. T., Grassian, V. H. and Thorne, P. S. 2014. Toxicity assessment of zinc oxide nanoparticles using sub-acute and sub-chronic murine inhalation models. *Particle and Fibre Toxicology* 11.15. doi: 10.1186/1743-8977-11-15.

Adams, L. K., Lyon, D. Y. and Alvarez, P. J. 2006. Comparative eco-toxicity of nanoscale TiO_2, SiO_2 and ZnO water suspensions. *Water Research* 40.19: 3527-3532.

Adam-Vizi, V. and Seregi, M. 1982. Receptor independent stimulatory effect of noradrenaline on Na, K-ATPase in rat brain homogenate. Role of lipid peroxidation. *Biochemical Pharmacology* 31.13: 2231-2236.

Adham, I. M., Nayernia, K., Burkhardt-Go¨ttges, E., Topaloglu, O., Dixken, C., Holstein A. F. and Engel, W. 2001. Teratozoospermia in mice lacking the transition protein 2 (Tnp2). *Molecular Human Reproduction* 7.6: 513–520.

Afifi, M., Almaghrabi, O. A. and Kadasa, N. M. 2015. Ameliorative effect of zinc oxide nanoparticles on antioxidants and sperm characteristics in streptozotocin-induced diabetic rat testes. *Biomedical Research International* DOI: 10.1155/2015/153573.

Ahamed, M., Akhtar, M. J., Raja, M., Ahmad, I., Siddiqui, M. K., AlSalhi, M. S. and Alrokayan, S. A. 2011. ZnO nanorod-induced apoptosis in human alveolar

adenocarcinoma cells via p53, survivin and bax/bcl-2 pathways: role of oxidative stress. *Nanomedicine* 7.6: 904–913.

Ahamed, M., Majeeed Khan, M. A., Akhtar, M. J., Alhadlaq, H. A. Alshamsan, A. 2016. Role of Zn doping in oxidative stress mediated cytotoxicity of TiO_2 nanoparticles in human breast cancer MCF-7 cells. *Scientific reports* 6:30196.doi:10.1038/srep30196.

Ahmad, A., Senapati, S., Khan, M. I., Kumar, R. and Sastry, M. 2005. Extra-/intracellular biosynthesis of gold nanoparticles by an alkalotolerant fungus, *Trichothecium sp. Journal of Biomedical Nanotechnology* 1.1: 47-53

Aitken, R. J. and De Luliis, G. N. 2007. Origins and consequences of DNA damage in male germ cells. *Reproductive BioMedicine Online* 14.6: 727-733.

Aitken, R. J. and De Luliis, G. N. 2010. On the possible origins of DNA damage in human spermatozoa. *Molecular Human Reproduction* 16.1: 3-13.

Akhtar, M. J., Ahamed, M., Kumar, S., Khan, M. A., Ahamed, J. and Alrokayan, S. A. 2012. Zinc oxide nanoparticles selectively induced apoptosis in human cancer cells through reactive oxygen species. *International Journal of Nanomedicine* 7: 845-857.

Akyil, D., Eren, Y., Konuk, M., Tepekozcan, A. and Saglam, E. 2015. Determination of mutagenicity and genotoxicity of indium tin oxide and micronucleus assay. *Toxicology and Industrial Health* 32.9: 1720-1728.

Alabi, O. A. and Bakare, A. A. 2011. Genotoxicity and mutagenicity of electronic waste leachates using animal bioassays. *Toxicological and Environmental Chemistry* 93.5: 1073-1088.

Alarifi, S., Ali, D., Alkahtani, S. and Alhader, M. S. 2014. Iron oxide nanoparticles Induce oxidative stress, DNA damage and caspase activation in the human breast cancer cell line. *Biological Trace Element Research* 159.1-3: 416-424.

Alimba, C. G. and Bakare, A. A. 2016. *In vivo* micronucleus test in the assessment of cytogenotoxicity of landfill leachates in three animal models from various ecological habitats. *Ecotoxicology* 25.2: 310-319.

Allen, J. W., Liang, J. C., Carrano, A. V. and Preston, R. J. 1986. Review of literature on chemical-induced aneuploidy in mammalian male germ cells. *Mutation Research* 167. 1-2: 123-137.

Almansour, M., Jarrar, Q., Battah, A. and Jarrar, B. 2015. Morphometric alterations induced by the toxicity of variable sizes of silver nanoparticles. *International Journal of Morphology* 33.2: 544-552.

Almofti, M. R., Ichikawa, T., Yamashita, K., Terada, H. and Shinohara, Y. 2003. Silver ion induces a cyclosporine a – insensitive permeability transition in rat liver mitochondria and release of apoptogenic cytochrome C. *Journal of Biochemistry* 134.1: 43-49.

Amara, S., Slama, I. B., Mrad, I., Rihane, N., Khemissi, W., El Mir, L., Rhouma, K. B., Abdelmelek, H. and Salky, M. 2014. Effects of zinc oxide nanoparticles and/or zinc chloride on biochemical parameters and mineral levels in rat liver and kidney. *Human and Experimental Toxicology* 33.11:1150-1157.

Amelar, R. D. 1966. The semen analysis. In: Infertility in men. F. A. Davis Company, Philadelphia, U.S.A pp 30-53.

Andersson, P. O., Lejon, C., Ekstrand-Hammarstrom. B., Akfur. C., Ahlinder. L., Bucht. A. and Osterlund, L. 2011. Polymorph- and size-dependent uptake and toxicity of TiO_2 Nanoparticles in living lung epithelial cells. *Small* 7.4: 514–523.

Arora, S., Jain, J., Rajwade, J. M. and Paknikar, K. M. 2009. Interactions of silver nanoparticles with primary mouse fibroblasts and liver cells. *Toxicology and Applied Pharmacology* 236.3: 310-318.

Asakura M., Sasaki, T., Sugiyama, T., Takaya, M., Koda, S., Nagano, K., Arito, H. and Fukushima, S. 2010. Genotoxicity and cytotoxicity of multi-wall carbon nanotubes in cultured Chinese Hamster lung cells in comparison with chrysolite A fibers. *Journal Occupational Health* 52.3: 155-166.

AshaRani, P. V., Mun, G. L. K., Hande, M. P. and Valiyaveettil, S. 2009. Cytotoxicity and genotoxicity of silver nanoparticles in human cells. *ACS Nano* 3.2: 279-290.

Ashby, M. F., Ferreira, P. J. and Schodek, D. L. 2009. Nanomaterials, nanotechnologies and design: an introduction for Engineers and Architects. Butterworth-Heinemann. pp560.

Attia, A. A. 2014. Evaluation of the testicular alterations induced by silver nanoparticles in male mice: biochemical, histological and ultrastructural studies. *Research Journal of Pharmaceutical, Biological and Chemical Sciences* 5.4: 1558-1589.

Awasthi, K. K., Verma, R., Awasthi, A., Awasthi, K., Soni, I. and John, P. J. 2015. *In vivo* genotoxic assessment of silver nanoparticles in liver cells of Swiss albino mice using the comet assay. *Advanced Materials Letters* 6.3: 187-193.

Baarends, W. M., Hoogerbrugge, J. W., Roest, H. P., Ooms, M., Vreeburg, J., Hoeijmakers, J.H. and Grootegoed, J.A. 1999. Histone ubiquitination and

chromatin remodeling in mouse spermatogenesis. *Developmental Biology* 207:322–333.

Baek, M., Chung, H., Yu, J., Lee, J. A., Kim, T. H., Oh, J. M., Lee, W. J., Paek, S. M., Lee, J.K., Jeong, J., Choy, J. H. and Choi, S. J. 2012. Pharmacokinetics, tissue distribution and excretion of zinc oxide nanoparticles. *International Journal of Nanomedicine* 7: 3081-3097.

Bailey, S. A., Zidell, R. H. and Perry, R. W. 2004. Relationships between organ weight and body/brain weight in the rat: what is the best analytical endpoint? *Toxicologic Pathology* 32.4: 448-66.

Balasubramanyam, A., Sailaja, N., Mahboob, M., Rahman, M. F., Hussain, S. M. and Grover, P. 2009a. *In vivo* genotoxicity assessment of aluminum oxide nanomaterials in rat peripheral blood cells using the comet assay and micronucleus test. *Mutagenesis* 24.3: 245-251.

Balasubramanyam, A., Sailaja, N., Mahboob, M., Rahman, M. F., Misra, S., Hussain, S. M. and Grover, P. 2009b. Evaluation of genotoxic effects of oral exposure to aluminum oxide nanomaterials in rat bone marrow. *Mutation Research* 676.1-2: 41-47.

Ballmer, P. E. 2001. Causes and mechanisms of hypoalbuminaemia. *Clinical Nutrition* 20.3: 271-273.

Barillet, S., Jugan, M. L., Laye, M., Leconte, Y., Herlin-Boime, N., Reynaud, C. and Carriere, M. 2010. *In vitro* evaluation of SiC nanoparticles impact on A549 pulmonary cells: cyto-, genotoxicity and oxidative stress. *Toxicology Letters* 198.3: 324–330.

Barkhordari, A., Hekmatimoghaddam, S., Jebali, A., Khalili, A., Talebi, A. and Noorani, M. 2013. Effect of zinc oxide nanoparticles on viability of human spermatozoa. *Iranian Journal of Reproductive Medicine* 11.9: 767-771.

Barnes, C. A., Elsaesser, A., Arkusz, J., Smok, A., Palus, J., Les´niak, A., Salvati, A, Hanrahan, J. P., Jong W. H., Dziubaltowoska, E., Stepnik, M., Rydzynski, K., McKerr, G., Lynch, I., Dawson, K. A. and Howard, C. V. 2008. Reproducible comet assay of amorphous silica nanoparticles detects no genotoxicity. *Nano Letters* 8.9: 3069–3074.

Bartels, H. and Bohmer, M. 1972. A colourimetric method for determination of serum creatinine. *Clinica Chimica Acta* 37: 193.

Bartke, A., Weir, J. A., Mathison, P., Roberson, C. and Dalterio, S. 1974. Testicular function in mouse strains with different age of sexual maturation. *Journal of Hereditary* 65.4: 204-208.

Baskerville, A., Fitzgeorge, R. B., Gilmour, M. I., Dowsett, A. B., Williams, A. and Featherstone, A. S. 1988. Effects of inhaled titanium dioxide dust on the lung and on the course of experimental Legionnaires' disease. *British Journal of Experimental Pathology* 69.6: 781-792.

Baum, N., Dichoso, C. C. and Carlton, C. E. 1975. Blood urea nitrogen and serum creatinine. Physiology and Interpretations. *Urology* 5.5: 583-858.

Beatty, R. A. 1970. The genetics of the mammalian gamete. *Biological Reviews* 45:73 - 119.

Bebington, C., Doherty, F. J. and Fleming, S. D. 2001. The possible biological and reproductive functions of ubiquitin. *Human Reproduction Update* 7:102–111.

Begnum, A., HariKrishna, S. and Khan, I. 2009. Analysis of heavy metals in water, sediments and fish samples of Madivala lakes of Bangalore, Karnataka. *International Journal of ChemTech Research* 1.2: 245-249.

Bektas, M., Savas, B., Cetinkaya, H., Ensari, A., Oztas, E., Can, B. and Ozden, A. 2008. An unusual presentation of tangier disease with gall bladder involvement. *Acta Gastro enterologica Belgica* 71: 397-400.

Benigni, R., Bossa, C., Tcheremenskaia ,O., Battistelli ,C. L. and Crettaz, P. 2012. The new ISSMIC database on *in vivo* micronucleus and its role in assessing genotoxicity testing strategies. *Mutagenesis*27: 87–92.

Ben-Slama, I., Amara, S., Mrad, I., Rihane, N., Omri, K., El Ghoul, J., El Mir, L., Rhouma, K. B., Abdelmelek, H. and Sakly, M. 2015. Sub-acute oral toxicity of zinc oxide nanoparticles in male rats. *Journal of Nanomedicine and Nanotechnology* 6.284 DOI: 10.4172/2157-7439.1000284.

Bermudez, E., Mangum, J. B., Asgharian, B., Wong, B. A., Reverdy, E. E., Janszen, D. B., Hext, P. M., Warheit, D. B. and Everitt, J. I. 2002. Long-term pulmonary responses of three laboratory rodent species to subchronic inhalation of pigmentary titanium dioxide particles. *Toxicological Sciences* 70.1: 86–97.

Bermudez, E., Mangum, J. B., Wong, B. A., Asgharian, B., Hext, P. M., Warheit, D. B. and Everitt, J. I. 2004. Pulmonary responses of mice, rats and hamsters to subchronic inhalation of ultrafine titanium dioxide particles. *Toxicological Sciences* 77.2: 347–357.

Bermudez, V., Cano, R., Cano, C., Bermudez, F., Arraiz, N., Acosta, L., Finol, F., Pabon, M. R., Amell, A., Reyna, N., Hidalgo, J., Kendall, P., Manuel, V. and Hernandez, R. 2008. Pharmacologic management of isolated low high-density lipoprotein syndrome. *American Journal of Therapeutics* 15.4: 377-388.

Bernard, B. K., Osheroff, M. R., Hofmann, A. and Mennear, J. H. 1990. Toxicology and carcinogenesis studies of dietary titanium dioxide-coated mica in male and female Fischer 344 rats. *Journal of Toxicology and Environmental Health Part A* 29.4: 417–429.

Bebb, R. A., Bradley, D. A., Christenses, R. B., Paulsen, C. A., Bremmer, W. J. and Matsumoto, A. M. 1996. Combined administration of Levonorgestrel and testosterone induces more rapid and effective suppression of spermatogenesis than testosterone alone: a promising male contraceptive approach. *Journal of Clinical Endocrinology Metabolism* 81.2: 757-762.

Beutler, E., Duron, O. and Kelly, B. M. 1963. Improved method for determination of blood glutathione. *The Journal of Laboratory and Clinical Medicine* 61: 882-888.

Bhatnagar, D., Soran, H. and Durrington, P. N. 2008. Hypercholesterolaemia and its management. *BMJ* 337: a993.

Bhattacharya, K., Davoren, M., Boertz, J., Schins, R. P., Hoffmann, E. and Dopp, E. 2009. Titanium dioxide nanoparticles induce oxidative stress and DNA-adduct formation but not DNA-breakage in human lung cells. *Particle and Fibre Toxicology* 6: 17. doi: 10.1186/1743-8977-6-17.

Bianco, A. and Prato, M. 2003. Can Carbon Nanotubes be Considered Useful Tools for Biological Applications? *Advanced Materials* 15.20: 1765-1768.

Bitzur, R., Cohen, H., Kamari, Y., Shaish, A. and Harats, D. 2009. Triglycerides and HDL Cholesterol: Stars or second leads in diabetes? *Diabetes Care* 32.S2: S373-S377.

Boller, K. and Schmid. W. 1970. Chemische Mutagenese beim Sauger. Das knochenmark des Chinesischen Hamsters als in vivo-testsystem. Haematologische befunde nach Behandlung mit Trenimon. *Humangenetik* 11: 35–54.

Bollu, V. S., Nethl, S. K., Dasari, R. K., Rao, S. S., Misra, S. and Patra, C. R. 2016a. Evaluation of *in vivo* cytogenetic toxicity of europium hydroxide nanorods (EHNs) in male and female Swiss albino mice. *Nanotoxicology* 10.4: 413-425. DOI: 10.3109/17435390.2015.1073398.

Bollu, V. S., Soren, G., Jamil, K., Bairi, A. and Yashmaina, S. 2016b. Genotoxic and histopathological evaluation of zinc oxide nanorods *in vivo* in swiss albino mice. *Journal of Evolution of Medical and Dental Sciences* 5.83: 6186-6191.

Bonassi, S., El-Zein, R., Bolognesi, C. and Fenech, M. 2011. Micronuclei frequency in peripheral blood lymphocytes and cancer risk: evidence from human studies. *Mutagenesis* 26: 93–100.

Bonassi, S., Znao,r A., Ceppi, M., Lando, C., Chang, W. P., Holland, N., Kirsch-Volders, M., Zeiger, E., Ban, S., Barale, R., Bigatti, M. P., Bolognesi, C., Cebulska-Wasilewska, A., Fabianova, E., Fucic, A., Hagmar, L., Joksic, G., Martelli, A., Migliore, L., Mirkova, E., Scarfi, M. R., Zijno, A., Norppa, H. and Fenech, M. 2006. An increased micronucleus frequency in peripheral blood lymphocytes predicts the risk of cancer in humans. *Carcinogenesis* 28.3: 625–31.

Bondarenko, O., Juganson, K., Ivask, A., Kasemets, K., Mortimer, M. and Kahru, A. 2013. Toxicity of Ag, CuO and ZnO nanoparticles to selected environmentally relevant test organisms and mammalian cells in vitro: A critical review. *Archives of Toxicology* 87.7: 1181-1200.

Boverhof, D. R. and David, R. M. 2010. Nanomaterial characterisation: considerations and needs for hazard assessment and safety evaluation. *Analytical and Bioanalytical Chemistry* 396.3: 953- 961.

Boxall, A. B., Tiede, K. and Chaudhry, Q. 2007. Engineered nanomaterials in soils and water: how do they behave and could they pose a risk to human health? *Nanomedicine (London)* 2.6: 919-927.

Braydich-Stolle, L., Hussain, S., Schlager, J. J. and Hofmann, M. 2005. *In vitro* cytotoxicity of nanoparticles in mammalian germline stem cells. *Toxicological Sciences* 88.2: 412–419.

Brinkworth, M. H. 2000. Paternal transmission of genetic damage: Findings in animals and humans. *International Journal of Andrology* 23.3: 123-135.

Brendler-Schwaab, S., Hartmann, A., Pfuhler, S. and Speit, G. 2005. The *in vivo* comet assay: use and status in genotoxicity testing. *Mutagenesis* 20: 245–54.

Brohmann, H., Pinnecke, S. and Hoyer-Fender, S. 1997. Identification and characterisation of new cDNAs encoding outer dense fiber proteins of rat sperm. *Journal of Biological Chemistry* 272:10327–10332.

Browning, C. L., The, T., Mason, M. D. and Wise Sr, J. P. 2014. Titanium dioxide nanoparticles are not cytotoxic or clastogenic in human skin cells. *Journal of Environmental and Analytical Toxicology* 4.6: 239. Doi: 10.4172/2161-0525.1000239.

Bruce, W. R., Furrer, R., Wyrobek, A. J. 1974. Abnormalities in the shape of murine sperm after acute testicular X-irradiation. *Mutation Research* 23: 381-386.

Bu, Q., Yan, G., Deng, P., Peng, F., Lin, H., Xu, Y., Cao, Z., Zhou, T., Xue, A., Wang, Y., Cen, X. and Zhao, Y. L. 2010. NMR-based metabonomic study of the sub-acute toxicity of titanium dioxide nanoparticles in rats after oral administration. *Nanotechnology* 21.12: 125105.

Burnett, M. E. and Wang, S. Q. 2011. Current sunscreen controversies: a critical review. *Photodermatology Photoimmunology and Photomedicine* 27.2: 58–67.

Buzea, C., Pacheco, I. I. and Robbie, K. 2007. Nanomaterials and nanoparticles: Sources and toxicity. *Biointerphases* 2.4: MR17-MR71.

Calderon, R., Schenider, R. H., Alexander, C. N., Myers, H. F., Nidich, S. I. and Haney, C. 1999. Stress, stress reduction and hypercholesterolemia in African Americans: a review. *Ethinicity & Disease* 9.3: 451-462.

Calza, L., Manfredi, R. and Chiodo, F. 2004. Dyslipidaemia associated with antiretroviral in HIV-infected patients. *Journal of Antimicrobial Chemotherapy* 53.1: 10-14.

Cambier, S., Gogeberg, M., Georgantzopoulou, A., Serchi, T., Karlsson, C., Verhaegen, S., Iversen, T., Guignard, C., Kruszewski, M., Hoffmann, L., Audinot, J., Ropstad, E. and Gutleb, A. C. 2018. Fate and effects of silver nanoparticles on early life-stage development of zebrafish (*Danio rerio*) in comparison to silver nitrate. *Science of the Total Environment* 610-611: 972-982.

Cañas, J. E., Long, M., Nations, S., Vadan, R., Dai, L., Luo, M., Ambikapathi, R., Lee, E. H and Olszyk, D. 2008. Effects of functionalised and non-functionalised single-walled carbon nanotubtes on root elongation of select crop species. *Environmental Toxicology and Chemistry* 27.9: 1922-1931.

Catalan, J., Jarventaus, H., Vippola, M., Savolainen, K. and Norppa, H. 2012. Induction of chromosomal aberrations by carbon nanotubes and titanium dioxide nanoparticles in human lymphocytes *in vitro*. *Nanotoxicology* 6: 825-836.

Chan, V. S. 2006. Nanomedicine: an unresolved regulatory issue. *Regulatory Toxicology and Pharmacology* 46.3: 218–224.

Chandra, A. K., Chatterjee, A., Ghosh, R., Sarkar, M. and Chaube, S. K. 2007. Chromium induced testicular impairment in relation to adrenocortical activities in adult albino rats. *Reproductive Toxicology* 24.3-4: 388-396.

Chandra, A. K., Chatterjee, A., Ghosh, R. and Sarkar, M. 2010. Vitamin E-supplementation protects chromium (VI)-induced spermatogenic and steoidogenic disorders in testicular tissues of rats. *Food and Chemical Toxicology* 48: 972-979.

Chatterjee, T., Chakraborti, S., Joshi, P., Singh, S. P., Gupta, V. and Chakrabarti, P. 2010. The effect of zinc oxide nanoparticles on the structure of the periplasmic domain of the Vibrio cholerae ToxR protein. *FEBS Journal*277.20: 4184–4194.

Cheesbrough, M. 2005. District Laboratory practice in tropical countries: Haematological test Part 2. 2nd ed. Cambridge Low Price Editions. Pp 263-347.

Chen, H. W., Su, S. F., Chien, C. T., Lin, W. H., Yu, S. L., Chou, C. C., Chen, J. J. and Yang, P. C. 2006. Titanium dioxide nanoparticles induce emphysema-like lung injury in mice. *Federation of American Societies for Experimental Biology Journal* 20.13: 2393-2395.

Chen, J., Dong, X., Zhao, J. and Tang, G. 2009. *In vivo* acute toxicity of titanium dioxide nanoparticles to mice after intraperitioneal injection. *Journal of Applied Toxicology* 29.4: 330–337.

Chen, J., Zhou, H., Santulli, A. C. and Wong, S. S. 2010. Evaluating cytotoxicity and cellular uptake from the presence of variously processed TiO_2 nanostructured morphologies. *Chemical Research in Toxicology* 23.5: 871–879.

Chen, S., Allam, J. P., Duan, Y. G. and Haidl, G. 2013. Influence of reactive oxygen species on human sperm functions and fertilizing capacity including therapeutical approaches. *Archives of Gynecology and Obstetrics* 288.1: 191-199. DOI: 10.1007/s00404-013-2801-4.

Chen, T., Yan, J. and Li, Y. 2014. Genotoxicity of titanium dioxide nanoparticles. *Journal of Food and Drug Analysis* 22.1: 95-104.

Chen, Y., Xue, Z., Zheng, D., Xia, K., Zhao, Y., Liu, T., Long, Z. and Xia, J. 2003. Sodium chloride modified silica nanoparticles on a non viral vector with a high efficiency of DNA transfer into cells. *Current Gene Therapy* 3.3: 273-279.

Cheraghi, J., Hosseini, E., Hoshmandfar, R. and Sahraei, R. 2013. Hematologic parameters study of male and female rats treated with different concentrations of Silver Nanoparticles. *International Journal of Agriculture and Crop Sciences* 5.7: 789-796.

Cho, C., Jung-Ha, H., William, W. D., Goulding, E. H., Stein, P., Xu Z, Schultz, R. M., Hecht, N. B. and Eddy, E. M.. 2003. Protamine 2 deficiency leads to sperm DNA damage and embryo death in mice. *Biology of Reproduction* 69.1: 211–217.

Cho, W. S., Duffin, R., Poland, C. A., Duschl, A., Oostingh, G. J., Macnee, W., Bradley, M., Megson, I. L. and Donalson, K. 2012. Differential pro-inflammatory effects of metal oxide nanoparticles and their soluble ions *in vitro* and *in vivo*; zinc and copper nanoparticles, but not their ions, recruit eosinophils to the lungs. *Nanotoxicology* 6.1: 22–35.

Cho, W. S., Kang, B. C., Lee, J. K., Jeong, J., Che, J. H. and Seok, S. H. 2013. Comparative absorption, distribution and excretion of titanium dioxide and zinc oxide nanoparticles after repeated oral administration. *Particle and Fibre Toxicology* 10: 9. doi: 10.1186/1743-8977-10-9.

Choi, J., Kim, H., Kim, P., Jo, E., Kim, H. M., Lee, M. Y., Jin, S. M. and Park, K. 2015. Toxicity of zinc oxide nanoparticles in rats treated by two different routes: single intravenous injection and single oral administration. *Journal of Toxicology and Environmental Health* Part A 78.4: 226-243.

Choi, M. R., Stanton-Maxey, K. J., Stanley, J. K., Levin, C. S., Bardhan, R., Akin, D., Badve, S., Sturgis, J., Robinson, J. P. and Bashir, R. 2007. A cellular trojan horse for delivery of therapeutic nanoparticles into tumours. *Nano Letters* 7.12: 3759-3765.

Choi, S., Lee, J., Jeong, J. and Jin-Ho, C. 2013. Toxicity evaluation of inorganic considerations and challenges. *Molecular and Cell Toxicology* 9.3: 205-210.

Chow, E., Herrmann, J., Barton, C.S., Raguse, B. and Wieczorek, L. 2009. Inkjet-printed gold nanoparticle chemiresistors: Influence of film morphology and ionic strength on the detection of organics dissolved in aqueous solution. *Analytica Chimica Acta* 632.1: 135-142.

Chung, H. E., Yu, J., Baek, M., Lee, J. A., Kim, M. S., Kim, S. H., Maeng, E. H., Lee, J. K., Jeong, J. and Choi, S. J. 2012. Toxicokinetics of zinc oxide nanoparticles in rats. *Journal of Physics: Conferences Series*. 429.1. doi: 10.1088/1742-6596/429/1/012037.

CIOMS. 1985. International guiding principles for biomedical research involving animals. http://www.cioms.ch/publications/guidelines/1985_texts_of_guidelines.htm (Available online; accessed on 23 August 2014).

Claiborne, A. 1985. Catalase activity. In: Wald RAG (ed) CRC Handbook of Methods for Oxygen Radical Research, CRC Press, Boca Raton, FL, USA, pp 283-284.

Clark, J. M. 2006. The epidemiology of non alcoholic fatty liver disease in adults. *Journal of Clinical Gastroenterology* 40: S5-10.

Cooke, M. S., Evans, M. D., Dizdaroglu, M. and Lunec, J. 2003. Oxidative DNA damage: mechanisms, mutation and disease. *Federation of American Societies of Experimental Biology* 17.10: 1195–1214.

Couto, N., Malys, N., Gaskell, S. and Barber, J. 2013. Partition and Turnover of Glutathione Reductase from Saccharomyces cerevisiae: a Proteomic Approach. *Journal of Proteomic Research* 12.6:2885-2894.

Countryman, P. I. and Heddle, J. A. 1976. The production of micronuclei from chromosome aberrations in irradiated cultures of human lymphocytes. *Mutation Research* 41: 321–32.

Cox, R. A. and García-Palmieri, M. R. 1990. Cholesterol, Triglycerides and Associated Lipoproteins. In: Walker, H. K., Hall, W. D. and Hurst, J.W., editors. Clinical Methods: The History, Physical and Laboratory Examinations. 3rd edition. Boston: Butterworths; Chapter 31. Available from: https://www.ncbi.nlm.nih.gov/books/NBK351/

Cui, Y., Chen, X., Zhou, Z., Lei, Y., Ma, M., Cao, R., Sun, T., Xu, J., Huo, M., Cao, R., Wen, C. and Che, Y. 2014. Prenatal exposure to nanoparticulate titanium dioxide enhances depressive-like behaviours in adult rats. *Chemosphere* 96: 99-104.

Cui, Y., Liu, H., Zhou, M., Duan, Y., Li, N., Gong, X., Hu, R., Hong, M. and Hong, F. 2011. Signaling pathway of inflammatory responses in the mouse liver caused by TiO_2 nanoparticles. *Journal of Biomedical Materials Research Part A* 96.1: 221–229.

Dabla, P. K. 2010. Renal function of diabetic nephropathy. *World Journal of Diabetes* 1.2: 48-56.

Dalton, R. N. 2010. Serum creatinine and glomerular filtration rate: perception and reality. *Clinical Chemistry* 55.5: 687-689.

Daniel, S. P. and Marshal, M. P. 2007. Laboratory test. In: Schiff's diseases of the liver, 10th edition, volume 1, Eugene, R. S, Michael, F. S, Willis, C. M. Lippincott Williams and Wilkins pp19-54.

Dankovic, D., Kuempel, E. and Wheeler, M. 2007. An approach to risk assessment for TiO_2. *Inhalation Toxicology* 19(Suppl 1): 205–212.

Darroudi, M., Sabouri, Z., Oskuee, R. K. Kargar, H. and Hosseini, H. A. 2014. Neuronal toxicity of biopolymer-template synthesised ZnO nanoparticles. *Nanomedicine Journal* 1.2: 93-98.

De Boer, P., de Vries, M. and Ramos, L. 2015. A mutation study of sperm head shape and motility in the house: lessons for the clinic. *Andrology* 3: 174-202.

Demir, E., Akca, H., Kaya, B., Burgucu, D., Tokgun, O., Turna, F., Aksakal, S., Vales, G., Creus, A. and Marcos, R. 2014. Zinc oxide nanoparticles: Genotoxicity, interactions with UV-light and cell-transforming potential. *Journal of Hazardous Materials* 264: 420-429.

Demir, E., Akca, H., Turna, F., Aksakal, S., Burgucu, D., Kaya, B., Tokgun, O., Vales, G., Creus, A. and Marcos, R. 2015. Genotoxic and cell-transforming effects of titanium dioxide nanoparticles. *Environmental Research* 136: 300-308.

Deng, Z. J., Mortimer, G., Schiller, T., Musumeci, A., Martin, D. and Minchin, R. F. 2009. Differential plasma protein binding to metal oxide nanoparticles. *Nanotechnology* 20.45: 455101.

Dhawan, A., Sharma, V. and Parmar, D. 2009. Nanomaterials: a challenge for toxicologists. *Nanotoxicology* 3.1: 1–9.

Di Virgilio, A. L., Regiosa, M., Arnal, P. M. and Fernandez Lorenzo de Mele, M. 2010. Comparative study of the cytotoxic and genotoxic effects of titanium dioxide and aluminum oxide nanoparticles in Chinese hamster ovary (CHO-K1) cells. *Journal of Hazardous Materials* 177.1-3: 711-718.

Dimkpa, C. O., Calder, A., Britt, D. W., McLean, J. E. and Anderson, A. J. 2011. Responses of a soil bacterium, pseudomonas chlorophis O6 to commercial metal oxide nanoparticles compared with responses to metal ions. *Environmental Pollution* (Oxford, UK) 159.7: 1749-1756.

Dobrzynska, M. M., Gajowik, A., Radzikowska, J., Lankoff, A., Dusinska, M. and Kruszewski, M. 2014. Genotoxicity of silver and titanium dioxide nanoparticles in bone marrow cells of rats *in vivo*. *Toxicology* 315: 86-91.

Don, B. R. and Kaysen, G. 2004. Serum albumin: relationship to inflammation and nutrition. *Seminars in Dialysis* 17.6: 432-437.

Dorman, D. C., McManus, B. E., Parkinson, C. U., Manuel, C. A., McElveen, A. M., Everitt, J. I. 2004. Nasal toxicity of manganese sulfate and manganese phosphate in young male rats following subchronic (13-week) inhalation exposure. *Inhalation Toxicology* 16.6-7: 481–488.

Doudi, M. and Setorki, M. 2013. The effect of gold nanoparticles on renal function in rats. *Nanomedicine Journal* 1.3: 171-179.

Du, H., Zhu, X., Fan, C., Xu, S., Wang, Y. and Zhou, Y. 2012. Oxidative damage and OGG1 Expression induced by a combined effect of titanium dioxide nanoparticles and lead acetate in human hepatocytes. *Environmental Toxicology* 27.10: 590-597.

Du, Y. and Wang, C. 2009. Preparation Ru, Bi monolayer modified Pt nanoparticles as the anode catalyst for methanol oxidation. *Materials Chemistry and Physics* 113.2-3: 927-932.

Duffaud, F., Orsiere, T., Digue, L., Villani, P., Volot, F., Favre, R. and Botta, A. 1999. Micronucleated lymphocyte rates from head-and-neck cancer patients. *Mutation Research* 439: 259–66.

Dumas, B. T., Watson, W. A. and Biggs, H. G. 1997. Albumin standards and the measurement of serum albumin with bromocresol green 1971. *International Journal of Clinical Chemistry* 258.1: 21-30.

Durrington, P. 2003. Dyslipidaemia. *The Lancet* 362.9385: 717-731.

Dusinska, M., Fjellsbø, L. M., Magdolenova, Z., Ravnum, S., Rinna, A. and Rundén-Pran, E. 2011. Safety of Nanoparticles in Medicine. In: Nanomedicine in Health and Disease. Preedy, V. R. Ed. USA: Science Publishers, Chap. 11, pp. 203–226.

Dusinska, M., Rundén-Dusinska, M., Rundén-Pran, E., Carreira, S. C. and Saunders, M. 2012. *In vitro* and *in vivo* toxicity test methods. Chapter 4. Critical evaluation of toxicity tests. In: Fadeel, B., Pietroiusti, A., Shvedova, A. editors. Adverse effects of engineered nanomaterials: exposure, toxicology and impact on human health. Elsevier; pp. 63–84.

Dutta, R. K., Nenavathu, B. P., Gangishetty, M. K. and Reddy, A. V. 2013. Antibacterial effect of chronic exposure of low concentration ZnO nanoparticles on *E coli*. *Journal of Environmental Science and Health Part A: Toxic/Hazardous Substances and Environmental Engineering* 48.8: 871-878.

El Khoury, P., Plengpanich, W., Frisdal, E., Le Goff, W., Khovidhunkit, W., Guerin, M. 2014. Improved plasma cholesterol efflux capacity from human macrophages in patients with hyperaliphalipoproteinemia. *Atherosclerosis* 234.1: 193-199.

Elder, A. and Oberdörster, G. 2006. Translocation and effects of ultrafine particles outside of the lung. *Clinics in Occupational Environmental Medicine* 5.4:785-796.

El-Morshedi, N., AlZahrani, I., Kizilbash, N. A. and Al-Fayez, H. A. A. 2014. Toxic effect of zinc oxide nanoparticles on some organs in experimental male wistar rats. *International Journal of Advanced Research* 2.4: 907-915.

Ema, M., Kobayashi, N., Naya, M., Hanai, S. and Nakanishi, J. 2010. Reproductive and developmental toxicity studies of manufactured nanomaterials. *Reproductive Toxicology* 30.3: 343-352.

Environmental Defense and DuPont. 2013. Nano Risk Framework. 21 June. http//www.NanoRiskFramework.com.(Available online: Accessed August 10, 2013).

Escalier, D., Bai, X., Silvius, D., Xu, P. and Xu, X. Spermatid nuclear and sperm periaxonemal anomalies in the mouse *Ube2b* null mutant. 2003. *Molecular Reproduction and Development* 65: 298-308.

Esmaeillou, M., Moharamnejad, M., Hsankhani, R., Tehrani, A. A. and Maadi, H. 2013. Toxicity of ZnO nanoparticles in healthy adult mice. *Environmental Toxicology and Pharmacology* 35.1:67-71.

Esterhuizen, A. D., Franken, D. R., Lourens, J. G., Prinsloo, E. and van Rooyen, L. H. 2000. Sperm chromatin packaging as an indicator of in vitro fetrilisation rates. *Human Reproduction* 15: 657-661.

EU - European Commission Recommendation on the definition of nanomaterial. http://osha.europa.eu/en/news/eu-european-commissionrecommendation-on-the-definition-of-nanomaterial.

Evelyn, A., Mannick, S. and Sermon, P. A. 2003. Unusual carbon-based nanofibers and chains among diesel emitted particles. *Nano letters* 3.1: 63-64.

Evenson, D. P., Jost, L. K., Baer, R. K., Turner, T. W. and Schader, S. M. 1991. Individuality of DNA denaturation patterns in human sperm as measured by the sperm chromatin structure assay. *Reproductive Toxicology* 5.2: 115-125.

Eydner, M., Schaudien, D., Creutzenberg, O., Ernst, H., Hansen, T., Baumgartner, W. and Rittinghausen, S. 2012. Impacts after inhalation of nano- and fine-sized titanium dioxide particles: morphological changes, translocation within the rat lung and evaluation of particle deposition using the relative deposition index. *Inhalation Toxicology* 24.9: 557–569.

Fabian, E., Landsiedel, R., Ma-Hock, L., Wiench, K., Wohlleben, W. and Ravenzwaay, B. V. 2008. Tissue distribution and toxicity of intravenously treated titanium dioxide nanoparticles in rats. *Archives of Toxicology* 82.3: 151-157.

Falck, G. C. M., Lindberg, H. K., Suhonen, S., Vippola, M., Vanhala, E., Catalan, J., Savolainen, K. and Norppa, H. 2009. Genotoxic effects of nanosized and fine TiO_2. *Human and Experimental Toxicology* 28.6-7: 339-352.

Farrell, G. C. and Larter, C. Z. 2006. Nonalcoholic fatty acid disease: from steatosis to cirrhosis. *Hepatology* 43.2S1: S99-S112.

Fawcett, D. W. and Chemes, H. E. 1979. Changes in distribution of nuclear pores during differentiation of the male germ cells. *Tissue Cell* 11:147–162.

Federici, G., Shaw, B. J. and Handy, R. D. 2007. Toxicity of titanium dioxide nanoparticles to rainbow trout (*Oncorrhynchus mykiss*): Gill injury,

oxidative stress and other physiological effects. *Aquatic toxicology* 84.4: 415-430.

Fenech, M. 2000. The *in vitro* micronucleus technique. *Mutation Research* 455: 81–95.

Fenech, M. 2007. Cytokinesis-block micronucleus cytome assay. *Nature protocols* 2:1084–104.

Fenech, M. 2010. The lymphocyte cytokinesis-block micronucleus cytome assay and its application in radiation biodosimetry. *Health Physics* 98: 234–43.

Fenech, M. and Morley, A. A. 1985. Measurement of micronuclei in lymphocytes. *Mutation Research* 147: 29–36.

Fenech, M., Holland, N., Chang, W. P., Zeiger, E. and Bonassi, S. 1999. The Human Micronucleus Project-An international collaborative study on the use of the micronucleus technique for measuring DNA damage in humans. *Mutation Research* 428: 271–83.

Feng, J., Liu, H., Bhakoo, K. K., Lu, L. and Chen, Z. 2011. A metabolomic analysis of organ specific response to USPIO administration. *Biomaterials* 32.27: 6558–6569.

Ferin, J., Oberdorster, G. and Penney, D. P. 1992. Pulmonary retention of ultrafine and fine particles in rats. *American Journal of Respiratory Cell and Molecular Biology* 6.5: 535–542.

Fernandez, J. L., Muriel, L., Rivero, M. T., Goyanes, V., Vazquez, R. and Alvarez, J. G. 2003. The sperm chromatin dispersion test: a simple method for the determination of sperm DNA fragmentation. *Journal of Andrology* 24.1: 59-66.

Fernandez, J. L., Vazquez-Gundin, F., Delgado, A., Goyanes, V. J., Ramiro-Diaz, J., de la Torre, J. and Gosalvez, J. 2005. DNA breakage detection-FISH (DBD-FISH) in human spermatozoa: technical variants evidence different structural features. *Mutation Research* 453.1: 77-82.

Ferreira, G. K., Cardoso, E., Vuolo, F. S., Michels, M., Zanoni, E. T., Carvalho-Silva, M., Gomes, L. M., Dal-Pizzol, F., Rezin, G. T., Streck, E. L. and Paula, M. M. 2015. Gold nanoparticles alter parameters of oxidative stress and energy metabolism in organs of adult rats. *Biochemistry and Cell Biology* 93.6: 548-557.

Filipe, P., Silva, J. N., Silva, R., Cirne de Castro, J. L., Marques Gomes, M., Alvs, L. C., Santus, R. and Pinheiro, T. 2009. Stratum corneum is an effective barrier to TiO_2 and ZnO nanoparticles percutaneous absorption. *Skin Pharmacology and Physiology* 22.5: 266–275.

Finn, A. V., Nakano, M., Narula, J., Kolodgic, F. D. and Virmani, R. 2010. Concept of vulnerable/unstable plaque. *Arteriosclerosis, thrombosis and vascular biology* 30.7: 1282-1292.

Fiorini, C., Tilloy-Ellul, A., Chevalier, S., Charuel, C. and Pointis, G. 2004. Sertoli cell junctional proteins as early targets for different classes of reproductive toxicants. *Reproductive Toxicology* 18.3: 413-421.

Fischer, H. C. and Chan, W. C. 2007. Nanotoxicity: the growing need for *in vivo* study. *Current Opinion in Biotechnology* 18.6: 565-571.

Foldberg, R., Dang, D. A. and Autrup, H. 2011. Cytotoxicity and genotoxicity of silver nanoparticles in the human lung cancer cell line, A549. *Archives of Toxicology* 85.7: 743-750.

Franken, D. R. and Oehninger, S. 2012. Semen analysis and sperm function testing. *Asian Journal of Andrology* 14.1: 6-13.

Franklin, N. M., Rogers, N. J., Apte, S. C., Batley, G. E., Gadd, G. E. and Casey, P. S. 2007. Comparative toxicity of nanoparticulate ZnO, bulk ZnO and $ZnCl_2$ to a freshwater microalga (*Pseudokirchneriella subcapitata*): the importance of particle solubility. *Environmental Science and Technology* 41.24: 8484–8490.

Fujita, K., Horie, M., Kato, H., Endoh, S., Suzuki, M., Nakamura, A., Miyauchi, A., Yamamoto, K., Kinugasa, S. and Nishio, K. 2009. Effects of ultrafine TiO_2 particles on gene expression profile in human keratinocytes without illumination: involvement of extracellular matrix and cell adhesion. *Toxicology Letters* 191.2-3: 109–117.

Future Markets Inc. 2013.The global market for metal oxide nanoparticles to 2020, 322. Available:http://www.researchandmarkets.com/research/jkjd5k/the_global_market.Assessed 10 June, 2013.

Gaharwar, U. S. and Paulraj, R. 2015. Iron oxide nanoparticles induced oxidative damage in peripheral blood cells of rat. *Journal of Biomedical Science and Engineering* 8.4: 274-286.

Gallagher, J. C. and Seligson, D. 1962. Significance of abnormally low blood urea levels. *New England Journal of Medicine* 266: 492-495.

Gao, G., Ze, Y., Li, B., Zhao, X., Zhang, T., Sheng, L., Hu, R., Gui, S., Sang, X., Sun, Q., Cheng, J., Cheng, Z., Wang, L., Tang, M. and Hong, F. 2012. Ovarian dysfunction and gene-expressed characteristics of female mice caused by long-term exposure to titanium dioxide nanoparticles. *Journal of Hazardous Material* 243: 19-27.

Gao, G., Ze, Y., Zhao, X., Sang, X., Zheng, L., Ze, X., Gui, S., Sheng, L., Sun, Q., Hong, J., Yu, X., Wang, L., Hong, F. and Zhang, X. 2013. Titanium dioxide nanoparticles-induced testicular damage, spermatogenesis suppression and gene expression alterations in male mice. *Journal of Hazardous Materials* 258-259:133-143.

Garcia, T. X., Costa, G. M. J., Franca, L. R. and Hofmann, M. 2014. Sub-acute intravenous administration of silver nanoparticles in male mice alters Leydig cell function and testosterone levels. *Reproductive Toxicology* 45: 59-70.

Garcovich, M., Zocco, M. A. and Gasbarrini, A. 2009. Clinical use of albumin in hepatology. *Blood Transfusion* 7.4: 268-277.

Geim, A. K. and Novoselov, K. S. 2007. The rise of graphene. *Nature Materials* 6.3: 183-191.

Geiser, M. and Kreyling, W. G. 2010. Deposition and biokinetics of inhaled nanoparticles. *Particle and Fibre Toxicology* 7: 2.

Georgantzopoulou, A., Balachandran, Y. L., Rosenkranz, P., Dusinska, M., Lankoff, A., Wojewodzka, M., Hruszewski, M., Guignard, C., Audinot, J. N., Girija, S., Hoffmann, L and Gutleb, A. C. 2013. Ag nanoparticles: size- and surface-dependent effects on model aquatic organisms and uptake evaluation with NanoSIMS. *Nanotoxicology* 7:1168–78.

Georgantzopoulou, A., Serchi, T., Cambier, S., Leclercq, C. C., Renaut, J., Shao, J., Kruszewski, M., Lentzen, E., Grysan, P., Eswara, S., Audinot, J., Contal, S., Ziebel, J., Guignard, C., Hoffmann, L., Murk, A. and Gutleb, A. C. 2016. Effects of silver nanoparticles and ions on a co-culture model for the gastrointestinal epithelium. *Particle and Fibre Toxicology* 13:9 DOI 10.1186/s12989-016-0117-9.

George, S., Pokhrel, S., Xia, T., Gilbert, B., Ji, Z., Schwalter, M., Rosenauer, A., Damolseaux, R., Bradley, K. A., Madler, L. and Nel, A. E. 2010. Use of a rapid cytotoxicity screening approach to engineer a safer zinc oxide nanoparticle through iron doping. *ACS Nano* 4.1: 15–29.

Ghosh, M., Bandyopadhyay, M. and Mukherjee, A. 2010. Genotoxicity of titanium dioxide (TiO_2) nanoparticles at two trophic levels: plant and human lymphocytes. *Chemosphere*, 81.10: 1253–1262.

Ghosh, M., Jana, A., Sinha, S., Jothiramajayam, M., Nag, A., Chakraborty, A., Mukherjee, A. and Mukherjee, A. 2016. Effects of ZnO nanoparticles in plants: cytotoxicity, genotoxicity, deregulation of antioxidant defenses and cell-cycle arrest. *Mutation Research- Genetic Toxicology and Environmental Mutagenesis* 807: 25-32.

Ghosh, M., Sinha, J. M., Chakraborty, A., Mallick, S. K., Bandyopadhyay, M. and Mukherjee, A. 2012. *In vitro* and *in vivo* genotoxicity of silver nanoparticles. *Mutation research/Genetic Toxicology and Environmental Mutagenesis* 749.1-2: 60-69.

Giannini, E., Risso, D., Botta, F., Chiarbonello, B., Fasoli, A., Malfatti, F., Romagnoli, P., Testa, E., Ceppa, P. and Testa, R. 2003. Validity and clinical utility of the aspartate aminotransferase-alanine aminotransferase ratio in assessing disease severity and prognosis in patients with hepatitis c virus-related chronic liver disease. *Archives of Internal Medicine* 163.2: 218-224.

Giri, S., Prasad, S. B., Giri, A. and Sharma, G. D. 2002. Genotoxic effects of malathion: an organophosphorus insecticide, using three mammalian bioassays *in vivo*. *Mutation research* 514: 223-231.

Gonzalez, L., Thomassen, L. C., Plas, G., Rabolli, V., Napierska, D., Decordier, I., Roelants, M., Hoet, P. H., Kirschhock, C. E., Martens, J. A., Lison, D. and Kirsch-Volders, M. 2010. Exploring the aneugenic and clastogenic potential in the nanosize range: A549 human lung carcinoma cells and amorphous monodisperse silica nanoparticles as models. *Nanotoxicology* 4: 382–395.

Gopalan, R. C., Osman, I. F., Amani, A., De Matas, M. and Anderson, D. 2009. The effect of zinc oxide and titanium dioxide nanoparticles in the Comet assay with UVA photoactivation of human sperm and lymphocytes. *Nanotoxicology* 3.1: 33-39.

Gorczyca, W., Traganos, F., Jesionowska, H. and Darzynkiewicz, Z. 1993. Presence of DNA strand breaks and increased sensitivity of DNA in situ to denaturation in abnormal human sperm cells: analogy to apoptosis of somatic cells. *Experimental Cell Research* 207.1: 202-205.

Gornal, A. G., Bardawill, C. J. and David, M. M. 1949. Determination of serum protein by means of biuret reaction. *Journal of Biological Chemistry* 177.2: 751-756.

Gowda, S., Desai, P., Hull, V. V., Math, A. A. K. Vernekar, S. N. and Kulkarni, S. S. 2009. A review on laboratory liver function tests. *Pan African Medical Journal* 3: 17.

Grissa, I., Elghoul, J., Ezzi, L., Chakroun, S., Kerkeni, E., Hassine, M., Mir, L. E., Mehdi, M., Cheikh, H. B. and Haouas, Z. 2015. Anaemia and genotoxicity induced by sub-chronic intragastric treatment of rats with titanium dioxide nanoparticles. *Mutation Research/ Genetic Toxicology and Environmental Mutagenesis* 794: 25-31.

Gromadzka-Ostrowska, J., Dziendzikowska, K., Lankoff, A., Dodrzynska, M., Instanes, C., Brunborg, G., Gajowik, A., Radzikowska, J., Wojewodzka, M. and

Kruszewski, M. 2012. Silver nanoparticles effects on epididymal sperm in rats. *Toxicology Letters* 214.3: 251-258.

Guan, R., Kang, T., Lu, F., Zhang, Z., Shen, H. and Liu, M. 2012. Cytotoxicity, oxidative stress and genotoxicity in human hepatocytes and embryonic kidney cells treated with ZnO nanoparticles. *Nanoscale Research Letters* 7.1: 602.

Guerrini, L., Garcia-Ramos, J. V., Domingo, C. and Sanchez-Cortes, S. 2009. Sensing polycyclic aromatic hydrocarbons with dithiocarbamate-functionalised Ag nanoparticles by surface-enhanced raman scattering. *Analytical Chemistry* 81.3: 953-960.

Gulson, B., McCall., M., Korsch, M., Gomez, L., Casey, P., Oylam, Y., Taylor, A., McCulloch, M., Trotter, J., Kinsley, L. and Greenoak, G. 2010. Small amounts of zinc from zinc oxide particles in sunscreens applied outdoors are absorbed through human skin. *Toxicological Science* 123.1: 264-280.

Guo, D., Wu, C., Jiang, H., Li, Q., Wang, X. and Chen, B. 2008. Synergistic cytotoxic effect of different sized ZnO nanoparticles and daunorubicin against leukemia cancer cells under UV irradiation. *Journal of Photochemistry and Photobiology* 93.3: 119-126.

Gurr, J. R., Wang, A. S., Chen, C. H. and Jan, K. Y. 2005. Ultrafine titanium dioxide particles in the absence of photoactivation can induce oxidative damage to human bronchial epithelial cells. *Toxicology* 213.1-2: 66–73.

Guyton, A. and Hall, J. 2006. Textbook of Medical Physiology. 11th Ed. Elsevier Inc.1600 John F. Kennedy Blvd., Suite 1800 Philadelphia, Pennsylvania 19103-2899. 1152pp.

Hackenberg, S., Scherzed, A., Harnisch, W., Froelich, K., Ginzkey, C., Koehler, C., Hagen, R. and Kleinsasser. 2012. Antitumour activity of photo-stimulated zinc oxide nanoparticles combined with paclitaxel or cisplatin in HNSCC cell lines. *Journal of Photochemistry and Photobiology B: Biology* 114: 87-93.

Hackenberg, S., Scherzed, A., Technau, A., Kessler, M., Froelich, K., Ginzkey, C., Koehler, C., Burghartz, M., Hagen, R. and Kleinsasser, N. 2011. Cytotoxic, genotoxic and pro-inflammatory effects of zinc oxide nanoparticles in human nasal mucosa cells *in vitro*. *Toxicology in vitro* 25.3:657–663.

Hagen, W. I., Oomen, A. G., de Jong, W. H., Cassee, F. R. and Sips, A. 2007. What do we (need to) know about the kinetic properties of nanoparticles in the body? *Regulatory Toxicology and Pharmacology* 49.3: 217–229.

Hamada, S., Ohyama, W., Takashima, R., Shimada, K., Matsumoto, K., Kawakami, S., Uno, F., Sui, H., Shimada, Y., Imamura, T., Matsumura, S., Sanada, H.,

Inoue, K., Muto, S., Ogawa, I., Hayashi, A., Takayanagi, T., Ogiwara, Y., Maeda, A., Okada, E., Terashima, Y., Takasawa, H., Narumi, K., Wako, Y., Kawasako, K., Sano, M., Ohashi, N., Morita, T., Kojima, H., Honma, M. and Hayashi, M. 2015. Evaluation of the repeated-dose liver and gastrointestinal tract micronucleus assays with 22 chemicals using young adult rats: Summary of the collaborative study by the Collaborative Study Group for the Micronucleus Test (CSGMT)/The Japanese Environmental Mutagen Society (JEMS) – Mammalian Mutagenicity Study Group (MMS). *Mutation Research* 780-781:2–17.

Han, D., Tian, Y., Zhang, T., Ren, G. and Yang, Z. 2011. Nano-zinc oxide damages spatial cognition capability via over-enhanced long-term potentiation in hippocampus of Wistar rats. *International Journal of Nanomedicine* 6: 1453–1461.

Handy, R. D., Henry, T. B., Scown, T. M., Johnston, B. D. and Tyler, C. R. 2008b. Manufactured nanoparticles: their uptake and effects on fish–a mechanistic analysis. *Ecotoxicology* 17.5: 396–409.

Handy, R. D., Owen, R. and Valsami-Jones, E. 2008a. The ecotoxicology of nanoparticles and nanomaterials: current status, knowledge gaps, challenges and future needs. *Ecotoxicology* 17.5: 315–325.

Hankins, J. 2006. The Role of Albumin in Fluid and Electrolyte Balance. *Journal of Infusion Nursing* 29.5: 260-265.

Hanley, C., Thurber, A., Hanna, C., Punnoose, A., Zhang, J. and Wingett, D. 2009. The influences of cell type and ZnO nanoparticle size on immune cell cytotoxicity and cytokine induction. *Nanoscale Research Letters* 4.12: 1409-1420.

Hansen, S. F., Larsen, B. H., Olsen, S. I. and Baun, A. 2007. Categorisation framework to aid hazard identification of nanomaterials. *Nanotoxicology* 1.3: 243–250.

Hanukoglu, I. 1992. Steroidogenic enzymes: structure, function and role in regulation of steroid hormone biosynthesis. *Journal of Steroid Biochemistry and Molecular Biology* 43.8: 779-804.

Hao, L., Chen, L., Hao, J. and Zhong, N. 2013. Bioaccummulation and sub-acute toxicity of zinc oxide nanoparticles in juvenile carp (*Cyprinus carpio*): A comparative study with its bulk counterparts. *Ecotoxicology and Environmnetal Safety* 91: 52-60. DOI: 10.1016/j.ecoenv.2013.01.007.

Haseeb, A. K., Abdelhalim, M. A. K., Al-Ayed, M. S. and Alhomida, A. S. 2012. Effects of GNPs on glutathione and malondialdehyde levels in liver, lung, heart and kidney of rats *in vivo*. *Saudi Journal of Biological Science* 19: 461-464.

Hashimoto, M. and Imazato, S. 2015. Cytotoxic and genotoxic characterisation of aluminum and silicon oxide nanoparticles in macrophages. *Dental Materials* 31.5: 556-564.

Hayashi, M. 2016. The micronucleus test- most widely used in vivo genotoxicity test. *Genes and Environment* 38:18.

Hayashi, M., Sofuni, T. and Ishidate, Jr M. 1983. An application of acridine orange fluorescent staining to the micronucleus test. *Mutation Research* 120: 241–7.

Hayashi, M., Sutou, S., Shimada, H., Sato, S., Sasaki, Y. F. and Wakata, A. 1989. Difference between intraperitoneal and oral gavage application in the micronucleus test: The 3rd collaborative study by CSGMT/JEMS-MMS. *Mutation Research* 223: 329–344.

Heddle, J. A. 1973. A rapid *in vivo* test for chromosomal damage. *Mutation Research* 18:187–90.

Hein, M.S. 2003. Copper deficiency anaemia and nephrosis in zinc-toxicity: a case report. *South Dakota Journal of Medicine* 56.4:143–147.

Heinrich, U., Fuhst, R., Rittinghausen, S., Creutzenberg, O., Bellmann, B., Koch, W. and Levsen, K. 1995. Chronic inhalation exposure of Wistar rats and two different strains of mice to diesel engine exhaust, carbon black and titanium dioxide. *Inhalation Toxicology* 7.4: 533–556.

Hetrick, E. M., Shin, J. H., Paul, H. S. and Schoenfisch, M. H. 2009. Anti-biofilm efficacy of nitric oxide releasing silica nanoparticles. *Biomaterials* 30.14: 2782-2789.

Hirsch, L. R., Stafford, R. J., Bankson, J. A., Sershen, S. R., Rivera, B., Price, R. E., Hazle, J. D., Halas, N. J. and West, J. L. 2003. Nanoshell-mediated near infrared thermal therapy of tumours under magnetic resonance guidance. *Proceedings of the National Academy of Sciences of the United States of America* 100.23: 13549-13554.

Hodis, H. N., Mack, W. J., Krauss, R. M. and Alaupovic, P. 1996. Pathophysiology of triglyceride-rich lipoproteins in atherothrombosis: clinical aspects. *Clinical Cardiology* 22: 15-20.

Hong, F., Wang, Y., Zhou, Y., Zhang, Q., Ge, Y., Chen, M., Hong, J. and Wang, L. 2016. Exposure to TiO_2 nanoparticles induces immunological dysfunction in mouse testis. *Journal of Agricultural and Food Chemistry* 64: 346-355.

Hong, J. S., Park, M. K., Kim, M. S., Lim, J. H., Park, G.J., Maeng, E.H., Shin, J.H., Kim, M.K., Jeong, J., Park, J.A., Kim, J.C. and Shin, H.C. 2014. Prenatal

development toxicity study of zinc oxide nanoparticles in rats. *International Journal of Nanomedicine* 9.S2: 159-171.

Hooper, H. L., Jurkschat, K., Morgan, A. J., Bailey, J., Lawlor, A. J., Spurgeon, D. J. and Svendsen, C. 2011. Comparative chronic toxicity of nanoparticulate and ionic zinc to the earthworm *Eisenia veneta* in a soil matrix. *Environmental International* 37.6: 1111-1117.

Horne, M., Heitz, U. and Swearingen, P. 1991. Fluid, Electrolyte and Acid-Base Balance: A Case Study Approach. St. Louis: Mosby Year Book. 451 pp.

Hougaard, K. S., Jackson, P., Jensen, K. A., Sloth, J. J., Loschner, K., Larsen, E. H., Birkedal, R. K., Vibenholt, A., Boisen, A. M., Wallin, H. and Vogel, U. 2010. Effects of prenatal exposure to surface-coated nanosized titanium dioxide (UV-Titan). A study in mice. *Particle and Fibre Toxicology* 7: 16.

Hsiao, I. L. and Huang, Y. J. 2011. Titanium oxide shell coatings decrease the cytotoxicity of ZnO nanoparticles. *Chemical Research in Toxicology* 24.3: 303–313.

http://mnt.globalwatchonline.com/epicentric_portal/site/MNT/menuitem.f279ff2f60faf0ea7e61083267d001a0/ The Nanotechnology Knowledge Transfer Network. Gateshead, U.K. Available online. Accessed 12/05/2014.

http://ruby.colorado.edu/~smyth/min/tio2.html. Accessed 12/05/2014.

http://thesceneisdead.com/2013/05/05/edc-vegas-protip-48-be-prepared-for-cigarette-smoke. Accessed 12/05/2014.

http://www.dailymail.co.uk/news/article-1351064/Japan-raises-alert-following-volcanos-biggest-eruption-50-years.html. Accessed 12/05/2014.

http://www.ecoforumjournal.org/forest-fires-2/. Accessed 12/05/2014.

http://www.luxresearchinc.com Sizing Nanotechnology's Value Chain (2004). Lux Research Inc. New York, U.S.A. Available online. Accessed12/05/2014.

http://www.telegraph.co.uk/news/science/science-news/9209597/Exhaust-fumes-are-twice-as-deadly-as-roads-study-claims.html. Accessed 12/05/2014.

http://www.blogs.law.widener.edu/nanolaw/category/nanoparticles/. Accessed 09/05/2014

Hubbard, S. R., Mohammadi, M. and Schlessinger, J. 1998. Autoregulatory mechanisms in protein-tyrosine kinases. *Journal of Biological Chemistry* 273: 11987-11990.

Hu, J. Q., Chen, C. Y., Bai, R., Zhen, S., Du, X. M., Zang, J. J., Li, J. C., Gu, Y. Q. and Jia, G. 2010a. Effect of nano-TiO_2 intratracheal instillation on lipid

metabolism of AopE gene-knockout mice. *Zhonghua Yu Fang Yi Xue Za Zhi* 44.9: 780–784.

Hu, R., Gong, X., Duan, Y., Li, N., Che, Y., Cui, Y., Zhou, M., Liu, C., Wang, H. and Hong, F. 2010b. Neurotoxicological effects and the impairment of spatial recognition memory in mice caused by exposure to TiO_2 nanoparticles. *Biomaterials* 31.31: 8043–8050.

Huang, C. C., Aronstam, R. S., Chen, D. R. and Huang, Y. W. 2010. Oxidative stress, calcium homeostasis and altered gene expression in human lung epithelial cells treated with ZnO nanoparticles. *Toxicology In vitro* 24.1:45–55.

Huang, S., Chueh, P. J., Lin, Y. W., Shih, T. S. and Chuang, S. M. 2009. Disturbed mitotic progression and genome segregation are involved in cell transformation mediated by nano-TiO_2 long-term exposure. *Toxicology and Applied Pharmacology* 241.2: 182–194.

Hughes, C. M., Lewis, S. E., McKelvey-Martin, V. J. and Thompson, W. 1996. A comparison of baseline and induced DNA damage in human spermatozoa from fertile and infertile men, using a modified comet assay. *Molecular Human Reproduction* 2.8: 613-619.

Iarmarcovai, G., Ceppi, M., Botta, A., Orsiere, T. and Bonassi, S. 2008. Micronuclei frequency in peripheral blood lymphocytes of cancer patients: a meta-analysis. *Mutation Research* 659: 274–83.

Iavicoli, I., Leso, V. and Bergamaschi, A. 2012. Toxicological effects of titanium dioxide nanoparticles: a review of *in vivo* studies. *Journal of Nanomaterials* 2012: 1-36. Doi.org/10.1155/2012/964381.

Incardona, J. P. and Eaton, S. 2000. Cholesterol in signal transduction. *Current Opinion in Cell Biology* 12.2:193-203.

Institute for Laboratory Animal Research, (ILAR) 2011. Guide for the care and use of laboratory animals. 8th edition. The National Academies Press. Washington DC. 246pp.

IPPIC (International Paint and Printing Ink Council). 2012. http://www.ippic.org/site/assets/docs/Public%20AFWG/IPPIC%20%20Zinc%20oxide%20%20regulatory%20status%20final%20Draft%20March%201%202012.pdf

Ismail, M., Gul, S., Khan, M. A. and Khan, M. I. 2016. Plant mediated Green Synthesis of Anti-Microbial Silver Nanoparticles- A review of recent trends. *Reviews in Nanoscale and Nanotechnology* 5.2: 119-135.

Iso, H., Ikeda, A., Inoue, M., Sato, S., Tsugane, S. and JPHC study group. 2009. Serum Cholesterol levels in relation to the incidence of cancer: the JPHC study cohorts. *International Journal of Cancer* 125.11: 2679-2686.

Iwagami, Y. 1996. Changes in the ultrasonic of human cells related to certain biological responses under hyperthermic culture conditions. *Human Cell* 9.4: 353-366.

Jacob, N. J. and VanDemark, P. J. 1960. The purification and properties of the α-glycerophosphate-oxidizing enzyme of *Streptococcus faecalis* 10C1. *Archives of Biochemistry and Biophysics* 88.2: 250-255.

Jain, K. K. 2010. Advances in the field of nanooncology. *BMC Medicine* 8: 83.

Jamsai, D. and O'Bryan, M. K. 2011. Mouse models in male fertility research. *Asian Journal of Andrology* 13.1: 139-151.

Jang, J., Lim, D. H. and Choi, I. H. 2010. The impact of nanomaterials in immune system. *Immune Network* 10.3: 85-91.

Jemec, A., Drobne, D., Remškar, M., Sepcic, K., Tišler, T. 2008. Effects of ingested nano-sized titanium dioxide on terrestrial isopods (*Porcellio scaber*). *Environmental Toxicology and Chemistry* 27.9: 1904-1914.

Jendrassik, L. and Grof, P. 1938. Colourimetric method of determination of bilirubin. *Biochemische Zeitschrift* 297:81-82.

Jia, F., Sun, Z., Yan, X., Zhou, B. and Wang, J. 2014. Effect of pubertal nano-TiO_2 exposure on testosterone synthesis and spermatogenesis in mice. *Archives of Toxicology* 88.3: 781-788.

Jiang, X., Dias, J. A. and He, X. 2014. Structural biology of glycoprotein hormones and their receptors: insights to signaling. *Molecular and Cellular Endocrinology* 382.1: 424-451.

Jiang, X., Liu, H., Chen, X, Chen, P. H., Fischer, D., Sriraman, V., Yu, H. N., Arkinstall, S. and He, X. 2012. Structure of the follicle-stimulating hormone in complex with the entire ectodomain of its receptor. *Proceedings of the National Academy of Sciences USA* 109.31: 12491-12496.

Jiang, Y., Sun, Y., Liu, H., Zhu, F. and Yin, H. 2008. Solar photocatalytic decolourisation of C.I. Basic Blue 41 in an aqueous suspension of TiO_2-ZnO. *Dyes and Pigments* 78.1: 77-83.

Jo, E., Seo, G., Kwon, J. T., Lee, M., Lee, B. C., Eom, I., Kim, P. and Choi, K. 2013. Exposure to zinc oxide nanoparticles affects reproductive development and

biodistribution in offsprings of rats. *Journal of Toxicological Science* 38.4: 525-530.

Johansen, A., Pedersen, A. L., Jensen, K. A., Karlson, U., Hansen, B. M., Scott-Fordsmand, J. J. and Winding, A. 2008. Effects of C60 fullerene nanoparticles on soil bacteria and protozoans. *Environmental Toxicology and Chemistry* 27.9: 1895-1903.

Jones, N. C., Thornton, C. A., Mark, D. and Harrison, R. M. 2000. Indoor/outdoor relationships of particulate matter in domestic homes with roadside, urban and rural locations. *Atmospheric Environment* 34.16: 2603-2612.

Jurado, R. and Mattix, H. 1998. The decreased serum urea nitrogen-creatinine ratio. *Archives of Internal Medicine* 158.22: 2509-2511.

Kakafika, A., Athyros, V. G., Tziomalos, K., Karagiannis, A. and Dimitri, P. 2008. High density lipoprotein cholesterol and statin trials. *Current Medical Chemistry* 15.22: 2265-2270.

Kang, S. H., Kwon, J. Y., Lee, J. K. and Seo, Y. R. 2013. Recent advances in *in vivo* genotoxicity testing: prediction of carcinogenic potential using comet and micronucleus assay in animal models. *Journal of Cancer Prevention* 18.4: 277-288.

Kang, S. J., Kim, B. M., Lee, Y. J. and Chung, H. W. 2008. Titanium dioxide nanoparticles trigger p53-mediated damage response in peripheral blood lymphocytes. *Environmental and Molecular Mutagenesis* 49.5: 399-405.

Kang, S. J., Lee, Y. J., Kim, B. M., Choi, Y. J. and Chung, H. W. 2011. Cytotoxicity and genotoxicity of titanium dioxide nanoparticles in UVA-irradiated normal peripheral blood lymphocytes. *Drug and Chemical Toxicology* 34.3: 277-284.

Kansara, K., Patel, P., Shah, D., Shukla, R. K., Singh, S., Kumar, A. and Dhawan, A. 2015. TiO_2 nanoparticles induce DNA double strand breaks and cell cycle arrest in human alveolar cells. *Environmental and Molecular Mutagenesis* 56.2: 204-217.

Karlsson, H. L., Cronholm, P., Gustafsson, J. and Möller, L. 2008. Copper oxide nanoparticles are highly toxic: a comparison between metal oxide nanoparticles and carbon nanotubes. *Chemical Research in Toxicology* 21: 1726–1732.

Katsifis, S. P., Kinney, P. L., Hosselet, S., Burns, F. J. and Christie, N. T. 1996. Interaction of nickel with mutagens in the induction of sister chromatid exchanges in human lymphocytes. *Mutation Research* 359.1: 7-15.

Kaysen, G. A. and de Sain-van der Velden, M. G. 1999. New insights into lipid metabolism in the nephrotic syndrome. *Kidney International Supplement* 71: S18-21.

Kaysen, G. A., Dubin, J. A., Muller, H. G., Rosales, L., Levin, N. W., Mitch, W. E. and HEMO Group. 2004. Inflammation and reduced albumin synthesis associated with stable decline in serum albumin in hemodialysis patients. *Kidney International* 65:1408-1415.

Keen-Kim, D., Nooraie, F. and Rao, P. N. 2008. Cytogenetic biomarkers for human cancer. *Frontiers in Bioscience*13: 5928.

Kierszenbaum, A. L., Gil, M., Rivkin, E. and Tres, L. L. 2002a. Ran, a GTP-binding protein involved in nucleocytoplasmic transport and microtubule nucleation, relocates from the manchette to the centrosome region during rat spermiogenesis. *Molecular Reproduction and Development* 63:131–140.

Kierszenbaum, A. L. 2001. Spermatid manchette: plugging proteins to zero into the sperm tail. *Molecular Reproduction and Development* 59: 347–349.

Kierszenbaum, A. L. 2002b. Intramanchette transport (IMT): managing the making of the spermatid head, centrosome and tail. *Molecular Reproduction and Development* 63: 1–4.

Kierszenbaum, A. L. and Tres, L. L. 2004. The acrosome-acroplaxome manchette complex and the shaping of the spermatid head. *Archives of Histology and Cytology* 67: 271–284.

Kierszenbaum, A. L., Rivkin, E., Tres, L. L., Yoder, B. K., Haycraft, C. J., Bornens, M. and Rios, R. M. 2011. GMAP210 and IFT88 are present in the spermatid golgi apparatus and participate in the development of the acrosome-acroplaxome complex, head-tail coupling apparatus and tail. *Developmental Dynamics* 240: 723–736.

Kim, J. S., Sung, J. H., Ji, J. H., Song, K. S., Lee, J. H., Kang, C. S. and Yu, J. J. 2011. *In vivo* genotoxicity of silver nanoparticles after 90-day silver nanoparticle inhalation exposure. *Safety Health Work* 2.1: 34-38.

Kim, K. M., Kim, T. H., Kim, H. M., Kim, H. J., Gwak, G., Peak, S. and Oh, J. 2012. Colloidal behaviours of ZnO nanoparticles in various aqueous media. *Toxicology and Environmental Health Sciences* 4.2: 121-131.

Kim, K., Song, J. H., Kim, M., Chung, S. T., Jeong, J., Yang, J., Choi, A., Choi, H. and Oh, J. 2014a. Physicochemical analysis methods for nanomaterials considering their toxicological evaluations. *Molecular and Cellular Toxicology* 10.4: 347-360.

Kim, Y. R., Park, J., Lee, J. E., Park, H, S., Seong, N. W., Kim, J. H., Kim, Y. G., Meang, E. H., Hong, J. S., Kim, S. H., Koh, S. B., Kim, M. S., Kim, C. S., Kim, S. K., Son, S. W., Seo, Y. R., Kang, B. H., Han, B. S., An, S. S., Yun, H. I. and Kim, M. K. 2014b. Toxicity of 100 nm zinc oxide nanoparticles: A report of 90-day repeated oral administration in Sprague Dawley rats. *International Journal of Nanomedicine* 9.18: 109-126.

Kim, Y. S., Kim, J. S., Cho, H. S., Rha, D. S., Kim, J. M., Park, J. D., Choi, B. S., Lim, R., Chang, H. K., Chung, Y. H., Kwon, I. H., Jeong, J., Han, B. S. and Yu, I. J. 2008. Twenty-eight-day oral toxicity, genotoxicity and gender-related tissue distribution of silver nanoparticles in sprague-dawley rats. *Inhalation Toxicology* 20.6: 575-583.

Kittleson, D. B. 2001. Recent measurements of nanoparticles emission from engines. *Current Research on Diesel Exhaust Particles, Japan Association of Aerosol Science and Technology*.

Klaine, S. J., Alvarez, P. J. J., Batley, G. E., Fernandes, T. F., Handy, R. D., Lyon, D. Y., Mahendra, S., McLaughlin, M. J. and Lead, J. R. 2008. Nanomaterials in the environment: behaviour, fate, bioavailability and effects. *Environmental Toxicology and Chemistry* 27.9: 1825-1851.

Kobayashi, N., Naya, M., Endoh, S., Maru, J., Yamamoto, K. and Nakanishi, J. 2009. Comparative pulmonary toxicity study of nano-TiO_2 particles of different sizes and agglomerations in rats: different short- and long-term post-instillation results. *Toxicology* 264.1-2: 110–118.

Kocbek, P., Teskac, K., Kreft, M.E. and Kristl, J. 2010. Toxicological aspects of long-term treatment of keratinocytes with ZnO and TiO_2 nanoparticles. *Small* 6.17: 1908–1917.

Koditschek, L. K. and Umbreit, W. W. 1969. Alpha-glycerophosphate oxidase in Streptococcus faecium F24. *Journal of Bacteriology* 98.3: 1063-1068.

Koedrith, P., Boonprasert, R., Kwon, J. Y., Kim, I. and Seo, Y. R. 2014. Recent toxicological investigations of metal or metal oxide nanoparticles in mammalian models *in vitro* and *in vivo*: DNA damaging potential and relevant physicochemical characteristics. *Molecular and Cellular Toxicology* 10.2: 107-126.

Koenig, G. and Seneff, S. 2015. Gamma-Glutamyltransferase: A Predictive Biomarker of Cellular Antioxidant Inadequacy and Disease Risk. *Disease Markers* 2015: 1-18. DOI: 10.1155/2015/818570.

Koken, M. H., Hoogerbrugge, J. W., Jasper-Dekker, I., de Wit, J., Willemsen, R., Roest, H. P., Grootegoed, J. A. and Hoeijmakers, J. H. 1996. Expression of the ubiquitin-conjugating DNA repair enzymes HHR6A and B suggests a role

in spermatogenesis and chromatin modification. *Developmental Biology* 173:119–132.

Komatsu, T., Tabata, M., Kubo-Irie, M., Shimizu, T., Suzuki, K., Nihei, Y. and Takeda, K. 2008. The effects of nanoparticles on mouse testis Leydig cells *in vitro*. *Toxicology in Vitro* 22.8: 1825-1831.

Kool, P. L., Oritz, M. D. and van Gestel, C. A. 2011. Chronic toxicity of ZnO nanoparticles, non-nano ZnO and $ZnCl_2$ to *Folsomia candida* (Collembola) in relation to bioavailability in soil. *Environmental Pollution* 159.10: 2713-2719.

Krishna, G and Hayashi, M. 2000. *In vivo* rodent micronucleus assay; protocol, conduct and data interpretation. *Mutation Research* 20.455(1-2):155-66.

Krug, H.F. and Wick, P. 2011. Nanotoxicology: An Interdisciplinary Challenge. *Angewandte Chemie International Edition* 50.6: 1260-1278.

Kruszewski, M., Brzoska, K., Brunborg, G., Asare, N., Dobrzynska, M., Dusinska, M., Fjellsbo, L. M., Georgantzopoulou, A., Gromadzka-Ostrowska, J., Gutleb, A. C., Lankoff, A., Magdolenova, Z., Pran, E.R, Rinna, A., Instanes, C., Sandberg, W. J., Schwartze, Per., Stepkowski, T., Wojewodzka, M. and Refsnes, M. 2011. *Toxicity of silver nanomaterials in higher eukaryotes: In advances in molecular toxicology Volume 5.* Chapter 5, pp.179–218.

Kumar, A. and Dhawan, A. 2013. Genotoxic and carcinogenic potential of engineered nanoparticles: an update. *Archives of Toxicology* 87.11: 1883-1900.

Kumar, A., Najafzadeh, M., Jacob, B. K., Dhawan, A. and Anderson, D. 2015. Zinc oxide nanoparticles affect the expression of p53, Ras p21 and JNKs: an *ex vivo/in vitro* exposure study in respiratory disease patients. *Mutagenesis* 30.2: 237-245.

Kumar, A., Pandey, A. K., Singh, S. S., Shanker, R. and Dhawan, A. 2011. A flow cytometric method to assess nanoparticle uptake in bacteria. *Cytometry A* 79.9: 707–712.

Kumari, M., Singh, S. P., Chinde, S., Rahman, M. F., Mahboob, M. and Grover, P. 2014. Toxicity study of cerium oxide nanoparticles in human neuroblastoma cells. *International Journal of Toxicology* 33.2: 86-97.

Kurzawa-Zegota, M., Sharma, V., Najafzadeh, M., Reynolds, D. P., Davies, J. P., Shukla, R. K., Dhawan, A. and Anderson, D. 2017. Titanium dioxide nanoparticles induce DNA damage in peripheral blood lymphocytes from polyposis coli, colon cancer patients and healthy individuals: an*ex vivo/in vitro* study. *Journal of Nanoscience and Nanotechnology* 17:1-12.

Kwon, J. P., Koedrith, P. and Seo, Y. R. 2014a. Current investigations into the genotoxicity of zinc oxide and silica nanoparticles in mammalian models *in vitro* and in vivo: carcinogenic/genotoxic potential, relevant mechanisms and biomarkers, artifacts and limitations. *International Journal of Nanomedicine* 9.S2: 271-286.

Kwon, J. Y., Lee, S. Y., Koedrith, P., Lee, J. Y., Kim, K., Oh. J., Yang, S. I. K., Kim., M., Lee, J. K., Jeong, J., Maeng, E. H., Lee, B. J. and Seo. Y. R. 2014b. Lack of genotoxic potential of ZnO nanoparticles in *in vitro* and *in vivo* tests. *Mutation Research/Genetic Toxicology and Environmental Mutagenesis* 761: 1-9.

Lademann, J., Richter, H., Teichmann, A., Otberg, N., Blume-Peytavi, U., Luengo, J., Weiss, B., Schaefer, U. F., Lehr, C. M, Wepf, R. and Sterry, W. 2008. Nanoparticles – an efficient carrier for drug delivery into the hair follicles. *European Journal of Pharmaceutics and Biopharmaceutics* 66.2: 159-164.

Lademann, J., Weigmann, H. J., Rickmeyer, C., Barthelmes, H., Schaefer, H., Mueller, G. and Sterry, W. 2006. Penetration of titanium dioxide microparticles in a sunscreen formulation into the horny layer and the follicular orifice. *Skin Pharmacology and Applied Skin Physiology* 12.5: 247–256.

Lan, Z. and Yang, W. X. 2012. Nanoparticles and spermatogenesis: how do nanoparticles affect spermatogenesis and penetrate the blood-testis barrier. *Nanomedicine* 7.4: 579-596.

Landsiedel, R., Ma-Hock, L., Van Ravenzwaay, B., Schulz, M., Wiench, K., Champ, S., Schulte, S., Wohlleben, W. and Oesch, F. 2010. Genotoxicity studies on titanium dioxide and zinc oxide nanomaterials used for UV-protection in cosmetic formulations. *Nanotoxicology* 4: 364-81.

Lankveld, D. P. K., Oomen, A. G., Krystek, P., Neig, A., Troost-De Jong, A., Noorlander, C. W., Van Eijkeren, J. C., Geertsma, R. E. and De Jong, W. 2010. The kinetics of the tissue distribution of silver nanoparticles of different sizes. *Biomaterials* 31.32: 8350-8361.

Le, N.A. and Walter, M. F. 2007. The role of hypertriglyceridemia in atherosclerosis. *Current Atherosclerosis Reports* 9.2: 110-115.

Lee, D., Lim, J., Yang, J., Ha, M. and Jacobs, D. R. 2005. Serum gamma-glutamyltransferase within its normal range predicts a chronic elevation of alanine aminotransferase: A four year follow-up study. *Free Radical Research* 39.6: 589-593.

Lee, K. P., Trochimowicz, H. J. and Reinhardt, C. F. 1985. Pulmonary response of rats treated with titanium dioxide (TiO_2) by inhalation for two years. *Toxicology and Applied Pharmacology* 79.2: 179–192.

Lee, S., Chung, H., Kim, S. and Lee, I. 2013. The genotoxic effect of ZnO and CuO nanoparticles on early growth of buckwheat, *Fagopyrum esculentum*. *Water, Air, Soil Pollution* 224:1668. Doi: 10.1007/s11270-013-1668-0.

Lemieux, I., Pascot, A., Couillard, C., Lamarche, B., Tchernof, A., Almeras, N., Bergeron, J., Gaudet, D., Tremblay, G., Prud'homme, D., Nadeau, A. and Despres, J. P. 2000. Hypertriglyceridemic waist: a marker of the atherogenic metabolic triad (hyperinsulinemia; hyperapolipoprotein B; small, dense LDL) in men? *Circulation* 102.2: 179-184.

Li, C., Shen, C., Cheng, Y., Huang, S., Wu, C., Kao, C., Liao, J. and Kang J. 2012. Organ biodistribution, clearance and genotoxicity of orally treated zinc oxide nanoparticles in mice. *Nanotoxicology* 6.7: 746-756.

Li, N., Duan, Y., Hong, M., Zheng, L., Fei, M., Zhao, X., Wang, J., Cui, Y., Liu, H., Cai, J., Gong, S., Wang, H. and Hong, F. 2010c. Spleen injury and apoptotic pathway in mice caused by titanium dioxide nanoparticles. *Toxicology Letters* 195.2-3: 161-168.

Li, N., Ma, L., Wang, J., Zheng, L., Liu, J., Duan, Y., Liu, H., Zhao, X., Wang, S., Wang, H., Hong, F. and Xie, Y. 2010a. Interaction between nano-anatase TiO_2 and liver DNA from mice *in vivo*. *Nanoscale Research Letters* 5.1: 108–115.

Li, S., Zhu, H., Zhu, R., Sun, X., Yao, S. and Wang S. 2008b. Impact and mechanism of TiO_2 nanoparticles on DNA synthesis *in vitro*. *Science China Series B Chemistry* 51: 367-372.

Li, S. Q., Zhu, R. R., Zhu, H., Xue, M., Sun, X. Y., Yao, S. D. and Wang, S. L. 2008a. Nanotoxicity of TiO_2 nanoparticles to erythrocyte *in vitro*. *Food and Chemical Toxicology* 46.12: 3626–3631.

Li, Y., Li, J., Yin, J., Li, W., Kang, C., Huang, Q. and Li, Q. 2010b. Systematic influence induced by 3 nm titanium dioxide following intratracheal instillation of mice. *Journal of Nanoscience and Nanotechnology* 10.12: 8544–8549.

Li, Y., Sun, L., Jin, M., Du, Z., Liu, X., Guo, C., Li, Y., Huang, P. and Sun, Z. 2011. Size-dependent cytotoxicity of amorphous silica nanoparticles in human hepatoma HepG2 cells. *Toxicology in vitro* 25.7: 1343-1352.

Li, W. Q., Wang, F., Liu, Z. M., Wang, Y. C., Wang, J. and Sun, F. 2013. Gold nanoparticles elevate plasma testosterone levels in male mice without affecting fertility. *Small* 9.9-10: 1708-1714.

Liang, G., Pu, Y., Yin, L., Liu, R., Ye, B., Su, Y. and Li, Y. 2009. Influence of different sizes of titanium dioxide nanoparticles on hepatic and renal functions in rats with correlation to oxidative stress. *Journal of Toxicology and Environmental Health, Part A* 72.11-12: 740-745.

Limdi, J. K. and Hyde, G. M. 2003. Evaluation of abnormal liver function tests. *Postgraduate Medical Journal* 79.932: 307-312.

Lin, D. and Xing, B. 2008. Phytotoxicity of nanoparticles: inhibition of seed germination and root growth. *Environmental Pollution* 150.2: 243-250.

Lin, W. S., Xu, Y., Huang, C. C., Ma, Y., Shannon, K. B., Chen, D.R. and Huang, Y. 2009. Toxicity of nano- and micro-sized ZnO particles in human lung epithelial cells. *Journal of Nanoparticle Research* 11.1: 25-39.

Lindberg, H. K., Falck, G. M., Catalan, J., Koivisto, A. J., Suhonen, S., Jarventaus, H., Rossi, E. M., Nykasenoja, H., Peltonen, Y., Moreno, C., Alenius, H., Tuomi, T., Savolainen, K. M. and Norppa, H. 2012. Genotoxicity of inhaled nanosized TiO_2 in mice. *Mutation Research* 745.1-2: 58-64.

Liu, D. Y. and Baker, H. W. 1990. Relationships between human sperm acrosin, acrosomes, morphology and fertilisation in vitro. *Human Reproduction* 5: 298-303.

Liu, D. Y. and Baker, H. W. 1992. Morphology of spermatozoa bound to the zona pellucida of human oocytes that failed to fertilize in vitro. *Journal of Reproduction and Fertility* 94: 71-84.

Liu, H., Ma, L., Zhao, J., Liu, J., Yan, J., Ruan, J. and Hong, F. 2009a. Biochemical toxicity of nano-anatase tio_2 particles in mice. *Biological Trace Element Research* 129.1-3: 170-180.

Liu, K., Lin, X. and Zhao, J. 2013. Toxic effects of the interaction of titanium dioxide nanoparticles with chemicals or physical factors. *International Journal of Nanomedicine* 8: 2509-2520.

Liu, Q., Hong, Z., Guo, B., Zhang, Y., Li, Y. and Liu, J. 2006. Experimental study on toxicity of nanosized titanium dioxide. *Modern Preventive Medicines* 33: 1211–1212.

Liu, R., Yin, L., Pu, Y., Liang, G., Zhang, J., Su, Y., Xiao, Z. and Ye, B. 2009b. Pulmonary toxicity induced by three forms of titanium dioxide nanoparticles via intra-tracheal instillation in rats. *Progress in Natural Science* 19.5: 573–579.

Liu, R., Zhang, X., Pu, Y., Yin, L., Li, Y., Zhang, X., Liang, G., Li, X. and Zhang, J. 2010a. Small-sized titanium dioxide nanoparticles mediate immune toxicity in rat pulmonary alveolar macrophages *in vivo*. *Journal of Nanoscience and Nanotechnology* 10.8: 5161–5169.

Liu, W., Wu, Y., Wang, C., Li, H. C., Wang, T., Liao, C. Y., Cui, L., Zhou, Q. F., Yan, B. and Jiang, G. B. 2010b. Impact of silver nanoparticles on human cells: effect of particle size. *Nanotoxicology* 4.3: 319-330.

Long, T. C., Saleh, N., Tilton, R. D., Lowry, G. V. and Veronesi, B. 2006. Titanium dioxide (P25) produces reactive oxygen species in immortalised brain microglia (BV2): implications for nanoparticle neurotoxicity. *Environmental Science and Technology* 40.14: 4346-4352.

Lopes, S., Ribeiro, F., Wojnarowicz, J., Lojkowski, W., Jurkschat, K., Crossley, A., Soares, A. M. and Loureiro, S. 2014. Zinc oxide nanoparticles toxicity to Daphnia magna: size-dependent effects and dissolution. *Environmental Toxicology Chemistry* 33.1: 190-198.

Louvet, J., Harman, S. and Ross, G. 1975. Effects of human chrionic gonadotrophin, human interstitial cell stimulating hormone and human follicle stimulating hormone on ovarian weights in estrogen-primed hypophysectomised immature female rats. *Endocrinology* 96.5: 1179-1186.

Lovric, J., Bazzi, H. S., Cuie, Y., Fortin, G. R., Winnik, F. M. and Maysinger, D. 2005. Differences in subcellular distribution and toxicity of green and red emitting CdTe quantum dots. *Journal of Molecular Medicine* 83.5: 377-385.

Lozovska, Y. V., Naleskina, L. A., Lukyanowa, N. Y., Todor, I. M. and Chekhun, V. F. 2015. Assessment of the Geno- and Cytotoxic Action of Colloidal Gold Nanoparticles on the Bone Marrow Erythroid Cell Lines and Tumours in Animals with Ehrlich Ascites Carcinoma. *Cytology and Genetics* 49.1: 42-48.

Lu, S.C. 2009. Regulation of glutathione synthesis. *Molecular Aspects of Medicine* 30.1-2: 42-59.

Luo, J., Gupta, V., Kern, B., Tash, J. S., Sanchez, G., Blanco, G. and Kinsey, W. H. 2012. Role of FYN kinase in spermatogenesis: defects characteristic of Fyn-null sperm in mice. *Biology of Reproduction* 86.1: 1–8.

Luther, W. and Malanoswski, N. 2004. ´Das wirtschaftliche Potenzial der Nanotechnologie´, Technikfolgenabschätzung – *Theorie und Praxis* 2:26-33.

Ma, H., Wallis, L. K., Diamond, S., Li, S., Canas-Carell, J. and Parra, A. 2014. Impact of solar UV radiation on toxicity of ZnO nanoparticles through photocatalytic reactive oxygen species (ROS) generation and photo-induced dissolution. *Environmental Pollution* 193: 165-172.

Ma, L., Zhao, J., Wang, J., Liu, J., Duan, Y., Liu, H., Li, N., Yan, J., Ruan, J., Wang, H. and Hong, F. 2009. The acute liver injury in mice caused by nano-anatase TiO_2. *Nanoscale Research Letters* 4.11: 1275–1285.

Ma, L., Liu, J., Li, N., Wang, J., Duan, Y., Yan, J., Liu, H., Wang, H. and Hong, F. 2010. Oxidative stress in the brain of mice caused by translocated nanoparticulate TiO_2 delivered to the abdominal cavity. *Biomaterials* 31.1: 99–105.

MacGregor, J. T., Wehr, C. M. and Gould, D. H. 1980. Clastogen-induced micronuclei in peripheral blood erythrocytes: The basis of an improve micronucleus test. *Environmental Mutagen* 2: 509–14.

MacGregor, J. T., Wehr, C. M. and Langlois, R. G. 1983. A simple fluorescent staining procedure for micronuclei and RNA in erythrocytes using Hoechst 33258 and pyronin Y. *Mutation Research* 120: 269–275.

Magdolenova, Z., Bilanicova, D., Pojana, G., Fjellsbo, L. M., Hudecova, A., Hasplova, K., Marcomini, A. and Dusinska, M. 2012. Impact of agglomeration and different dispersions of titanium dioxide nanoparticles on the human related *in vitro* cytotoxicity and genotoxicity. *Journal of Environmental Monitoring* 14.2: 455-464.

Magdolenova, Z., Collins, A., Kumar, A., Dhawan, A., Stone, V. and Dusinska, M. 2014. Mechanisms of genotoxicity. A review of *in vitro* and *in vivo* studies with engineered nanoparticles. *Nanotoxicology* 8.3: 233–278.

Manke, A., Wang, L. and Rojanasakul, Y. 2013. Mechanisms of nanoparticle-induced oxidative stress and toxicity. *BioMed Research International* 2013. DOI: 10.1155/2013/942916.

Martin, R. H. 2003. Chromosomal abnormalities in human sperm. In advances in male mediated developmental toxicity Volume 518. Edited by: Robaire, B. and Hales, B. E. New York, Plenum Press. pp 181-188.

Martin, R. H., Ko, E. and Barclay, L. 1994. Human sperm karyotypes. In: Human chromosomes: manual of basic techniques Edited by: Verma, R. S. and Babu, A. New York, McGraw-Hill. pp 56-65.

Masala, O. and Seshadri, R. 2004. Synthesis routes for large volumes of nanoparticles. *Annual Review of Materials Research* 34: 41-81.

Mateuca, R., Lombaert, N. and Kirsch-Volders, M. 2006. Chromosomal changes: induction, detection methods and applicability in human biomonitoring. *Biochimie* 88: 1515–31.

Mathias, F. T., Romano, R. M., Kizys, M. M. L., Kasamatsu, T., Giannocco, G., Chiamolera, M. I., Dias-da-Silva, M. R. and Romano, M. A. 2015. Daily

exposure to silver nanoparticles during prepubertal development decreases adult sperm and reproductive parameters. *Nanotoxicology* 9.1: 64-70.

Mazzaferro, E. M., Rudloff, E. and Kirby, R. 2002. The role of albumin replacement in the critically ill veterinary patient. *Journal of Veterinary Emergency and Critical Care* 12.2: 113-124.

McNeil, S. E. 2005. Nanotechnology for the biologist. *Journal of Leukocyte Biology* 78.3: 585–94.

Meena, R., Kajal, K. and Paulraj, R. 2015. Cytotoxic and genotoxic effects of titanium dioxide nanoparticles in testicular cells of male wistar rat. *Applied Biochemistry and Biotechnology* 175.2: 825-840.

Meistrich, M. L., Trostle-Weige, P. K. and Russell, L. D. 1990. Abnormal manchette development in spermatids of azh/azh mutant mice. *American Journal of Anatomy* 188: 74 – 86.

Mendoza, S., Lutmer, R. F. and Glueck, C. J., Chen, C. Y., Steiner, P. M., Fallat, R. W. and Kashyap, M. L. 1976. Composition of HDL-2 and HDL-3 in familial hyperalphalipoproteinemia. *Atherosclerosis* 25.1: 131-136.

Mendoza-Lujambio, I., Burfeind, P., Dixkens, C., Meinhardt, A., Hoyer-Fender, S., Engel, W. and Neesen, J. 2002. The *Hook1* gene is non-functional in the abnormal spermatozoon head shape (azh) mutant mouse. *Human Molecular Genetics* 11.14: 1647-1658.

Menkveld, R., El-Garem, Y., Schill, W. B. and Henkel, R. 2003. Relationship between human sperm morphology and acrosomal function. *Journal of Assisted Reproduction and Genetics* 20: 432.438.

Menzel, F., Reinert, T., Vogt, J. and Butz, T. 2004. Investigations of percutaneous uptake of ultrafine TiO_2 particles at the high energy ion nanoprobe LIPSION. *Nuclear Instruments and Methods in Physics Research Section B: Beam interactions with materials and atoms* 219-220: 82-86.

Meyer, K., Rajanahalli, P., Ahamed, M., Rowe, J. J. and Hong, Y. 2011. ZnO nanoparticles induce apoptosis in human dermal fibroblasts via p53 and p38 pathways. *Toxicology In vitro* 25.8: 1721–1726.

Mikkelsen, S. H., Hansen, E. and Christensen, T. B., Baun, A., Hansen, S. F. and Binderup, M. 2011. Survey on basic knowledge about exposure and potential environmental and health risks for selected nanomaterials. The Danish Ministry of the Environment Enivronmental Protection Agency. Environmental Project No. 1370.

Mistra, H. and Fridovich, I. 1972. The role of superoxide anion in the autooxidation of epinephrine and a simple assay for superoxide dismutase. *Journalof Biology and Chemistry* 247.10: 3170-3175.

Mohammadipour, A., Fazel, A., Haghir, H., Motejaded, F., Rafatpanah, H., Zabihi, H., Hosseini, M. and Bideskan, A. E. 2014. Maternal exposure to titanium dioxide nanoparticles during pregnancy; impaired memory and decreased hippocampal cell proliferation in rat offspring. *Environmental Toxicology and Pharmacology* 37.2: 617-625.

Monopoli, M. P., Walczyk, D., Campbell, A., Elia, G., Lynch, I., Baldelli Bombelli, F. and Dawson, K. A. 2011. Physical-chemical aspects of protein corona: relevance to *in vitro* and *in vivo* biological impacts of nanoparticles. *Journal of the American Chemical Society* 133.8: 2525–2534.

Montazer, M. and Seifollahzadeh, S. 2011. Enhanced self-cleaning, antibacterial and UV protection properties of nano TiO_2 treated textile through enzymatic pretreatment. *Photochemistry and Photobiology* 87.4: 877–883.

Monteiro-Riviere, N. A., Wiench, K., Landsiedel, R., Schulte, S., Inman, A. O. and Riviere, J. E. 2011. Safety evaluation of sunscreen formulations containing titanium dioxide and zinc oxide nanoparticles in UVB sunburned skin: an *in vitro* and *in vivo* study. *Toxicological Sciences* 123.1: 264–280.

Mooradian, A. D., Morley, J. E. and Korenman, S. G. 1987. Biological actions of androgens. *Endocrine Reviews* 8.1: 1–28.

Moos, P. J., Olszewski, K., Honeggar, M., Cassidy, P., Leachman, S., Woessner, D., Cutler, N. S. and Veranth, J. M. 2011. Responses of human cells to ZnO nanoparticles: a gene transcription study. *Metallomics* 3.11: 1199–1211.

Moretti, E., Terzuoli, G., Renieri, T., Iacoponi, F., Castellini, C., Giordano, C. and Collodel, G. 2013. *In vitro* effect of gold and silver nanoparticles on human spermatozoa. *Andrologia* 45.6: 392-396.

Morishita, Y., Yoshioka, Y., Satoh, H., Nojiri, N., Nagano, K., Abe, Y., kamada, H., Tsunoda, S., Nabeshi, H., Yoshikawa, T. and Tsutsumi, Y. 2012. Distribution and histologic effects of intravenously treated amorphous nanosilica particles in the testes of mice. *Biochemical and Biophysical Research Communications* 420.2: 297-301.

Morita, T., Asano, N., Awogi, T., Sasaki, Y. F., Sato, S., Shimada, H., Sutou, S., Suzuki, T., Wakata, A., Sofuni, T. and Hayashi, M. 1997. Evaluation of the rodent micronucleus assay in the screening of IARC carcinogens (Groups 1, 2A and 2B). The summary report of the 6th collaborative study by CSGMT/JEMS·MMS. *Mutation Research* 389: 3–122.

Morsy, G. M., El-Ala, K. S. and Ali, A. A. 2016. Studies on fate and toxicity of nanoalumina in male albino rats: lethality, biaccummulation and genotoxicity. *Toxicology and Industrial Health* 32.2: 344-359.

Mroz, R. M., Schins, R. P., Li, H., Jimenez, L. A., Dorst, E. M., Holownia, A., MacNee, W. and Donaldson, K. 2008. Nanoparticle-driven DNA damage mimics irradiation-related carcinogenesis pathways. *European Respiratory Journal* 31.2:241-251.

Mousavi, Z., Hassanpourezatti, M., Najafizadeh, P., Rezagolian, S., Rhamanifar, M. S. and Nosrati, N. 2016. Effects of subcutaneous injection MnO_2 micro- and nanoparticles on blood glucose level and lipid profile in rat. *Iranian Journal of Medical Science* 41.6:518-524.

Mueller, N. C. and Nowack, B. 2008. Exposure modeling of engineered nanoparticles in the environment. *Environmental Science and Technology* 42.12: 4447-4453.

Muller, J., Decordier, I., Hoet, P. H., Lombaert, N., Thomassen, L., Huaux, F., Lison, D. and Kirsch-Volders, M. 2008. Clastogenic and aneugenic effects of multi-wall carbon nanotubes in epithelial cells. *Carcinogenesis* 29.2: 427-433.

Murgia, E., Ballardin, M., Bonassi, S., Rossi, A. M. and Barale, R. 2008. Validation of micronuclei frequency in peripheral blood lymphocytes as early cancer risk biomarker in a nested case-control study. *Mutation Research* 639: 27–34.

Najafzadeh, H., Ghoreishi, S. M., Mohammadian, B., Raimi, E., Afzalzadeh, M. R., Kazemivarnamkhasti, M. and Ganjealidarani, H. 2013. Serum biochemical and histopatological changes in liver and kidney in lambs after Zinc Oxide nanoparticles administration. *Veterinary World* 6.8: 534-537.

Nam, D., Lee, B., Eom, I., Kim, P. and Yeo, M. 2014. Uptake and bioaccumulation of titanium- and silver- nanoaparticles in aquatic ecosystems. *Molecular and Cellular Toxicology* 10: 9-17.

Namvar, F., Rahman, H. S., Mohamad, R., Azizi, S., Tahir, P. M., Chartrand, M. S. and Yeap, S. K. 2015. Cytotoxic effects of biosynthesised zinc oxide nanoparticles on murine cell lines. *Evidence-Based Complementary and Alternative Medicine* 2015:593014. doi: 10.1155/2015/593014.

Nemmar, A., Melghit, K. and Ali, B. H. 2008. The acute proinflammatory and prothrombotic effects of pulmonary exposure to rutile TiO_2 nanorods in rats. *Experimental Biology and Medicine* 233.5: 610-619.

Newman, M. D., Stotland, M. and Ellis, J. I. 2009. The safety of nanosized particles in titanium dioxide- and zinc oxide-based sunscreens. *Journal of the American Academy of Dermatology* 61.4: 685–692.

Ng, K. W., Khoo, S. P., Heng, B. C., Seryawati, M. I., Tan, E. C., Zhao, X., Xiong, S., Fang, W., Leong, D. T. and Loo, J. S. 2011. The role of the tumour suppressor p53 pathway in the cellular DNA damage response to zinc oxide nanoparticles. *Biomaterials* 32: 8218-8822.

Ning, Z., Cheung, C. S., Fu, J., Liu, M. A. and Schnell, M. A. 2006. Experimental study of environmental tobacco smoke particles under actual indoor environment. *Science of the Total Environment* 367.2-3: 822-830.

Niska, K., Pyszka, K., Tukaj, C., Wozniak, M., Radomski, M. W. and Inkielewicz-Stepniak, I. 2015. Titanium dioxide nanoparticles enhance production of superoxide anion and alter the antioxidant system in human osteoblast cells. *International Journal of Nanomedicine* 10:1095-1107.

Nitsche, E. K. 2004. Erythrocytosis in dogs and cats: Diagnosis and management. *Compendium* 26.2: 104-119.

Noble, R. W. and Gibson, Q. H. 1970. The reaction of ferrous horseradish peroxidase with hydrogen peroxide. *The Journal of Biological Chemistry* 245.9: 2409-2413.

Nohynek, G. J., Dufour, E. K. and Roberts, M. S. 2008. Nanotechnology, cosmetics and the skin: is there a health risk? *Skin Pharmacology and Physiology* 21.3: 136–149.

Nohynek, G. J., Lademann, J., Ribaud, C. and Roberts, M. S. 2007. Grey goo on the skin? Nanotechnology, cosmetic and sunscreen safety. *Critical Review in Toxicology* 37.3: 251-277.

Noori, A., Karimi, F., Fatahian, S. and Yazdani, F. 2014. Effects of zinc oxide nanoparticles on renal function in mice. *International Journal of Biosciences* 5.9: 140-146.

Oberdörster, G. 2001. Pulmonary effects of inhaled ultrafine particles. *International Archives of Occupational and Environmental Health* 74.1: 1-8.

Oberdörster, G., Ferin, J. and Lehnert, B. E. 1994. Correlation between particle size, *in vivo* particle persistence and lung injury. *Environmental Health Perspectives* 102 (Suppl 5): 173–179.

Oberdörster, G., Finkelstein, J. N., Johnston, C., Gelein, R., Cox, C., Baggs, R. and Elder, A. C. 2000. Acute pulmonary effects of ultrafine particles in rats and mice. *Research Report Health Effects Institute* 96: 5–74.

Oberdörster, G., Oberdörster, E. and Oberdörster, J. 2005. Nanotoxicology: an emerging discipline evolving from studies of ultrafine particles. *Environmental Health Perspectives* 113.7: 823-839.

OECD guideline (420) for testing of chemicals, acute oral toxicity-fixed dose procedure. Adopted on 17 December 2001. Paris: Organisation for Economic Corporation and Development.

Omura, T. and Morohashi, K. 1995. Gene regulation of steroidogenesis. *Journal of Steroid Biochemistry and Molecular Biology* 53.1-6: 19-25.

Ono, K., Ono, T. and Matsumata, T. 1995. The pathogenesis of decreased aspartate aminotransferase and alanine aminotransferase activity in the plasma of hemodialysis patients: the role of vitamin B6 deficiency. *Clinical Nephrology* 43.6:405-408.

Ono, N., Oshio, S., Niwata, Y., Yoshida, S., Tsukue, N., Sugawara, I., Takano, H. and Takeda, K. 2007. Prenatal Exposure to Diesel Exhaust Impairs Mouse Spermatogenesis. *Inhalation Toxicology* 19.3: 275-281.

Osman, I. F., Baumgartner, A., Cemeli, E., Fletcher, J. N. and Anderson, D. 2010. Genotoxicity and cytotoxicity of zinc oxide and titanium dioxide in HEp-2 cells. *Nanomedicine* 5.8: 1193–1203.

Osmond, M. J. and McCall, M. J. 2010. Zinc oxide nanoparticles in modern sunscreens: an analysis of potential exposure and hazard. *Nanotoxicology* 4.1: 15–41.

Owen, R. and Handy, R. 2007. Formulating the problems for environmental risk assessment of nanomaterials. *Environmental Science and Technology* 41.16: 5582-5588.

Oztas, Y. 2016. Hypocholesterolemia: A negelected laboratory finding. *Acta Medica* 47.1: 19-22.

Park, E. J., Yi, J., Kim, Y., Choi, K. and Park, K. 2010. Silver nanoparticles induce cytotoxicity by a trojan-horse type mechanism. *Toxicology in Vitro* 24.3: 872-878.

Park, H., Shin, S., Meang, E., Hong, J., Park, J., Kim, S., Koh, S., Lee, S., Jang, D., Lee, J., Sun, Y., Kang, J., Kim, Y., Kim, M., Jeong, J., Lee, J., Son, W. and Park, J. 2014. A 90-day study of subchronic oral toxicity of 20 nm, negatively charged zinc oxide nanoparticles in Sprague Dawley rats. *International Journal of Nanomedicine* 9: 79-92.

Pastore, A., Piemonte, F., Locatelli, M., Lo Russo, A. L., Gaeta, L. M., Giulia, T. and Federici, G. 2001. Determination of blood total, reduced andoxidised glutathione in pediatric subjects. *Clinical Chemistry* 47.8: 1467-1469.

Pasupuleti, S., Alapati, S., Ganapathy, S., Anumolu, G., Pully, N. R. and Prakhya, B. M. 2012a. Toxicity of zinc oxide nanoparticles through oral route. *Toxicology and Industrial Health* 28.8: 675-686.

Pasupuleti, S., Kishore, A. S., Srinivas, A. and Selvam, G. 2012b. Repeated dose dermal toxicity study of nano zinc oxide with Sprague-Dawley rats. *Cutaneous and Ocular Toxicology* 31.1: 26-32.

Patlolla, A. K., Hussain, S. M., Sohlager, J. J., Patlolla, S. and Tchounwou, P. B. 2010. Comparative Study of the Clastogenicity of Functionalised and Nonfunctionalised Multiwalled Carbon Nanotubes in Bone Marrow Cells of Swiss-Webster Mice. *Environmental Toxicology* 25.6: 608-621.

Patlolla, A. K., Patra, P. K., Flountan, M. and Tchounwou, P. B. 2016. Cytogenetic evaluation of functionalised single-walled carbon nanotube in mice bone marrow cells. *Environmental Toxicology* 31.19: 1091-1102.

Payne, A. H. and Hales, D. B. 2004. Overview of steriodogenic enzymes in the pathway from cholesterol to active steroid hormones. *Endocrine Reviews* 25.6: 947-970.

Payne, A. H. and Youngblood, G. L. 1995. Regulation of expression of steriodogenic enzymes in Leydig cells. *Biology of Reproduction* 52.2: 217-225.

Perreault, F., Pedroso Melegari, S., Henning de Costa, C., de Oliveira Franco Rossetto, A. L., Popovic, R. and Gerson Matias, W. 2012. Genotoxic effects of copper oxide nanoparticles in Neuro 2A cell cultures. *Science of the Total Environment* 441: 117-124.

Petkovic, J., Zegura, B., Stevanovic, M., Drnovšek, N., Uskokovic, D., Novak, S. and Filipic, M. 2011. DNA damage and alterations in expression of DNA damage responsive genes induced by TiO_2 nanoparticles in human hepatoma HepG2 cells. *Nanotoxicology* 5.3: 341–53.

Piao, M. J., Kang, K. A., Lee, I. K., Kim, H. S., Kim, S., Choi, J. Y., Choi, J. and Hyun, J. W. 2011. Silver nanoparticles induce oxidative cell damage in human liver cells trough inhibition of reduced glutathione and induction of mitochondria-involved apoptosis. *Toxicology Letters* 201.1: 92-100.

Piccinno, F., Gottschalk, F., Seeger, S. and Nowack, B. 2012. Industrial production quantities and uses of ten engineered nanomaterials for Europe and the world. *Journal of Nanoparticle Research* 14: 1109–1120.

Pompella, A., Visvikis, A., Paolicchi, A., De Tata, V. and Casini, A.F. 2003. The changing faces of glutathione, a cellular protagonist. *Biochemical Pharmacology* 66.8:1499-1503.

Pott, F. and Roller, M. 2005. Carcinogenicity study with nineteen granular dusts in rats. *European Journal of Oncology* 10.4: 249-281.

Pourhamzeh, M., Mahmoudian, Z. G., Saidijam, M., Asari, M. J. and Alizadeh, Z. 2016. The effects of silver nanoparticles on the biochemical parameters of liver function in serum and the expression of caspase-3 in the liver tissues of male rats. *Avicenna Journal of Medical Biochemistry* 4.2:e35557.

Pratheepa, S. N., Kaur, S., Reddy, K. S. and Vivekanandam, S. 2008. Micronucleus Index: an early diagnosis in oral carcinoma. *Journal of the Anatomical Society of India* 57: 8–13.

Qu, X., Wang, J., Yao, C. and Zhang, Z. 2008. Two-photon imaging of lymphoma cells targeted by gold nanoparticles. *Chinese Optics Letters* 6.12: 879-881.

Rahman, Q., Lohani, M., Dopp, E., Pemsel, H., Jonas, L., Weiss, D. G. and Schiffmann, D. 2002. Evidence that ultrafine titanium dioxide induces micronuclei and apoptosis in Syrian hamster embryo fibroblasts. *Environmental Health Perspectives* 110.8: 797-800.

Rajapurohitam, V., Bedard, N. and Wing, S. S. 2002. Control of ubiquitination of proteins in rat tissues by ubiquitin conjugating enzymes and isopeptidases. *American Journal of Physiology-Endocrinology and Metabolism* 282: E739–745.

Rajapurohitam, V., Morales, C. R., El-Alfy, M., Lefrancois, S., Bedard, N. and Wing, S. S. 1999. Activation of a UBC4-dependent pathway of ubiquitin conjugation during postnatal development of the rat testis. *Developmental Biology* 212:217–228.

Ramaty, E., Maor, E., Peltz-Sinvani, N., Brom, A., Grinfeld, A., Kivity, S., Segev, S., Sidi, Y., Kessler, T., Sela, B. A. and Segal, G. 2014. Low ALT blood levels predict long-term all-cause mortality among adults. A historical prospective cohort study. *European Journal of Internal Medicine* 25.10: 919-921.

Ramdhan, D. H., Ito, Y., Yanagiba, Y., Yamagishi, N., Hayashi, Y., Li, C., Taneda, S., Suzuki, A. K., Watanabe, G., Taya, K., Kamijima, M. and Nakajima, T. 2009. Nanoparticle-rich diesel exhaust may disrupt testosterone biosynthesis and metabolism via growth hormone. *Toxicology Letters* 191.2-3: 103-108.

Ramesh, M., Palanisamy, K., Babu, K. and Sharma, N. K. 2014. Effects of bulk and nano-titanium dioxide and zinc oxide on physio-morphological changes in *Triticum aestivum* linn. *Journal of Global Biosciences* 3.2: 415-422.

Ramsden, C. S., Smith, T. J., Shaw, B. J. and Handy, R. D. 2009. Dietary exposure to titanium dioxide nanoparticles in rainbow trout (*Oncorhynchus mykiss*): no effect on growth, but subtle biochemical disturbances in the brain. *Ecotoxicology* 18.7: 939–951.

Ramsden, C. S., Henry, T. B. and Handy, R. D. 2013. Sub-lethal effects of titanium dioxide nanoparticles on the physiology and reproduction of zebrafish. *Aquatic Toxicology* 126: 404–413.

Rattner, J. B. and Brinkley, B. R. 1972. Ultrastructure of mammalian spermiogenesis. 3. The organisation and morphogenesis of the manchette during rodent spermiogenesis. *Journal of Ultrastructure Research* 41: 209–218.

Ray, P.C., Yu, H. and Fu, P.P. 2009. Toxicity and environmental risks of nanomaterials: challenges and future needs. *Journal of Environmental Science and Health Part C Environmental Carcinogenesis and Ecotoxicology Reviews* 27.1: 1-35.

Razin, S. and Tully, J. G. 1970. Cholesterol requirement of mycoplasmas. *Journal of Bacteriology* 102.2: 306-310.

Reddy, U. A., Prabhakar, P. V. Mahboob, M. 2015. Biomarkers of oxidative stress for *in vivo* assessment of toxicological effects of iron oxide nanoparticles. *Saudi Journal of Biological Sciences* http://doi.org/10.1016/j.sjbs.2015.09.029.

Reeves, J. F., Davies, S. J., Dodd, N. J. K. and Jha, A. N. 2008. Hydroxyl radicals (.OH) are associated with titanium dioxide (TiO_2) nanoparticle-induced cytotoxicity and oxidative DNA damage in fish cells. *Mutation Research* 640.1-2: 113-122.

Reichling, J. J. and Kaplan, M. M. 1988. Clinical use of serum enzymes in liver disease. *Digestive Diseases and Sciences* 33.12:1601-1614.

Reitman, S. and Frankel, S. A. 1957. A colourimetric method for the determination of serum glutamic oxalacetic and glutamic pyruvic transaminases. *American Journal of Clinical Patholoys* 28.1: 56-63.

Repine, J. E., Bast, A. and Lankhorst, I. 1997. Oxidative stress in chronic obstructive pulmonary disease. *American Journal of Respiratory and Critical Care Medicine* 156. 2 Pt 1: 341-357.

Reshma, V. G. and Mohanan, P. V. 2016. Induction of cytotoxicity and oxidative stress of dextran coated ferrite nanoparticles (dfnps) on a549 cell lines. *Journal of Pharmacology and Clinical Research* 1.5. DOI: 10.19080/JPCR.2016.01.555572.

Rice-Evans, C., Omorphos, C. and Baysal, E. 1986. Sickle cell membrane and oxidative damage. *Biochemistry Journal* 237.1: 265-269.

Rivkin, E., Cullinan, E. B., Tres, L. L. and Kierszenbaum, A. L. 1997. A protein associated with the manchette during rat spermiogenesis is encoded by a gene of the TBP-1-like subfamily with highly conserved ATPase and

protease domains. *Molecular Reproduction and Developmental Journal* 48:77–89.

Roest, H. P., van Klaveren, J., de Wit, J., van Gurp, C. G., Koken, M. H., Vermey, M., van Roijen, J. H., Hoogerbrugge, J. W., Vreeburg, J. T., Baarends, W. M., Bootsma, D., Grootegoed, J. A. and Hoeijmakers, J.H. 1996. Inactivation of the HR6B ubiquitin-conjugating DNA repair enzyme in mice causes male sterility associated with chromatin modification. *Cell* 86:799–810.

Rossi, E. M., Pylkkanen, L., Koivisto, A. J., Vippopa, M., Jensen, K. A., Miettinen, M., Sirola, K., Nykasenoja, H., Karisola, P., Stjernvall, T., Vanhala, E., Kiilunen, M., Pasanen, P., Makinen, M., Hameri, K., Joutsensaari, J., Tuomi, T., Jokiniemi, J., Wolff, H., Savolainen, K., Matikainen, S. and Alenius, H. 2010. Airway Exposure to Silica-Coated TiO_2 Nanoparticles Induces Pulmonary Neutrophilia in Mice. *Toxicological Sciences* 113.2: 422–433.

Roursgaard, M., Jensen, K. A., Poulsen, S. S., Jensen, N. E., Poulsen, L. K., Hammer, M., Nielsen, G. D. and Larsen, S. T. 2011. Acute and subchronic airway inflammation after intratracheal instillation of quartz and titanium dioxide agglomerates in mice. The *Scientific World Journal* 11: 801–825.

Russell, L. D., Russell, J. A., MacGregor, G. R. and Meistrich, M. L. 1991. Linkage of manchette microtubules to the nuclear envelope and observations of the role of the manchette in nuclear shaping during spermiogenesis in rodents. *American Journal of Anatomy* 192: 97–120.

Ryu, H. J., Seo, M. Y., Jung, S. K., Maeng, E. H., Lee, S. Y., Jang, D. H., Lee, T. J., Jo, K. Y., Kim, Y. R., Cho, K. B., Kim, M. K., Lee, B. J. and Son, S. W. 2014. Zinc oxide nanoparticles: a 90-day repeated dose dermal toxicity study in rats. *International Journal of Nanomedicine* 9.S2: 137-144.

Sadeghiani, N., Barbosa, L. S., Silva, L. P., Azevedo, R. B., Morais, P. C. and Lacava, Z. G. M. 2005. Genotoxicity and inflammatory investigation in mice treated with magnetitie nanoparticles surface coated with polyasoartic acid. *Journal of Magnetism and Magnetic Materials* 289: 466-468.

Sadek, S. A., Soliman, A. M. and Marzouk, M. 2016. Ameliorative effect of *Allolobophora caliginosa* extract on hepatotoxicity induced by silicon dioxide nanoparticles. *Toxicology and Industrial* Health 32.8: 1358-1372.

Sadiq, R., Bhalli, J. A., Yan, J., Woodruff, R. S., Pearce, M. G., Li, Y., Mustafa, T., Watanabe, F., Pack, L. M., Biris, A. S., Khan, Q. M. and Chen, T. 2012. Genotoxicity of TiO_2 anatase nanoparticles in B6C3F1 male mice evaluated using *Pig-a* and flow cytometric micronucleus assays. *Mutation Research* 745.1-2: 65-72.

Sahu, D., Kannan, G. M., Vijayaraghavan, R., Anand, T. and Khanum, F. 2013. Nanosized zinc oxide induces toxicity in human lung cells. *International Scholarly research Notices Toxicology* 8. DOI:10.1155/2013/316075.

Sang, X., Zheng, L., Sun, Q., Li, N., Cui, Y., Hu, R., Gao, G., Cheng, Z., Cheng, J., Gui, S., Liu, H., Zhang, Z. and Hong, F. 2012. The chronic spleen injury in mice following long-term exposure to titanium dioxide nanoparticles. *Journal of Biomedical Material Research A* 100.4: 894-902.

Sarkar, A. and Sil, P. 2014. Iron oxide nanoparticles mediated cytotoxicity via PI3K/AKT pathway: Role of quercetin. *Food and Chemical Toxicology* 71: 106-115.

Sarkheil, M., Johari, S. A., An, H. J., Asghari, S., Park, H. S., Sohn, E. K. and Yu, I J. 2018. Acute toxicity, uptake, and elimination of zinc oxide nanoparticles (ZnO NPs) using saltwater microcrutacean, Artemia franciscana. *Environmental Toxicology and Pharmacology* 57: 181-188.

Sasaki, Y. F., Kawaguchi, S., Kamaya, A., Ohshita, M., Kabasawa, K., Iwama, K., Taniguchi, K. and Tsuda, S. 2002. The comet assay with 8 mouse organs: results with 39 currently used food additives. *Mutation Research*519.1-2: 103–119.

Savage, J. R. 1988. A comment on the quantitative relationship between micronuclei and chromosomal aberrations. *Mutation Research* 207: 33–36.

Sayes, C. M., Reed, K. L. and Warheit, D. B. 2007. Assessing toxicity of fine and nanoparticles: comparing *in vitro* measurements to *in vivo* pulmonary toxicity profiles. *Toxicological Sciences* 97.1: 163–180.

Sayes, C. M., Wahi, R., Kurian, P. A., Liu, Y., West, J. L., Ausman, K. D., Warheit, D. B. and Colvin, V. L. 2006. Correlating nanoscale titania structure with toxicity: a cytotoxicity and inflammatory response study with human dermal fibroblasts and human lung epithelial cells. *Toxicology Science* 92.1: 174-185.

Schumacher, J. M., Artzt, K. and Braun, R. E. 1998. Spermatid perinuclear acid-binding protein binds microtubules and associates with abnormal manchettes *in vivo* in mice. *Biology of Reproduction* 59: 69-76.

Schilling, K., Bradford, B., Castelli, D., Dufour, E., Nash, J. F., Pape, W., Schlte, S., Tooley, I., van den Bosch, J. and Schellauf, F. 2010. Human safety review of "nano" titanium dioxide and zinc oxide. *Photochemical and Photobiological Sciences* 9.4: 495–509.

Schmid, W. 1975. The micronucleus test. *Mutation Research* 31.1:9-15.

Scott-Fordsmand, J. J., Krogh, P. H., Schaefer, M. and Johansen, A. 2008. The toxicity testing of double-walled nanotubes-contaminated food to *Eisenia veneta* earthworms. *Ecotoxicology and Environmental Safety* 71.3: 616-619.

Scown, T. M., Van Aerle, R. and Tyler, C. R. 2010. Review: Do engineered nanoparticles pose a significant threat to the aquatic environment? *Critical Reviews in Toxicology* 40.7: 653-670.

Scown, T. M., van Aerle, R. Y., Johnston, B. D., Cumberland, S., Lead, J. R., Owen, R. and Tyler, C. R. 2009. High doses of intravenously treated titanium dioxide nanoparticles accumulate in the kidneys of rainbow trout but no observable impairment of renal function. *Toxicology Science* 109.2: 372-380.

Seabra, A. B. and Duran, N. 2015. Nanotoxicology of Metal Oxide Nanoparticles. *Metals* 5.2: 934-975.

Seok, S. H., Cho, W., Park, J. S., Na, Y., Jang, A., Kim, H., Cho, Y., Kim, T., You, J., Ko, S., Kang, B., Lee, J. K., Jeong, J. and Che, J. 2013. Rats pancreatitis produced by 13-week administration of zinc oxide nanoparticles: biopersistence of nanoparticles and possible solutions. *Journal of Applied Toxicology* 33.10: 1089-1096.

Setyawati, M. I., Tay, C. Y., Docter, D., Stauber, R. H. and Leong, D. T. 2015. Understanding and exploiting nanoparticles intimacy with the blood vessel and blood. *Chemical Society Reviews* 44: 8174-8199.

Setyawati, M. I., Mochalin, V. N. and Leong, D. T. 2016. Tuning endothelial permeability with functionalized nanodiamonds. ACS NANO 10: 1170-1181.

Shao, X., Tarnasky, H. A., Lee, J. P., Oko, R. and van der Hoorn, F. A. 1999. Spag4, a novel sperm protein, binds outer dense-fiber protein odf1 and localizes to microtubules of manchette and axoneme. *Developmental Biology* 211: 109-123.

Sharghi, H., Khalifeh, R. and Doroodmand, M. M. 2009. Copper Nanoparticles on Charcoal for Multicomponent Catalytic Synthesis of 1,2,3-Triazole Derivatives from Benzyl Halides or Alkyl Halides, Terminal Alkynes and Sodium Azide in Water as a "Green" Solvent. *Advanced Synthesis and Catalysis* 351.1-2: 207-218.

Sharma, V., Anderson, D. and Dhawan, A. 2012b. Zinc oxide nanoparticles induce oxidative DNA damage and ROS-triggered mitochondria mediated apoptosis in human liver cells (HepG2). *Apoptosis* 17.8: 852-870.

Sharma, V., Shukla, R., Saxena N., Parmar, D., Das, M. and Dhawan, A. 2009. DNA damaging potential of zinc oxide nanoparticles in human epidermal cells. *Toxicology Letters* 185.3: 211-218.

Sharma, V., Singh, P., Pandey, A. and Dhawan, A. 2012a. Induction of oxidative stress, DNA damage and apoptosis in mouse liver after sub-acute oral exposure to zinc oxide nanoparticles. *Mutation Research* 745.1-2: 84-91.

Sharma, V., Singh, S. K., Anderson, D., Tobin, D. J. and Dhawan, A. 2011. Zinc oxide nanoparticles induced genotoxicity in primary human epidermal keratinocytes. *Journal of Nanoscience and Nanotechnology* 11.5: 3782–3788.

Shaymurat, T., Gu, J., Xu, C., Yang, Z., Zhao, Q., Liu, Y. and Liu, Y. 2012. Phytotoxic and genotoxic effects of ZnO nanoparticles on garlic (*Allium sativum* L.): A morphological study. *Nanotechnology* 6.3: 241-248.

Sheth, S. G., Flamm, S. L., Gordon, F. D. and Chopra, S. 1998. AST/ALT ratio predicts cirrhosis in patients with chronic hepatitis C virus infection. *American Journal of Gastroenterology* 93.1: 44-48.

Shi, H., Magaye, R., Castranova, V. and Zhao, J. 2013. Titanium dioxide nanoparticles: a review of current toxicological data. *Particle and Fibre Toxicology* 10: 15. DOI: 10.1186/1743-8977-10-15.

Shi, J. P., Evans, D. E., Khan, A. A. and Harrison, R. M. 2001. Sources and concentration of naoparticles (< 10 nm diameter) in the urban atmosphere. *Atmospheric Environment* 35.7: 1193-1202.

Shi, Y., Zhang, J., Jiang, M., Zhu, L. Tan, H. and Lu, B. 2010. Synergistic Genotoxicity Caused by Low Concentration of Titanium Dioxide Nanoparticles and p,p'-DDT in Human Hepatocytes. *Environmental and Molecular Mutagenesis* 51.3: 192-204.

Shinohara, N., Matsumoto, K., Endoh, S., Maru, J. and Nakanishi, J. 2009. *In vitro* and *in vivo* genotoxicity tests on fullerene C60 nanoparticles. *Toxicology Letters* 191.2-3: 289–296.

Shokouhian, A., Soheilli, S., Moradhaseli, S., Fazli, L., Ardestani, M. and Ghorbani, M. 2013. Toxicity of zinc oxide nanoparticles in lung tissue after repeated oral administration. *American Journal of Pharmacology and Toxicology* 8.4:148-154.

Shrivastava, R., Kushwaha, P., Butia, Y. C. and Flora, S. J. S. 2014b. Oxidative stress induced following exposure to silver and gold nanoparticles in mice. *Toxicology and Industrial Health* 32.8: 1391-1404.

Shrivastava, R., Raza, S., Yadav, A., Kushwaha, P. and Flora, S. J. S. 2014a. Effects of subacute exposure to TiO_2, ZnO and Al_2O_3 nanoparticles on oxidative stress and histological changes in mouse liver and brain. *Drug and Chemical Toxicology* 37.3: 336-347.

Shukla, R. K., Kumar, A., Gurbani, D., Pandey, A. K., Singh, S. and Dhawan A. 2013. TiO_2 nanoparticles induce oxidative DNA damage and apoptosis in human liver cells. *Nanotoxicology* 7.1: 48-60.

Shukla, R. K., Kumar, A., Vallabani, N. V. S., Pandey, A. and Dhawan, A. 2014. Titanium dioxide nanoparticle-induced oxidative stress triggers DNA damage and hepatic injury in mice. *Nanomedicine* 9.9: 1423-1434.

Shukla, R. K., Sharma, V., Pandey, A. K., Singh, S., Sultana, S. and Dhawan, A. 2011. ROS-mediated genotoxicity induced by titanium dioxide nanoparticles in human epidermal cells. *Toxicology in vitro* 25.1: 231–241.

Sich, D., Saudi, Y., Giral, P., Lagrost, L., Egloff, M., Auer, C., Gautier, V., Turpin, G. and Beucler, I. 1998. Hyperalphalipoproteinemia: charcaterisation of a carioprotective profile associating increased high-density lipoprotein 2 levels and decreased hepatic lipase activity. *Metabolism* 47.8: 965-973.

Siemianowicz, K., Gminski, J., Stajszczyk, M., Wojakowski, W., Goss, M., Machalski, M., Telega, A., Brulinski, K. and Magiera-Molendowska, H. 2000. Serum total cholesterol and triglycerides levels in patient with lung cancer. *International Journal of Molecular Medicine* 5.2: 201-205.

Sies, H., Stahl, W. and Sevanian, A. 2005. Nutritional, dietary and postprandial oxidative stress. *Journal of Nutrition* 135.5: 969-972.

Sikka, S. C. and Hellstrom, W. J. G. 2016. Current updates on laboratory techniques for the diagnosis of male reproductive failure. *Asian Journal of Andrology* 18.3: 392-401.

Silva, A. H., Locatelli, C., Filho, U. P. R., Gomes, B. F., de Carvalho Junior, R. M., de Gois, J. S., Borges, D. L. G. and Creczynski-Pasa, T. B. 2017. Visceral fat increase and signals of inflammation in adipose tissue after administration of titanium dioxide nanoparticles in mice. *Toxicology and Industrial Health* 33.2: 147-158.

Silvente-Poirot, S. and Poirot, M. 2012. Cholesterol metabolism and cancer: the good, the bad and the ugly. *Current Opinion in Pharmacology* 12.6: 673-676.

Singh, R. and Lillard, J. W. 2009. Nanoparticle-based targeted drug delivery. *Experimental and Molecular Pathology* 86.3: 215-223.

Singh, S. P., Kumari, M., Kumari, S. I., Rahman, M. F., Maboob, M. and Grover, P. 2013. Toxicity assessment of manganese oxide macro and nanoparticles in wistar rats after 28 days of repeated oral exposure. *Journal of Applied Toxicology* 33.10: 1165-1179.

Singh, S., Shi, T., Duffin, R., Albrecht, C., van Berlo, D., Hohr, D., Fubini, B., Martra, G., Fenoglio, I., Born, P. J. A. and Schins, R. P. F. 2007. Endocytosis, oxidative stress and IL-8 expression in human lung epithelial cells upon treatment with fine and ultrafine TiO_2: Role of the specific surface area and of surface methylation of the particles. *Toxicology and Applied Pharmacology* 222: 141-151.

Sioutas, C., Delfino, R. J. and Singh, M. 2005. Exposure assessment for atmospheric ultrafine particles (UFPs) and implications in epidemiologic research. *Environmental Health Perspectives* 113.8: 947-955.

Sleiman, H. K., Romano, R. M., Oliveira, C. A. and Romano, M. A. 2013. Effects of prepubertal exposure to silver nanoparticles on reproductive parameters in adult male Wistar rats. *Journal of Toxicology and Environmental Health Part A* 76.17: 1023-1032.

Smith, C. J., Shaw, B. J. and Handy, R. D. 2007. Toxicity of single walled carbon nanotubes on rainbow trout (*Oncorhynchus mykiss*): respiratory toxicity, organ pathologies and other physiological effects. *Aquatic Toxicology* 82.2: 94–109.

Smith, D. J. 2015. Nanomaterials Using Transmission Electron Microscopy, in Nano Characterisation: In Royal Society of Chemistry Nanoscience & Nanotechnology. Pp 1-29.

Smith, M. A., Michael, R., Aravindan, R. G., Dash, S., Shah, S. I., Galileo, D. S. and Martin-DeLeon, P. A. 2015. Anatase titanium dioxide nanoparticles in mice: evidence for induced structural and functional sperm defects after short-, but not long-, term exposure. *Asian Journal of Andrology* 17: 261-268.

Smith, T. T. and Yanagimachi, R. 1990. The viability of hamster sperm stored in the isthmus of the oviduct: the importance of sperm-epithelium contact for sperm survival. *Biology of Reproduction* 42: 450–457.

Soliman, M. M., Attia, H. F., Hussein, M. M., Mohamed, E. H. and Ismail, T. A. 2013. Protective effect of n-acetylcysteine against titanium dioxide nanoparticles modulated immune responses in male albino rats. *American Journal of Immunology* 9.4: 148-158.

Som, C., Berges, M., Chaudhry, Q., Dusinska, M., Fernandes, T. F., Olsen, S. I., Nowack, B. 2010. The importance of life cycle concepts for the development of safe nanoproducts. *Toxicology* 269.2-3: 160–169.

Song, M., Li, Y., Kasai, H. and Kawai, K. 2012. Metal nanoparticle-induced micronuclei and oxidative damage in mice. *Journal of Clinical Biochemistry and Nutrition* 50.3: 211-216.

Sriram, M. I., Kanth, S. B., Kalishwaralal, L. and Gurunathan, S. 2010. Antitumour acitivity of silver nanoparticles in Dalton's lymphoma ascites tumour model. *International Journal of Nanomedicine* 5: 753-762.

Srivastav, A. K., Kumar, M., Ansari, N. G., Jain, A. K, Shankar, J., Arjaria, N, Jagdale, P. and Singh, D. 2016. A comprehensive toxicity study of zinc oxide nanoparticles versus their bulk in Wistar rats: Toxicity study of zinc oxide nanoparticles. *Human and Experimental Toxicology* 35.12: 1286-1304.

Srivastava, R. K., Rahman, Q., Kashyap, M. P., Lohani, M. and Pant, A. B. 2011. Ameliorative effects of dimetylthiourea and N-acetylcysteine on nanoparticles induced cyto-genotoxicity in human lung cancer cells-A549. *PLoS One* 6.9:e25767.

Srivastava, R. K., Rahman, Q., Kashyap, M. P., Singh, A. K., Jain, G., Jahan, S., Lohani, M., Lantow, M. and Pant, A. B. 2013. Nano-titanium dioxide induces genotoxicity and apoptosis in human lung cancer cell line, A549. *Human and Experimental Toxicology* 32.2:153-166.

Stefani, D., Wardman, D. and Lambert, T. 2005. The implosion of the Calgary General Hospital: ambient air quality issues. *Journal of the Air and Waste Management Association* 55.1: 52-59.

Stocco, D. M. 2001. StAR protein and the regulation of steroid hormone biosynthesis. *Annual Review of Physiology* 63: 193-213.

Stone, V., Johnston, H. and Schins, R. P. 2009. Development of *in vitro* systems for nanotoxicology: methodological considerations. *Critical Reviews in Toxicology* 39.7: 613–626.

Stone, V., Nowack, B., Baun, A., van den Brink, N., Kammer, F., Dusinska, M., Handy, R., Hankin, S., Hassellov, M., Joner, E. and Fernandes, T. F. 2010. Nanomaterials for environmental studies: classification, reference material issues and strategies for physicochemical characterisation. *Science of the Total Environment* 408.7: 1745-1754.

Stratton, M. R., Campbell, P. J. and Futreal, P. A. 2009. The cancer genome. *Nature* 458: 719–24.

Strojny, B., Kurantowicz, N., Sawosz, E., Grodzki, M., Jaworski, S., Kutwin, M., Wierzbicki, M., Hotowy, A., Lipinska, L. and Chwalibog, A. 2015. Long term influence of carbon nanoparticles on health and liver status in rats. *PLoS ONE* 10.12: e0144821.

Styrna J., Imai, H. T. and Moriwaki, K. 1991. An increased level of sperm abnormalities in mice with a partial deletion of the Y chromosome. *Genetics Research Cambridge* 57:195–199.

Su, D. 2017. Advanced electron microscopy characterisation of nanomaterials for catalysis. *Green Energy and Environment* 2.2: 70-83.

Suarez, S. S. 1987. Sperm transport and motility in the mouse oviduct: obsevations *in situ*. *Biology of Reproduction* 36: 203–210.

Sun, F., Ko, E. and Martin, R. H. 2006. Is there a relationship between sperm chromosome abnormalities and sperm morphology? *Reproductive Biology and Endocrinology* 4:1.

Sun, L., Singh, A. K., Vig, K., Pillai, S. R. and Singh, S. R. 2008. Silver nanoparticles inhibit replication of respiratory syncytial virus. *Journal of Biomedical Nanotechnology* 4.2:149-158.

Suzuki, H., Ikeda, N., Kobayashi, K., Terashima, Y., Shimada, Y., Suzuki, T., Hagiwara, T., Hatakeyama, S., Nagaoka, K., Yoshida, J., Saito, Y., Tanaka, J. and Hayashi, M. 2005. Evaluation of liver and peripheral blood micronucleus assays with 9 chemicals using young rats: A study by the Collaborative Study Group for the Micronucleus Test (CSGMT)/Japanese Environmental Mutagen Society (JEMS)-Mammalian Mutagenicity Study Group (MMS). *Mutation Research* 583:133–45.

Suzuki, Y., Nagae, Y., Li, J., Sakaba, H., Mozawa, K., Takahashi, A. and Shimizu, H. 1989. The micronucleus test and erythropoiesis. Effects of erythropoietin and a mutagen on the ratio of polychromatic to normochromatic erythrocytes (P/N ratio). *Mutagenesis* 4.6: 420-424.

Syama, S., Reshma, S. C., Leji, B., Anju, M., Sreekanth, P. J., Varma, H. K. and Mohanan, P. V. 2014. Toxicity evaluation of dextran coated ferrite nanomaterials after acute oral exposure to wistar rats. *Journal of Allergy and Therapy* 5:166. DOI: 10.4172/2155-6121.1000166.

Sycheva, L. P., Zhurkov, V. S., Lurchenko, V. V., Daugel-Dauge, N. O., Kovalenko, M. A., Krivtsova, E. K. and Durnev, A. D. 2011. Investigation of genotoxic and cytotoxic effects of micro- and nanosized titanium dioxide in six organs of mice *in vivo*. *Mutation Research* 726.1: 8-14.

Szasz, G. 1969. A kinetic photometric method for serum gamma-glutamyl transpeptidase. *Clinical Chemistry* 15.2: 124-136.

Talebi, A. R., Khorsandi, L. and Moridian, M. 2013. The effect of zinc oxide nanoparticles on mouse spermatogenesis. *Journal of Assisted Reproduction and Genetics* 30.9: 1203-1209.

Taniguchi, N. 1974. On the Basic Concept of Nanotechnology. *Proceedings of the International Conference on Production Engineering, Tokyo*. p 18-23.

Tao, Y., Zhang, H., Gao, B., Guo, J., Hu, Y. and Su, Z. 2011.Water-soluble chitosan nanoparticles inhibit hypercholesterolemia induced by feeding a high-fat diet in male sprague-dawley rats. *Journal of Nanomaterials* 2011. doi:10.1155/2011/814606.

Tassinari, R., Cubadda, F., Moracci, G., Aureli, F., D'Amato, M., Valeri, M., De Berardis, B., Raggi, A., Mantovani, A., Passeri, D., Rossi, M. and Maranghi, F. 2014. Oral, short-term exposure to titanium dioxide nanoparticles in Sprague-Dawley rat: focus on reproductive and endocrine systems and spleen. *Nanotoxicology* 8.6: 654-662.

Tavares, A. M., Louro, H., Antunes, S., Quarre, S., Simar, S., De Temmerman, P, J., Verleysen, E., Mast, J., Jensen, K. A., Norppa, H., Nesslany, F. and Silva, M. J. 2014. Genotoxicity evaluation of nanosized titanium dioxide, synthetic amorphous silica and multi-walled carbon nanotubes in human lymphocytes. *Toxicology In vitro* 28.1: 60-69.

Taylor, D. A. 2002. Dust in the wind. *Environmental Health Perspective* 110.2: A80-A87.

Thakur, M., Gupta, H., Singh, D., Mohanty, I. R., Maheswari, U., Vanage, G. and Joshi, D. S. 2014. Histopathological and ultra structural effects of nanoparticles on rat testis following 90 days (Chronic study) of repeated oral administration. *Journal of Nanobiotechnology* 12:42.

Thatcher, T. L. and Layton, D. W. 1995. Deposition, resuspension and penetration of particles within a residence. *Atmospheric Environment* 29.13: 1487-1497.

The Collaborative Study Group for the Micronucleus Test. 1986. Sex difference in the micronucleus test. *Mutation Research* 172: 151–63.

Thurnherr, T., Brandenberger, C., Fischer, K., Diener, L., Manser, P., Maeder-Althaus, X., Kaiser, J., Krug, H. F., Rothen-Rutishauser, B. and Wick, P. 2011. A comparison of acute and long-term effects of industrial mutliwalled carbon nanotubes on human lung and immune cells in vitro. *Toxicology Letters* 200.3: 176-186.

Tian, B., Zheng, X., Kempa, T. J., Fang, Y., Yu, N., Yu, G., Huang, J. and Lieber, C. M. 2007. Coaxial silicon nanowires as solar cells and nanoelectronic power sources. *Nature* 449: 885-889.

Tietz, N. W. 1990. Clinical guide to laboratory tests, Second Edition W. B. Saunders Company, Philadelphia, USA 554-556.

Tilly, J. L. 1998. Molecular and genetic basis of normal and toxicant-induced apoptosis in female germ cells. *Toxicology Letters* 102-103: 497-501.

Toblli, J. E., Cao, G., Oliveri, L. and Angerosa, M. 2011. Assessment of the extent of oxidative stress induced by intravenous ferumoxytol, ferric carboxymaltose, iron sucrose and iron dextran in a nonclinical model. *Arzneimittel-Forschung* 61.7: 399–410.

Tomankova, K., Horakova, J., Harnanova, M., Malina, L., Soukupova, J., Hradilova, S., Kejlova, K., Malohlava, J., Licman, L., Dvorakova, M., Jirova, D. and Kolarova, H. 2015. Cytotoxicity, cell uptake and microscopic analysis of titanium dioxide and silver nanoparticles *in vitro*. *Food and Chemical Toxicology* 82:106-115.

Topham, J. C. 1980b. Chemically induced transmissible abnormalities in sperm head shape. *Mutation Research* 70: 109–114.

Topham, J. C. 1980a. The detection of carcinogen induced sperm head abnormalities in mice. *Mutation Research* 69: 149–155.

Torjesen, P. A. and Sandnes, L. 2004. Serum testosterone in women as measured by n automated immunoassay and a RIA. *Clinical Chemistry* 50.3: 678-679.

Toth, P. P. 2005. The "good cholesterol" high-density lipoprotein. *Circulation* 111.5: e89-91.

Touvier, M., Fassier, P., His, M., Norat, T., Chan, D. S. M., Blacher, J., Hercberg, S., Galan, P., Druesne-Pecollo, N. and Latino-Martel, P. 2015. Cholesterol and breast cancer risk: a systematic review and meta-analysis of prospective studies. *British Journal of Nutrition* 114.3: 347-357.

Traynor, J., Mactier, R., Geddes, C. C. and Fox, J. G. 2006. How to measure renal function in clinical practice. *BMJ* 333.7571: 733-737.

Trinder, P. 1969. Determination of glucose in blood using glucose oxidase with an alternative oxygen receptor. *Annals of Clinical Biochemistry* 6: 24 – 27.

Trouiller, B., Reliene, R., Westbrook, A., Solaimani, P. and Schiestl, R. H. 2009. Titanium dioxide nanoparticles induce DNA damage and genetic instability *in vivo* in mice. *Cancer Research* 69.22: 8784-8789.

Tsai, S. J., Ada, E., Isaacs, J. A. and Ellenbecker, M. J. 2009. Airborne nanoparticle exposures associated with the manual handling of nanoalumina and nanosilver in fume hoods. *Journal of Nanoparticle Research* 11.1: 147-161.

Tu, M., Huang, Y., Li, H. and Gao, Z. 2012. The stress caused by nitrite with titanium dioxide nanoparticles under UVA irradiation in human keratinocyte cell. *Toxicology* 299.1: 60-68.

Turkez, H. 2011. The role of ascorbic acid on titanium dioxide-induced genetic damage assessed by the comet assay and cytogenetic tests. *Experimental and Toxicologic Pathology* 63.5: 453-457.

Uboldi, C., Urban, P.,Gillilard, D., Bajak, E., Valsami-Jones, E., Ponti. And Rossi, F. 2016. Role of the crystalline form of titanium dioxide nanoparticles: rutile, and not anatase induces toxic effects in balb3T3 mouse fibroblasts. *Toxicology In Vitro* 31: 137-145.

Umrani, R. D. and Paknikar, K. M. 2014. Zinc oxide nanoparticles show antidiabetic activity in streptozotocin-induced Type 1 and 2 diabetic rats. *Nanomedicine* 9.1: 89-104.

Unnithan, J., Rehman, M. U., Ahmad, F. J. and Samim, M. 2011. Aqueous synthesis and concentration-dependent dermal toxicity of TiO_2 nanoparticles in Wistar rats. *Biological Trace Element Research* 143.3: 1682–1694.

Valdiglesias, V., Costa, C., Sharma, V., Killc, G., Pasaro, E., Teixeira, J. P., Dhawan, A. and Laffon, B. 2013. Comparative study on effects of two different types of titanium dioxide nanoparticles on human neuronal cells. *Food and Chemical Toxicology* 57:352-361.

Valerino, D. M. and McCormack, J. J. 1971. Xanthine oxidase-mediated oxidation of epinephrine. *Biochemical Pharmacology* 20.1: 47-55.

Van der Steeg, W. A., Holme, I., Boekholdt, S. M., Larsen, M. L., Lindahl, C., Stroes, E. S., Tikkanen, M. J., Wareham, N. J., Faergeman, O., Olsson, A. G., Pedersen, T. R., Khaw, K. T. and Kastelein, J. J. 2008. High-density lipoprotein cholesterol, high-density lipoprotein particle size and apolipoprotein A-I: significance for cardiovascular risk: the IDEAL and EPIC-Norfolk studies. *Journal of the American College of Cardiology* 51.6: 634 – 642.

Vasan, S. S. 2011. Semen analysis and sperm function test: How much to test? *Indian Journal of Urology* 27.1: 41-48.

Vaseem, M., Umar, A. and Hahn, Y. B. 2010. Chapter 4: ZnO nanoparticles: growth, properties and application. In: Umar, A. and Hahn, Y. B. (Eds.), Metal Oxide Nanostructures and Their Applications, 4th edition. *American Scientific Publishers* 5: 1-36.

Vega-Villa, K. R., Takemoto, J. K., Yáñez, J. A., Remsberg, C. M., Forrest, M. L. and Davies N. M. 2008. Clinical toxicities of nanocarrier systems. *Advanced Drug Delivery Reviews* 60.8: 929–938.

Vernet, P., Aitken, R. J. and Drevet, J. R. 2004. Antioxidant strategies in the epididymis. *Molecular and Cellular Endocrinology* 216.1-2: 31-39.

Vevers, W. F. and Jha, A. N. 2008. Genotoxic and cytotoxic potential of titanium dioxide (TiO_2) nanoparticles on fish cells *in vitro*. *Ecotoxicology* 17.5: 410-420.

Wakata, A., Miyamae, Y., Sato, S., Suzuki, T., Morita, T., Asano, N., Awogi, T., Kondo, K. and Hayashi, M. 1998. Evaluation of the rat micronucleus test with bone marrow and peripheral blood: Summary of the 9th collaborative study by CSGMT/JEMS·MMS. *Environmental and Molecular Mutagenesis* 32: 84–100.

Walenta, J. H., Didier, A. J., Liu, X. and Kramer, H. 2001. The golgi associated hook3 protein is a member of a novel family of microtubule binding proteins. *Journal of Cell Biology* 152: 923–934.

Wang, B., Feng, W., Wang, M., Wang, T., Gu, Y., Zhu, M., Ouyang, H., Shi J., Zhang, F., Zhao, Y., Chai, Z., Wang, H. and Wang, J. 2008a. Acute toxicological impact of nano- and submicro-scaled zinc oxide powder on healthy adult mice. *Journal of Nanoparticle Research* 10.2: 263-276.

Wang, C. and Li, Y. 2012. Interaction and nanotoxic effect of TiO_2 nanoparticle on fibrinogen by multi-spectroscopic method. *Science of the Total Environment* 429: 156–160.

Wang, D., Hu, J., Irons, D. and Wang, J. 2011. Synergistic toxic effect of nano-TiO_2 and As(V) on *Ceriodaphnia dubia*. *Science of the Total Environment* 409.7: 1351-1356.

Wang, D., Li, H., Liu, Z., Zhou, J. and Zhang, T. 2017a. Acute toxicological effects of zinc oxide nanoparticles after intratracheal instillation. *International Journal of Occupational and Environmental Health*. 23.1: 11-19.

Wang, E., Huang, Y., Du, Q. and Sun, Y. 2017b. Silver nanoparticle induced toxicity to human sperm by increasing ROS (reactive oxygen species) production and DNA damage. *Environmental Toxicology and Pharmacology* DOI: http://dx.doi.org:10.1016/j.etap.2017.04.010

Wang, H., Wick, R. L. and Xing, B. 2009. Toxicity of nanoparticulate and bulk ZnO, Al_2O_3 and TiO_2 to the nematode *Caenorhabditis elegans. Environmental Pollution* 157.4: 1171-1177.

Wang, J., Liu, Y., Jiao, F., Lao, F., Li, W., Gu, Y., Li, Y., Ge, C., Zhou, G., Li, B., Zhao, Y., Chai, Z. and Chen, C. 2008b. Time-dependent translocation and potential impairment on central nervoussystem by intranasally instilled TiO_2 nanoparticles. *Toxicology* 254. 1-2: 82–90.

Wang, J., Zhou, G., Chen, C., Yu, H., Wang, T., Ma, Y., Jia, G., Gao, Y., Li, B., Sun, J., Li, Y., Jiao, F, Zhao, Y. and Chai, Z. 2007. Acute toxicity and

biodistribution of different sized titanium dioxide particles in mice after oral administration. *Toxicology Letters* 168.2: 176-185.

Wang, L., Wang, L., Ding, W. and Zhang, F. 2010. Acute toxicity of ferric oxide and zinc oxide nanoparticles in rats. *Journal of Nanoscience and Nanotechnology* 10.12: 8617–8624.

Warburg, O. 1956. On the origin of cancer cells. *Science* 123.3191: 309-314.

Ward, M. A. 2005. Intracytoplasmic sperm injection effects in infertile *azh* mutant mice. *Biology of Reproduction* 73.1: 193-200.

Ward, M. A. and Burgoyne, P. S. 2006. The effects of deletions of the mouse Y chromosome long arm on sperm function-intracytoplasmic sperm injection (ICSI)-based analysis. *Biology of Reproduction* 74: 652–658.

Warheit, D. B., Hansen, J. F., Yuen, I. S., Kelly, D. P., Snajdr, S. I. and Hartsky, M. A. 1997. Inhalation of high concentrations of low toxicity dusts in rats results in impaired pulmonary clearance mechanisms and persistent inflammation. *Toxicology and Applied Pharmacology* 145.1: 10–22.

Warheit, D. B., Hoke, R. A., Finlay, C., Donner, E. M., Reed, K. L. and Sayes, C. M. 2007a. Development of a base set of toxicity tests using ultrafine TiO_2 particles as a component of nanoparticle risk management. *Toxicology Letters* 171.3: 99-110.

Warheit, D. B., Sayes, C. M. and Reed, K. L. 2009. Nanoscale and fine zinc oxide particles: can *in vitro* assays accurately forecast lung hazards following inhalation exposures? *Environmental Science and Technology* 43.20: 7939–7945.

Warheit, D. B., Webb, T. R., Reed, K. L., Frerichs, S. and Sayes, C. M. 2007b. Pulmonary toxicity study in rats with three forms of ultrafine-TiO_2 particles: Differential responses related to surface properties. *Toxicology* 230.1: 90-104.

Warheit, D. B., Webb, T. R., Sayes, C. M., Colvin, V. L. and Reed, K. L. 2006. Pulmonary instillation studies with nanoscale TiO_2 rods and dots in rats: toxicity is not dependent upon particle size and surface area. *Toxicological Sciences* 91.1: 227–236.

Warheit, D. B., Yuen, I. S., Kelly, D. P., Snajdr, S. and Hartsky, M. A. 1996. Subchronic inhalation of high concentrations of low toxicity, low solubility particulates produces sustained pulmonary inflammation and cellular proliferation. *Toxicology Letters* 88.1-3: 249–253.

Warth, M. R., Arky, R. A. and Knopp, R. H. 1975. Lipid metabolism in pregnancy. altered lipid composition in intermediate, very low, low and high-density lipoprotein fractions. *Journal of Clinical Endocrinology Metabolism* 41.4: 649-655.

Weatherburn, M. W. 1967. Phenol-hypocholrite reaction for determination of ammonia. *Analytical Chemistry* 39.8: 917 – 974.

Wei, Y., Zhao, M., Yang, F., Mao, Y., Xie, H. and Zhou, O. 2016. Iron overload by superparamagnetic iron oxide nanoparticles is a high risk factor in cirrhosis by a systems toxicology assessment. *Scientific Reports* 6: 29110. DOI: 10.1038/srep29110.

Weir, A., Westerhoff, P., Fabricius, L., Hristovski, K. and von Goetz, N. 2012. Titanium dioxide nanoparticles in food and personal care products. *Environmental Science and Technology* 46.4: 2242–2250.

Weisburger, J. H. and Williams, G. M. 1981. Carcinogen testing: current problems and new approaches. *Science* 214: 401–407.

Welty, F. K. 2014. Hypobetalipoproteinemia and abetalipoproteinemia. *Current Opinion in Lipidology* 25.3: 161-168.

Westerdahl, D., Fruin, S., Sax, T., Fine, P. M. and Sioutas, C. 2005. Mobile platform measurements of ultrafine particles and associated pollutant concentrations on freeways and residential streets in Los Angeles. *Atmospheric Environment* 39.20: 3597-3610.

Wickline, S. A., Neubauer, A. M., Winter, P., Caruthers, S. and Lanza, G. 2006. Applications of nanotechnology to atherosclerosis, thrombosis and vascular biology. *Arteriosclerosis, thrombosis and vascular biology* 26.3: 435-41.

Williams, D., Amman, M., Autrup, H., Bridges, J., Cassee, F., Donaldson, K., Fattal, E., Janssen, C., De Jong, W., Jung, T., Marty, J. P. and Rydzynski, K. 2005. The appropriateness of existing methodologies to assess the potential risks associated with engineered and adventitious products of nanotechnologies. *In: risks Scoeanih, editor: European commission health and consumer protection directorate general*. p 1-78.

World Health Oragnisation. 2010. WHO laboratory manual for the examination and processing of human semen. 5th edition Geneva: World Health Organisation. 287 pp. http://www.who.int/iris/handle/10665/44261

Wu, J., Liu, W., Xue, C., Zhou, S., Lan, F., Bi, L., Xu, H., Yang, X. and Zeng, F. D. 2009. Toxicity and penetration of TiO_2 nanoparticles in hairless mice and porcine skin after subchronic dermal exposure. *Toxicology Letters* 191.1: 1–8.

Wu, W., Samet, J. M., Peden, D. B. and Bromberg, P. A. 2010. Phosphorylation of p65 is required for zinc oxide nanoparticle-induced interleukin 8 expression in human bronchial epithelial cells. *Environmental Health Perspectives* 118.7: 982–987.

Wyrobek, A. J. and Bruce, W. R. 1975. Chemical induction of sperm abnormalities in mice. *Proceedings of the National Academy of Science USA* 72.11: 4425-4429.

Wyrobek, A. J.,Gordon, L. A., Burkhart, J. G., Francis, M. W., Kapp Jr, R. W., Letz, G., Malling, H. G., Topham, J. C. and Whorton, M. D. 1983. An evaluation of the mouse sperm morphology test and other sperm tests in non-human mammals. A report of the United States Environmental Protection Agency Gene–Tox Programme. *Mutation Research* 115.1: 1-72.

Xia, B., Chen, J. and Zhou, Y. 2011. Cellular Oxidative Damage of HEK293T Cells Induced by Combination of $CdCl_2$ and Nano-TiO_2. *Journal of Huazhong University of Science and Technology (Medical Science)* 31.3: 290-294.

Xia, T., Kovochich, M., Liong, M., Madler, L., Gilbert, B., Shi, H. B., Yeh, J. L., Zink, J. L. and Nel, A. E. 2008. Comparison of the mechanism of toxicity of zinc oxide and cerium oxide nanoparticles based on dissolution and oxidative stress properties. *ACS Nano* 2.10: 2121-2134.

Xia, T., Zhao, Y., Sager, T., George, S., Pokhrel, S., Li, N., Schoenfeld, D., Meng, H., Lin, S., Wang, X., Wang, M., Ji, Z., Zink, J. I., Madler, L., Castranova, V., Lin, S. and Nel, A.E. 2011. Decreased dissolution of ZnO by iron doping yields nanoparticles with reduced toxicity in the rodent lung and zebrafish embryos. *ACS Nano.* 5.2: 1223–1235.

Xiao, L., Takada, H., Maeda, K., Haramoto, M. and Miwa, N. 2005. Antioxidant effects of water-soluble fullerene derivatives against ultraviolet ray or peroxylipid through their action of scavenging the reactive oxygen species in human skin keratinocytes. *Biomedicine and Pharmacotherapy* 59.7: 351-358.

Xie, G. P., Wang, C., Sun, J. and Zhong, G. R. 2011. Tissue distribution and excretion of intravenously treated titanium dioxide nanoparticles. *Toxicology Letters* 205.1: 55-61.

Xu, J., Futakuchi, M., Alexander, D. B., Fukamachi, K., Numano, T., Suzui, M., Shimizu, H., Omori, T., Kanno, J., Hirose, A. and Tsuda, H. 2014. Nanosized zinc oxide particles do not promote DHPN-induced lung carcinogenesis but cause reversible epithelial hyperplasis of terminal bronchioles. *Archives of Toxicology* 88.1: 65-75.

Xu, J., Sagawa, Y., Futakuchi, M., Fukamachi, K., Alexander, D. B., Furukawa, F., Ikarashi, Y., Uchino, T., Nishimura, T., Morita, A., Suzui, M. and Tsuda,

H. 2011. Lack of promoting effect of titanium dioxide particles on ultraviolet B-initiated skin carcinogenesis in rats. *Food and Chemical Toxicology* 49.6: 1298–1302.

Xu, Z. P., Niebert, M., Porazik, K., Walker, T. L., Cooper, H. M., Middleberg, A. P., Gray, P. P., Bartlett, P. F. and Lu, G. Q. 2008. Subcellular compartment targeting of layered double hydroxide nanoparticles. *Journal of Controlled Release* 130.1: 86-94.

Xue, C., Liu, W., Wu, J., Yang, X. and Xu, H. 2011. Chemoprotective effect of N-acetylcysteine (NAC) on cellular oxidative damages and apoptosis induced by nano titanium dioxide under UVA irradiation. *Toxicology In Vitro* 25.1: 110-116.

Yaar, M. and Gilchrest, B. 2003. *Aging of skin* In: I.M. Freedberg, A.Z. Eisen, K. Wolff, K.F. Austen, L.A. Goldsmith, S.I. Katz (Eds.), Fitzpatrick's dermatology in general medicine, McGraw Hill, New York, pp. 1386–1398.

Yah, C. S., Simate, G. S. and Iyuke, S. E. 2012. Nanoparticles toxicity and their routes of exposures. *Pakistan Journal of Pharmaceutical Science*s 25.2: 477-491.

Yamagishi, Y., Watari, A., Hayata, Y., Li, X., Kondoh, M., Yoshioka, Y., Tsutsumi, Y. and Yagi, K. 2013. Acute and Chronic nephrotoxicity of platinum nanoparticles in mice. *Nanoscale Research letters* 8.1:395.

Yamashita, K., Yoshioka, Y., Higashisaka, K., Mimura, K., Morishita, Y., Nozaki, M., Yoshida, T., Ogura, T., Nabeshi, H., Nagano, K., Abe, Y., Kamada, H., Monobe, Y., Imazawa, T., Aoshima, H., Shishido, K., Kawai, Y., Mayumi, T., Tsunoda, S., Itoh, N., Yoshihawa, T., Yanagihara, I., Saito, S. and Tsutsumi, Y. 2011. Silica and titanium dioxide nanoparticles cause pregnancy complications in mice. *Nature Nanotechnology* 6.5: 321-328.

Yang, H., Liu, C., Yang, D. F., Zhang, H. S. and Xi, Z. 2009. Comparative study of cytotoxicity, oxidative stress and genotoxicity induced by four typical nanomaterials: The role of particle size, shape and composition. *Journal of Applied Toxicology* 29.1: 69–78.

Yasuda, K., Okuda, K., Endo, N., Ishiwatari, Y., Ikeda, R., Hayashi, H., Yokozeki, K., Kobayashi, S. and Irie, Y. 1995. Hypoaminotransferasemia in patients undergoing long-term hemodialysis: clinical and biochemical appraisal. *Gastroenterology* 109.4: 1295-1300.

Yazdi, A. S., Guarda, G., Riteau, N., Drexler, S. K., Tradivel, A., Couillin, I. and Tschopp, J. 2010. Nanoparticles activate the NLR pyrin domain containing 3 (Nlrp3) inflammasome and cause pulmonary inflammation through release of IL-1α and IL-1β. *Proceedings of the National Academy of Science U S A* 107.45: 19449–19454.

Yin, J., Liu, J., Ehrenshaft, M., Roberts, J. E., Fu, P. P., Mason, R. P. and Zhao, B. 2012. Photoxicity of nano titanium dioxides in HaCat keratinocytes-Generation of reactive oxygen species and cell damage. *Toxicology and Applied Pharmacology* 263.1: 81-88.

Yoisungern, T., Choi, Y., Han, J. W., Kang, M., Das, J., Gurunathan, S., Kwon, D., Co, S., Park, C., Chang, W., K., Chang, B., Parnpai, R. and Kim, J. 2015. Internalisation of silver nanoparticles into mouse spermatozoa results in poor fertilisation and compromised embryo development. *Scientific Report* DOI: 10.1038/srep11170.

Yoshida, R., Kitamura, D. and Maenosono, S. 2009a. Mutagenicity of water-soluble ZnO nanoparticles in Ames test. *Journal of Toxicology Sciences* 34.1: 119–122.

Yoshida, S., Hiyoshi, K., Ichinose, T., Takano, H., Oshio, S., Sugawara, I., Takeda, K. and Shibamoto, T. 2008. Effect of nanoparticles on the male reproductive system of mice. *International Journal of Andrology* 32.4: 337-342.

Yoshida, S., Sagai, M., Oshio, S., Umeda, T., Ihara, T., Sugamata, M., Sugawara, I., and Takeda, K. 1999. Exposure to diesel exhaust affects the male reproductive system of mice. *International Journal of Andrology* 22: 307–315.

Yoshida, S., Hiyoshi, K., Ichinose, T., Takano, H., Oshio, S., Sugawara, I., Takeda, K. and Shibamoto, T. 2009b. Effect of nanoparticles on the male reproductive system of mice. *International Journal of Andrology* 32.4:337–342.

Yoshikawa, T. and Naito, Y. 2002. What is Oxidative Stress? *JMAJ* 45.7: 271-276.

Yuan, G., Al-Shali, K. Z. and Hegele, R. A. 2007. Hypertriglyceridemia: Its etiology, effects and treatment. *Canadian Mecical Association Journal* 176.8: 1113-1120.

Yuan, Y., Ding, J., Xu, J., Deng, J. and Guo, J. 2010. TiO_2 nanoparticles co-doped with silver and nitrogen for antibacterial application. *Journal of Nanoscience and Nanotechnology* 10.8: 4868–4874.

Zhang, H., Chen, B., Jiang, H., Wang, C., Wang, H. and Wang, X. 2011a. A strategy for ZnO nanorod mediated multi-mode cancer treatment. *Biomaterials* 32.7: 1906–1914.

Zhang, H., Yang, D., Yang, H. and Liu, H. 2008. Effect on conception and offspring development in female parental rats following intratracheal instillation of nano-C ZnO and C-ZnO composite nanoparticles. *Wei Sheng Yan Jiu* 37.6: 654-656.

Zhang, J., Song, W., Guo, J., Sun, Z., Li, L., Ding, F. and Gao, M. 2013. Cytotoxicity of different sized TiO_2 nanoparticles in mouse macrophages. *Toxicology and Industrial Health* 29.6: 523-533.

Zhang, R., Bai, Y., Zhang, B., Chen, L. and Yan B. 2012. The potential health risk of titania nanoparticles. *Journal of Hazardous Materials* 211-212: 404– 413.

Zhang, R., Niu, Y., Li, Y., Zhao, C., Song, B., Li, Y. and Zhou, Y. 2010. Acute toxicity study of the interaction between titanium dioxide nanoparticles and lead acetate in mice. *Environmental Toxicology and Pharamacology* 30.1: 52-60.

Zhang, W. X. 2003. Nanoscale iron particles for environmental remediation: An overview. *Journal of Nanoparticle Research* 5.3: 323-332.

Zhang, W., Jiang, P., Chen, W., Zheng, B., Mao, Z., Antipov, A., Correia, M., Larsen, E. H. and Gao, C. 2016. Genotoxicity of copper oxide nanoparticles with different surface chemistry on rat bone marrow mesenchymal stem cells. *Journal of Nanoscience and Nanotechnology* 16.6: 5489-5497.

Zhang, X. D., Wu, D., Shen, X., Liu, P. X., Yang, N., Zhao B., Zhang, H., Sun, Y., Zhang, L. and Fan, F. 2011b. Size-dependent *in vivo* toxicity of PEG-coated gold nanoparticles. *International Journal of Nanomedicine* 6: 2071-2081.

Zhang, X., Choi, Y., Han, J. W., Kim, E., Park, J. H., Gurunathan, S. and Kim, J. 2015. Differential nanoreprotoxicity of silver nanoparticles in male somatic cells and spermatogonial stem cells. *International Journal of Nanomedicine* 10: 1335-1357.

Zhao, W. A., Pacard, E., Chaix-Bauvais, C., Pichot, C. and Brook, M. A. 2009. Covalent assembly of silica nanoparticle aggregates for oligonucleotide synthesis. *Colloids and Surfaces A - Physicochemical and Engineering Aspects* 339.1-3: 26-34.

Zhao, X., Sheng, L., Wang, L., Hong, J., Yu, X., Sang, X., Sun, Q., Ze, Y. and Hong, F. 2014. Mechanisms of nanosized titamium dioxide-induced testicular oxidative stress and apoptosis in male mice. *Particle and Fibre Toxicology* 11.1: 47.

Zheng, D., Wang, N., Wang, X., Tang, Y., Zhu, L., Huang, Z., Tang, H., Shi, Y., Wu, Y., Zhang, M. and Lu, B. 2012. Effects of the interaction of TiO_2 nanoparticles with bisphenol A on their physicochemical properties and *in vitro* toxicity. *Journal of Hazardous Materials* 199-200: 426-432.

Zhong, X. H., Wang, R., Liu, L. B., Kang, M., Wen, Y. Y., Hou, F., Feng, J. M. and Li, Y. L. 2012. Structures and characterisation of bundles of collapsed double-walled carbon nanotubes. *Nanotechnology* 23.50: 505712.

Zhu, H., Han, J., Xiao, J. Q. and Jin, Y. 2008. Uptake, translocation and accumulation of manufactured iron oxide nanoparticles by pumpkin plants. *Journal of Environmental Monitoring* 10.6: 713-717.

Zhu, X., Zhou, J. and Cai, Z. 2011. The toxicity and oxidative stress of TiO_2 nanoparticles in marine abalone (*Haliotis diversicolor* supertexta). *Marine Pollution Bulletin* 63. 5-12: 334-338.

APPENDIX 1

UNIVERSITY OF IBADAN, IBADAN, NIGERIA
DEPARTMENT OF VETERINARY PATHOLOGY

Cables & Telegrams: UNIVERSITY IBADAN
E-mail: uivetpath@yahoo.com
Fax: 02-8103043, 02-8103118
Tel: 022-8103168, 022-8103380

19th January, 2015.

Dr. A.A. Bakare,
Dept. of Zoology ,
University of Ibadan,
Ibadan.

RE: APPLICATION FOR ETHICAL APPROVAL ON UI-ACUREC/014/1

On behalf of the University of Ibadan **Animal Care and Use Research Ethics Committee (UI-ACUREC)**, I write to grant you an **Ethical Approval** for a study on the "***In Vivo Evaluation of Genotoxicity and Mutagenicity of Metal and Metal Oxide Nanoparticles in Animal Models***" **strictly as outlined in your final proposal submitted for assessment.**

Please quote **UI-ACUREC/App/2015/005** as reference for this approval.

You are to note that **UI-ACUREC** reserves the right to monitor and conduct compliance visit to your research site without previous notification.

Thank you.

19/01/2015

Prof. V.O. Taiwo
Chairperson, U.I ACUREC

Cc: Dean, FVM
Director, Research Management Office

APPENDIX 2


ALDRICH
Titanium(IV) oxide, anatase
ALDRICH
Zinc oxide
HAZARDOUS WASTE
AUTOCLAVABLE
DISPOSAL BAG
HAZARDOUS
WASTE
SANDELIN

APPENDIX 3

1. Alanine Aminotransferase

Pipetted into test tubes

Procedure

	Reagent blank	Sample
Sample	-	0.1 mL
Buffer (R1)	0.5 mL	0.5 mL
Distilled H_2O	0.1 mL	-

The solution was properly mixed and incubated at 37°C for exactly 30 minutes

2, 4-dinitrophenylhydrazine (R2)	0.5 mL	0.5 mL

The solution was properly mixed again, and then allowed to stand at 20 to 25°C for exactly 20 minutes

NaOH (0.4 mol/L)	5.0 mL	5.0 mL

The solution was read at 546 nm against the reagent blank.

ALT activity (U/L) was read off the standard curve

2. Aspartate Aminotransferase

Pipetted into test tubes

Procedure

	Reagent blank	Sample
Sample	-	0.1 mL

Buffer (R1)	0.5 mL	0.5 mL
Distilled H_2O	0.1 mL	-

The solution was properly mixed and incubated at 37°C for exactly 30 minutes

2, 4-dinitrophenylhydrazine (R2)	0.5 mL	0.5 mL

The solution was properly mixed again, and then allowed to stand at 20 to 25°C for exactly 20 minutes

NaOH (0.4 mol/L)	5.0 mL	5.0 mL

The solution was read at 546 nm against the reagent blank.

AST activity (U/L) was read off the standard curve

3. γ- Glutamyl transferases

Working reagent

One vial of substrate R1b (L-γ-glutamyl-3-carboxy-4-nitroanilide) was reconstituted with 3.0 mL of R1a (Buffer/Glycylglycine), which was stable for 21 days.

Procedure

Pipetted into the cuvette:

Sample - 0.10 mL

Reagent (25°C, 30°C, 37°C) - 1.00 mL

The initial absorbance of the solution was read at 0 seconds, 1, 2 and 3 minutes at 405 nm.

Calculation

$$GGT\ (U/L) = \frac{A_{3min}-A_{0min}}{3} \times 1158$$

4. Total bilirubin

Pipetted into test tubes

Procedure

	Sample
Sulphanilic acid (R1)	200 µL
Sodium Nitrite (R2)	50 µL
Caffeine (R3)	1000 µL
Sample	200 µL

Mixed, incubated for exactly 10 minutes at 20 – 25 ^{o}C

Tartrate (R4)	1000 µL

Mixed and further incubated for 30 minutes at 25°C. Read at 578 nm against the reagent blank.

Calculation

T. Bilirubin (mg/dL) = 10.8 x A_{TB} (578 nm)

Direct bilirubin

Pipetted into test tubes

Procedure

	Sample
Sulphanilic acid (R1)	200 µL
Sodium Nitrite (R2)	50 µL

0.9 % NaCl	2000 µL
Sample	200 µL

Mixed, incubated for exactly 10 minutes at 20 – 25 ^{o}C. Read at 546 nm against the reagent blank.

Calculation

D. Bilirubin (mg/dL) = 14.4 x A_{DB} (546 nm)

5. Albumin

Pipette into test tubes

Procedure

	Reagent	Standard	Sample
Distilled H_2O	0.01 mL	-	-
Standard	-	0.01 mL	-
Sample	-	-	0.01 mL
BCG reagent (R1)	3 mL	3 mL	3 mL

The solution was properly mixed and incubated at 20 – 25°C for 5 minutes. The standard and sample absorbances were read against distilled H_2O at 630 nm.

Calculation

$$\text{ALB (g/dL)} = \frac{A_{sample}}{A_{standard}} \times \text{Concentration of the standard (4.55 g/dL)}$$

6. Urea

Working reagents

R1 = Rla (Urease) + R1b (Sodium nitroprusside)

R2 = Dilute R2 (phenol concentrate) with 660 mL of distilled water

R3 = Dilute R3 (Hypochlorite concentrate with 750 mL of distilled water)

Pipetted into test tubes

Procedure

Blank	Standard	Sample
Sample	-	-	10 µL
Standard	-	10 µL	-
Distilled water	10 µL	-	-
Reagent 1	100 µL	100 µL	100 µL

Mixed and incubated at 37°C for 10 minutes

Reagent 2	2.5 mL	2.5 mL	2.5 mL
Reagent 3	2.5 mL	2.5 mL	2.5 mL

The solution was immediately mixed and incubated for 15 minutes at 37°C

The standard and sample absorbances were read against distilled H_2O at 546 nm.

Calculation

$$\text{Urea (mg/dL)} = \frac{A_{sample}}{A_{standard}} \times \text{Concentration of the standard (76.87 mg/dL)}$$

7. Creatinine

Working reagent = equal volumes of solutions R1a (picric acid) + R1b (sodium hydroxide)

Pipetted into the cuvette	Standard	Sample
Working reagent	1.0 mL	1.0 mL
Sample	0.1 mL	-
Standard	0.1 mL	-

Solutions were mixed and read at 492 nm after 30 seconds (A_{30sec}) and 2 minutes ($A_{2minutes}$) respectively against distilled water

Change in absorbance = $A_{2minutes}$-A_{30sec}

Calculation

$$\text{Creatinine (mg/dL)} = \frac{\text{Change in absorbance of sample}}{\text{Change in absorbance of standard}} \times \text{Standard concentration}$$

8. Cholesterol

Pipetted into test tubes

Procedure

Reagent	Blank	Standard	Sample
Distilled water	10 µL	-	-
Standard	-	10 µL	-
Sample	-	-	10 µL
Reagent	1000 µL	1000 µL	1000 µL

Mixed and incubated at 37°C for 5 minutes and read at 546 nm against the reagent blank

Calculation

$$\text{Cholesterol (mg/dL)} = \frac{\Delta A_{sample}}{\Delta A_{standard}} \times \text{concentration of standard (208 mg/dL)}$$

9. High-density lipoprotein

Working reagent = Phosphotungstic acid (R1) + 20 mL redistilled water

Precipitation

Sample/Standard	200 µL
Diluted Precipitant (R1)	500 µL

The solution was properly mixed and allowed to stand at room temperature for 10 minutes. Thereafter, it was spun for 10 minutes at 4 000 rpm.

The clear supernatant was separated and used in determining HDL-cholesterol by the CHOD-PAP method

HDL- cholesterol CHOD-PAP method

Pipetted into the test tubes

Reagent	Blank	Standard	Sample
Distilled water	100 µL	-	-
Supernatant	-	-	100 µL
Standard supernatant	-	100 µL	-
Reagent	1000 µL	1000 µL	1000 µL

The solution was mixed and incubated for 10 minutes at 25°C. The sample and standard absorbances were measured against distilled H_2O at 546 nm.

Calculation

$$\text{HDL-Cholesterol (mg/dL)} = \frac{\Delta A_{sample}}{\Delta A_{standard}} \times \text{Concentration of the standard (208 mg/dL)}$$

10. Triglycerides

Working reagent = 15 mL of R1a (buffer) was added to one vial of enzyme reagent R1b

Procedure

Pipetted into test tubes

Reagent	Blank	Standard	Sample
Sample	-	-	10 µL
Standard	-	10 µL	-
Working Reagent	1000 µL	1000 µL	1000 µL

The solution was properly mixed and incubated at 20 – 25°C for 10 minutes. The absorbances of the standard and sample were measured against the reagent blank at 546 nm.

Calculation

$$\text{TRI (mg/dL)} = \frac{A_{sample}}{A_{standard}} \times \text{Concentration of the standard (192 mg/dL)}$$

11. Estimation of proteins

Reagents

0.2 M sodium hydroxide (NaOH)

Sodium hydroxide (8g) was dissolved in distilled H_2O and the solution made up to a litre.

Biuret reagent

Copper sulphate (3g of $CuSO_4.5H_2O$) and 9g of sodium potassium tartarate were dissolved in 0.2 M NaOH (500 mL). Potassium Iodide (5g KI) was added to the solution, and thereafter topped up to 1000 mL with 0.2 M NaOH.

3. Stock Bovine Serum Albumin (standard)

7.4 g of BSA was dissolved in 100 mL of 0.9 % NaCl so that the final concentration gave 7.4 g/100 mL.

4. Standard BSA curve by the Biuret method

Stock solution was made into several dilutions of 2 – 10 mg protein/mL. Biuret reagent (4 mL) was added into the test tubes containing 1 mL of each protein standard. The solution was incubated for 30 minutes at room temperature while the wave length was read at 540 nm. A plot of protein concentration (X axis) against optical densities (Y axis) was made.

Table1: Protein estimate determined according to Gornal *et al*. (1949)

Test tube number	1	2	3	4	5	6	7	8	9
Stock BSA (mL)	0.1	0.2	0.3	0.4	0.5	0.6	0.7	0.8	0.9
Distilled water (mL)	0.9	0.8	0.7	0.6	0.5	0.4	0.3	0.2	0.1
Biuret reagent (mL)	4	4	4	4	4	4	4	4	4
BSA concentration (mg/mL)	0.05	0.10	0.20	0.30	0.40	0.50	0.60	0.70	0.80
Absorbance (540 nm)	0.004	0.006	0.008	0.014	0.0185	0.024	0.028	0.042	0.042

Protein estimate in samples

Procedure

The supernatants (post mitochondrial fractions) of the liver, kidney and testes were diluted 5 times with distilled water. Biuret reagent (3 mL) was added to 1 mL of the supernatant in the test tubes. The solution was incubated for 30 minutes at room temperature. The optical density was read at 540 nm while distilled water served as a blank. The actual amount of the protein was obtained by multiplying the protein content of the samples by 5.

12. Determination of Superoxide Dismutase Activity

Reagents

1. 0.05 M Carbonate Buffer, pH 10.2

$Na_2CO_3.10H_2O$ (14.3 g) and $NaHCO_3$ (4.2 g) were dissolved in distilled water (900 mL) and then topped up to 1000 mL.

2. 0.3 M of adrenaline.

Adrenaline (epinephrine) (0.0137 g) was freshly prepared prior to the experiment by dissolving in distilled water (200 mL) and then topped up to 250 mL.

Procedure

A 1 in 10 dilution was made by diluting the sample (1 mL) and distilled water (9 mL). Within a cuvette, 0.3 mL of 0.3 mM adrenaline was added to the mixture of 2.5 mL of 0.05 M carbonate buffer (pH 10.2) and 0.2 mL of the diluted sample to initiate the reaction. After proper mixing by inversion, the mixture was read at every 30 seconds interval for a total of 150 seconds. The blank consisted of distilled water (0.2 mL), adrenaline (0.3 mL) and carbonate buffer (2.5 mL).

Calculation

$$\text{Increase in absorbance per minute} = \frac{A_3 - A_0}{2.5}$$

Where A_0 = absorbance after 0 seconds

A_3 = absorbance after 150 seconds

$$\% \text{ inhibition} = \frac{\text{Increase in absorbance for substrate}}{\text{Increase in absorbance of blank}} \times \frac{100}{1}$$

1 unit of SOD activity was given as the amount of SOD necessary to cause 50% inhibition of the oxidation of adrenaline.

13. Determination of Catalase Activity

Reagents

1. Phosphate buffer (0.05 M, pH 7.4)

Distilled water (90 mL) was added to dissolve potassium dihydrogen phosphate (0.265 g) and dipotassium hydrogen phosphate trihydrate ($K_2HPO_4.3H_2O$) (0.696 g). Distilled water was added to make up 100 mL after adjusting the pH to 7.4.

2. Hydrogen peroxide (H_2O_2) (19 mM)

Phosphate buffer (pH 7.4) (50 mL) was added to hydrogen peroxide (30 %) (215.3 µL) and topped up to 100 mL using the same phosphate buffer.

Procedure

The cuvette contained 50 µL of the sample and 2.95 mL of 19 mM H_2O_2. The solution was properly mixed and immediately read at 240 nm for every 15 sec for 1 min for the liver and kidney homogenates, and every 1 min for 5 min for the testis homogenate.

Calculation

$$\text{Catalase activity} = \frac{\Delta A240/\text{min} \times \text{reaction volume} \times \text{dilution factor}}{0.0436 \times \text{sample volume} \times \text{mg protein/mL}}$$

$$= \mu\text{mole } H_2O_2/\text{min/mg protein}$$

14. Estimation of Reduced Glutathione (GSH) level

Reagents

Reduced Glutathione (GSH) working standard

Phosphate buffer (0.1 M, pH 7.4) was used in dissolving 40 mg of GSH in a beaker, and topped up to 100 mL with the same phosphate buffer.

0.1 M Phosphate buffer (pH 7.4)

7.1628 g of $Na_2HPO_4.12H_2O$ (Mol.Wt. 358.22) was dissolved in 200 mL of distilled water.

100 mL of distilled water was used in dissolving 1.5603 g of $NaH_2PO_4.2H_2O$.

200 mL of (a) and 100 mL of (b) were added up to produce 0.1 M phosphate buffer. HCl or NaOH was used to adjust the pH to 7.4.

Ellman's Reagent [5', 5'-dithiobis-(2-nitrobenzoate) (DTNB)]

0.1 M phosphate buffer was used in dissolving 40 mg of Ellman's reagent and then topped up to 100 mL using the same phosphate buffer. DNTB is stable for at least 3 weeks in the refrigerator.

Precipitating Solution.

Sulphosalicyclic acid (4 g) in little quantity was dissolved in 100 mL of distilled water in a standard volumetric flask.

Procedure

0.1 mL of diluted homogenate was further diluted with 0.9 mL of distilled water to give 1 in 10 dilutions. 3 mL of 4% sulphosalicyclic acid solution (precipitating solution) was added to the diluted test sample to deproteinize it. The mixture was centrifuged at 3000 rpm for 5 minutes. 4.5 mL of Ellman's Reagent was added to 0.5 mL of the supernatant. Reaction mixture of 4 mL of 0.1 M phosphate buffer, 0.5 mL of the diluted precipitating solution (addition of 3 mL of precipitating solution and 2 mL of distilled water) and 4.5 mL of Ellman's Reagent was the blank. The absorbances of the samples were read at 412 nm.

Table 2: Calibration for GSH standard curve

Stock	PO_4	Ellman's Reagent	Absorbance (412nm)	GSH Conc.(ug/ml)
0.02	0.48	4.50	0.033	8
0.05	0.45	4.50	0.099	20
0.10	0.40	4.50	0.246	40
0.20	0.30	4.50	0.346	60
0.30	0.20	4.50	0.505	80
0.40	0.10	4.50	0.683	100

15. Assessment of lipid peroxidation

Reagents

30% Trichloroacetic acid (TCA)

100 mL of distilled water was used in dissolving 30 g of TCA and stored at 4^0C.

0.75 % Thiobarbituric acid (TBA) in 0.1M HCl

10 mL of 0.1 M HCl was used in dissolving 0.075 g of TBA. It was freshly prepared by boiling in a water bath.

0.1 M Tris- KCl buffer, pH 7.4

Distilled water was used in dissolving 1.12 g of KCl and 2.36 g of Tris base and topped up to 100 mL with distilled water. The pH 7.4 was obtained using concentrated HCl.

Procedure

0.5 mL of 30 % TCA was added to a mixture of 1.6 mL of Tris-KCl buffer and 0.4 mL of the sample. Within each test tube was added 0.5 mL of 0.75 % TBA and boiled in a water bath for 45 min at 80^0C. This was cooled on ice and spun for 15 minutes at 3000 rpm. The pink solution formed was measured at an absorbance of 532 nm against distilled water (reagent blank). The method of Adam-Vizi and Sergi (1982) was used in calculating the MDA level. A molar extinction coefficient of 1.56 x $10^5 M^{-1} Cm^{-1}$ was computed with lipid peroxidation in units /mg protein or gram tissue.

Calculation

$$\text{MDA (units/mg protein)} = \frac{\text{Absorbance x Volume of mixture}}{E_{532nm} \text{ x Volume of Sample x mg Protein}}$$

16. Assessment of Luteinizing Hormone

Reagents

Microwells coated with Streptavidin, LH Standards, LH enzyme conjugate, TMB Substrate, Stop Solution and Wash concentrate (20X).

Working reagent

1X Wash buffer = 25 mL of the Wash concentrate in 475 mL of distilled water stored at room temperature (18-26°C).

Procedure: The desired numbers of coated wells were placed in a microplate holder. Then 25 µL of the LH standards and mice sera were pipetted into the microwells and 100 µL of the enzyme conjugate was added to all wells. This was incubated at room temperature (18-26°C) for 60 minutes. The mixtures were discarded and wash three times with the 1X wash buffer, blotted dry on an absorbent paper. Thereafter, 100 µL of the TMB substrate was added to the wells and incubated at room temperature for 15 minutes in the dark. Finally, 50 µL of the stop solution was added to the wells and shaken gently to stop the reaction. The absorbance was read within 15 minutes after the addition of the stop solution at 450 nm. The colour intensity was proportional to the absorbance at 450 nm.

Table 3: Calibration for LH standard curve

Standard	Values (mIU/mL)	OD (450 nm)
1	0	0.010
2	5	0.278
3	25	0.988
4	50	1.543
5	100	2.104
6	200	2.681

17. Assessment of Follicle Stimulating Hormone

Reagents

Microwells coated with Streptavidin, FSH Standards, FSH enzyme conjugate, TMB Substrate, Stop Solution and Wash concentrate (20X).

Working reagent

1X Wash buffer = 25 mL of the Wash concentrate in 475 mL of distilled water stored at room temperature (18-26°C).

Procedure: The desired numbers of coated wells were placed in a microplate holder. Then 50 µL of the FSH standards and mice sera were pipetted into the microwells and 100 µL of the enzyme conjugate was added to all wells. This was incubated at room temperature (18-26°C) for 60 minutes. The mixtures were discarded and wash three times with the 1X wash buffer, blotted dry on an absorbent paper. Thereafter, 100 µL of the TMB substrate was added to the wells and incubated at room temperature for 15 minutes in the dark. Finally, 50 µL of the stop solution was added to the wells and shaken gently to stop the reaction. The absorbance was read within 15 minutes after the addition of the stop solution at 450 nm. The colour intensity was proportional to the absorbance at 450 nm.

Table 4: Calibration for FSH standard curve

Standard	Values (mIU/mL)	OD (450 nm)
1	0	0.09
2	5	0.20
3	10	0.32
4	25	0.69
5	50	1.31
6	100	2.46

18. Assessment of Testosterone Hormone

Reagents

Microwells coated with Mouse Anti-Testosterone, Testosterone Standards, Enzyme Conjugate (20X), Assay Diluent, TMB Substrate, Stop Solution and Wash concentrate (20X).

Working reagent

1X Enzyme conjugate = 0.1 mL of the Testosterone enzyme conjugate concentrate to 1.9 mL of the assay diluent.

1X Wash buffer = 25 mL of the Wash concentrate in 475 mL of distilled water stored at room temperature (18-26°C).

Procedure

The desired numbers of coated wells were placed in a microplate holder. Then 25 µL of the Testosterone standards and mice sera were pipetted into the microwells and 100 µL of the Testosterone-enzyme conjugate reagent was added to all wells and swirled for 30 seconds. This was incubated at room temperature (18-26°C) for 60 minutes. The liquid

from all wells were discarded and wash three times with the 1X wash buffer, blotted dry on an absorbent paper. Thereafter, 100 µL of the TMB substrate was added to the wells and incubated at room temperature for 15 minutes in the dark. Finally, 50 µL of the stop solution was added to the wells and shaken gently to stop the reaction. The absorbance was read within 15 minutes after the addition of the stop solution at 450 nm. The colour intensity was inversely proportional to the absorbance at 450 nm.

Table 5: Calibration for Testosterone standard curve

Standard	Values (mIU/mL)	Absorbance (450 nm)
1	0	2.38
2	0.1	1.75
3	0.5	1.02
4	2.0	0.59
5	6.0	0.34
6	18.0	0.17